

PROGRESS TOWARD THE ASYMMETRIC TOTAL SYNTHESIS OF VARIECOLIN
AND
GAS-PHASE STUDIES OF THE TWISTED AMIDE 2-QUINUCLIDONE

Thesis by
Michael Raymond Krout

In Partial Fulfillment of the Requirements for the Degree of
Doctor of Philosophy

California Institute of Technology

Pasadena, California

2010

(Defended September 4, 2009)

© 2010

Michael Raymond Krout

All Rights Reserved

To my mother

ACKNOWLEDGEMENTS

I would like to express my utmost gratitude toward my advisor and mentor, Professor Brian Stoltz. The enthusiasm that Brian brings to chemistry is as contagious as his laugh. Brian fosters a group of highly skilled and creative co-workers that strive to address significant problems in our field, and the ceaseless progression of science is exciting to be a part of. Brian expected nothing but the best from everyone, and his high standards (and the accomplishments of those before me) were a continual source of motivation. His support, friendship, and advice throughout my experience in graduate school have been invaluable. I also share a personal connection with Brian in that we are both alumni from IUP. During my time at IUP I had never envisioned the possibility of attaining such a distinguished accolade, and for that reason, I sincerely have to thank Brian for this opportunity.

I would also like to extend my appreciation to the members of my thesis committee: Professors John Bercaw, Bob Grubbs, and Sarah Reisman. They have been highly supportive of my research, and their insightful questioning and advice during the various meetings throughout my time at Caltech have forced me to think of my research and proposals from new perspectives, greatly improving their quality and depth. I would also like to thank Professors Dave MacMillan and Bill Goddard for their tenure on my committee.

I owe my primary interest in science to Mr. Daryl Dreese and his challenging class in 7th grade physical science. Mr. Dreese had a remarkable ability to relate science beyond common facts published in a textbook. I enjoyed his unconventional teaching style and

was intrigued by his labs that were a constant exercise in creativity, critical thinking, and fun.

A significant shift in my scientific interests occurred when I audited an organic chemistry course by John T. Wood at IUP. I was a major in biochemistry at the time and had only a minor interest in organic chemistry. Despite this, a personal invitation from Dr. Wood's was impossible to pass up. He was an extraordinary teacher that persistently encouraged students to achieve more and provided me with the knowledge and confidence that I could accomplish anything as long as I'm willing to work hard enough. His efforts were not without the help of fellow student Chrysa Malosh, who was a regular in all of Dr. Wood's courses. I value her friendship and admire her tenacious approach to organic chemistry.

I was extremely fortunate to obtain several summer internships to augment my coursework at IUP. My first adventure into the lab (outside of general organic lab) was as a summer student in Professor William Bailey's lab at the University of Connecticut. This summer was mostly about the fundamentals, and thanks to Dr. Matt Luderer, I was able to conduct several experiments with *t*-BuLi! I then spent a summer and eight months in the Medicinal Chemistry Department at Merck in West Point, PA, and am grateful for my time working with Mr. Robert Gomez and Dr. Yuntae Kim. Bob and Yuntae were constructive mentors that exposed me to the chemical and biological aspects of medicinal chemistry, and both took an active role in my preparation for graduate school. I thank for their time and help at such an influential point of my career.

I have developed various friendships throughout my years in the Stoltz lab that have enhanced my Caltech experience. Professor Neil Garg has been a great friend, always

offering advice and encouragement. His creativity, hard work, and success have raised the bar of expectations for the Stoltz lab, and are characteristics that I strove to emulate during my time at Caltech. I have always looked up to Neil and thank him for all of his guidance. Professor Uttam Tambar was a very friendly, easygoing, and optimistic co-worker. I admire Uttam for his quiet confidence and tenacious enthusiasm for chemistry despite the many challenges we are often faced with in graduate school. Dr. Dan Caspi has been a like a brother, providing invaluable advice during my last year here. I have always enjoyed our discussions and his interesting outlook on life. There is always a good time to be had when hanging out with Dan, and also very little sleep. Dr. JT Mohr has been my best friend at Caltech, and one of the most intelligent people that I have ever met. His knowledge of random facts is uncanny, and our shared interest in sports and the outdoors was a great outlet from chemistry. Still waters run deep. I have also developed a close friendship with JT's wonderful wife, Sarah, and was lucky to be around during the birth of their daughter, Marie Elise. It was fun watching them grow into a family, and I look forward to our lifelong friendship. I also owe a lot of gratitude to Dr. John Phillips, Dr. Dave White, and Dr. Nolan McDougal for their friendship, advice, and numerous good times outside of the lab.

I feel extremely fortunate to have worked with Samantha Levine during her SURF and Dalton Fund fellowships. Sam's ability to assimilate reactions and techniques, coupled with her diligent work ethic, enabled her to become a successful chemist and one of the first undergraduates in the Stoltz lab to achieve a publication. I thoroughly enjoyed my time as Sam's mentor and will remember it as one of my most rewarding experiences at Caltech. I wish her the best in graduate school at Colorado State and beyond.

As I approached the conclusion of my graduate studies, I was joined on the variecolin project by two exceptional and talented chemists, Thomas Jensen and Dr. Chris Henry. The fresh ideas and meticulous work that Thomas and Chris have contributed to the project have enabled the development of a fascinating story that is nearing completion. I cannot express enough gratitude for their efforts and friendship, and I wish them the best of luck in attaining finality with the project and with their careers. I also owe thanks to Allen Hong and Nathan Bennett for their ongoing efforts on the ring contraction project.

There were various opportunities in the Stoltz lab to collaborate with labs outside of organic chemistry, and I'm grateful to have participated in the mass spectrometry studies of 2-quinuclidone with Professor Ryan Julian of UC Riverside. My interactions with his students Don Pham and Tony Ly were constructive, and together we uncovered some interesting chemistry with this quintessential twisted amide.

The entire Stoltz lab has been very supportive and a wonderful environment to explore ideas. Many people have passed through the lab over my time, including many graduate students, postdocs, visiting scholars, and undergraduates, and each person has influenced me professionally and personally. I want to thank the rest of classmates Mike Meyer, JT Mohr, Jennifer Roizen, and Jenn Stockdill for their friendship, collaboration, and advice with everyday things. The various Friday club meetings were instrumental in my maturation as a chemist, and I would like to thank anyone who has ever participated in them. They were rewarding to both the audience and the presenter, and I found them to be well worth the extra effort. I also would like to sincerely thank Dr. Chris Douglas and Dr. Tom Driver for their informative discussions and challenging questions.

Several people have been essential to my sanity outside of the chemistry lab. Habib Ahmad and I first met during recruiting weekend in early 2003, and his friendship over this time has been indispensable. I valued our times outside of the lab, whether it involved going to the beach, grabbing lunch, or going go-karting, and am grateful for his availability to discuss ideas and suggestions. I had a great time rooming with Chiraj Dalal in the Cats apartments for two years. Chiraj is an incredibly kind and intelligent person, easy going, and an extremely talented at almost any sport. I am fortunate to have met a fellow adrenaline junkie, Lenny Lucas, at an early time during graduate school. We've gone on many epic mountain bike rides in the San Gabriel's and faced some extremely sketchy trails (and crashes), but they were some of my best times. Ryan Zeidan and I share a passion for sports, and he has been a great friend to discuss football and anything else other than chemistry. I am appreciative of Jean Li for her friendship and our many late night discussions as I was finishing my Ph.D. Most of the time we would complain about unimportant things, but I found it to be therapeutic during the stressful times writing this thesis. Thanks Jean! I would also like to thank the playmakers (championship!) flag football team, anyone who has ever played (and lost to) me in racquetball, the stereoablators softball team, weekly pick-up basketball games, and everyone else that used sports to divert me from the bench.

I would like to express my appreciation for my long-term baymates Dr. Haiming Zhang, Dr. Eric Ferreira, Dr. Charles Liu, Dr. Christian Defieber, and Alex "rookie" Goldberg. Their work ethic and enthusiasm for chemistry has been a constant source of inspiration. I have gained a lot from the diverse skills of each individual, and the daily interactions with these guys have contributed to my enjoyable graduate experience. I also

owe an enormous thanks to Kevin Allan, Chris Gilmore, Alex Goldberg, Dr. Chris Henry, Allen Hong, Thomas Jensen, Dr. Amanda Jones, Sandy Ma, Dr. Andrew McClory, Dr. Nolan McDougal, Narae Park, Jennifer Roizen, and Pamela Tadross for proofreading portions of this document. Their thorough efforts have greatly improved its quality.

The contents of this thesis would not have been possible without the support of the entire staff at Caltech. I would specifically like to acknowledge the NMR facilities (Dr. Scott Ross, Dr. Dave VanderVelde), mass spec facilities (Dr. Mona Shahgholi, Naseem Torian), X-ray facilities (Larry Henling, Dr. Mike Day), Rick Gerhart (and all of his glass blowing marvels), Tom Dunn, Anne Penney, Lynne Martinez, and Joe Drew. In addition to heading the Catalysis Center, Dr. Scott Virgil is a regular presence in our group, and his insight and creative suggestions have added a new dimension to our lab.

To my extended family—the Longacres and Daxes—your love and support has been invaluable. I am grateful that my brothers Jan and Eric were able to visit and experience CA while I was here. It was difficult living on the opposite coast from my family, and their conversations and encouragement made it manageable. I would also like to acknowledge my niece and nephews—Lorin, Tobin, and Collin—for their love and eagerness for phone calls. Eric's fiancée, Jill, has been a great friend, and I wish them the best in their marriage and life together. To my wife Kristy, your unwavering love and support has meant the world to me. I have always enjoyed your sense of humor and appreciate your willingness to enhance my mood, as difficult as it was at times. You are my rock, my love, my best friend, and a huge component to me crossing the finish line. I sincerely thank you for all that you have done. And last, but certainly not least, I owe an

enormous amount of appreciation to my mother. She is the epitome of a role model, always leading by example, refusing to allow the challenges she faces to deter her from succeeding. She has sacrificed a great deal to ensure that I could pursue my dreams, and I cannot thank her enough for this support. I have a great deal of respect for my mother and I share this accomplishment with her. Thanks!

ABSTRACT

Biologically active natural products and pharmaceuticals often present intriguing structural features that can challenge the state of the art in catalysis and synthetic methodology for their preparation. The identification of unique targets thus stimulates the development of new strategies and methods for chemical synthesis. The complex architecture representative of the variecolin family of sesterterpenes has inspired our pursuit of new tactics that has enabled the expansion of methods from our laboratory.

First, progress toward the asymmetric total synthesis of variecolin is discussed. Our convergent synthetic approach bisects the target into two complex fragments to address the main structural challenges. A microwave-promoted tandem Wolff/Cope rearrangement of vinyl cyclobutyl diazocarbonyls has been developed that provides access to functionalized, fused eight-membered rings and is used to construct the central B ring of variecolin. In addition, the utility of our Pd-catalyzed enantioselective alkylation method is extended to a new vinylogous ester substrate class to produce a quaternary ketone in excellent yield with high selectivity that is an exceptional substrate for an efficient ring contraction to the cyclopentene D ring system. The successful asymmetric preparation of our two devised fragments has facilitated initial studies toward their coupling and completion of variecolin.

Second, a preliminary examination of the substrate scope for the asymmetric alkylation of the vinylogous β -ketoester substrate class is described. Derivatives that perturb substrate electronics display enhanced reactivity and selectivity, generating products with excellent selectivities and expanding the potential of this versatile class of substrates. Furthermore, their utility is underscored as the key enantioselective transformation en route to the synthesis of the sesquiterpenoid (+)-carissone.

Finally, gas-phase studies of the twisted amide 2-quinuclidone are described. Proton affinity experiments have quantified its high basicity, which is comparable to a tertiary amine. A gas-phase synthesis of 2-quinuclidone via elimination of water and subsequent fragmentation further highlight the unusual characteristics of extremely twisted amides.

TABLE OF CONTENTS

Acknowledgements	iv
Abstract	xi
Table of Contents	xii
List of Figures	xviii
List of Schemes	xxix
List of Tables	xxxiii
List of Abbreviations	xxxvi

CHAPTER 1

1

Natural Products and Pharmaceuticals as Inspiration for the Development of Enantioselective Catalysis

1.1 Introduction	1
1.2 Historical Overview of Enantioselective Methods	2
1.3 Recent Developments in Enantioselective Catalysis	7
1.3.1 β -Enamino Amide Hydrogenations — Januvia	8
1.3.2 C(sp ³)–C(sp ³) Cross-Couplings — Fluvirucinine A ₁	12
1.3.3 Intramolecular Heck Cyclizations — Minfiensine	15
1.3.4 Indole Friedel–Crafts Alkylations — Flustramine B	17
1.3.5 Pictet–Spengler Cyclizations — Harmicine	19
1.3.6 Phase Transfer Alkylations — Indacrinone	21
1.3.7 Pd-Catalyzed Enolate Alkylation — Cyanthiwigin F	23
1.3.8 Trimethylenemethane Cyclizations — Marcfortine B	26
1.4 Outlook	28
1.5 Notes and References	30

CHAPTER 2

38

The Variocolin Family of Sesterterpenoids

2.1 Introduction and Background	38
2.1.1 Isolation and Structural Elucidation	38
2.1.2 Biosynthetic Proposal	41

	xiii
2.2 Biological Activity.....	43
2.2.1 Antihypertensive Properties	43
2.2.2 Immunomodulatory Properties	44
2.2.3 CCR5 Antagonist	45
2.2.4 Antibiotic and Antifungal Properties.....	45
2.3 Synthetic Studies toward Variecolin.....	45
2.3.1 Piers' Approach to the CD Ring System	46
2.3.2 Molander's Approach to the B Ring.....	51
2.3.3 Molander's Second-Generation Approach	54
2.4 Conclusion	59
2.5 Notes and References	60

CHAPTER 3

64

Progress toward the Asymmetric Total Synthesis of Variecolin

3.1 Introduction and Synthetic Strategy	64
3.1.1 Introduction	64
3.1.2 Retrosynthetic Analysis	66
3.2 A Wolff/Cope Approach to the AB Ring System	67
3.2.1 Model Studies of the Wolff/Cope Rearrangement toward Construction of the Eight- Membered AB Ring	68
3.2.1.1 Model Wolff/Cope Substrate Synthesis	68
3.2.1.2 Model Wolff/Cope Rearrangement Investigations.....	74
3.2.2 Asymmetric Synthesis of the AB Ring Fragment of Variecolin Employing the Wolff/Cope Rearrangement.....	77
3.2.2.1 Asymmetric Synthesis of Wolff/Cope Substrate toward Variecolin.....	77
3.2.2.2 α -Diazoketone Synthesis and Wolff/Cope Studies.....	80
3.3 Catalytic Asymmetric Synthesis of a D-Ring Fragment.....	83
3.3.1 Optimization of the Pd-Catalyzed Asymmetric Alkylation of Cyclic Seven-Membered Vinylogous β -Ketoesters	84
3.3.2 Ring Contraction Investigations and Determination of the Absolute Stereochemistry	86
3.3.3 Completion of the D-Ring Fragment.....	91
3.4 Studies toward the Fragment Coupling of the AB and D-Ring Fragments toward Variecolin	92
3.4.1 Model Studies for Fragment Coupling and C-Ring Annulation.....	93
3.4.1.1 Model Reductive Enone Alkylation and Hydrosilylation/Alkylation	93

	xiv
3.4.1.2 Model C-Ring Radical Cyclization	94
3.4.2 Coupling Studies regarding the Asymmetric AB Ring Fragment of Variocolin	95
3.4.2.1 Enone Reductive Alkylation of the Asymmetric AB Ring Fragment.....	95
3.4.2.2 Enone Hydrosilylation of the Asymmetric AB Ring Fragment	98
3.5 Proposed Completion of Variocolin	99
3.6 Conclusion	100
3.7 Experimental Section	102
3.7.1 Materials and Methods.....	102
3.7.2 Preparative Procedures.....	105
3.7.2.1 Tricarbonyliron-Cyclobutadiene Fragments	105
3.7.2.2 AB Ring Model System Fragments	108
3.7.2.3 AB Ring Asymmetric Fragments.....	125
3.7.2.4 D-Ring Fragments.....	143
3.7.2.5 Model Fragment Coupling and C-Ring Annulation.....	162
3.7.2.6 Asymmetric AB Ring and D-Ring Fragment Coupling	172
3.8 Notes and References	176

APPENDIX 1 **188**
Synthetic Summary toward the Asymmetric Total Synthesis of Variocolin

APPENDIX 2 **192**
Spectra Relevant to Chapter 3: Progress toward the Asymmetric Total Synthesis of Variocolin

APPENDIX 3 **299**
X-Ray Crystallography Reports Relevant to Chapter 3: Progress toward the Asymmetric Total Synthesis of Variocolin

A3.1 Crystal Structure Analysis of 215	299
A3.2 Crystal Structure Analysis of 233	307

CHAPTER 4 **317**
Enantioselective Allylic Alkylations of Vinylogous β -Ketoester Derivatives: Total Synthesis of (+)-Carissone

4.1 Introduction.....	317
-----------------------	-----

4.2	Enantioselective Decarboxylative Alkylations of Vinylogous β -Ketoester Derivatives	318
4.2.1	Effect of Solvent	319
4.2.2	Effect of Substrate Substitution	320
4.2.3	Extensions to Six-Membered Rings	322
4.2.4	Future Studies of Vinylogous β -Ketoester Substrates	324
4.3	Catalytic Enantioselective Approach to the Eudesmane Sesquiterpenoids	325
4.3.1	Background of the Eudesmane Sesquiterpenoids	325
4.3.2	Retrosynthetic Analysis of the Eudesmane Carbocyclic Core	327
4.3.3	Total Synthesis of (+)-Carissone	328
4.3.3.1	Pd-Catalyzed Enantioselective Alkylation of Vinylogous Ester Derivatives	328
4.3.3.2	Preparation of the Bicyclic Core	329
4.3.3.3	Completion of (+)-Carissone and a Formal Synthesis of (–)- α -Eudesmol	331
4.4	Conclusion	332
4.5	Experimental Section	334
4.5.1	Materials and Methods	334
4.5.2	Preparative Procedures	336
4.5.2.1	Asymmetric Alkylation of Vinylogous β -Ketoester Derivatives	336
4.5.2.2	Enantioselective Total Synthesis of (+)-Carissone	349
4.6	Notes and References	371

APPENDIX 4 **378**
Spectra Relevant to Chapter 4: Enantioselective Allylic Alkylations of Vinylogous β -Ketoester Derivatives: Total Synthesis of (+)-Carissone

CHAPTER 5 **409**
Synthesis, Structural Analysis, and Gas-Phase Studies of 2-Quinuclidonium Tetrafluoroborate

5.1	Introduction and Background	409
5.1.1	The Amide Linkage	409
5.1.2	2-Quinuclidone	410
5.2	The Synthesis and Characterization of 2-Quinuclidonium Tetrafluoroborate	412
5.2.1	Synthesis of 2-Quinuclidonium via an Intramolecular Schmidt–Aubé Cyclization	413
5.2.2	Characterization, Properties, and Reactivity	415
5.3	Gas-Phase Studies	417
5.3.1	Proton Affinity via the Extended Kinetic Method	417

	xvi
5.3.2	Collision-Induced Dissociation Pathway..... 419
5.3.3	Gas-Phase Synthesis of 2-Quinuclidonium by Eliminating Water..... 423
5.3.4	Comparison to 6,6,7,7-Tetramethyl-2-quinuclidone 424
5.4	Future Studies..... 426
5.4.1	1-Azabicyclo[2.2.1]heptan-2-one 427
5.4.2	1-Azabicyclo[3.3.3]undecan-2-one..... 428
5.5	Conclusion 430
5.6	Experimental Section 431
5.6.1	Materials and Methods..... 431
5.6.1.1	Chemical Synthesis 431
5.6.1.2	Extended Kinetic Methods, Gas-Phase Synthesis, and Calculations..... 432
5.6.2	Preparative Procedures..... 434
5.6.3	Computationally Optimized Structures 449
5.6.4	Extended Kinetic Methods Plots..... 452
5.6.5	MS ² Spectra of Isotopically Labeled Derivatives and their Hydrolysis Products 453
5.7	Notes and References 456

APPENDIX 5 **462**
Spectra Relevant to Chapter 5: Synthesis, Structural Analysis, and Gas-Phase Studies of 2-Quinuclidonium Tetrafluoroborate

APPENDIX 6 **501**
An Improved and Highly Efficient Copper(I)-Catalyzed Preparation of (S)-t-Bu-PHOX

A6.1	Introduction and Background..... 501
A6.2	Reaction Optimization 502
A6.3	Crystallization and Improved Purification..... 504
A6.4	Conclusion 505
A6.5	Experimental Section 507
A6.5.1	Materials and Methods 507
A6.5.2	Preparative Procedures 509
A6.6	Notes and References 511

APPENDIX 7**514**

Spectra Relevant to Appendix 6: An Improved and Highly Efficient Copper(I)-Catalyzed Preparation of (S)-t-Bu-PHOX

APPENDIX 8**517**

X-Ray Crystallography Reports Relevant to Appendix 6: An Improved and Highly Efficient Copper(I)-Catalyzed Preparation of (S)-t-Bu-PHOX

A8.1 Crystal Structure Analysis of (S)-55.....517

APPENDIX 9**524**

Notebook Cross-Reference

Comprehensive Bibliography.....529
Index.....565
About the Author.....569

LIST OF FIGURES

CHAPTER 2*The Variocolin Family of Sesterterpenoids*

Figure 2.1.1. Proposed structure of variocolin.....	39
Figure 2.1.2. Variocolin family of sesterterpenoids.....	41

CHAPTER 3*Progress toward the Asymmetric Total Synthesis of Variocolin*

Figure 3.1.1. Variocolin family of sesterterpenes.....	65
Figure 3.2.1 Comparison of the strain-releasing Cope rearrangements of 204 and 206	76
Figure 3.2.2. X-ray crystal structure of acetal 215 . The molecular structure is shown with 50% probability ellipsoids. a) Side view. b) Top view.....	79
Figure 3.3.1. X-ray crystal structure of semicarbazone 233 . The molecular structure is shown with 50% probability ellipsoids.....	91

APPENDIX 2*Spectra Relevant to Chapter 3: Progress toward the Asymmetric Total Synthesis of Variocolin*

Figure A2.1. ¹ H NMR spectrum (500 MHz, CDCl ₃) of 178	193
Figure A2.2. Infrared spectrum (neat film/NaCl) of 178	194
Figure A2.3. ¹³ C NMR spectrum (126 MHz, CDCl ₃) of 178	194
Figure A2.4. ¹ H NMR spectrum (500 MHz, CDCl ₃) of 180	195
Figure A2.5. Infrared spectrum (neat film/NaCl) of 180	196
Figure A2.6. ¹³ C NMR spectrum (75 MHz, CDCl ₃) of 180	196
Figure A2.7. ¹ H NMR spectrum (500 MHz, CDCl ₃) of 181	197
Figure A2.8. Infrared spectrum (neat film/NaCl) of 181	198
Figure A2.9. ¹³ C NMR spectrum (126 MHz, CDCl ₃) of 181	198
Figure A2.10. ¹ H NMR spectrum (300 MHz, C ₆ D ₆) of 183	199
Figure A2.11. ¹ H NMR spectrum (300 MHz, C ₆ D ₆) of 184	200
Figure A2.12. Infrared spectrum (neat film/NaCl) of 184	201
Figure A2.13. ¹³ C NMR spectrum (126 MHz, C ₆ D ₆) of 184	201

Figure A2.14. ^1H NMR spectrum (500 MHz, C_6D_6) of 185	202
Figure A2.15. Infrared spectrum (neat film/ NaCl) of 185	203
Figure A2.16. ^{13}C NMR spectrum (126 MHz, C_6D_6) of 185	203
Figure A2.17. ^1H NMR spectrum (300 MHz, CDCl_3) of 186	204
Figure A2.18. ^1H NMR spectrum (500 MHz, CDCl_3) of 187	205
Figure A2.19. ^1H NMR spectrum (300 MHz, C_6D_6) of 188	206
Figure A2.20. Infrared spectrum (neat film/ NaCl) of 188	207
Figure A2.21. ^{13}C NMR spectrum (126 MHz, C_6D_6) of 188	207
Figure A2.22. ^1H NMR spectrum (500 MHz, CDCl_3) of 189	208
Figure A2.23. Infrared spectrum (neat film/ NaCl) of 189	209
Figure A2.24. ^{13}C NMR spectrum (126 MHz, CDCl_3) of 189	209
Figure A2.25. ^1H NMR spectrum (500 MHz, CDCl_3) of 190	210
Figure A2.26. Infrared spectrum (neat film/ NaCl) of 190	211
Figure A2.27. ^{13}C NMR spectrum (126 MHz, CDCl_3) of 190	211
Figure A2.28. ^1H NMR spectrum (500 MHz, CDCl_3) of 191	212
Figure A2.29. Infrared spectrum (neat film/ NaCl) of 191	213
Figure A2.30. ^{13}C NMR spectrum (126 MHz, CDCl_3) of 191	213
Figure A2.31. ^1H NMR spectrum (300 MHz, CDCl_3) of 192	214
Figure A2.32. ^1H NMR spectrum (500 MHz, CDCl_3) of 193	215
Figure A2.33. Infrared spectrum (neat film/ NaCl) of 193	216
Figure A2.34. ^{13}C NMR spectrum (126 MHz, CDCl_3) of 193	216
Figure A2.35. ^1H NMR spectrum (500 MHz, CDCl_3) of 197	217
Figure A2.36. Infrared spectrum (neat film/ NaCl) of 197	218
Figure A2.37. ^{13}C NMR spectrum (126 MHz, CDCl_3) of 197	218
Figure A2.38. ^1H NMR spectrum (500 MHz, CDCl_3) of 198	219
Figure A2.39. Infrared spectrum (neat film/ NaCl) of 198	220
Figure A2.40. ^{13}C NMR spectrum (126 MHz, CDCl_3) of 198	220
Figure A2.41. ^1H NMR spectrum (500 MHz, CDCl_3) of 200	221
Figure A2.42. Infrared spectrum (neat film/ NaCl) of 200	222
Figure A2.43. ^{13}C NMR spectrum (126 MHz, CDCl_3) of 200	222
Figure A2.44. ^1H NMR spectrum (500 MHz, C_6D_6) of 201	223
Figure A2.45. ^1H NMR spectrum (500 MHz, CDCl_3) of 201	224
Figure A2.46. Infrared spectrum (neat film/ NaCl) of 201	225
Figure A2.47. ^{13}C NMR spectrum (126 MHz, CDCl_3) of 201	225
Figure A2.48. ^1H NMR spectrum (500 MHz, CDCl_3) of 203	226

Figure A2.49. Infrared spectrum (neat film/NaCl) of 203	227
Figure A2.50. ^{13}C NMR spectrum (126 MHz, CDCl_3) of 203	227
Figure A2.51. ^1H NMR spectrum (300 MHz, CDCl_3) of 208	228
Figure A2.52. ^1H NMR spectrum (500 MHz, CDCl_3) of 209	229
Figure A2.53. Infrared spectrum (neat film/NaCl) of 209	230
Figure A2.54. ^{13}C NMR spectrum (126 MHz, CDCl_3) of 209	230
Figure A2.55. ^1H NMR spectrum (500 MHz, CDCl_3) of 211	231
Figure A2.56. Infrared spectrum (neat film/NaCl) of 211	232
Figure A2.57. ^{13}C NMR spectrum (126 MHz, CDCl_3) of 211	232
Figure A2.58. ^1H NMR spectrum (500 MHz, C_6D_6) of 212	233
Figure A2.59. Infrared spectrum (neat film/NaCl) of 212	234
Figure A2.60. ^{13}C NMR spectrum (126 MHz, CDCl_3) of 212	234
Figure A2.61. ^1H NMR spectrum (500 MHz, CDCl_3) of 213	235
Figure A2.62. Infrared spectrum (neat film/NaCl) of 213	236
Figure A2.63. ^{13}C NMR spectrum (126 MHz, CDCl_3) of 213	236
Figure A2.64. ^1H NMR spectrum (500 MHz, CDCl_3) of 214	237
Figure A2.65. Infrared spectrum (neat film/NaCl) of 214	238
Figure A2.66. ^{13}C NMR spectrum (126 MHz, CDCl_3) of 214	238
Figure A2.67. ^1H NMR spectrum (600 MHz, CDCl_3) of 215	239
Figure A2.68. Infrared spectrum (neat film/NaCl) of 215	240
Figure A2.69. ^{13}C NMR spectrum (126 MHz, CDCl_3) of 215	240
Figure A2.70. ^1H NMR spectrum (500 MHz, CDCl_3) of 216	241
Figure A2.71. Infrared spectrum (neat film/NaCl) of 216	242
Figure A2.72. ^{13}C NMR spectrum (126 MHz, CDCl_3) of 216	242
Figure A2.73. ^1H NMR spectrum (500 MHz, CDCl_3) of 217	243
Figure A2.74. Infrared spectrum (neat film/NaCl) of 217	244
Figure A2.75. ^{13}C NMR spectrum (126 MHz, CDCl_3) of 217	244
Figure A2.76. ^1H NMR spectrum (600 MHz, CDCl_3) of 218	245
Figure A2.77. Infrared spectrum (neat film/NaCl) of 218	246
Figure A2.78. ^{13}C NMR spectrum (126 MHz, CDCl_3) of 218	246
Figure A2.79. ^1H NMR spectrum (500 MHz, CDCl_3) of 220	247
Figure A2.80. Infrared spectrum (neat film/NaCl) of 220	248
Figure A2.81. ^{13}C NMR spectrum (126 MHz, CDCl_3) of 220	248
Figure A2.82. ^1H NMR spectrum (500 MHz, CDCl_3) of 221	249
Figure A2.83. Infrared spectrum (neat film/NaCl) of 221	250

Figure A2.84. ^{13}C NMR spectrum (126 MHz, CDCl_3) of 221	250
Figure A2.85. ^1H NMR spectrum (500 MHz, CDCl_3) of 222	251
Figure A2.86. Infrared spectrum (neat film/ NaCl) of 222	252
Figure A2.87. ^{13}C NMR spectrum (126 MHz, CDCl_3) of 222	252
Figure A2.88. ^1H NMR spectrum (600 MHz, CDCl_3) of 223	253
Figure A2.89. Infrared spectrum (neat film/ NaCl) of 223	254
Figure A2.90. ^{13}C NMR spectrum (126 MHz, CDCl_3) of 223	254
Figure A2.91. ^1H NMR spectrum (500 MHz, CDCl_3) of 224	255
Figure A2.92. Infrared spectrum (neat film/ NaCl) of 224	256
Figure A2.93. ^{13}C NMR spectrum (126 MHz, CDCl_3) of 224	256
Figure A2.94. ^1H NMR spectrum (500 MHz, CDCl_3) of 225	257
Figure A2.95. Infrared spectrum (neat film/ NaCl) of 225	258
Figure A2.96. ^{13}C NMR spectrum (126 MHz, CDCl_3) of 225	258
Figure A2.97. ^1H NMR spectrum (300 MHz, CDCl_3) of 227	259
Figure A2.98. ^1H NMR spectrum (500 MHz, CDCl_3) of 228	260
Figure A2.99. Infrared spectrum (neat film/ NaCl) of 228	261
Figure A2.100. ^{13}C NMR spectrum (126 MHz, CDCl_3) of 228	261
Figure A2.101. ^1H NMR spectrum (500 MHz, CDCl_3) of 229	262
Figure A2.102. Infrared spectrum (neat film/ NaCl) of 229	263
Figure A2.103. ^{13}C NMR spectrum (126 MHz, CDCl_3) of 229	263
Figure A2.104. ^1H NMR spectrum (500 MHz, CDCl_3) of 231	264
Figure A2.105. Infrared spectrum (neat film/ NaCl) of 231	265
Figure A2.106. ^{13}C NMR spectrum (75 MHz, CDCl_3) of 231	265
Figure A2.107. ^1H NMR spectrum (300 MHz, CDCl_3) of 232	266
Figure A2.108. Infrared spectrum (neat film/ NaCl) of 232	267
Figure A2.109. ^{13}C NMR spectrum (75 MHz, CDCl_3) of 232	267
Figure A2.110. ^1H NMR spectrum (500 MHz, CDCl_3) of 233	268
Figure A2.111. Infrared spectrum (neat film/ NaCl) of 233	269
Figure A2.112. ^{13}C NMR spectrum (126 MHz, CDCl_3) of 233	269
Figure A2.113. ^1H NMR spectrum (300 MHz, CDCl_3) of 235	270
Figure A2.114. Infrared spectrum (neat film/ NaCl) of 235	271
Figure A2.115. ^{13}C NMR spectrum (75 MHz, CDCl_3) of 235	271
Figure A2.116. ^1H NMR spectrum (500 MHz, CDCl_3) of 236	272
Figure A2.117. Infrared spectrum (neat film/ NaCl) of 236	273
Figure A2.118. ^{13}C NMR spectrum (75 MHz, CDCl_3) of 236	273

Figure A2.119. ^1H NMR spectrum (500 MHz, CDCl_3) of 237	274
Figure A2.120. Infrared spectrum (neat film/ NaCl) of 237	275
Figure A2.121. ^{13}C NMR spectrum (126 MHz, CDCl_3) of 237	275
Figure A2.122. ^1H NMR spectrum (300 MHz, CDCl_3) of 238	276
Figure A2.123. Infrared spectrum (neat film/ NaCl) of 238	277
Figure A2.124. ^{13}C NMR spectrum (75 MHz, CDCl_3) of 238	277
Figure A2.125. ^1H NMR spectrum (500 MHz, C_6D_6) of 239	278
Figure A2.126. Infrared spectrum (neat film/ NaCl) of 239	279
Figure A2.127. ^{13}C NMR spectrum (126 MHz, C_6D_6) of 239	279
Figure A2.128. ^1H NMR spectrum (300 MHz, CDCl_3) of 240	280
Figure A2.129. Infrared spectrum (neat film/ NaCl) of 240	281
Figure A2.130. ^{13}C NMR spectrum (75 MHz, CDCl_3) of 240	281
Figure A2.131. ^1H NMR spectrum (500 MHz, CDCl_3) of 241	282
Figure A2.132. Infrared spectrum (neat film/ NaCl) of 241	283
Figure A2.133. ^{13}C NMR spectrum (126 MHz, CDCl_3) of 241	283
Figure A2.134. ^1H NMR spectrum (500 MHz, CDCl_3) of 242	284
Figure A2.135. Infrared spectrum (neat film/ NaCl) of 242	285
Figure A2.136. ^{13}C NMR spectrum (126 MHz, CDCl_3) of 242	285
Figure A2.137. ^1H NMR spectrum (500 MHz, CDCl_3) of the major diastereomer of 243	286
Figure A2.138. Infrared spectrum (neat film/ NaCl) of the major diastereomer of 243	287
Figure A2.139. ^{13}C NMR spectrum (126 MHz, CDCl_3) of the major diastereomer of 243	287
Figure A2.140. ^1H NMR spectrum (500 MHz, CDCl_3) of the minor diastereomer of 243	288
Figure A2.141. Infrared spectrum (neat film/ NaCl) of the minor diastereomer of 243	289
Figure A2.142. ^{13}C NMR spectrum (neat film/ NaCl) of the minor diastereomer of 243	289
Figure A2.143. ^1H NMR spectrum (500 MHz, CDCl_3) of 245	290
Figure A2.144. Infrared spectrum (neat film/ NaCl) of 245	291
Figure A2.145. ^{13}C NMR spectrum (126 MHz, CDCl_3) of 245	291
Figure A2.146. ^1H NMR spectrum (300 MHz, CDCl_3) of 253	292
Figure A2.147. Infrared spectrum (neat film/ NaCl) of 253	293
Figure A2.148. ^{13}C NMR spectrum (75 MHz, CDCl_3) of 253	293
Figure A2.149. ^1H NMR spectrum (600 MHz, CDCl_3) of 254	294
Figure A2.150. Infrared spectrum (neat film/ NaCl) of 254	295
Figure A2.151. ^{13}C NMR spectrum (126 MHz, CDCl_3) of 254	295
Figure A2.152. ^1H NMR spectrum (300 MHz, CDCl_3) of 255	296
Figure A2.153. ^1H NMR spectrum (300 MHz, CDCl_3) of 256	297

Figure A2.154. Infrared spectrum (neat film/NaCl) of 256	298
Figure A2.155. ¹³ C NMR spectrum (126 MHz, CDCl ₃) of 256	298

APPENDIX 3

X-Ray Crystallography Reports Relevant to Chapter 3: Progress toward the Asymmetric Total Synthesis of Variocolin

Figure A3.1.1. Acetal 215 is shown with 50% probability ellipsoids. Crystallographic data have been deposited at the CCDC, 12 Union Road, Cambridge CB2 1EZ, UK, and copies can be obtained on request, free of charge, by quoting the publication citation and the deposition number 718289.....	299
Figure A3.1.2. Acetal 215	302
Figure A3.2.1. Semicarbazone 233 is shown with 50% probability ellipsoids. Crystallographic data have been deposited at the CCDC, 12 Union Road, Cambridge CB2 1EZ, UK, and copies can be obtained on request, free of charge, by quoting the publication citation and the deposition number 686849.....	307
Figure A3.2.2. Semicarbazone 233	311

CHAPTER 4

Enantioselective Allylic Alkylations of Vinylogous β -Ketoester Derivatives: Total Synthesis of (+)-Carissone

Figure 4.1.1. Representative transformations of vinylogous esters.....	318
Figure 4.3.1. Representative eudesmane sesquiterpenoids.....	326

APPENDIX 4

Spectra Relevant to Chapter 4: Enantioselective Allylic Alkylations of Vinylogous β -Ketoester Derivatives: Total Synthesis of (+)-Carissone

Figure A4.1. ¹ H NMR spectrum (500 MHz, CDCl ₃) of 275	379
Figure A4.2. Infrared spectrum (neat film/NaCl) of 275	380
Figure A4.3. ¹³ C NMR spectrum (126 MHz, CDCl ₃) of 275	380
Figure A4.4. ¹ H NMR spectrum (500 MHz, CDCl ₃) of 276	381
Figure A4.5. Infrared spectrum (neat film/NaCl) of 276	382
Figure A4.6. ¹³ C NMR spectrum (126 MHz, CDCl ₃) of 276	382
Figure A4.7. ¹ H NMR spectrum (300 MHz, CDCl ₃) of 277	383
Figure A4.8. Infrared spectrum (neat film/NaCl) of 277	384

Figure A4.9. ^{13}C NMR spectrum (75 MHz, CDCl_3) of 277	384
Figure A4.10. ^1H NMR spectrum (300 MHz, CDCl_3) of 278	385
Figure A4.11. Infrared spectrum (neat film/ NaCl) of 278	386
Figure A4.12. ^{13}C NMR spectrum (75 MHz, CDCl_3) of 278	386
Figure A4.13. ^1H NMR spectrum (500 MHz, CDCl_3) of (+)-carissone (279).....	387
Figure A4.14. Infrared spectrum (neat film/ NaCl) of (+)-carissone (279).....	388
Figure A4.15. ^{13}C NMR spectrum (126 MHz, CDCl_3) of (+)-carissone (279).....	388
Figure A4.16. ^1H NMR spectrum (500 MHz, CDCl_3) of 287	389
Figure A4.17. ^1H NMR spectrum (500 MHz, CDCl_3) of 288	390
Figure A4.18. Infrared spectrum (neat film/ NaCl) of 288	391
Figure A4.19. ^{13}C NMR spectrum (126 MHz, CDCl_3) of 288	391
Figure A4.20. ^1H NMR spectrum (300 MHz, CDCl_3) of 289	392
Figure A4.21. ^1H NMR spectrum (500 MHz, C_6D_6) of 290	393
Figure A4.22. Infrared spectrum (neat film/ NaCl) of 290	394
Figure A4.23. ^{13}C NMR spectrum (126 MHz, C_6D_6) of 290	394
Figure A4.24. ^1H NMR spectrum (500 MHz, C_6D_6) of 292	395
Figure A4.25. Infrared spectrum (neat film/ NaCl) of 292	396
Figure A4.26. ^{13}C NMR spectrum (126 MHz, C_6D_6) of 292	396
Figure A4.27. ^1H NMR spectrum (500 MHz, C_6D_6) of 293	397
Figure A4.28. Infrared spectrum (neat film/ NaCl) of 293	398
Figure A4.29. ^{13}C NMR spectrum (126 MHz, C_6D_6) of 293	398
Figure A4.30. ^1H NMR spectrum (500 MHz, C_6D_6) of 294	399
Figure A4.31. Infrared spectrum (neat film/ NaCl) of 294	400
Figure A4.32. ^{13}C NMR spectrum (126 MHz, C_6D_6) of 294	400
Figure A4.33. ^1H NMR spectrum (500 MHz, CDCl_3) of 295	401
Figure A4.34. Infrared spectrum (neat film/ NaCl) of 295	402
Figure A4.35. ^{13}C NMR spectrum (126 MHz, CDCl_3) of 295	402
Figure A4.36. ^1H NMR spectrum (500 MHz, CDCl_3) of 304	403
Figure A4.37. Infrared spectrum (neat film/ NaCl) of 304	404
Figure A4.38. ^{13}C NMR spectrum (126 MHz, CDCl_3) of 304	404
Figure A4.39. ^1H NMR spectrum (300 MHz, CDCl_3) of 307	405
Figure A4.40. ^1H NMR spectrum (300 MHz, CDCl_3) of 308	406
Figure A4.41. ^1H NMR spectrum (500 MHz, C_6D_6) of the major diastereomer of 309	407
Figure A4.42. Infrared spectrum (neat film/ NaCl) of the major diastereomer of 309	408
Figure A4.43. ^{13}C NMR spectrum (126 MHz, C_6D_6) of the major diastereomer of 309	408

CHAPTER 5

Synthesis, Structural Analysis, and Gas-Phase Studies of 2-Quinuclidonium Tetrafluoroborate

Figure 5.1.1. Resonance stabilization of a typical amide.	410
Figure 5.1.2. a) Woodward's failed synthesis of 311 from amino acid 310 . b) Facile amide bond formation to afford constitutional isomer 313	411
Figure 5.2.1. ORTEP drawing of 311 •HBF ₄	415
Figure 5.3.1. Data from kinetic method experiments showing the relative PA versus natural log of the ratio of ion intensities minus protonation entropies. Three representative collision energies are shown for each reference base. The collinearity of all three lines indicates few entropic effects. The PA of 311 is determined to be 230.4 kcal/mol by the extended kinetic method.	419
Figure 5.3.2. Representative amide and amine experimentally determined PAs (kcal/mol).....	419
Figure 5.3.3. i) CID spectrum of 311 •H ⁺ (m/z = 126) with a single fragment being detected. ii) CID spectrum of 310 •H ⁺ (m/z = 144). The loss of water generates 311 •H ⁺ , which simultaneously fragments. iii) MS ³ CID spectrum of the reisolated peak at m/z 126 from spectrum ii confirming that 311 •H ⁺ is generated by the loss of water.	420
Figure 5.3.4. i) CID spectrum of 318 •H ⁺ (m/z = 182). ii) CID spectrum of 346 •H ⁺ (m/z = 200). In this case, the synthesis proceeds cleanly without spontaneous fragmentation. iii) MS ³ CID spectrum showing that all fragment peaks are reproduced when the gas-phase product is compared to the bona-fide sample in spectrum i.	426
Figure 5.4.1. a) Comparison of strain energies of related bicyclic systems (kcal/mol). ³⁷ b) Comparison of proton affinity values for select bicyclic twisted amides (kcal/mol).	427
Figure 5.4.2. Bicyclo[3.3.3] bridgehead amide 355 and amine 356	429
Figure 5.6.1. Optimized structure of 2-quinuclidone (311).	449
Figure 5.6.2. Optimized structure of N-protonated 2-quinuclidone (311 •H ⁺).	450
Figure 5.6.3. Optimized structure of 6,6,7,7-tetramethyl-2-quinuclidone (318).	450
Figure 5.6.4. Optimized structure of N-protonated 6,6,7,7-tetramethyl-2-quinuclidone (318 •H ⁺)... ..	451
Figure 5.6.5. Plot of the extended kinetic method of 311 with direct entropy correction.....	452
Figure 5.6.6. Entropy corrected kinetic plot using bulky bases.	453
Figure 5.6.7. MS ² spectrum of 332 (¹⁵ N).	454
Figure 5.6.8. MS ² spectrum of 333 (¹³ C ₂).	454
Figure 5.6.9. MS ² spectrum of 334 (D).	455
Figure 5.6.10. MS ² spectrum of 335 (D ₂).	455

APPENDIX 5*Spectra Relevant to Chapter 5: Synthesis, Structural Analysis, and Gas-Phase Studies of 2-Quinuclidonium Tetrafluoroborate*

Figure A5.1. ^1H NMR spectrum (300 MHz, CD_3CN) of 333 • HBF_4	463
Figure A5.2. ^{13}C NMR spectrum (75 MHz, CD_3CN) of 333 • HBF_4	464
Figure A5.3. ^1H NMR spectrum (300 MHz, CD_3CN) of 334 • HBF_4	465
Figure A5.4. ^2H NMR spectrum (76 MHz, CH_3CN) of 334 • HBF_4	466
Figure A5.5. ^1H NMR spectrum (300 MHz, CD_3CN) of 335 • HBF_4	467
Figure A5.6. ^2H NMR spectrum (75 MHz, CH_3CN) of 335 • HBF_4	468
Figure A5.7. ^1H NMR spectrum (300 MHz, CDCl_3) of 339	469
Figure A5.8. ^{13}C NMR spectrum (75 MHz, CDCl_3) of 339	470
Figure A5.9. ^1H NMR spectrum (300 MHz, CDCl_3) of 340	471
Figure A5.10. ^{13}C NMR spectrum (75 MHz, CDCl_3) of 340	472
Figure A5.11. ^1H NMR spectrum (300 MHz, CDCl_3) of 341	473
Figure A5.12. ^{13}C NMR spectrum (75 MHz, CDCl_3) of 341	474
Figure A5.13. ^1H NMR spectrum (300 MHz, CDCl_3) of 344	475
Figure A5.14. ^2H NMR spectrum (76 MHz, CHCl_3) of 344	476
Figure A5.15. ^{13}C NMR spectrum (75 MHz, CDCl_3) of 344	476
Figure A5.16. ^1H NMR spectrum (300 MHz, CDCl_3) of 345	477
Figure A5.17. ^2H NMR spectrum (76 MHz, CHCl_3) of 345	478
Figure A5.18. ^{13}C NMR spectrum (75 MHz, CDCl_3) of 345	478
Figure A5.19. ^1H NMR spectrum (300 MHz, CDCl_3) of 363	479
Figure A5.20. Infrared spectrum (neat film/ NaCl) of 363	480
Figure A5.21. ^{13}C NMR spectrum (125 MHz, CDCl_3) of 363	480
Figure A5.22. ^1H NMR spectrum (300 MHz, CDCl_3) of 364	481
Figure A5.23. Infrared spectrum (neat film/ NaCl) of 364	482
Figure A5.24. ^{13}C NMR spectrum (75 MHz, CDCl_3) of 364	482
Figure A5.25. ^1H NMR spectrum (500 MHz, CD_3OD) of 365	483
Figure A5.26. Infrared spectrum (neat film/ NaCl) of 365	484
Figure A5.27. ^{13}C NMR spectrum (125 MHz, CD_3OD) of 365	484
Figure A5.28. ^1H NMR spectrum (300 MHz, CDCl_3) of 366	485
Figure A5.29. Infrared spectrum (neat film/ NaCl) of 366	486
Figure A5.30. ^{13}C NMR spectrum (75 MHz, CDCl_3) of 366	486
Figure A5.31. ^1H NMR spectrum (300 MHz, CD_3OD) of 368	487
Figure A5.32. ^{13}C NMR spectrum (75 MHz, CD_3OD) of 368	488

Figure A5.33. ^1H NMR spectrum (300 MHz, CDCl_3) of 369	489
Figure A5.34. ^{13}C NMR spectrum (75 MHz, CDCl_3) of 369	490
Figure A5.35. ^1H NMR spectrum (300 MHz, CD_3OD) of 370	491
Figure A5.36. ^2H NMR spectrum (76 MHz, CH_3OH) of 370	492
Figure A5.37. ^{13}C NMR spectrum (75 MHz, CD_3OD) of 370	492
Figure A5.38. ^1H NMR spectrum (300 MHz, CDCl_3) of 371	493
Figure A5.39. ^2H NMR spectrum (76 MHz, CHCl_3) of 371	494
Figure A5.40. ^{13}C NMR spectrum (75 MHz, CDCl_3) of 371	494
Figure A5.41. ^1H NMR spectrum (300 MHz, CDCl_3) of 372	495
Figure A5.42. ^2H NMR spectrum (76 MHz, CHCl_3) of 372	496
Figure A5.43. ^{13}C NMR spectrum (125 MHz, CDCl_3) of 372	496
Figure A5.44. ^1H NMR spectrum (300 MHz, CD_3OD) of 373	497
Figure A5.45. ^2H NMR spectrum (76 MHz, CH_3OH) of 373	498
Figure A5.46. ^{13}C NMR spectrum (75 MHz, CD_3OD) of 373	498
Figure A5.47. ^1H NMR spectrum (300 MHz, CDCl_3) of 374	499
Figure A5.48. ^2H NMR spectrum (76 MHz, CHCl_3) of 374	500
Figure A5.49. ^{13}C NMR spectrum (75 MHz, CDCl_3) of 374	500

APPENDIX 6

An Improved and Highly Efficient Copper(I)-Catalyzed Preparation of (S)-t-Bu-PHOX

Figure A6.3.1. X-ray crystal analysis of (S)-t-Bu-PHOX ((S)- 55). The molecular structure is drawn with 50% probability ellipsoids.....	505
---	-----

APPENDIX 7

Spectra Relevant to Appendix 6: An Improved and Highly Efficient Copper(I)-Catalyzed Preparation of (S)-t-Bu-PHOX

Figure A7.1. ^1H NMR spectrum (300 MHz, CDCl_3) of 55	515
Figure A7.2. ^{31}P NMR spectrum (121 MHz, CDCl_3) of 55	516
Figure A7.3. ^{13}C NMR spectrum (126 MHz, CDCl_3) of 55	516

APPENDIX 8

X-Ray Crystallography Reports Relevant to Appendix 6: An Improved and Highly Efficient Copper(I)-Catalyzed Preparation of (S)-t-Bu-PHOX

<i>Figure A8.1.1. (S)-t-Bu-PHOX ((S)-55) is shown with 50% probability ellipsoids. Crystallographic data have been deposited at the CCDC, 12 Union Road, Cambridge CB2 1EZ, UK, and copies can be obtained on request, free of charge, by quoting the publication citation and the deposition number 646767.</i>	517
<i>Figure A8.1.2. (S)-t-Bu-PHOX ((S)-55).</i>	520

LIST OF SCHEMES

CHAPTER 1

Natural Products and Pharmaceuticals as Inspiration for the Development of Enantioselective Catalysis

<i>Scheme 1.2.1. Enantioselective Diels–Alder cycloaddition and enantioselective ketone reduction en route to prostaglandins</i>	<i>3</i>
<i>Scheme 1.2.2. a) Enantioselective enamide hydrogenation toward α-amino acids. b) Enantioselective alkene epoxidation toward Crixivan. c) Enantioselective isomerization of an allyl amine toward menthol</i>	<i>5</i>
<i>Scheme 1.2.3. Enantioselective intramolecular aldol condensation toward steroids</i>	<i>6</i>
<i>Scheme 1.2.4. Convergent application of various enantioselective methods toward the synthesis of phorboxazole B</i>	<i>7</i>
<i>Scheme 1.3.1. Enantioselective hydrogenation of a β-enamino amide toward the synthesis of Januvia¹⁰</i>	
<i>Scheme 1.3.2 Enantioselective C(sp³)–C(sp³) cross-couplings toward fluvirucinine A₁.....</i>	<i>14</i>
<i>Scheme 1.3.3. Enantioselective intramolecular Heck reaction toward minfiensine</i>	<i>16</i>
<i>Scheme 1.3.4. Enantioselective Friedel–Crafts alkylation toward flustramine B.....</i>	<i>18</i>
<i>Scheme 1.3.5. Enantioselective Pictet–Spengler cyclization toward harmicine</i>	<i>20</i>
<i>Scheme 1.3.6. Phase-transfer alkylation toward indacrinone.....</i>	<i>22</i>
<i>Scheme 1.3.7. Pd-catalyzed enolate alkylations toward cyanthiwigin F.....</i>	<i>24</i>
<i>Scheme 1.3.8. a) Pd-catalyzed TMM-[3 + 2]-cycloaddition toward marcfortine B. b) Enantioselective TMM-cyclization.....</i>	<i>27</i>

CHAPTER 2

The Variocolin Family of Sesterterpenoids

<i>Scheme 2.1.1. Assignment of the absolute configuration of variocolin.....</i>	<i>40</i>
<i>Scheme 2.1.2. Hensens' biosynthetic proposal for variocolin.....</i>	<i>42</i>
<i>Scheme 2.3.1. Piers' stereoselective CD ring preparation.....</i>	<i>47</i>
<i>Scheme 2.3.2. Piers' annulation of the B ring</i>	<i>48</i>
<i>Scheme 2.3.3. Completion of the ABCD tetracycle via A-ring annulation.....</i>	<i>49</i>
<i>Scheme 2.3.4. Piers' end game progress toward completion of variocolin.....</i>	<i>50</i>
<i>Scheme 2.3.5. Samarium(II) iodide-promoted medium ring synthesis</i>	<i>51</i>
<i>Scheme 2.3.6. Molander's first-generation synthesis of A-ring fragment.....</i>	<i>52</i>

Scheme 2.3.7. Molander's first-generation synthesis of a CD ring fragment.....	54
Scheme 2.3.8. Molander's revised A-ring synthesis	55
Scheme 2.3.9. Molander's revised CD ring synthesis.....	56
Scheme 2.3.10. Molander's Sm(II)-promoted fragment coupling studies.....	57
Scheme 2.3.11. Alternate Sm(II)-promoted fragment coupling studies	58
Scheme 2.3.12. Molander's attempted installation of the C(11) quaternary stereocenter.....	59

CHAPTER 3

Progress toward the Asymmetric Total Synthesis of Variocolin

Scheme 3.1.1. Retrosynthetic analysis of variocolin.....	67
Scheme 3.2.1. Preparation of trichloroacetimidate 185	69
Scheme 3.2.2. Tethered cycloaddition of alcohol (\pm)- 187	70
Scheme 3.2.3. Termini-differentiating ozonolysis of cyclobutene 189	70
Scheme 3.2.4. Proposed ozonolytic cleavage of cyclobutene 189	72
Scheme 3.2.5. Optimized synthesis of α -diazoketone 200	74
Scheme 3.2.6. Initial Wolff/Cope studies on α -diazoketone 200	75
Scheme 3.2.7. Successful Wolff/Cope rearrangement of α -diazoketone 200	76
Scheme 3.2.8. Asymmetric synthesis of intramolecular cycloaddition substrate 212	78
Scheme 3.2.9. Cycloaddition, ozonolysis, and olefination toward an asymmetric Wolff/Cope substrate	79
Scheme 3.2.10. α -Diazoketone synthesis and Wolff/Cope rearrangement.....	80
Scheme 3.2.11. Optimized rearrangement of α -diazoketone 221 to α -methyl cyclooctadienone 223	83
Scheme 3.3.1. Proposed ring contraction approach to acylcyclopentene 225	83
Scheme 3.3.2. Vinylogous β -ketoester substrate synthesis and Pd-catalyzed asymmetric alkylation... ..	85
Scheme 3.3.3. Large-scale enantioselective alkylation of β -ketoester (\pm)- 181	86
Scheme 3.3.4. Reduction of ketone 229 and preliminary ring contraction.....	87
Scheme 3.3.5. Scale-up, derivatization, and enantioenrichment of acylcyclopentene 225	90
Scheme 3.3.6. Completion of D-ring fragment 237	92
Scheme 3.4.1. Model studies for B–D ring coupling.....	94
Scheme 3.4.2. Model radical cyclization for annulation of the C ring	95
Scheme 3.4.3. Efforts toward the direct reductive alkylation of enones 222 and 223 with iodide 237	96
Scheme 3.4.4. Diastereoselective reductive alkylation of 222 with methyl iodide or allyl bromide....	97
Scheme 3.4.5. Soft enolization of ketones 244 and 248	97
Scheme 3.4.6. Hydrosilylation investigations of enones 222 and 223	98

Scheme 3.5.1. Proposed end game strategy for completion of variecolin	100
---	-----

APPENDIX 1

Synthetic Summary toward the Asymmetric Total Synthesis of Variecolin

Scheme A1.1. Retrosynthetic analysis of variecolin	188
Scheme A1.2. Intramolecular cycloaddition and unsymmetrical ozonolysis toward the AB ring.....	189
Scheme A1.3. α -Diazoketone synthesis and Wolff/Cope rearrangement to AB ring fragments.....	189
Scheme A1.4. Asymmetric alkylation and ring contraction to the D-ring fragment.....	190
Scheme A1.5. Enrichment of acylcyclopentene 225 for the D-ring fragment.....	190
Scheme A1.6. AB ring reductive alkylation and soft enolization poised for fragment coupling.....	191
Scheme A1.7. Proposed completion of variecolin	191

CHAPTER 4

Enantioselective Allylic Alkylations of Vinylogous β -Ketoester Derivatives: Total Synthesis of (+)-Carissone

Scheme 4.3.1. Retrosynthetic analysis of the eudesmanes.....	327
Scheme 4.3.2. Enantioselective synthesis of the eudesmane bicyclic core.....	331
Scheme 4.3.3. End game for (+)-carissone (279) and the formal synthesis of (–)- α -eudesmol (281)	332

CHAPTER 5

Synthesis, Structural Analysis, and Gas-Phase Studies of 2-Quinuclidonium Tetrafluoroborate

Scheme 5.1.1. Synthesis of methyl-substituted 2-quinuclidone derivatives	412
Scheme 5.2.1. Retrosynthetic analysis of 2-quinuclidone using the Schmidt–Aubé reaction	413
Scheme 5.2.2. Preparation of ketoazide 320	414
Scheme 5.2.3. Synthesis of 2-quinuclidonium tetrafluoroborate (311 •HBF ₄)	414
Scheme 5.3.1. a) Proposed CID fragmentation mechanism of 311 •H ⁺ . b) Isotopically labeled mechanistic probes.....	421
Scheme 5.3.2. Synthetic route for the preparation of isotopically labeled mechanistic probes. a) ¹⁵ N-labeled 332 •HBF ₄ ; b) ¹³ C ₂ -labeled 333 •HBF ₄ ; c) D-labeled 334 •HBF ₄ ; d) D ₂ -labeled 335 •HBF ₄	422
Scheme 5.3.3. Gas-phase elimination of water to construct 311 •H ⁺ and 318 •H ⁺	424
Scheme 5.4.1. Proposed synthesis of 349 •H ⁺ employing the Schmidt–Aubé cyclization	428

Scheme 5.4.2. Proposed synthesis of **355** using the Schmidt–Aubé cyclization..... 430

APPENDIX 6

An Improved and Highly Efficient Copper(I)-Catalyzed Preparation of (S)-t-Bu-PHOX

Scheme A6.1.1. Original CuI-catalyzed coupling for the preparation of (S)-t-Bu-PHOX..... 502

LIST OF TABLES

CHAPTER 2

The Variocolin Family of Sesterterpenoids

Table 2.2.1. Immunosuppressant activity of the variocolin sesterterpenes.....	44
---	----

CHAPTER 3

Progress toward the Asymmetric Total Synthesis of Variocolin

Table 3.2.1. Equilibration of acetal 191	73
Table 3.2.2. Wolff/Cope solvent studies of α -diazoketone 221	82
Table 3.3.1. Asymmetric alkylation screen of vinylogous β -ketoester (\pm)- 181	86
Table 3.3.2. Ring contraction investigations of 231	89

APPENDIX 3

X-Ray Crystallography Reports Relevant to Chapter 3: Progress toward the Asymmetric Total Synthesis of Variocolin

Table A3.1.1. Crystal data and structure refinement for 215 (CCDC 718289).....	300
Table A3.1.2. Atomic coordinates ($\times 10^4$) and equivalent isotropic displacement parameters ($\text{\AA}^2 \times 10^3$) for acetal 215 (CCDC 718289). $U(\text{eq})$ is defined as the trace of the orthogonalized U^{ij} tensor.....	303
Table A3.1.3. Bond lengths [\AA] and angles [$^\circ$] for acetal 215 (CCDC 718289)	304
Table A3.1.4. Anisotropic displacement parameters ($\text{\AA}^2 \times 10^4$) for acetal 215 (CCDC 718289). The anisotropic displacement factor exponent takes the form: $-2\pi^2 [h^2 a^{*2} U^{11} + \dots + 2 h k a^* b^* U^{12}]$	305
Table A3.1.5. Hydrogen coordinates ($\times 10^4$) and isotropic displacement parameters ($\text{\AA}^2 \times 10^3$) for acetal 215 (CCDC 718289)	306
Table A3.2.1 Crystal data and structure refinement for 233 (CCDC 686849).....	307
Table A3.2.2. Atomic coordinates ($\times 10^4$) and equivalent isotropic displacement parameters ($\text{\AA}^2 \times 10^3$) for semicarbazone 233 (CCDC 686849). $U(\text{eq})$ is defined as the trace of the orthogonalized U^{ij} tensor	311
Table A3.2.3. Bond lengths [\AA] and angles [$^\circ$] for semicarbazone 233 (CCDC 686849)	313

Table A3.2.4. Anisotropic displacement parameters ($\text{\AA}^2 \times 10^4$) for semicarbazone 233 (CCDC 686849). The anisotropic displacement factor exponent takes the form: $-2\pi^2 [h^2 a^{*2} U^{11} + \dots + 2 h k a^* b^* U^{12}]$	315
Table A3.2.5. Hydrogen bonds for semicarbazone 233 (CCDC 686849) [\AA and $^\circ$].....	316

CHAPTER 4

Enantioselective Allylic Alkylations of Vinylogous β -Ketoester Derivatives: Total Synthesis of (+)-Carissone

Table 4.2.1. Solvent screen for the Pd-catalyzed alkylation of vinylogous β -ketoester (\pm)- 181	320
Table 4.2.2. Variation of the vinylogous functional group for improved stereoselectivity.....	322
Table 4.2.3. Six-membered vinylogous β -ketoester substrates.....	323
Table 4.3.1. Asymmetric allylation of vinylogous ester derivatives.....	329

CHAPTER 5

Synthesis, Structural Analysis, and Gas-Phase Studies of 2-Quinuclidonium Tetrafluoroborate

Table 5.2.1. Comparison of structural parameters for 311 • HBF_4 and formamide.....	416
---	-----

APPENDIX 6

An Improved and Highly Efficient Copper(I)-Catalyzed Preparation of (S)-t-Bu-PHOX

Table A6.2.1. Optimization of the coupling conditions.....	503
Table A6.2.2. Inorganic base screen.....	504

APPENDIX 8

X-Ray Crystallography Reports Relevant to Appendix 6: An Improved and Highly Efficient Copper(I)-Catalyzed Preparation of (S)-t-Bu-PHOX

Table A8.1.1. Crystal data and structure refinement for (S)- 55 (CCDC 664767).....	518
Table A8.1.2. Atomic coordinates ($\times 10^4$) and equivalent isotropic displacement parameters ($\text{\AA}^2 \times 10^3$) for (S)- 55 (CCDC 664767). $U(\text{eq})$ is defined as the trace of the orthogonalized U^{ij} tensor	521
Table A8.1.3. Bond lengths [\AA] and angles [$^\circ$] for (S)- 55 (CCDC 664767).....	522

Table A8.1.4. Anisotropic displacement parameters ($\text{\AA}^2 \times 10^4$) for (S)- 55 (CCDC 664767). The anisotropic displacement factor exponent takes the form: $-2\pi^2 [h^2 a^{*2} U^{11} + \dots + 2 h k a^* b^* U^{12}]$	523
--	-----

APPENDIX 9

Notebook Cross-Reference

Table A9.1. Notebook cross-reference for compounds of Chapter 3 and Appendix 2.....	525
Table A9.2. Notebook cross-reference for compounds of Chapter 4 and Appendix 4.....	526
Table A9.3. Notebook cross-reference for compounds of Chapter 5 and Appendix 5.....	527
Table A9.4. Notebook cross-reference for compounds of Appendix 6 and Appendix 7.....	528

LIST OF ABBREVIATIONS

Å	Ångstrom
$[\alpha]_D$	specific rotation at wavelength of sodium D line
Ac	acetyl
Anal.	combustion elemental analysis
APCI	atmospheric pressure chemical ionization
app	apparent
aq	aqueous
AIBN	2,2'-azobisisobutyronitrile
Ar	aryl
atm	atmosphere
BBN	borabicyclononane
Bn	benzyl
Boc	<i>tert</i> -butyloxycarbonyl
bp	boiling point
br	broad
Bu	butyl
<i>i</i> -Bu	<i>iso</i> -butyl
<i>n</i> -Bu	butyl
<i>t</i> -Bu	<i>tert</i> -Butyl
Bz	benzoyl
<i>c</i>	concentration for specific rotation measurements
°C	degrees Celsius
ca.	about (Latin circa)
calc'd	calculated

CAN	ceric ammonium nitrate
cat	catalytic
Cbz	carbobenzyloxy
CCDC	Cambridge Crystallographic Data Centre
CDI	1,1'-carbonyldiimidazole
cf.	compare (Latin confer)
CI	chemical ionization
CID	collision-induced dissociation
cm ⁻¹	wavenumber(s)
comp	complex
Cy	cyclohexyl
d	doublet
D	deuterium
dba	dibenzylideneacetone
DBU	1,8-diazabicyclo[5.4.0]undec-7-ene
DCE	dichloroethane
dec	decomposition
DIAD	diisopropyl azodicarboxylate
DMA	<i>N,N</i> -dimethylacetamide
DMAP	4-dimethylaminopyridine
dmdba	bis(3,5-dimethoxybenzylidene)acetone
DMF	<i>N,N</i> -dimethylformamide
DMSO	dimethyl sulfoxide
DNA	(deoxy)ribonucleic acid
dppb	1,4-bis(diphenylphosphino)butane
dppf	1,1'-bis(diphenylphosphino)ferrocene
dr	diastereomeric ratio

E_A	activation energy
EC ₅₀	median effective concentration (50%)
EDC	<i>N</i> -(3-dimethylaminopropyl)- <i>N'</i> -ethylcarbodiimide
ee	enantiomeric excess
EI	electron impact
e.g.	for example (Latin <i>exempli gratia</i>)
equiv	equivalent
ESI	electrospray ionization
Et	ethyl
FAB	fast atom bombardment
FID	flame ionization detector
g	gram(s)
GC	gas chromatography
gCOSY	gradient-selected correlation spectroscopy
h	hour(s)
HIV	human immunodeficiency virus
HMDS	1,1,1,3,3,3-hexamethyldisilazane
HMPA	hexamethylphosphoramide
HOBt	1-hydroxybenzotriazole
HPLC	high-performance liquid chromatography
HRMS	high-resolution mass spectroscopy
HSV	herpes simplex virus
$h\nu$	light
Hz	hertz
IC ₅₀	median inhibition concentration (50%)
i.e.	that is (Latin <i>id est</i>)
IR	infrared (spectroscopy)

<i>J</i>	coupling constant
kcal	kilocalorie
KDA	potassium diisopropylamide
KHMDS	potassium hexamethyldisilazide
λ	wavelength
L	liter
LDA	lithium diisopropylamide
lit.	literature value
LTQ	linear trap quadrupole
m	multiplet; milli
<i>m</i>	meta
<i>m/z</i>	mass to charge ratio
M	metal; molar; molecular ion
Me	methyl
MHz	megahertz
μ	micro
μ waves	microwave irradiation
min	minute(s)
MM	mixed method
mol	mole(s)
MOM	methoxymethyl
mp	melting point
Ms	methanesulfonyl (mesyl)
MS	molecular sieves
n	nano
N	normal
nbd	norbornadiene

NBS	<i>N</i> -bromosuccinimide
NIST	National Institute of Standards and Technology
NMO	<i>N</i> -methylmorpholine <i>N</i> -oxide
NMR	nuclear magnetic resonance
NOE	nuclear Overhauser effect
NOESY	nuclear Overhauser enhancement spectroscopy
Nu	nucleophile
[O]	oxidation
<i>o</i>	ortho
<i>p</i>	para
PA	proton affinity
PCC	pyridinium chlorochromate
PDC	pyridinium dichromate
Ph	phenyl
pH	hydrogen ion concentration in aqueous solution
PhH	benzene
PhMe	toluene
PHOX	phosphinooxazoline
Piv	pivaloyl
<i>pKa</i>	<i>pK</i> for association of an acid
PMB	<i>p</i> -methoxybenzyl
pmdba	bis(4-methoxybenzylidene)acetone
PPL	porcine pancreas lipase
ppm	parts per million
PPTS	pyridinium <i>p</i> -toluenesulfonate
Pr	propyl
<i>i</i> -Pr	isopropyl

Py	pyridine
q	quartet
ref	reference
R	generic for any atom or functional group
R_f	retention factor
rt	room temperature
s	singlet or strong or selectivity factor
sat.	saturated
SET	single electron transfer
S_N2	second-order nucleophilic substitution
sp.	species
t	triplet
TBAF	tetrabutylammonium fluoride
TBHP	<i>tert</i> -butyl hydroperoxide
TBS	<i>tert</i> -butyldimethylsilyl
TCDI	1,1'-thiocarbonyldiimidazole
TCNE	tetracyanoethylene
Tf	trifluoromethanesulfonyl (trifyl)
TFA	trifluoroacetic acid
TFE	2,2,2-trifluoroethanol
THF	tetrahydrofuran
TIPS	triisopropylsilyl
TLC	thin-layer chromatography
TMEDA	<i>N,N,N',N'</i> -tetramethylethylenediamine
TMS	trimethylsilyl
TOF	time-of-flight
Tol	tolyl

TON	turnover number
t_R	retention time
Ts	<i>p</i> -toluenesulfonyl (tosyl)
UV	ultraviolet
<i>v/v</i>	volume to volume
w	weak
<i>w/v</i>	weight to volume
X	anionic ligand or halide

CHAPTER 1

Natural Products and Pharmaceuticals as Inspiration for the Development of Enantioselective Catalysis[†]

1.1 INTRODUCTION

Biologically active natural products and pharmaceuticals often contain particularly challenging structural features and functionalities in terms of synthesis. Perhaps the greatest difficulties are those caused by issues of stereochemistry. A useful strategy for synthesizing such molecules is to devise methods of bond formation that provide opportunities for using enantioselective catalysis. In using this tactic, the desire for a particular target structure ultimately drives the development of catalytic methods. New enantioselective catalytic methods contribute to a greater fundamental understanding of how bonds can be constructed and lead to valuable synthetic technologies that are useful for a variety of applications. The lack of methods available for installing functionalities or structural motifs during chemical synthesis can at first be frustrating. However,

[†] This review was written in collaboration with Justin T. Mohr and a similar version has been published. See: Mohr, J. T.; Krout, M. R.; Stoltz, B. M. *Nature* **2008**, *455*, 323–332.

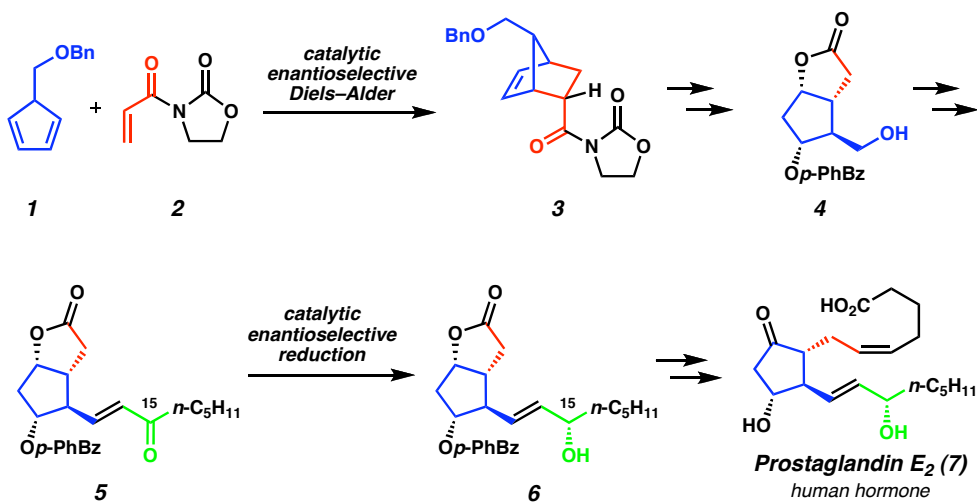
retrosynthetic analysis,¹ a way of viewing the target molecule as a series of structurally simpler precursors, can greatly aid in planning how to generate a valuable chemical substance. Despite this, difficulties in preparing materials enriched in a particular enantiomer persist because of the limited number of catalytic enantioselective transformations available.² One fruitful strategy is to design a synthesis that depends on a bond-forming reaction for which there is no known enantioselective variant. This approach thus provides the impetus for developing novel transformations and leads to a greater understanding of methods of bond construction and catalysis. Herein, several recent examples of novel catalytic enantioselective transformations are described in order to illustrate the effectiveness of this strategy for preparing important structural motifs found in biologically active molecules. Each of these transformations has contributed not only an effective means of generating a particular target structure but also a useful new tool for a variety of applications in synthetic chemistry.

1.2 HISTORICAL OVERVIEW OF ENANTIOSELECTIVE METHODS

To provide an overview of established catalytic enantioselective methods that have been developed for total synthesis, several notable examples of enantioselective reactions in total synthesis are highlighted in Scheme 1.2.1 through Scheme 1.2.4. In each of these cases, the target molecules posed particular challenges that had yet to be solved by enantioselective catalysis. Although, in some instances (e.g., the Diels–Alder reaction, Scheme 1.2.1), the methods were developed before their first application in total synthesis, the demonstrated value of the transformation highlighted the need for enantioselective variants. Following the development of the [4 + 2] cycloaddition

reaction in the 1920s,³ studies of this transformation elucidated several key facets of the stereochemical outcome of the reaction (e.g., the “endo rule,” regioselectivity, and diastereoselectivity). These intrinsic stereochemical control elements proved useful when the Diels–Alder reaction was first featured in a total synthesis with Stork’s stereocontrolled synthesis of cantharidin⁴ in 1951. Subsequently, the thermal Diels–Alder reaction was used for several total syntheses, perhaps most famously in Woodward’s landmark synthesis of reserpine.⁵ Enantioselectivity in this transformation remained elusive, however, and perhaps was considered unattainable at the time.

Scheme 1.2.1. Enantioselective Diels–Alder cycloaddition and enantioselective ketone reduction en route to prostaglandins



One key practical improvement in the Diels–Alder reaction was the discovery that Lewis acids markedly increased the reaction rate.⁶ Many laboratories sought to exploit this and to develop asymmetric versions of the Diels–Alder reaction catalyzed by chiral Lewis acids, culminating in a report of the first highly enantioselective catalytic Diels–

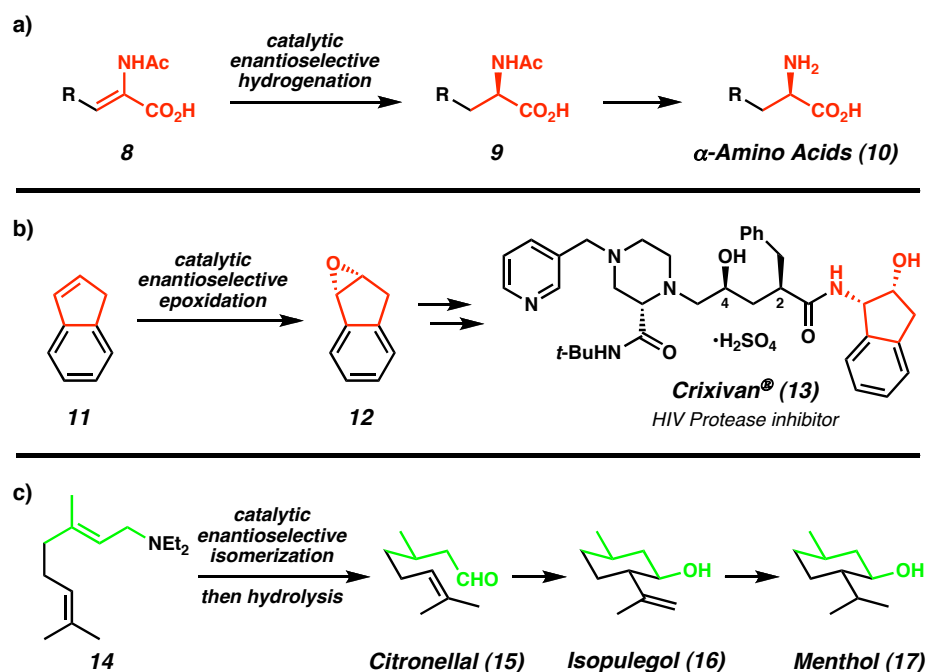
Alder reaction in 1979.⁷ The interface between reaction development, study of the mechanism, and synthesis is readily apparent from the multitude of chiral Diels–Alder catalysts and accompanying enantioselective total syntheses that have been reported.⁸ These successes validate the extensive efforts directed at realizing this important goal.

Other methods were developed to address more general problems in synthesis (e.g., synthesis of chiral alcohols by means of enantioselective ketone reduction, Scheme 1.2.1); however, the key structures are embedded in a variety of important natural products and pharmaceutical compounds. In the case of Corey’s approach to the synthesis of prostaglandins⁹ first reported in the 1960s, control of the configuration of the sidechain allylic alcohol at C(15) required stoichiometric chiral reducing agents until a solution to this long-standing problem was found in the 1980s.¹⁰ Interestingly, the oxazaborolidine catalyst discovered in these explorations has had other varied applications in synthesis and catalysis,^{8b,11} demonstrating the versatility of privileged molecular frameworks¹² for enantioselective catalysis.

The practical application of enantioselective catalysis is apparent in myriad industrial applications (e.g., Scheme 1.2.2), for which the limits of catalysis must be examined to minimize costs. Important industrial applications include the synthesis of chiral building blocks (e.g., amino acids¹³ (**10**)), novel biologically active pharmaceuticals (e.g., Crixivan¹⁴ (indinavir sulfate, **13**)), and commodity chemicals (cheap chemicals sold in bulk) with various important uses (e.g., menthol¹⁵ (**17**)). Only the most efficient methods are feasible for large-scale industrial synthesis, and in many ways these protocols represent the pinnacle of modern enantioselective catalysis.¹⁶ A viable commercial operation must account for more than simply effective asymmetric induction; factors

including turnover frequency, catalyst availability, catalyst recovery, catalyst toxicity, and feasible large-scale handling procedures must all be considered for industrial applications. These daunting challenges underscore the demand for increasingly efficient catalyst systems.

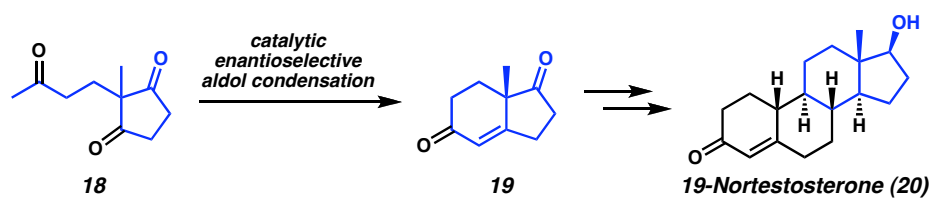
Scheme 1.2.2. a) Enantioselective enamide hydrogenation toward α -amino acids. b) Enantioselective alkene epoxidation toward Crixivan. c) Enantioselective isomerization of an allyl amine toward menthol



To maximize the usefulness of the stereochemistry attained by these key asymmetric transformations, subsequent diastereoselective reactions may be used to control the formation of many stereocenters based on a single enantioselective transformation (e.g., Scheme 1.2.3). The Hajos–Parrish ketone (**19**), first prepared in the context of steroid synthesis, has been used extensively in other synthetic efforts and has proved to be a

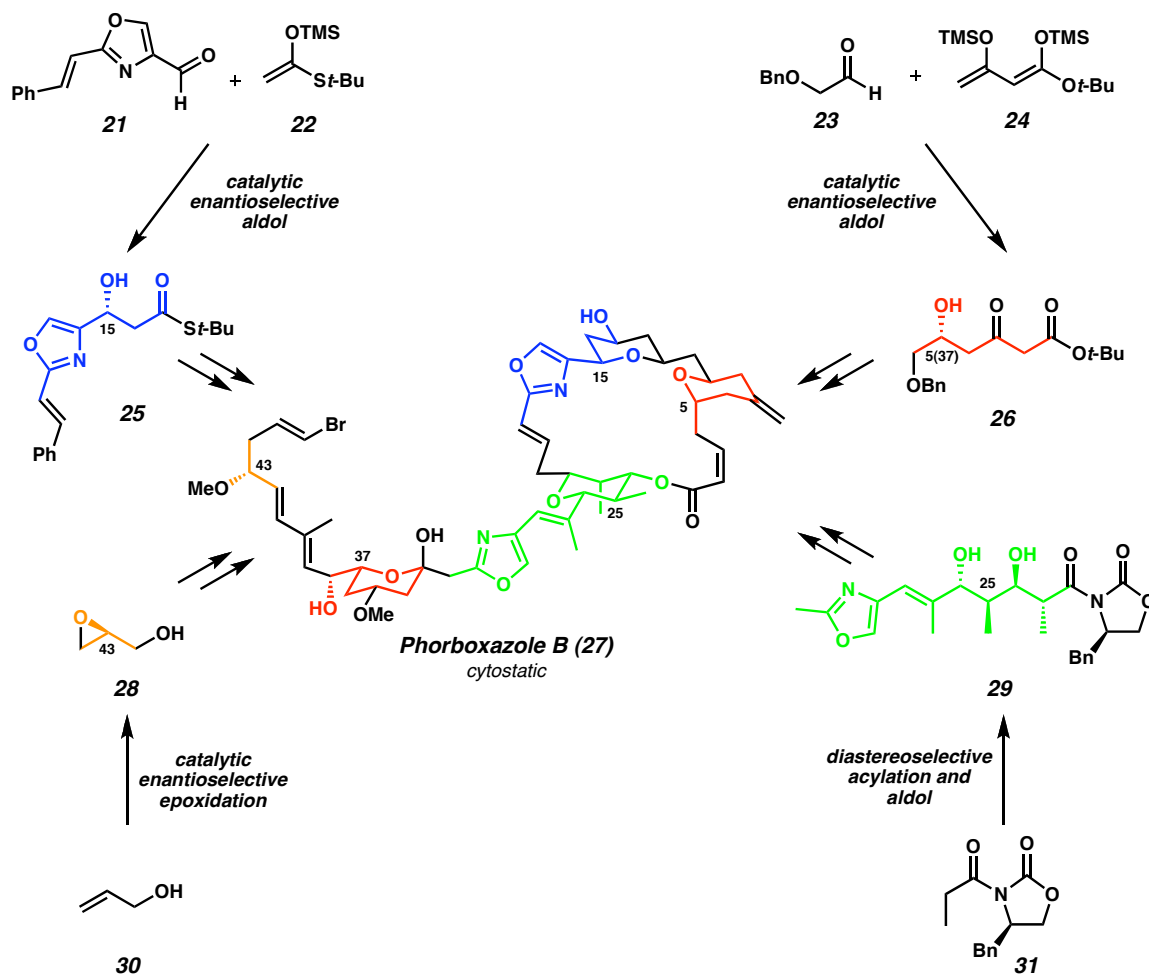
versatile chiral-pool starting material.¹⁷ The amino acid catalyst system developed for this intramolecular aldol condensation provided a sound basis for the recent use of organic molecules as catalysts for a variety of enantioselective transformations (see subsection 1.3.4).

Scheme 1.2.3. Enantioselective intramolecular aldol condensation toward steroids



The use of several different enantioselective reactions to prepare enantioenriched fragments of complex molecules improves efficiency through convergency. The importance of this strategy is shown by the variety of extraordinarily complex polyketide natural products that have been prepared through asymmetric intermolecular aldol reactions (e.g., phorboxazole B¹⁸ (**27**), Scheme 1.2.4). The challenging structure of these molecules has required the development of several related protocols to address the subtle differences in substitution patterns and functionality present in substrates, and, despite many successes, studies are ongoing.¹⁹

Scheme 1.2.4. Convergent application of various enantioselective methods toward the synthesis of phorboxazole B



1.3 RECENT DEVELOPMENTS IN ENANTIOSELECTIVE CATALYSIS

In this section, recent representative developments made by using this approach—that is, by using target structures to inspire the development of enantioselective catalysts—for the construction of biologically important target molecules are described. Most of these methods involve the formation of a carbon–carbon bond, the fundamental structure of organic molecules. These cases were selected to illustrate some of the latest developments in enantioselective catalysis for complex molecule synthesis. Special

attention has been given to reactions that address some of the most important challenges in synthetic chemistry today: increasing functional group tolerance, generating new carbocyclic and heterocyclic rings, and forming all-carbon quaternary stereocenters. The examples are also intended to show the important symbiosis between total synthesis and method development, and to show that improvements in one branch of synthetic chemistry have an impact on the others.

1.3.1 β -ENAMINO AMIDE HYDROGENATIONS — JANUVIA

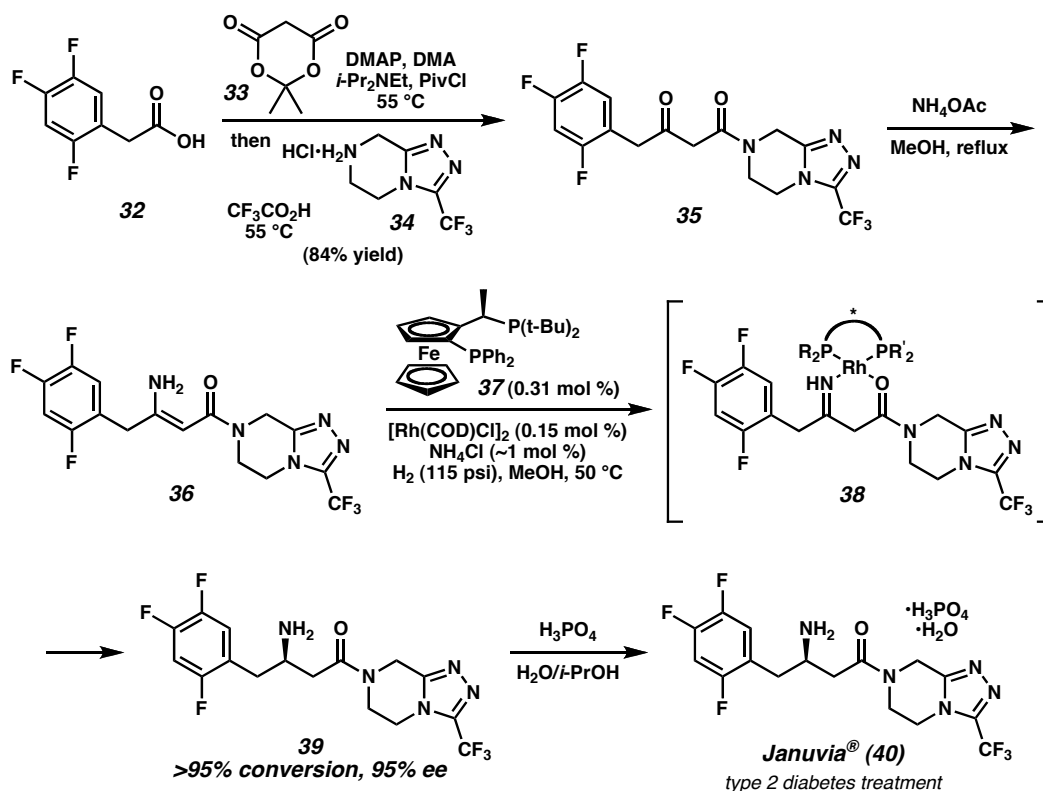
Catalytic enantioselective hydrogenation has become one of the most effective and powerful methods for the synthesis of chiral α -amino acids for numerous applications.¹³ Over the past decade, the usefulness of the homologous building blocks, β -amino acids, in pharmaceutical, agrochemical, β -peptide, and natural substances has become evident, highlighting the need for a general and effective means for their preparation.²⁰ Undoubtedly, the implementation of a catalytic asymmetric hydrogenation of *N*-acyl- β -enamino esters seemed to be the most efficient pathway toward their synthesis, although initial investigations achieved poor selectivities.²¹ Additional syntheses using the chiral pool, auxiliaries, and more recently the catalytic asymmetric generation of C–C and C–N bonds have been successful in satisfying the increased demand for β -amino acids.^{20b} These valuable methods allow flexible strategies for the synthesis of a variety of analogs; however, most examples are limited by the requirement for further chemical manipulation that is often necessary to produce the functionality of the desired β -amino acids.

Despite initial difficulties, the asymmetric hydrogenation of *N*-acyl- β -enamino esters has been developed into a useful method over the past 15 years.²² This fruitful endeavor has demonstrated that several transition metal and ligand combinations are competent for preparing *N*-acyl- β -amino acids with good-to-excellent enantioselectivities. A notable drawback to this strategy, however, is the requirement for the seemingly indispensable *N*-acyl group on the β -enamino esters; this group is needed for metal chelation, which improves reactivity and selectivity. The introduction of this moiety often produces enamine alkene isomers that can be difficult to separate, and, importantly, the individual isomers are typically hydrogenated with differing rates and selectivities. Moreover, these difficulties are magnified by the necessary removal of this group, a seemingly cumbersome artifact of an otherwise powerful strategy. Nonetheless, this advance has allowed a variety of β -amino acids to be prepared.^{20b}

An innovative solution to this problem was demonstrated by a group at Merck en route to synthesizing Januvia (sitagliptin phosphate; **40**, Scheme 1.3.1), which has recently been approved by the U. S. Food and Drug Administration for the treatment of type 2 diabetes.²³ The optimal target contains an unfunctionalized β -amino amide. A strategy was sought to install this moiety directly by asymmetric hydrogenation of unsubstituted β -enamino ester and amide derivatives²⁴ (e.g., **36**). A traditional hydrogenation route for the production of amino acids is a proven, cost-effective method for the synthesis of chiral building blocks. The industrial infrastructure is already in place to realize this goal; however, in this case, the reduction of unprotected β -enamino acids was not effective with existing chiral catalysts. A crucial component in addressing such limitations was Merck's high-throughput screening facility, which allowed rapid

screening of catalyst structures and reaction conditions (an essential component for the success of any asymmetric catalytic process).²⁵ One potential complication for this hydrogenation strategy was avoided when it was observed that the preparation of the β -enamino ester and amide substrates (e.g., **35** \rightarrow **36**) proceeded with complete selectivity for the *Z*-isomer, presumably owing to hydrogen bonding in the products.

Scheme 1.3.1. Enantioselective hydrogenation of a β -enamino amide toward the synthesis of Januvia



During the screening, a survey of transition metals and ligands revealed that rhodium complexes of the Josiphos (e.g., **37**, Scheme 1.3.1) family of ligands efficiently catalyze the hydrogenation of a variety of substrates to give high yields with excellent enantioselectivities. The remarkable functional-group tolerance of this catalyst allowed

the strategic implementation of this asymmetric transformation as the penultimate step of the synthesis, thereby maximizing the usefulness of the process and materials. Thus, phenylacetic acid derivative **32** was converted into β -ketoamide **35** in a one-pot procedure via acylation of Meldrum's acid (**33**), followed by treatment with triazole salt **34**.²⁶ Exposure to ammonium acetate converted this into β -enamino amide **36** as a single enamine isomer. Hydrogenation of amide **36** in the presence of 0.30 mol % of rhodium(I) and ligand **37** provided β -amino amide **39** in >95% conversion and 95% enantiomeric excess. Subsequent recrystallization and salt formation with phosphoric acid gave Januvia (**40**). Efforts to optimize efficiency and examine the mechanism of the asymmetric process revealed that reactivity and selectivity were dependent on the pH of the reaction solution.²⁷ It was found that ~1 mol % of a mild acid (i.e., ammonium chloride) was essential for the reaction to proceed reproducibly on a large scale. In addition, it was observed that hydrogenation of a related substrate under identical conditions with a deuterium gas atmosphere resulted in deuterium incorporation at the β -position only, suggesting that an imine is an intermediate (**38**) and that an enamine–imine tautomerization process plays an important part in the mechanism.²⁴ Interestingly, intermediates such as **38** have a striking similarity to asymmetric β -carbonyl hydrogenations pioneered by Noyori and co-workers.²⁸

This example demonstrates the development of asymmetric catalysis into a state-of-the-art science through maximizing the efficiency by minimizing unnecessary functionality, by using atom economy, and by using extremely active catalysts. Moreover, the development of the catalyst system for the synthesis of Januvia exemplifies the continued need for subtly different catalysts to meet new synthetic

demands. Building on the experience obtained during the development of a highly efficient enamide reduction toward α -amino acids, such large-scale industrial synthesis of important β -amino acids has been a relatively rapid process.

1.3.2 $C(sp^3)$ – $C(sp^3)$ CROSS-COUPPLINGS – FLUVIRUCININE A₁

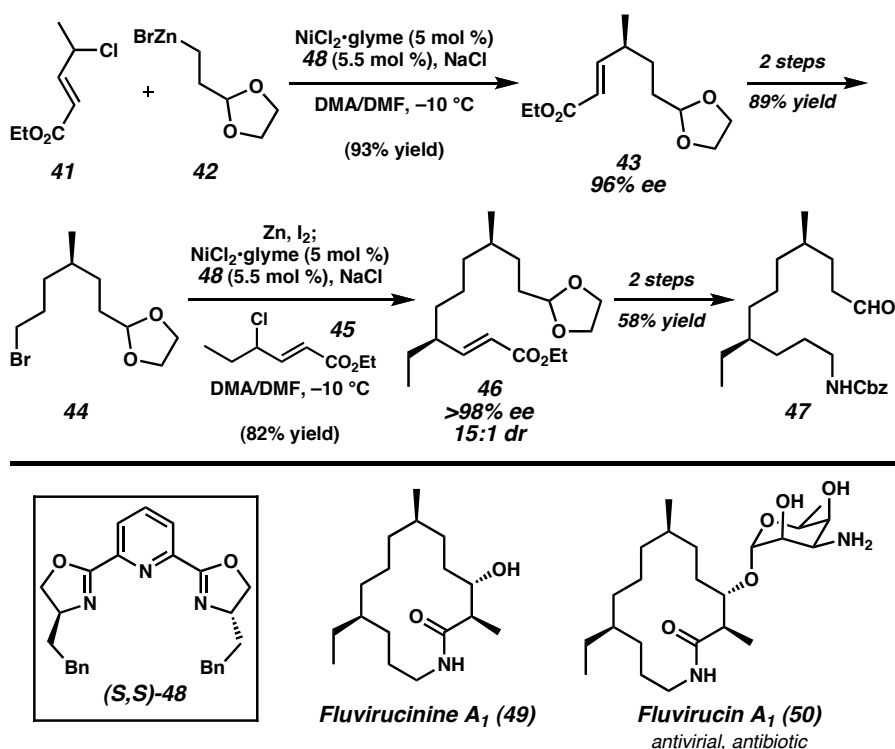
Transition metal-catalyzed cross-coupling reactions have been used extensively for constructing C–C bonds and, consequently, have had a substantial effect on the field of complex molecule synthesis.²⁹ The predominance of palladium and nickel catalysts in cross-coupling technologies and their extraordinary functional-group tolerance increases the efficiency of this process by allowing a large degree of functionalization before coupling. Moreover, the efficacy of this cross-coupling strategy for streamlining synthesis has allowed retrosynthetic analyses that had been thought impossible with standard, nonmetal reactions. Until recently, however, most cross-coupling methods involved $C(sp^2)$ – $C(sp^2)$ or $C(sp^2)$ – $C(sp)$ centers, limiting the application potential. Two crucial issues associated with expanding the substrate scope to include $C(sp^3)$ – $C(sp^3)$ couplings are the relatively low reactivity of alkyl halides toward oxidative addition and the propensity of σ -alkyl organometallic complexes to undergo rapid β -hydrogen elimination reactions.³⁰ Practical solutions to this problem were first presented by Suzuki and Knochel, followed more recently by Fu.^{30b,31} In general, the reaction scope now encompasses a variety of primary and secondary halides and pseudohalides as the electrophilic component, with organoboranes, boronic acids, alkylmagnesium halides and alkylzinc halides as the nucleophilic component.^{30b} Although perhaps not developed in the context of a particular target molecule, progress in these cross-coupling methods has

allowed retrosynthetic disconnections that were not practical previously. Asymmetric cross-coupling protocols could, in turn, allow the direct formation of remote stereocenters in relatively unfunctionalized molecules.

Early examples of catalytic asymmetric cross-coupling reactions involving C(sp³)-C(sp²) centers were explored by Kumada and co-workers in the late 1970s and produced moderate enantioselectivities.³² Despite these initial reports and the subsequent evolution of cross-coupling methods and asymmetric catalysis, a deficiency in the development of catalytic asymmetric methods for C(sp³)-C(sp³) couplings existed until Fu and co-workers³³ reported an asymmetric Negishi coupling in 2005. Before this report, researchers in the Fu laboratory observed the proficiency of tridentate pybox ligands (e.g., **48**, Scheme 1.3.2) at enabling the room temperature nickel-catalyzed Negishi coupling of symmetric secondary alkyl bromides and iodides.³⁴ It was postulated that the tridentate nature of pybox ligands prevented the undesired β -hydrogen-elimination pathway, which would require a vacant coordination site. Reaction optimization facilitated the development of several asymmetric variations that generate challenging stereocenters applicable to complex molecule synthesis, as demonstrated in Fu's formal total synthesis of fluvirucinine A₁ (**49**), the aglycon of the macrolactam antibiotic fluvirucin A₁ (**50**).³⁵ A key nickel(II)-catalyzed asymmetric cross-coupling of racemic allylic chloride **41** and alkylzinc reagent **42** in the presence of (*S,S*)-**48** generated γ -disubstituted enone **43** in an excellent yield and 96% enantiomeric excess. Elaboration over two steps to a bromide (**44**), followed by conversion to the alkylzinc form and a second nickel(II)-catalyzed asymmetric Negishi cross-coupling with racemic allylic chloride **45**, provided the ester **46** in a good yield and with >98% enantiomeric excess

and a 15:1 ratio of diastereomers. A subsequent two-step conversion to the aldehyde **47** intersected Suh's synthesis of fluvirucine A₁ (**49**).³⁶ This method exemplifies the efficiency of the C(sp³)-C(sp³) cross-coupling and presents a creative solution to the particularly difficult challenge of remote stereochemical control.

Scheme 1.3.2 Enantioselective C(sp³)-C(sp³) cross-couplings toward fluvirucine A₁



At present, most examples of this technology require a stabilizing group adjacent to the site of the putative carbon-centered radical. Eliminating this condition would further improve the utility of this asymmetric cross-coupling method. In addition, stereogenic organometallic coupling partners (e.g., secondary alkylzinc reagents) have not yet been reported in this asymmetric transformation. A potential goal for this synthetic method would be the combination of a racemic secondary alkyl halide and a racemic secondary

alkylmetal reagent to form vicinal stereocenters along an alkyl chain with high levels of enantioselectivity and diastereoselectivity.

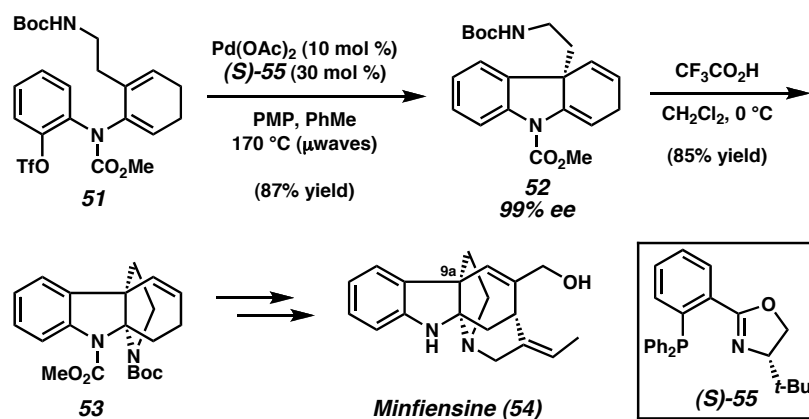
1.3.3 INTRAMOLECULAR HECK CYCLIZATIONS — MINFIENSINE

The enantioselective generation of all-carbon quaternary stereocenters is a considerable challenge for synthetic chemists.³⁷ As quaternary stereocenters are found in many natural product structures, convenient enantioselective methods for their formation would be useful. One such method is the Heck reaction,³⁸ in which a palladium(0) catalyst promotes the vinylation of an aryl halide, vinyl halide, or trifluoromethane sulfonate. The large body of literature on palladium catalysis and mechanisms,²⁹ as well as an ever-growing collection of chiral ligands for transition-metal catalysis, greatly increased the potential of using this method to carry out asymmetric catalysis. In addition, many synthetic endeavors using diastereoselective or nonstereoselective intramolecular Heck reactions have been reported,³⁹ increasing the significance of an enantioselective process. In 1989, the laboratories of Shibasaki⁴⁰ and Overman⁴¹ independently reported the first variants of an intramolecular catalytic asymmetric Heck reaction. Initial levels of enantioselectivity were moderate; however, subsequent optimizations realized good-to-excellent selectivities in the generation of tertiary and all-carbon quaternary stereocenters.⁴²

Indole alkaloids encompass a large number of natural and pharmaceutical substances with a wide range of biological activities.⁴³ The plant alkaloid minfiensine (**54**, Scheme 1.3.3) is a compelling example of the all-carbon quaternary stereocenter motif in biologically active natural products. Minfiensine and related alkaloids have been used in

traditional medicines and have promising anticancer activity.⁴⁴ The intriguing polycyclic structure and biological relevance of minfiensine prompted the Overman laboratory⁴⁵ to explore a catalytic enantioselective Heck reaction to generate the sole quaternary stereocenter at C(9a). It was discovered that the palladium-catalyzed intramolecular Heck reaction of dienyl aryl trifluoromethane sulfonate **51** in the presence of the phosphinooxazoline ligand (*S*)-**55** under microwave conditions produced indoline **52** in good yield and with 99% enantiomeric excess. Subsequent acid-promoted carbamate cyclization produced the tricyclic core of minfiensine (**53**), which was then converted to the natural product. The efficiency and selectivity of the catalytic asymmetric Heck reaction facilitated completion of the target, where the remaining stereocenters are derived from this initial transformation.

Scheme 1.3.3. Enantioselective intramolecular Heck reaction toward minfiensine



Despite numerous examples of the asymmetric Heck reaction in total synthesis,⁴² there are several features that could be improved. Reactions typically require high temperatures and relatively high catalyst loadings, and the development of chiral ligands

that greatly increase the reactivity of the transition metal while maintaining an adequate asymmetric environment would be greatly beneficial.

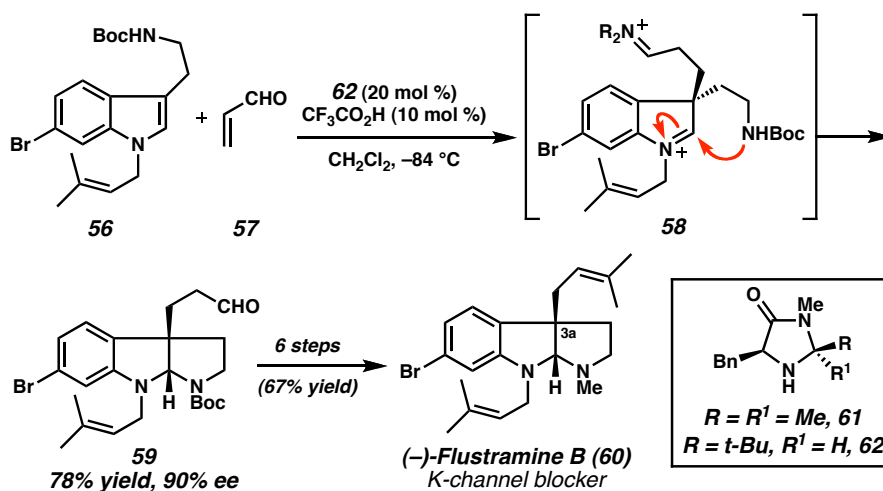
As most enantioselective Heck reactions use an sp^2 -hybridized organohalide component, another frontier lies in the application of unactivated alkyl carbon electrophiles that have β -hydrogens in both intramolecular and intermolecular cases, an area currently in its infancy.⁴⁶

1.3.4 *INDOLE FRIEDEL–CRAFTS ALKYLATIONS — FLUSTRAMINE B*

Numerous methods have been developed for the generation of substituted indoles;⁴⁷ however, enantioselective indole functionalization has been far less explored. To address the deficiencies in the indole functionalization literature, Jørgensen⁴⁸ and MacMillan⁴⁹ independently developed strategies for asymmetric Friedel–Crafts alkylation of conjugate acceptors with electron-rich heteroaromatics. MacMillan's method uses a secondary amine catalyst (**61**, Scheme 1.3.4) that facilitates the LUMO-lowering activation of α,β -unsaturated aldehydes for a variety of transformations.⁵⁰ Although imidazolidinone **61** was a sufficient catalyst for the Friedel–Crafts alkylation of pyrroles, generating good yields and excellent enantioselectivities,⁴⁹ application of less-activated indole substrates resulted in sluggish reactivity with considerably diminished selectivities.⁵¹ Kinetic investigations of iminium-catalyzed reactions revealed that the overall reaction rate was influenced by the efficiency of formation for both the iminium ion and the C–C bond, prompting the development of a modified imidazolidinone catalyst (**62**). This refinement minimized the steric bulk around one face of the catalyst, thereby exposing the lone pair of electrons on the secondary amine nitrogen. This structural change translated into

increased reactivity that enabled the asymmetric Friedel–Crafts alkylation of a variety of indoles with good-to-excellent yields and very high enantioselectivities.⁵¹

Scheme 1.3.4. Enantioselective Friedel–Crafts alkylation toward flustramine B



Pyrroloindoline alkaloids are a family of polyindole alkaloids of diverse structural complexity and biological relevance.⁵² Diastereoselective syntheses of the core of these compounds have focused on the control of the C(3a) all-carbon quaternary stereocenter as a key design element.⁵³ With a powerful and mild indole alkylation method in hand, MacMillan and co-workers⁵⁴ devised a cascade strategy for the catalytic asymmetric preparation of the C(3a) stereocenter and the pyrroloindoline core of the potassium-channel blocker **(-)-flustramine B (60)**, Scheme 1.3.4) in one step. In this key transformation, tryptamine derivative **56** and 2-propenal (acrolein, **57**), in the presence of catalyst **62**, underwent the asymmetric Friedel–Crafts alkylation to provide iminium intermediate **58**. Subsequent carbamate cyclization and hydrolysis to regenerate the catalyst provided the core (**59**) with a good yield and 90% enantiomeric excess.

Importantly, this allowed completion of (–)-flustramine B (**60**) in just six steps and with good overall yield, highlighting the efficiency of this cascade approach. It is noteworthy that this strategy also has the potential to be applied to the synthesis of various polycyclic indolines such as the diazamide family of cytotoxic alkaloids.⁵⁴ It is also interesting to note that both the intramolecular Heck reaction (see subsection 1.3.3) and the indole Friedel–Crafts alkylation can generate similar indoline structural motifs despite the markedly different bond-connecting strategies of these reactions. The success of these dissimilar strategies allows a great deal of flexibility in the planning of syntheses.

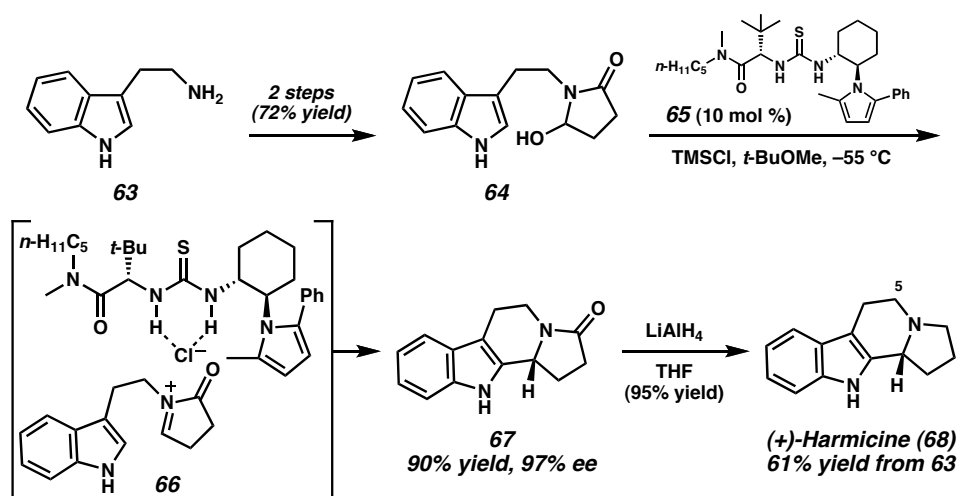
Iminium-activation methods with chiral amine catalysts have been successful for numerous transformations, but catalyst loading, turnover frequency, and excesses of certain reagents limit the large-scale industrial application of these methods. In addition, in some cases, the organic catalyst may be more difficult to remove from the reaction products than a metal catalyst. However, the typically air- and moisture-stable reaction conditions, low cost of some catalysts, and often metal-free conditions are attractive. The variety of asymmetric transformations (some proceeding through substantially different reaction pathways) that have been realized with chiral amine catalysts so far indicates a burgeoning field in which there are many useful enantioselective catalysts.

1.3.5 *PICTET–SPENGLER CYCLIZATIONS — HARMICINE*

Since Pictet and Spengler reported the intramolecular cyclization of an aromatic ring onto an iminium species in 1911,⁵⁵ this transformation has been of great use in the synthesis of many important alkaloid natural products.⁵⁶ Indeed, the need for asymmetric variants of this reaction was recognized, and several diastereoselective protocols have

been devised.⁵⁶ A common approach to diastereoselective Pictet–Spengler cyclization has been to use tryptophan derivatives to control the stereochemistry of the cyclization. However, using this type of technique for the synthesis of a natural product such as harmicine (**68**, Scheme 1.3.5), which is active against the disease leishmaniasis, necessitates the removal of the stereocontrol element at C(5), following the diastereoselective cyclization. Nonetheless, Allin and co-workers⁵⁷ proved this to be a viable method in 2007. This particular structure, however, highlighted a challenge for enantioselective catalysis and an opportunity to improve synthetic efficiency.

Scheme 1.3.5. Enantioselective Pictet–Spengler cyclization toward harmicine



When considering prospects for asymmetric induction, Jacobsen and Taylor considered activated *N*-acyl-iminium ions as a template and reasoned that a chiral thiourea derivative might be effective in promoting cyclization.⁵⁸ In practice, these Brønsted acids,⁵⁸ as well as other Brønsted acids investigated later by other groups,⁵⁹ proved to be excellent catalysts for enantioselective indole annulations with in situ-

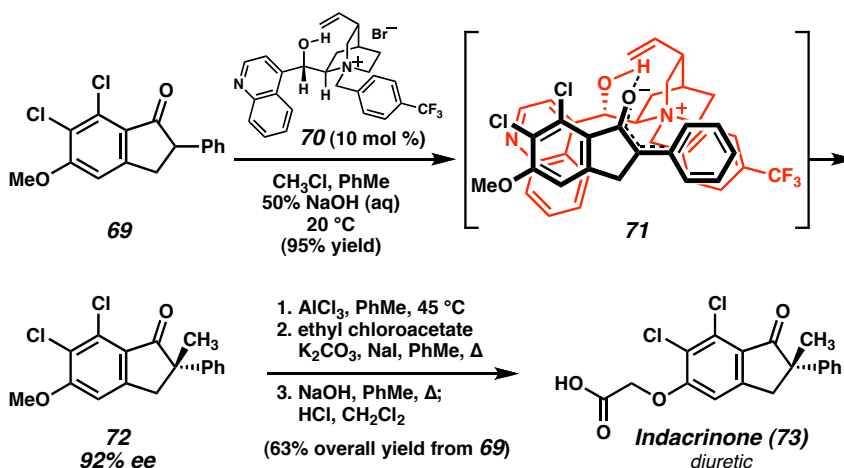
generated *N*-acyl-iminium species (e.g., **66**, Scheme 1.3.5). In later studies by Jacobsen and co-workers, it was found that hydroxylactams (e.g., **64**) are convenient precursors to *N*-acyl-iminium ions, which in turn enable access to various polycyclic structures.⁶⁰ Given this effective protocol, an efficient catalytic asymmetric synthesis of harmicine (**68**) was realized in four steps from tryptamine (**63**). Several mechanistic experiments have suggested that asymmetric induction is controlled by a complex of the Brønsted acid catalyst (**65**) and a chloride counterion closely associated with the iminium ion (e.g., **66**) that effectively blocks approach to one face of the electrophile, providing annulated products (e.g., **67**) with excellent enantiomeric excesses. This insight into the remarkable mechanism of this transformation has led to a related C–C bond-forming process using oxocarbenium ions.⁶¹ Further exploitation of this unusual proposed catalyst–anion interaction could lead to a variety of other asymmetric addition reactions, such as intermolecular alkylation of *N*-acyl-iminium ions. In common with the history of the Diels–Alder reaction (see section 1.2), the exploration of the Pictet–Spengler cyclization has provided a useful method to access many heterocyclic structures embedded in alkaloid natural products using a classical reaction with well-established synthetic applications.

1.3.6 PHASE TRANSFER ALKYLATIONS — INDACRINONE

Enolate alkylations exemplify the fundamental usefulness of the carbonyl group for C–C bond formation. Strategies to induce asymmetry in these reactions have included chiral auxiliaries and chiral ligands, although few examples are catalytic. A particularly challenging class of product targets is all-carbon quaternary stereocenters adjacent to

carbonyl groups. One example of an important target bearing this motif is the diuretic drug candidate indacrinone (**73**, Scheme 1.3.6).⁶² Given the lack of efficient methods for synthesizing this structure, researchers at Merck envisaged an enantioselective phase-transfer alkylation method based on a quaternary ammonium salt derived from a naturally occurring cinchona alkaloid (e.g., **70**). In the event, readily prepared indanone **69** was methylated, producing ketone **72** with 95% yield and 92% enantiomeric excess, and **72** was then converted to indacrinone (**73**) in three additional steps.

Scheme 1.3.6. Phase-transfer alkylation toward indacrinone



Although successful in achieving enantioselective enolate alkylation, the mechanism for this process seems to be complex;⁶³ however, enantiofacial selectivity in the alkylation event may be rationalized through the hypothetical transition state **71** (Scheme 1.3.6). Three key interactions are thought to control selectivity: a hydrogen bond between the enolate oxygen and the catalyst hydroxyl group, and two π -system stacking interactions between the four aromatic rings. Perhaps as a consequence of the complex

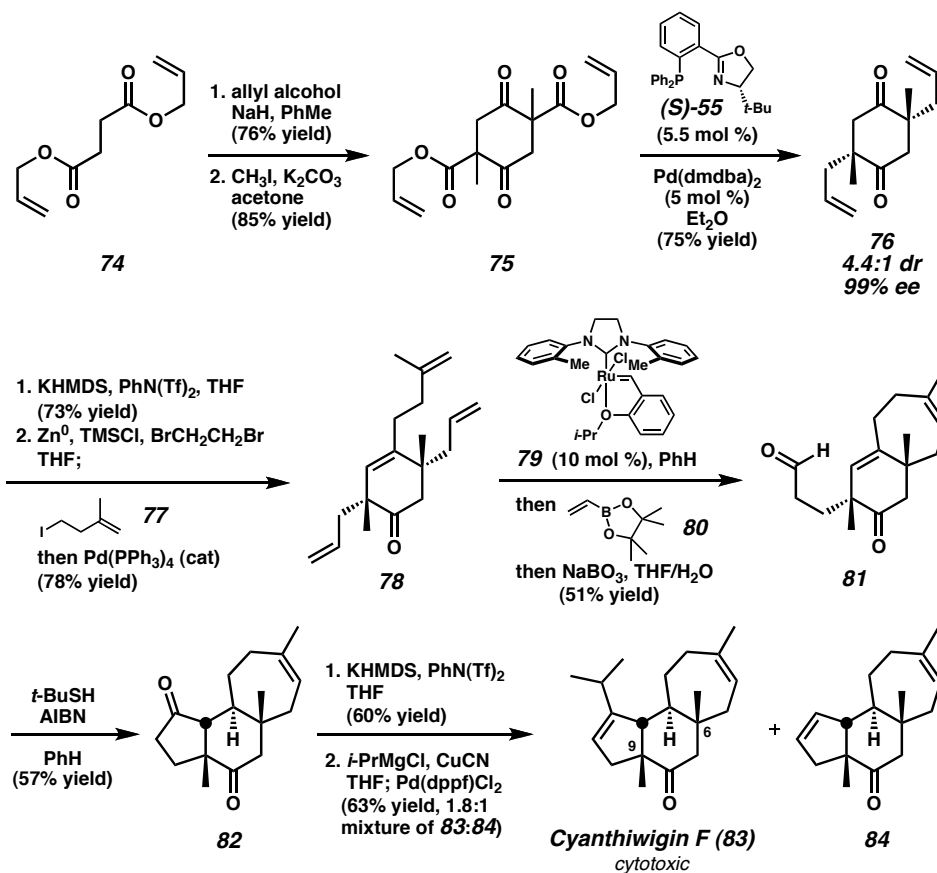
mechanism, the range of substrates for enolate alkylation is limited, and other solutions to this problem are still needed. However, these initial results have led to several related catalytic enantioselective reactions using cinchoninium salts or related organic ammonium complexes as catalysts.⁶⁴ The discovery of these useful catalysts has provided not only an alternative to related transformations using metal catalysts but also a means of accessing chiral environments that are simply not possible with metal-based catalysts. Moreover, eliminating metal waste materials is attractive from an industrial and environmental standpoint. Ultimately, the studies directed toward an enantioselective synthesis of indacrinone demonstrate the versatility of privileged catalysts developed for the synthesis of target molecules for a range of other applications.

1.3.7 *Pd*-CATALYZED ENOLATE ALKYLATION — CYANTHIWIGIN F

A recent case of enantioselective enolate alkylation is the synthesis of cyanthiwigin F (**83**, Scheme 1.3.7), a cytotoxic natural product from a sea sponge. The cyanthiwigin family is composed of more than 30 diterpenoids, most of which bear two quaternary stereocenters, at C(6) and C(9), and a syn relationship of the methyl groups in the central ring. These core stereochemical elements are a complicating factor for a convergent strategy that might seek to couple the five- and seven-membered ring portions and subsequently form the six-membered ring. To avoid this difficulty, Enquist and Stoltz chose instead to address these two central stereocenters at an early stage and append the five- and seven-membered rings to the assembled cyclohexane.⁶⁵ Accordingly, a synthetic strategy was devised that involved a one-pot double-enantioselective enolate alkylation reaction to form both quaternary stereocenters simultaneously. Although such

enantioselective alkylations have proved difficult, recent studies have identified palladium catalysts that might provide a solution to this problem and enable the synthesis of a variety of targets containing quaternary carbon stereocenters, including the cyanthiwigins.⁶⁶

Scheme 1.3.7. Pd-catalyzed enolate alkylations toward cyanthiwigin F



The implementation of this retrosynthetic strategy began with a Claisen–Dieckmann sequence that converted diallyl succinate (**74**, Scheme 1.3.7) to bis(β-ketoester) **75** as a 1:1 mixture of racemic and meso diastereomers. On exposure to the catalyst derived from Pd(dmdba)₂ and phosphinooxazoline ligand **(S)-55**,⁶⁶ each stereoisomer of **75** was

transformed to bis(allylated) ketone **76** with 75% yield and 99% enantiomeric excess as a 4.4:1 mixture of diastereomers. With both quaternary centers in place, elaboration of this stereochemically rich core structure to the natural product was achieved in six further steps. Enol triflate formation and Negishi coupling (**76** + **77** → **78**) preceded a tandem ring-closing metathesis–cross-metathesis sequence with Grubbs' ruthenium catalyst **79**.⁶⁷ Aldehyde–alkene radical cyclization generated the final ring of the cyanthiwigin core (**81** → **82**), and enol triflate formation and palladium-catalyzed cross-coupling formed (–)-cyanthiwigin F (**83**), together with reduction product **84**. Choosing to confront the difficult stereochemical elements of the cyanthiwigin structure at an early stage led to a direct synthetic route proceeding in nine steps from diallyl succinate. This strategy was made possible by the intriguing reaction mechanism of the enantioselective decarboxylative allylation, in which all three stereoisomers of bis(β-ketoester) **75** were converted to a specific stereoisomer of product (**76**) with high selectivity, through a stereoablative process.⁶⁸ In addition, of the nine steps required for the synthesis, seven form C–C bonds, and four form *multiple* C–C bonds. Directly addressing the carbon framework of the target molecule and the stereochemical challenges embedded within ultimately led to an efficient synthetic sequence for this important molecule.

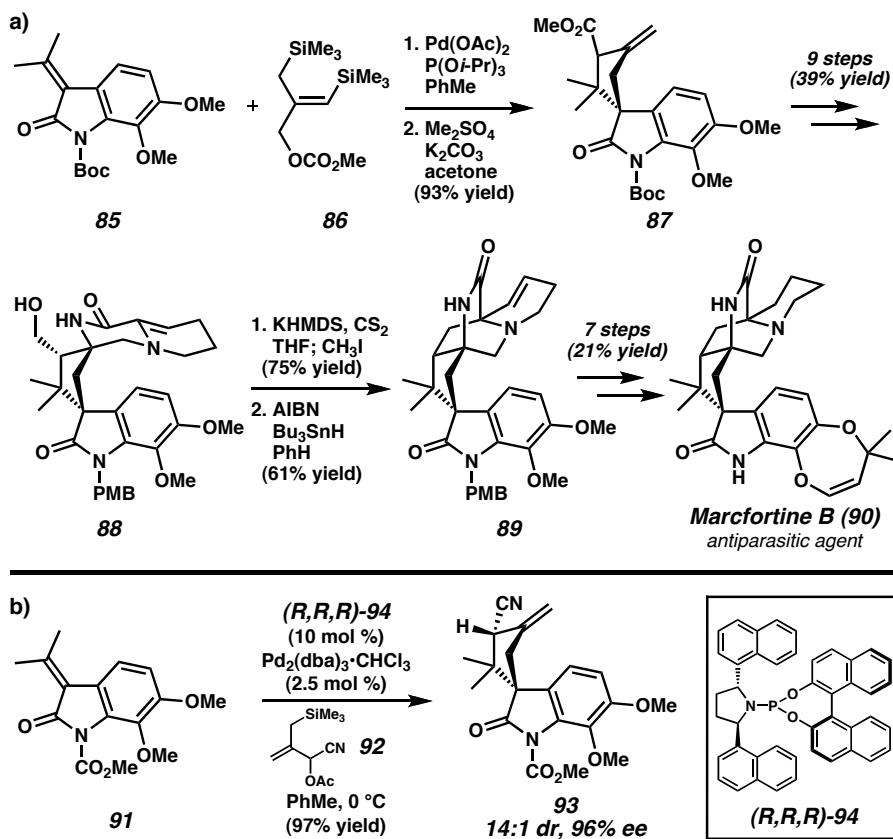
Recently, the proposed chiral palladium enolate was shown to be intercepted by allyl or proton electrophiles.^{66,69} Although the synthesis of cyanthiwigin F demonstrates the versatility of allyl moieties for further derivatization, the direct use of alternative electrophiles would provide a more general and direct method for transition metal-mediated enolate functionalization.⁷⁰

1.3.8 TRIMETHYLENEMETHANE CYCLIZATIONS — MARCFORTINE B

Of the many fundamental approaches to the formation of five-membered rings from acyclic precursors, the [3 + 2] cycloaddition is among the most convergent strategies. A useful method of achieving such a cyclization is via a trimethylenemethane (TMM) intermediate.⁷¹ This interesting non-Kekulé molecule was first prepared and studied through photolytic decomposition of a cyclic diazene precursor. However, the free diyl is prone to several undesired reaction pathways and does not lend itself to asymmetric catalysis. Despite this, intramolecular diyl-trapping reactions are valuable methods of cyclopentane formation.⁷¹ Recognizing the synthetic utility of TMM, Trost and co-workers developed an array of 2-(trimethylsilyl)-2-propenyl acetate reagents that generate a metal•TMM complex when exposed to a palladium catalyst.⁷² A recent application of this transformation in total synthesis is the approach to marcfortine B (**90**, Scheme 1.3.8a), a member of a family of antiparasitic agents.⁷³ The strategy used sought to forge the [2.2.2]bicycle via an intramolecular radical cyclization and install the spiro all-carbon quaternary stereocenter by the cycloaddition of oxindole **85** with TMM precursor **86**. In the event, an excellent yield was observed for the annulation reaction yielding spirooxindole **87** as a 1:1 mixture of diastereomers. Over the course of nine additional steps, spirocycle **87** was transformed into amide **88**. Preparation of the xanthate derivative of alcohol **88** allowed radical cyclization, generating the challenging [2.2.2]bicycle **89**. Seven further steps produced (±)-marcfortine B (**90**).

Scheme 1.3.8. a) Pd-catalyzed TMM-[3 + 2]-cycloaddition toward marcfortine B.

b) Enantioselective TMM-cyclization



Although this strategy demonstrated several intriguing ring-forming reactions, an asymmetric synthesis of **90** would require an enantioselective variant of the key TMM-[3 + 2] cycloaddition, a goal that has remained elusive.⁷⁴ The first asymmetric palladium-catalyzed [3 + 2] cycloaddition with various bis(phosphine) ligands was reported by Ito and co-workers,⁷⁵ but with only moderate enantiomeric excess (up to 78%) and diastereomeric ratio (up to 4:1 trans:cis). Thereafter, Trost and co-workers explored bulky monodentate phosphoramidite ligands (e.g., (*R,R,R*)-**94**, Scheme 1.3.8b) for the transformation and observed very high enantioselectivity for the first time.⁷⁶ Of particular interest is the enantioselective addition of substituted TMM reagents to

functionalized oxindole derivatives.^{76b} The use of oxindole **91** and TMM-precursor **92** in the palladium-catalyzed cyclization with ligand (*R,R,R*)-**94** yielded spirooxindole **93** with 14:1 diastereomeric ratio and 96% enantiomeric excess for the major diastereomer. Although a completed asymmetric synthesis of marcfortine B (**90**) from intermediate **93** has not been reported, many of the key functional groups are in place and the challenging spiroquaternary stereocenter has been installed (cf. **87** and **93**). The development of this valuable asymmetric transformation highlights the ongoing efforts to devise new and useful techniques for the construction of important molecules.

1.4 OUTLOOK

The representative synthetic efforts presented here demonstrate the crucial interplay between target-directed synthesis and the development of novel reaction methods. Although many useful asymmetric technologies are currently available, the specific challenges posed by important natural products and pharmaceutical compounds highlight deficiencies in the current technology. Envisaging strategies to construct these relevant molecules through means beyond the current arsenal of enantioselective transformations will aid the evolution of both synthetic planning and reaction development. The symbiotic relationship between total synthesis and method development can continue to expand the understanding of synthetic strategy and catalysis on both fundamental and practical levels.

Despite the substantial advances that have been made so far, significant challenges remain for both multistep synthesis and catalysis. In addition to improvements to efficiency and selectivity, better reactivity and handling stability are constantly required

to implement and improve industrial processes for existing methods. Exceptionally reliable methods will aid in the discovery of new biologically active compounds by using high-throughput combinatorial screening techniques that are well established in the pharmaceutical industry, although these techniques are limited by the number of readily accessible chiral building blocks. Existing methods may be improved by identifying systems with better functional-group tolerances that might obviate the need for protecting and masking groups. Similarly, known privileged chiral frameworks may be modified to control chiral space more effectively for especially challenging transformations, a technique conspicuously successful for Trost's TMM cyclizations (see subsection 1.3.8).

Overall, creative solutions are required to address specific organic transformations that remain significant impediments to efficient syntheses, namely forming multiple stereocenters and rings, forming multiple C–C bonds, generating vicinal quaternary stereocenters, and achieving C–H and C–C functionalization reactions. Cyclic structures often present particular challenges owing to the unique strain and steric elements imparted by their connectivity. As a result, many highly strained or complex polycyclic structures are daunting targets for synthesis. Finally, the discovery of new natural products will undoubtedly result in new challenges for synthetic chemistry and catalysis. In this thesis, examples of the development of useful enantioselective transformations for the synthesis of natural products will be presented. These reactions were initially conceived as solutions to synthetic problems in the context of total synthesis efforts and have led to various derivative applications and methodologies with broad utility.

1.5 NOTES AND REFERENCES

- (1) Corey, E. J.; Cheng, X.-M. *The Logic of Chemical Synthesis*; Wiley: New York, 1995; pp 1–91.
- (2) For reviews, see: (a) *Comprehensive Asymmetric Catalysis, Vol. I–III*; Jacobsen, E. N., Pfaltz, A., Yamamoto, H., Eds.; Springer-Verlag: Berlin, 2000. (b) *Comprehensive Asymmetric Catalysis, Supplement 1 & 2*; Jacobsen, E. N., Pfaltz, A., Yamamoto, H., Eds.; Springer-Verlag: Berlin, 2004. (c) Hoveyda, A. H. Asymmetric Catalysis in Target-Oriented Synthesis. In *Stimulating Concepts in Chemistry*; Vögtle, F., Stoddart, J. F., Shibasaki, M., Eds.; Wiley-VCH: Weinheim, 2000; pp 145–160. (d) Trost, B. M. *Proc. Natl. Acad. Sci. U.S.A.* **2004**, *101*, 5348–5355. (e) Taylor, M. S.; Jacobsen, E. N. *Proc. Natl. Acad. Sci. U.S.A.* **2004**, *101*, 5368–5373.
- (3) Diels, O.; Alder, K. *Justus Liebigs Ann. Chem.* **1928**, *460*, 98–122.
- (4) Stork, G.; van Tamalen, E. E.; Friedman, L. J.; Burgstahler, A. W. *J. Am. Chem. Soc.* **1951**, *73*, 4501.
- (5) Woodward, R. B.; Bader, F. E.; Bickel, H.; Frey, A. J.; Kierstead, R. W. *J. Am. Chem. Soc.* **1956**, *78*, 2023–2025.
- (6) Yates, P.; Eaton, P. *J. Am. Chem. Soc.* **1960**, *82*, 4436–4437.
- (7) Hashimoto, S.-i.; Komeshima, N.; Koga, K. *J. Chem. Soc., Chem. Commun.* **1979**, 437–438.
- (8) For examples, see: (a) Hayashi, Y. Catalytic Asymmetric Diels–Alder Reactions. In *Cycloaddition Reactions in Organic Synthesis*; Kobayashi, S., Jørgensen, K.

- A., Eds.; Wiley-VCH: Weinheim, 2002; pp 5–55. (b) Corey, E. J. *Angew. Chem., Int. Ed.* **2002**, *41*, 1650–1667. (c) Nicolaou, K. C.; Snyder, S. A.; Montagnon, T.; Vassilikogiannakis, G. *Angew. Chem., Int. Ed.* **2002**, *41*, 1668–1698.
- (9) Corey, E. J.; Andersen, N. H.; Carlson, R. M.; Paust, J.; Vedejs, E.; Vlattas, I.; Winter, R. E. K. *J. Am. Chem. Soc.* **1968**, *90*, 3245–3247.
- (10) Corey, E. J.; Bakshi, R. K.; Shibata, S.; Chen, C.-P.; Singh, V. K. *J. Am. Chem. Soc.* **1987**, *109*, 7925–7926.
- (11) Corey, E. J.; Helal, C. J. *Angew. Chem., Int. Ed.* **1998**, *37*, 1986–2012.
- (12) Yoon, T. P.; Jacobsen, E. N. *Science* **2003**, *229*, 1691–1693.
- (13) Nájera, C.; Sansano, J. M. *Chem. Rev.* **2007**, *107*, 4584–4671.
- (14) Senanayake, C. H.; Jacobsen, E. N. Chiral (Salen)Mn(III) Complexes in Asymmetric Epoxidations: Practical Synthesis of *cis*-Aminoindanol and Its Application to Enantiopure Drug Synthesis. In *Process Chemistry in the Pharmaceutical Industry*; Gadamasetti, K. G., Ed.; Marcel Dekker, New York, 1999; pp 347–368.
- (15) Akutagawa, S.; Tani, K. Asymmetric Isomerization of Allylamines. In *Catalytic Asymmetric Synthesis*; Ojima, I., Ed.; Wiley-VCH: New York, 2002; pp 145–161.
- (16) For reviews concerning industrial-scale synthesis, see: (a) Nugent, W. A.; RajanBabu, T. V.; Burk, M. J. *Science* **2002**, *259*, 479–483. (b) Farina, V.; Reeves, J. T.; Senanayake, C. H.; Song, J. J. *Chem. Rev.* **2006**, *106*, 2734–2793. (c) *Asymmetric Catalysis on Industrial Scale: Challenges, Approaches and Solutions*; Blaser, H.-U., Schmidt, E., Eds.; Wiley-VCH: Weinheim, 2004.

- (17) (a) Eder, U.; Sauer, G.; Wiechert, R. *Angew. Chem., Int. Ed. Engl.* **1971**, *10*, 496–497. (b) Hajos, Z. G.; Parrish, D. R. *J. Org. Chem.* **1973**, *38*, 3244–3249. (c) Hajos, Z. G.; Parrish, D. R. *J. Org. Chem.* **1974**, *39*, 1615–1621.
- (18) Evans, D. A.; Fitch, D. M.; Smith, T. E.; Cee, V. J. *J. Am. Chem. Soc.* **2000**, *122*, 10033–10046.
- (19) Palomo, C., Oiarbide, M., García, J. M. *Chem.—Eur. J.* **2002**, *8*, 37–44.
- (20) (a) Ma, J.-A. *Angew. Chem., Int. Ed.* **2003**, *42*, 4290–4299. (b) *Enantioselective Synthesis of β -Amino Acids*; Juaristi, E., Soloshonok, V. A., Eds; Wiley & Son: Hoboken, 2005.
- (21) Vineyard, B. D.; Knowles, W. S.; Sabacky, M. J.; Bachman, G. L.; Weinkauff, D. *J. J. Am. Chem. Soc.* **1977**, *99*, 5946–5952.
- (22) (a) Lubell, W. D.; Kitamura, M.; Noyori, R. *Tetrahedron: Asymmetry* **1991**, *2*, 543–554. (b) Drexler, H.-J.; You, J.; Zhang, S.; Fischer, C.; Baumann, W.; Spannenberg, A.; Heller, D. *Org. Process Res. Dev.* **2003**, *7*, 355–361.
- (23) Drucker, D.; Easley, C.; Kirkpatrick, P. *Nat. Rev. Drug Discovery* **2007**, *6*, 109–110.
- (24) Hsiao, Y.; Rivera, N. R.; Rosner, T.; Krska, S. W.; Njolito, E.; Wang, F.; Sun, Y.; Armstrong, J. D., III; Grabowski, E. J. J.; Tillyer, R. D.; Spindler, F.; Malan, C. *J. Am. Chem. Soc.* **2004**, *126*, 9918–9919.
- (25) Shultz, C. S.; Krska, S. W. *Acc. Chem Res.* **2007**, *40*, 1320–1326.
- (26) Xu, F.; Armstrong, J. D., III; Zhou, G. X.; Simmons, B.; Hughes, D.; Ge, Z.; Grabowski, E. J. *J. Am. Chem. Soc.* **2004**, *126*, 13002–13009.

- (27) Clausen, A. M.; Dziadul, B.; Cappuccio, K. L.; Kaba, M.; Starbuck, C.; Hsiao, Y.; Dowling, T. M. *Org. Process Res. Dev.* **2006**, *10*, 723–726.
- (28) Noyori, R.; Kitamura, M.; Ohkuma, T. *Proc. Natl. Acad. Sci. U.S.A.* **2004**, *101*, 5356–5362.
- (29) (a) *Handbook of Organopalladium Chemistry for Organic Synthesis*; Negishi, E.-i., de Meijere, A., Eds.; Wiley & Sons: New York, 2002; Vol 1. (b) *Metal-Catalyzed Cross-Coupling Reactions*; de Meijere, A., Diederich, F., Eds.; Wiley-VCH: Weinheim, 2004; Vols. 1 and 2.
- (30) (a) Luh, T.-Y.; Leung, M.-k.; Wong, K.-T. *Chem. Rev.* **2000**, *100*, 3187–3204. (b) Frisch, A. C.; Beller, M. *Angew. Chem., Int. Ed.* **2005**, *44*, 674–688.
- (31) Netherton, M. R.; Fu, G. C. Palladium-Catalyzed Cross-Coupling Reactions of Unactivated Alkyl Electrophiles with Organometallic Compounds. In *Topics in Organometallic Chemistry: Palladium in Organic Synthesis*; Tsuji, J., Ed.; Springer: New York, 2005; pp 85–108.
- (32) (a) Kiso, Y.; Tamao, K.; Miyake, N.; Yamamoto, K.; Kumada, M. *Tetrahedron Lett.* **1974**, *15*, 3–6. (b) Hayashi, T.; Konishi, M.; Fukushima, M.; Mise, T.; Kagotani, M.; Tajika, M.; Kumada, M. *J. Am. Chem. Soc.* **1982**, *104*, 180–186.
- (33) (a) Fischer, C.; Fu, G. C. *J. Am. Chem. Soc.* **2005**, *127*, 4594–4595. (b) Arp, F. O.; Fu, G. C. *J. Am. Chem. Soc.* **2005**, *127*, 10482–10483.
- (34) Zhou, J.; Fu, G. C. *J. Am. Chem. Soc.* **2003**, *125*, 14726–14727.
- (35) Son, S.; Fu, G. C. *J. Am. Chem. Soc.* **2008**, *130*, 2756–2757.

- (36) Suh, Y.-G.; Kim, S.-A.; Jung, J.-K.; Shin, D.-Y.; Min, K.-H.; Koo, B.-A.; Kim, H.-S. *Angew. Chem., Int. Ed.* **1999**, *38*, 3545–3547.
- (37) Douglas, C. J.; Overman, L. E. *Proc. Natl. Acad. Sci. U.S.A.* **2004**, *101*, 5363–5367.
- (38) Heck, R. F. *Acc. Chem. Res.* **1979**, *12*, 146–151.
- (39) Overman, L. E. *Pure Appl. Chem.* **1994**, *66*, 1423–11430.
- (40) Sato, Y.; Sodeoka, M.; Shibasaki, M. *J. Org. Chem.* **1989**, *54*, 4738–4739.
- (41) Carpenter, N. E.; Kucera, D. J.; Overman, L. E. *J. Org. Chem.* **1989**, *54*, 5846–5848.
- (42) Dounay, A. B.; Overman, L. E. *Chem. Rev.* **2003**, *103*, 2945–2963.
- (43) *Indoles. Part Four. The Monoterpenoid Indole Alkaloids*; Saxton, J. E., Ed.; Wiley & Sons: New York, 1983.
- (44) Dounay, A. B.; Overman, L. E.; Wroblewski, A. D. *J. Am. Chem. Soc.* **2005**, *127*, 10186–10187.
- (45) Dounay, A. B.; Humphreys, P. G.; Overman, L. E.; Wroblewski, A. D. *J. Am. Chem. Soc.* **2008**, *130*, 5368–5377.
- (46) Kirmansjah, L.; Fu, G. C. *J. Am. Chem. Soc.* **2008**, *129*, 11340–11341.
- (47) (a) Sundberg, R. J. *Indoles*; Academic Press: San Diego, 1996. (b) Humphrey, G. R.; Kuethe, J. T. *Chem. Rev.* **2006**, *106*, 2875–2911.

- (48) Jensen, K. B.; Thorhauge, J.; Hazell, R. G.; Jørgensen, K. A. *Angew. Chem., Int. Ed.* **2001**, *40*, 160–163.
- (49) Paras, N. A.; MacMillan, D. W. C. *J. Am. Chem. Soc.* **2001**, *123*, 4370–4371.
- (50) (a) Lelais, G.; MacMillan, D. W. C. *Aldrichimica Acta* **2006**, *39*, 79–87.
(b) Erkkilä, A.; Majander, I.; Pihko, P. M. *Chem. Rev.* **2007**, *107*, 5416–5470.
- (51) Austin, J. F.; MacMillan, D. W. C. *J. Am. Chem. Soc.* **2002**, *124*, 1172–1173.
- (52) Hino, T.; Nakagawa, M. Chemistry and Reactions of Cyclic Tautomers of Tryptamines and Tryptophans. In *The Alkaloids*; Brossi, A., Ed.; Academic Press: San Diego, 1988; Vol. 34, pp 1–75.
- (53) (a) Overman, L. E.; Paone, D. V.; Stearns, B. A. *J. Am. Chem. Soc.* **1999**, *121*, 7702–7703. (b) Overman, L. E.; Larrow, J. F.; Stearns, B. A.; Vance, J. M. *Angew. Chem., Int. Ed.* **2000**, *39*, 213–215. (c) Depew, K. M.; Marsden, S. P.; Zatorska, D.; Zatorski, A.; Bornmann, W. G.; Danishefsky, S. J. *J. Am. Chem. Soc.* **1999**, *121*, 11953–11963.
- (54) Austin, J. F.; Kim, S.-G.; Sinz, C. J.; Xiao, W.-J.; MacMillan, D. W. C. *Proc. Natl. Acad. Sci. U.S.A.* **2004**, *101*, 5482–5487.
- (55) Pictet, A.; Spengler, T. *Ber. Dtsch. Chem. Ges.* **1911**, *44*, 2030–2036.
- (56) Cox, E. D.; Cook, J. M. *Chem. Rev.* **1995**, *95*, 1797–1842.
- (57) Allin, S. M.; Gaskell, S. N.; Elsegood, M. R. J.; Martin, W. P. *Tetrahedron Lett.* **2007**, *48*, 5669–5671.
- (58) Taylor, M. S.; Jacobsen, E. N. *J. Am. Chem. Soc.* **2004**, *126*, 10558–10559.

- (59) (a) Seayad, J.; Seayad, A. M.; List, B. *J. Am. Chem. Soc.* **2006**, *128*, 1086–1087.
(b) Wanner, M. J.; van der Haas, R. N. S.; de Cuba, K. R.; van Maarseveen, J. H.; Hiemstra, H. *Angew. Chem., Int. Ed.* **2007**, *46*, 7485–7487.
- (60) (a) Raheem, I. T.; Thiara, P. S.; Peterson, E. A.; Jacobsen, E. N. *J. Am. Chem. Soc.* **2007**, *129*, 13404–13405. (b) Raheem, I. T.; Thiara, P. S.; Jacobsen, E. N. *Org. Lett.* **2008**, *10*, 1577–1580.
- (61) Reisman, S. E.; Doyle, A. G.; Jacobsen, E. N. *J. Am. Chem. Soc.* **2008**, *130*, 7198–7199.
- (62) Dolling, U.-H.; Davis, P.; Grabowski, E. J. J. *J. Am. Chem. Soc.* **1984**, *106*, 446–447.
- (63) Hughes, D. L.; Dolling, U.-H.; Ryan, K. M.; Schoenewaldt, E. F.; Grabowski, E. J. J. *J. Org. Chem.* **1987**, *52*, 4745–4752.
- (64) *Asymmetric Phase Transfer Catalysis*; Maruoka, K., Ed.; Wiley-VCH: Weinheim, 2008.
- (65) Enquist, J. A., Jr.; Stoltz, B. M. *Nature* **2008**, *453*, 1228–1231.
- (66) (a) Behenna, D. C.; Stoltz, B. M. *J. Am. Chem. Soc.* **2004**, *126*, 15044–15045.
(b) Mohr, J. T.; Behenna, D. C.; Harned, A. M.; Stoltz, B. M. *Angew. Chem., Int. Ed.* **2005**, *44*, 6924–6927. (c) Mohr, J. T.; Stoltz, B. M. *Chem.–Asian J.* **2007**, *2*, 1476–1491.
- (67) Stewart, I. C.; Ung, T.; Pletnev, A. A.; Berlin, J. M.; Grubbs, R. H.; Schrodi, Y. *Org. Lett.* **2007**, *9*, 1589–1592.
- (68) Mohr, J. T.; Ebner, D. C.; Stoltz, B. M. *Org. Biomol. Chem.* **2007**, *5*, 3571–3576.

- (69) (a) Mohr, J. T.; Nishimata, T.; Behenna, D. C.; Stoltz, B. M. *J. Am. Chem. Soc.* **2006**, *128*, 11348–11349. (b) Marinescu, S. C.; Nishimata, T.; Mohr, J. T.; Stoltz, B. M. *Org. Lett.* **2008**, *10*, 1039–1042.
- (70) Further studies on trapping of the enolate with other carbon-based electrophiles have been successful. Streuff, J.; White, D. E.; Virgil, S. C.; Stoltz, B. M. *Nat. Chem.* **2010**, *2*, 192–196.
- (71) Yamago, S.; Nakamura, E. *Org. React.* **2002**, *61*, 1–217.
- (72) (a) Trost, B. M.; Chan, D. M. T. *J. Am. Chem. Soc.* **1979**, *101*, 6429–6432. (b) Trost, B. M.; Chan, D. M. T. *J. Am. Chem. Soc.* **1979**, *101*, 6432–6433.
- (73) Trost, B. M.; Cramer, N.; Bernsmann, H. *J. Am. Chem. Soc.* **2007**, *129*, 3086–3087.
- (74) Le Marquand, P.; Tam, W. *Angew. Chem., Int. Ed.* **2008**, *47*, 2926–2928.
- (75) Yamamoto, A.; Ito, Y.; Hayashi, T. *Tetrahedron Lett.* **1989**, *30*, 375–378.
- (76) (a) Trost, B. M.; Stambuli, J. P.; Silverman, S. M.; Schwörer, W. *J. Am. Chem. Soc.* **2006**, *128*, 13328–13329. (b) Trost, B. M.; Cramer, N.; Silverman, S. M. *J. Am. Chem. Soc.* **2007**, *129*, 12396–12397. (c) Trost, B. M.; Silverman, S. M.; Stambuli, J. P. *J. Am. Chem. Soc.* **2007**, *129*, 12398–12399.

CHAPTER 2

The Variocolin Family of Sesterterpenoids

2.1 INTRODUCTION AND BACKGROUND

The variocolin family of sesterterpenoids has emerged as an intriguing class of biologically relevant natural products. Members of this family possess an array of biological activities including anti-HIV, antihypertensive, and immunosuppressant properties. Structurally, the variocolin-type sesterterpenoids are defined by their complex molecular architecture including a central eight-membered ring, a high degree of stereocomplexity, and a low degree of oxidation. Thus, this important class of natural products constitutes a formidable challenge for chemical synthesis.

2.1.1 ISOLATION AND STRUCTURAL ELUCIDATION

Hensens and co-workers at Merck first isolated variocolin (**95**) in 1991 as a bioactive component of the fungi imperfecti *Aspergillus varicolor*.¹ Extensive structural elucidation via 2D NMR spectroscopy and ¹H–¹H coupling constant analysis revealed a sesterterpenoid with a novel tetracyclic ring skeleton possessing the relative

stereochemistry as shown in Figure 2.1.1. The absolute stereochemistry was proposed as *ent*-**95** due to biosynthetic considerations and structural similarity to the ceriferene class of sesterterpenoids (e.g., Flocerol (**96**)), which contains an analogous CD ring system.²

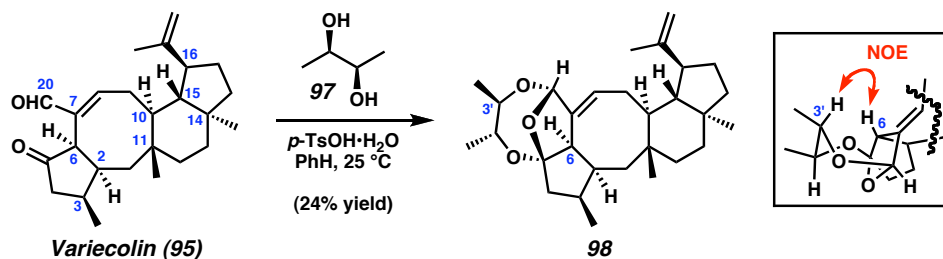
Figure 2.1.1. Proposed structure of variocolin.[†]



Variocolin (**95**) was later identified from the fungus *Emericella aurantiobrunnea* nine years after its first isolation.^{3,4} Although direct confirmation of the absolute configuration was not feasible, Fujimoto and co-workers obtained structural verification through derivatization. Functionalization of **95** with (2*R*,3*R*)-(-)-butane-2,3-diol (**97**) generated chiral polycyclic acetal **98**, which, upon structural analysis, revealed four possible conformations—two derived from each enantiomer of **95**—that could be distinguished by NOESY correlation (Scheme 2.1.1). In a key NOE experiment a sole interaction of 6–9% was observed between H6 and H3', indicating that variocolin possesses a C(6) *R*-configuration, opposite to that of the biosynthetic proposal by Hensens. Butler provided further validation of the relative stereochemistry by X-ray crystal analysis of **95**, although the absolute configuration could not be determined.⁵

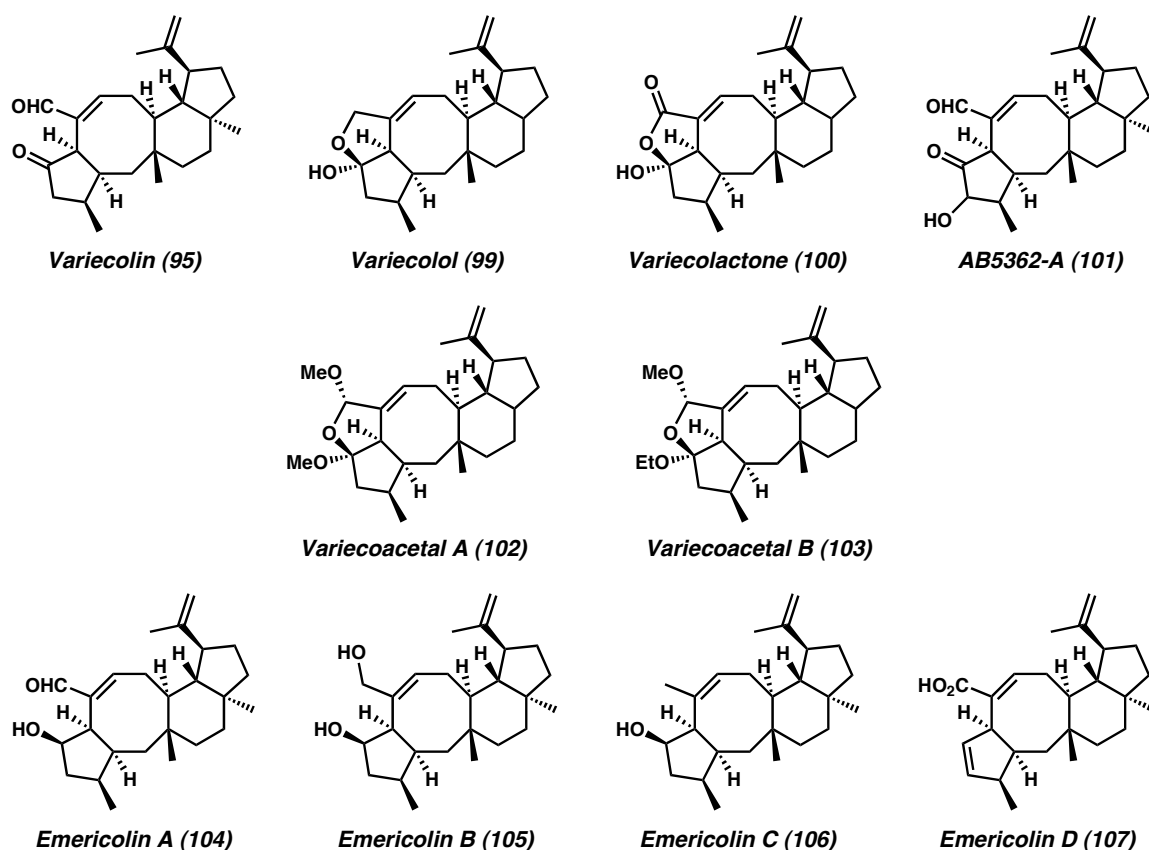
[†] <http://www.ibioo.com/picture/microorganism/2009/6888.html>

Scheme 2.1.1. Assignment of the absolute configuration of variecolin



In subsequent reports, variecolin (**95**) has been isolated from the related fungi *Emericella purpurea*⁶ and *Phoma* sp.⁷ Several variecolin congeners (**99–107**, Figure 2.1.2) have also been identified from the aforementioned fungi extracts^{3,5–8} and share a common ABCD ring system with identical CD rings and subtle oxidation state variations in the A and B rings. In addition to the structural data of **95**, the absolute stereochemistry of variecolol (**99**) has been confirmed by semisynthesis^{3,6b} and the relative stereochemistry of variicolactone (**100**) has been verified by X-ray crystal analysis.^{6b} The structural information and origin of isolation for the members of this family suggests the absolute stereochemistry of all related members is that depicted in Figure 2.1.2, and thus based on the revised assignment of variecolin.

Figure 2.1.2. Variocolin family of sesterterpenoids.

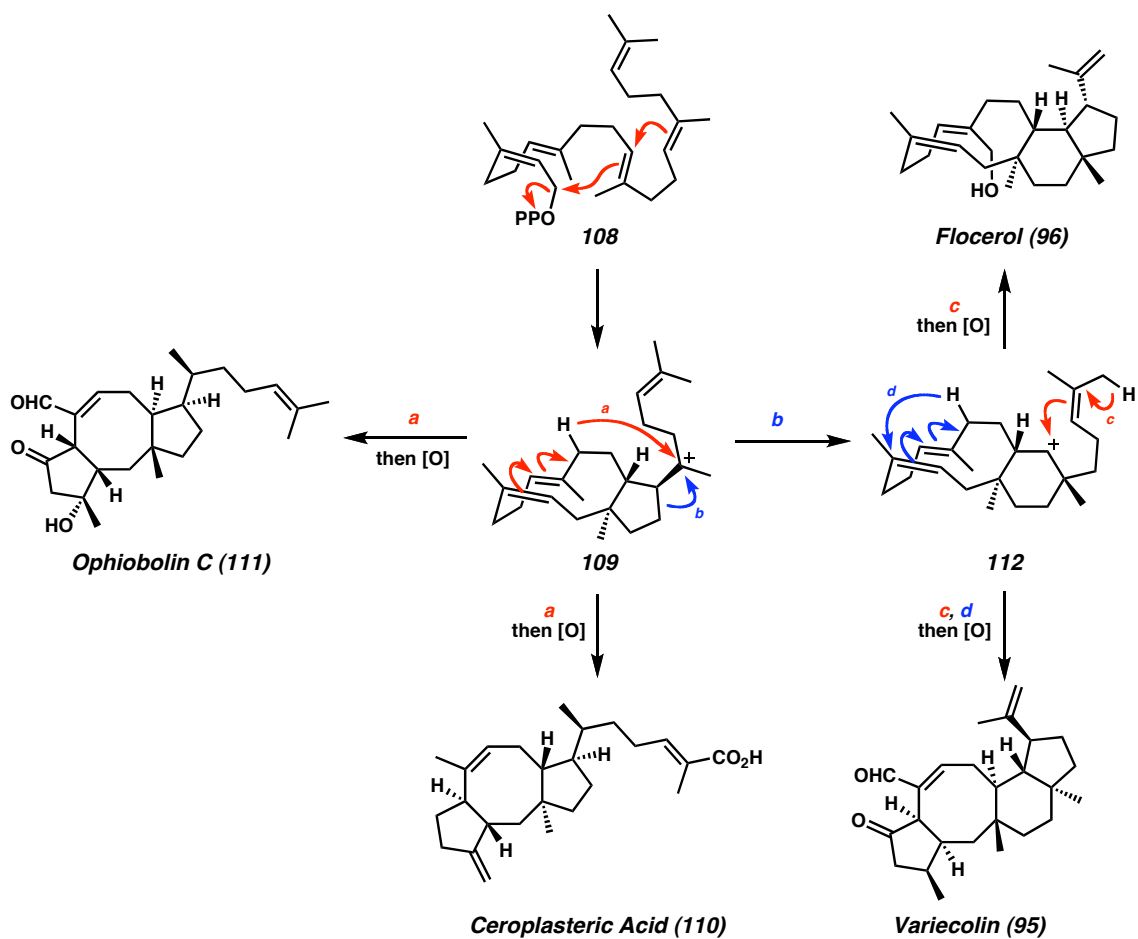


2.1.2 BIOSYNTHETIC PROPOSAL

A detailed study of the variocolin family sesterterpenoid² biosynthesis has not been reported. The authors from the original isolation work surmised that a potential biogenetic link existed between the ophiobolin and ceriferene class of sesterterpenoids, of which variocolin is thought to be descended.¹ Utilizing the reported biosynthetic studies of the ophiobolins^{2a} and triterpenoids⁹ as a premise, Hensens proposed that the variocolin sesterterpenoids arise from geranylarnesyl diphosphate (**108**) of the mevalonate biosynthetic pathway. An initial cyclization cascade with displacement of pyrophosphate generates intermediate **109**, which is perceived as a divergent intermediate (Scheme

2.1.2). One potential fate of this intermediate is cyclization concomitant with a hydride shift (path a) and oxidation to generate the ring system of the ophiobolanes ceroplasteric acid (**110**) or ophiobolin C (**111**). Alternatively, a ring-expanding C–C migration (path b) affords ceriferene intermediate **112** that can undergo a cyclization (path c) to afford the floccerol (**96**), or cyclization followed by a H-shift cyclization (paths c and d) to give variocolin (**95**). This unified scheme effectively links all three classes to this divergent intermediate (**109**).¹⁰

Scheme 2.1.2. Hensens' biosynthetic proposal for variocolin



2.2 BIOLOGICAL ACTIVITY

Variocolin and related sesterterpenes exhibit diverse biological activities. Numerous studies describe the general activity of this family toward a distinct biological target; however, details regarding specificity and mode of action are nonexistent at this time.

2.2.1 ANTIHYPERTENSIVE PROPERTIES

The initial isolation by Hensens indicated variocolin (**95**) as an angiotensin II antagonist that was shown to inhibit ^{125}I -labeled angiotensin II binding in rabbit aortic or bovine adrenal cortical membranes ($\text{IC}_{50} = 3.6 \pm 1 \mu\text{M}$).¹ Angiotensin II is a blood hormone that acts as a vasoconstrictor that contributes to the pathogenesis of hypertension, cardiovascular disease, and affects water and ion homeostasis in the kidneys.¹¹ Angiotensin II antagonists have been shown to be effective toward treating hypertension as well as for the prevention of congestive heart failure. Although variocolin has shown modest antagonist activity, inhibition of carbachol-induced inositol phosphate accumulation indicates a possible nonspecific inhibition of the angiotensin response.¹

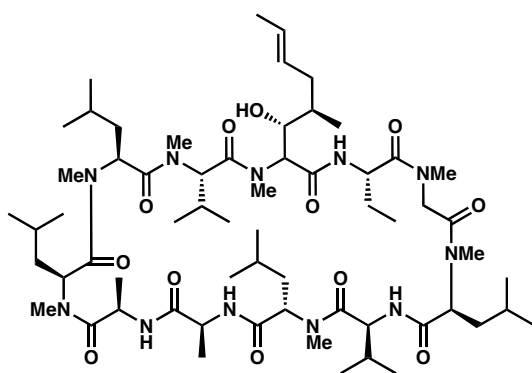
Several years later, a Japanese patent claimed variocolactone (**100**) to be an effective endothelin antagonist that inhibits binding to endothelin A (ET_A , $\text{IC}_{50} = 0.765 \mu\text{M}$) and endothelin B (ET_B , $\text{IC}_{50} = 0.683 \mu\text{M}$) receptors.⁸ Endothelin is a potent vasoconstrictor peptide that has similar physiological effects as the angiotensin II peptide.¹² This finding suggests **100** as a potential therapy for hypertension, cardiovascular diseases, cerebrovascular diseases, renal disease, asthma, and pulmonary hypertension.

2.2.2 IMMUNOMODULATORY PROPERTIES

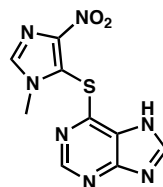
Variocolin and related sesterterpenes have been shown to possess immunosuppressive properties against both humoral (B-cell, LPS-induced) and cell-mediated (T-cell, Con A-induced) proliferations of splenic lymphocytes (Table 2.2.1).³ Of those examined, variocolin was the most active at suppressing the immune responses, suggesting an important role of the ketone and aldehyde functionalities. The activity compared to other classic immunosuppressants shows comparable data up to the strong binder FK506 (**115**).

Table 2.2.1. Immunosuppressant activity of the variocolin sesterterpenes

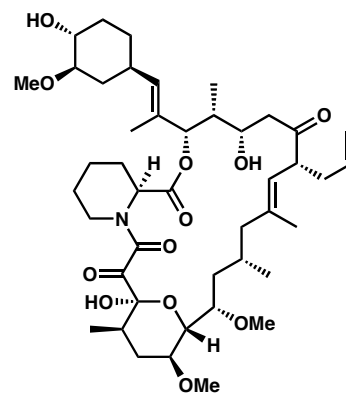
compound	Con A-induced IC ₅₀ (μg/mL)	LPS-induced IC ₅₀ (μg/mL)
Variocolin (95)	0.4	0.1
Variocolactone (100)	8.0	2.5
Variecoacetal A (102)	4.5	1.5
Variecoacetal B (103)	6.5	2.2
Variocolol (99)	1.7	0.6
Azathioprine (114)	2.7	2.7
Cyclosporin A (113)	0.04	0.07
FK506 (115)	1.5 × 10 ⁻⁵	1.6 × 10 ⁻³



Cyclosporin A (**113**)



Azathioprine (**114**)



FK506 (**115**)

2.2.3 CCR5 ANTAGONIST

Butler and co-workers showed in 2004 that variocolin (**95**) and variocolol (**99**) both compete with macrophage inflammatory protein (MIP)-1 α for binding to human CCR5 receptor ($IC_{50} = 9$ and $32 \mu\text{M}$, respectively).⁵ Chemokine receptor CCR5 is a key co-receptor involved in the uptake of HIV-1 into target cells.¹³ As a result, CCR5 plays a major role in the early transmission of HIV-1, the major cause of AIDS. Observation that the inhibition of CCR5 retards viral uptake while maintaining immune competence suggests this receptor as an emerging target for anti-HIV therapeutics. It should be noted that emericolins A–D (**104–107**) showed no activity toward CCR5, further indicating an important role for the ketone and aldehyde functionalities present in **95**.

2.2.4 ANTIBIOTIC AND ANTIFUNGAL PROPERTIES

A 1998 Japanese patent disclosed the potential antibacterial and antifungal properties of variocolin (**95**), variocolactone (**100**), and AB5362-A (**101**).⁷ It was observed that **100** displays 100% antifungal activity at 10 ppm against *Pseudoperonospora cubensis* without damaging a cucumber, highlighting its potential as a herbicide.

2.3 SYNTHETIC STUDIES TOWARD VARIECOLIN

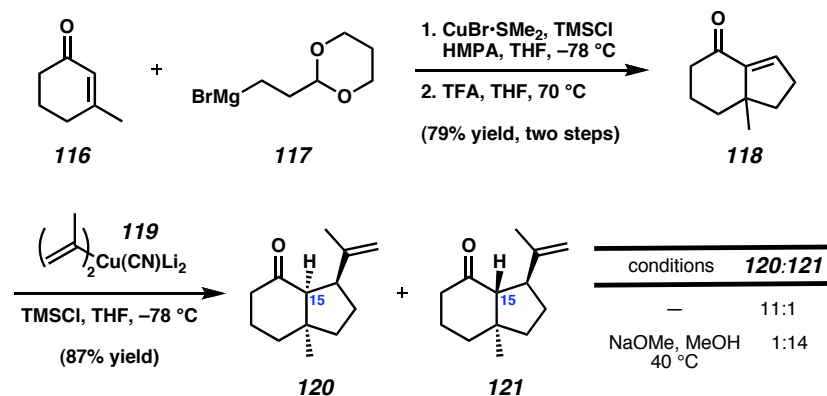
The variocolin family of sesterterpenes has received only modest attention from the synthetic community in the 18 years since the first discovery of variocolin despite their intriguing structure and biological relevance. At the onset of our studies toward variocolin (**95**), two laboratories have disclosed synthetic efforts en route to this

sesterterpenoid. Despite significant progress in this area, these distinct approaches have not yet culminated in the completion of variocolin or any member of this class (Figure 2.1.2).

2.3.1 *PIERS' APPROACH TO THE CD RING SYSTEM*

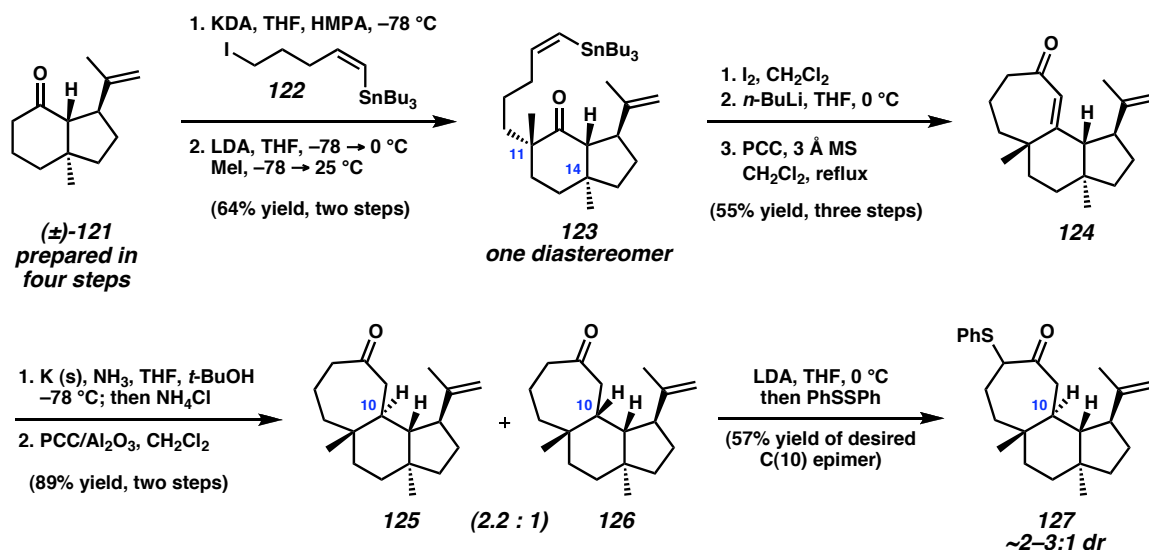
In the first report of a synthetic approach toward variocolin, Piers and Boulet demonstrated their key method for the stereoselective generation of the CD ring system.¹⁴ Starting racemic enone **118** was prepared in two steps from 3-methylcyclohexenone (**116**), followed by a diastereoselective conjugate addition of a higher-order 2-propenyl cuprate to afford a mixture of C(15)¹⁵ epimers **120** and **121** (11:1) in 86% yield (Scheme 2.3.1). An important feature of this transformation is the generation of the relative anti stereochemistry of the all-carbon quaternary stereocenter and the newly installed 2-propenyl group. However, the *cis* stereochemistry of the ring juncture is opposite to that required for variocolin. Thus, a thermodynamic equilibration with NaOMe in methanol facilitated a C(15) epimerization to favor the desired *trans*-fused isomer, **121** (14:1 of **121:120**), the bicyclic CD system of which maps on to **95** as well as several other diterpenoids.¹⁴

Scheme 2.3.1. Piers' stereoselective CD ring preparation



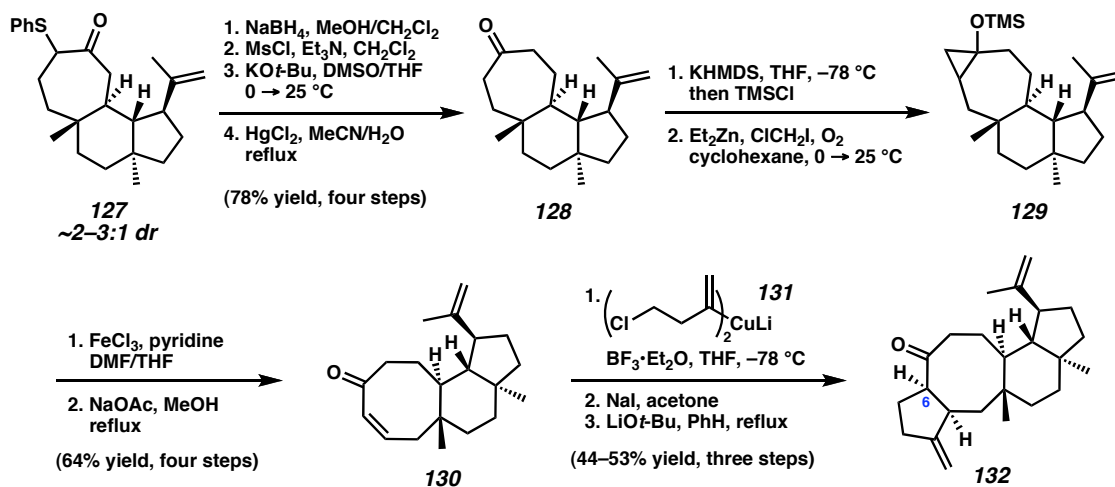
With an effective preparation of this key bicyclic intermediate (**121**), graduate student Shawn Walker explored its utility toward the total synthesis of variecolin.¹⁶ Their devised synthetic strategy employing this intermediate involved the linear, stepwise annulation of the B and A rings on to this key CD ring fragment. Accordingly, sequential alkylation of intermediate (\pm)-**121** provided ketone **123** as a single diastereomer, possessing the correct relative quaternary stereochemistry at C(11) (Scheme 2.3.2). Functional group interconversion to a vinyl iodide, followed by lithium–halogen exchange with carbonyl addition, then a PCC-mediated allylic alcohol transposition with oxidation afforded the annulated tricycle **124**. The stereochemistry at C(10) was achieved via Birch reduction of this cycloheptenone (**124**) using potassium in ammonia, moderately favoring the desired C(10) epimer **125** as a 2.2:1 mixture of inseparable isomers (**125**:**126**). Further transformation via α -functionalization of the carbonyl with diphenyldisulfide afforded separable compounds at the C(10) stereocenter to provide **127** in modest yield.

Scheme 2.3.2. Piers' annulation of the B ring



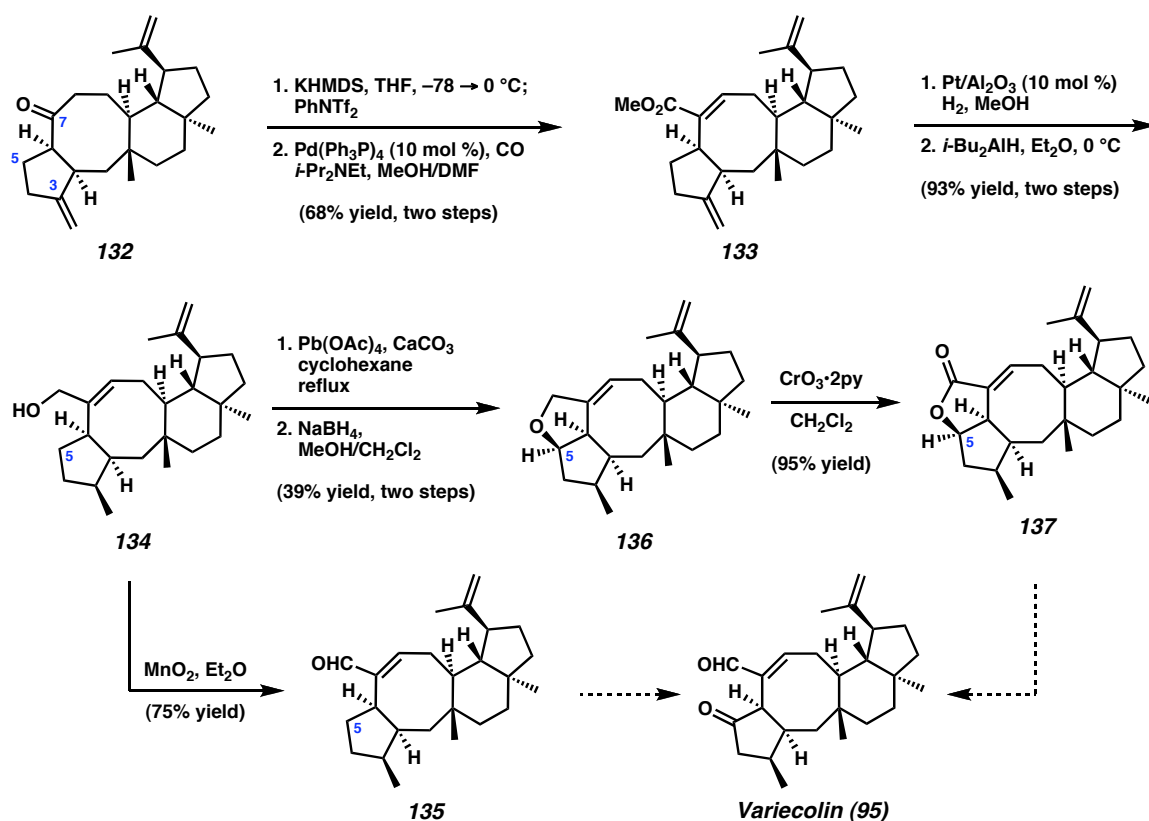
Carbonyl transposition of **127** over four steps provided ketone **128** which was then utilized for a one-carbon ring expansion via a cyclopropanation–cleavage sequence (Scheme 2.3.3). Ketone enolization and cyclopropanation afforded **129**, which upon FeCl_3 -mediated radical cleavage followed by β -chloro elimination completed the B-ring expansion to generate cyclooctenone **130** in 64% yield over four steps. With the BCD carbocyclic skeleton in place, annulation of the final A ring was accomplished utilizing a bifunctional cuprate reagent (**131**), first to achieve the conjugate 1,4-addition, succeeded by an alkylation event (i.e., **130** \rightarrow **132**). The C(6) stereocenter readily epimerized during the final alkylation event and, consequently, modest conversions employing LiOt-Bu were necessary to overcome this difficulty. Importantly, the preparation of tetracycle **132** comprised the complete ABCD ring structure of variocolin.

Scheme 2.3.3. Completion of the ABCD tetracycle via A-ring annulation



The remaining transformations toward completion of variocolin involved the functionalization of the A and B rings. Accordingly, conversion of ketone **132** to an enol triflate and palladium-catalyzed carbonylation generated ester **133** (Scheme 2.3.4). This trisolefin intermediate was then chemo- and stereoselectively hydrogenated at C(3), followed by ester reduction to form (±)-5-deoxymericolin B (**134**). Allylic oxidation using MnO₂ provided (±)-deoxymericolin A (**135**), whereas oxidation using Pb(OAc)₄ afforded (±)-5-deoxyvariocolol (**136**). Further oxidation using Collins reagent gave (±)-5-deoxyvariocolactone (**137**).

Scheme 2.3.4. Piers' end game progress toward completion of variocolin

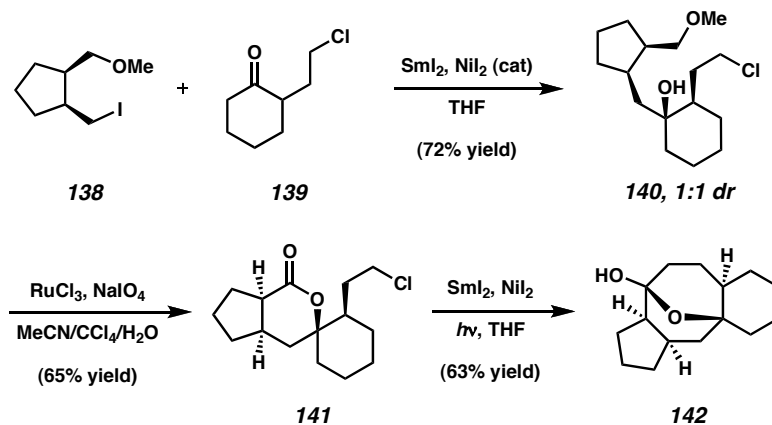


The preparation of highly advanced deoxy analogues of variocolin and related sesterterpenes set the stage for further C(5) oxidation and completion of the targets, although “material constraints” have hindered this progress. Indeed, this synthetic sequence is highly linear, requiring 28 steps for the longest linear sequence. The incorporation of the central eight-membered B ring is tedious, requiring 12 steps to achieve a one-carbon ring expansion. An issue yet to be addressed is the incorporation of asymmetry, which would have to occur at the beginning of the synthesis due to linearity.¹⁷ Nonetheless, Piers' impressive synthetic effort has highlighted various reactivity and selectivity features of this system and enabled the preparation of highly advanced intermediates.

2.3.2 MOLANDER'S APPROACH TO THE B RING

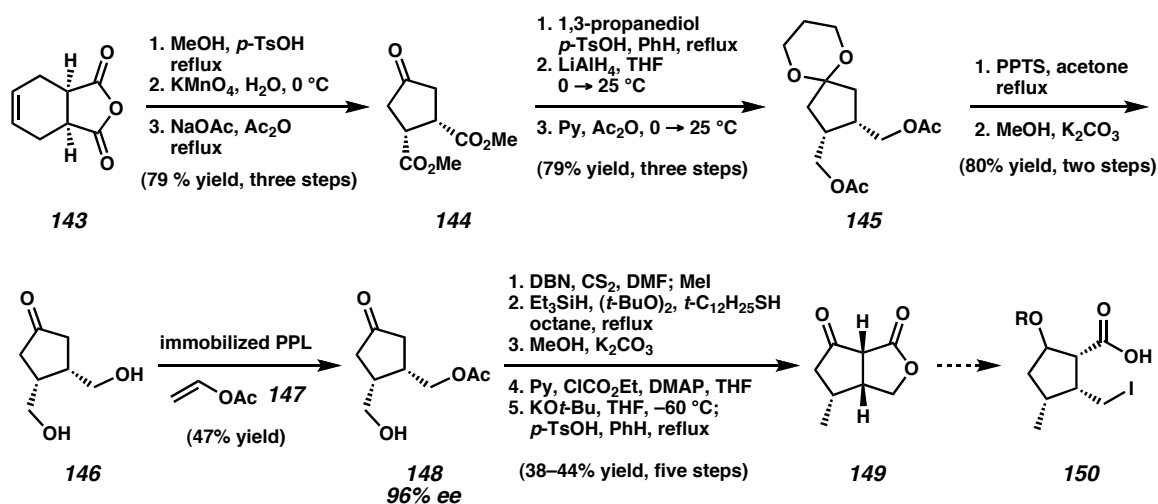
The Molander laboratory disclosed a samarium(II) iodide-promoted annulative approach toward variocolin in 2001.¹⁸ This strategy was derived from previous work in their laboratory delineating SmI_2 -promoted sequential reactions for the rapid and stereoselective construction of medium-sized carbocycles.¹⁹ A model system was devised to rapidly explore a carbonyl addition–nucleophilic acyl substitution reaction en route to the carbocyclic core of variocolin. The samarium(II) iodide-promoted intermolecular Barbier reaction of ketochloride **139** and alkyl iodide **138** furnished chloroalcohol **140** (Scheme 2.3.5). Oxidation of the methyl ether moiety with concomitant lactonization gave spirocyclic lactone **141**, a substrate for the intramolecular nucleophilic acyl substitution reaction studies. The samarium(II) iodide-promoted reductive cyclization occurred under photochemical conditions to generate **142**, which possesses the ABC carbocyclic core of variocolin.

Scheme 2.3.5. Samarium(II) iodide-promoted medium ring synthesis



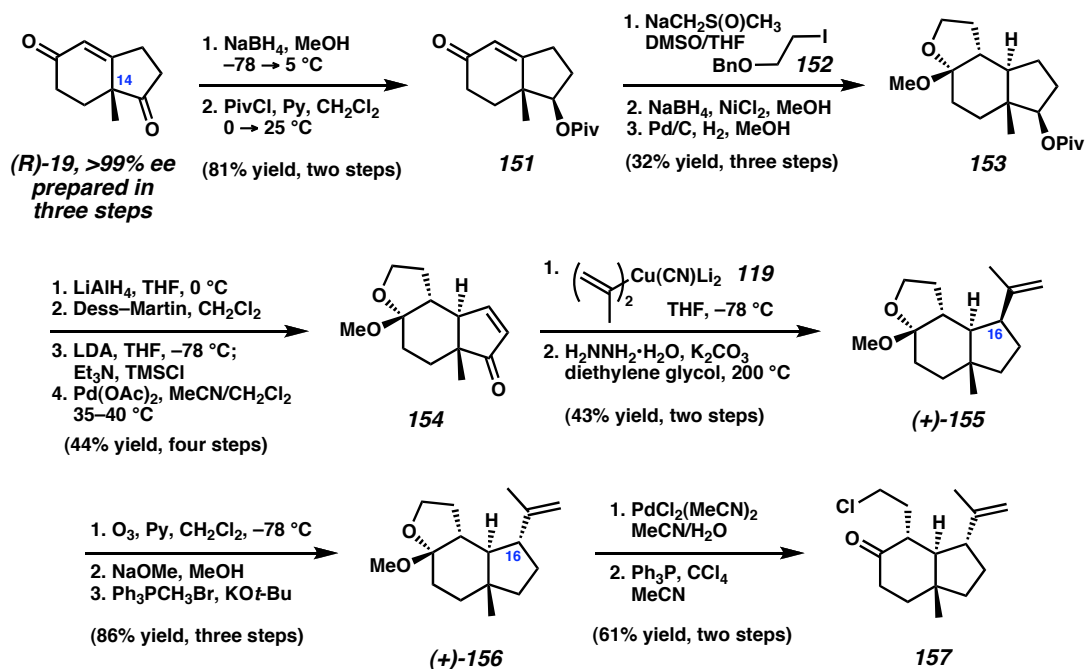
With a viable strategy in hand, Molander and co-workers pursued enantioselective syntheses of suitable A- and CD ring fragments to explore their key sequential samarium-promoted coupling toward *ent*-**95**.²⁰ Accordingly, the A-ring fragment was asymmetrically synthesized from *meso*-diol **146**, which was prepared in eight steps from tetrahydrophthalic anhydride (**143**, Scheme 2.3.6). Acidic methanolysis of **143**, oxidative olefin cleavage and intramolecular Dieckmann cyclization with decarboxylation generated *meso*-cyclopentanone **144**. Ketone protection, ester reduction and exposure to Ac₂O afforded protected *meso*-bisacetate **145**, upon which all protecting groups were cleaved to form *meso*-diol **146** (50% yield over eight steps). Enzymatic desymmetrization via acylation produced monoacetate **148** in 47% yield and 96% ee, which was elaborated to β-ketolactone **149** over five steps. Advancement of this material toward an intermediate analogous to **150**, what would be suitable for the key samarium coupling, was not described.

Scheme 2.3.6. Molander's first-generation synthesis of A-ring fragment



The targeted CD ring fragment was prepared from Hajos–Parrish ketone (*R*)-**19**, which is readily available in >99% ee (Scheme 2.3.7). Stereoselective ketone reduction and protection as a pivalate ester generated **151**. α -Alkylation of this intermediate with iodide **152** was achieved from the thermodynamic enolate of enone **151** using sodium dimsylate, and subsequent stereoselective 1,4-reduction and benzyl cleavage steps provided acetal **153**. This material was advanced to enone **155** in four steps to set the stage for a diastereoselective 2-propenyl cuprate (**119**) addition followed a Wolff–Kishner reduction to afford acetal (+)-**155**, albeit in modest yield with the undesired C(16) stereochemistry.¹⁵ This was rectified with a three-step ozonolysis, epimerization, and Wittig olefination sequence to provide thermodynamic product (+)-**156**. Acetal cleavage and conversion to an alkyl chloride gave desired intermediate **157**. These efforts have demonstrated enantioselective approaches to A-ring fragment **149** and CD ring fragment **157**, although details of the potential samarium-promoted coupling and further functionalization toward variocolin were not described.

Scheme 2.3.7. Molander's first-generation synthesis of a CD ring fragment



2.3.3 MOLANDER'S SECOND-GENERATION APPROACH

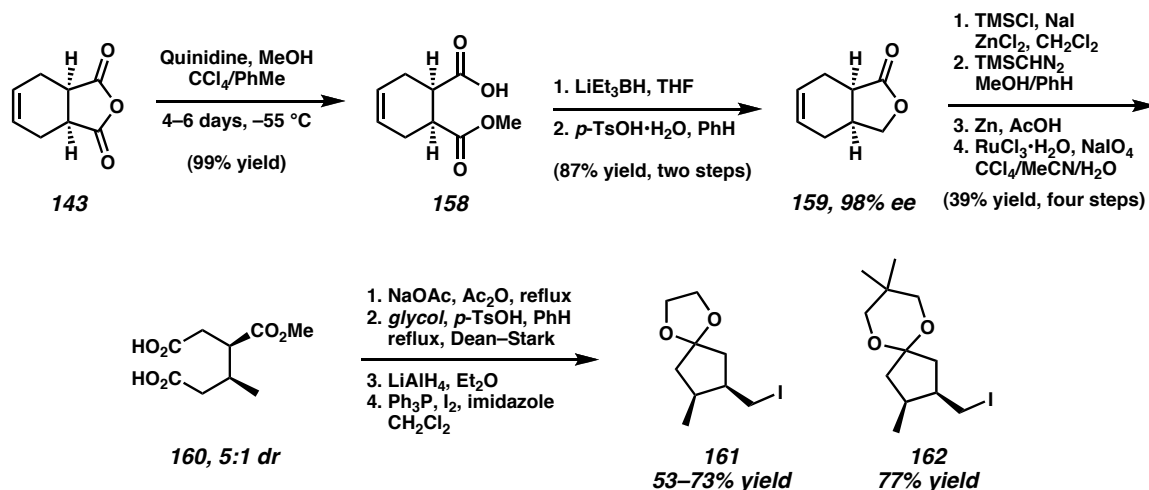
Graduate student Kelly George of the Molander laboratory disclosed a second-generation approach to variocolin in 2005.²¹ The overall synthetic strategy incorporating the key sequential samarium coupling remained the same. However, the synthetic sequences to the A- and CD ring fragments were improved and coupling studies were explored.

The revised stereoselective synthesis of a viable A-ring fragment began with the asymmetric desymmetrization of *meso*-anhydride **143** with quinidine to produce monoacid **158** in 99% yield (Scheme 2.3.8). Chemoselective ester reduction and cyclization provided γ -lactone **159** in 98% ee and 87% yield over two steps. Lactone functionalization and olefin oxidative cleavage over four steps afforded acyclic diacid

160 which was transformed into iodides **161** and **162** in good overall yield (four steps).

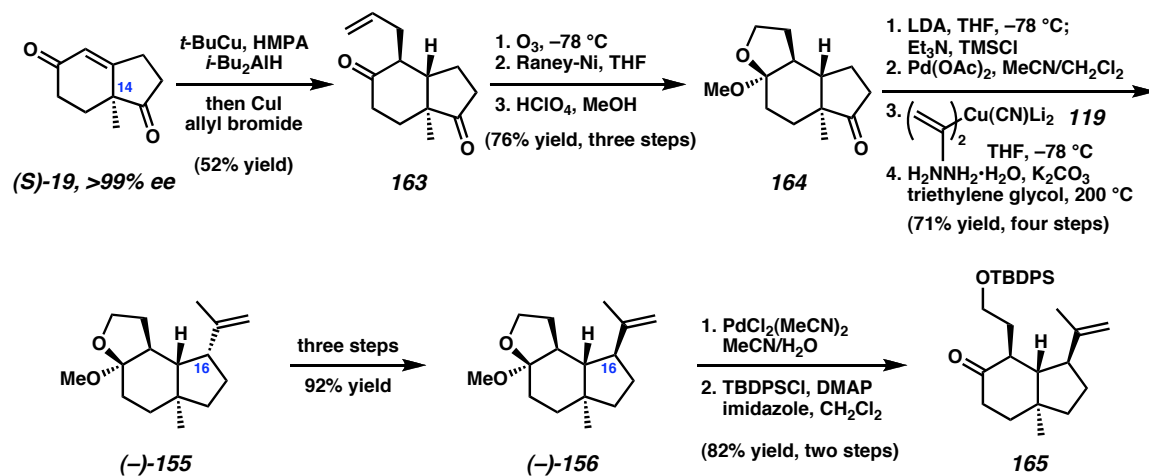
This reaction sequence provided the A-ring intermediates in 11 steps, a marked improvement over the previous generation synthesis (>14 steps).²²

Scheme 2.3.8. Molander's revised A-ring synthesis



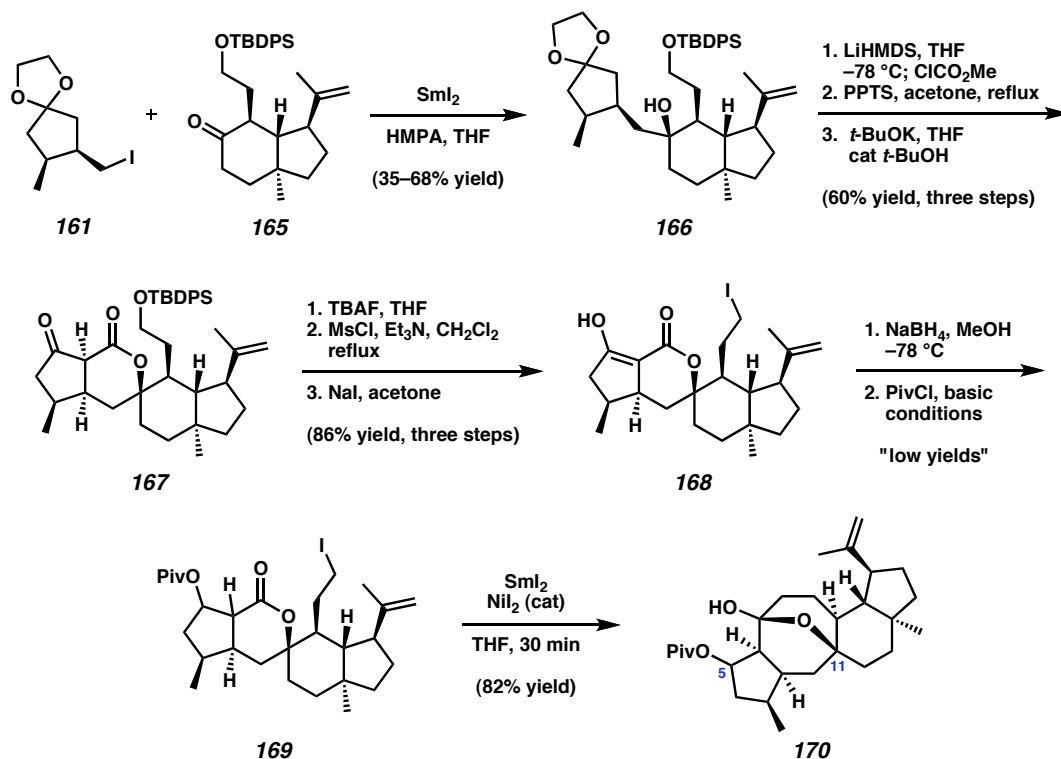
Molander's revised approach to the CD ring proceeded from the correct enantiomer of the Hajos–Parrish ketone ((*S*)-**19**) (Scheme 2.3.9). Enone reduction with copper hydride and diastereoselective allylation of the resulting enolate furnished allyl ketone **163**. Oxidative cleavage of the allyl group, aldehyde reduction and acetylation gave acetal **164**. Typical D-ring functionalization installed the C(16) 2-propenyl moiety in the wrong configuration ((-)-**155**). This was advanced to acetal (-)-**156** by a similar three-step sequence as above (cf. Scheme 2.3.7) to achieve the correct C(16) stereochemistry, and acetal cleavage with alcohol protection provided a suitable coupling partner (**165**). The revised CD ring fragment synthesis was accomplished in 14 steps, a modest improvement over the previous 16-step sequence.

Scheme 2.3.9. Molander's revised CD ring synthesis



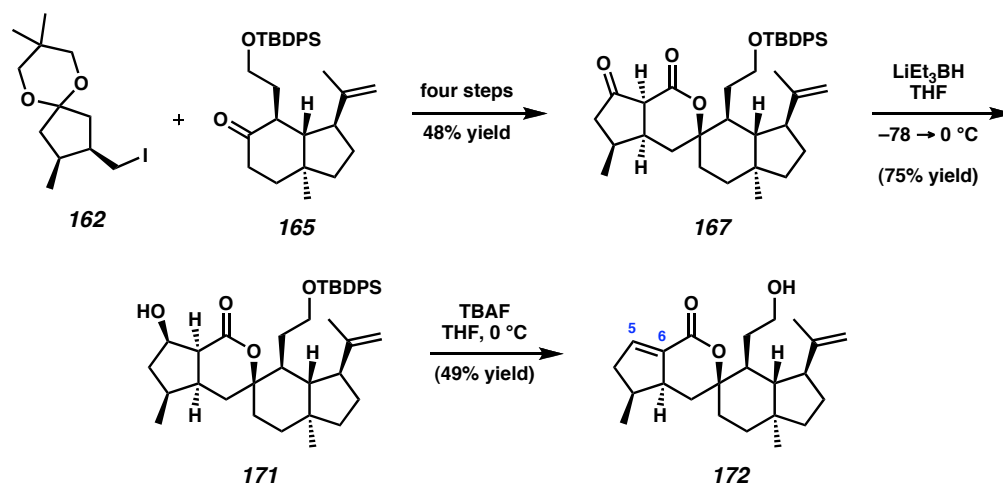
The development of scalable asymmetric syntheses of both the A- and CD ring fragments enabled the exploration of the samarium-promoted coupling strategy. In the event, the intermolecular samarium-promoted Barbier coupling of iodide **161** and chloroketone **165** generated intermediate **166** in variable yields (Scheme 2.3.10). This material was advanced to β -ketolactone **167** over three steps. Silyl cleavage and alcohol conversion to an alkyl iodide afforded **168**; however, the β -ketoester moiety existed in the enolized form removing the C(6) stereochemistry. Ketone reduction and protection as a pivalate under various conditions provided iodolactone **169** in low yields. In the key reaction, it was found that the samarium-promoted intramolecular nucleophilic acyl substitution of this iodolactone proceeded efficiently, constructing **170** in 82% yield. While this method successfully generated the ABCD carbocyclic core of variocolin, low and variable yields as well as C(5) stereochemical issues hampered further progress.

Scheme 2.3.10. Molander's Sm(II)-promoted fragment coupling studies



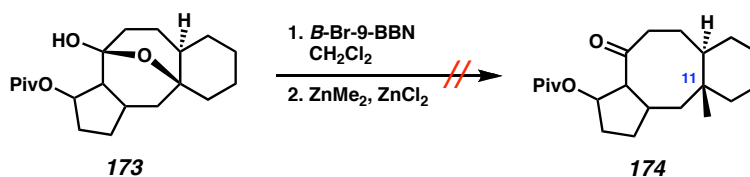
To overcome these difficulties, Molander and co-workers investigated a revised reaction sequence altering the order of operations. The new route involved the samarium-promoted coupling of iodide **162** and ketone **165** over four steps to produce β -ketoester **167** in 48% yield (Scheme 2.3.11). Importantly, the revised A-ring ketone protecting group and modified reaction conditions improved yields and minimized the troublesome C(6) enolization. Diastereoselective ketone reduction with super hydride produced β -hydroxyketone **171** and subsequent fluoride-mediated silyl cleavage resulted in β -hydroxy elimination to form α,β -unsaturated lactone **172**, removing the C(5) and C(6) stereocenters. Efforts to circumvent this problem have not been described.

Scheme 2.3.11. Alternate Sm(II)-promoted fragment coupling studies



The progress of Molander and co-workers toward variocolin appears to have stalled at this intermediate (**172**). The apparent difficulties observed with this sequential samarium-promoted coupling strategy seem to be involved with the order of chemical operations on sensitive intermediates as well as lengthy preparations of these intermediates. In addition to these issues, the strategy necessitates the late installation of the C(11) all-carbon quaternary stereocenter after the final intramolecular nucleophilic acyl substitution reaction. However, model system studies to forge this bond by reported methods²³ resulted with intractable mixtures and no quaternary stereocenter formation (Scheme 2.3.12). Thus, the strategy must be further revised to incorporate this stereocenter at an earlier intermediate via a separate method, which would obviate the designed sequential samarium couplings.

Scheme 2.3.12. Molander's attempted installation of the C(11) quaternary stereocenter



2.4 CONCLUSION

The variocolin sesterterpenes are a structurally complex and biologically active class of natural products isolated from various fungal sources. Biological investigations of this family have indicated anti-HIV, antihypertension, immunomodulatory, and antibacterial properties. The extraordinary tetracyclic core defined by a central eight-membered ring with a high degree of stereocomplexity has inspired valiant synthetic efforts from the Piers and Molander laboratories. These unique approaches to variocolin highlight various stereochemical and functional group attributes for this unusual system. Despite significant progress in this area, completion of variocolin or any of its congeners has yet to be reported.

2.5 NOTES AND REFERENCES

- (1) Hensens, O. D.; Zink, D.; Williamson, J. M.; Lotti, V. J.; Chang, R. S. L.; Goetz, M. A. *J. Org. Chem.* **1991**, *56*, 3399–3403.
- (2) For reviews of sesterterpenoids, see: (a) Hanson, J. R. *Nat. Prod. Rep.* **1986**, *3*, 123–132. (b) Hanson, J. R. *Nat. Prod. Rep.* **1992**, *9*, 481–489. (c) Hanson, J. R. *Nat. Prod. Rep.* **1996**, *13*, 529–535. (d) Liu, Y.; Wang, L.; Jung, J. H.; Zhang, S. *Nat. Prod. Rep.* **2007**, *24*, 1401–1429.
- (3) Fujimoto, H.; Nakamura, E.; Okuyama, E.; Ishibashi, M. *Chem. Pharm. Bull.* **2000**, *48*, 1436–1441.
- (4) The ascomycetes *Emericella* sp. reproduce sexually and are the sexual (perfect) state of the hyphomycetes *Aspergillus* sp.
- (5) Yoganathan, K.; Rossant, C.; Glover, R. P.; Cao, S.; Vittal, J. J.; Ng, S.; Huang, Y.; Buss, A. D.; Butler, M. S. *J. Nat. Prod.* **2004**, *67*, 1681–1684.
- (6) (a) Kawai, K.-i.; Nozawa, K.; Nakajima, S. *J. Chem. Soc., Perkin Trans. 1* **1994**, 1673–1674. (b) Takahashi, H.; Hosoe, T.; Nozawa, K.; Kawai, K.-i. *J. Nat. Prod.* **1999**, *62*, 1712–1713.
- (7) Tezuka, Y.; Takahashi, A.; Maruyama, M.; Tamamura, T.; Kutsuma, S.; Naganawa, H.; Takeuchi, T. Novel Antibiotics, AB5362-A, B, and C, Their Manufacture, Their Use as Fungicides, and Phoma Species AB5362. Japan Patent JP 10045662, 1998.
- (8) For a separate reported isolation of variocolactone (**100**) from *E. aurantiobrunnea*, see: Sato, A.; Morishita, T.; Hosoya, T. S-19777 as Endothelin

Antagonist, Its Manufacture with *Emericella Aurantiobrunnea*, and Its Use as Pharmaceutical. Japan Patent JP 10306087, 1998.

- (9) Harrison, D. M. *Nat. Prod. Rep.* **1988**, *5*, 387–415.
- (10) At the time of this biosynthetic proposal, the hypothesized configuration of variocolin adequately linked to this divergent scheme. The revised stereochemical assignment of variocolin, however, would necessitate the enantiomer of divergent intermediate **109** (i.e., *ent*-**109**), as would ophiobolin C (**111**).
- (11) For a recent review of angiotensin II, see: Bader, M.; Ganten, D. *J. Mol. Med.* **2008**, *86*, 615–621 and references therein.
- (12) For a recent review of endothelin, see: Barton, M.; Yanagisawa, M. *Can. J. Physiol. Pharmacol.* **2008**, *86*, 485–498 and references therein.
- (13) For information on the CCR5 receptor and its relation to HIV, see: (a) Moore, J. P.; Stevenson, M. *Nat. Rev. Mol. Cell. Biol.* **2000**, *1*, 40–49. (b) De Clercq, E. *Med. Res. Rev.* **2002**, *22*, 531–565. (c) Lehner, T. *Trends Immunol.* **2002**, *23*, 347–351. (d) Kedzierska, K.; Crowe, S. M.; Turville, S.; Cunningham, A. L. *Rev. Med. Virology* **2003**, *13*, 39–56. (e) Newman, D. J.; Cragg, G. M. *J. Nat. Prod.* **2007**, *70*, 461–477.
- (14) Piers, E.; Boulet, S. L. *Tetrahedron Lett.* **1997**, *38*, 8815–8818.
- (15) Atom numbering follows that of variocolin (see ref 1).
- (16) Walker, S. D. A Synthetic Approach to the Variocolin Class of Sesterterpenoids: Total Synthesis of (\pm)-5-Deoxyvariocolin, (\pm)-5-Deoxyvariocolol and (\pm)-5-

- Deoxyvariecolactone. A New Cycloheptenone Annulation Method Employing the Bifunctional Reagent (Z)-5-Iodo-1-tributylstannylpent-1-ene. Ph.D. Thesis, University of British Columbia, Vancouver, Canada, 2002.
- (17) A method for the catalytic asymmetric synthesis of bicycle **118** has recently been reported. See: (a) d'Augustin, M.; Palais, L.; Alexakis, A. *Angew. Chem., Int. Ed.* **2005**, *44*, 1376–1378. (b) Vuagnoux-d'Augustin, M.; Alexakis, A. *Chem.—Eur. J.* **2007**, *13*, 9647–9662.
- (18) Molander, G. A.; Quirnbach, M. S.; Silva, Jr., L. F.; Spencer, K. C.; Balsells, J. *Org. Lett.* **2001**, *3*, 2257–2260.
- (19) (a) Molander, G. A.; Harris, C. R. *J. Am. Chem. Soc.* **1995**, *117*, 3705–3716.
(b) Molander, G. A.; Alonso-Alija, C. J. *J. Org. Chem.* **1998**, *63*, 4366–4373.
(c) Molander, G. A.; Harris, C. R. *Tetrahedron* **1998**, *54*, 3321–3354.
(d) Molander, G. A.; Machrouhi, F. *J. Org. Chem.* **1999**, *64*, 4119–4123.
- (20) At the time of Molander and co-workers' initial synthetic efforts, the absolute configuration of variecolin had not yet been determined. Consequently, their plans toward an asymmetric route were dependent upon the original (and incorrect) biosynthetic proposal by Hensens; see ref 1.
- (21) George, K. M. Natural Product Total Synthesis: I. The Total Synthesis of (+)-Isoschizandrin. II. Progress Toward the Total Synthesis of Variocolin. Ph.D. Thesis, University of Pennsylvania, Philadelphia, PA, 2005.
- (22) Molander's first-generation synthesis of an A-ring fragment required 14 steps and does not include the additional transformations necessary to produce a viable coupling fragment.

- (23) (a) Reetz, M. T.; Wenderoth, B.; Peter, R.; Steinbach, R.; Westerman, J. J. *Chem. Soc., Chem. Commun.* **1980**, 1202–1204. (b) Reetz, M. T.; Steinbach, R.; Wenderoth, B. *Synth. Commun.* **1981**, *11*, 261–266.

CHAPTER 3

Progress toward the Asymmetric

Total Synthesis of Variocolin[†]

3.1 INTRODUCTION AND SYNTHETIC STRATEGY

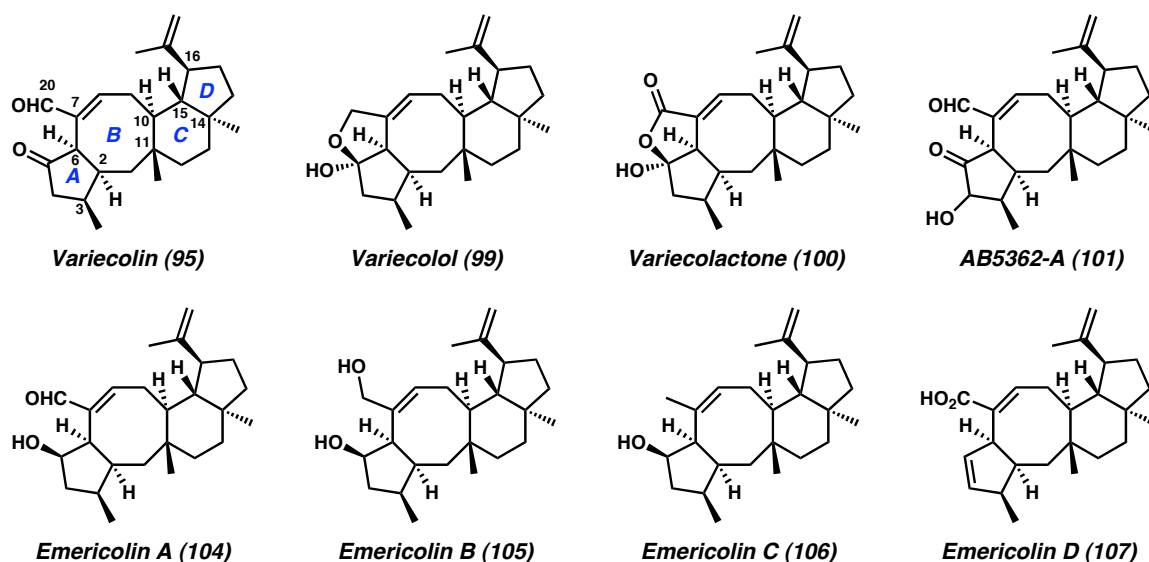
3.1.1 INTRODUCTION

Variocolin (**95**) is a complex sesterterpenoid isolated from extracts of the fungi *Asperigillus* sp. and *Emericella* sp.¹ It belongs to a growing class of sesterterpene natural products defined by a tetracyclic core possessing a central eight-membered ring, comprising varicolol (**99**), varicolactone (**100**),² AB5362-A (**101**), and emericolins A–D (**104–107**) (Figure 3.1.1). This family exhibits an array of biological activities, including antihypertensive,^{1a,2} anti-HIV,^{1f} immunosuppressive,^{1e} and antifungal^{1c} properties. Our interest in the pursuit of an effective and general synthetic strategy toward these bioactive natural products focused on variocolin, as it represents the most widely studied and biologically relevant member. The inherent synthetic challenges

[†] This work was performed in collaboration with Thomas Jensen, a visiting scholar from the Technical University of Denmark, and Dr. Chris Henry, a postdoctoral scholar in the Stoltz group.

posed by the complex tetracyclic core representative of this sesterterpene family provide inspiration to utilize and expand the state of the art in catalysis and synthetic methodology.

Figure 3.1.1. Variocolin family of sesterterpenes.



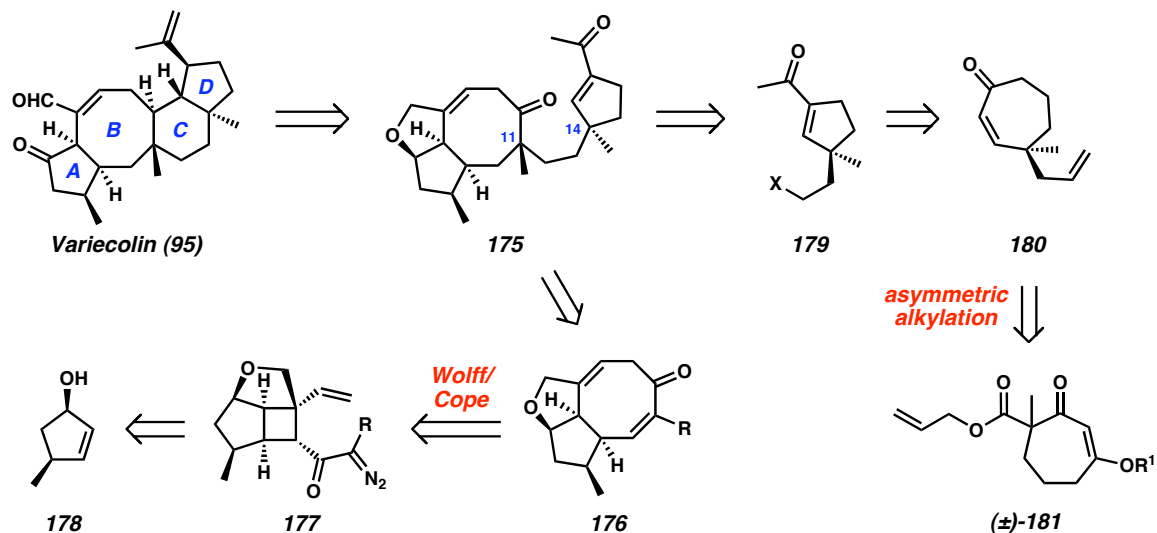
The 25-carbon tetracyclic core of variocolin (**95**) consists of a central eight-membered ring and possesses eight stereocenters, including two all-carbon quaternary stereocenters at C(11) and C(14)³ of the B–C and C–D ring fusions, respectively.^{1a,e,f} Synthetic control of the relative and absolute stereochemistry of these trans-fused rings poses a significant challenge for the design of critical bond-forming reactions. Herein we present a convergent approach to variocolin that harnesses methods developed in our laboratories to construct these key structural features and provides opportunities to explore new reactivity. At the outset of our investigations, two laboratories had published efforts

toward variocolin, although all members of this family have thus far continued to elude chemical synthesis.⁴

3.1.2 RETROSYNTHETIC ANALYSIS

Our retrosynthetic approach toward variocolin (**95**) focused on the construction of the central eight-membered ring and two all-carbon quaternary stereocenters,⁵ with the intention of improving synthetic efficiency through the coupling of two highly substituted fragments. We envisioned a critical C-ring disconnection, through bisketone **175**, to AB ring fragment **176** and D-ring fragment **179** (Scheme 3.1.1). Our laboratory recently developed a powerful tandem Wolff/Cope rearrangement for the facile generation of functionalized fused bicyclic cycloheptadienones from vinyl cyclopropyl diazo ketones.⁶ Using this technology, we anticipated that AB ring synthon **176** could be accessed through a Wolff/Cope rearrangement of highly functionalized cyclobutane **177**, which may in turn be assembled via a tethered cycloaddition of alcohol **178**. We surmised that the crucial all-carbon quaternary stereocenter of D-ring synthon **179** could be installed through an enantioselective Pd-catalyzed alkylation of in situ-generated cyclic enolates recently developed in our laboratories.⁷ Accordingly, **179** could originate from a ring contraction of cycloheptenone **180**, which itself would arise from the asymmetric palladium-catalyzed alkylation of racemic vinylogous β -ketoester (\pm)-**181**.

Scheme 3.1.1. Retrosynthetic analysis of variocolin



3.2 A WOLFF/COPE APPROACH TO THE AB RING SYSTEM

Eight-membered rings are common structural motifs that occur in widely diverse terrestrial plants, insects, marine organisms, and fungi. The theoretical and synthetic intrigue of these medium-sized carbocyclic structures has stimulated the development of various strategies for their preparation, many of which have been applied toward the synthesis of complex molecular targets.⁸ Inasmuch as we are restricted by the limitations of reaction scope in the state of the art, the selective preparation of eight-membered rings remains a noteworthy and continuing challenge to modern chemical methods.⁹

The design of tandem reaction sequences for the rapid generation of molecular complexity is an area of constant investigation in our laboratory.¹⁰ We have recently developed a tandem Wolff/Cope rearrangement for the facile construction of functionalized seven-membered rings.⁶ A critical component to the success of this method was the identification of photochemical or silver-catalyzed sonochemical

conditions to allow direct access to a variety of [*n*-7] fused bicyclic systems in excellent yields. In drawing inspiration from this efficient process, a primary objective of the devised synthetic plan toward variocolin (**95**) is the development of a tandem Wolff/Cope rearrangement to forge fused carbocyclic eight-membered ring systems. Application of this key transformation for the construction of the central B ring of **95** would expand the reaction scope, and furthermore, could provide new tools and strategies for the general preparation of natural and nonnatural substances containing this eight-membered ring motif.

3.2.1 MODEL STUDIES OF THE WOLFF/COPE REARRANGEMENT TOWARD CONSTRUCTION OF THE EIGHT-MEMBERED AB RING

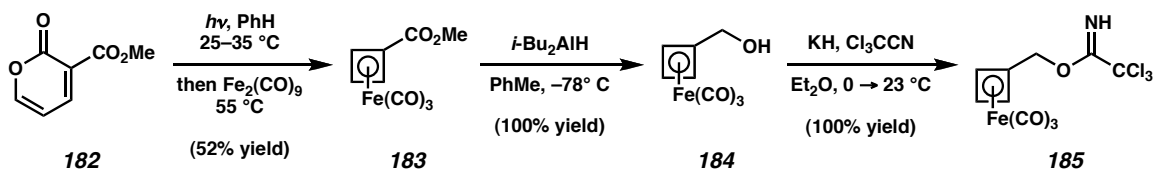
In order to investigate the tandem Wolff/Cope rearrangement toward eight-membered AB ring fragment (**176**), we sought an expedient, stereoselective synthesis of a highly substituted cyclobutane substrate (e.g., **177**). During the course of our efforts, we elected to use an exceedingly effective cyclobutadiene–olefin cycloaddition for the rapid construction of this cyclobutane moiety.¹¹ Model studies pursued toward this goal provided insight into the physical properties and identification of reaction intermediates using a readily available cyclopentenol analogue.

3.2.1.1 MODEL WOLFF/COPE SUBSTRATE SYNTHESIS

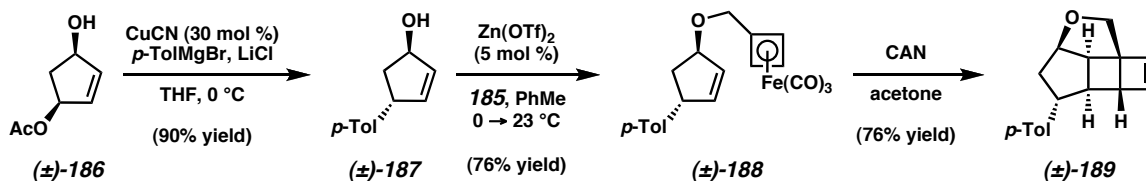
We initiated investigations toward an AB ring model system by preparing a suitable tricarbonyliron-cyclobutadiene derivative with sufficient electrophilicity to enable

alcohol alkylations under mild conditions.¹² Conversion of pyrone **182** into tricarbonyliron-cyclobutadiene complex **183**,¹³ followed by ester reduction produced alcohol **184** (Scheme 3.2.1). Alkoxide generation using KH and exposure to trichloroacetonitrile effectively formed trichloroacetimidate **185** in quantitative yield.

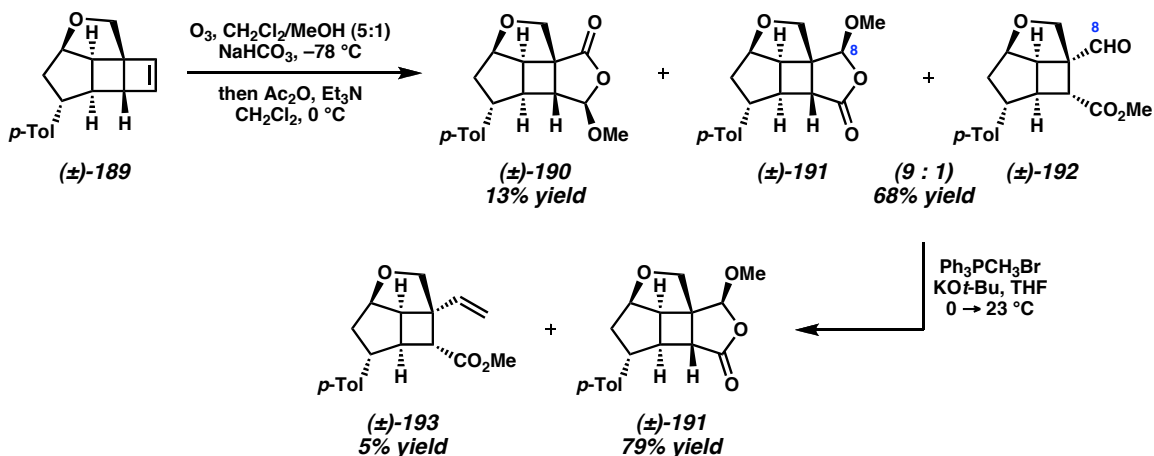
Scheme 3.2.1. Preparation of trichloroacetimidate **185**



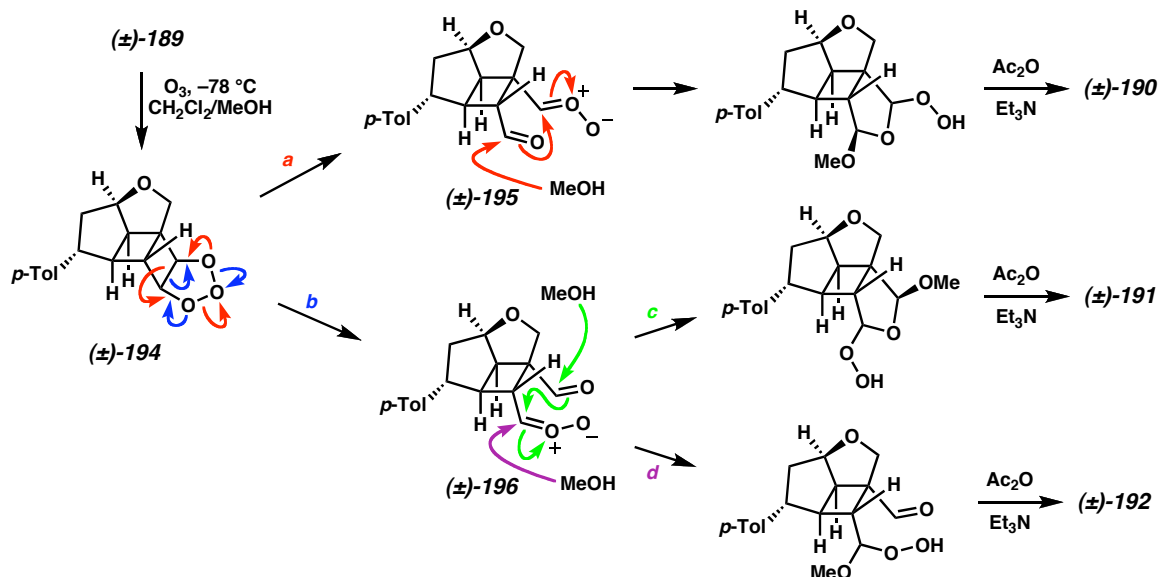
The stereoselective synthesis of a chiral cyclopentenol was achieved utilizing precedented cuprate chemistry.¹⁴ Readily available *anti*-cyclopentenol (\pm)-**187**^{14b} was prepared from monoacetate (\pm)-**186**¹⁵ by a copper(I) cyanide-catalyzed S_N2 displacement using *p*-tolylmagnesium bromide (Scheme 3.2.2). Zinc(II)-catalyzed alkylation¹⁶ of *anti*-cyclopentenol **187** with trichloroacetimidate **185** afforded the requisite intramolecular cycloaddition substrate **188** in 76% yield.¹² Oxidative liberation of cyclobutadiene promoted by ceric ammonium nitrate (CAN), with subsequent olefin cycloaddition rapidly assembled the desired cyclobutene **189** in 76% yield, establishing the stereoselective preparation of a model for our highly substituted cyclobutane intermediate.

Scheme 3.2.2. Tethered cycloaddition of alcohol (\pm)-**186**

We next considered regioselective functionalization of the cyclobutene moiety via construction of cycloadduct **189** en route to a Wolff/Cope substrate. To this end, we explored a method for the ozonolytic cleavage of olefins to terminally differentiated products in CH_2Cl_2 and methanol popularized by Schreiber.^{17,18} Exposure of cycloadduct **189** to typical reaction conditions provided a mixture of compounds including undesired acetal **190** in 13% yield and an inseparable 9:1 mixture of acetal **191** and desired aldehyde **192** in 68% yield (Scheme 3.2.3). Direct Wittig methylation of the mixture afforded pure acetal **191** in addition to minor quantities of desired olefin **193**.

Scheme 3.2.3. Termini-differentiating ozonolysis of cyclobutene **189**

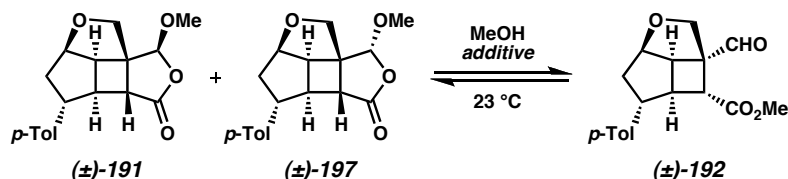
The production of acetals **190** and **191** from this unsymmetrical ozonolysis indicates diverging reaction pathways (Scheme 3.2.4). Cycloaddition of ozone to cyclobutene **189** generates primary ozonide **194**, which fragments in one of two ways. Cleavage of the primary ozonide to **195** (path *a*) positions the carbonyl oxide on the fully substituted carbon. Subsequent addition of methanol to this intermediate and dehydration with $\text{Ac}_2\text{O}/\text{Et}_3\text{N}$ generates acetal **190**. Conversely, primary ozonide cleavage in the opposite manner produces **196** (path *b*) with the carbonyl oxide positioned on the less-substituted carbon. This intermediate further reacts by another of two possible pathways: (1) addition of methanol from the reaction medium (path *c*) and dehydration to generate acetal **191**, or (2) methanol addition to the carbonyl oxide (path *d*) and dehydration to furnish aldehyde **192**. Although desired aldehyde **192** is a minor component of this reaction, the selectivity for the cleavage of primary ozonide **194** via the desired path *b* is favored in an approximate 3:1 ratio, and is presumably the result of steric influences of the cyclobutene moiety.¹⁹

Scheme 3.2.4. Proposed ozonolytic cleavage of cyclobutene **189**

The isolation of aldehyde **192** as a minor product from the unsymmetrical ozonolysis of cyclobutene **189** hindered progress toward a model Wolff/Cope substrate. Fortuitously, we recognized that acetal **191** and aldehyde **192** arise from the same fragmentation pathway (path *b*, Scheme 3.2.4) and thus possess the same aldehyde oxidation state at C(8)³ (cf. Scheme 3.2.3). To exploit this result, we explored potential equilibration conditions to determine the propensity for formation of aldehyde **192** from the isomeric aldehyde/acetal mixture (Table 3.2.1). Our primary investigations revealed that solvation of pure acetal **191** in methanol effected the equilibration to favor aldehyde **192** and produced minor quantities of acetal diastereomer **197** (entries 1 and 2). A survey of various Lewis acids identified the proficiency of divalent triflate salts in shifting the equilibrium to further favor **192** (entries 3–6).²⁰ Similarly, molecular sieves and combinations thereof with Lewis acids proved to be efficient for the conversion to **192** (entries 7–10). As a result of this screen of conditions, we elected to proceed in the

synthesis using 4 Å MS in our optimal conditions because they provide a nearly 3:1 ratio of **192:191 + 197** and enhanced operational efficiency.²¹

Table 3.2.1. Equilibration of acetal **191**



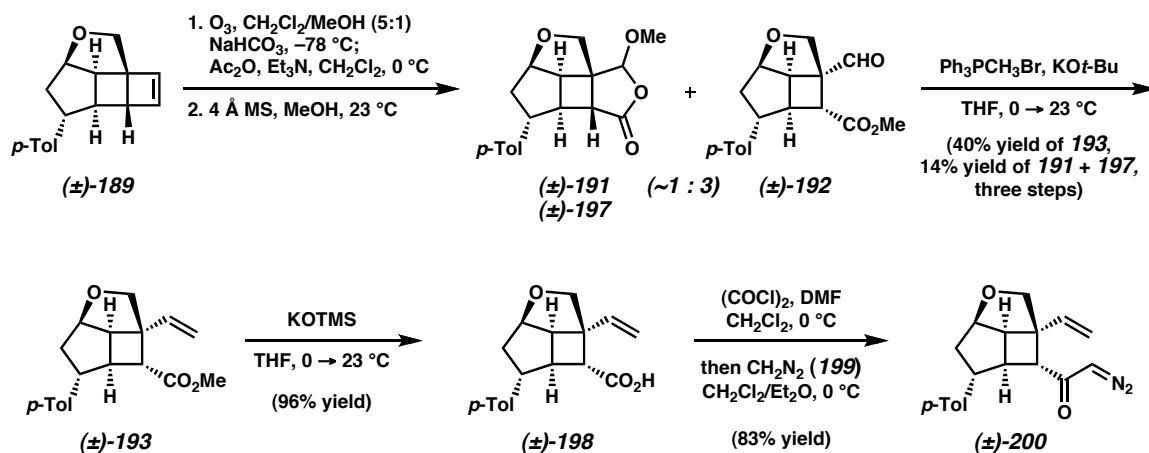
entry ^a	additive ^b	191 + 197 : 192 ^c
1	—	66 : 34
2	— ^d	39 : 61
3	CuCl ₂	75 : 25
4	ZnCl ₂	41 : 59
5	Cu(OTf) ₂	36 : 64
6	Zn(OTf) ₂	30 : 70
7	3 Å MS	32 : 68
8	4 Å MS	29 : 71
9	4 Å MS/Zn(OTf) ₂	27 : 73
10	4 Å MS/Cu(OTf) ₂	28 : 72

^a Each entry started from pure acetal **191**. ^b Lewis acids were used in 20 mol %; molecular sieves were used in 0.5 g/mmol. ^c Ratio determined by ¹H NMR analysis of crude reaction filtrate after 20–24 h. ^d At 50 °C.

The equilibration of acetal **191** to desired aldehyde **192** considerably improved the overall reaction sequence for the preparation of a Wolff/Cope α -diazoketone substrate (e.g., **177**). In the event, the unsymmetrical ozonolysis of cyclobutene **189** followed by equilibration with 4 Å MS in methanol afforded a ~1:3 ratio of acetals **191 + 197** and aldehyde **192** (Scheme 3.2.5). Wittig methylenation of this mixture produced the desired olefin **193** in 40% yield over three steps, while the recovery of acetals **191** and **197** in 14% yield enabled recycling of material.²² Hydrolysis of ester **193** with KOTMS and

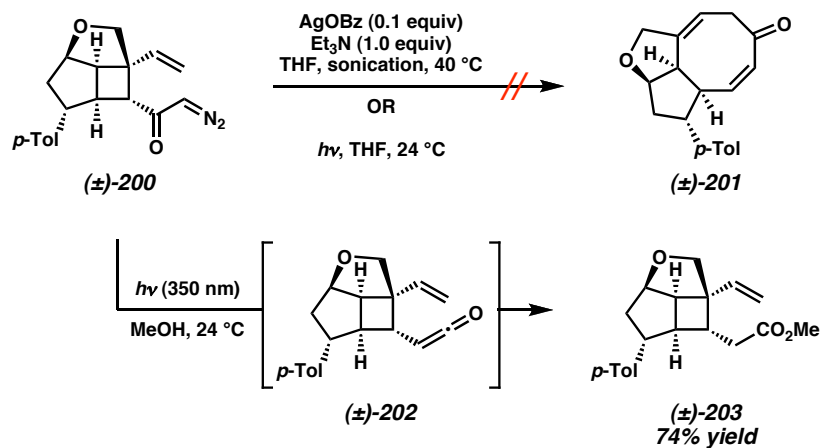
conversion to α -diazoketone **200** by way of an acid chloride and diazomethane (**199**) proceeded in excellent yield.

Scheme 3.2.5. Optimized synthesis of α -diazoketone **200**



3.2.1.2 MODEL WOLFF/COPE REARRANGEMENT INVESTIGATIONS

The synthesis of α -diazoketone **200** enabled the examination of our key Wolff/Cope rearrangement toward the eight-membered B ring of variocolin. Thorough investigations of this transformation utilizing various photochemical or silver(I)-catalyzed sonochemical conditions afforded only intractable mixtures (Scheme 3.2.6). The lack of useful information acquired from these initial experiments required us to examine the tandem process in a stepwise manner. Accordingly, irradiation of α -diazoketone **200** in methanol with a 350 nm light induced the photochemical Wolff rearrangement to form homologated²³ ester **203** as the sole product, confirming the intermediacy of ketene **202**. We were thus able to conclude that the ketene vinyl cyclobutane rearrangement does not readily occur under the conditions surveyed.

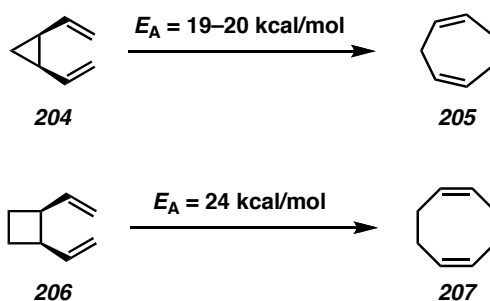
Scheme 3.2.6. Initial Wolff/Cope studies on α -diazoketone **200**

To rationalize the difficulty of the *cis*-ketene vinyl cyclobutane rearrangement of **202**, we considered the analogous *cis*-divinyl cyclobutane rearrangement.²⁴ A comparison of the experimental activation energy (E_A) for a strain-releasing Cope rearrangement of *cis*-divinyl cyclopropane (**204**) to that of *cis*-divinyl cyclobutane (**206**) reveals a higher activation barrier of the latter by roughly 4–5 kcal/mol (Figure 3.2.1).²⁵ The related decrease in reaction rate constant is consistent with the slightly elevated reaction temperatures known to be required for *cis*-divinyl cyclobutane rearrangements. This difference, when coupled with our observations that the ketene vinyl cyclopropane rearrangement to afford substituted cycloheptadienones occurs under mild conditions,⁶ suggested that thermolysis of the intermediate ketene should facilitate the rearrangement. In the event, a photochemical Wolff rearrangement with subsequent thermolysis at 80 °C provided cyclooctenone **201** in 59% yield (Scheme 3.2.7).

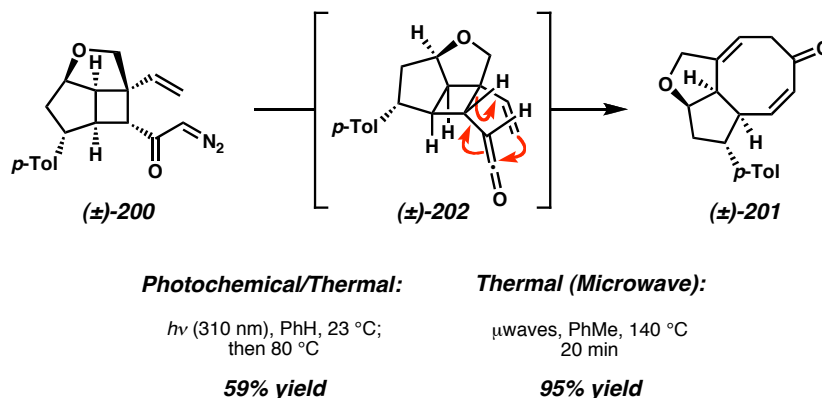
With the success of this tandem reaction, we recognized that the high reactivity of a ketene intermediate and the time between photolysis/thermolysis could account for the

moderate yield of **201** and furthermore might hinder material throughput. In our search for alternative conditions, we investigated reports harnessing microwave irradiation to promote Wolff rearrangements, where we anticipated that the surplus energy could facilitate the Cope rearrangement.²⁶ Indeed, microwave irradiation for 20 minutes at 140 °C in toluene afforded cyclooctadienone **201** in 95% yield. These model system results thereby confirm the Wolff/Cope strategy for the synthesis of the AB fragment of variocolin (**95**), and provide new tools for the construction of substituted eight-membered rings

Figure 3.2.1 Comparison of the strain-releasing Cope rearrangements of **204** and **206**.



Scheme 3.2.7. Successful Wolff/Cope rearrangement of α -diazoketone **200**

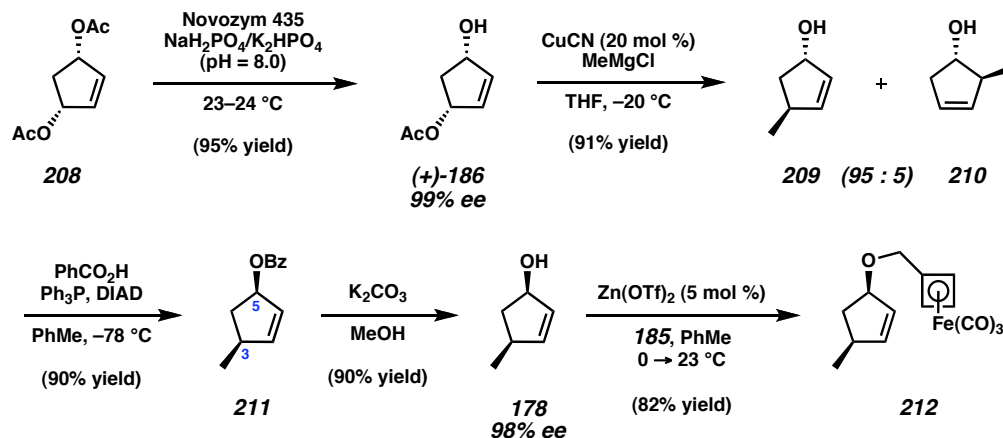


3.2.2 ASYMMETRIC SYNTHESIS OF THE AB RING FRAGMENT OF VARIECOLIN EMPLOYING THE WOLFF/COPE REARRANGEMENT

Having established a viable route toward the AB ring system of variocolin through model system studies, we then pursued an asymmetric synthesis of this fragment.

3.2.2.1 ASYMMETRIC SYNTHESIS OF WOLFF/COPE SUBSTRATE TOWARD VARIECOLIN

The application of our proven intramolecular cycloaddition strategy for an asymmetric synthesis of the AB ring fragment (i.e., **176**, Scheme 3.1.1) originated from a chiral cyclopentenol possessing syn stereochemistry. An enzymatic desymmetrization of *meso*-bisacetate **208** provided monoacetate (+)-**186** in excellent yield and 99% ee (Scheme 3.2.8).²⁷ Copper(I) cyanide-catalyzed S_N2 displacement using methylmagnesium chloride with monoacetate **186** afforded a 95:5 mixture of alcohols **209** and **210** in 91% yield.^{14a} Mitsunobu inversion of this alcohol mixture using benzoic acid produced allylic benzoate **211**, possessing the desired syn stereochemistry between C(3) and C(5).^{3,28} Benzoate methanolysis and zinc(II)-catalyzed coupling¹⁶ with tricarbonyliron-cyclobutadiene trichloroacetimidate **185** gave the requisite intramolecular cycloaddition substrate (**212**).

Scheme 3.2.8. Asymmetric synthesis of intramolecular cycloaddition substrate **212**

Efforts toward the intramolecular cyclobutadiene–olefin cycloaddition of **212** promoted by CAN resulted in low yields and complex mixtures of products, presumably the result of competing intermolecular dimerization reactions. Snapper has established that the rapid oxidative decomplexation of tricarbonyliron–cyclobutadiene complexes using CAN provides sufficient access to cycloadducts of substrates predisposed for the intramolecular cycloaddition (e.g., **188**).^{11f} Oxidations using trimethylamine-*N*-oxide, however, enact a slow release of cyclobutadiene to enable access to cycloadducts of substrates with a lower reactivity for this process (e.g., **212**). The gradual liberation of the highly reactive intermediate favors an intramolecular cycloaddition process by disfavoring intermolecular reaction pathways. Application of trimethylamine-*N*-oxide to facilitate the oxidative decomplexation of **212** in refluxing acetone smoothly generated cycloadduct **213** (Scheme 3.2.9).^{29,30} Subsequent unsymmetrical ozonolysis of **213**, acetal equilibration promoted by 4 Å MS in refluxing methanol and Wittig methylenation afforded a 2.7:1 ratio olefins **216** and **217**, in addition to acetals **214** and **215**. This reaction sequence provided desired olefin **216** in 16% yield over four steps, together with

17% yield of recyclable acetal **214**.³¹ Critically, acetal **215** was sufficiently crystalline to enable X-ray analysis, providing further confirmation of the desired relative stereochemistry of this polycyclic fragment (Figure 3.2.2).³²

Scheme 3.2.9. Cycloaddition, ozonolysis, and olefination toward an asymmetric Wolff/Cope substrate

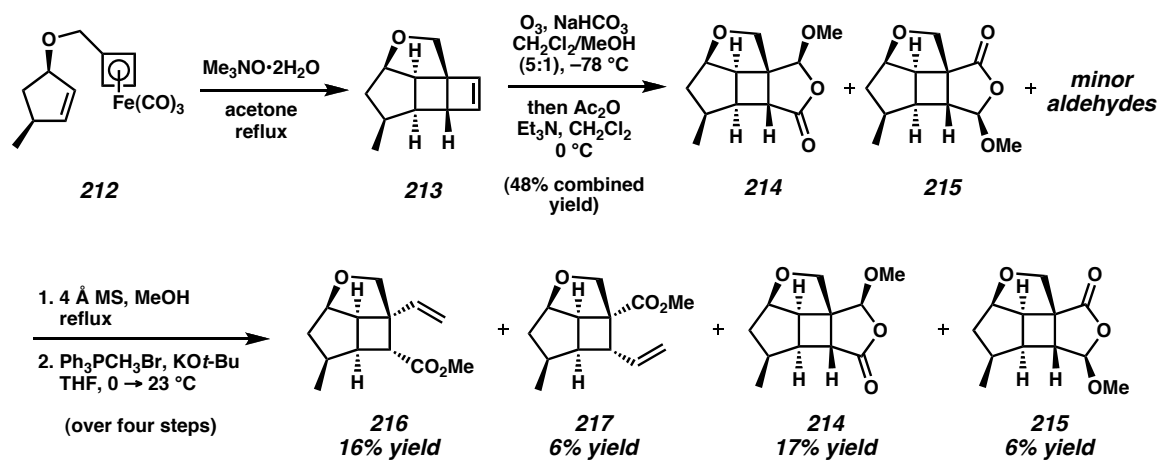
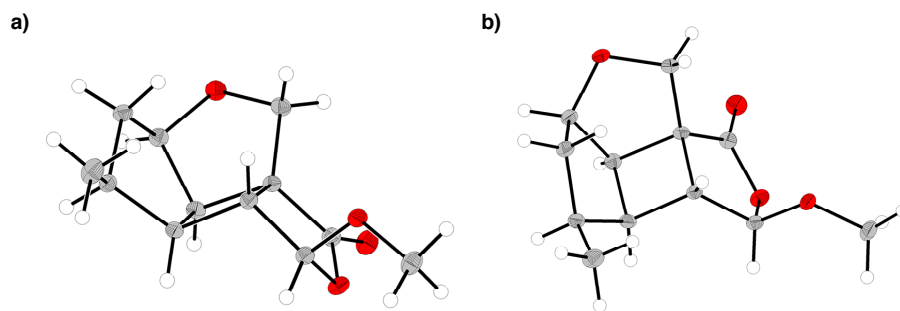


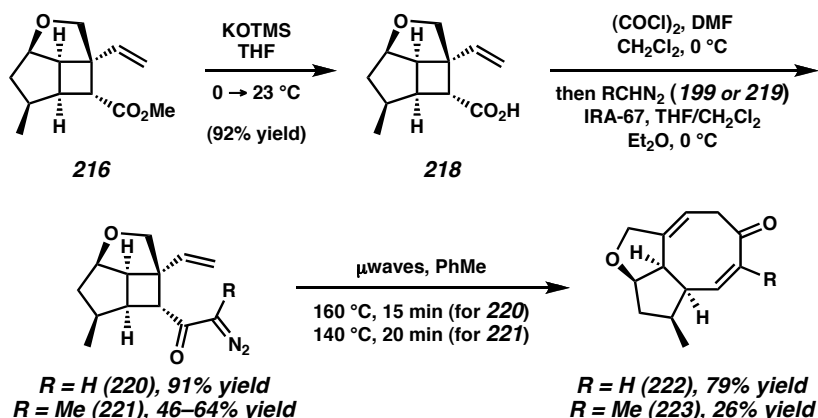
Figure 3.2.2. X-ray crystal structure of acetal **215**. The molecular structure is shown with 50% probability ellipsoids. a) Side view. b) Top view.



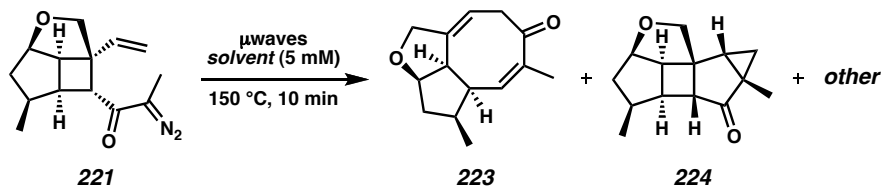
3.2.2.2 α -DIAZOKETONE SYNTHESIS AND WOLFF/COPE STUDIES

In the synthesis of our asymmetric AB ring fragment, we desired cyclooctadienone products **176** where R = H, Me, or alkyl (Scheme 3.1.1). Model studies have demonstrated the tandem rearrangement where R = H (i.e., **200** \rightarrow **201**, see subsection 3.2.1.2). However, alkyl substitution had not yet been explored for the Wolff/Cope rearrangement and thus represented an unprecedented extension of the methodology. Advancing to the target α -diazoketones, hydrolysis of ester **216** to acid **218** and conversion to the acid chloride and treatment with either diazomethane (**199**, R = H) or diazoethane (**219**, R = Me) produced α -diazoketones **220** and **221**, respectively (Scheme 3.2.10). Although diazomethane generated **220** in 91% yield, we were surprised by the inconsistent and lower-yielding results obtained using diazoethane.³³ Despite extensive efforts toward optimization, however, improvements in yield could not be realized.³⁴ Nonetheless, the microwave-promoted tandem Wolff/Cope rearrangement of both substrates resulted in the successful construction of their respective cyclooctadienones (**222** and **223**).

Scheme 3.2.10. α -Diazoketone synthesis and Wolff/Cope rearrangement



The notably low yield of α -substituted cyclooctadienone **223** using microwave irradiation is a direct result of the formation of numerous byproducts.³⁵ Inspection of these various compounds revealed that cyclopropane **224** is a major side product (~1:1 ratio of **223:224**) of this reaction, formed through a carbene intermediate. Two mechanisms have been proposed for the Wolff rearrangement: 1) a concerted group migration with nitrogen expulsion to a ketene or 2) the stepwise loss of nitrogen to generate an α -carbonyl carbene intermediate that can either undergo the desired Wolff rearrangement to a ketene or participate in other intra- or intermolecular reactions.³⁶ A complicating factor in our analysis of the rearrangement of **221** is that the two mechanisms often operate competitively with high substrate dependence. However, we noted the influence of solvent toward substrate conformation (**224**) and its impact on the mechanistic pathway,³⁷ and thus posited that solvent variation might facilitate an increase in the production of our targeted cyclooctadienone **223** (Table 3.2.2).³⁸ We observed that high-polarity solvents such as acetonitrile or 1,2-dichloroethane favored cyclopropane formation decidedly over the Wolff rearrangement (entries 1 and 2). Less-polar solvents, such as THF, ethyl acetate, and toluene, reversed the selectivity and improved the formation of desired product **223** (entries 3–6). Furthermore, the nonpolar solvents methylcyclohexane and heptane reversed the reaction selectivity to favor the desired **223** as a major product, in a 3:1 ratio (entries 7 and 8). Although solvent polarity roughly reflects product selectivity, in which less-polar solvents favor the Wolff rearrangement, the complex reaction profile makes it difficult to conclusively correlate solvent polarity to reaction pathway.

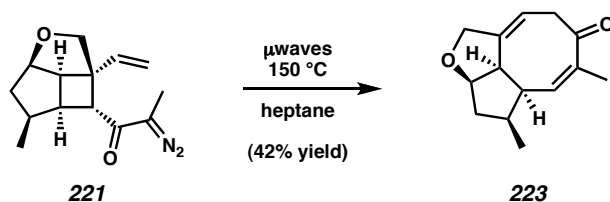
Table 3.2.2. Wolff/Cope solvent studies of α -diazoketone **221**

entry ^a	solvent	dielectric constant (ϵ)	223 : 224 ^b
1	acetonitrile	37.5	1 : 4
2	DCE	10.4	1 : 2.8
3	THF	7.58	1 : 1.1
4	EtOAc	6.02	1 : 1.3
5	toluene	2.38	1.1 : 1
6	1,4-dioxane	2.21	1 : 1.7
7	methylcyclohexane	2.02	3 : 1
8	heptane	1.92	3 : 1

^a Starting material was consumed in all reactions. ^b Ratios determined by ¹H NMR analysis of crude reaction mixtures.

The application of these optimized reaction conditions with heptane enabled the microwave-promoted rearrangement of **221** to produce α -methyl cyclooctadienone **223** in 42% isolated yield (Scheme 3.2.11). The success of this rearrangement is significant as it represents the first example of the tandem Wolff/Cope rearrangement of a substrate possessing α -alkyl functionality. Moreover, the combined results from all substrates in this study (i.e., **200**, **220**, and **221**) highlight the utility of microwave energy to facilitate tandem rearrangements and expand the collection of eight-membered rings available by this method. This Wolff/Cope approach to variecolin AB ring systems **222** and **223** provided advanced material to support fragment coupling studies toward completion of the natural product.

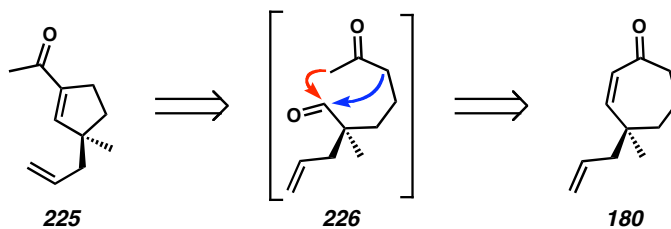
Scheme 3.2.11. Optimized rearrangement of α -diazoketone **221** to α -methyl cyclooctadienone **223**



3.3 CATALYTIC ASYMMETRIC SYNTHESIS OF A D-RING FRAGMENT

D-ring fragment **179** presents an all-carbon quaternary stereocenter contained within the cyclopentene core as the key synthetic challenge. Literature reports of approaches to similar quaternary acylcyclopentenones are remarkably limited,³⁹ and thus we sought a novel route to construct these potentially useful substances. Structures analogous to **179** have been assembled both from five-membered rings⁴⁰ and as the products of six-membered ring contractions.^{41,42} In our design of a synthetic route to D-ring fragment **225** we envisioned the contraction of cycloheptenone **180** via a retro-aldol/aldol sequence⁴³ to enable the direct formation of a cyclopentene intermediate (Scheme 3.3.1).

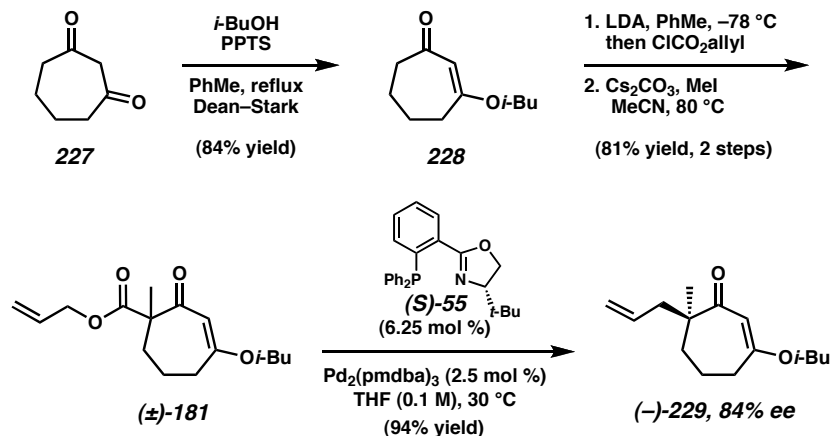
Scheme 3.3.1. Proposed ring contraction approach to acylcyclopentene **225**



The palladium-catalyzed enantioselective alkylation of unstabilized, prochiral ketone enolates has been an area of intense investigation in our laboratory.⁷ This technology has enabled the preparation of a wide variety of cyclic carbonyl compounds possessing adjacent quaternary stereocenters with high levels of selectivity and excellent yields. To explore this ring contraction pathway, we pursued the enantioselective construction of the C(14) quaternary stereocenter via the asymmetric alkylation of racemic vinylogous⁴⁴ β -ketoester (\pm)-**181**.

3.3.1 OPTIMIZATION OF THE Pd-CATALYZED ASYMMETRIC ALKYLATION OF CYCLIC SEVEN-MEMBERED VINYLOGOUS β -KETOESTERS

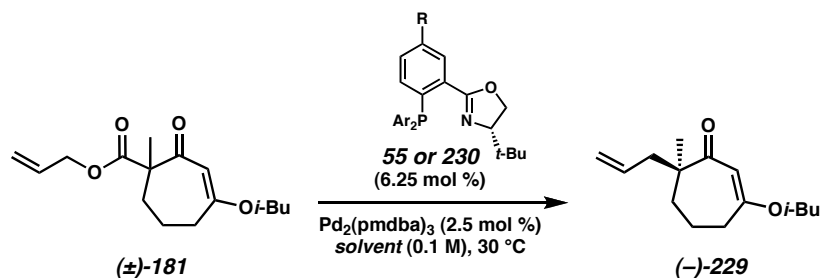
The synthesis of a suitable β -ketoester substrate initiated with the production of vinylogous ester **228** from cycloheptane-1,3-dione (**227**)⁴⁵ (Scheme 3.3.2). Ketone enolization and acylation with allyl chloroformate formed an intermediate β -ketoester that was subsequently alkylated with methyl iodide to produce racemic β -ketoester (\pm)-**181**. In the presence of our standard alkylation conditions employing a catalyst complex generated in situ from Pd₂(pmdba)₃ and (*S*)-*t*-Bu-PHOX ((*S*)-**55**) in THF at 30 °C, vinylogous β -ketoester was transformed to α -quaternary ketone ($-$)-**229** in 94% yield and 84% ee.

Scheme 3.3.2. Vinylogous β -ketoester substrate synthesis and Pd-catalyzed asymmetric alkylation

Although allyl ketone **229** was produced in excellent yield, we sought to improve the enantioselectivity of the process. A survey of common solvents afforded similar yields of allyl ketone **229** with a distinct enhancement of enantioselectivity (Table 3.3.1). Etheral solvents enabled a modest selectivity increase to 86% ee in Et_2O (entries 1–3), while aromatic solvents provided a more substantial improvement to 88% ee in toluene (entries 4 and 5). In addition, we altered the electronics of our ligand, using fluorinated derivative **230**⁴⁶ to produce allyl ketone **229** in 90% ee, albeit with diminished yield at higher catalyst loading (entry 6). Since the diminished reactivity⁴⁷ of the electronically deficient palladium complex derived from **230** required increased catalyst loadings and resulted in lower yields, we elected to use the standard *t*-Bu-PHOX ligand (**55**) in toluene to carry out our asymmetric alkylation. The large-scale application of this method was facilitated by lower catalyst loadings (2.4 mol %) and increased reaction concentrations (0.2 M) to smoothly form allyl ketone **229** in 98% yield and 88% ee, a critical result that enhanced the practicality of the transformation (Scheme 3.3.3). Moreover, the optimal conditions for this class of cyclic vinylogous esters provide us with a new variety of

substrates for our asymmetric alkylation methodology as we continue to seek new synthetic applications for this chemistry.

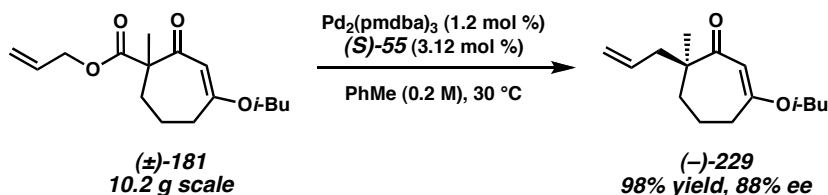
Table 3.3.1. Asymmetric alkylation screen of vinylogous β -ketoester (\pm)-**181**



entry ^a	ligand	solvent	yield (%) ^b	ee (%) ^c
1	55 ($R = H$, $Ar = Ph$)	THF	94	84
2	55 ($R = H$, $Ar = Ph$)	TBME	88	85
3	55 ($R = H$, $Ar = Ph$)	Et ₂ O	93	86
4	55 ($R = H$, $Ar = Ph$)	benzene	84	86
5	55 ($R = H$, $Ar = Ph$)	toluene	91	88
6 ^d	230 ($R = CF_3$, $Ar = 4-CF_3-C_6H_4$)	benzene	57	90

^a pmdba = bis(4-methoxybenzylidene)acetone. ^b Isolated yield. ^c Enantiomeric excess determined by chiral HPLC. ^d 5 mol % Pd₂(pmdba)₃ and 12.5 mol % **230** were used to reach complete conversion.

Scheme 3.3.3. Large-scale enantioselective alkylation of β -ketoester (\pm)-**181**

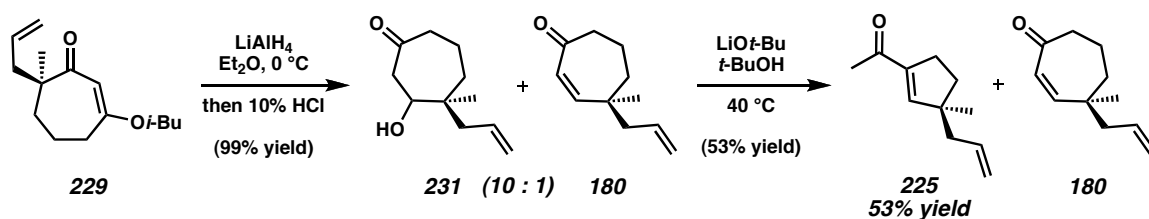


3.3.2 RING CONTRACTION INVESTIGATIONS AND DETERMINATION OF THE ABSOLUTE STEREOCHEMISTRY

A scalable and efficient asymmetric preparation of allyl ketone **229** enabled our pursuit of the targeted D-ring fragment **179**. Reduction of vinylogous ester **229** with

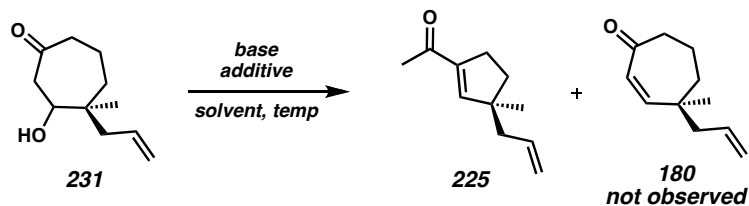
acidic workup furnished a 10:1 mixture of β -hydroxyketone **231** and enone **180** in 99% overall yield (Scheme 3.3.4). Exposure of this crude mixture to aldol conditions using LiOt-Bu in *t*-BuOH produced the desired ring-contracted acylcyclopentene **225** in 53% yield. Our isolation of the desired product in greater than 10% yield indicated to us that β -hydroxyketone **231** is readily converted to **225**, whereas the minor cycloheptenone **180** remained in the reaction after consumption of **231**. Since β -hydroxyketone **231** is equivalent to the first step of the retro-aldol/aldol sequence (through water addition to the enone) and is available as the major product from the reduction of **229**, it thus provided us with an ideal substrate on which to pursue further studies.⁴⁸

Scheme 3.3.4. Reduction of ketone **229** and preliminary ring contraction



Our subsequent efforts to maximize the efficiency of this transformation focused on the ring contraction of the major reduction product, β -hydroxyketone **231**. Given our early result using LiOt-Bu (Scheme 3.3.4), we examined numerous aldol conditions that consisted of a variety of non-nucleophilic bases (Table 3.3.2).⁴⁹ We observed that several *t*-butoxides in *t*-BuOH and THF effected substrate conversion to the desired product (**225**) in good yields (entries 1–4), noting that the rate of product formation was comparatively slower with LiOt-Bu than that of Na- and KOt-Bu. The use of various hydroxides revealed a similar trend, where NaOH and KOH generated **225** in 4 hours

with improved yields over their respective *t*-butoxides (entries 5 and 6). In contrast, the reactivity of LiOH was comparatively sluggish, providing **225** in low yield with the formation of various intermediates (entry 7).⁵⁰ To harness the mild reactivity of LiOH while improving the yield of **225**, we investigated the effect of alcohol additives to modulate the efficacy of the transformation. The combination of *t*-BuOH and LiOH in THF increased the yield of **225** to a similar level as that observed with LiO*t*-Bu, although the reaction continued to proceed at a slow rate (entry 8). Application of more acidic, non-nucleophilic alcohols such as trifluoroethanol (TFE) and hexafluoroisopropanol (HFIP)⁵¹ demonstrated exceptional reactivity with LiOH to efficiently produce **225** in high yields (entries 9 and 10).⁵² This is reflective of the recently reported use of fluorinated lithium alkoxides to promote Horner–Wadsworth–Emmons olefinations of sensitive substrates and underscores their mild reactivity and efficacy.⁵³ The data from our study further recognize the unique properties of these mild bases and suggest their application may be examined in a broader context. While a number of bases are effective in the production of **225** in good yields, we selected the combination of LiOH and TFE as our optimal conditions for scale-up efforts. Importantly, none of the conditions surveyed for the ring contraction studies generated the β -elimination product, cycloheptenone **180**, providing further validation that β -hydroxyketone **231** is an ideal substrate for this transformation.⁵⁴

Table 3.3.2. Ring contraction investigations of **231**

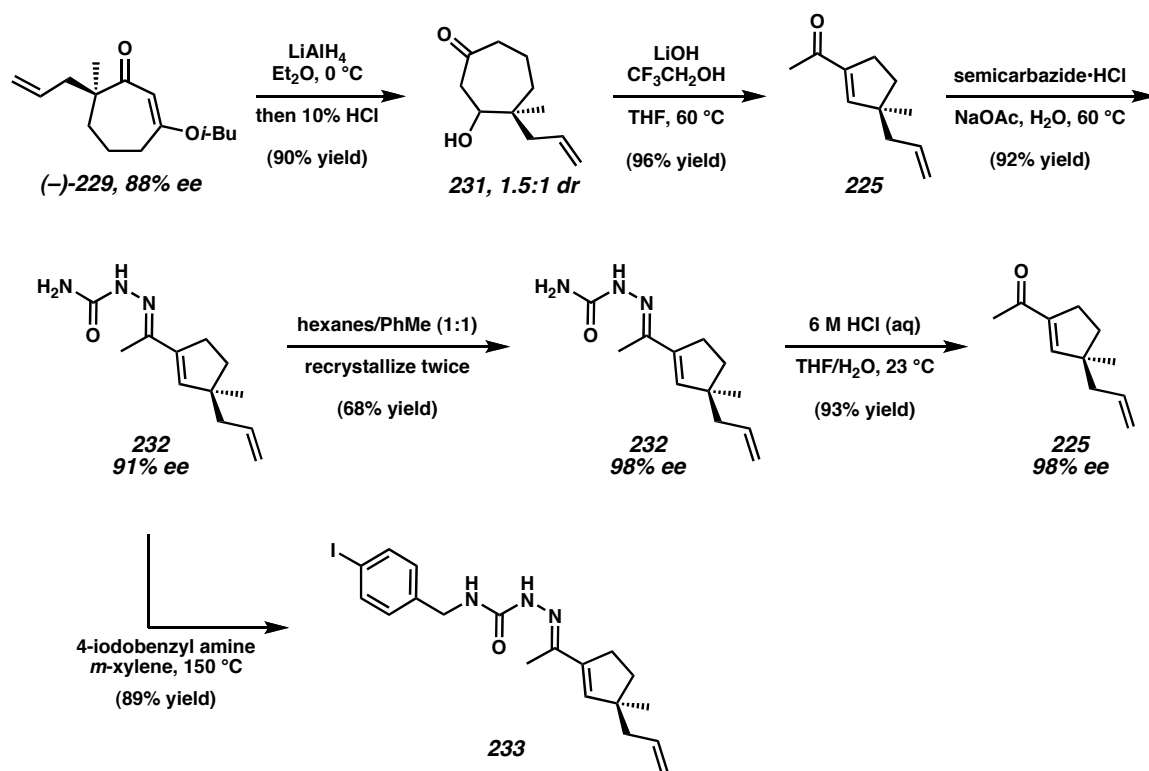
entry ^{a,b}	base	additive	solvent	temp (°C)	t (h)	conversion (%) ^c	yield (%) ^c
1	LiO <i>t</i> -Bu	—	<i>t</i> -BuOH	40	9	100	71
2	LiO <i>t</i> -Bu	—	THF	40	8	100	60
3	NaO <i>t</i> -Bu	—	THF	40	5	100	81
4	KO <i>t</i> -Bu	—	THF	40	5	100	85
5	NaOH	—	THF	60	4	100	89
6	KOH	—	THF	60	4	100	87
7	LiOH	—	THF	60	24	78	19 ^d
8	LiOH	<i>t</i> -BuOH	THF	60	24	98	78
9	LiOH	TFE	THF	60	12.5	99	96
10	LiOH	HFIP	THF	60	12.5	99	87

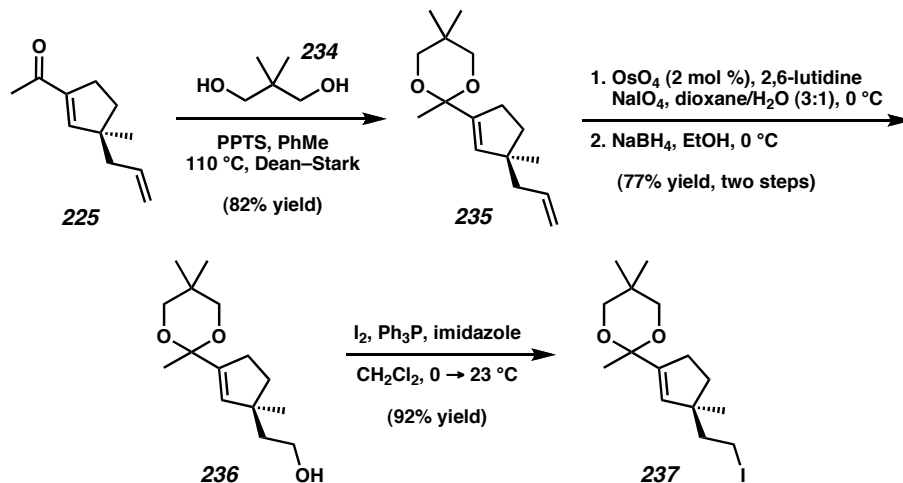
^a TFE = 2,2,2-trifluoroethanol; HFIP = hexafluoro-2-propanol. ^b Reactions performed with 1.5 equiv each of base and additive at 0.1 M in solvent. ^c Determined by GC analysis using an internal standard. ^d Several intermediates observed by TLC and GC analysis.

The reduction of allyl ketone **229** with acidic workup furnished β -hydroxyketone **231** in 90% yield and 1:1.5 dr (Scheme 3.3.5). Application of the devised ring contraction conditions consisting of LiOH and TFE in THF at 60 °C facilitated the preparation of desired acylcyclopentene **225** in 96% yield, and enabled access to multigram quantities of this important intermediate. The production of allyl ketone **229** in 88% ee from the asymmetric allylic alkylation reaction was satisfactory for our synthetic efforts, but we were interested in identifying an appropriate crystalline derivative to enhance the optical purity of our material. We thus pursued the derivatization of acylcyclopentene **225** by conversion to semicarbazone **232** in 92% yield and with a marginal increase in ee to 91%.⁵⁵ Recrystallization of this material provided semicarbazone **232** in 98% ee, which was readily cleaved under acidic conditions to reveal the desired acylcyclopentene (**225**). Further functionalization of semicarbazone **232** with 4-iodobenzyl amine furnished **233**,

and enabled X-ray crystal structure analysis to confirm the absolute stereochemistry of the asymmetric alkylation (Figure 3.3.1).⁵⁶

Scheme 3.3.5. Scale-up, derivatization, and enantioenrichment of acylcyclopentene **225**



Scheme 3.3.6. Completion of D-ring fragment **237**

3.4 STUDIES TOWARD THE FRAGMENT COUPLING OF THE AB AND D-RING FRAGMENTS TOWARD VARIECOLIN

The asymmetric syntheses of AB ring fragments **222** and **223** and D-ring fragment **237** allowed the evaluation of C-ring annulation strategies toward completion of the target. We envisioned that construction of the final two bonds of the tetracyclic core of variocolin could be achieved by a convergent, strategic operation from these advanced intermediates. An important characteristic of the cyclooctadienones generated by the Wolff/Cope rearrangement is the ability of the enone functionality to provide regiocontrol for the reductive generation of nonsymmetrical ketone enolates.⁵⁹ We planned to harness this regiospecific enolate generation to carry out a diastereoselective C(11)³ alkylation of D-ring iodide **237** to produce a derivative of coupled diketone **175** (Scheme 3.1.1). With the fusion of fragments **223** and **237** to produce a derivative of diketone **175**, we envisioned that the final C-ring closure would occur via radical addition

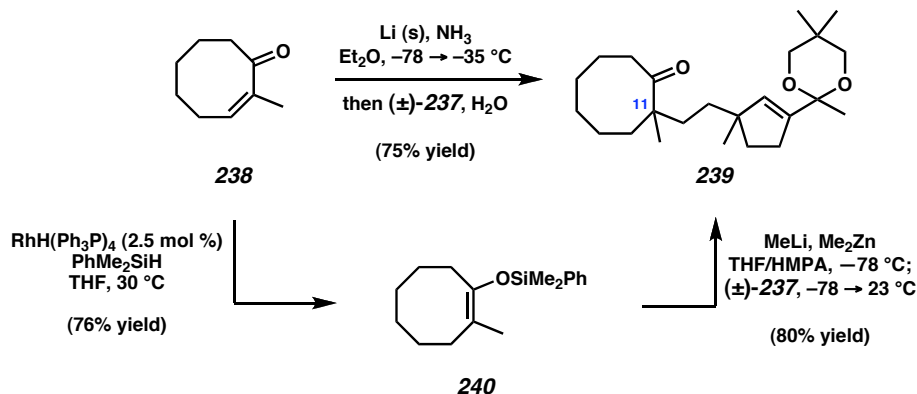
to the conjugated enone. Toward this end, we examined model compounds to determine the feasibility of this convergent approach for the construction of the C ring.

3.4.1 MODEL STUDIES FOR FRAGMENT COUPLING AND C-RING ANNULATION

3.4.1.1 MODEL REDUCTIVE ENONE ALKYLATION AND HYDROSILYLATION/ALKYLATION

The availability of 2-methyl cyclooctenone (**238**) as a model α -substituted eight-membered enone allowed us to evaluate various reductive methods to install the C(11) all-carbon quaternary stereocenter of variocolin (**95**). This can be readily accomplished with **238** in a one-pot dissolving metal (Li/NH₃) reductive alkylation procedure⁶⁰ to generate an intermediate lithium enolate that was subsequently alkylated with D-ring iodide **237** to construct ketone **239** in 75% yield as a mixture of diastereomers (Scheme 3.4.1). An alternative two-step method used a rhodium(I)-catalyzed hydrosilylation of enone **238** with PhMe₂SiH to produce isolable enol silane **240**.⁶¹ This was next exposed to Noyori's⁶² alkylation conditions with D-ring iodide **237** to furnish the desired quaternary ketone (**239**) in 61% yield over two steps. The results of this model study establish a reasonable precedent for the construction of the C(11) quaternary stereocenter via alkylation, and importantly underscore the reactivity of D-ring iodide **237** with a congested lithium enolate (derived from **238**).

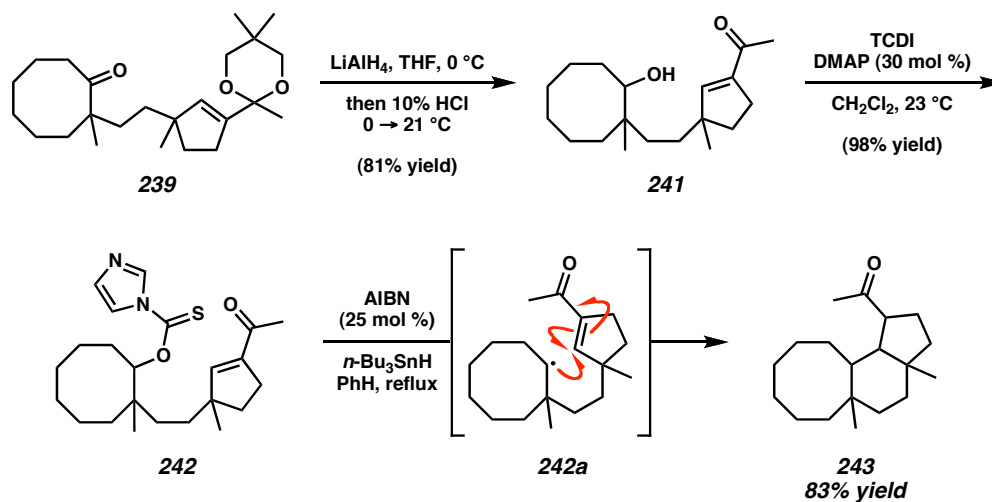
Scheme 3.4.1. Model studies for B–D ring coupling



3.4.1.2 MODEL C-RING RADICAL CYCLIZATION

With a plausible unification of the model fragments to form BD ring ketone **239** established, we pursued a radical-mediated formation of the final C–C bond to complete the C-ring annulation.⁶³ The requisite substrate was prepared from LiAlH_4 reduction of ketone **239** with acidic workup to effect protecting group cleavage and reveal cyclopentene **241** as a mixture of four diastereomers (Scheme 3.4.2). Conversion of the alcohol into imidazolyl thiocarbonate **242** followed by the AIBN-initiated radical cyclization with slow addition of tri-*n*-butyltin hydride formed the final C–C bond of our model BCD ring core (i.e., **243**) for the variocolin sesterterpenes. This significant result provides firm precedent for the C-ring annulation approach for completion of the tetracyclic core of this family, although information concerning the stereochemistry of our model cyclization product could not be conclusively discerned from this system owing to the number of diastereomers present in the starting material and product mixtures.

Scheme 3.4.2. Model radical cyclization for annulation of the C ring



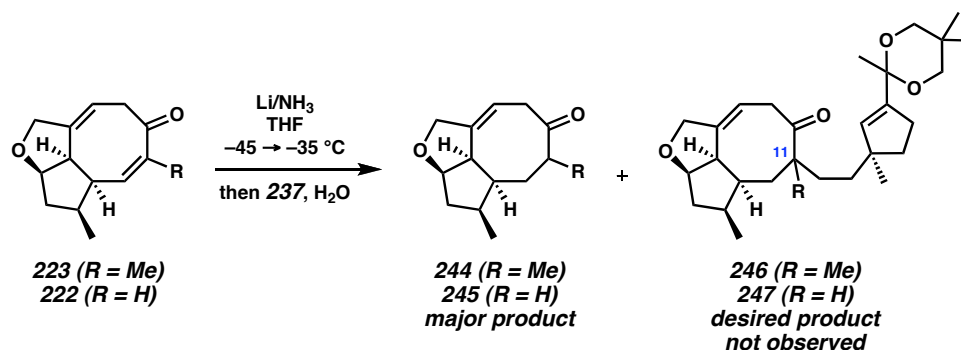
3.4.2 COUPLING STUDIES REGARDING THE ASYMMETRIC AB RING FRAGMENT OF VARIECOLIN

3.4.2.1 ENONE REDUCTIVE ALKYLATION OF THE ASYMMETRIC AB RING FRAGMENT

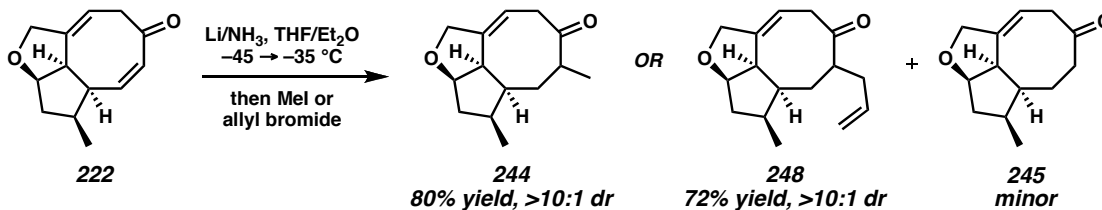
The confirmation of our model alkylation/radical cyclization sequence to form the C ring of variocolin prompted application toward the total synthesis. The direct formation of the C(11) quaternary stereocenter was initially examined using the one-pot reductive alkylation procedure. In the event, dissolving metal reduction of α -substituted cyclooctadienone intermediate **223** and exposure to an excess of D-ring iodide **237** resulted in a number of products, with saturated ketone **244**—the 1,4-reduction product of **223**—as the major component (Scheme 3.4.3). Unfortunately, the desired α -quaternary ketone **246** was not observed. Further investigation of this direct reductive alkylation of

AB ring fragment **222** yielded similar results, thus indicating that D-ring iodide **237** is not sufficiently reactive toward enolates derived from **222** and **223**.

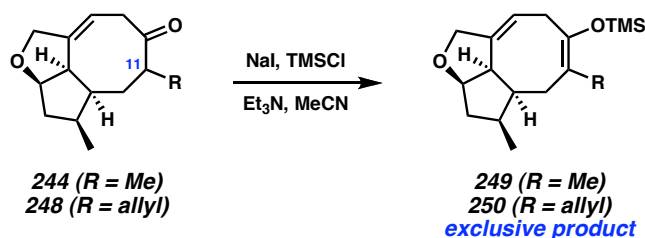
Scheme 3.4.3. Efforts toward the direct reductive alkylation of enones **222** and **223** with iodide **237**



To understand the reactivity difference of the alkylation model system (**238**) and AB ring nucleophiles (**222** and **223**) toward the D-ring iodide (**237**), we explored more reactive electrophiles. Interestingly, the reductive alkylation of enone **222** using either methyl iodide or allyl bromide produced the desired α -tertiary ketones **244** and **248** in good yield and diastereoselectivity with only minor quantities of reduced ketone **245** (Scheme 3.4.4).⁶⁴ These observations provide further evidence that D-ring iodide **237** is not sufficiently reactive toward AB ring nucleophiles derived from **222** and **223**. Due to limited quantities of α -substituted cyclooctadienone **223**, we are currently unable to assess the potential of a direct reductive alkylation with reactive electrophiles (e.g., allyl bromide) to generate the C(11) quaternary stereocenter.

Scheme 3.4.4. Diastereoselective reductive alkylation of **222** with methyl iodide or allyl bromide

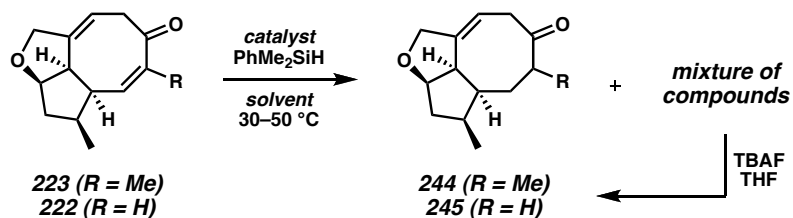
Although we are currently unable to construct the C(11) quaternary stereocenter using a direct reductive alkylation of D-ring iodide **237**, the availability of saturated α -substituted ketones **244** and **248** encouraged us to determine the plausibility for regioselective enolate formation for this alkylative step. Soft enolization conditions employing TMSI/Et₃N⁶⁵ smoothly transformed ketones **244** and **248** to tetrasubstituted enol silanes **249** and **250**, respectively, as the exclusive reaction products (Scheme 3.4.5). The preparation of various latent enolate equivalents thus expands our investigations to include a host of enolate alkylation conditions that will promote the formation of the C(11) all-carbon quaternary stereocenter.

Scheme 3.4.5. Soft enolization of ketones **244** and **248**

3.4.2.2 ENONE HYDROSILYLATION OF THE ASYMMETRIC AB RING FRAGMENT

After identifying an effective two-step procedure to generate substituted enol silanes in model studies (see subsection 3.4.1.1), we explored a potential one-step transformation using a transition-metal catalyzed hydrosilylation reaction. We applied conditions optimized using model studies to α -substituted enone **223** that provided a number of compounds by TLC analysis, including saturated ketone **244** (Scheme 3.4.6).⁶⁶ We were unable to determine if any of the remaining products were the desired silyl enol ether due to difficulties encountered during purification of the side products. Purification of **244** and exposure of the mass balance to TBAF provided **244**, suggesting that some of the products formed under the reaction conditions are isomeric to the desired enol silane. The use of enone **222**, which does not possess α -substitution, yielded similar results, demonstrating a unique conformational preference for the fused [5–5–8] system that inhibits the desired reactivity observed in the model system. The inability to generate a pure enol silane product and isolation difficulties halted further hydrosilylation efforts.

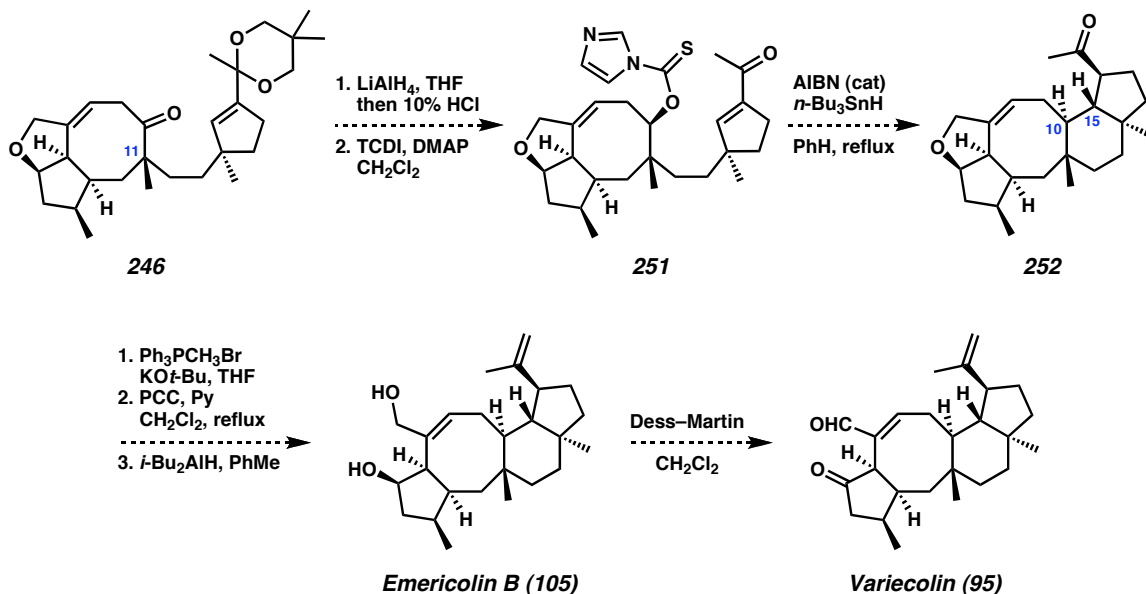
Scheme 3.4.6. Hydrosilylation investigations of enones **222** and **223**



3.5 PROPOSED COMPLETION OF VARIECOLIN

The regioselective preparation of enol silane **249** provides optimism for advancing the AB and D-ring fragments toward variocolin (**95**). Potential access to a variety of D-ring derivatives through our synthetic route, and the observed stereoselective alkylation (**222** → **244**, Scheme 3.4.4) are key elements that predict the success of this strategy. In the event of the desired C(11) alkylation with a suitable D-ring fragment to form ketone **246**, we anticipate that the following transformations will enable the rapid completion of the total synthesis (Scheme 3.5.1). Reduction of ketone **246** and acylation with thiocarbonyldiimidazole (TCDI) should form the imidazolyl thiocarbonate **251**. Radical generation and diastereoselective cyclization should accomplish the C(10)–C(15) ring closure to complete the tetracyclic core of variocolin (i.e., **252**). Carbonyl methylenation, allylic ether oxidation with PCC/pyridine,^{4b,13} and lactone reduction with *i*-Bu₂AlH will produce emericolin B (**105**). Diol oxidation using Dess–Martin periodinane⁶⁷ will then furnish variocolin (**95**).

Scheme 3.5.1. Proposed end game strategy for completion of variocolin



3.6 CONCLUSION

In summary, we have achieved significant progress toward a general, convergent asymmetric approach for the total synthesis of the variocolin sesterterpenoids. Our critical disconnection bisected variocolin into two highly substituted fragments containing the central eight-membered ring and an important all-carbon quaternary stereocenter. The AB ring preparation features an intriguing regioselective cleavage of a fused cyclobutene to terminally differentiated products en route to several advanced α -diazoketones, and set the stage for a key tandem Wolff/Cope rearrangement to construct the eight-membered ring. Importantly, our investigations revealed the proficiency of microwave energy to promote this tandem process, and provided first examples of α -substituted cyclooctadienones to further expand the collection of eight-membered rings available by this method. Our synthetic route to the D ring features a

palladium-catalyzed enantioselective alkylation of racemic vinylogous β -ketoester (\pm)-**181** for the construction of the C(14) quaternary stereocenter. The efficient, large-scale preparation of ketone **229** enabled our development of a new strategy for the synthesis of enantioenriched quaternary cyclopentenones that harnesses the exceptional reactivity of fluorinated lithium alkoxides, and moreover, provides a new variety of substrates for our Pd-catalyzed asymmetric alkylation methodology. We believe that the results achieved from this synthetic endeavor highlight intriguing reactivity and expand synthetic methods that can be of general use for the preparation of natural and non-natural substances. Studies directed toward the coupling of these highly substituted AB and D-ring fragments for the final C-ring annulation and completion of the synthesis are ongoing.

3.7 EXPERIMENTAL SECTION

3.7.1 MATERIALS AND METHODS

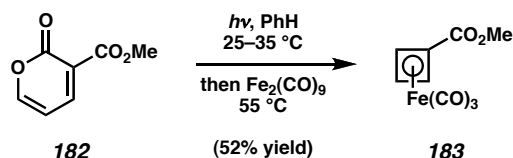
Unless otherwise stated, reactions were performed in flame-dried glassware under an argon or nitrogen atmosphere using dry, deoxygenated solvents. Solvents were dried by passage through an activated alumina column under argon. Reagent grade acetone was used as received. Water (18 M Ω) used as reaction medium was obtained from a Millipore MiliQ water purification system. All starting materials were purchased from commercial sources and used as received, unless otherwise stated. Liquids and solutions were transferred via syringe or positive-pressure cannulation. Brine solutions refer to saturated aqueous sodium chloride solutions. Diiron nonacarbonyl was stored and handled in a glove box. Triethylamine, diisopropylamine, and *t*-BuOH were distilled from CaH₂ prior to use. The following liquids were purified by distillation and stored in a Schlenk tube under nitrogen: acetic acid (from CrO₃), hexamethylphosphoramide (from CaH₂), and oxalyl chloride. Zinc dust was activated over 1% HCl. Solutions of *n*-BuLi, MeLi, *p*-TolMgBr, and MeMgCl were titrated prior to use. Molecular sieves were dried and stored in a 115 °C oven. Anhydrous granular LiOH was pulverized using a mortar and pestle. Lithium wire was stored over mineral oil and washed with hexanes, then methanol, then hexanes prior to use. Previously reported methods were used to prepare Pd₂(pmdba)₃,⁶⁸ (*S*)-*t*-Bu-PHOX ((*S*)-**55**),⁶⁹ fluorinated PHOX ligand **230**,⁴⁶ and RhH(Ph₃P)₄.⁷⁰ Diazomethane (**199**) was freshly prepared from *N*-methyl-*N*-nitroso-*p*-toluenesulfonamide (Diazald) as a solution in Et₂O using a Diazald kit. Diazoethane (**219**) was freshly prepared from *N*-ethyl-*N*-nitrosourea⁷¹ as a solution in Et₂O using a

Diazald kit. Diazoalkane solutions were dried over KOH pellets for ca. 30 min at or below 0 °C and cannula (Teflon) transferred under nitrogen to a dry Erlenmeyer flask prior to use. Reaction temperatures were controlled by an IKA Mag temperature modulator. Ozonolysis reactions were performed with an OzoneLab OL80 Desktop ozone generator. Photochemical irradiation was performed in septum sealed quartz tubes with a Luzchem Photochemical reactor or with a water-cooled Hanovia 450 W medium pressure mercury-vapor immersion lamp. Microwave reactions were performed with a Biotage Initiator Eight 400 W apparatus at 2.45 GHz. Thin-layer chromatography was performed using E. Merck silica gel 60 F254 precoated plates (0.25 mm) and visualized by UV fluorescence quenching, *p*-anisaldehyde, potassium permanganate, or ceric ammonium molybdate staining. SiliCycle SiliaFlash P60 Academic Silica Gel (particle size 40–63 μm; pore diameter 60 Å) was used for flash chromatography. Analytical chiral HPLC was performed with an Agilent 1100 Series HPLC utilizing a Chiralpak OD-H column (4.6 mm x 25 cm) obtained from Daicel Chemical Industries, Ltd. with 1 mL/min mobile phase and visualization at 254 nm. Analytical achiral GC was performed on an Agilent 6850 GC with FID detector using an Agilent DB-WAX (30.0 m x 0.25 mm) column at 1.0 mL/min He carrier gas flow. Chiral GC was performed on an Agilent 6850 GC with FID detector using a Chiraldex GTA column (30.0 m x 0.25 mm, purchased from Bodman Industries) at 1.0 mL/min He carrier gas flow. Optical rotations were measured with a Jasco P-1010 polarimeter at 589 nm using spectrophotometric grade solvents. ¹H and ¹³C NMR spectra were recorded on a Varian Mercury 300 (at 300 MHz and 75 MHz respectively), Varian Inova 500 (at 500 MHz and 126 MHz, respectively) or Varian Inova 600 (at 600 MHz), and are reported relative to Me₄Si (δ 0.0

ppm).⁷² Data for ¹H NMR spectra are reported as follows: chemical shift (δ ppm) (multiplicity, coupling constant (Hz), integration). IR spectra were recorded on a Perkin Elmer Paragon 1000 spectrometer and are reported in frequency of absorption (cm^{-1}). Melting points were acquired using a Buchi Melting Point B-545 instrument and the values are uncorrected. High-resolution mass spectra were acquired using an Agilent 6200 Series TOF with an Agilent G1978A Multimode source in ESI, APCI, or MM (ESI/APCI) ionization mode, in addition to the Caltech Mass Spectral Facility. Crystallographic data have been deposited at the CCDC, 12 Union Road, Cambridge CB2 1EZ, UK, and copies can be obtained on request, free of charge, by quoting the publication citation and the deposition number.

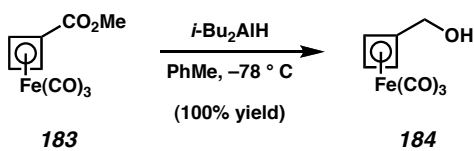
3.7.2 PREPARATIVE PROCEDURES

3.7.2.1 TRICARBONYLIRON-CYCLOBUTADIENE FRAGMENTS



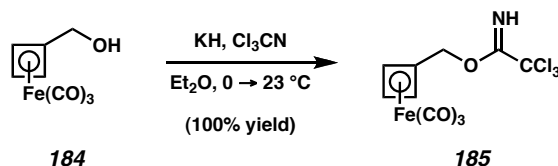
Tricarbonyliron-cyclobutadiene methyl ester 183.^{13b} Pyrone **182** (5.086 g, 33.00 mmol, 1.0 equiv) was dissolved in spectrophotometric grade benzene (1 L, 0.033 M) in a flame-dried 1 L photochemical reactor containing a stir bar, the reactor and lamp were assembled and the solution was sparged with N₂ for 30 min. The resulting degassed solution was irradiated with a Hanovia medium-pressure mercury-vapor lamp affixed with a pyrex filter until consumption of pyrone **182** by TLC (5:1 CH₂Cl₂/EtOAc, typically requires 20 h to 5 d; T_{internal} = 25–35 °C). The lamp was removed from the reactor and the solution was transferred to a dry 3 L flask containing a stir bar, washing the photoreaction with excess benzene (2 x 30 mL). Fe₂(CO)₉ (14.4 g, 39.6 mmol, 1.2 equiv) was weighed into a glass jar in a glove box, transferred out of the box, and added to the reaction. The resulting suspension was warmed to 50 °C (internal) in an oil bath (T = 55–60 °C) and after 2 h at 50 °C, a second portion of Fe₂(CO)₉ (2.40 g, 6.60 mmol, 0.2 equiv) was added to the reaction. After another 1 h, the turbid reaction was cooled to room temperature and filtered through a plug of basic alumina (5 x 8 cm) capped with Celite (5 x 16 cm) washing with excess Et₂O (ca. 400 mL) until the eluent was colorless. The dark yellow solution was concentrated under reduced pressure to a turbid, yellow/brown oil. The crude material was purified by flash chromatography on SiO₂ (2.5

x 24 cm, 15:1 → 9:1 → 4:1 hexanes/Et₂O) to afford tricarbonyliron-cyclobutadiene methyl ester **183** (4.2585 g, 17.03 mmol, 52% yield) as a dark yellow/brown oil that solidified in a -20 °C freezer. $R_f = 0.54$ (2:1 hexanes/EtOAc); ¹H NMR (300 MHz, C₆D₆) δ 3.84 (s, 2H), 3.22 (s, 3H), 3.20 (s, 1H). All other spectral data are consistent with reported values.



Hydroxymethyl cyclobutadiene 184. To a solution of cyclobutadiene ester **183** (9.066 g, 36.27 mmol, 1.0 equiv) in PhMe (120 mL, 0.3 M) at -78 °C was added neat *i*-Bu₂AlH (14.54 mL, 81.60 mmol, 2.25 equiv) dropwise over 15 min with vigorous stirring. Upon consumption of **183** by TLC analysis (typically as last of *i*-Bu₂AlH is added), EtOAc (3.54 mL, dried over MgSO₄, 1.0 equiv) was added and after 5 min the reaction was placed in a 0 °C ice bath. After 30 min the reaction was slowly quenched with a 1 M solution of Na/K tartrate (100 mL) with vigorous stirring. After 5 min, the cooling bath was removed and EtOAc (50 mL) was added to the thick suspension. When the layers became homogeneous (typically 5–8 h), the layers were separated and the aq phase was extracted with Et₂O (2 x 50 mL). The combined organic layers were dried with MgSO₄, filtered, and concentrated in vacuo. The thick oil was dried under high vacuum until a constant mass was achieved to afford hydroxymethyl cyclobutadiene **184** (8.105 g, 36.51 mmol, 100% yield) as a pale brown solid. $R_f = 0.29$ (2:1 hexanes/EtOAc); ¹H NMR (300 MHz, C₆D₆) δ 3.37 (s, 3H), 3.34 (s, 1H), 3.26 (s, 1H), 0.62 (t, $J = 5.9$ Hz, 1H); ¹³C NMR (126 MHz, C₆D₆) δ 214.9, 85.0, 63.9, 62.2, 58.0; IR

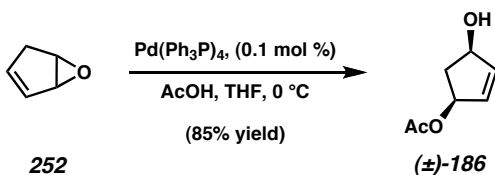
(Neat Film NaCl) 3326 (br), 2932, 2872, 2046, 1963, 1448, 1297, 1070, 997, 822, 613 cm^{-1} ; HRMS (EI+) m/z calc'd for $\text{C}_8\text{H}_6\text{O}_4\text{Fe} [\text{M}]^+$: 221.9616, found 221.9615.



Cyclobutadiene trichloroacetimidate 185. To a round-bottom flask charged with KH (41 mg, 1.0 mmol, 0.057 equiv) and Et_2O (43 mL) at 0°C was added a solution of hydroxymethyl cyclobutadiene **184** (3.86 g, 17.4 mmol, 1.0 equiv) in Et_2O (43 mL, 0.2 M total) by cannula. After 10 min, trichloroacetonitrile (8.7 mL, 87 mmol, 5.0 equiv) was added to the light orange solution dropwise by syringe. Over the course of the addition, the reaction turned dark brown. After 15 min, the ice bath was removed and the reaction was allowed to warm to room temperature. Upon reaching ambient temperature the volatiles were removed in vacuo and the remaining dark brown oil was taken up in hexane (20 mL, from solvent column) with *vigorous* shaking. This solution was filtered through a pad of Celite, and the reaction flask was washed with an additional portion of hexane (20 mL) and filtered. The combined filtrate was concentrated in vacuo to afford trichloroacetimidate **185** (6.38 g, 17.4 mmol, 100% yield) as a clear, pale red oil. This oil was immediately used in the next step without further purification and is not stable to prolonged storage. $R_f = \text{unstable to SiO}_2$; $^1\text{H NMR}$ (500 MHz, C_6D_6) δ 8.22 (br s, 1H), 4.25 (s, 2H), 3.49 (s, 2H), 3.30 (s, 1H); $^{13}\text{C NMR}$ (126 MHz, C_6D_6) δ 214.5, 162.6, 92.0, 76.8, 65.7, 64.9, 64.5; IR (Neat Film NaCl) 3344, 2049, 1971, 1666, 1449, 1368, 1304,

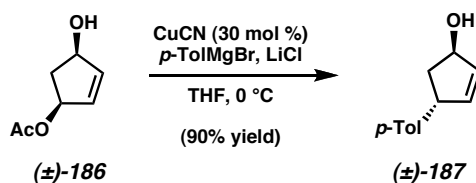
1288 cm^{-1} ; HRMS (FAB+) m/z calc'd for $\text{C}_9\text{H}_6\text{Cl}_3\text{FeNO}_3$ $[\text{M} - \text{CO}]^+$: 336.8763, found 336.8769.

3.7.2.2 AB RING MODEL SYSTEM FRAGMENTS

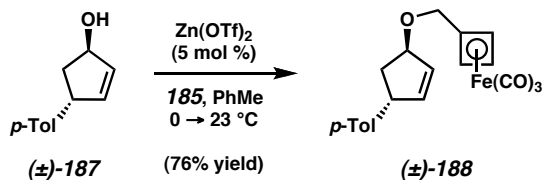


Monoacetate 186.¹⁵ A 1 L 3-neck flask fitted with an addition funnel was charged with $\text{Pd}(\text{Ph}_3\text{P})_4$ (595 mg, 0.515 mmol, 0.001 equiv) and dissolved in THF (258 mL, 2 M). The catalyst solution was cooled to 0 °C and a solution of epoxide **252** (42.29 g corrected, 515.1 mmol, 1.0 equiv) in THF (86 mL) was transferred to the addition funnel via cannulation. To the catalyst solution was added AcOH (29.5 mL, 515.1 mmol, 1.0 equiv) via syringe, followed by the solution of **252** via addition funnel over 20 min. Upon consumption by TLC (reaction turns orange in color when complete) the solution was transferred to a flask washing with EtOAc and concentrated in vacuo. The crude material was purified by flash chromatography on SiO_2 (7 x 5 cm, dry load onto SiO_2 , flush with Et_2O until product elutes by TLC) to afford monoacetate **(±)-186** as a yellow semisolid. This was diluted with heptane (100 mL), concentrated and dried under high vacuum to afford a pale yellow semisolid (62.30 g, 438.3 mmol, 85.1% yield) that completely solidified in a -20 °C freezer. $R_f = 0.33$ (1:1 hexanes/EtOAc); ^1H NMR (300 MHz, CDCl_3) δ 6.12 (ddd, $J = 5.61, 2.07, 1.30$ Hz, 1H), 5.99 (ddd, $J = 5.57, 2.04, 1.06$ Hz, 1H), 5.52–5.47 (m, 1H), 4.76–4.69 (m, 1H), 2.81 (app dt, $J = 14.7, 7.4$ Hz, 1H),

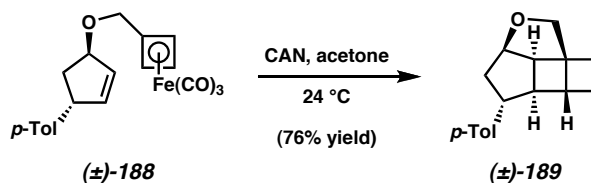
2.06 (s, 3H), 1.72 (br s, 1H), 1.66 (app dt, $J = 14.6, 3.8$ Hz, 1H). All other spectral data are consistent with reported values.



Aryl cyclopentenol 187.^{14b} A flask was charged with LiCl (896.4 mg, 21.1 mmol, 4.0 equiv), flame-dried under vacuum and cooled under nitrogen. To this was added CuCN (142 mg, 1.59 mmol, 0.3 equiv) and the solids were partially dissolved in THF (20 mL) and cooled to 0 °C. To this suspension was added a solution *p*-TolMgBr (15.9 mL, 15.9 mmol, 1 M in Et₂O). After 5 min, a solution of monoacetate (±)-**186** (751.5 mg, 5.29 mmol, 1.0 equiv) in THF (15 mL) over 5 min via cannulation and the flask was washed with additional THF (2 x 1 mL) for a quantitative transfer. Upon consumption of **186** by TLC (ca. 1.5 h), the reaction was slowly quenched with sat aq NH₄Cl (10 mL) and water (5 mL) and stirred vigorously for 30 min. The homogeneous phases were separated, the aq layer was extracted with EtOAc (3 x 30 mL), and the combined organics were dried over MgSO₄, filtered, and concentrated in vacuo. The crude material was purified by flash chromatography on SiO₂ (6:1 → 3:1 → 1:1 hexanes/Et₂O) to afford aryl cyclopentenol **187** (829.7 mg, 4.76 mmol, 90% yield) as a pale yellow oil. $R_f = 0.63$ (1:1 hexanes/EtOAc); ¹H NMR (500 MHz, CDCl₃) δ 7.10 (d, $J = 7.83$, 2H), 7.03 (d, $J = 8.0$ Hz, 2H), 6.04–6.01 (comp m, 2H), 5.05 (d, $J = 5.1$ Hz, 1H), 4.13–4.10 (m, 1H), 2.32 (s, 3H), 2.27 (ddd, $J = 14.1, 8.0, 2.7$ Hz, 1H), 2.09 (ddd, $J = 14.1, 7.0, 5.5$, 1H). All other spectral data are consistent with reported values.

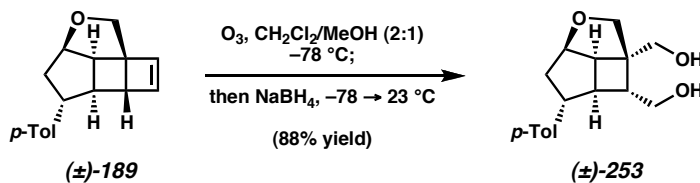


Aryl cyclopentenol ether 188. To a round-bottom flask charged with zinc(II) triflate (14.9 mg, 0.041 mmol, 5 mol %) and PhMe (0.2 mL) at 0 °C was added aryl cyclopentenol **187** (151.3 mg, 0.868 mmol, 1.0 equiv) by syringe. To this suspension was added a solution of cyclobutadiene trichloroacetimidate **185** (370 mg, 1.01 mmol, 1.2 equiv) in PhMe (0.2 mL) by cannula transfer, with further washing by additional PhMe (0.2 mL). A yellow precipitate was observed at the beginning of the addition, and this turned into a thick slurry upon completion of the addition. The ice bath was allowed to expire over 1.5 h and the reaction was stirred for an additional 6 h at ambient temperature. The crude reaction mixture was transferred directly onto a 5 g silica gel loading cartridge and purified with a Teledyne ISCO CombiFlash system using a 40 g silica column (1:0 → 9:1 hexanes/EtOAc) to afford ether **188** (250.8 mg, 0.663 mmol, 76% yield) as a pale yellow oil. $R_f = 0.56$ (4:1 hexanes/EtOAc); $^1\text{H NMR}$ (300 MHz, C_6D_6) δ 7.00 (d, $J = 7.8$ Hz, 2H), 6.94 (d, $J = 7.9$ Hz, 2H), 5.88–5.85 (m, 1H), 4.45–4.44 (m, 1H), 3.96–3.94 (m, 1H), 3.55 (d, $J = 1.2$ Hz, 2H), 3.46 (s, 2H), 3.33 (s, 1H), 2.28 (ddd, $J = 13.8, 6.9, 5.4$ Hz, 1H), 2.14 (s, 3H), 1.86 (ddd, $J = 13.7, 6.9, 5.4$ Hz, 1H); $^{13}\text{C NMR}$ (126 MHz, C_6D_6) δ 215.0, 142.3, 140.1, 135.9, 131.6, 129.5, 127.4, 84.9, 82.5, 64.6 (two lines), 64.0, 62.3, 50.1, 41.2, 21.0; IR (Neat Film NaCl) 2863, 2044, 1959, 1513, 1075, 1048, 613 cm^{-1} ; HRMS (FAB+) m/z calc'd for $\text{C}_{20}\text{H}_{18}\text{O}_4\text{Fe}$ $[\text{M}]^+$: 378.0554, found 378.0551.



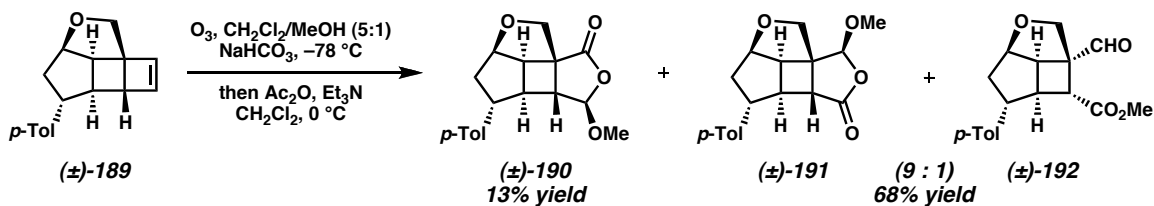
Aryl cyclobutene 189. To a vigorously stirring solution of aryl cyclopentenol ether **188** (683 mg, 1.806 mmol, 1.0 equiv) in acetone (1.81 mL, 1 mM) was added CAN (1.98 g, 3.61 mmol, 2.0 equiv) under ambient atmosphere. After 15 min, a second portion of CAN (1.98 g, 3.61 mmol, 2.0 equiv) was added. After 5 min, TLC showed consumption of **188** (4:1 hexanes/Et₂O, developed twice) and the reaction was quenched by addition of sat aq NaHCO₃ (50 mL). After 15 min, stirring was ceased, the solids were allowed to settle and the supernatant was decanted into a flask (to prevent bumping) and concentrated in vacuo to ca. 50 mL. This slurry and the remnants of the flask were transferred to a separatory funnel with minimal acetone, diluted with brine (10 mL) and pentane (200 mL). The layers were separated, the organic phase was washed with water (2 x 100 mL), and the combined aq layers were extracted with 1:1 hexanes/Et₂O (200 mL). The combined organic layers were concentrated to ca. 25 mL, transferred to a sep funnel and diluted with CH₂Cl₂ (30 mL) and brine (25 mL). The layers were separated, the aq was extracted with CH₂Cl₂ (2 x 30 mL), the organics were dried over MgSO₄, filtered, and concentrated to a dark orange oil. The crude material was purified by flash chromatography on SiO₂ (2.5 x 21 cm, 15:1 → 9:1 hexanes/Et₂O, slow gradient) to afford aryl cyclobutene **189** (326.2 mg, 1.37 mmol, 76% yield) as a colorless oil that solidified in a -20 °C freezer. *R_f* = 0.54 (4:1 hexanes/Et₂O, developed twice); ¹H NMR (500 MHz, CDCl₃) δ 7.11 (d, *J* = 8.2 Hz, 2H), 7.08 (d, *J* = 8.2 Hz, 2H), 6.35 (d, *J* = 2.1

Hz, 1H), 6.31 (d, $J = 2.3$ Hz, 1H), 4.71–4.69 (m, 1H), 3.91 (d, $J = 9.8$ Hz, 1H), 3.87 (d, $J = 9.8$ Hz, 1H), 3.27 (ddd, $J = 8.6, 8.6, 3.9$ Hz, 1H), 3.06 (app t, $J = 3.1$ Hz, 1H), 2.94 (s, 1H), 2.46 (ddd, $J = 13.8, 7.0, 2.3$ Hz, 1H), 2.35 (app t, $J = 4.8$ Hz, 1H), 2.32 (s, 3H), 2.03 (ddd, $J = 13.8, 8.8, 4.9$ Hz, 1H); ^{13}C NMR (126 MHz, CDCl_3) δ 142.9, 140.3, 138.4, 135.6, 129.3, 127.2, 84.1, 71.2, 59.6, 54.9, 52.6, 50.3, 46.5, 44.6, 21.1; IR (Neat Film NaCl) 3025, 2949, 1514, 1074, 1041, 1025, 811, 744 cm^{-1} ; HRMS (FAB+) m/z calc'd for $\text{C}_{17}\text{H}_{17}\text{O}$ $[\text{M} + \text{H} - \text{H}_2]^+$: 237.1279, found 237.1271.



Diol 253. To a solution of aryl cyclobutene **189** (18.0 mg, 75.5 μmol , 1.0 equiv) in a 2:1 mixture of CH_2Cl_2 (1.0 mL) and MeOH (0.5 mL) was added a solution of Sudan Red 7b (25 μL of a 0.05 wt % in MeOH) and cooled to $-78\text{ }^\circ\text{C}$. The resulting pink solution was sparged with a gentle stream of oxygen for ~ 1 min, then ozonolyzed until consumption of **189** by TLC (indicator typically turned colorless just prior to completion). The solution was sparged with oxygen for another 1 min, and NaBH_4 (28.8 mg, 0.76 mmol, 10 equiv) was added and the bath was removed. When the reaction reached room temperature, CH_2Cl_2 (2 mL) was added followed by quenching with 10% HCl (1 mL). The layers were separated, the aq extracted with CH_2Cl_2 (3 x 2 mL), the organics were dried over Na_2SO_4 , filtered, and concentrated in vacuo. The crude material was purified by flash chromatography on SiO_2 to afford diol **253** (18.2 mg, 66.3 μmol , 88% yield) as a colorless oil. $R_f = 0.31$ (3:1 hexanes/EtOAc); ^1H NMR (300 MHz,

CDCl₃) δ 7.09 (d, J = 8.1 Hz, 2H), 7.00 (d, J = 8.0 Hz, 2H), 4.60 (app t, J = 4.3 Hz, 1H), 4.24 (d, J = 11.5 Hz, 1H), 4.10 (d, J = 9.2 Hz, 1H), 3.88–3.78 (comp m, 2H), 3.69 (d, J = 9.2 Hz, 1H), 3.55 (d, J = 11.5 Hz, 1H), 3.42 (ddd, J = 10.6, 7.1, 3.8 Hz, 1H), 3.09 (br s, 2H), 2.82 (dd, J = 8.5, 5.3 Hz, 1H), 2.58 (dd, J = 14.0, 7.2 Hz, 1H), 2.36 (dd, J = 11.0, 5.4 Hz, 1H), 2.31 (s, 3H), 1.99 (app dt, J = 8.7, 4.4 Hz, 1H), 1.73 (ddd, J = 13.9, 10.5, 3.4 Hz, 1H); ¹³C NMR (75 MHz, CDCl₃) δ 143.1, 135.7, 129.3, 127.0, 86.2, 80.6, 63.5, 63.4, 51.4, 50.8, 50.7, 49.1, 44.8, 42.2, 21.1; IR (Neat Film NaCl) 3332 (br), 2922, 1514, 1436, 1100, 1037, 811 cm⁻¹; HRMS (FAB+) m/z calc'd for C₁₇H₂₁O₃ [M + H – H₂]⁺: 273.1491, found 273.1485.

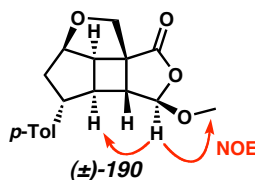


Ozonolysis of cyclobutene **189** to form acetals **190** and **191**, along with aldehyde

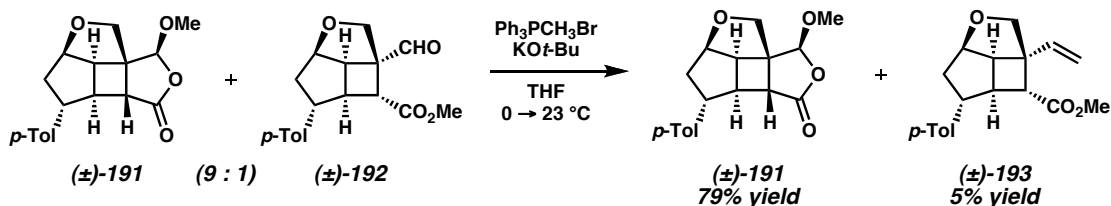
192. To a solution of aryl cyclobutene **189** (49.6 mg, 0.208 mmol, 1.0 equiv) in a 5:1 mixture of CH₂Cl₂ (1.75 mL) and MeOH (0.35 mL, 0.1 M total) was added NaHCO₃ (5.2 mg, 63 μ mol, 0.3 equiv) and a solution of Sudan Red 7b (75 μ L of a 0.05 wt % solution in MeOH). The resulting pink-colored solution was cooled to –78 °C, sparged with a stream of oxygen for 1 min, then ozonolyzed until consumption of **189** by TLC (typically just as indicator turns colorless). The solution was sparged with oxygen for 1 min, the gas inlet was removed and the flask was fitted with a drying tube and warmed to room temperature. The crude reaction was filtered through a cotton plug with CH₂Cl₂ (2 x 1 mL) and benzene (1 mL). The filtrate was concentrated to ca. 0.5 mL in vacuo,

diluted with 5 mL of benzene, and further concentrated to ca. 0.5 mL. This crude was dissolved in CH_2Cl_2 (2.1 mL), cooled to 0 °C, and Ac_2O (58.5 μL , 0.624 mmol, 3 equiv) and Et_3N (37.7 μL , 0.270 mmol, 1.3 equiv) were added. After 5 min the bath was removed and the reaction was stirred at room temperature for 5 h, at which point the reaction was diluted with CH_2Cl_2 (25 mL), washed with 5% H_2SO_4 (3 x 5 mL), sat aq NaHCO_3 (3 x 5 mL), brine, and dried over Na_2SO_4 . The crude pale yellow oil was purified by flash chromatography on SiO_2 (4:1 \rightarrow 3:1 \rightarrow 1:1 hexanes/ EtOAc) to furnish acetal **190** (8.3 mg, 27.6 μmol , 13% yield) as a colorless oil and an inseparable 9:1 mixture of acetal **191** and aldehyde **192** (42.6 mg, 0.142 mmol, 68% yield) as a pale yellow oil.

Acetal 190. $R_f = 0.52$ (1:2 hexanes/ Et_2O); ^1H NMR (500 MHz, CDCl_3) δ 7.13 (d, $J = 7.8$ Hz, 2H), 7.05 (d, $J = 8.1$ Hz, 2H), 5.36 (s, 1H), 4.75 (dd, $J = 5.2, 4.0$ Hz, 1H), 4.13 (d, $J = 9.7$ Hz, 1H), 4.01 (d, $J = 9.7$ Hz, 1H), 3.56 (app t, $J = 6.3$ Hz, 1H), 3.49 (s, 3H), 3.48–3.45 (m, 1H), 2.58–2.52 (comp m, 3H), 2.33 (s, 3H), 1.80 (ddd, $J = 14.4, 10.9, 3.7$ Hz, 1H); ^{13}C NMR (126 MHz, CDCl_3) δ 175.5, 141.3, 136.3, 129.5, 127.2, 109.0, 85.9, 73.0, 56.8, 55.5, 51.9, 51.3, 51.2, 44.5, 44.2, 21.1; IR (Neat Film NaCl) 2927, 1773, 1515, 1353, 1182, 1143, 1118, 1018, 990, 930, 814 cm^{-1} ; HRMS (FAB+) m/z calc'd for $\text{C}_{18}\text{H}_{21}\text{O}_4$ $[\text{M} + \text{H}]^+$: 301.1440, found 301.1448. Relative stereochemistry determined by NOE interactions shown below.



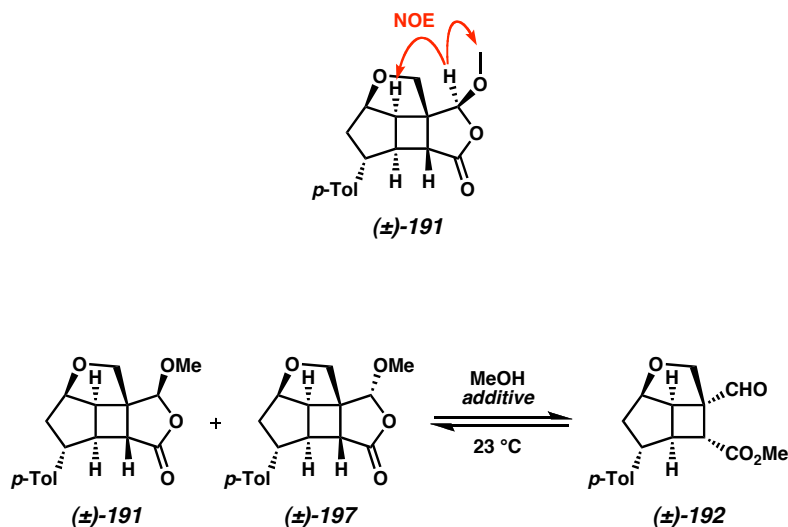
Mix of acetal **191 and aldehyde **192**.** Aldehyde **192** was difficult to isolate as a pure compound, as it usually contained varying quantities of acetal **191**. It has the following spectrum: $^1\text{H NMR}$ (300 MHz, CDCl_3) δ 9.76 (s, 1H), 7.10 (d, $J = 8.3$ Hz, 2H), 7.04 (d, $J = 8.2$ Hz, 2H), 4.69 (dd, $J = 4.5, 3.9$ Hz, 1H), 4.10 (d, $J = 9.6$ Hz, 1H), 3.91 (d, $J = 9.7$ Hz, 1H), 3.70 (s, 3H), 3.59 (dd, $J = 8.3, 5.3$ Hz, 1H), 3.45 (ddd, $J = 10.7, 7.1, 3.7$ Hz, 1H), 3.06–2.97 (comp m, 2H), 2.63 (dd, $J = 14.2, 7.3$ Hz, 1H), 2.31 (s, 3H), 1.81 (ddd, $J = 14.1, 10.6, 3.4$ Hz, 1H).



Wittig methylenation to form olefin **193 and recover acetal **191**.** To a suspension of methyltriphenylphosphonium bromide (23.6 mg, 66 μmol , 0.58 equiv) in THF (0.4 mL) at 0°C was added $\text{KO}t\text{-Bu}$ (6.4 mg, 57 μmol , 0.5 equiv) in one portion. The white suspension immediately turned bright yellow in color and was stirred for 15 min, at which point a solution of a $\sim 9:1$ mixture acetal **191** and aldehyde **192** (34.2 mg, 114 μmol , 1.0 equiv) in THF (0.2 mL) was quantitatively transferred via cannulation. After 30 min, the reaction was quenched with 0.5 mL water and diluted with CH_2Cl_2 (3 mL). The layers were separated, the aq layer was extracted with CH_2Cl_2 (3 x 2 mL), the organics were dried over Na_2SO_4 , filtered, and concentrated in vacuo. The crude material was purified by preparative TLC on SiO_2 (2:1 hexanes/ EtOAc) to give olefin **193** (1.8 mg, 6.0 μmol , 5% yield) as a colorless oil and recovered acetal **191** (27.1 mg, 90.2 μmol , 79% yield) as a colorless oil.

Olefin 193. $R_f = 0.62$ (2:1 hexanes/EtOAc); ^1H NMR (500 MHz, CDCl_3) δ 7.09 (d, $J = 8.0$ Hz, 2H), 7.05 (d, $J = 8.2$ Hz, 2H), 5.94 (dd, $J = 17.5, 10.8$ Hz, 1H), 5.18 (dd, $J = 10.8, 1.1$ Hz, 1H), 5.14 (dd, $J = 17.5, 1.1$ Hz, 1H), 4.64 (app t, $J = 4.3$ Hz, 1H), 4.03 (d, $J = 9.2$ Hz, 1H), 3.62 (s, 3H), 3.57 (d, $J = 9.2$ Hz, 1H), 3.40 (ddd, $J = 10.7, 7.3, 3.8$ Hz, 1H), 3.26 (dd, $J = 8.5, 5.2$ Hz, 1H), 3.04–3.01 (m, 1H), 2.98 (d, $J = 5.5$ Hz, 1H), 2.64 (dd, $J = 14.1, 7.3$ Hz, 1H), 2.31 (s, 3H), 1.78 (ddd, $J = 14.0, 10.5, 3.3$ Hz, 1H); ^{13}C NMR (126 MHz, CDCl_3) δ 173.3, 142.6, 135.6, 134.7, 129.2, 127.1, 116.3, 86.5, 78.9, 55.2, 53.0, 51.6, 51.2, 51.1, 45.0, 40.8, 21.1; IR (Neat Film NaCl) 2952, 2922, 1733, 1515, 1435, 1210, 1158, 1055, 1037, 919, 812 cm^{-1} ; HRMS (EI+) m/z calc'd for $\text{C}_{19}\text{H}_{22}\text{O}_3$ $[\text{M}]^+$: 298.1569, found 298.1580.

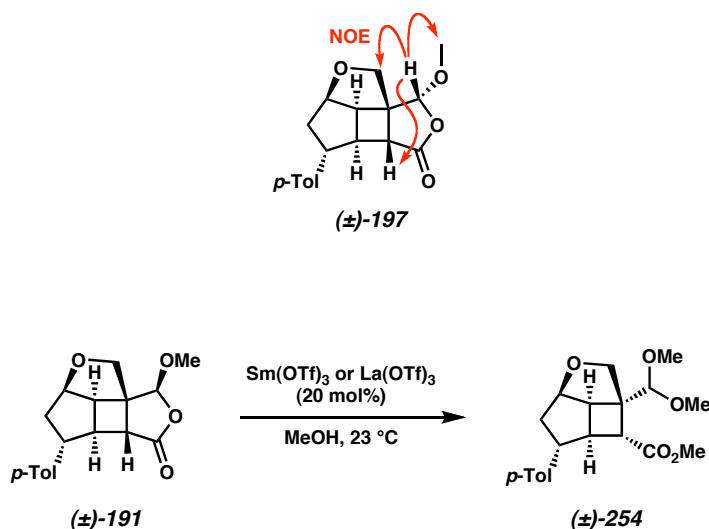
Acetal 191. $R_f = 0.33$ (1:2 hexanes/ Et_2O); ^1H NMR (500 MHz, CDCl_3) δ 7.09 (d, $J = 8.0$ Hz, 2H), 7.06 (d, $J = 8.1$ Hz, 2H), 5.40 (s, 1H), 4.71 (dd, $J = 5.4, 3.1$ Hz, 1H), 4.08 (d, $J = 10.5$ Hz, 1H), 3.78 (d, $J = 10.5$ Hz, 1H), 3.55 (app pentet, $J = 6.1$ Hz, 1H), 3.48 (s, 3H), 3.31 (dd, $J = 7.4, 5.7$ Hz, 1H), 2.89 (d, $J = 2.4$ Hz, 1H), 2.66 (ddd, $J = 7.6, 5.2, 2.4$ Hz, 1H), 2.53 (dd, $J = 13.8, 6.7$ Hz, 1H), 2.31 (s, 3H), 1.76 (ddd, $J = 13.9, 11.7, 3.2$ Hz, 1H); ^{13}C NMR (126 MHz, CDCl_3) δ 177.7, 140.1, 136.1, 129.4, 127.1, 106.3, 85.7, 71.8, 56.8, 55.0, 51.1, 50.0, 47.9, 46.2, 43.9, 21.1; IR (Neat Film NaCl) 2925, 2847, 1772, 1516, 1352, 1207, 1168, 1144, 1108, 1042, 943, 814, 729, 705 cm^{-1} ; HRMS (FAB+) m/z calc'd for $\text{C}_{18}\text{C}_{21}\text{O}_4$ $[\text{M} + \text{H}]^+$: 301.1440, found 301.1444. Relative stereochemistry determined by NOE interactions shown below.



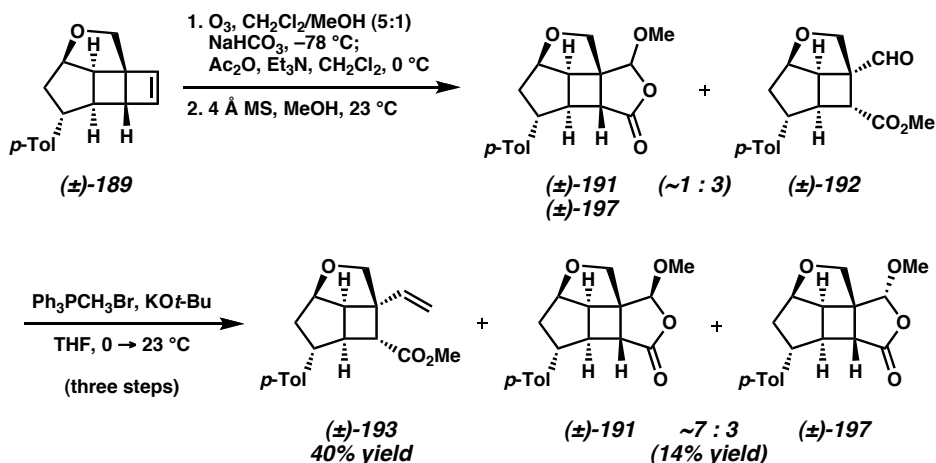
Equilibration of acetal 191. To a solution of pure acetal **191** in MeOH (25 mM) as added the appropriate additive (MS = 0.5 mg/ μmol ; Lewis acid = 20 mol %). The reaction atmosphere was purged with nitrogen, capped and stirred at ambient temperature. After 20–24 h the reaction was diluted with Et₂O, filtered through a small plug of SiO₂ and concentrated in vacuo. The crude filtrate was then analyzed by ¹H NMR analysis. In addition to acetal **191** and aldehyde **192**, acetal diastereomer **197** was identified as a minor product.

Acetal 197. R_f = 0.19 (1:2 hexanes/Et₂O); ¹H NMR (500 MHz, CDCl₃) δ 7.1 (d, J = 8.0 Hz, 2H), 7.06 (d, J = 8.1 Hz, 2H), 5.30 (s, 1H), 4.68 (dd, J = 5.6, 3.3 Hz, 1H), 4.07 (d, J = 9.5 Hz, 1H), 3.72 (dd, 7.2, 6.2 Hz, 1H), 3.69 (d, J = 9.5 Hz, 1H), 3.63 (s, 3H), 3.52–3.47 (m, 1H), 2.85 (d, J = 2.7 Hz, 1H), 2.66 (ddd, J = 7.7, 5.0, 2.7 Hz, 1H), 2.54 (dd, J = 13.9, 6.8 Hz, 1H), 2.31 (s, 3H), 1.79 (ddd, J = 14.0, 11.5, 3.3 Hz, 1H); ¹³C NMR (126 MHz, CDCl₃) δ 175.8, 140.8, 136.1, 129.4, 127.1, 104.0, 86.0, 72.7, 58.7, 54.5, 50.2 (two lines), 47.7, 44.8, 44.0, 21.1; IR (Neat Film NaCl) 2922, 1770, 1515, 1450, 1386, 1209, 1170, 1106, 1041, 995, 942, 813 cm⁻¹; HRMS (MM: ESI/APCI) m/z calc'd for

$C_{18}H_{21}O_4$ $[M + H]^+$: 301.1434, found 301.1432. Relative stereochemistry determined by NOE analysis as shown below.



Dimethyl acetal 254. To a solution of acetal **191** (1.0 equiv) in MeOH (25 mM) was added either $La(OTf)_3$ or $Sm(OTf)_3$ (20 mol %). The reaction was stirred until complete conversion by TLC, diluted with Et_2O , filtered through a plug of Celite, and concentrated in vacuo. The crude 1H NMR showed dimethyl acetal **254** as the exclusive product. $R_f = 0.36$ (1:2 hexanes/ Et_2O); 1H NMR (600 MHz, $CDCl_3$) δ 7.08 (d, $J = 7.9$ Hz, 2H), 7.04 (d, $J = 8.1$ Hz, 2H), 4.69 (s, 1H), 4.58 (dd, $J = 4.8, 3.8$ Hz, 1H), 3.88 (d, $J = 9.2$ Hz, 1H), 3.86 (d, $J = 9.2$ Hz, 1H), 3.67 (s, 3H), 3.51 (s, 3H), 3.39 (s, 3H), 3.36 (ddd, $J = 10.7, 7.4, 3.8$ Hz, 1H), 3.23 (dd, $J = 8.7, 5.3$ Hz, 1H), 2.93 (ddd, $J = 9.1, 5.6, 3.8$ Hz, 1H), 2.82 (d, $J = 5.7$ Hz, 1H), 2.60 (dd, $J = 14.1, 7.4$ Hz, 1H), 2.30 (s, 3H), 1.75 (ddd, $J = 14.0, 10.3, 3.5$ Hz, 1H); ^{13}C NMR (126 MHz, $CDCl_3$) δ 174.1, 142.7, 135.6, 129.2, 127.1, 105.0, 85.8, 75.0, 58.3, 56.6, 54.5, 52.1, 51.7, 51.4, 49.4, 45.0, 42.4, 21.1; IR (Neat Film NaCl) 2952, 1727, 1515, 1435, 1362, 1210, 1069, 1042, 977, 813 cm^{-1} ; HRMS (FAB+) m/z calc'd for $C_{20}H_{25}O_5$ $[M + H - H_2]^+$: 345.1702, found 345.1701.

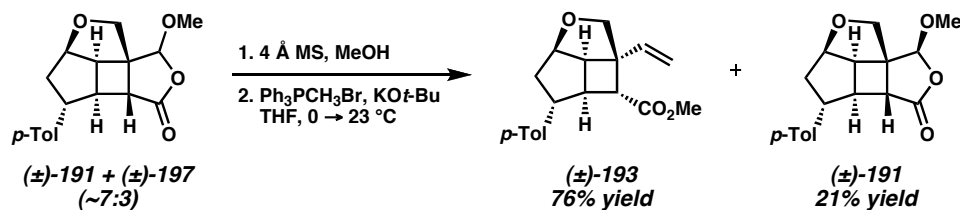


Conversion of cyclobutene 189 over three steps to olefin 193 and acetals 191 and 197. A solution of cyclobutene **189** (326.2 mg, 1.369 mmol, 1.0 equiv) in $\text{CH}_2\text{Cl}_2/\text{MeOH}$ (5:1, 27.4 mL, 0.05 M) containing NaHCO_3 (34.5 mg, 0.411 mmol, 0.3 equiv) and Sudan Red 7b (150 μL of a 0.05 wt % solution in MeOH) at $-78\text{ }^\circ\text{C}$ was sparged with a stream of oxygen for ~ 1 min and ozonolyzed until consumption by TLC analysis (typically as indicator turned colorless). After sparging with oxygen for an additional 3 min, the reaction was capped with a drying tube and warmed to room temperature. The solution was filtered through a cotton plug, washing with benzene (3 mL). The reaction was concentrated in vacuo to ~ 2 mL, and to this flask was added a stir bar, septum, and the flask was evacuated/purged briefly (3x). To the crude was added CH_2Cl_2 (13.7 mL), the solution was cooled to $0\text{ }^\circ\text{C}$, and to this was added Ac_2O (387 μL , 4.11 mmol, 3.0 equiv) and Et_3N (286 μL , 2.05 mmol, 1.5 equiv). The bath was removed and the reaction was stirred at room temperature for 8 h, diluted with CH_2Cl_2 (25 mL), washed with 2% HCl (10 mL), then 10% NaOH (10 mL), dried over MgSO_4 , filtered, and concentrated in vacuo to a pale yellow oil. The crude oil was purified by flash chromatography on SiO_2 (2.5 x 8 cm, 4:1 \rightarrow 1:1 hexanes/ Et_2O) to afford acetal **190** (61.5 g, 0.205 mmol, 15%

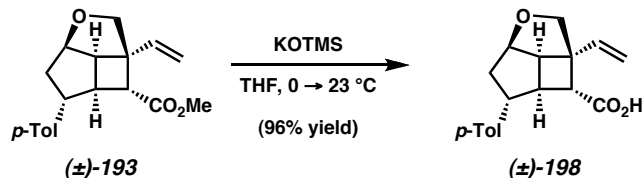
yield) and a mixture of aldehyde **192** and acetals **191** and **197** (293.5 mg, 0.977 mmol, 71% yield).

The mixture of desired isomers (293.5 mg) was dissolved in MeOH (19.5 mL, 0.05 M) and to this was added oven-dried 4 Å MS (489 mg, 0.5 g/mmol). After 24 h at room temperature, the reaction was diluted with EtOAc (20 mL), filtered through a plug of Celite, and concentrated to a turbid yellow oil. This was dissolved in CH₂Cl₂ and passed through a small SiO₂ plug and concentrated in vacuo to afford a pale yellow oil (312.1 mg).

To a solution of methyltriphenylphosphonium bromide (390 mg, 1.09 mmol, 1.05 equiv) at 0 °C was added KO^t-Bu (105 mg, 0.935 mmol, 0.9 equiv). The resulting bright yellow solution was stirred for 1 h, and a solution of aldehyde **192** and acetals **191** and **197** (312.1 mg) in THF (2 mL) was quantitatively transferred via cannulation. After 10 min, the bath was removed and at 5 h the reaction was quenched with water (5 mL) and diluted with Et₂O (5 mL). The layers were separated, the aq was extracted with Et₂O (2 x 10 mL), the combined organics were dried over Na₂SO₄, filtered, and concentrated in vacuo to a pale yellow oil. The crude material was purified by flash chromatography on SiO₂ (2.5 x 15 cm, 9:1 → 1:1 hexanes/Et₂O) to afford olefin **193** (162.2 mg, 0.544 mmol, 40% yield over three steps) and a ~7:3 mixture of acetals **191** and **197** (59.5 mg, 0.198 mmol, 14% yield over three steps).

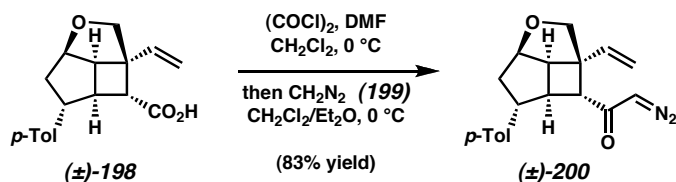


Recycling of acetals **191 and **197**.** A ~7:3 mixture of acetals **191** and **197** (60.7 mg, 0.202 mmol) were equilibrated in MeOH with 4 Å MS to ~3:1 mixture of aldehyde **192** and acetals **191** and **197**, and the resulting crude was olefinated as detailed above with methyltriphenylphosphonium bromide (1.5 equiv) and KO*t*-Bu (1.25 equiv) and purified by flash chromatography on SiO₂ to provide olefin **193** (46.2 mg, 0.155 mmol, 76% yield over two steps) and acetal **191** (13.0 mg, 0.432 mmol, 21% yield over two steps).



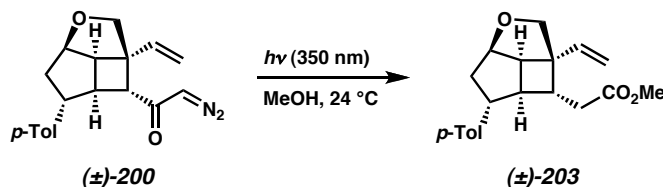
Acid **198.** To a solution of olefin **193** (162.2 mg, 0.544 mmol, 1.0 equiv) in THF (10.9 mL, 0.05 M) at 0 °C was added KOTMS (698 mg, 5.44 mmol, 10 equiv) in one portion. The cooling bath was removed and the reaction was stirred until consumption of **193** by TLC analysis (typically 5–6 h). The reaction was cooled to 0 °C and slowly quenched with 1 N HCl (10 mL), diluted with EtOAc (20 mL) and brine (5 mL). The layers were separated, the aq was extracted with EtOAc (3 x 20 mL), the combined organics were dried over Na₂SO₄, filtered, and concentrated to a pale yellow semisolid. The crude material was purified by flash chromatography on SiO₂ (1:1 hexanes/EtOAc) to give acid **198** (148.7 mg, 0.523 mmol, 96% yield) as a white solid. $R_f = 0.23$ (2:1 hexanes/EtOAc); ¹H NMR (500 MHz, CDCl₃) δ 7.09 (d, $J = 8.0$ Hz, 2H), 7.04 (d, $J = 8.1$ Hz, 2H), 6.00 (dd, $J = 17.4, 10.8$ Hz, 1H), 5.21 (dd, $J = 10.8, 1.1$ Hz, 1H), 5.17 (dd, $J = 17.6, 1.2$ Hz, 1H), 3.64 (dd, $J = 4.7, 3.7$ Hz, 1H), 4.04 (d, $J = 9.3$ Hz, 1H), 3.57 (d, $J = 9.3$

Hz, 1H), 3.40 (ddd, $J = 10.6, 7.3, 3.6$ Hz, 1H), 3.26 (dd, $J = 8.2, 5.2$ Hz, 1H), 3.00–2.95 (comp m, 2H), 2.64 (d, $J = 14.2, 7.3$ Hz, 1H), 2.31 (s, 3H), 1.78 (ddd, $J = 14.0, 10.5, 3.3$ Hz, 1H); ^{13}C NMR (126 MHz, CDCl_3) δ 177.7, 142.6, 135.7, 134.4, 139.3, 127.7, 116.6, 86.6, 79.0, 54.9, 53.2, 51.1 (two lines), 44.9, 40.8, 21.1; IR (Neat Film NaCl) 2923, 1729, 1700, 1515, 1418, 1223, 1053, 992, 918, 812 cm^{-1} ; HRMS (FAB+) m/z calc'd for $\text{C}_{18}\text{H}_{21}\text{O}_3$ $[\text{M} + \text{H}]^+$: 285.1491, found 285.1495.



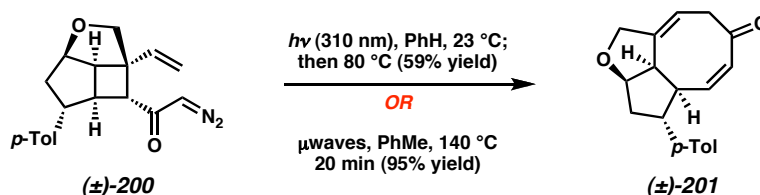
α -Diazoketone 200. To a solution of acid **198** (14.7 mg, 51.7 μmol , 1.0 equiv) in CH_2Cl_2 (2 mL, 0.025 M) at 0 $^\circ\text{C}$ was added a solution of oxalyl chloride (107 μL of a 1.45 M solution in CH_2Cl_2 , 155 μmol , 3.0 equiv), followed by 1 drop of DMF. The reaction was stirred for 1 h, at which point the stir bar was removed and the volatiles were removed on a rotovap purged with argon. The septum and stir bar were replaced and the crude material was further dried under high vacuum for 10 min. The resulting crude semisolid was partially dissolved in CH_2Cl_2 (1 mL) and transferred quantitatively via Teflon cannula to a vigorously stirring solution of excess diazomethane (**199**, 5–8 mL) at 0 $^\circ\text{C}$. After 30 min the cooling bath was removed, and after a further hour the diazomethane was pulled off via water aspirator. The pale yellow solution was filtered through a small SiO_2 plug (Et_2O) and concentrated in vacuo. The crude material was purified by flash chromatography on SiO_2 (9:1 \rightarrow 3:1 hexanes/ EtOAc) to afford α -diazoketone **200** (13.2 mg, 42.8 μmol , 83% yield) as a bright yellow oil that solidified

in a $-20\text{ }^{\circ}\text{C}$ freezer. $R_f = 0.31$ (2:1 hexanes/EtOAc); $^1\text{H NMR}$ (500 MHz, CDCl_3) δ 7.07 (d, $J = 7.9$ Hz, 2H), 7.03 (d, $J = 7.9$ Hz, 2H), 6.01 (dd, 17.5, 10.8 Hz, 1H), 5.17 (d, $J = 10.8$ Hz, 1H), 5.11–5.06 (br m, 2H), 4.64 (app t, $J = 4.0$ Hz, 1H), 3.97 (br d, $J = 9.1$ Hz, 1H), 3.66 (br d, $J = 8.6$ Hz, 1H), 3.36 (ddd, $J = 10.6, 7.7, 3.5$ Hz, 1H), 3.19 (br s, 1H), 3.11 (br s, 1H), 2.92 (br s, 1H), 2.64 (dd, $J = 14.2, 7.3$ Hz, 1H), 2.30 (s, 3H), 1.78 (ddd, $J = 13.7, 10.5, 3.0$ Hz, 1H); $^{13}\text{C NMR}$ (126 MHz, CDCl_3) δ 193.6, 142.5, 135.7, 134.9, 129.3, 127.1, 116.0, 86.5, 78.6, 60.8, 55.3, 53.6, 51.4, 44.9, 40.5, 30.4, 21.1; IR (Neat Film NaCl) 2955, 2921, 2100, 1633, 1514, 1370, 1352, 1048, 812 cm^{-1} ; HRMS (FAB+) m/z calc'd for $\text{C}_{19}\text{H}_{21}\text{O}_2\text{N}_2$ $[\text{M} + \text{H}]^+$: 309.1603, found 309.1619.



Homologated ester 203. A solution of α -diazoketone **200** (3.2 mg, 104 μmol) in MeOH (5.2 mL, 2 mM) in a dried quartz tube was irradiated in a Luzchem rayonette ($\lambda = 350$ nm) for 1.5 h. The solution was concentrated in vacuo and revealed homologated ester **203** as the sole product by crude $^1\text{H NMR}$. An analytical sample was obtained from purification by preparative TLC on SiO_2 (2:1 hexanes/EtOAc) to give **203** (2.4 mg, 7.7 μmol , 74% yield) as a colorless oil. $R_f = 0.43$ (2:1 hexanes/EtOAc); $^1\text{H NMR}$ (500 MHz, CDCl_3) δ 7.07 (d, $J = 7.5$ Hz, 2H), 7.02 (d, $J = 7.5$ Hz, 2H), 5.89 (dd, $J = 16.9, 10.2$ Hz, 1H), 5.22 (d, $J = 10.7$ Hz, 1H), 5.13 (d, $J = 17.5$ Hz, 1H), 4.64 (app t, $J = 3.9$ Hz, 1H), 3.97 (d, $J = 8.7$ Hz, 1H), 3.51 (s, 3H), 3.50 (d, $J = 8.7$ Hz, 1H), 3.46–3.42 (m, 1H), 3.23 (dd, $J = 7.9, 5.8$ Hz, 1H), 2.61 (dd, $J = 14.1, 7.3$ Hz, 1H), 2.54–2.36 (comp

m, 3H), 2.30 (s, 3H), 2.11 (app dt, $J = 7.7, 3.8$ Hz, 1H), 1.78 (ddd, $J = 12.7, 10.4, 2.1$ Hz, 1H); ^{13}C NMR (126 MHz, CDCl_3) δ 173.1, 143.6, 135.5, 135.3, 129.2, 127.1, 116.4, 86.7, 79.2, 52.4, 51.9, 51.6, 50.1, 47.0, 46.9, 45.0, 37.2, 21.1; IR (Neat Film NaCl) 2951, 2922, 1736, 1514, 1435, 1207, 1163, 1041, 916, 808 cm^{-1} ; HRMS (EI+) m/z calc'd for $\text{C}_{20}\text{H}_{24}\text{O}_3$ $[\text{M}]^+$: 312.1726, found 312.1725.

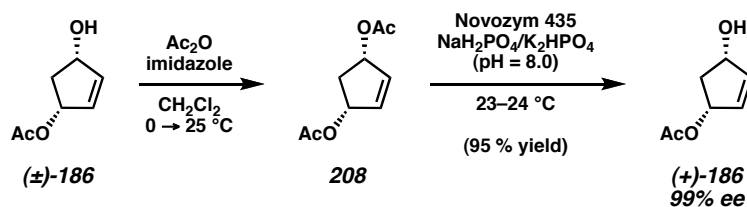


Cyclooctadienone 201. *Photochemical/Thermal:* A solution of α -diazoketone **200** (3.5 mg, 11.4 μmol) in PhH (5.7 mL, 2 mM) in a dried quartz tube was irradiated in a Luzchem photochemical reactor ($\lambda = 310$ nm) for 10 min, and then the lamp was turned off and the quartz tube was placed in an 80 °C oil bath for 2 h. The reaction was concentrated in vacuo and purified by preparative TLC on SiO_2 (1:1 hexanes/ Et_2O , developed twice) to give cyclooctadienone **201** (1.9 mg, 6.8 μmol , 59% yield) as a colorless oil.

Microwave (thermal): A solution of α -diazoketone **200** (2.3 mg, 7.5 μmol) in PhMe (1.5 mL, 5 mM) was prepared in a nondried microwave vial containing a stir bar under ambient atmosphere. The vial was sealed and irradiated in a Biotage Initiator microwave reactor at 400 W until the temperature reached 140 °C, and the temperature was maintained for 20 min. The vial was cooled to room temperature, the seal was removed, and the contents were concentrated in vacuo. Reaction conversion was monitored by crude ^1H NMR analysis (C_6D_6). The crude material was purified by preparative TLC on

SiO₂ (2:1 hexanes/EtOAc) to give **201** (2.0 mg, 7.1 μmol, 95% yield) as a colorless oil that solidified in a -20 °C freezer. $R_f = 0.32$ (3:1 hexanes/EtOAc); ¹H NMR (CDCl₃, 500 MHz) δ 7.17–7.13 (comp m, 4H), 5.80–5.73 (comp m, 2H), 5.63–5.59 (m, 1H), 4.76 (d, $J = 5.2$ Hz, 1H), 3.66 (dd, $J = 10.8, 5.9$ Hz, 1H), 3.41 (dd, $J = 14.7, 8.1$ Hz, 1H), 3.23 (app t, $J = 11.3$ Hz, 1H), 3.13–3.05 (comp m, 2H), 2.34 (s, 3H), 2.30 (dd, $J = 13.8, 5.9$ Hz, 1H), 1.93 (ddd, $J = 13.8, 12.1, 4.6$ Hz, 1H); ¹³C NMR (126 MHz, CDCl₃) δ 203.3, 146.8, 139.7, 138.4, 136.9, 129.7, 129.2, 127.9, 144.2, 85.3, 72.2, 53.9, 50.6, 48.1, 45.4, 41.4, 21.2; ¹H NMR (500 MHz, C₆D₆) δ 6.99 (d, $J = 7.7$ Hz, 2H), 6.86 (d, $J = 6.9$ Hz, 2H), 5.78–5.75 (m, 1H), 5.55 (d, $J = 13.6$ Hz, 1H), 5.11–5.08 (m, 1H), 4.35 (app t, $J = 5.13$ Hz, 1H), 4.24 (d, $J = 13.1$ Hz, 1H), 4.11 (d, $J = 13.2$ Hz, 1H), 3.04–2.89 (comp m, 4H), 2.70 (app t, $J = 11.3$ Hz, 1H), 2.20 (dd, $J = 13.6, 5.9$ Hz, 1H), 2.15 (s, 3H), 1.53–1.46 (m, 1H); ¹³C NMR (126 MHz, C₆D₆) δ 201.9, 147.2, 139.2, 138.6, 136.8, 130.1, 130.0, 128.7, 114.4, 85.5, 72.5, 53.8, 51.2, 48.3, 45.9, 41.9, 21.3; IR (Neat Film NaCl) 3015, 2922, 1693, 1661, 1516, 1435, 1318, 1208, 1062, 1030, 817 cm⁻¹; HRMS (MM: ESI/APCI) m/z calc'd for C₁₉H₁₉O₂ [M - H]⁺: 279.1319, found 279.1384.

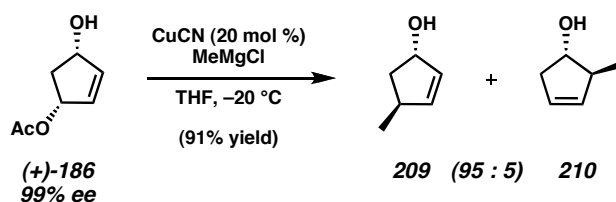
3.7.2.3 AB RING ASYMMETRIC FRAGMENTS



Monoacetate (+)-186.²⁷ To a solution of monoacetate (\pm)-**186** (40.43 g, 284.4 mmol, 1.0 equiv) in CH_2Cl_2 (47 mL, 6 M) was added imidazole (21.11 g, 310 mmol, 1.09 equiv), and after the contents were completely dissolved, the solution was cooled to 0 °C and Ac_2O (29.3 mL, 310 mmol, 1.09 equiv) was added over 5–7 min via syringe. After 10 min, the bath was removed and the solution was stirred for 22 h at room temperature, at which EtOAc (150 mL) was added and the contents were poured into ice-cold 1 N HCl (150 mL). The layers were separated and the aq layer was saturated with NaCl (s) and extracted with Et_2O (2 x 100 mL, 1 x 50 mL). The combined organics were washed with sat. aq NaHCO_3 (100 mL), this aq layer was saturated with NaCl (s) and extracted with Et_2O (2 x 100 mL). The combined organics were dried over MgSO_4 , filtered, concentrated, and dried under high vacuum to afford *meso*-bisacetate **208** (50.88 g, 276.2 mmol, 97% yield) as a pale yellow oil. This material could be used in subsequent reactions as is, or can be purified by short-path distillation (bp = 74–98 °C, ~0.8 torr) to give **208** as a colorless oil in 89% yield. $R_f = 0.75$ (Et_2O); $^1\text{H NMR}$ (300 MHz, CDCl_3) δ 6.09 (d, $J = 0.9$ Hz, 2H), 5.54 (ddd, $J = 7.6, 3.8, 0.9$ Hz, 2H), 2.88 (app dt, $J = 15.1, 7.6$ Hz, 1H), 2.06 (s, 6H), 1.74 (app dt, $J = 15.0, 3.8$ Hz, 1H). All other spectral data are consistent with reported values.^{27c}

meso-Bisacetate **208** (33.15 g, 180.0 mmol, 1.0 equiv) was added to a purified water triple-rinsed 1 L Erlenmeyer flask containing a stir bar and partially dissolved in aq $\text{NaH}_2\text{PO}_4/\text{K}_2\text{HPO}_4$ buffer (0.05 M, pH = 8.0). To this solution was added Novozym 435 (4.0 g), the flask was covered with parafilm and stirred gently to at room temperature until consumption of **208** by TLC analysis (5–8 h). The contents were vacuum filtered and the supported enzyme was washed with water (150 mL) and EtOAc (2 x 150 mL).

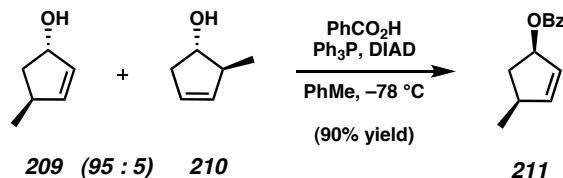
The filtrate layers were separated and the aq layer was saturated with NaCl (200 g), extracted with EtOAc (5 x 200 mL, follow by TLC), and the combined organics were dried over MgSO₄, filtered, and concentrated in vacuo. The crude oil was dissolved in Et₂O (150 mL) and heptane was added (150 mL), followed by concentration in vacuo to afford a white semisolid. This was repeated one more time and the solid was dried under high vacuum to provide monoacetate (+)-**186** (24.36 g, 171 mmol, 95% yield) as a white semisolid. The crude material is >95% pure by ¹H NMR, but can be purified by flash chromatography on SiO₂ (1:2 hexanes/Et₂O, dry load onto SiO₂) to provide **186** in 89% yield. The material displayed the same spectral properties as above,^{27a,b} mp = 45–49 °C; [α]_D^{22.5} +61.2° (c 1.28, CHCl₃, 99% ee). GC conditions: 100 °C isothermal, GTA column, t_R (min): major = 30.5, minor = 27.6. We have reused the recovered Novozym 435 up to four times and observed slightly lower activity for each subsequent use with identical selectivities.



anti-Cyclopentenols 209 and 210. A 2 L 3-neck flask was charged with CuCN (2.01 g, 112.2 mmol, 0.2 equiv) and THF (280 mL), and the suspension was cooled to ca. –20 °C (internal) using a cryocool. To this was added a solution of MeMgCl (109 mL, 337 mmol of a 3.1 M solution in THF) and the internal temperature warmed to –14 °C. After 30 min at –20 °C, a solution of monoacetate (+)-**186** (15.95 g, 112.2 mmol, 1.0 equiv) in THF (40 mL) was slowly transferred (quantitative) via cannulation at such a

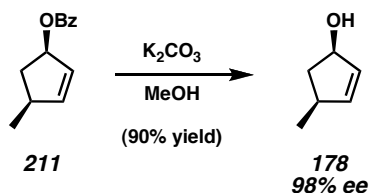
rate that the temperature does not rise above $-10\text{ }^{\circ}\text{C}$ (requires $\sim 1\text{ h}$). After 30 min the reaction was slowly quenched with sat. aq NH_4Cl (100 mL), 50% sat. brine (100 mL), the cooling bath was removed and the viscous suspension was stirred vigorously for several hours. Additional water (200 mL) and 3% HCl (100 mL) was added and the layers were separated. The aq layer was extracted with Et_2O (3 x 200 mL), the combined organics were dried over MgSO_4 , filtered, and concentrated carefully (water bath = $5\text{ }^{\circ}\text{C}$, down to 30 torr) to a pale yellow oil. The crude material was purified by short path distillation (bp = $88\text{--}92\text{ }^{\circ}\text{C}$, 40 torr) to afford a 95:5 mixture of *anti*-cyclopentenols **209** and **210** (8.847 g, 90.2 mmol, 80% yield). The early distillation fractions and washing from the apparatus were combined and purified by flash chromatography on SiO_2 (2.5 x 27 cm, 6:1 \rightarrow 1:1 pentane/ Et_2O) to provide another 1.049 g of **209** and **210**. The combined yield obtained was 9.996 g, 101.9 mmol, 91% yield. R_f (**210**) = 0.35 (1:1 hexanes/ EtOAc); R_f (**209**) = 0.29 (1:1 hexanes/ EtOAc); bp = $88\text{--}92\text{ }^{\circ}\text{C}$ (40 torr).

An analytical sample of **209** was obtained from the column conditions above. ^1H NMR (500 MHz, CDCl_3) δ 5.89 (dd, $J = 5.5, 1.9\text{ Hz}$, 1H), 5.79 (ddd, $J = 4.6, 2.2, 2.2\text{ Hz}$, 1H), 4.88–4.86 (m, 1H), 2.99–2.91 (m, 1H), 1.96 (ddd, $J = 14.0, 7.5, 2.6\text{ Hz}$, 1H), 1.71 (ddd, $J = 14.0, 7.1, 5.2\text{ Hz}$, 1H), 1.48 (br s, 1H), 1.03 (d, $J = 7.1\text{ Hz}$, 3H); ^{13}C NMR (126 MHz, CDCl_3) δ 142.0, 132.1, 77.6, 42.7, 38.5, 21.0; IR (Neat Film NaCl) 3338 (br), 2956, 2870, 1354, 1088, 1017, 982, 742 cm^{-1} ; HRMS (EI+) m/z calc'd for $\text{C}_6\text{H}_{10}\text{O}$ $[\text{M}]^+$: 98.07317, found 98.07171; $[\alpha]_{\text{D}}^{21}$ -272.2° (c 0.39, CHCl_3 , 99% ee). GC conditions: $45\text{ }^{\circ}\text{C}$ isothermal, GTA column, t_{R} (min): major = 37.7, minor = 36.7.



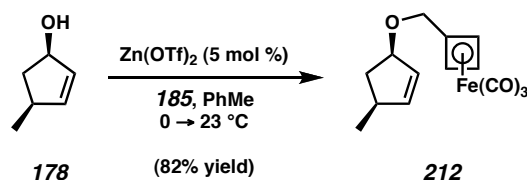
syn-Benzoate 211. To a suspension of Ph_3P (13.41 g, 51.12 mmol, 1.2 equiv) and benzoic acid (6.243 g, 51.12 mmol, 1.2 equiv) in PhMe (237 mL) at $-75\text{ }^\circ\text{C}$ (internal) was added DIAD (10.1 mL, 51.12 mmol, 1.2 equiv) dropwise, neat over 15 min. The resulting yellow suspension was stirred vigorously for 30 min, at which point a solution of **209** and **210** (4.1806 g, 42.60 mmol, 1.0 equiv) in PhMe (47 mL, 0.15 M total) was transferred via cannula quantitatively over 30 min (observed maximum temperature increase to $-70\text{ }^\circ\text{C}$). When $\sim 1/3$ of this solution was added, the reaction mixture turned homogeneous. After complete addition of **209** and **210**, the reaction was stirred for an additional 30 min (white precipitate has formed) and quenched with sat. aq NaHCO_3 (100 mL) and water (100 mL) and the contents were warmed to room temperature. The layers were separated, the aq was extracted with Et_2O (2 x 50 mL), and the combined organics were shaken with 3% aq H_2O_2 until TLC showed disappearance of Ph_3P . The layers were separated, the aq was extracted with Et_2O (1 x 50 mL), and the combined organics were dried over MgSO_4 , filtered, and concentrated to a pale yellow solid. The crude material was purified by flash chromatography on SiO_2 (7 x 7.5 cm, 1:0 \rightarrow 24:1 hexanes/ Et_2O , dry loaded onto SiO_2) to give *syn*-benzoate **211** (7.792 g, 38.53 mmol, 90% yield) as a pale yellow oil. $R_f = 0.57$ (3:1 hexanes/ EtOAc); $^1\text{H NMR}$ (500 MHz, CDCl_3) δ 8.04 (dd, $J = 8.2, 1.2$ Hz, 2H), 7.56–7.53 (m, 1H), 7.43 (app t, $J = 7.8$ Hz, 2H), 6.03 (dd, $J = 4.4, 2.0$ Hz, 1H), 5.90–5.86 (comp m, 2H), 2.80–2.73 (m, 1H), 2.65 (ddd, $J = 14.0, 7.8, 7.8$ Hz, 1H), 1.51 (ddd, $J = 14.0, 4.4, 4.4$ Hz, 1H), 1.16 (d, $J = 7.0$ Hz, 3H);

^{13}C NMR (126 MHz, CDCl_3) δ 166.6, 142.9, 132.9, 130.8, 129.7, 128.6, 128.4, 80.9, 38.9, 38.7, 21.7; IR (Neat Film NaCl) 2961, 1716, 1451, 1340, 1315, 1272, 1110, 711 cm^{-1} ; HRMS (EI+) m/z calc'd for $\text{C}_{13}\text{H}_{14}\text{O}_2$ $[\text{M}]^+$: 202.0994, found 202.0957; $[\alpha]_{\text{D}}^{25.7} +123.8^\circ$ (c 1.175, CHCl_3 , 98–99% ee). For a chiral analytical assay, see *syn*-diol **178**.



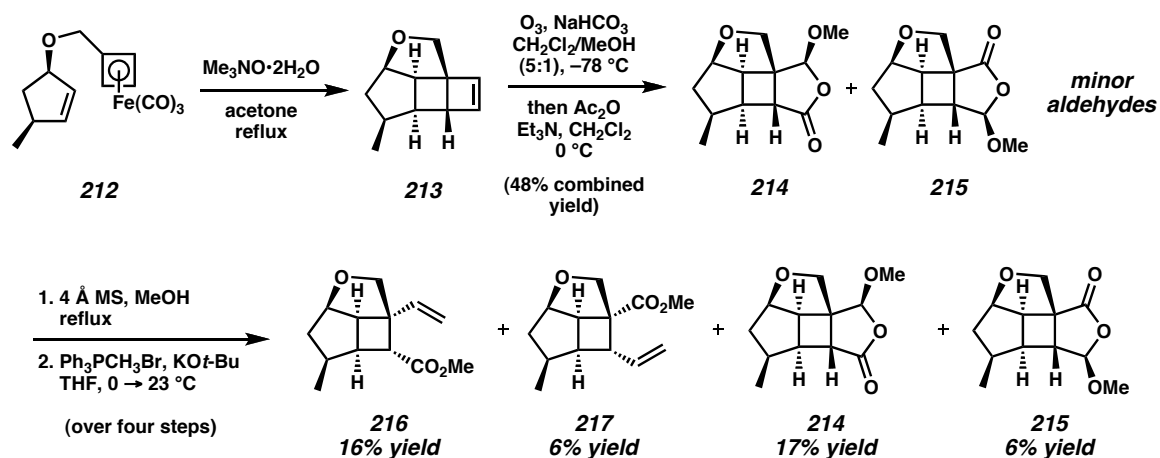
***syn*-Cyclopentenol 178.** To a solution of benzoate **211** (6.255g, 30.93 mmol, 1.0 equiv) in MeOH (62 mL, 0.5 M) was added K_2CO_3 (8.549 g, 61.85 mmol, 2.0 equiv) in one portion. After completion as judged by TLC analysis (3 h, 3:1 hexanes/EtOAc), the reaction was concentrated carefully in vacuo to a slurry (~5–10 mL). The white slurry was diluted with brine (25 mL) and extracted with Et_2O (4 x 25 mL, follow by TLC), the organics were dried over MgSO_4 , filtered, and concentrated carefully in vacuo. The crude material was purified by flash chromatography on SiO_2 (5 x 12 cm, 6:1 \rightarrow 1:1 pentane/ Et_2O) and concentrated down to 100 torr until ^1H NMR analysis revealed the absence of solvent to afford *syn*-cyclopentenol **178** (2.728 g, 27.79 mmol, 90% yield) as a colorless oil. $R_f = 0.25$ (3:1 hexanes/EtOAc); ^1H NMR (500 MHz, CDCl_3) δ 5.82 (app dt, $J = 5.5, 1.5$ Hz, 1H), 5.73 (app dt, $J = 5.5, 2.0$ Hz, 1H), 4.79 (br s, 1H), 2.66–2.59 (m, 1H), 2.52 (ddd, $J = 13.4, 7.6, 7.6$ Hz, 1H), 1.79 (br s, 1H), 1.17 (app dt, 13.4, 5.4 Hz, 1H), 1.09 (d, $J = 7.0$ Hz, 3H); ^{13}C NMR (126 MHz, CDCl_3) δ 140.4, 132.8, 77.8, 42.6, 39.0, 22.0; IR (Neat Film NaCl) 3338 (br), 3048, 2959, 2870, 1456, 1356, 1322, 1115,

1051, 755 cm^{-1} ; HRMS (EI+) m/z calc'd for $\text{C}_6\text{H}_{10}\text{O}$ $[\text{M}]^+$: 98.07317, found 98.06857; $[\alpha]_{\text{D}}^{27}$ -23.0° (c 0.475, CHCl_3 , 98.2% ee). GC conditions: 50 $^\circ\text{C}$ isothermal, GTA column, t_{R} (min): major = 21.2, minor = 20.7.



Cyclobutadiene-iron ether complex 212. To a round-bottom flask containing zinc(II) triflate (271 mg, 0.745 mmol, 5 mol%) and PhMe (3.7 mL) at 0 $^\circ\text{C}$ was added cyclopentenol **178** (1.45 g, 14.8 mmol, 1.0 equiv) by syringe. To this suspension was added a solution of cyclobutadiene trichloroacetimidate **185** (6.38 g, 17.4 mmol, 1.2 equiv) in PhMe (2.0 mL) by cannula transfer, with further washing by PhMe (1.7 mL). A yellow precipitate was observed at the beginning of the addition, and this turned into a viscous slurry upon completion of the addition. The ice bath was allowed to expire over 1.5 h and the reaction was stirred for an additional 0.5 h at ambient temperature. The crude reaction mixture was transferred directly onto a 25 g silica gel loading cartridge and purified with a Teledyne ISCO CombiFlash system using a 125 g silica column (1:0 \rightarrow 19:1 hexanes/EtOAc) to afford cyclobutadiene-ether complex **212** (3.65 g, 12.2 mmol, 82% yield) as a pale yellow oil. R_f = 0.73 (4:1 hexanes/EtOAc); ^1H NMR (500 MHz, C_6D_6) δ 5.72 (app dt, J = 5.6, 1.9 Hz, 1H), 5.66 (app dt, J = 5.6, 1.6 Hz, 1H), 4.27–4.24 (m, 1H), 3.54 (d, J = 9.1 Hz, 1H), 3.52 (d, J = 9.1 Hz, 1H), 3.48 (s, 2H), 3.32 (s, 1H), 2.43–2.39 (m, 1H), 2.15 (app dt, J = 13.3, 7.6 Hz, 1H), 1.26 (ddd, J = 17.0, 11.2, 6.9 Hz, 1H), 0.98 (d, J = 7.0 Hz, 3H); ^{13}C NMR (126 MHz, C_6D_6) δ 215.0, 140.5, 130.5,

85.2, 82.6, 64.6 (two lines), 64.0, 62.2, 39.1, 38.9, 21.6; IR (Neat Film NaCl) 2961, 2871, 2046, 1965, 1359, 1076, 1055, 757 cm^{-1} ; HRMS (FAB+) m/z calc'd for $\text{C}_{14}\text{H}_{14}\text{FeO}_4$ $[\text{M}]^+$: 302.0242, found 302.0244; $[\alpha]_{\text{D}}^{25}$ +22.7° (c 0.86, hexane, 98% ee).



Cycloaddition to cyclobutene 213. A solution of ether **212** (2.3582 g, 7.806 mmol, 1.0 equiv) dissolved in acetone (780 mL, 10 mM) in a 1 L round-bottom flask fitted with a reflux condenser was warmed in a 70°C oil bath. When the solution approached reflux, the condenser was momentarily removed and $\text{Me}_3\text{NO}\cdot 2\text{H}_2\text{O}$ (8.77 g, 78.9 mmol, 10 equiv) was added in a single portion. The solution was allowed to reflux and within 10 min the reaction vessel was filled with a rust colored precipitate. After 4 h a second portion of $\text{Me}_3\text{NO}\cdot 2\text{H}_2\text{O}$ (4.35 g, 45.9 mmol, 5.8 equiv) was added. The solution was heated at reflux for an additional 17 h after which the reaction was judged to be complete by TLC analysis (4:1 hexanes/EtOAc). The solution was cooled to room temperature and poured directly onto a SiO_2 column (25 x 5 cm) packed in pentane. The column was washed with $0 \rightarrow 10\%$ Et_2O in pentane, and all fractions containing cyclobutene **213** were combined and concentrated carefully to a volume of ~ 30 mL by atmospheric

pressure distillation. This solution was purified by flash chromatography on SiO₂ (pack with pentane, elute with 20:1 pentane/Et₂O). The fractions containing product were combined and concentrated to a volume of ~10 mL by atmospheric pressure distillation. This pale yellow cyclobutene solution in pentane was used directly in the following reaction. An analytical sample of cyclobutene **213** could be prepared by further chromatography and exhaustive distillation of solvent. $R_f = 0.39$ (3:1 hexanes/Et₂O); ¹H NMR (500 MHz, CDCl₃) δ 6.27 (d, $J = 2.2$ Hz, 1H), 6.22 (s, 1H), 4.84 (dd, $J = 14.4, 7.1$ Hz, 1H), 4.04 (d, $J = 9.1$ Hz, 1H), 3.94 (d, $J = 8.6$ Hz, 1H), 3.00 (s, 1H), 2.89 (dd, $J = 19.7, 13.8$ Hz, 1H), 2.27–2.18 (m, 1H), 2.10–2.05 (comp m, 2H), 1.37 (ddd, $J = 13.0, 13.0, 7.0$ Hz, 1H), 0.97 (d, $J = 6.7$ Hz, 3H); ¹³C NMR (126 MHz, CDCl₃) δ 140.2, 138.4, 84.7, 70.3, 57.9, 52.0, 47.8, 44.8, 39.0, 37.3, 14.3; IR (Neat Film NaCl) 2955, 2865, 1458, 1334, 1089, 1075, 1057, 1032, 931, 740 cm⁻¹; HRMS (EI⁺) m/z calc'd for C₁₁H₁₄O [M]⁺: 162.1045, found 162.1026; an optical rotation was not obtained due to the volatility of this compound. Cyclobutene **213** was found to possess an optical purity (ee) of 98% by chiral GC analysis; GC conditions: 110 °C isothermal, GTA column, t_R (min): major = 13.6, minor = 13.3.

Ozonolysis, equilibration, and methylenation to olefins 216 and 217, and acetals 214 and 215. In a 250 mL round-bottom flask, the cyclobutene solution prepared above was diluted with CH₂Cl₂ (130 mL) and methanol (26 mL, 5:1, 0.05 M total). To this was added NaHCO₃ (205.2 mg, 2.44 mmol, 0.3 equiv) and a few drops of Sudan Red (0.05 wt % in MeOH) until the solution became a persistent pink color (ca. 10 drops). The reaction vessel was cooled to -78 °C and the solution was sparged with O₂ gas (0.5 L/min) for 2 min. The reaction was then ozonolyzed (setting the ozone generator to

“5” with an O₂ flow rate of 0.5 L/min) for 60 min, at which point the pink color of the solution had disappeared and the reaction was judged to be complete by TLC analysis. The ozone was sparged with O₂ gas (1 L/min) through the solution for 2 min, and the pale yellow solution was warmed to room temperature and filtered through a cotton plug to remove the solid NaHCO₃. The cotton plug was washed with PhH (10 mL) and the filtrate was concentrated to a small volume (ca. 3–4 mL). The resulting crude yellow oil was dissolved in CH₂Cl₂ (78 mL), cooled to 0 °C, and to this was added Et₃N (1.63 mL, 11.7 mmol, 1.5 equiv) and Ac₂O (2.21 mL, 23.4 mmol, 3.0 equiv) dropwise via syringe. After 6 h, the reaction was quenched by the addition of 2 M HCl (25 mL), the organic layer was separated and washed with 2 M NaOH (25 mL), and the combined aqueous layers were extracted with CH₂Cl₂ (5 x 25 mL). The organics were dried over MgSO₄, filtered, and concentrated to afford a pale brown oil which was passed through a SiO₂ plug eluting with EtOAc, and concentrated to afford a pale yellow oil (0.8504 g, 3.8 mmol, three steps, 48% crude yield) containing mostly acetals **214** and **215**.

The crude pale yellow oil prepared above was azeotroped from PhH (2 x 10 mL) in a 250 mL round-bottom flask and dissolved in MeOH (76 mL, 0.05 M). To this was added oven dried 4 Å MS (1.90 g, 0.5 g/mmol) and the flask was fitted with a reflux condenser and heated to reflux using an 80 °C oil bath. After 6 h, a reaction aliquot was judged complete by ¹H NMR analysis and the reaction was cooled to room temperature. Most of the 4 Å MS were removed by filtration through Celite eluting with EtOAc. The filtrate was concentrated and the resultant turbid oil was further purified by filtration through a SiO₂ plug with EtOAc. This filtrate was concentrated to afford a yellow oil (0.8420 g)

containing mostly aldehydes derived from **214** and **215** with acetals **214** and **215**.

This was used directly in the following reaction.

A flask containing $\text{Ph}_3\text{PCH}_3\text{Br}$ (1.62 g, 4.54 mmol, 1.2 equiv) was partially dissolved with THF (15 mL) and cooled to 0 °C. To this was added $\text{KO}t\text{-Bu}$ (423 mg, 3.77 mmol, 1.0 equiv) in one portion, and the solution immediately displayed a bright yellow color. The crude yellow oil of aldehydes/acetals (0.8420 g, ~3.7 mmol) prepared above was azeotroped from PhH (2 x 10 mL), dissolved in THF (7.5 mL), cooled to 0 °C, and transferred dropwise via positive pressure cannulation into the solution of phosphorane over ca. 10 min. The flask was then washed with a second portion of THF (7.5 mL) to ensure quantitative transfer. The reaction was gradually allowed to warm to room temperature. After 18 h the reaction was quenched by the addition of H_2O (25 mL) and extracted with Et_2O (4 x 20 mL) then EtOAc (2 x 20 mL). The combined organics were dried with MgSO_4 , filtered and concentrated in vacuo. The crude yellow residue was purified flash chromatography on SiO_2 (15 x 2 cm, 20:1 → 4:1 hexanes/ EtOAc) to afford olefins **216** and **217** (384.4 mg, 1.729 mmol, 2.7:1 ratio, 22.2% yield over four steps from ether **212**) as a colorless oil and acetals **214** and **215** (400.5 mg, 1.786 mmol; 2.7:1 ratio, 22.9% yield over four steps from ether **212**) as pale yellow oil. Olefins **216** and **217** could be separated by further flash chromatography on SiO_2 (20:1 → 9:1 hexanes/ EtOAc), and acetals **214** and **215** could be separated by further flash chromatography on SiO_2 (3:1 → 1:1 hexanes/ EtOAc).

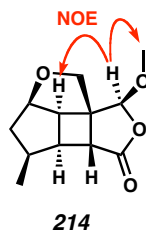
Olefin 216. $R_f = 0.46$ (9:1 hexanes/ EtOAc , developed thrice); $^1\text{H NMR}$ (500 MHz, CDCl_3) δ 5.95 (dd, $J = 17.5, 10.8$ Hz, 1H), 5.15 (dd, $J = 10.8, 1.2$ Hz, 1H), 5.11 (dd, $J = 17.5, 1.2$ Hz, 1H), 4.59 (ddd, $J = 6.3, 6.3, 1.5$ Hz, 1H), 3.99 (d, $J = 9.0$ Hz, 1H), 3.64 (s,

3H), 3.54 (d, $J = 9.0$ Hz, 1H), 3.16 (d, $J = 7.1$ Hz, 1H), 3.02 (app t, 7.1 Hz, 1H), 2.95 (dd, $J = 7.5, 7.4$ Hz, 1H). 2.43–2.34 (m, 1H), 2.18 (ddd, $J = 14.7, 10.4, 5.7$ Hz, 1H), 1.71 (ddd, $J = 14.6, 6.3, 1.7$ Hz, 1H), 1.02 (d, $J = 7.0$ Hz, 3H); ^{13}C NMR (126 MHz, CDCl_3) δ 173.6, 134.9, 115.9, 87.1, 78.7, 52.6, 51.6, 51.4, 44.8, 42.5, 38.9, 37.2, 17.2; IR (Neat Film NaCl) 2954, 1736, 1436, 1363, 1236, 1206, 1162, 1042, 920 cm^{-1} ; HRMS (MM: ESI/APCI) m/z calc'd for $\text{C}_{13}\text{H}_{18}\text{O}_3$ $[\text{M} + \text{H}]^+$: 223.13287, found 223.13255; $[\alpha]_{\text{D}}^{16.8} -4.73^\circ$ (c 1.18, CH_2Cl_2 , 98% ee).

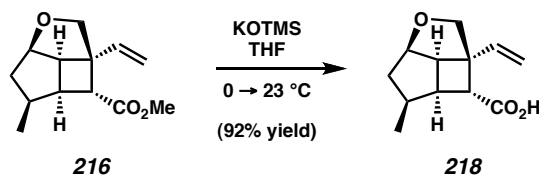
Olefin 217. $R_f = 0.39$ (9:1 hexanes/EtOAc, developed thrice); ^1H NMR (500 MHz, CDCl_3) δ 5.86 (ddd, $J = 17.0, 10.3, 7.8$ Hz, 1H), 5.05 (ddd, $J = 17.1, 1.5, 1.5$ Hz, 1H), 5.02 (ddd, $J = 10.3, 1.4, 1.4$ Hz, 1H), 4.67 (ddd, $J = 6.6, 6.6, 2.8$ Hz, 1H), 4.02 (d, $J = 9.4$ Hz, 1H), 3.88 (d, $J = 9.4$ Hz, 1H), 3.68 (s, 3H), 3.30 (app t, $J = 7.2$ Hz, 1H), 3.00 (app t, $J = 7.2$ Hz, 1H), 2.54 (app q, 7.16 Hz, 1H), 2.35 (d septuplets, $J = 9.6, 7.1$ Hz, 1H), 2.18 (ddd, $J = 14.5, 9.7, 6.3$ Hz, 1H), 1.67 (ddd, $J = 14.5, 7.7, 2.8$ Hz, 1H), 1.01 (d, $J = 7.0$ Hz, 3H); ^{13}C NMR (126 MHz, CDCl_3) δ 172.3, 137.9, 115.9, 87.1, 76.0, 55.8, 51.7, 48.9, 44.9, 43.6, 41.8, 38.0, 16.2; IR (Neat Film NaCl) 2953, 5873, 1731, 1436, 1295, 1207, 1041, 917 cm^{-1} ; HRMS (EI+) m/z calc'd for $\text{C}_{13}\text{H}_{18}\text{O}_3$ $[\text{M}]^+$: 222.1256, found 222.1216; $[\alpha]_{\text{D}}^{15.1} -0.49^\circ$ (c 0.72, CH_2Cl_2 , 98% ee).

Acetal 214. $R_f = 0.29$ (2:1 hexanes/EtOAc); ^1H NMR (500 MHz, CDCl_3) δ 5.39 (s, 1H), 4.80 (ddd, $J = 6.5, 6.5, 4.5$ Hz, 1H), 4.00 (d, $J = 10.6$ Hz, 1H), 3.98 (d, $J = 10.7$ Hz, 1H), 3.48 (s, 3H), 3.13 (app t, $J = 6.7$ Hz, 1H), 2.89 (d, $J = 3.3$ Hz, 1H), 2.61 (ddd, $J = 6.9, 6.9, 3.3$ Hz, 1H), 2.39–2.30 (m, 1H), 2.06 (ddd, $J = 14.4, 8.4, 6.3$ Hz, 1H), 1.60 (ddd, $J = 13.3, 8.5, 4.5$ Hz, 1H), 1.11 (d, $J = 7.0$ Hz, 3H); ^{13}C NMR (126 MHz, CDCl_3) δ 179.0, 107.4, 86.7, 70.9, 56.8, 52.4, 51.5, 44.7, 40.8, 38.6, 37.2, 16.9; IR (Neat Film NaCl)

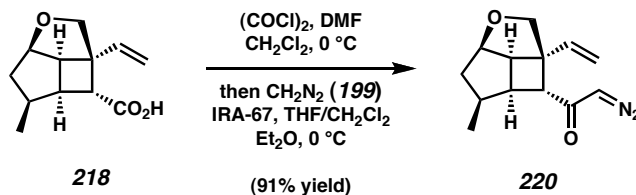
2961, 2877, 1772, 1353, 1150, 1128, 1100, 1062, 936, 710 cm^{-1} ; HRMS (EI+) m/z calc'd for $\text{C}_{12}\text{H}_{16}\text{O}_4$ $[\text{M}]^+$: 224.1049, found 224.1052; $[\alpha]_{\text{D}}^{18.3} +73.0^\circ$ (c 1.13, CH_2Cl_2 , 98% ee). Relative stereochemistry determined by NOE interactions shown below.



Acetal 215. $R_f = 0.19$ (2:1 hexanes/EtOAc); mp = 151.5–153 $^\circ\text{C}$ (Et_2O); ^1H NMR (600 MHz, CDCl_3) δ 5.30 (s, 1H), 4.89 (dd, $J = 12.9, 7.2$ Hz, 1H), 4.19 (d, $J = 9.6$ Hz, 1H), 4.11 (d, $J = 9.6$ Hz, 1H), 3.49 (s, 3H), 3.33 (dd, $J = 7.0, 6.3$ Hz, 1H), 2.58 (d, $J = 4.0$ Hz, 1H), 2.40 (ddd, $J = 10.0, 6.0, 4.1$ Hz, 1H), 2.30–2.22 (m, 1H), 2.16 (ddd, $J = 14.5, 7.4, 7.4$ Hz, 1H), 1.55 (ddd, $J = 14.0, 11.1, 5.7$ Hz, 1H), 1.03 (d, $J = 6.8$ Hz, 3H); ^{13}C NMR (126 MHz, CDCl_3) δ 177.2, 108.4, 86.6, 73.2, 56.5, 55.5, 50.1, 42.8, 41.2, 38.7, 38.2, 15.3; IR (Neat Film NaCl) 2934, 1766, 1460, 1359, 1199, 1171, 1143, 1130, 1115, 1063, 1045, 916, 904, 691 cm^{-1} ; HRMS (EI+) m/z calc'd for $\text{C}_{12}\text{H}_{16}\text{O}_4$ $[\text{M}]^+$: 224.1049, found 224.1044; $[\alpha]_{\text{D}}^{17.9} -56.7^\circ$ (c 0.62, CH_2Cl_2 , 98% ee). Crystals suitable for X-ray analysis were obtained by slow evaporation from Et_2O . See Appendix 3 for the crystallography report.

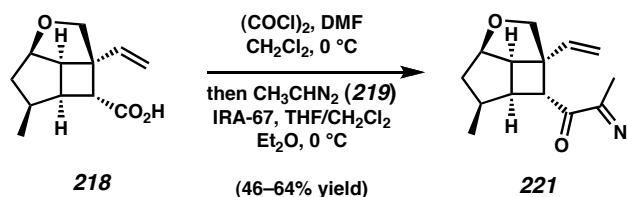


Acid 218. To a solution of olefin **216** (41.0 mg, 0.184 mmol, 1.0 equiv) in THF (3.7 mL, 0.05 M) cooled to 0 °C was added KOTMS (236 mg, 1.84 mmol, 10 equiv) in one portion. After 5 min the reaction was warmed to room temperature and monitored by TLC. At 12 h the reaction was cooled to 0 °C and slowly quenched with 10% HCl (4 mL) and diluted with brine (4 mL) and EtOAc (10 mL). The layers were separated and the aq layer was extracted with EtOAc (3 x 10 mL), the combined organics were dried over Na₂SO₄, filtered, and concentrated to a pale yellow oil. The crude was purified by flash chromatography on SiO₂ (6:1 → 3:1 hexanes/EtOAc, CH₂Cl₂ load) to afford acid **218** (35.2 mg, 0.169 mmol, 92% yield) as a white solid. $R_f = 0.21$ (2:1 hexanes/EtOAc); ¹H NMR (600 MHz, CDCl₃) δ 6.04 (dd, $J = 17.5, 10.8$ Hz, 1H), 5.20 (dd, $J = 10.8, 1.2$ Hz, 1H), 5.17 (dd, $J = 17.5, 1.2$ Hz, 1H), 4.61 (ddd, $J = 6.4, 6.4, 1.6$ Hz, 1H), 4.02 (d, $J = 9.1$ Hz, 1H), 3.54 (d, $J = 9.1$ Hz, 1H), 3.22 (d, $J = 7.3$ Hz, 1H), 3.05 (app t, $J = 7.1$ Hz, 1H), 2.91 (app q, $J = 7.6$ Hz, 1H), 2.40 (d septuplets, $J = 10.4, 7.0$ Hz, 1H), 2.20 (ddd, $J = 14.7, 10.4, 5.8$ Hz, 1H), 1.73 (ddd, $J = 14.7, 6.3, 1.7$ Hz, 1H), 1.05 (d, $J = 7.1$ Hz, 3H); ¹³C NMR (126 MHz, CDCl₃) δ 178.6, 134.5, 116.2, 87.2, 78.8, 52.8, 51.2, 44.7, 42.5, 39.0, 37.2, 17.2; IR (Neat Film NaCl) 3085 (br), 2958, 2930, 1731, 1704, 1418, 1283, 1241, 1086, 1041, 996, 921 cm⁻¹; HRMS (EI+) m/z calc'd for C₁₂H₁₆O₃ [M]⁺: 208.1100, found 208.1094; $[\alpha]_D^{15.3} +28.3^\circ$ (c 0.97, CH₂Cl₂, 98% ee).

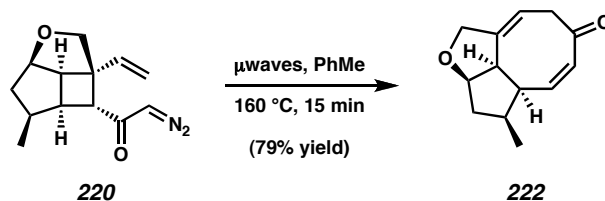


Diazoketone 220. To a solution of acid **218** (62.5 mg, 0.300 mmol, 1.0 equiv) in CH_2Cl_2 (6.0 mL, 0.05 M) at 0 °C was added a solution of oxalyl chloride (353 μL of a 1.7 M solution in CH_2Cl_2 , 0.600 mmol, 2.0 equiv), followed by 1 drop of DMF. The reaction was stirred for 45 min at 0 °C, at which point the stir bar was removed, PhMe was added (6 mL), and the volatiles were removed on a rotovap purged with argon. The septum and stir bar were replaced and the crude material was further dried under high vacuum for 10 min. The resulting crude semisolid was partially dissolved in CH_2Cl_2 (2 mL) and THF (4 mL) and transferred quantitatively via Teflon cannula to a vigorously stirring solution of excess diazomethane (**199**, ca. 30 mL) containing IRA-67 (161 mg, ca. 0.9 mmol, 3.0 equiv) at 0 °C. The flask was further washed with CH_2Cl_2 (4 mL) and THF (2 mL) and quantitatively transferred. After 3.5 h the cooling bath was removed and the diazomethane was pulled off via water aspirator. The pale yellow solution was filtered through a small SiO_2 plug (Et_2O) and concentrated in vacuo. The crude material was purified by flash chromatography on SiO_2 (6:1 \rightarrow 2:1 hexanes/ Et_2O) to afford α -diazoketone **220** (63.2 mg, 0.272 mmol, 91% yield) as a bright yellow oil that solidifies in a -20 °C freezer. $R_f = 0.24$ (3:1 hexanes/ EtOAc); ^1H NMR (500 MHz, CDCl_3) δ 6.01 (dd, $J = 17.5, 10.8$ Hz, 1H), 5.15 (d, $J = 10.9$ Hz, 1H), 5.10 (br s, 1H), 5.05 (d, $J = 17.5$ Hz, 1H), 4.59 (app t, $J = 6.1$ Hz, 1H), 3.92 (d, $J = 9.0$ Hz, 1H), 3.63 (d, $J = 9.0$ Hz, 1H), 3.11 (br d, $J = 14.8$, 2H), 2.96 (app t, $J = 6.9$ Hz, 1H), 2.44–2.35 (m, 1H), 2.20 (ddd, $J = 15.4, 10.5, 5.8$ Hz, 1H), 1.70 (dd, $J = 14.7, 6.3$ Hz, 1H), 0.99 (d, $J = 7.0$ Hz, 3H); ^{13}C NMR (126 MHz, CDCl_3) δ 193.7, 134.9, 115.7, 87.2, 78.3, 54.8, 53.3, 51.9, 50.4, 42.6, 38.3, 37.3, 17.2; IR (Neat Film NaCl) 3081, 2956, 2100, 1635, 1373,

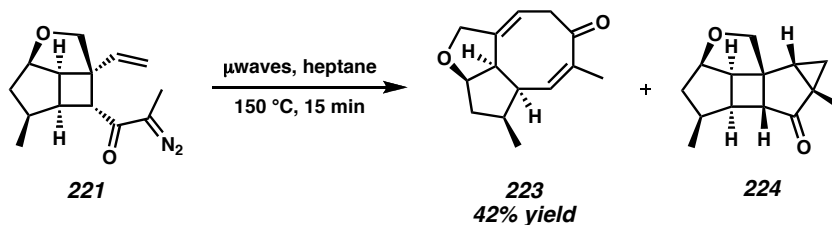
1047, 919 cm^{-1} ; HRMS (FAB+) m/z calc'd for $\text{C}_{13}\text{H}_{17}\text{N}_2\text{O}_2$ $[\text{M} + \text{H}]^+$: 233.1290, found 233.1296; $[\alpha]_{\text{D}}^{20.2} -66.3^\circ$ (c 0.99, CH_2Cl_2 , 98% ee).



Diazoketone 221. α -Diazoketone was prepared by the same procedure as described for diazoketone **220** using acid **218** (17.3 mg, 83.1 μmol , 1.0 equiv), but with freshly prepared and KOH-dried diazoethane (**219**, ca. 20 mL). After 4 h at 0 $^\circ\text{C}$ the excess diazoethane was removed via water aspirator. The pale orange solution was filtered through a small SiO_2 plug (Et_2O) and concentrated in vacuo. The crude material was purified by flash chromatography on SiO_2 (6:1 \rightarrow 4:1 hexanes/ Et_2O , CH_2Cl_2 load) to afford α -diazoketone **221** (13.0 mg, 52.8 μmol , 64% yield) as a bright yellow oil. $R_f = 0.38$ (2:1 hexanes/ Et_2O); ^1H NMR (500 MHz, CDCl_3) δ 5.95 (dd, $J = 17.5, 10.9$ Hz, 1H), 5.10 (d, $J = 10.8$ Hz, 1H), 5.05 (d, $J = 17.6$ Hz, 1H), 4.57 (app t, $J = 5.7$ Hz, 1H), 3.86 (d, $J = 9.3$ Hz, 1H), 3.66 (d, $J = 9.3$ Hz, 1H), 3.34 (d, $J = 6.8$ Hz, 1H), 3.28 (dd, $J = 14.9, 7.5$ Hz, 1H), 2.93 (app t, $J = 6.9$ Hz, 1H), 2.45–2.36 (m, 1H), 2.16 (ddd, $J = 15.1, 10.6, 5.7$ Hz, 1H), 1.94 (s, 3H), 1.70 (dd, $J = 14.5, 5.9$ Hz, 1H), 0.98 (d, $J = 7.1$ Hz, 3H); ^{13}C NMR (126 MHz, CDCl_3) δ 14.3, 134.8, 115.5, 87.0, 77.3, 53.0, 52.5, 47.7, 42.3, 36.7, 36.3, 17.3, 8.3; IR (Neat Film NaCl) 2957, 2926, 2064, 1631, 1286, 1050 cm^{-1} ; HRMS (FAB+) m/z calc'd for $\text{C}_{14}\text{H}_{19}\text{O}_2\text{N}_2$ $[\text{M} + \text{H}]^+$: 247.1447, found 247.1457; $[\alpha]_{\text{D}}^{19.9} +71.6^\circ$ (c 0.57, CH_2Cl_2 , 98% ee).



Cyclooctadienone 222. A solution of α -diazoketone **220** (69.2 mg, 0.271 mmol) in PhMe (54 mL, 5 mM) was partitioned equally into three nondried 20 mL microwave reaction vessels containing a stir bar under ambient atmosphere. Each vial was sealed and irradiated in a Biotage Initiator microwave reactor at 400 W until the temperature reached 160 °C, and the temperature was maintained for 15 min. The vial was cooled to room temperature, the seal was removed, and the contents were concentrated in vacuo. Reaction conversion was monitored by crude ^1H NMR analysis (CDCl_3). The crude material was purified by flash chromatography on SiO_2 (9:1 \rightarrow 6:1 \rightarrow 3:1 hexanes/EtOAc) to give **222** (43.9 mg, 0.215 mmol, 79% yield) as a colorless oil that solidifies in a -20 °C freezer. $R_f = 0.35$ (3:1 hexanes/EtOAc); ^1H NMR (500 MHz, CDCl_3) δ 6.08 (dd, $J = 12.4, 6.5$ Hz, 1H), 5.93 (app dt, $J = 12.4, 1.9$ Hz, 1H), 5.54 (dtdd, $J = 4.8, 3.2, 2.6, 1.7$ Hz, 1H), 4.59 (dd, $J = 14.1, 6.9$ Hz, 1H), 4.38 (d, $J = 12.1$ Hz, 1H), 4.32 (d, $J = 12.2$ Hz, 1H), 3.44 (ddd, $J = 9.4, 2.2, 1.0$ Hz, 1H), 3.28 (dd, $J = 14.3, 9.8$ Hz, 1H), 3.18–3.13 (m, 1H), 2.99 (ddd, $J = 14.3, 6.2, 1.2$ Hz, 1H), 2.41–2.32 (m, 1H), 2.18 (dddd, $J = 13.1, 7.1, 6.1, 1.2$ Hz, 1H), 1.44 (ddd, $J = 13.2, 13.2, 5.9$ Hz, 1H), 1.11 (s, 3H); ^{13}C NMR (126 MHz, CDCl_3) δ 204.4, 146.1, 139.2, 131.6, 114.2, 85.1, 74.6, 52.9, 47.8, 40.1, 38.9, 15.0; IR (Neat Film NaCl) 2958, 2874, 1691, 1666, 1116, 1064, 1032, 974, 867 cm^{-1} ; HRMS (FAB+) m/z calc'd for $\text{C}_{13}\text{H}_{17}\text{O}_2$ $[\text{M} + \text{H}]^+$: 205.1229, found 205.1223; $[\alpha]_D^{20.4} -642^\circ$ (c 1.38, CH_2Cl_2 , 98% ee).

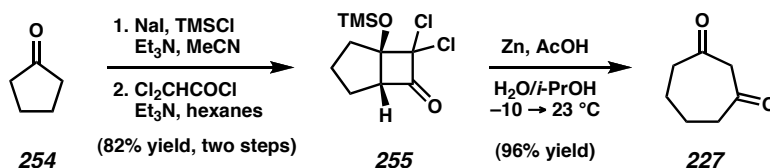


Wolff/Cope rearrangement for cyclooctadienone 223 and cyclopropane 224. A solution of α -diazoketone **221** (17.7 mg, 71.9 μmol) in heptane (14.4 mL, 5 mM) was prepared in a nondried 20 mL microwave reaction vessel under ambient atmosphere and sealed. The contents were irradiated in a Biotage Initiator microwave reactor at 400 W until the temperature reached 150 $^\circ\text{C}$, and the temperature was maintained for 10 min. The reaction was cooled to room temperature and TLC analysis showed consumption of **221**. The solution was concentrated in vacuo and purified by preparative TLC on SiO_2 (3:1 hexanes/EtOAc, develop twice) to afford α -methyl cyclooctadienone **223** (6.6 mg, 30.2 μmol , 42% yield) as a colorless oil and cyclopropane **224** as a single diastereomer.

Cyclooctadienone 223. $R_f = 0.41$ (3:1 hexanes/EtOAc); $^1\text{H NMR}$ (600 MHz, CDCl_3) δ 5.80 (app dq, $J = 7.2, 1.3$ Hz, 1H), 5.52–5.48 (m, 1H), 4.58 (ddd, $J = 7.3, 7.3, 6.2$ Hz, 1H), 4.38 (d, $J = 12.1$ Hz, 1H), 4.31 (ddd, $J = 10.7, 3.0, 1.6$ Hz, 1H), 3.36 (dddd, $J = 9.3, 8.1, 2.4, 1.1$ Hz, 1H), 3.24 (dd, $J = 15.6, 9.5$ Hz, 1H), 3.02–2.98 (comp m, 2H), 2.36–2.14 (m, 1H), 2.16 (ddd, $J = 13.2, 7.1, 1.0$ Hz, 1H), 1.84 (app t, $J = 1.5$ Hz, 3H), 1.47 (ddd, $J = 13.3, 13.3, 5.9$ Hz, 1H), 1.08 (d, $J = 6.9$ Hz, 3H). $^{13}\text{C NMR}$ (126 MHz, CDCl_3) δ 207.6, 146.6, 137.2, 132.5, 113.7, 85.1, 74.5, 53.3, 47.0, 46.8, 40.3, 38.9, 20.8, 15.0; IR (Neat Film NaCl) 2956, 2923, 2874, 1693, 1667, 1452, 1375, 1076, 1045, 1020, 973, 873, 838 cm^{-1} ; HRMS (MM: ESI/APCI) m/z calc'd for $\text{C}_{14}\text{H}_{19}\text{O}_2$ $[\text{M} + \text{H}]^+$: 219.1380, found 219.1379; $[\alpha]_D^{25} -573^\circ$ (c 0.35, CHCl_3 , 98% ee)

Cyclopropane 224. $R_f = 0.36$ (3:1 hexanes/EtOAc); ^1H NMR (500 MHz, CDCl_3) δ 4.80 (ddd, $J = 7.2, 7.2, 6.0$ Hz, 1H), 3.94 (d, $J = 9.3$ Hz, 1H), 3.84 (d, $J = 9.3$ Hz, 1H), 2.86 (d, $J = 1.8$ Hz, 1H), 2.84 (dd, $J = 7.4, 5.8$ Hz, 1H), 2.25 (d, $J = 2.9$ Hz, 1H), 2.16 (dddd, $J = 10.5, 10.5, 8.6, 4.1$ Hz, 1H), 2.12–2.07 (m, 1H), 2.04 (ddd, $J = 9.0, 4.6, 1.8$ Hz, 1H), 1.56–1.54 (comp m, 2H), 1.49 (ddd, $J = 13.6, 10.9, 5.8$ Hz, 1H), 1.22 (s, 3H), 0.96 (d, $J = 6.7$ Hz, 3H); ^{13}C NMR (126 MHz, CDCl_3) δ 198.7, 86.3, 74.3, 67.1, 57.9, 51.0, 49.7, 46.7, 43.1, 38.8, 37.4, 32.7, 15.2, 9.4; IR (Neat Film NaCl) 2953, 2923, 2868, 1776, 1449, 1073, 1015, 937 cm^{-1} ; HRMS (MM: ESI/APCI) m/z calc'd for $\text{C}_{14}\text{H}_{19}\text{O}_2$ $[\text{M} + \text{H}]^+$: 219.1380, found 219.1382; $[\alpha]_{\text{D}}^{25} +46.1^\circ$ (c 0.38, CHCl_3 , 98% ee)

3.7.2.4 D-RING FRAGMENTS



Cycloheptane-1,3-dione (227).⁴⁵ NaI (156.74 g, 1.046 mol, 1.25 equiv) was placed in a 3 L 3-neck flask and dried under high vacuum at 90 °C for 12 h and then cooled to ambient temperature under N_2 . CH_3CN (1.3 L, 0.65 M) was added to dissolve the NaI and to the resulting solution was added cyclopentanone (**254**, 70.7 g, 74.3 mL, 0.840 mol, 1.0 equiv) followed by Et_3N (106.25 g, 146.3 mL, 1.050 mol, 1.25 equiv). The flask was fitted with an oven-dried addition funnel and was charged with TMSCl (104.03 g, 122 mL, 0.958 mol, 1.15 equiv), which was added dropwise over 30 min. The resulting suspension was stirred for an additional 1 h at ambient temperature. Pentane (1.0 L) was

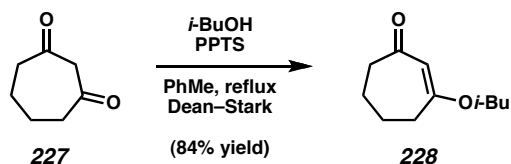
added and the biphasic system was stirred vigorously for 10 min. The layers were separated and the CH₃CN layer was extracted with pentane (3 x 400 mL). The combined pentane extracts were washed with H₂O (2 x 500 mL), brine (500 mL), dried over Na₂SO₄, filtered, and carefully concentrated under reduced pressure (down to 100 torr) to afford the desired silyl enol ether (131.4 g, 0.840 mol, quantitative yield) as a colorless oil. This material was used directly in the following reaction without further purification. $R_f = 0.83$ (4:1 hexanes/EtOAc); ¹H NMR (300 MHz, CDCl₃) δ 4.78 (dt, $J = 3.9, 2.0$ Hz, 1H), 2.45–2.33 (comp m, 4H), 1.89–1.79 (comp m, 2H), 0.27 (s, 9H). All other spectral data are consistent with reported values.

The obtained silyl enol ether (89.7 g, 0.574 mol, 1.0 equiv) was placed in a 3 L 3-neck round-bottom flask fitted with a stopper, an addition funnel, and an overhead stirrer. Hexanes (900 mL) were added followed by Et₃N (80.7 g, 111.2 mL, 0.798 mol, 1.4 equiv). Dichloroacetyl chloride (101.70 g, 66.4 mL, 0.690 mol, 1.2 equiv) was dissolved in hexanes (400 mL), transferred to the closed addition funnel, and added dropwise to the reaction over 9.5 h with vigorous stirring. After 18 h of stirring at 23 °C, the brown suspension was vacuum filtered through a coarse sintered-glass funnel. The filter cake was thoroughly rinsed with EtOAc (3 x 500 mL) while agitating the precipitate with a stirring rod. The clear brown solution was concentrated under reduced pressure and then filtered through a pad of Al₂O₃ (neutral, 7 x 18 cm) eluting with EtOAc. The resulting solution was concentrated under reduced pressure to afford dichlorocyclobutanone **255** (124.7 g, 0.467 mol, 82% yield) as a dark brown oil that crystallized in a –20 °C freezer. This material was used directly in the next reaction without further purification. $R_f = 0.58$ (6:1 hexanes/EtOAc); ¹H NMR (300 MHz, CDCl₃)

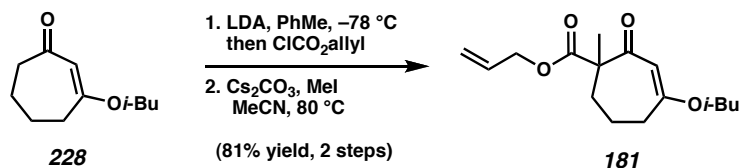
δ 3.66 9d, $J = 8.4$ Hz, 1H), 2.55 (dd, $J = 13.3, 6.8$ Hz, 1H), 2.12–1.84 (comp m, 4H), 1.64–1.51 (m, 1H), 0.25 (s, 9H). All other spectral data are consistent with reported values.

The above dichlorocyclobutanone **255** (53.4 g, 0.200 mol, 1.0 equiv) was placed in a 3 L 3-neck round-bottom flask fitted with a thermometer, an addition funnel and an overhead stirrer. This material was dissolved in *i*-PrOH and purified water (170 mL each). The suspension was cooled to -10 °C (internally) in a MeOH/ice bath. To this cooled solution was added Zn dust (58.8 g, 0.899 mol, 4.5 equiv) in four portions (5 min between each). The addition funnel was charged with a solution of AcOH (66.1 g, 63 mL, 1.10 mol, 5.5 equiv) dissolved in purified water (130 mL) and this solution was added to the reaction in a dropwise manner at such a rate to keep the internal temperature below 0 °C (typically added over 1.5 h). Upon complete addition, the suspension was stirred for an additional 30 min at -10 °C (internal) and then the cooling bath was removed and the reaction was allowed to warm to ambient temperature. After 8.5 h, the reaction mixture was filtered through a coarse sintered-glass funnel and rinsed with *i*-PrOH (100 mL). The filtrate was cooled to 0 °C and slowly neutralized by portionwise addition of K_2CO_3 (74.6 g, 0.54 mol, 2.7 equiv) with vigorous stirring (overhead stirrer). The viscous suspension was filtered and rinsed with H_2O (100 mL) and EtOAc (300 mL). The biphasic system was concentrated under reduced pressure to ~ 200 mL to remove a large portion of the *i*-PrOH and extracted with CH_2Cl_2 (100 mL portions until TLC clear). The combined organics were dried over $MgSO_4$, filtered, and concentrated under reduced pressure to afford cycloheptane-1,3-dione (**227**) (24.2 g, 0.192 mol, 96% yield) as a pale orange oil. $R_f = 0.16$ (4:1 hexanes/EtOAc); 1H NMR (300 MHz, $CDCl_3$) δ 3.59 (s, 2H),

2.60–2.56 (comp m, 4H), 2.02–1.94 (comp m, 4H). All other spectral data are consistent with reported values.



Vinylogous ester 228. To a solution of **227** (35.8 g, 0.284 mol, 1.0 equiv) in toluene (280 mL, 1 M) in a flask fitted with a Dean–Stark trap and reflux condenser was added *i*-BuOH (168.3 g, 208 mL, 2.27 mol, 8.0 equiv) and PPTS (1.07 g, 4.26 mmol, 0.0015 equiv). The solution was immersed into an oil bath at 130 °C and monitored by TLC. Upon consumption of the starting material (typically within 4–6 h), the reaction was allowed to cool to room temperature and the resulting dark orange solution was washed with sat. aq NaHCO₃ (200 mL). The aqueous phase was extracted with EtOAc (3 x 150 mL), the combined organics were washed with brine, dried over MgSO₄, filtered and concentrated under reduced pressure to afford a thick dark orange oil. The crude oil was flushed through a plug of silica gel (7 x 9 cm SiO₂, 1:4 → 3:7 → 1:1 hexanes/Et₂O) to afford the vinylogous ester **228** (43.5 g, 0.239 mol, 84% yield) as a pale orange oil. *R_f* = 0.22 (2:1 hexanes/EtOAc); ¹H NMR (500 MHz, CDCl₃) δ 5.37 (s, 1H), 3.49 (d, *J* = 6.6 Hz, 2H), 2.60–2.56 (comp m, 4H), 2.00 (septuplet, *J* = 6.6 Hz, 1H), 1.88–1.77 (comp m, 4H), 0.96 (d, *J* = 6.8 Hz, 6H); ¹³C NMR (126 MHz, CDCl₃) δ 202.5, 176.6, 106.0, 75.0, 41.9, 33.1, 27.9, 23.7, 21.5, 19.3; IR (Neat Film NaCl) 2958, 2872, 1646, 1607, 1469, 1237, 1190, 1174 cm⁻¹; HRMS (EI+) *m/z* calc'd for C₁₁H₁₈O₂ [M]⁺: 182.1307; found 182.1310.



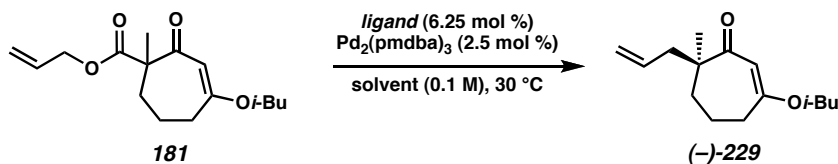
Vinylogous β -ketoester (\pm)-181. To a solution of *i*-Pr₂NH (3.06 mL, 21.9 mmol, 2.05 equiv) in PhMe (75 mL) cooled to $-78\text{ }^\circ\text{C}$ was added a solution of *n*-BuLi (8.36 mL, 21.3 mmol, 2.0 equiv; 2.55 M in hexane) via syringe. The flask was placed in a $0\text{ }^\circ\text{C}$ ice bath for 10 min, and then cooled back to $-78\text{ }^\circ\text{C}$ at which point a solution of **228** (1.9434 g, 10.7 mmol, 1.0 equiv) in PhMe (7 mL) was added dropwise via cannula. The flask was washed with extra PhMe (5 mL) to ensure complete transfer. After 30 min, allyl chloroformate (1.25 mL, 11.7 mmol, 1.1 equiv) was added dropwise and the cooling bath was removed. After 1 h at room temperature the reaction was quenched with 1 N KHSO₄ (25 mL) and the layers were separated. The aq layer was extracted with Et₂O (2 x 40 mL) and the combined organics were washed with brine, dried over Na₂SO₄, filtered, and concentrated to a viscous yellow oil.

The crude oil was dissolved in MeCN (43 mL, 0.25 M) and to this was added Cs₂CO₃ (4.34 g, 13.3 mmol, 1.25 equiv) and MeI (2.0 mL, 32.0 mmol, 3.0 equiv). The flask was fitted with a reflux condenser and placed in an $80\text{ }^\circ\text{C}$ oil bath with vigorous stirring. After 6–8 h the reaction was warmed to room temperature, diluted with EtOAc (50 mL), dried over MgSO₄, filtered, and concentrated in vacuo. The crude material was purified by flash chromatography on SiO₂ (9:1 \rightarrow 6:1 \rightarrow 3:1 hexanes/EtOAc, PhMe load) to give vinylogous β -ketoester (\pm)-**181** (2.4416 g, 8.71 mmol, 81% yield over two steps) as a pale yellow oil. $R_f = 0.43$ (4:1 hexanes/EtOAc); ¹H NMR (500 MHz, CDCl₃) δ 5.86

(dddd, $J = 17.1, 10.7, 5.6, 5.6$ Hz, 1H), 5.39 (s, 1H), 5.29 (ddd, $J = 17.1, 2.9, 1.5$ Hz, 1H), 5.20 (app d, $J = 10.5$ Hz, 1H), 4.59 (dddd, $J = 19.0, 13.2, 5.6, 1.2$ Hz, 2H), 3.50 (dd, $J = 9.3, 6.8$ Hz, 1H), 3.47 (dd, $J = 9.3, 6.6$ Hz, 1H), 2.59 (ddd, $J = 17.8, 9.8, 3.9$ Hz, 1H), 2.45–2.38 (comp m, 2H), 2.02–1.94 (m, 1H), 1.84–1.75 (m, 1H), 1.70 (ddd, $J = 14.4, 7.3, 4.4$ Hz, 1H), 1.43 (s, 3H), 0.94 (d, $J = 6.6$ Hz, 6H); ^{13}C NMR (126 MHz, CDCl_3) δ 199.1, 174.0, 173.5, 132.0, 118.4, 105.2, 74.8, 65.8, 59.1, 34.3, 33.9, 27.9, 24.2, 21.4, 19.3; IR (Neat Film NaCl) 2959, 2936, 2875, 1734, 1650, 1613, 1456, 1384, 1233, 1170, 1115, 994 cm^{-1} ; HRMS (EI+) m/z calc'd for $\text{C}_{16}\text{H}_{24}\text{O}_4$ $[\text{M}]^+$: 280.1675; found 280.1686.

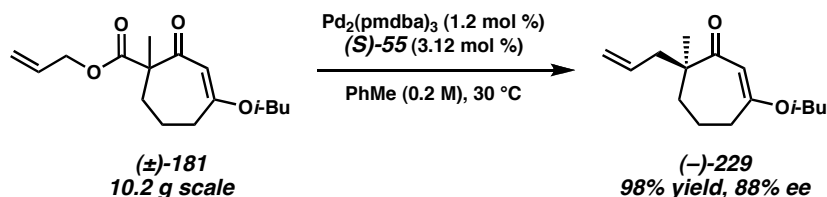
Alternative procedure using allyl cyanofornate. To a solution of *i*-Pr₂NH (4.66 g, 6.46 mL, 46.1 mmol, 1.2 equiv) in THF (180 mL) cooled to 0 °C in a 500 mL round-bottom flask was added *n*-BuLi (17.2 mL, 44.2 mmol, 2.57 M in hexanes, 1.15 equiv) dropwise over 15 min by use of syringe pump. After 15 min stirring at 0 °C, the mixture was cooled to –78 °C and a solution of vinylogous ester **228** (7.01 g, 38.4 mmol, 1.0 equiv) dissolved in THF (20 mL) and added in a dropwise manner over 20 min by use of a syringe pump. After an additional 1 h of stirring at –78 °C, allyl cyanofornate (4.69 g, 4.60 mL, 42.2 mmol, 1.1 equiv) was added in a dropwise manner over 10 min. The mixture was stirred at –78 °C for 2.5 h and quenched with 50% sat. aq NH₄Cl (60 mL) and allowed to warm to ambient temperature. The reaction mixture was diluted with Et₂O (100 mL) and the phases were separated. The aq phase was extracted with Et₂O (2 x 100 mL) and the combined organic phases were dried over MgSO₄, filtered and concentrated under reduced pressure to afford a pale orange oil (10.5 g, >100%, some allyl cyanofornate left).

The crude oil was converted to vinylogous β -ketoester **181** as above using CH_3CN (130 mL, 0.3 M), MeI (16.35 g, 7.2 mL, 115 mmol, 3.0 equiv), and Cs_2CO_3 (16.76 g, 49.9 mmol, 1.3 equiv). Purification by flash chromatography on SiO_2 (19:1 \rightarrow 9:1, hexanes/EtOAc, dry-loaded using Celite) afforded vinylogous β -ketoester (\pm)-**181** (8.51 g, 30.4 mmol, 79% yield over two steps) as a pale yellow oil.

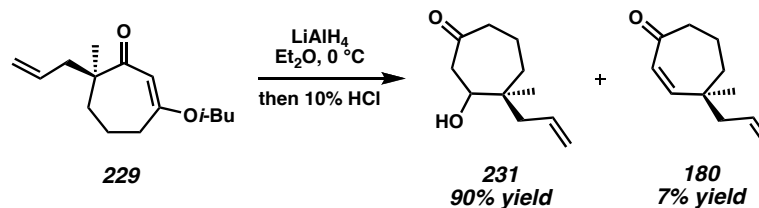


Screen for ketone (–)-229. To a dry flask was added $\text{Pd}_2(\text{pmdba})_3$ (2.5 mol %) and ligand (6.25 mol %) and the contents were evacuated/purged 3x with N_2 . To this was added solvent (0.1 M, most of it) and the contents were stirred for 30 min in a 30 °C oil bath, at which point a solution of (\pm)-**181** (1.0 equiv) in remaining solvent was transferred via cannula. When judged complete by TLC analysis, the reaction was filtered through a small plug of SiO_2 eluting with Et_2O and concentrated in vacuo. Purification by flash chromatography (15:1 \rightarrow 9:1 hexanes/EtOAc) or preparative TLC (4:1 hexanes/EtOAc) provided ketone **229** for analytical analysis. $R_f = 0.31$ (3:1 hexanes/ Et_2O); ^1H NMR (500 MHz, CDCl_3) δ 5.72 (dddd, $J = 16.6, 10.5, 7.3, 7.3$ Hz, 1H), 5.31 (s, 1H), 5.05–5.00 (m, 2H), 3.50 (dd, $J = 9.3, 6.6$ Hz, 1H), 3.47 (dd, $J = 9.3, 6.6$ Hz, 1H), 2.53–2.42 (m, 2H), 2.38 (dd, $J = 13.7, 7.1$ Hz, 1H), 2.20 (dd, $J = 13.7, 7.8$ Hz, 1H), 1.98 (app septuplet, $J = 6.6$ Hz, 1H), 1.86–1.70 (comp m, 3H), 1.62–1.56 (m, 1H), 1.14 (s, 3H), 0.95 (app d, $J = 6.6$ Hz, 6H); ^{13}C NMR (126 MHz, CDCl_3) δ 206.7, 171.3, 134.6, 117.9, 105.0, 74.5, 51.5, 45.4, 36.1, 35.2, 28.0, 25.2, 19.9, 19.3, 19.3; IR (Neat Film NaCl) 2960, 2933, 2873,

1614, 1470, 1387, 1192, 1171, 998, 912 cm^{-1} ; HRMS (EI+) m/z calc'd for $\text{C}_{15}\text{H}_{24}\text{O}_2$ $[\text{M}]^+$: 236.1776; found 236.1767. HPLC conditions: 1% *i*-PrOH in hexanes, OD-H column, t_R (min): major = 6.3, minor = 7.3.



Scale-up of ketone (-)-229. $\text{Pd}_2(\text{pmdba})_3$ (496 mg, 0.453 mmol, 0.0125 equiv) and ligand (*S*)-**55** (439 mg, 1.13 mmol, 0.0312 equiv) were placed in a 500 mL round-bottom flask and the flask was evacuated and backfilled with N_2 (3 cycles with 10 min evacuation per cycle). Toluene (150 mL, sparged with N_2 for 1 h immediately prior to use) was added and the dark purple suspension was immersed into a 30 °C oil bath. After 30 min stirring the solution had changed to a dark orange color and vinylogous β -ketoester (\pm)-**181** (10.16 g, 36.24 mmol, 1.0 equiv) dissolved in toluene (31 mL sparged with N_2 immediately before use) was added via positive pressure cannulation. Upon addition of (\pm)-**181**, the dark orange catalyst solution immediately turned olive green. The reaction mixture was stirred at 30 °C for 21 h (consumption by TLC), allowed to cool to ambient temperature, filtered through a small plug of SiO_2 (5.5 x 2 cm, Et_2O eluent) and concentrated under reduced pressure. Purification by flash chromatography on SiO_2 (5 x 15 cm, 19:1 hexanes/ EtOAc , dry-loaded on SiO_2) afforded ketone (-)-**229** (8.38 g, 35.46 mmol, 98% yield) as a pale yellow oil. $[\alpha]_D^{25.6} -69.04^\circ$ (c 1.08, CHCl_3 , 88% ee).

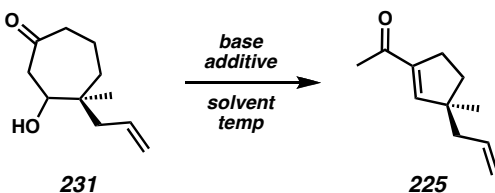


Reduction of ketone (–)-229. To a flask charged with Et₂O (15 mL) cooled to 0 °C was added LiAlH₄ (71.2 mg, 1.88 mmol, 0.55 equiv) in one portion. After 10 min, a solution of ketone **229** (806.1 mg, 3.41 mmol, 1.0 equiv) in Et₂O (2 mL) was added via cannula, washing the transfer flask with excess Et₂O to ensure quantitative transfer. After consumption of **229** by TLC analysis (1 h), the reaction was quenched by slow addition of 10% HCl (10 mL). The resulting biphasic system was allowed to warm to ambient temperature and stirred vigorously for 8–15 h. The layers were separated and the aq phase was extracted with Et₂O (3 x 20 mL). The combined organic phases were dried over Na₂SO₄, filtered and concentrated under reduced pressure. The crude product was azeotroped with toluene (3 x 5 mL) and purified by flash chromatography on SiO₂ (9:1 → 3:1 hexanes/EtOAc) to afford β-hydroxyketone **231** (558.8 mg, 3.07 mmol, 90% yield) as a colorless oil that forms a semisolid in a –20 °C freezer and cycloheptenone **180** (40.8 mg, 0.248 mmol, 7% yield) as a colorless oil.

β-Hydroxyketone 231. $R_f = 0.23$ (7:3 hexanes/EtOAc); ¹H NMR (500 MHz, CDCl₃) δ **major diastereomer:** 5.88 (dddd, $J = 15.1, 9.0, 7.6, 7.6$ Hz, 1H), 5.12–5.08 (m, 2H), 3.70 (dd, $J = 4.9, 3.9$ Hz, 1H), 2.86 (dd, $J = 15.6, 1.7$ Hz, 1H), 2.65 (dd, $J = 15.6, 7.3$ Hz, 1H), 2.54–2.43 (m, 2H), 2.24 (dd, $J = 13.7, 7.8$ Hz, 1H), 2.07 (dd, $J = 13.4, 7.3$ Hz, 1H), 1.99 (dd, $J = 15.9, 4.4$ Hz, 1H), 1.82–1.69 (comp m, 2H), 1.45–1.41 (m, 1H), 0.96 (s, 3H); **minor diastereomer:** 5.83 (dddd, $J = 14.9, 10.3, 7.6, 7.6$ Hz, 1H), 5.12–5.06 (m, 2H), 3.68 (dd, $J = 4.1, 2.4$ Hz, 1H), 2.80 (dd, $J = 15.4, 2.4$ Hz, 1H), 2.74 (dd, $J =$

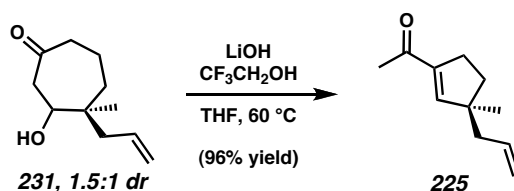
15.4, 8.1 Hz 1H), 2.46–2.38 (m, 2H), 2.18 (dd, $J = 13.9, 7.3$ Hz, 1H), 2.09 (dd, $J = 12.9, 7.8$ Hz, 1H), 1.82–1.65 (comp m, 3H) 1.50–1.47 (m, 1H), 1.02 (s, 3H); ^{13}C NMR (75 MHz, CDCl_3) δ **major diastereomer:** 213.2, 135.0, 118.1, 72.9, 46.7, 44.9, 44.2, 41.0, 36.3, 21.9, 18.9; **minor diastereomer:** 212.6, 134.2, 118.3, 73.3, 47.2, 42.8, 41.0, 35.9, 22.6, 18.7 one peak overlapping; IR (Neat Film NaCl) 3436 (br), 3074, 2932, 1692, 1638, 1443, 1403, 1380, 1352, 1318, 1246, 1168, 1106, 1069, 999, 913, 840 cm^{-1} ; HRMS (EI+) m/z calc'd for $\text{C}_{11}\text{H}_{18}\text{O}_2$ $[\text{M}]^+$: 182.1307; found 182.1313; $[\alpha]_{\text{D}}^{22.8} -57.1^\circ$ (c 2.56, CHCl_3 , 1.5:1 dr and 88% ee).

Cycloheptenone 180. $R_f = 0.54$ (7:3 hexanes/EtOAc); ^1H NMR (500 MHz, CDCl_3) δ 6.04 (dd, $J = 12.9, 0.7$ Hz, 1H), 5.82 (d, $J = 12.9$ Hz, 1H), 5.75 (dddd, $J = 17.1, 10.3, 7.8, 7.1$ Hz, 1H), 5.10 (dddd, $J = 10.3, 1.2, 1.2, 1.2$ Hz, 1H), 5.08–5.03 (m, 1H), 2.65–2.52 (m, 2H), 2.19 (app dd, $J = 13.7, 6.8$ Hz, 1H), 2.11 (app dd, $J = 13.7, 8.1$ Hz, 1H), 1.84–1.76 (m, 3H), 1.68–1.63 (m, 1H), 1.10 (s, 3H); ^{13}C NMR (75 MHz, CDCl_3) δ 204.7, 152.5, 133.8, 128.6, 118.6, 47.2, 45.1, 42.7, 38.2, 27.1, 18.4; IR (Neat Film NaCl) 3076, 3011, 2962, 2934, 2870, 1659, 1454, 1402, 1373, 1349, 1335, 1278, 1208, 1172, 997, 916, 874, 822, 772 cm^{-1} ; HRMS (EI+) m/z calc'd for $\text{C}_{11}\text{H}_{16}\text{O}$ $[\text{M}]^+$: 164.1201; found 164.1209; $[\alpha]_{\text{D}}^{21.0} -9.55^\circ$ (c 1.07, CHCl_3 , 88% ee).



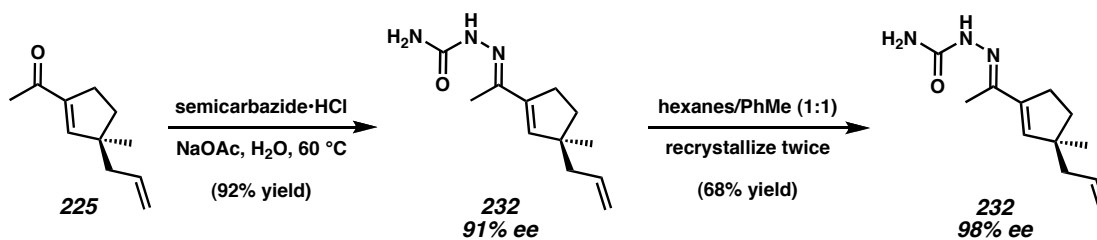
Ring contraction screen to produce acylcyclopentene 225. A benzene solution of β -hydroxyketone **231** was transferred to a dry 1-dram vial and concentrated in vacuo to

obtain a starting mass. To this vial was added a stir bar, 1,4-diisopropylbenzene (by mass, as internal standard), and the contents were solvated in either *t*-BuOH or THF (0.1 M). After complete solvation, an appropriate additive (*t*-BuOH, TFE, or HFIP; 1.5 equiv) followed by a base (1.5 equiv) were added, the head space of the vial was purged with nitrogen, and the vial was capped with a teflon-lined cap and placed on the appropriate heating block (40 or 60 °C). Reaction progress was initially followed by TLC analysis, and when necessary aliquots were removed and flushed through a small SiO₂ plug with EtOAc for GC analysis. GC conditions: 90 °C isothermal for 5 min, then ramp 10 °C/min to 250 °C, DB-WAX column, *t_R* (min): 1,4-diisopropylbenzene = 5.3, acylcyclopentene **225** = 9.3, β-hydroxyketone **231** = 17.1 and 17.2 (two diastereomers).



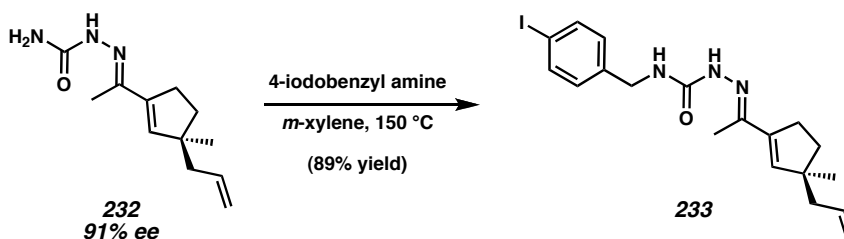
Scale-up of acylcyclopentene 225. To a solution of β-hydroxyketone **231** (6.09 g, 33.4 mmol, 1.0 equiv) dissolved in THF (334 mL, 0.1 M) in a 500 mL flask was added 2,2,2-trifluoroethanol (5.04 g, 3.67 mL, 50.1 mmol, 1.5 equiv) and LiOH (1.20 g, 50.1 mmol, 1.5 equiv). The flask was fitted with a reflux condenser, purged with a stream of N₂, and placed in a 60 °C oil bath. After 18 h the suspension was allowed to cool to ambient temperature, diluted with Et₂O (150 mL), dried over Na₂SO₄ (30 min stirring), filtered, and concentrated carefully under vacuum allowing for a film of ice to form on the outside of the flask. The crude product was purified by flash chromatography on SiO₂ (5 x 15 cm, 15:1 hexanes/Et₂O) and concentrated carefully to afford

acylcyclopentene **225** (5.29 g, 32.2 mmol, 96% yield) as a colorless fragrant oil. $R_f = 0.67$ (4:1 hexanes/EtOAc); $^1\text{H NMR}$ (500 MHz, CDCl_3) δ 6.45 (app t, $J = 1.7$ Hz, 1H), 5.76 (dddd, $J = 16.4, 10.7, 7.3, 7.3$ Hz, 1H), 5.07–5.03 (comp m, 2H), 2.59–2.48 (comp m, 2H), 2.21–2.14 (comp m, 2H), 2.30 (s, 3H), 1.85 (ddd, $J = 12.9, 8.3, 6.3$ Hz, 1H), 1.64 (ddd, $J = 6.1, 8.5, 12.9$ Hz), 1.11 (s, 3H); $^{13}\text{C NMR}$ (126 MHz, CDCl_3) δ 197.5, 151.9, 143.8, 134.9, 117.8, 50.0, 45.3, 36.0, 29.7, 26.8, 25.6; IR (Neat Film NaCl) 3077, 2956, 2863, 1668, 1635, 1616, 1454, 1435, 1372, 1366, 1309, 1265, 1213, 1177, 993, 914, 862 cm^{-1} ; HRMS (EI+) m/z calc'd for $\text{C}_{11}\text{H}_{16}\text{O}$ $[\text{M}]^+$: 164.1201; found 164.1216; $[\alpha]_{\text{D}}^{21.4} +17.3^\circ$ (c 0.955, CHCl_3 , 88% ee). GC conditions: 80 °C isothermal, GTA column, t_{R} (min): major = 54.7, minor = 60.2.



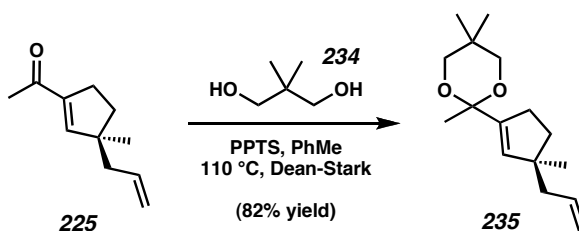
Semicarbazone 232. A 15 mL round-bottom flask was charged with sodium acetate (150 mg, 1.83 mmol, 1.2 equiv), and semicarbazide hydrochloride (204 mg, 1.83 mmol, 1.2 equiv). The solids were dissolved in purified water (1.7 mL). Acylcyclopentene **225** (250 mg, 1.52 mmol, 1.0 equiv) was added neat and the mixture was heated to 60 °C for 4 h. The slurry was allowed to cool to ambient temperature while stirring and vacuum filtered (water aspirator). The white solid was dried under reduced pressure to afford semicarbazone **232** (311 mg, 1.41 mmol, 92% yield). The ee of **232** at this point was found to be 91% (measured by hydrolysis to acylcyclopentene **225**). Semicarbazone **232**

Hydrolysis to acylcyclopentene 225. Semicarbazone **232** (191.8 mg, 0.867 mmol) was dissolved in THF (1.92 mL) and aq HCl (3.84 mL, 6 M) was added. The resulting biphasic mixture was stirred vigorously at 23 °C for 30 h. The reaction mixture was diluted with Et₂O (10 mL), the phases were separated, and the aqueous phase was extracted with Et₂O (2 x 10 mL). The combined organics were dried over MgSO₄, filtered and concentrated carefully under vacuum allowing for a film of ice to form on the outside of the flask. The residue was filtered through a short pad of SiO₂ (4:1 hexanes/Et₂O) to afford **225** (132.6 mg, 0.81 mmol, 93% yield); [α]_D^{21.2} +19.6° (*c* 1.035, CHCl₃, 97.9% ee).



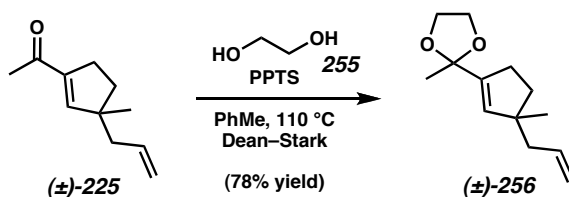
Iodoarene 233. To a solution of semicarbazone **232** (50 mg, 0.23 mmol, 91% ee, 1.0 equiv) in *m*-xylene (2.2 mL) was added 4-iodobenzylamine (63 mg, 0.27 mmol, 1.2 equiv). The resulting pale yellow solution was immersed in a 150 °C oil bath. After 9 h, the mixture was allowed to cool to ambient temperature and concentrated under reduced pressure to afford a pale yellow solid. The crude solid was purified by flash chromatography on SiO₂ (9:1 → 7:3 hexanes/EtOAc) to afford iodoarene **233** (88 mg, 0.20 mmol, 89% yield) as a white solid. X-ray-quality crystals were obtained by slow vapor diffusion of pentane into a chloroform solution of **233**. *R*_f = 0.52 (9:1 CHCl₃/MeOH); mp = 123–124°C (CHCl₃/*n*-pentane); ¹H NMR (500 MHz, CDCl₃) δ 7.88

(s, 1H), 7.66–7.64 (m, 2H), 7.08 (d, $J = 8.5$ Hz, 2H), 6.50 (t, $J = 6.1$ Hz, 1H), 5.86 (app t, $J = 1.5$ Hz, 1H), (dddd, $J = 16.9, 9.0, 7.6, 7.6$ Hz, 1H), 5.04–5.01 (comp m, 2H), 4.46 (d, $J = 6.3$ Hz, 2H), 2.60–2.49 (comp m, 2H), 2.18–2.10 (comp m, 2H); 1.95 (s, 3H), 1.82 (ddd, $J = 12.9, 8.5, 6.3$ Hz, 1H), 1.62 (ddd, $J = 12.9, 8.5, 6.1$ Hz, 1H), 1.07 (s, 3H); ^{13}C NMR (126 MHz, CDCl_3) δ 156.3, 144.5, 141.5, 141.4, 139.2, 137.8, 135.6, 129.4, 117.2, 92.6, 49.3, 45.9, 43.2, 36.2, 30.9, 26.3, 12.5; IR (Neat Film NaCl) 3411, 3194, 3075, 2946, 2920, 2863, 1677, 1528, 1486, 1401, 1323, 1259, 1142, 1114, 1057, 1000, 913, 845 cm^{-1} ; HRMS (FAB+) m/z calc'd for $\text{C}_{19}\text{H}_{25}\text{N}_3\text{OI}$ $[\text{M} + \text{H}]^+$: 438.1043; found 438.1036; $[\alpha]_{\text{D}}^{22.2} +31.4^\circ$ (c 0.385, CHCl_3 , 91% ee).



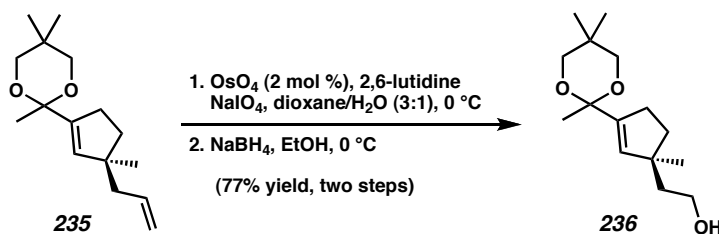
Acetal 235. To a solution of acylcyclopentene **225** (5.29 g, 32.2 mmol, 1.0 equiv) in toluene (322 mL) in a 1 L round-bottom flask was added neopentyl glycol (**234**) (20.1 g, 193.2 mmol, 6.0 equiv) and PPTS (809 mg, 3.22 mmol, 0.1 equiv). The flask was fitted with a Dean–Stark trap and a condenser and the mixture was placed in a 135 °C oil bath and heated to reflux. After 25 h the mixture was allowed to cool to ambient temperature, diluted with Et_2O (250 mL), and poured into sat. aq NaHCO_3 (100 mL). The aq phase was extracted with Et_2O (2 x 100 mL) and the combined organic phases were dried over Na_2SO_4 , filtered, and concentrated under reduced pressure to afford a white semisolid. The crude product was purified by flash chromatography on SiO_2 (1:0 \rightarrow 99:1 \rightarrow 98:2 hexanes/ EtOAc) to afford acetal **235** (6.59 g, 26.3 mmol, 82% yield) as a pale yellow oil.

$R_f = 0.62$ (7:3 hexanes/EtOAc); $^1\text{H NMR}$ (300 MHz, CDCl_3) δ 5.80 (dddd, $J = 16.7$, 9.3, 7.4, 7.4 Hz, 1H), 5.52 (app t, $J = 1.8$ Hz, 1H), 5.06–4.99 (comp m, 2H), 3.59 (dd, $J = 11.2$, 0.8 Hz, 1H), 3.51 (dd, $J = 11.2$, 0.8 Hz, 1H), 3.31 (d, $J = 11.2$ Hz, 2H), 2.37–2.19 (m, 2H), 2.13 (app dt, $J = 7.4$, 1.1 Hz, 2H), 1.853 (ddd, $J = 12.8$, 8.2, 6.4 Hz, 1H), 1.63 (ddd, $J = 12.8$, 8.8, 6.1 Hz, 1H), 1.41 (s, 3H), 1.17 (s, 3H), 1.07 (s, 3H), 0.69 (s, 3H); $^{13}\text{C NMR}$ (75 MHz, CDCl_3) δ 141.1, 138.2, 136.1, 116.9, 98.8, 71.8, 71.7, 49.0, 46.2, 36.4, 31.4, 29.8, 27.8, 26.9, 22.8, 22.2; IR (Neat Film NaCl) 3075, 2952, 2906, 2868, 1640, 1472, 1455, 1182, 1118, 1041, 996, 950, 911, 862 cm^{-1} ; HRMS (EI+) m/z calc'd for $\text{C}_{16}\text{H}_{27}\text{O}_2$ $[\text{M} + \text{H}]^+$: 251.2011; found 251.2011; $[\alpha]_{\text{D}}^{20.9} +11.5^\circ$ (c 1.01, CHCl_3 , 88% ee).



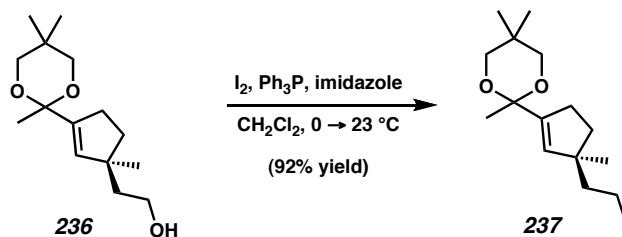
Dioxolane 256. To a solution of **225** (388.1 mg, 2.36 mmol, 1.0 equiv) in benzene (11.8 mL) in a 25 mL round-bottom flask was added ethylene glycol (**255**) (880 mg, 791 μL , 14.2 mmol, 6.0 equiv) and PPTS (59.4 mg, 0.24 mmol, 0.1 equiv). The flask was fitted with a condenser and a Dean–Stark trap and immersed into a 115 °C oil bath and heated to reflux. After 18 h at reflux, the mixture was allowed to cool to ambient temperature, diluted with Et_2O (50 mL), and washed with brine (10 mL). The aq phase was extracted with Et_2O (2 x 10 mL) and the combined organic phases were dried over Na_2SO_4 , filtered and concentrated under reduced pressure to give a colorless oil. The crude product was purified by flash chromatography on SiO_2 (15:1 \rightarrow 9:1 hexanes/EtOAc) to afford dioxolane **256** (381.4 mg, 1.83 mmol, 78% yield) as a colorless

oil. $R_f = 0.49$ (7:3 hexanes/EtOAc); $^1\text{H NMR}$ (300 MHz, CDCl_3) δ 5.76 (dddd, $J = 17.1, 9.3, 7.6, 7.6$ Hz, 1H), 5.50, (br s, 1H), 5.02–4.99 (comp m, 4H), 3.98–3.84 (comp m, 2H), 2.36 (dddd, $J = 10.3, 8.1, 5.9, 1.7$ Hz, 1H), 2.30 (dddd, $J = 10.3, 8.1, 6.1, 1.7$ Hz, 1H), 2.09 (d, $J = 7.3$ Hz, 2H), 1.82 (ddd, $J = 12.9, 8.5, 6.1$ Hz, 1H), 1.62 (ddd, $J = 12.7, 8.8, 5.9$ Hz, 1H), 1.48–1.47 (m, 3H), 1.03 (s, 3H); $^{13}\text{C NMR}$ (126 MHz, CDCl_3) δ 142.9, 136.0, 135.7, 116.8, 107.4, 64.7, 64.7 (two lines), 48.4, 46.1, 36.8, 30.6, 26.5, 24.0; IR (Neat Film NaCl) 2951, 2888, 1454, 1372, 1192, 1108, 1043, 996, 946, 912, 858 cm^{-1} ; HRMS (EI+) m/z calc'd for $\text{C}_{12}\text{H}_{17}\text{O}_2$ $[\text{M} - \text{CH}_3]^+$: 193.1229; found 193.1232.



Alcohol 236. To a solution of acetal **235** (1.51 g, 6.03 mmol, 1.0 equiv) in 1,4-dioxane (45 mL) and purified H_2O (15 mL) was added 2,6-lutidine (1.29 g, 1.40 mL, 12.0 mmol, 2.0 equiv). The mixture was cooled to 0°C and NaIO_4 (5.13 g, 24.0 mmol, 4.0 equiv) was added followed by OsO_4 (30.5 mg, 0.120 mmol, 0.02 equiv). The resulting suspension was stirred for 4.5 h at 0°C and then vacuum filtered, rinsing with EtOAc (100 mL). The aq phase was separated and extracted with EtOAc (2 x 25 mL), the combined organic phases were dried over Na_2SO_4 , filtered, and concentrated under reduced pressure to afford the desired product 1.82 g (>100%, contains some 2,6-lutidine) as a clear brown oil. This material was used in the subsequent step without purification.

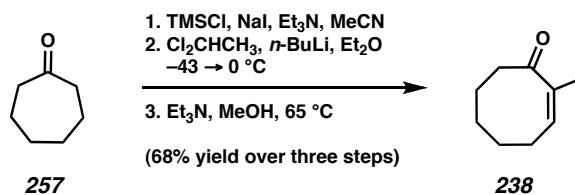
The crude product was dissolved in EtOH (7.5 mL) and cooled to $-21\text{ }^{\circ}\text{C}$ by use of a MeOH/ice bath. A solution of NaBH_4 (227.0 mg, 6.00 mmol, 1.0 equiv) dissolved in EtOH (7.5 mL) and precooled to $0\text{ }^{\circ}\text{C}$ was added dropwise over 25 min to the reaction mixture via positive pressure cannulation. After an additional 1 h stirring at $-21\text{ }^{\circ}\text{C}$, the reaction was quenched by slow addition of H_2O (4.5 mL). The reaction mixture was allowed to warm to $0\text{ }^{\circ}\text{C}$, concentrated under reduced pressure to ca. 10 mL and extracted with CH_2Cl_2 (3 x 25 mL), dried over Na_2SO_4 , filtered and concentrated under reduced pressure to afford a pale brown oil. The crude material was purified by flash chromatography on SiO_2 (19:1 \rightarrow 9:1 \rightarrow 4:1 hexanes/EtOAc) to afford alcohol **236** (1.18 g, 4.64 mmol, 77% yield over two steps) as a pale yellow oil. $R_f = 0.38$ (7:3 hexanes/EtOAc); ^1H NMR (500 MHz, CDCl_3) δ 5.57 (app t, $J = 1.7\text{ Hz}$, 1H), 3.71 (ddd, $J = 7.3, 7.3, 5.4\text{ Hz}$, 2H), 3.52 (app t, $J = 11.0\text{ Hz}$, 2H), 3.34 (11.0 Hz, 2H), 2.38–2.26 (comp m, 2H), 1.88 (ddd, $J = 12.9, 8.5, 6.1\text{ Hz}$, 1H), 1.71 (t, $J = 7.3\text{ Hz}$, 2H), 1.69 (ddd, $J = 12.9, 8.5, 5.9\text{ Hz}$, 1H), 1.42 (s, 3H), 1.21 (t, $J = 5.1\text{ Hz}$, 1H), 1.16 (s, 3H), 1.09 (s, 3H), 0.71 (s, 3H); ^{13}C NMR (75 MHz, CDCl_3) δ 141.1, 138.1, 98.6, 71.7, 60.2, 47.5, 44.1, 36.9, 31.1, 29.7, 27.4, 27.1, 22.7, 22.2; IR (Neat Film NaCl) 3428 (br), 3041, 2951, 2868, 1472, 1456, 1396, 1370, 1353, 1321, 1259, 1242, 1181, 1117, 1082, 1040, 1015, 950, 911, 862, 809, 793 cm^{-1} ; HRMS (FAB+) m/z calc'd for $\text{C}_{15}\text{H}_{27}\text{O}_3$ $[\text{M} + \text{H}]^+$: 255.1960; found 255.1951; $[\alpha]_{\text{D}}^{19.9} -3.25^{\circ}$ (c 0.99, CHCl_3 , 88% ee).



Iodide 237. A 25 mL flask was charged with PPh_3 (881.3 mg, 3.36 mmol, 1.5 equiv) and imidazole (457.5 mg, 6.72 mmol, 3.0 equiv) and the flask was evacuated and backfilled with Ar (3x). The solids were dissolved in CH_2Cl_2 (8.0 mL, typically solvated within 10 min). The flask was wrapped in aluminum foil and I_2 (869.6 mg, 3.36 mmol, 1.5 equiv) was added. After 10 min, the mixture was cooled to $0\text{ }^\circ\text{C}$ and a solution of alcohol **236** (571.2 mg, 2.24 mmol, 1.0 equiv) in CH_2Cl_2 (3.0 mL) was added via syringe. The reaction mixture was stirred at $0\text{ }^\circ\text{C}$ for 1 h and then allowed to warm to $23\text{ }^\circ\text{C}$. After an additional 3 h stirring, hexanes (11 mL) was added and the resulting slurry was filtered through a plug of Celite (5 x 1 cm) eluting with hexanes/ Et_2O (1:1, 100 mL). The filtrate was concentrated under reduced pressure, resuspended in hexanes (50 mL), filtered, and concentrated under reduced pressure. The crude material was purified by flash chromatography on SiO_2 (1:0 \rightarrow 99:1 \rightarrow 98:2 \rightarrow 90:10 hexanes/ Et_2O , dry-loaded on Celite) to afford iodide **237** (753 mg, 2.07 mmol, 92% yield) as a colorless oil. $R_f = 0.71$ (7:3 hexanes/ $EtOAc$); 1H NMR (500 MHz, $CDCl_3$) δ 5.51 (s, 1H), 3.50 (app t, 11.5 Hz, 2H), 3.34 (d, $J = 11.2$ Hz, 2H), 3.19–3.06 (comp m, 2H), 2.38–2.25 (comp m, 2H), 2.12–2.02 (comp m, 2H), 1.84 (ddd, $J = 13.2, 8.8, 5.9$ Hz, 1H), 1.67 (ddd, $J = 13.2, 8.8, 5.6$ Hz, 1H), 1.41 (s, 3H), 1.16 (s, 3H), 1.07 (s, 3H), 0.71 (s, 3H); ^{13}C NMR (126 MHz, $CDCl_3$) δ 142.5, 136.6, 98.6, 71.9, 71.9 (two lines), 51.2, 46.8, 36.1, 31.4, 29.8, 27.5, 26.4, 22.8, 22.3, 1.1; IR (Neat Film NaCl) 3039, 2956, 2863, 1470, 1450, 1390, 1365, 1315, 1254,

1173, 1119, 1083, 1039, 1011, 944, 915, 866, 814 cm^{-1} ; HRMS (FAB+) m/z calc'd for $\text{C}_{15}\text{H}_{26}\text{O}_2\text{I}$ $[\text{M} + \text{H}]^+$: 365.0978; found 365.0980; $[\alpha]_{\text{D}}^{20.3} +31.2^\circ$ (c 1.03, CHCl_3 , 88% ee).

3.7.2.5 MODEL FRAGMENT COUPLING AND C-RING ANNULATION



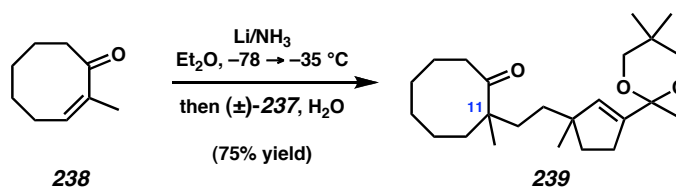
2-Methyl cyclooctenone (238). A 500 mL round-bottom flask was charged with NaI (18.74 g, 125 mmol, 1.25 equiv), MeCN (140 mL) was added, and the system was evacuated and backfilled with Ar. Cycloheptanone (**257**) (11.2 g, 11.8 mL, 100 mmol, 1.0 equiv) was added followed by Et₃N (16.7g, 17.4 mL, 125 mmol, 1.25 equiv) and dropwise addition of TMSCl (12.4 g, 14.6 mL, 114 mmol, 1.14 equiv). The resulting suspension was stirred at 23 °C for 30 min and then petroleum ether (100 mL) was added. The biphasic system was stirred vigorously for 10 min, the petroleum ether layer was decanted, and the MeCN layer was extracted with petroleum ether (3 x 50 mL). The combined petroleum ether layers were washed with H₂O (2 x 50 mL), brine (50 mL), dried over Na₂SO₄, filtered, and concentrated under reduced pressure. The crude oil was purified by short path distillation (8.7 torr, bp = 75–81°C) to afford the desired silyl enol ether (18.4 g, 99.8 mmol, 99.8% yield) as a colorless oil.

A solution of the above silyl enol ether (8.20 g, 44.5 mmol) in Et₂O (22.8 mL) and 1,1-dichloroethane (17.8 g, 15.1 mL, 180 mmol, 4.0 equiv) in a 250 mL round-bottom flask was cooled to -40 °C by use of a MeCN/CO_{2(s)} bath. To this was added *n*-BuLi

(58.7 mL, 135 mmol, 2.3 M in hexanes, 3.0 equiv) in a dropwise manner over 3 h by use of a syringe pump. The resulting mixture was stirred for an additional 1 h at $-40\text{ }^{\circ}\text{C}$, at which time the reaction was warmed to $0\text{ }^{\circ}\text{C}$ for 2 h, quenched with H_2O (20 mL) and allowed to warm to ambient temperature. The phases were separated and the organic phase was washed with H_2O (4 x 20 mL) until the aqueous phase showed neutral pH. The organic phase was dried over Na_2SO_4 , filtered, and concentrated under reduced pressure to afford the desired cyclopropane (11.1 g, 45.0 mmol, quantitative) as a clear, pale yellow oil. This material was used in the following reaction without further purification.

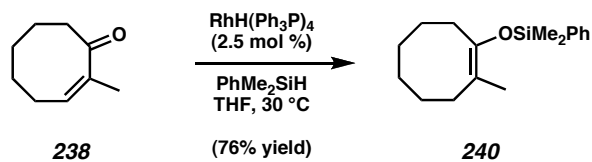
To a solution of the above cyclopropane (11.1 g, 45.0 mmol, 1.0 equiv) in MeOH (136 mL) was added Et_3N (41.0 g, 56 mL, 405 mmol, 9.0 equiv). The flask was fitted with a condenser and the mixture was immersed into a $85\text{ }^{\circ}\text{C}$ oil bath and heated to reflux. After 65 h, the mixture was allowed to cool to ambient temperature and concentrated carefully under reduced pressure (the compound is somewhat volatile). The residue was suspended in pentane (50 mL), filtered, and concentrated under reduced pressure. The final traces of Et_3N were removed by dissolving the residue in Et_2O (100 mL) and washing with KHSO_4 (20 mL, 1.0 M). The organic phase was dried over MgSO_4 , filtered, and concentrated under reduced pressure. The crude material was purified by flash chromatography on SiO_2 (1:0 \rightarrow 19:1 hexanes/ Et_2O) to 2-methyl cyclooctenone (**239**) (4.21 g, 30.5 mmol, 68% yield over three steps) as a colorless oil. $R_f = 0.43$ (4:1 hexanes/ Et_2O); ^1H NMR (300 MHz, CDCl_3) δ 6.09 (app tq, $J = 6.9, 1.5$ Hz, 1H), 2.65–2.61 (comp m, 2H), 2.42–2.35 (comp m, 2H), 1.86–1.77 (comp m, 3H), 1.84 (q, $J = 1.4$ Hz, 2H), 1.64–1.49 (comp m, 4H); ^{13}C NMR (75 MHz, CDCl_3) δ 208.9,

137.5, 135.0, 42.9, 28.6, 25.9, 23.3, 22.8, 21.1; IR (Neat Film NaCl) 2928, 1685, 1654, 1452, 1377, 1099, 850 cm^{-1} ; HRMS (MM: ESI/APCI) m/z calc'd for $\text{C}_9\text{H}_{15}\text{O}$ $[\text{M} + \text{H}]^+$: 139.1117, found 139.1114.

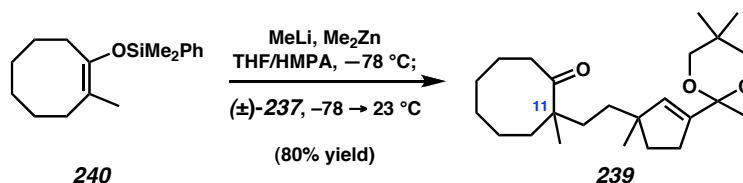


Ketone 239. Ammonia (ca. 5 mL) was condensed into a 2-neck round-bottom flask fitted with a septum, an argon inlet, and a glass-coated stir bar at $-78 \text{ }^\circ\text{C}$, and to this was added lithium wire (9.3 mg, 1.3 mmol, 3.0 equiv). The solution turned dark blue. The mixture was stirred for 20 min, at which point a solution of 2-methyl cyclooctenone (**238**, 60.2 mg, 0.436 mmol, 1.0 equiv) in a 0.21 M H_2O solution in Et_2O (2 mL, prepared by dissolving H_2O (94 μL) in Et_2O (25 mL) in a flame-dried round-bottom flask under argon) was added via cannula transfer. The vial was further washed and transferred with a portion of anhydrous Et_2O (1 mL). The bright blue color remained after addition and the solution was stirred for 10 min, at which point a solution of iodide (\pm)-**237** (324 mg, 0.980 mmol, 2.0 equiv) in Et_2O (2 mL) was added dropwise via cannula. During the addition of iodide (\pm)-**237**, the color of the solution changed from blue to colorless and stirring was continued in the acetone/ $\text{CO}_{2(\text{s})}$ bath. After 2 h, the cooling bath was replaced with a MeCN/ $\text{CO}_{2(\text{s})}$ cooling bath held between -45 and $-35 \text{ }^\circ\text{C}$. The mixture was stirred for an additional 2 h, at which point solid NH_4Cl (523 mg) was added, the cooling bath was removed, and the reaction was allowed to reach room temperature. After most of the ammonia had evaporated, the reaction was diluted with H_2O (10 mL)

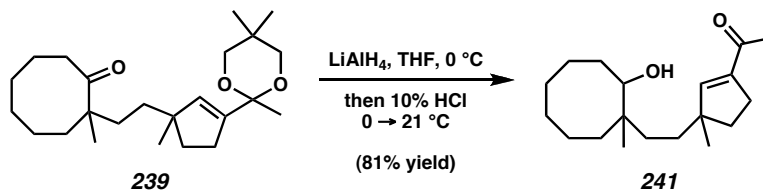
and Et₂O (25 mL). The aqueous layer was extracted with Et₂O (5 x 15 mL) and the combined organics were washed with brine (10 mL), dried with MgSO₄, filtered, and concentrated. The crude residue was purified by flash chromatography on SiO₂ (95:5 hexanes/EtOAc) to afford desired ketone **239** (122.9 mg, 0.326 mmol, 75% yield) as 1:1.2 mixture of diastereomers. $R_f = 0.70$ (3:7 hexanes/Et₂O); ¹H NMR (500 MHz, C₆D₆) δ **major diastereomer**: 5.58 (app t, $J = 1.7$ Hz, 1H), 3.55 (d, $J = 11.0$ Hz, 1H), 3.48 (d, $J = 11.0$ Hz, 1H), 3.31 (d, $J = 11.0$ Hz, 2H), 2.40–2.36 (comp m, 3H), 2.03 (ddd, $J = 10.7, 7.1, 3.4$ Hz, 1H), 1.81–1.69 (comp m, 3H), 1.62 (s, 3H), 1.60–1.50 (comp m, 3H), 1.42–1.22 (comp m, 8H), 1.19 (s, 3H), 1.18–1.10 (comp m, 3H), 1.02 (s, 3H), 1.00 (s, 3H), 0.53 (s, 3H); **minor diastereomer**: 5.56 (app t, $J = 1.7$ Hz, 1H), 3.52 (d, $J = 11.0$ Hz, 1H), 3.48 (d, $J = 10.7$ Hz, 1H), 3.30 (d, $J = 11.0$ Hz, 2H), 2.40–2.36 (comp m, 3H), 2.02 (ddd, $J = 10.7, 7.1, 3.4$ Hz, 1H), 1.81–1.69 (comp m, 3H), 1.62 (s, 3H), 1.62 (s, 3H), 1.60–1.50 (comp m, 3H), 1.42–1.22 (comp m, 8H), 1.19 (s, 3H), 1.18–1.10 (comp m, 3H), 1.03 (s, 3H), 1.00 (s, 3H), 0.52 (s, 3H); ¹³C NMR (126 MHz, C₆D₆) δ **mixture of two diastereomers**: 218.1 (two lines), 142.4 (two lines), 137.9, 137.8, 98.9 (two lines), 71.9, 71.8 (three lines), 49.8 (two lines), 48.7 (two lines), 36.9, 36.8, 36.5 (two lines), 35.9, 35.8, 34.6, 34.5, 34.2, 34.1, 31.9 (two lines), 30.4 (two lines), 29.7, 28.1, 28.0, 27.2, 27.1, 26.2, (two lines), 25.3 (two lines), 24.5, 22.9, 22.2, 22.1, 19.2, 19.1; IR (Neat Film NaCl) 2932, 2858, 1698, 1469, 1448, 1396, 1368, 1254, 1239, 1180, 1117, 1083, 1040, 950, 911, 863, 810, 793 cm⁻¹; HRMS (FAB+) m/z calc'd for C₂₄H₄₁O₃ [M + H]⁺: 377.3056; found 377.3043.



Silyl enol ether 240. Enone **238** (100 mg, 0.724 mmol, 1.0 equiv) was placed in a 1-dram vial, evacuated and backfilled with N₂ (3x), and solvated in THF (350 μL). A separate flask containing RhH(PPh₃)₄ (20.9 mg, 0.0181 mmol, 0.025 equiv) was evacuated and backfilled with N₂ (3 cycles with 5 min evacuation per cycle) and then THF (1.1 mL) was added. A separate vial containing an excess of PhMe₂SiH was degassed by evacuation/backfilling with N₂ (3x). The required amount of PhMe₂SiH (631 mg, 720 μL, 4.63 mmol, 6.4 equiv) was added to the catalyst suspension via syringe and the resulting clear orange solution was immersed in a 30 °C oil bath. After 10 min, the THF solution of enone **238** was added via positive pressure cannulation. After 25 h the reaction was allowed to cool to ambient temperature, filtered through a plug of SiO₂ (2 x 1 cm, Et₂O) and concentrated under reduced pressure to afford a pale orange oil. The crude material was purified by flash chromatography on SiO₂ (99:1 → 98:2 hexanes/PhH) to afford silyl enol ether **240** (150.2 mg, 0.547 mmol, 76% yield) as a colorless oil. *R_f* = 0.52 (hexanes); ¹H NMR (300 MHz, CDCl₃) δ 7.65–7.61 (comp m, 2H), 7.42–7.34 (comp m, 3H), 2.18–2.14 (comp m, 2H), 2.06–2.02 (comp m, 2H), 1.59 (s, 3H), 1.55–1.38 (comp m, 8H), 0.44 (s, 6H); ¹³C NMR (75 MHz, CDCl₃) δ 145.1, 138.7, 133.5, 129.6, 127.9, 113.9, 31.9, 31.6, 29.0, 28.7, 26.8, 26.5, 16.1, –0.4; IR (Neat Film NaCl) 3075, 2951, 2863, 1638, 1468, 1450, 1393, 1370, 1254, 1241, 1179, 1117, 1080, 1037, 1011, 995, 949, 910, 861, 809 cm⁻¹; HRMS (FAB+) *m/z* calc'd for C₁₇H₂₆OSi [M]⁺: 274.1753; found 274.1752.

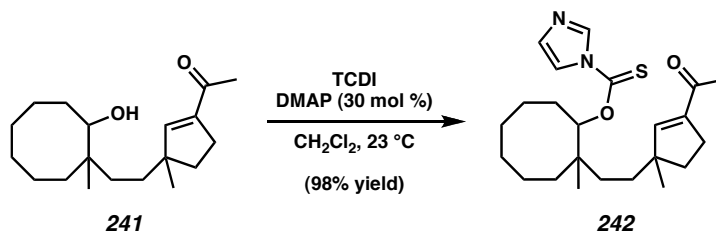


Ketone 239. Silyl enol ether **240** (39.7 mg, 0.145 mmol, 1.0 equiv) was placed in a 10 mL round-bottom flask, the flask was evacuated and backfilled with N₂ (3x), solvated in THF (1.45 mL, 0.1 M) and cooled to 0 °C. To this solution was added MeLi (57 μL, 0.152 mmol, 2.66 M in dimethoxymethane, 1.05 equiv) was added dropwise over 5 min. After an additional 1 h stirring at 0 °C, HMPA (260 mg, 252 μL, 1.45 mmol) was added in a dropwise manner over 5 min, at which point the reaction was cooled in a dry ice/acetone bath to -78 °C. The resulting clear solution mixture was stirred for 10 min followed by dropwise addition of Me₂Zn (145 μL, 0.145 mmol, 1.0 M in heptane, 1.0 equiv). After an additional 10 min, a solution of iodide (±)-**237** (63.4 mg, 0.0174 mmol) in THF (200 μL) was added dropwise over 2 min. After 1 h at -78 °C, the reaction was allowed to gradually warm to ambient temperature. After a further 21 h at 23 °C, the reaction mixture was diluted with Et₂O and washed with H₂O (10 mL). The aqueous phase was extracted with Et₂O (2 x 10 mL) and the combined organic phases were dried over Na₂SO₄, filtered, and concentrated under reduced pressure. The crude oil was purified by flash chromatography on SiO₂ (99:1 → 98:2 → 95:5 → 90:10 hexanes/Et₂O) to afford ketone **239** (43.9 mg, 0.117 mmol, 80% yield) as a 1:1.25 mixture of diastereomers.



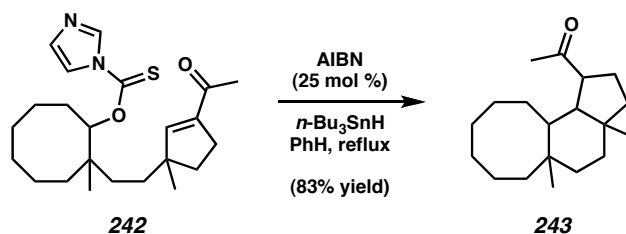
Ketoalcohol 241. To THF (12.5 mL) cooled to 0 °C was added LiAlH₄ (56.9 mg, 1.50 mmol, 1.2 equiv) followed by dropwise addition of a solution of ketone **239** (472 mg, 1.25 mmol, 1.0 equiv) in THF (4.7 mL). The suspension was stirred at 0 °C for 1.5 h and quenched by slow dropwise addition of 10% HCl (10 mL). The biphasic mixture was stirred at 0 °C for 2 h, allowed to warm to 23 °C and stirred for an additional 30 min. The reaction was diluted with Et₂O (25 mL), the phases were separated, and the aqueous phase was extracted with CH₂Cl₂ (2 x 25 mL). The combined organic phases were dried over MgSO₄, filtered, and concentrated under reduced pressure. The crude material was purified by flash chromatography on SiO₂ (7:3 hexanes/EtOAc) to afford a mixture of diastereomers of ketoalcohol **241** (296 mg, 1.01 mmol, 81% yield) as a colorless viscous oil. *R_f* = 0.22 (7:3 Hexanes-Et₂O); ¹H NMR (500 MHz, CDCl₃) δ **major set of diastereomers:** 6.48 (q, *J* = 1.7, 2H), 3.69 (app d, *J* = 7.1 Hz, 1H), 3.68 (app d, *J* = 7.1 Hz, 1H), 2.56–2.52 (comp m, 4H), 2.30 (s, 6H), 1.95–1.20 (comp m, 36 H), 1.10 (s, 6H), 1.09 (s, 6H); **minor set of diastereomers:** 6.47 (q, *J* = 2.2 Hz, 2H), 3.76 (app d, *J* = 8.8 Hz, 2H), 2.56–2.52 (comp m, 4H), 2.30 (s, 6H), 1.95–1.20 (comp m, 36 H), 0.96 (s, 3H), 0.95 (s, 3H), 0.78 (two lines, s, 3H each); ¹³C NMR (126 MHz, CDCl₃) δ **mixture of four diastereomers:** 197.7 (two lines), 152.9 (two lines), 152.8, 143.4 (two lines), 78.2 (two lines), 77.5, 50.1 (two lines), 50.0 (two lines), 40.3 (two lines), 39.6 (two lines), 36.3, 36.2, 35.3, 35.2, 34.7 (three lines), 34.5 (two lines), 33.6 (two lines), 32.3, 32.3 (three lines), 32.1, 29.7, 29.6, 29.1 (two lines), 28.1 (two lines), 27.9 (two

lines), 26.8, 26.6 (two lines), 26.0, 25.8, 25.6 (two lines), 25.5, 25.4, 23.7, 22.7, 22.2 (two lines), 19.3; IR (Neat Film NaCl) 3468, 3039, 2925, 2853, 1667, 1618, 1468, 1447, 1377, 1365, 1305, 1269, 1204, 1044, 964, 944, 871 cm^{-1} ; HRMS (EI+) m/z calc'd for $\text{C}_{19}\text{H}_{32}\text{O}_2$ $[\text{M}]^+$: 292.2402; found 292.2401.



Imidazolyl thiocarbonate 242. To a solution of ketoalcohol **241** (66.0 mg, 0.226 mmol, 1.0 equiv) in CH_2Cl_2 (4.7 mL) was added DMAP (8.28 mg, 0.068 mmol, 0.3 equiv) and 1,1'-thiocarbonyldiimidazole (TCDI) (201.4 mg, 1.13 mmol, 5.0 equiv). The resulting yellow solution was stirred at $23\text{ }^\circ\text{C}$. After 29 h, the reaction mixture was concentrated under reduced pressure and the crude material was purified by flash chromatography on SiO_2 (9:1 \rightarrow 4:1 hexanes/EtOAc) to afford imidazolyl thiocarbonate **242** (89.2 mg, 0.222 mmol, 98% yield) as a viscous colorless oil. $R_f = 0.19$ (7:3 hexanes/EtOAc); $^1\text{H NMR}$ (500 MHz, CDCl_3) δ **major set of diastereomers:** 8.32 (s, 1H), 8.30 (s, 1H), 7.60 (s, 2H), 7.03 (s, 2H), 6.37 (s, 1H), 6.34 (s, 1H), 5.65 (app d, $J = 8.5\text{ Hz}$, 2H), 2.63–2.53 (comp m, 2H), 2.53–2.42 (comp m, 2H), 2.23 (s, 3H), 2.21 (s, 3H), 2.09–2.03 (comp m, 2H), 1.84–1.22 (comp m, 34 H), 1.03 (s, 6H), 1.02 (two lines, s, 3H each); **minor set of diastereomers:** 8.30 (s, 1H), 8.29 (s, 1 H), 7.59 (s, 1H), 7.55 (s, 1H), 7.03 (s, 2H), 6.45 (s, 1H), 6.44 (s, 1H), 5.77 (app d, $J = 9.3\text{ Hz}$, 2H), 2.63–2.53 (comp m, 2H), 2.53–2.42 (comp m, 2H), 2.31 (two lines, s, 3H each), 2.09–2.03 (comp m, 2H), 1.84–1.22 (comp m, 34 H), 1.13 (two lines, s, 3H each), 0.95 (s, 3H), 0.94 (s,

3H) ; ^{13}C NMR (126 MHz, CDCl_3) δ **mixture of four diastereomers:** 197.5, 197.4 (two lines), 184.1, 152.0, 151.9 (two lines), 151.8, 143.8, 143.7, 143.6 (two lines), 136.8, 136.7, 130.9 (two lines), 118.0, 117.9, 117.8, 91.7, 91.6, 91.3, 91.2 50.0, 49.9, 49.7 (two lines), 40.2 (two lines), 39.9 (two lines), 36.3, 36.1 (two lines), 36.0, 35.2, 34.8, 34.7, 34.6, 34.5, 34.4, 32.5, 32.4, 32.3, 31.3, 30.5 (two lines), 29.9, 29.8, 29.7, 29.6, 28.7, 28.6, 27.6, 27.4 (two lines), 26.8 (two lines), 26.7, 26.4, 26.2, 25.7, 25.6, 25.3 (two lines), 25.1 (two lines), 23.3 (two lines), 22.6 (two lines), 22.1 (two lines), 21.5, 21.4; IR (Neat Film NaCl) 3158, 3121, 2930, 2853, 1664, 1618, 1530, 1460, 1383, 1328, 1282, 1228, 1099, 1037, 1013, 967, 889, 871, 830, 734 cm^{-1} ; HRMS (EI+) m/z calc'd for $\text{C}_{23}\text{H}_{34}\text{N}_2\text{O}_2\text{S}$ $[\text{M}]^+$: 402.2341; found 402.2354.



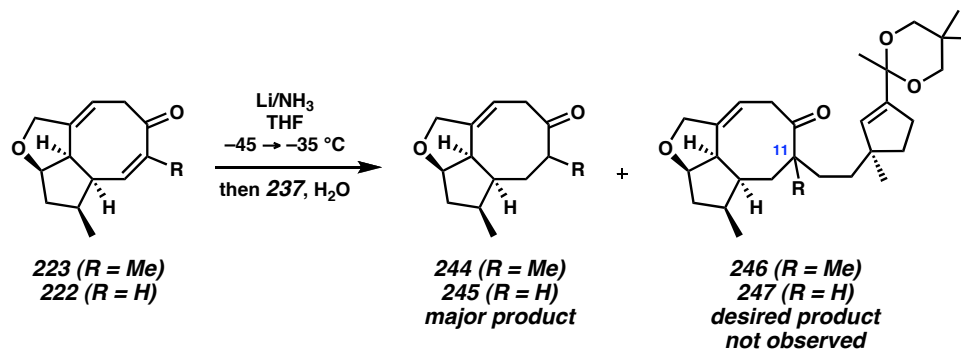
Ketone 243. Imidazolyl thiocarbonate **242** (41.2 mg, 0.102 mmol, 1.0 equiv) was placed in a 50 mL round-bottom 2-neck flask fitted with a condenser, solvated in PhH (18.4 mL), and the solution was sparged with N_2 for 1 h. The reaction mixture was immersed into an 85 °C oil bath and heated to reflux. A separate flask was charged with AIBN (4.19 mg, 0.026 mmol, 0.25 equiv), evacuated and backfilled with N_2 (3x), and PhH (2.0 mL, sparged with N_2 for 1 h prior to use) was added followed by $n\text{-Bu}_3\text{SnH}$ (59.4 mg, 54 μL , 0.204 mmol, 2.0 equiv). The solution of AIBN/ $n\text{-Bu}_3\text{SnH}$ was added dropwise to substrate **242** over 5 h via syringe pump. The reaction was stirred for an additional 12 h at reflux, allowed to cool to ambient temperature, and concentrated under

reduced pressure to afford a pale yellow oil. The crude oil was purified by flash chromatography on SiO₂ impregnated with AgNO₃ (hexanes eluent) to afford a mixture of diastereomers of the desired ketone **243** (23.4 mg, 0.0846 mmol, 83% yield) as a colorless oil. Samples of sufficient purity for characterization were obtained by flash chromatography (1:0 → 99:1 → 98:1 hexanes/Et₂O) and subsequent preparative TLC on SiO₂ (20 x 20 cm, PhMe, developed thrice) of the fractions containing mainly the desired set of diastereomers.

Major diastereomer. $R_f = 0.52$ (4:1 hexanes/Et₂O); ¹H NMR (600 MHz, CDCl₃) δ 3.27 (ddd, $J = 10.8, 7.3, 7.3$ Hz, 1H), 2.38 (app dt, $J = 7.0, 1.2$ Hz, 1H), 2.27–2.22 (m, 1H), 2.20 (s, 3H), 1.78–1.74 (m, 2H), 1.67–1.10 (comp m, 12H), 0.98 (s, 3H), 0.96 (s, 3H), 0.89–0.81 (comp m, 6H); ¹³C NMR (126 MHz, CDCl₃) δ 210.3, 56.9, 49.5, 42.7, 42.0, 37.9, 36.4, 34.6, 31.7, 31.6, 31.5, 30.9, 30.4, 26.8, 26.0, 25.6, 23.3, 23.0, 22.4; IR (Neat Film NaCl) 2920, 2853, 1708, 1460, 1377, 1199, 1179 cm⁻¹; HRMS (EI+) m/z calc'd for C₁₉H₃₂O [M]⁺: 276.2453; found 276.2450.

Minor set of diastereomers. $R_f = 0.58$ (4:1 hexanes/Et₂O); ¹H NMR (500 MHz, CDCl₃) δ 2.90 (ddd, $J = 10.0, 8.3, 5.6$ Hz, 1H), 2.71–2.64 (m, 1H), 2.35 (app t, $J = 7.3$ Hz, 1H), 2.17 (s, 3H), 2.16 (s, 3H), 2.07–1.85 (comp m, 4H), 1.76–1.06 (comp m, 33H), 1.04 (s, 3H), 1.03 (s, 3H), 1.00–0.82 (comp m, 6H), 0.77 (s, 3H), 0.76 (s, 3H); ¹³C NMR (126 MHz, CDCl₃) δ 211.5, 211.2, 58.8, 55.9, 44.6, 44.5, 41.3, 40.9 (two lines), 39.6, 36.4, 35.2, 34.6, 34.0, 33.1, 32.1, 32.0, 30.7, 29.9 (two lines), 29.5, 29.4, 29.2, 29.0, 28.8, 28.7, 27.9, 27.2, 26.4, 26.2, 25.8, 25.4, 24.6, 24.5, 24.3, 22.8, 22.1, 19.8; IR (Neat Film NaCl) 2919, 2848, 1737, 1711, 1460, 1383, 1352, 1261, 1173 cm⁻¹; HRMS (EI+) m/z calc'd for C₁₉H₃₂O [M]⁺: 276.2453; found 276.2441.

3.7.2.6 ASYMMETRIC AB RING AND D-RING FRAGMENT COUPLING

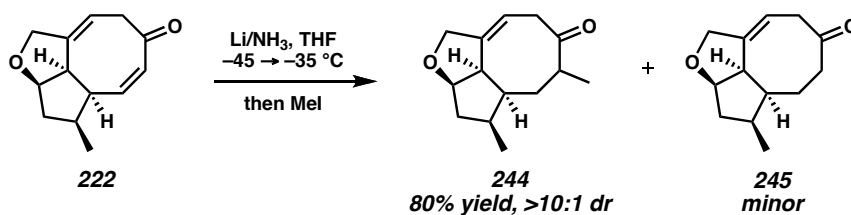
**Attempted reductive alkylation of the asymmetric AB and D-ring systems.**

Reductive alkylations of cyclooctadienones **223** and **222** were attempted using the Li/NH₃ conditions with a large excess of iodide **237** described above to afford the enolate protonation product ketones **244** and **245**, respectively, as the only products.

α -Methyl cyclooctanone 244. ¹H NMR (500 MHz, C₆D₆) δ 4.84–4.80 (m, 1H), 4.42–4.39 (m, 1H), 4.25 (dm, $J = 12.5$ Hz, 1H), 4.08 (dm, $J = 12.5$ Hz, 1H), 3.07 (dm, $J = 16.5$ Hz, 1H), 2.98 (br m, 1H), 2.61–2.54 (m, 1H), 2.39–2.32 (m, 1H), 1.79–1.76 (m, 3H), 1.66–1.58 (m, 1H), 1.44–1.38 (m, 1H), 1.15 (dm, $J = 14.0$ Hz, 1H), 0.88 (d, $J = 7.5$ Hz, 3H), 0.86 (d, $J = 3$ Hz).

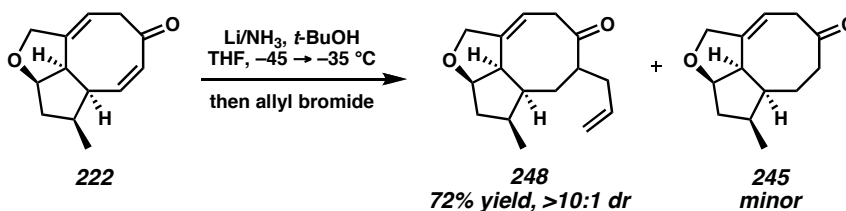
Cyclooctanone 245. $R_f = 0.28$ (3:1 hexanes/EtOAc); ¹H NMR (500 MHz, CDCl₃) δ 5.39–5.35 (m, 1H), 4.64 (ddd, $J = 6.5, 3.1, 3.1$ Hz, 1H), 4.43 (d pentets, $J = 12.6, 1.9$ Hz, 1H), 4.27–4.22 (m, 1H), 3.47–3.41 (m, 1H), 3.16–3.14 (m, 1H), 2.98–2.92 (m, 1H), 2.72 (ddd, $J = 13.6, 5.3, 2.7$ Hz, 1H), 2.38–2.32 (m, 1H), 2.20–2.04 (comp m, 3H), 1.83–1.78 (m, 1H), 1.77–1.75 (comp m, 2H), 0.91 (d, $J = 7.3$ Hz, 3H); ¹³C NMR (126 MHz, CDCl₃)

δ 213.8, 143.3, 112.6, 88.5, 73.3, 48.9, 47.4, 46.0, 44.6, 40.4, 38.1, 24.1, 16.5; IR (Neat Film NaCl) 2952, 2918, 1707, 1432, 1246, 1145, 1074 cm^{-1} ; HRMS (MM: ESI/APCI) m/z calc'd for $\text{C}_{13}\text{H}_{17}\text{O}_2$ $[\text{M} - \text{H}]^+$: 205.1234, found 205.1225; $[\alpha]_{\text{D}}^{25}$ -4.35° (c 0.953, CHCl_3 , 98% ee).



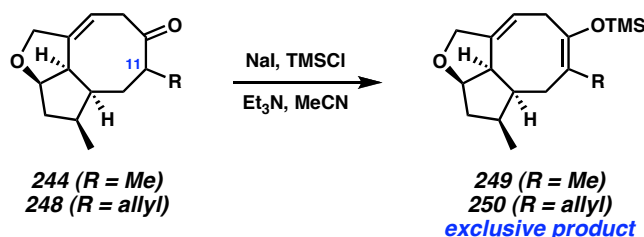
α -Methyl cyclooctanone 244. Ammonia (ca. 5 mL) was condensed into a 2-neck round-bottom flask fitted with a septum, an argon inlet, and a glass-coated stir bar cooled to -78°C , and to this was added lithium wire (3.3 mg, 0.5 mmol, 11 equiv). The solution turned dark blue. The cooling bath was replaced with a $\text{MeCN}/\text{CO}_2(\text{s})$ bath held between -45 and -35°C . The mixture was stirred for 20 minutes, at which point cyclooctadienone **22** (9.3 mg, 0.045 mmol, 1.0 equiv) in THF (1 mL) was added dropwise via cannula transfer. The vial was further washed and transferred with a portion of anhydrous THF (1 mL). The bright blue color remained after addition. As quickly as possible, MeI (100 μL , 1.61 mmol, 35 equiv) was added to the stirred solution by syringe, and the reaction color changed from blue to clear. After 1 h, solid NH_4Cl (100 mg) was added to the reaction, the cooling bath was removed, and the reaction was allowed to reach room temperature. After most of the ammonia had evaporated, the reaction was diluted with H_2O (10 mL) and Et_2O (25 mL). The aqueous layer was extracted with Et_2O (5 x 15 mL) and the combined organics were washed with brine (2 x 10 mL), dried with MgSO_4 , filtered and concentrated. The crude residue was purified by

flash chromatography on SiO₂ (2 x 10 cm, 25:1 → 10:1 hexanes/EtOAc) to afford α -methyl cyclooctanone **244** (8.0 mg, 36 μ mol, 80% yield) as a single major diastereomer with a minor amount of cyclooctanone **245**.



α -Allyl cyclooctenone 248. Ammonia (ca. 7 mL) was condensed into a 2-neck round-bottom flask fitted with a septum, an argon inlet, and a glass-coated stir bar cooled to -78 $^{\circ}$ C, and to this was added lithium wire (5.6 mg, 0.81 mmol, 45 equiv). The solution turned dark blue. The cooling bath was replaced with a MeCN/CO_{2(s)} bath held between -40 and -35 $^{\circ}$ C. The mixture was stirred for 20 minutes, at which point cyclooctadienone **222** (3.7 mg, 0.018 mmol, 1.0 equiv) dissolved in a 0.009 M *t*-BuOH solution in THF (2 mL, prepared by dissolving *t*-BuOH (21.5 μ L) in THF (25 mL) in a flamed dried round-bottom flask under argon) was transferred dropwise via cannula. The bright blue color remained after addition and the solution was stirred for 30 s, after which allyl bromide (200 μ L, 2.31 mmol, 128 equiv) was added by syringe. Stirring was continued for 30 min after which the cold bath was removed, NH₄Cl (420 mg) was added in a single portion and the reaction was allowed to reach room temperature. The reaction was diluted with H₂O (5 mL) and extracted with Et₂O (5 x 20 mL). The combined organics were washed with H₂O (5 mL) then brine (5 mL), dried with MgSO₄, and concentrated in vacuo. The crude residue was purified by flash chromatography on SiO₂ (15:1 → 4:1 hexanes/EtOAc) to afford α -allyl cyclooctanone **248** (3.2 mg, 13 μ mol, 72%

yield) as a single major diastereomer with a minor amount of cyclooctanone **245**. ^1H NMR (500 MHz, CDCl_3) δ 5.66–5.58 (m, 1H), 5.31–5.29 (m, 1H), 5.01–4.96 (m, 2H), 4.58–4.56 (m, 1H), 4.36 (d m, $J = 11$ Hz, 1H), 4.17 (m, $J = 11$ Hz, 1H), 3.44 (d m, $J = 15.5$ Hz, 1H), 3.07 (br m, 1H), 2.76–2.70 (m, 1H), 2.52–2.38 (m, 1H), 2.28–2.23 (m, 2H), 2.08–1.97 (m, 2H) 1.87–1.79 (m, 2H), 1.70–1.64 (m, 2H), 0.82 (d, $J = 7.5$ Hz, 3H).



Representative procedure for the soft enolization to silyl enol ethers **249** and **250**.

To a solution of sodium iodide (1.2 mg, 0.008 mmol, 2 equiv) and α -allyl cyclooctanone **248** (1.0 mg, 0.004 mmol, 1 equiv) in MeCN (0.5 mL) was added Et_3N (162 μL of a 0.05 M solution in MeCN, 0.008 mmol, 2 equiv) followed by TMSCl (121 μL of a 0.05 M solution in MeCN, 0.006 mmol, 1.5 equiv). After 1.5 h the solution was diluted with pentane (1 mL) and stirred for several minutes. The pentane was removed by pipette and the acetonitrile was further extracted with pentane (4 x 1 mL). The combined pentane extracts were dried with Na_2SO_4 , filtered and concentrated to afford crude silyl enol ether **250** (2.0 mg) as a single isomer by ^1H NMR analysis. This compound was used directly in subsequent reactions. $R_f = \text{unstable to SiO}_2$.

3.8 NOTES AND REFERENCES

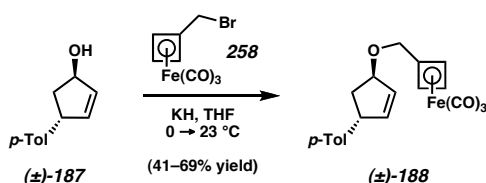
- (1) (a) Hensens, O. D.; Zink, D.; Williamson, J. M.; Lotti, V. J.; Chang, R. S. L.; Goetz, M. A. *J. Org. Chem.* **1991**, *56*, 3399–3403. (b) Kawai, K.-i.; Nozawa, K.; Nakajima, S. *J. Chem. Soc., Perkin Trans. I* **1994**, 1673–1674. (c) Tezuka, Y.; Takahashi, A.; Maruyama, M.; Tamamura, T.; Kutsuma, S.; Naganawa, H.; Takeuchi, T. Novel Antibiotics, AB5362-A, B, and C, Their Manufacture, Their Use as Fungicides, and Phoma Species AB5362. Japan Patent JP 10045662, 1998. (d) Takahashi, H.; Hosoe, T.; Nozawa, K.; Kawai, K.-i. *J. Nat. Prod.* **1999**, *62*, 1712–1713. (e) Fujimoto, H.; Nakamura, E.; Okuyama, E.; Ishibashi, M. *Chem. Pharm. Bull.* **2000**, *48*, 1436–1441. (f) Yoganathan, K.; Rossant, C.; Glover, R. P.; Cao, S.; Vittal, J. J.; Ng, S.; Huang, Y.; Buss, A. D.; Butler, M. S. *J. Nat. Prod.* **2004**, *67*, 1681–1684.
- (2) Sato, A.; Morishita, T.; Hosoya, T. S-19777 as Endothelin Antagonist, Its Manufacture with *Emericella Aurantiobrunnea*, and Its Use as Pharmaceutical. Japan Patent JP 10306087, 1998.
- (3) Variocolin number convention (ref 1a).
- (4) (a) Piers, E.; Boulet, S. L. *Tetrahedron Lett.* **1997**, *38*, 8815–8818. (b) Walker, S. D. A Synthetic Approach to the Variocolin Class of Sesterterpenoids: Total Synthesis of (±)-5-Deoxyvariocolin, (±)-5-Deoxyvaricolol and (±)-5-Deoxyvaricolactone. A New Cycloheptenone Annulation Method Employing the Bifunctional Reagent (Z)-5-Iodo-1-tributylstannylpent-1-ene. Ph.D. Thesis, University of British Columbia, Vancouver, Canada, 2002. (c) Molander, G. A.; Quirnbach, M. S.; Silva, Jr., L. F.; Spencer, K. C.; Balsells, J. *Org. Lett.* **2001**, *3*,

- 2257–2260. (d) George, K. M. Natural Product Total Synthesis: I. The Total Synthesis of (+)-Isoschizandrin. II. Progress Toward the Total Synthesis of Variocolin. Ph.D. Thesis, University of Pennsylvania, Philadelphia, PA, 2005.
- (5) For reviews of the synthesis of quaternary stereocenters, see: (a) Cozzi, P. G.; Hilgraf, R.; Zimmermann, N. *Eur. J. Org. Chem.* **2007**, *36*, 5969–5994. (b) Trost, B. M.; Jiang, C. *Synthesis* **2006**, 369–396. (c) *Quaternary Stereocenters: Challenges and Solutions for Organic Synthesis*; Christoffers, J., Baro, A., Eds.; Wiley: Weinheim, 2005. (d) Douglas, C. J.; Overman, L. E. *Proc. Natl. Acad. Sci. U.S.A.* **2004**, *101*, 5363–5367. (e) Denissova, I.; Barriault, L. *Tetrahedron* **2003**, *59*, 10105–10146.
- (6) (a) Sarpong, R.; Su, J. T.; Stoltz, B. M. *J. Am. Chem. Soc.* **2003**, *125*, 13624–13625. (b) Su, J. T.; Sarpong, R.; Stoltz, B. M.; Goddard, W. A., III. *J. Am. Chem. Soc.* **2004**, *126*, 24–25.
- (7) (a) Behenna, D. C.; Stoltz, B. M. *J. Am. Chem. Soc.* **2004**, *126*, 15044–15055. (b) Mohr, J. T.; Behenna, D. C.; Harned, A. M.; Stoltz, B. M. *Angew. Chem., Int. Ed.* **2005**, *44*, 6924–6927. (c) Seto, M.; Roizen, J. L.; Stoltz, B. M. *Angew. Chem., Int. Ed.* **2008**, *47*, 6873–6876. (d) For a review of the development of the enantioselective Tsuji allylation in our laboratory and others, see: Mohr, J. T.; Stoltz, B. M. *Chem.—Asian J.* **2007**, *2*, 1476–1491.
- (8) For reviews of the preparation of eight-membered rings, see: (a) Petasis, N. A.; Patane, M. A. *Tetrahedron* **1992**, *48*, 5757–5821. (b) Mehta, G.; Singh, V. *Chem. Rev.* **1999**, *99*, 881–930. (c) Maier, M. E. *Angew. Chem., Int. Ed.* **2000**, *39*,

- 2073–2077. (d) Yet, L. *Chem. Rev.* **2000**, *100*, 2963–3007. (e) Michaut, A.; Rodriguez, J. *Angew. Chem., Int. Ed.* **2006**, *45*, 5740–5750.
- (9) For recent advancements relevant to the construction of eight-membered rings, see: (a) Aloise, A. D.; Layton, M. E.; Shair, M. D. *J. Am. Chem. Soc.* **2000**, *122*, 12610–12611. (b) Lo, P. C.-K.; Snapper, M. L. *Org. Lett.* **2001**, *3*, 2819–2821. (c) Evans, P. A.; Robinson, J. E.; Baum, E. W.; Fazal, A. N. *J. Am. Chem. Soc.* **2002**, *124*, 8782–8783. (d) Barluenga, J.; Diéguez, A.; Rodríguez, F.; Flórez, J.; Fañanás, F. J. *J. Am. Chem. Soc.* **2002**, *124*, 9056–9057. (e) Marmster, F. P.; Murphy, G. K.; West, F. G. *J. Am. Chem. Soc.* **2003**, *125*, 14724–14725. (f) Takeda, K.; Haraguchi, H.; Okamoto, Y. *Org. Lett.* **2003**, *5*, 3705–3707. (g) Evans, P. A.; Baum, E. W. *J. Am. Chem. Soc.* **2004**, *126*, 11150–11151. (h) Wang, Y.; Wang, J.; Su, J.; Huang, F.; Jiao, L.; Liang, Y.; Yang, D.; Zhang, S.; Wender, P. A.; Yu, Z.-X. *J. Am. Chem. Soc.* **2007**, *129*, 10060–10061.
- (10) (a) May, J. A.; Stoltz, B. M. *J. Am. Chem. Soc.* **2002**, *124*, 12426–12427. (b) Tambar, U. K.; Kano, T.; Stoltz, B. M. *Org. Lett.* **2005**, *7*, 2413–2416. (c) Tambar, U. K.; Kano, T.; Zepernick, J. F.; Stoltz, B. M. *J. Org. Chem.* **2006**, *71*, 8357–8364. (d) Tambar, U. K.; Kano, T.; Zepernick, J. F.; Stoltz, B. M. *Tetrahedron Lett.* **2007**, *48*, 345–350.
- (11) (a) Watts, L.; Fitzpatrick, J. D.; Pettit, R. *J. Am. Chem. Soc.* **1965**, *87*, 3253–3254. (b) Grubbs, R. H.; Grey, R. A. *J. Am. Chem. Soc.* **1973**, *95*, 5765–5767. (c) Schmidt, E. K. G. *Angew. Chem., Int. Ed. Engl.* **1973**, *12*, 777–778. (d) Tallarico, J. A.; Randall, M. L.; Snapper, M. L. *J. Am. Chem. Soc.* **1996**, *118*, 9196–9197. (e) Limanto, J.; Snapper, M. L. *J. Org. Chem.* **1998**, *63*, 6440–6441.

(f) Limanto, J.; Tallarico, J. A.; Porter, J. R.; Khuong, K. S.; Houk, K. N.; Snapper, M. L. *J. Am. Chem. Soc.* **2002**, *124*, 14748–14758.

- (12) The preparation of tricarbonyliron-cyclobutadiene ether complexes of allylic alcohols is typically accomplished with bromide **258** (see ref. 11e). In our hands, this procedure was variable and furnished only modest yields of ether **188**.



(13) (a) Agar, J.; Kaplan, F.; Roberts, B. W. *J. Org. Chem.* **1974**, *39*, 3451–3452.

(b) Limanto, J.; Snapper, M. L. *J. Am. Chem. Soc.* **2000**, *122*, 8071–8072.

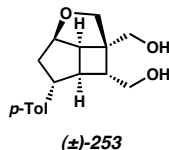
(14) (a) Ito, M.; Matsuumi, M.; Muruges, M. G.; Kobayashi, Y. *J. Org. Chem.* **2001**, *66*, 5881–5889. (b) Kobayashi, Y.; Nakata, K.; Ainai, T. *Org. Lett.* **2005**, *7*, 183–186.

(15) Deardorff, D. R.; Myles, D. C. *Organic Syntheses*; Wiley & Sons: New York, 1993; Collect. Vol. VIII, pp 13–15.

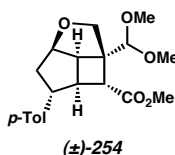
(16) Rai, A. N.; Basu, A. *Tetrahedron Lett.* **2003**, *44*, 2267–2269.

(17) (a) Schreiber, S. L.; Claus, R. E.; Reagan, J. *Tetrahedron Lett.* **1982**, *23*, 3867–3870. (b) Claus, R. E.; Schreiber, S. L. *Organic Syntheses*; Wiley & Sons: New York, 1990; Collect. Vol. VII, pp 168–171. (c) For a review of the unsymmetrical ozonolysis of cycloalkenes, see: Testero, S. A.; Suárez, A. G.; Spanevello, R. A.; Mangione, M. I. *Trends Org. Chem.* **2003**, *10*, 35–49.

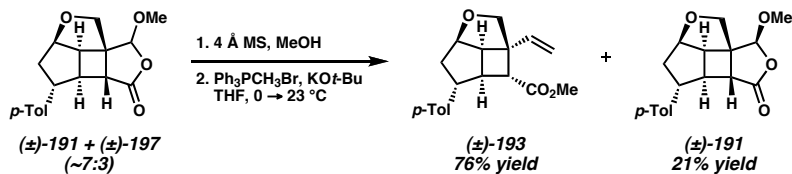
- (18) We also investigated the group-selective differentiation of diol **253** without success.



- (19) Kawamura, S.-i.; Yamakoshi, H.; Nojima, M. *J. Org. Chem.* **1996**, *61*, 5953–5958.
- (20) The Lewis acids La(OTf)₃ or Sm(OTf)₃ effect the conversion of acetal **191** to dimethyl acetal **254** as the sole product.



- (21) Our equilibration results suggest that the formation of acetal **191** is the kinetic product of the unsymmetrical ozonolysis, and is apparently due to the proximity of substituents attached to the cyclobutane ring.
- (22) The recycling of acetals **191** and **197** via this equilibration/olefination sequence provides olefin **193** and recovered acetal **191** in excellent yield over two steps.



- (23) Arndt, F.; Eistert, B. *Ber. Dtsch. Chem. Ges. B* **1935**, *68*, 200–208.

- (24) (a) Hammond, G. S.; DeBoer, C. D. *J. Am. Chem. Soc.* **1964**, *86*, 899–902.
(b) Trecker, D. J.; Henry, J. P. *J. Am. Chem. Soc.* **1964**, *86*, 902–905.
(c) Grimme, W. *J. Am. Chem. Soc.* **1972**, *94*, 2525–2526. (d) Berson, J. A.; Dervan, P. B. *J. Am. Chem. Soc.* **1972**, *94*, 7597–7598.
- (25) (a) Schneider, M. *Angew. Chem.* **1975**, *87*, 717–718. (b) Brown, J. M.; Golding, B. T.; Stofko, J. J., Jr. *J. Chem. Soc., Perkin Trans. 2* **1978**, 436–441.
(c) Gajewski, J. J.; Hawkins, C. M.; Jimenez, J. L. *J. Org. Chem.* **1990**, *55*, 674–679. (d) Özkan, I.; Zora, M. *J. Org. Chem.* **2003**, *68*, 9635–9642.
- (26) (a) Sudrik, S. G.; Chavan, S. P.; Chandrakumar, K. R. S.; Sourav, P.; Date, S. K.; Chavan, S. P.; Sonawane, H. R. *J. Org. Chem.* **2002**, *67*, 1574–1579. (b) Pisset, M.; Coquerel, Y.; Rodriguez, J. *J. Org. Chem.* **2009**, *74*, 415–418.
- (27) (a) Reetz, M. T.; Eipper, A.; Tielmann, P.; Mynott, R. *Adv. Synth. Catal.* **2002**, *344*, 1008–1016. (b) Tietze, L. F.; Stadler, C.; Böhnke, N.; Brasche, G.; Grube, A. *Synlett* **2007**, 485–487. (c) For a related example, see: Deardorff, D. R.; Windham, C. Q.; Craney, C. L. *Organic Syntheses*; Wiley & Sons, New York, 1998; Collect. Vol. IX, pp 487–492.
- (28) Alcohol isomer **210** is not reactive under these Mitsunobu conditions.
- (29) TLC analysis of the reaction progress indicated cycloadduct **213** as the major product, however, we are thus far unable to obtain isolated yields due to the volatility of this compound and its challenging isolation from a large volume of acetone.

- (30) The reactivity differences observed for this substrate (**212**) and the model system (**188**) underline the difference in the C(3) stereochemistry and its impact on the cycloaddition.
- (31) The reaction yield for the two steps post cycloaddition/ozonolysis is excellent (94%), indicating the low overall yield for the four steps is the result of either problematic cycloaddition or ozonolysis procedures. The difficulties we have encountered with the volatility and purification of cycloadduct **213** are suggestive of the major limitation of this reaction sequence.
- (32) The absolute stereochemistry of acetal **215** could not be determined from the X-ray diffraction data. See Appendix 3 for details.
- (33) For selected examples of α -diazoketone formation using diazoethane (**219**), see: (a) Wilds, A. L.; Meader, A. L., Jr. *J. Org. Chem.* **1948**, *13*, 763–779. (b) Veale, C. A.; Rheingold, A. L.; Moore, J. A. *J. Org. Chem.* **1985**, *50*, 2141–2145. (c) Kennedy, M.; McKervey, M. A. *J. Chem. Soc., Perkin Trans. 1* **1991**, 2565–2574. (d) Srikrishna, A.; Vijaykumar, D. *J. Chem. Soc., Perkin Trans. 1* **2000**, 2583–2589.
- (34) For alternative methods describing the preparation of α -diazoketones from carboxylic acids, see: (a) Hodson, D.; Holt, G.; Wall, D. K. *J. Chem. Soc. C* **1970**, 971–973. (b) Pettit, G. R.; Nelson, P. S. *Can. J. Chem.* **1986**, *64*, 2097–2102. (c) Ananda, G. D. S.; Steele, J.; Stoodley, R. J. *J. Chem. Soc., Perkin Trans. 1* **1988**, 1765–1771. (d) Nicolaou, K. C.; Baran, P. S.; Zhong, Y.-L.; Choi, H.-S.; Fong, K. C.; He, Y.; Yoon, W. H. *Org. Lett.* **1999**, *1*, 883–886. (e) Cuevas-Yañez, E.; García, M. A.; de la Mora, M. A.; Muchowski, J. M.; Cruz-Almanza,

- R. *Tetrahedron Lett.* **2003**, *44*, 4815–4817. (f) Wang, J.; Zhang, Z. *Tetrahedron* **2008**, *64*, 6577–6605.
- (35) Application of photochemical/thermal reaction conditions to α -diazoketone **221** produced similar results.
- (36) Kirmse, W. *Eur. J. Org. Chem.* **2002**, 2193–2256.
- (37) (a) Pecile, C.; Föffani, A.; Gherseti, S. *Tetrahedron* **1964**, *20*, 823–829. (b) Kaplan, F.; Meloy, G. K. *J. Am. Chem. Soc.* **1966**, *88*, 950–956. (c) Sorriso, S.; Piazza, G.; Foffani, A. *J. Chem. Soc. B* **1971**, 805–809. (d) Paliani, G.; Sorriso, S.; Cataliotti, R. *J. Chem. Soc., Perkin Trans. 2* **1976**, 707–710. (e) Wang, J.; Burdzinski, G.; Kubicki, J.; Platz, M. S. *J. Am. Chem. Soc.* **2008**, *130*, 11195–11209.
- (38) Variation of reaction temperature did not impact the ratio of products for the rearrangement of **221**.
- (39) Smith, A. B., III; Agosta, W. C. *J. Am. Chem. Soc.* **1974**, *96*, 3289–3295.
- (40) Schroeder, G. M.; Trost, B. M. *Chem.—Eur. J.* **2005**, *11*, 174–184.
- (41) For representative examples, see: (a) Wilson, S. R.; Turner, R. B. *J. Org. Chem.* **1973**, *38*, 2870–2873. (b) Gibbons, E. G. *J. Am. Chem. Soc.* **1982**, *104*, 1767–1769. (c) Paquette, L. A.; Dahnke, K.; Doyon, J.; He, W.; Wyant, K.; Friedrich, D. *J. Org. Chem.* **1991**, *56*, 6199–6205.
- (42) For a review on the direct formation of cyclopentanes via ring contraction, see: Silva, L. F., Jr. *Tetrahedron* **2002**, *58*, 9137–9161.

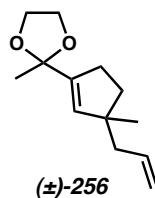
- (43) For a single example of the preparation of a cyclopentene via the ring contraction of a seven-membered ring, see: Jun, C.-H.; Moon, C. W.; Lim, S.-G.; Lee, H. *Org. Lett.* **2002**, *4*, 1595–1597.
- (44) Stork, G.; Danheiser, R. L. *J. Org. Chem.* **1973**, *38*, 1775–1776.
- (45) (a) Ragan, J. A.; Makowski, T. W.; am Ende, D. J.; Clifford, P. J.; Young, G. R.; Conrad, A. K.; Eisenbeis, S. A. *Org. Process Res. Dev.* **1998**, *2*, 379–381.
(b) Ragan, J. A.; Murry, J. A.; Castaldi, M. J.; Conrad, A. K.; Jones, B. P.; Li, B.; Makowski, T. W.; McDermott, R.; Sitter, B. J.; White, T. D.; Young, G. R. *Org. Process Res. Dev.* **2001**, *5*, 498–507. (c) Do, N.; McDermott, R. E.; Ragan, J. A. *Org. Synth.* **2008**, *85*, 138–146.
- (46) (a) Tani, K.; Behenna, D. C.; McFadden, R. M.; Stoltz, B. M. *Org. Lett.* **2007**, *9*, 2529–2531. (b) White, D. E.; Stewart, I. C.; Grubbs, R. H.; Stoltz, B. M. *J. Am. Chem. Soc.* **2008**, *130*, 810–811.
- (47) The catalyst derived from Pd(0) and fluorinated ligand **230** is highly effective for reactive substrates such as allyl enol carbonates (ref 46). However, alkylation reactions of vinylogous β -ketoester (\pm)-**181** using this catalyst proceed at a slow rate, even with 10 mol % of the palladium complex, presumably due to a slower rate of decarboxylation. The related increase in reaction times often result in catalyst decomposition prior to complete conversion of substrate.
- (48) The remarkable stability of β -hydroxyketone **231** is likely the result of transannular interactions or some other form of ring strain. This is comparable to the observation that cycloheptane-1,3-dione (**227**) exists exclusively in the diketo-

form in solution, and contrasts with propensity for six-membered analogue cyclohexane-1,3-dione to be completely enolized in solution. See ref 45b.

- (49) Preliminary investigations employing sodium methoxide/methanol conditions produced minor quantities of conjugate addition adducts of cycloheptenone **180**.
- (50) A number of intermediates are possible for the proposed retro-aldol/aldol sequence, such as ketoaldehyde **226** and several diastereomeric aldol addition adducts. ^1H NMR analysis of crude reaction filtrates exhibit a characteristic aldehyde peak, along with numerous other compounds. Addition of TFE to reactions containing these compounds facilitated the conversion to the desired acylcyclopentene **225**, further supporting their role as intermediates in the transformation.
- (51) For a discussion of the properties of fluorinated alcohols and their use, see: Bégué, J.-P.; Bonnet-Delpon, D.; Crousse, B. *Synlett* **2004**, 18–29.
- (52) We presume that the fluorinated lithium alkoxide is generated in situ due to the large difference in $\text{p}K_a$ values ($\text{H}_2\text{O} = 15.7$, TFE = 12.5, HFIP = 9.3 [water]; $\text{H}_2\text{O} = 31.2$, TFE = 23.5, HFIP = 18.2 [DMSO]).
- (53) Blasdel, L. K.; Myers, A. G. *Org. Lett.* **2005**, 7, 4281–4283.
- (54) Preliminary studies aimed at the conversion of pure cycloheptenone **180** to acylcyclopentene **225** using our optimal basic aldol conditions have not been successful.
- (55) Mohr, J. T.; Krout, M. R.; Stoltz, B. M. *Org. Synth.* **2009**, 86, 194–211.

(56) See Appendix 3 for details.

(57) Our initial studies employing derivative **256** revealed the propensity of the dioxolane protecting group toward cleavage under mild conditions.



(58) Yu, W.; Mei, Y.; Kang, Y.; Hua, Z.; Jin, Z. *Org. Lett.* **2004**, *6*, 3217–3219.

(59) For discussions regarding the utility of enones as a regiocontrol element for the generation of enolates, see: (a) Huddleston, R. R.; Krische, M. J. *Synlett* **2003**, 12–21. (b) Han, S. B.; Hassan, A.; Krische, M. J. *Synthesis* **2008**, 2669–2679.

(60) (a) Stork, G.; Rosen, P.; Goldman, N. L. *J. Am. Chem. Soc.* **1961**, *83*, 2965–2966. (b) Stork, G.; Rosen, P.; Goldman, N.; Coombs, R. V.; Tsuji, J. *J. Am. Chem. Soc.* **1965**, *87*, 275–286.

(61) Zheng, G. Z.; Chan, T. H. *Organometallics* **1995**, *14*, 70–79.

(62) Morita, Y.; Suzuki, M.; Noyori, R. *J. Org. Chem.* **1989**, *54*, 1785–1787.

(63) For reviews of radical cyclization reactions, see: (a) Crich, D.; Quintero, L. *Chem. Rev.* **1989**, *89*, 1413–1432. (b) Giese, B.; Kopping, B.; Gobel, T.; Dickhaut, J.; Thoma, G.; Kulicke, K. J.; Trach, F. *Org. React.* **1996**, *48*, 301–856.

(64) We are currently unable to determine the stereochemistry of the newly formed C(11) stereocenter.

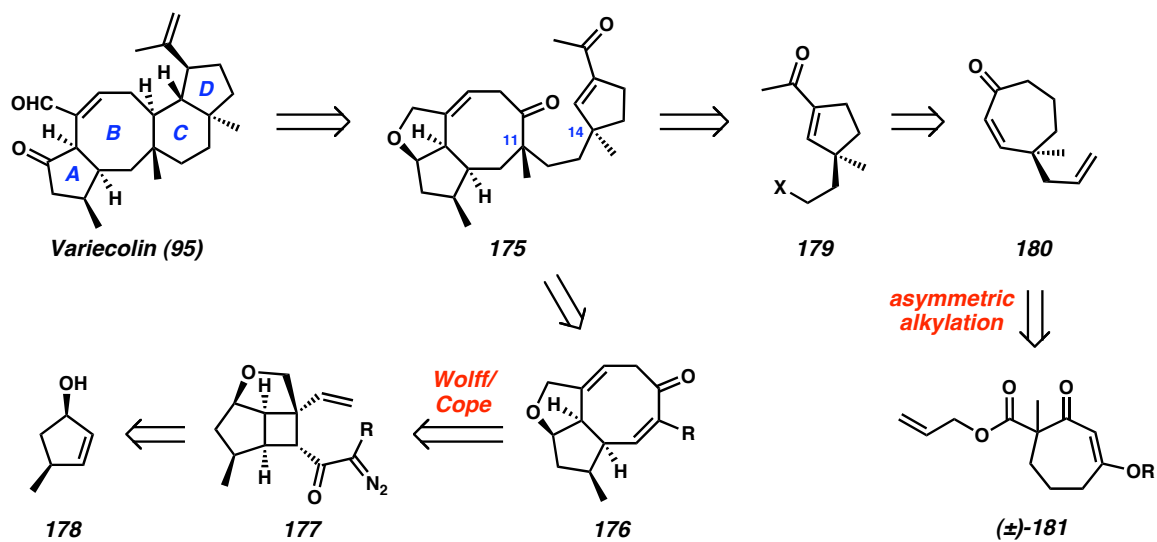
- (65) Cazeau, P.; Duboudin, F.; Moulines, F.; Babot, O.; Dunogues, J. *Tetrahedron* **1987**, *43*, 2075–2088.
- (66) We surveyed numerous conditions varying catalysts, solvents, silanes, and temperatures without further improvement.
- (67) Dess, D. B.; Martin, J. C. *J. Am. Chem. Soc.* **1991**, *113*, 7277–7287.
- (68) Ukai, T.; Kawazura, H.; Ishii, Y.; Bonnet, J. J.; Ibers, J. A. *J. Organomet. Chem.* **1974**, *65*, 253–266.
- (69) Krout, M. R.; Mohr, J. T.; Stoltz, B. M. *Org. Synth.* **2009**, *86*, 181–193.
- (70) Ahmad, N.; Robinson, S. D.; Uttley, M. F. *J. Chem. Soc., Dalton Trans.* **1972**, 843–847.
- (71) Werner, E. A. *J. Chem. Soc.* **1919**, 1093–1102.
- (72) Gottlieb, H. E.; Kotlyar, V.; Nudelman, A. *J. Org. Chem.* **1997**, *62*, 7512–7515.

APPENDIX 1

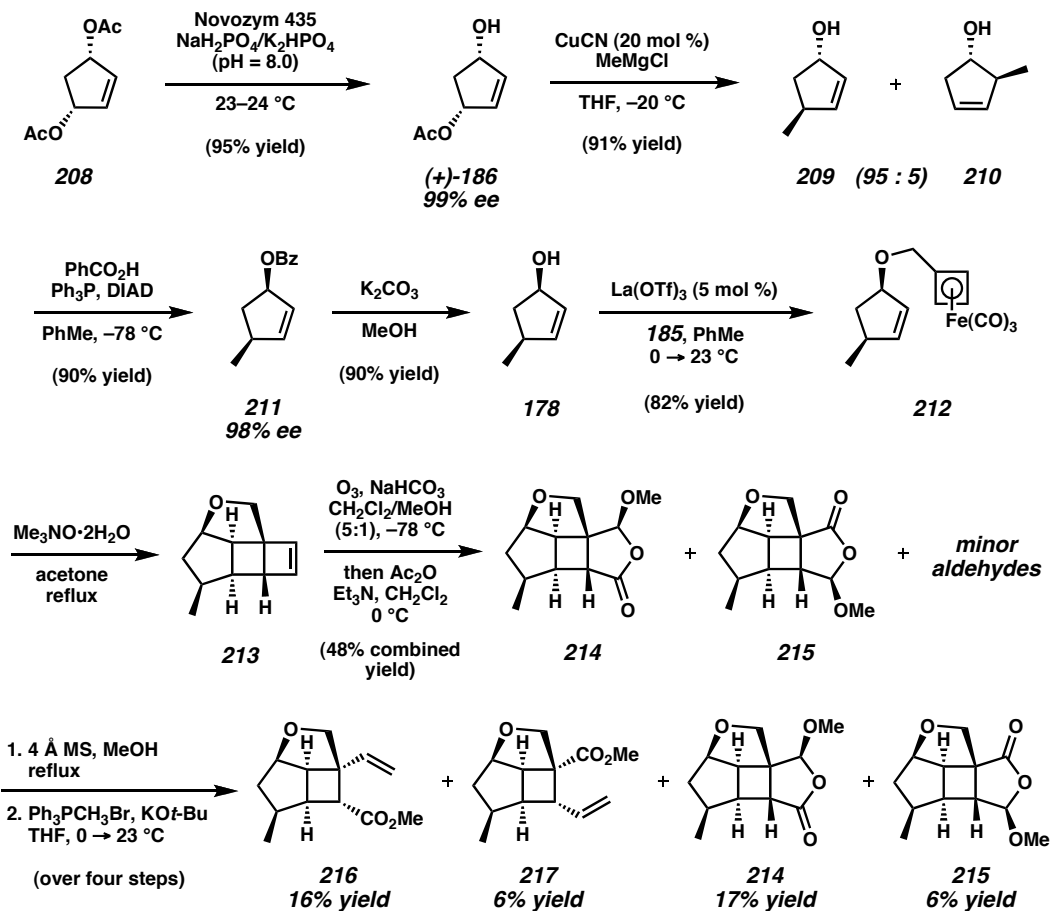
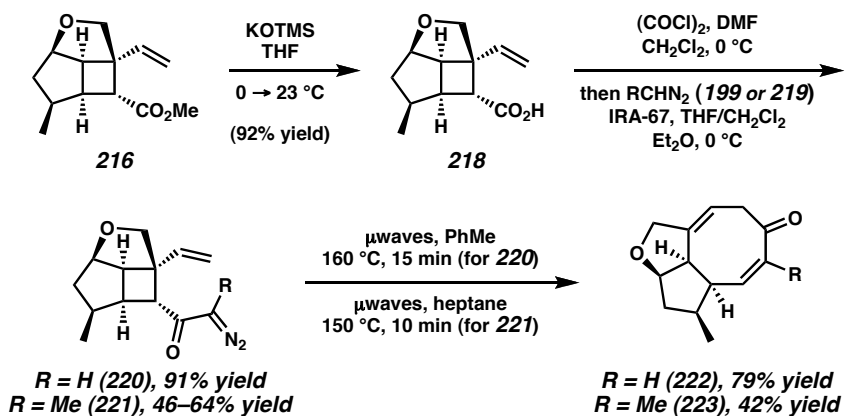
Synthetic Summary toward the Asymmetric

Total Synthesis of Variecolin

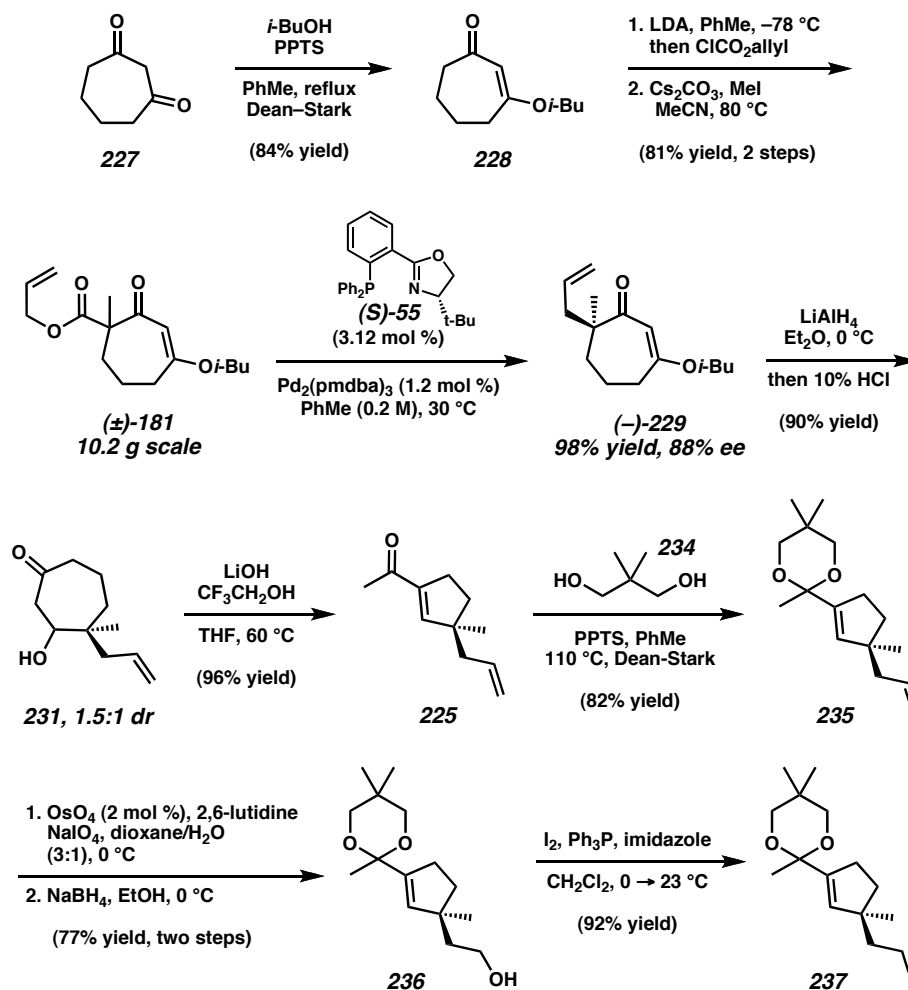
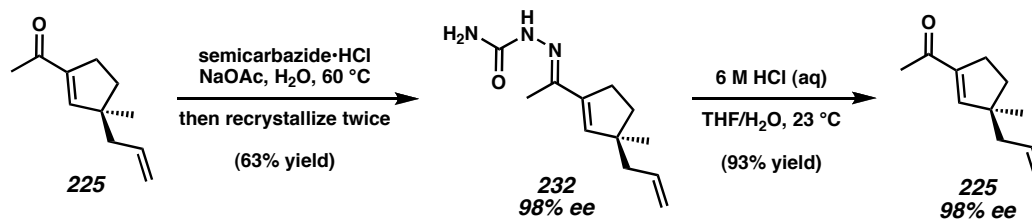
Scheme A1.1. Retrosynthetic analysis of variecolin



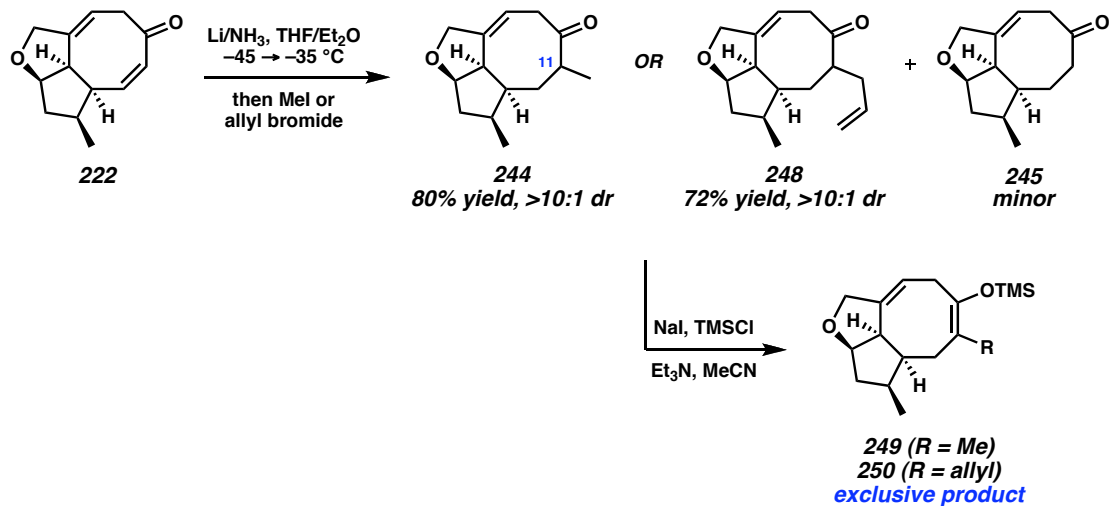
Scheme A1.2. Intramolecular cycloaddition and unsymmetrical ozonolysis toward the AB ring

Scheme A1.3. α -Diazoketone synthesis and Wolff/Cope rearrangement to AB ring fragments

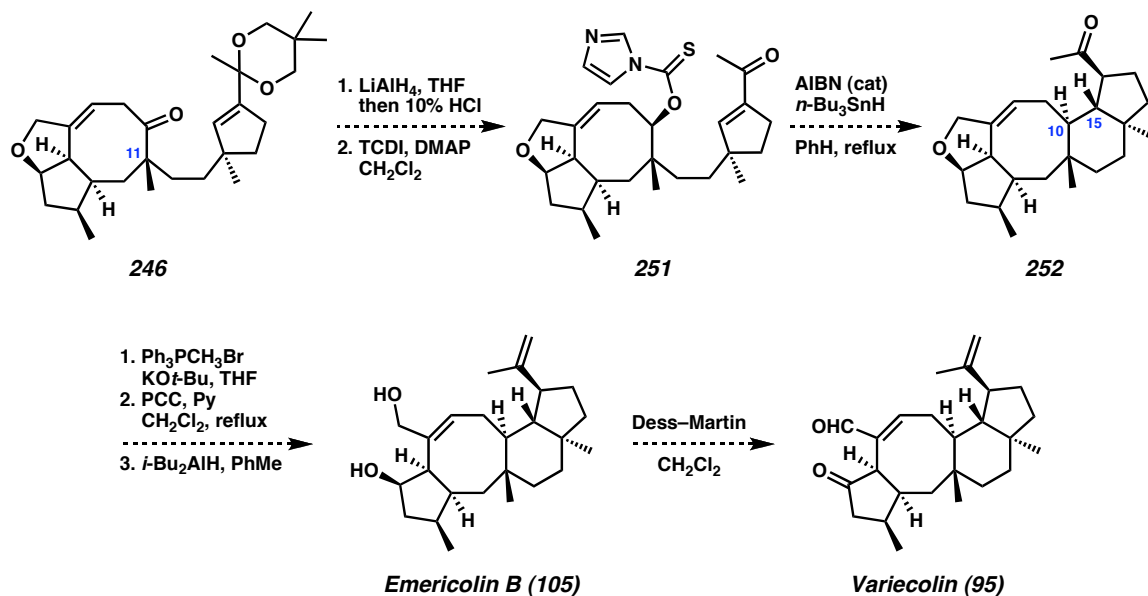
Scheme A1.4. Asymmetric alkylation and ring contraction to the D-ring fragment

Scheme A1.5. Enrichment of acylcyclopentene **225** for the D-ring fragment

Scheme A1.6. AB ring reductive alkylation and soft enolization poised for fragment coupling

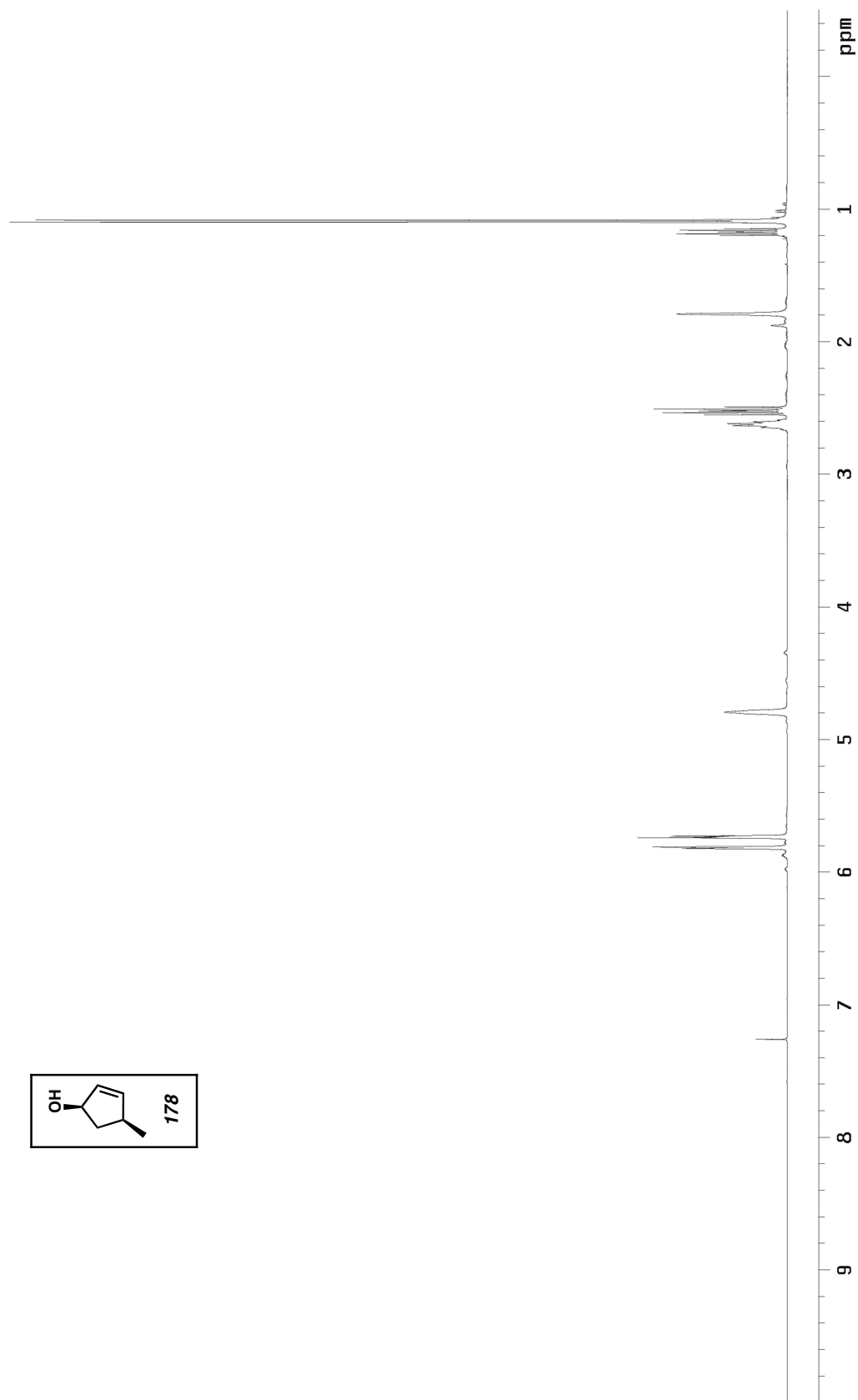


Scheme A1.7. Proposed completion of variocolin



APPENDIX 2

*Spectra Relevant to Chapter 3:
Progress toward the Asymmetric
Total Synthesis of Variocolin*

Figure A2.1. ^1H NMR spectrum (500 MHz, CDCl_3) of **178**.

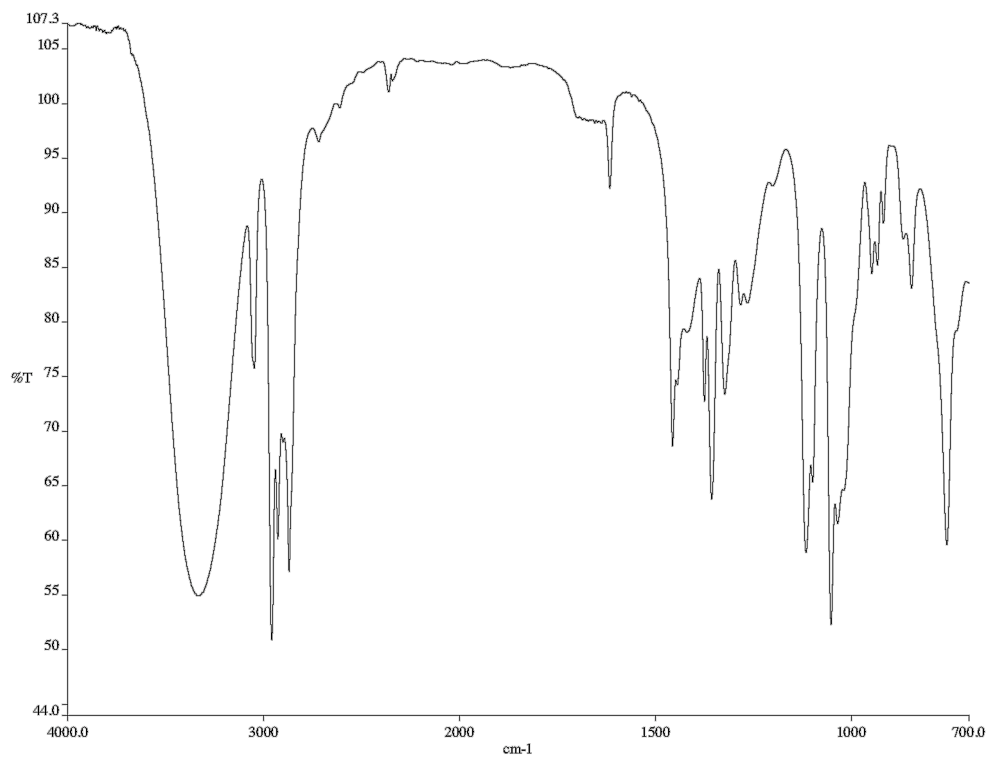


Figure A2.2. Infrared spectrum (neat film/NaCl) of **178**.

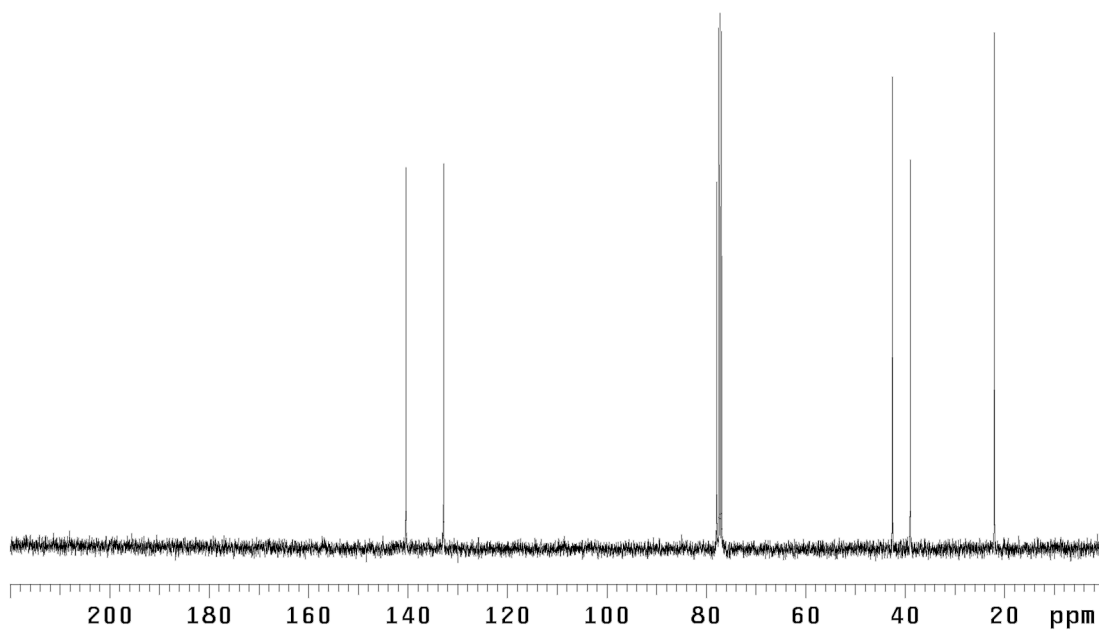
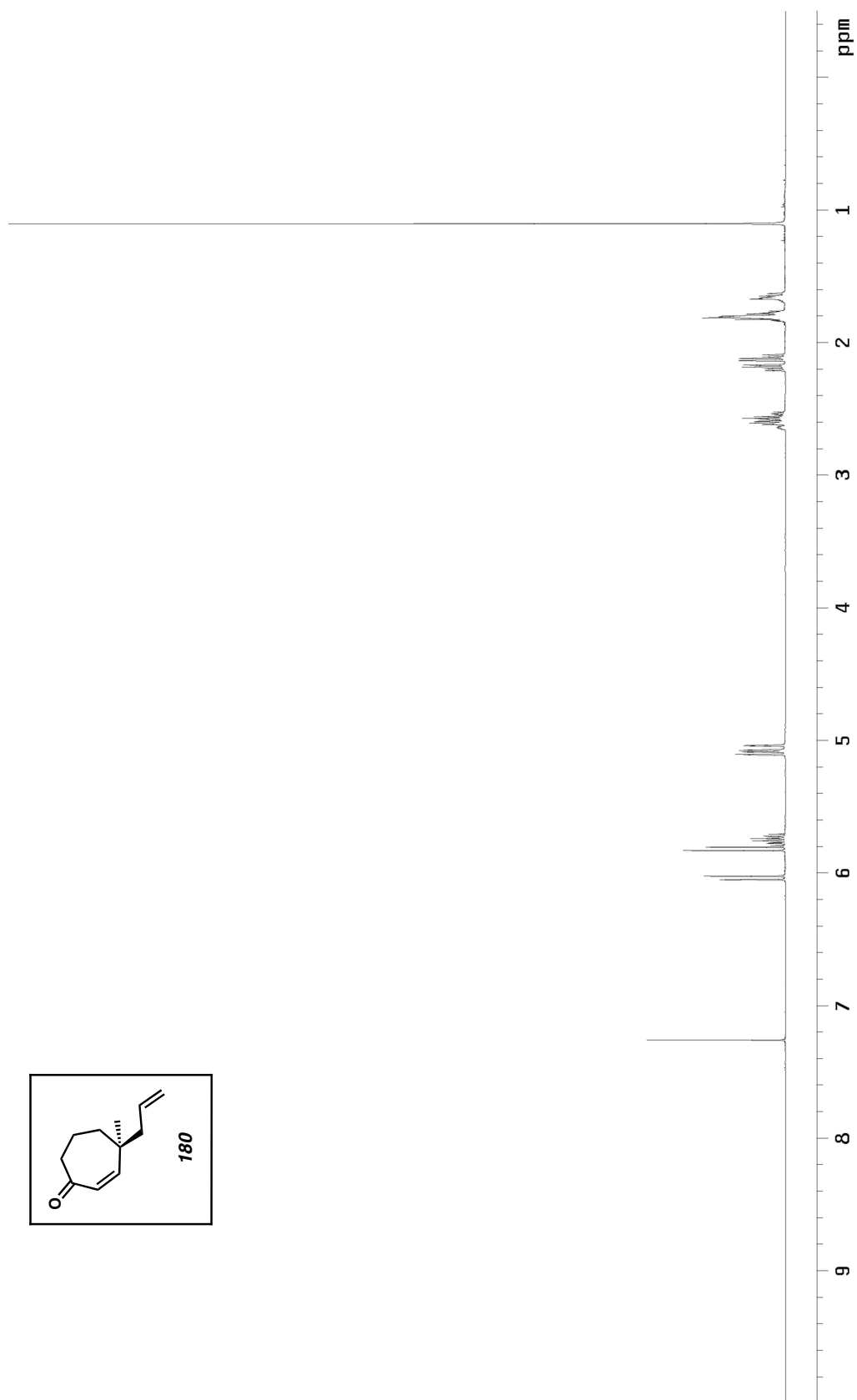


Figure A2.3. ¹³C NMR spectrum (126 MHz, CDCl₃) of **178**.

Figure A2.4. ^1H NMR spectrum (500 MHz, CDCl_3) of **180**.

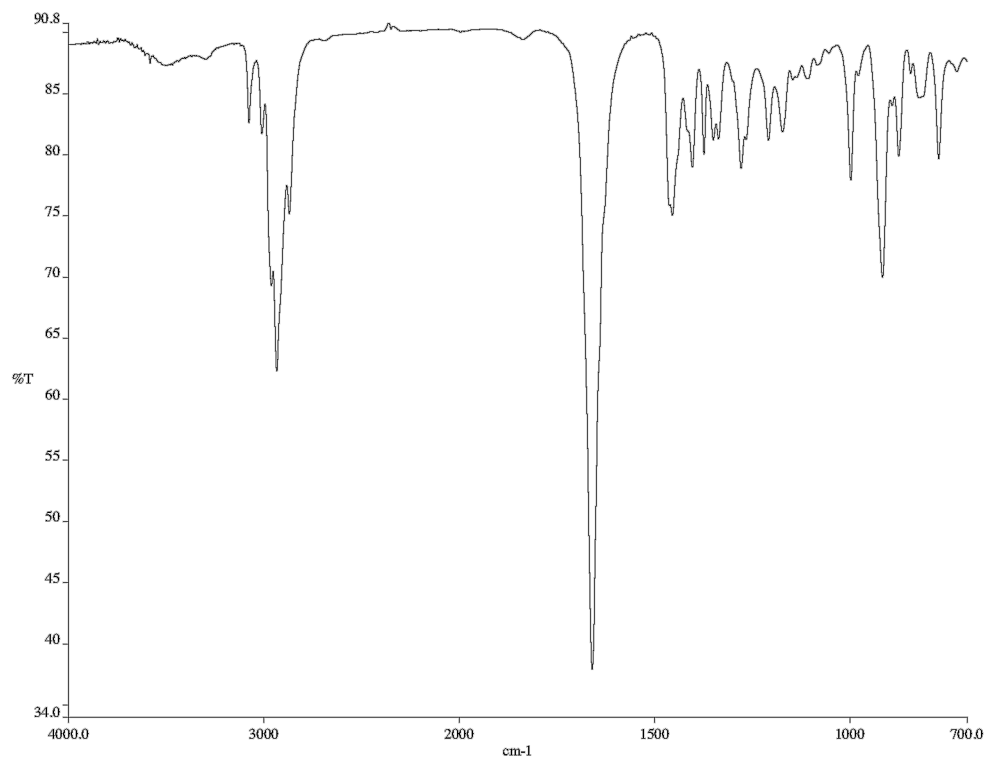


Figure A2.5. Infrared spectrum (neat film/NaCl) of **180**.

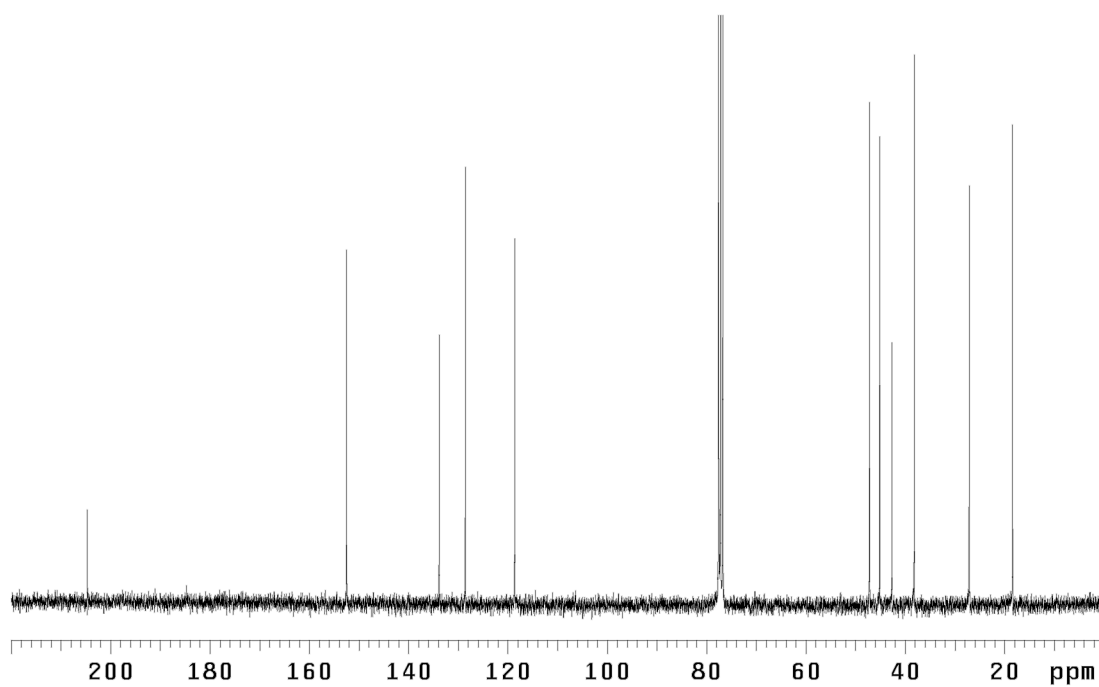
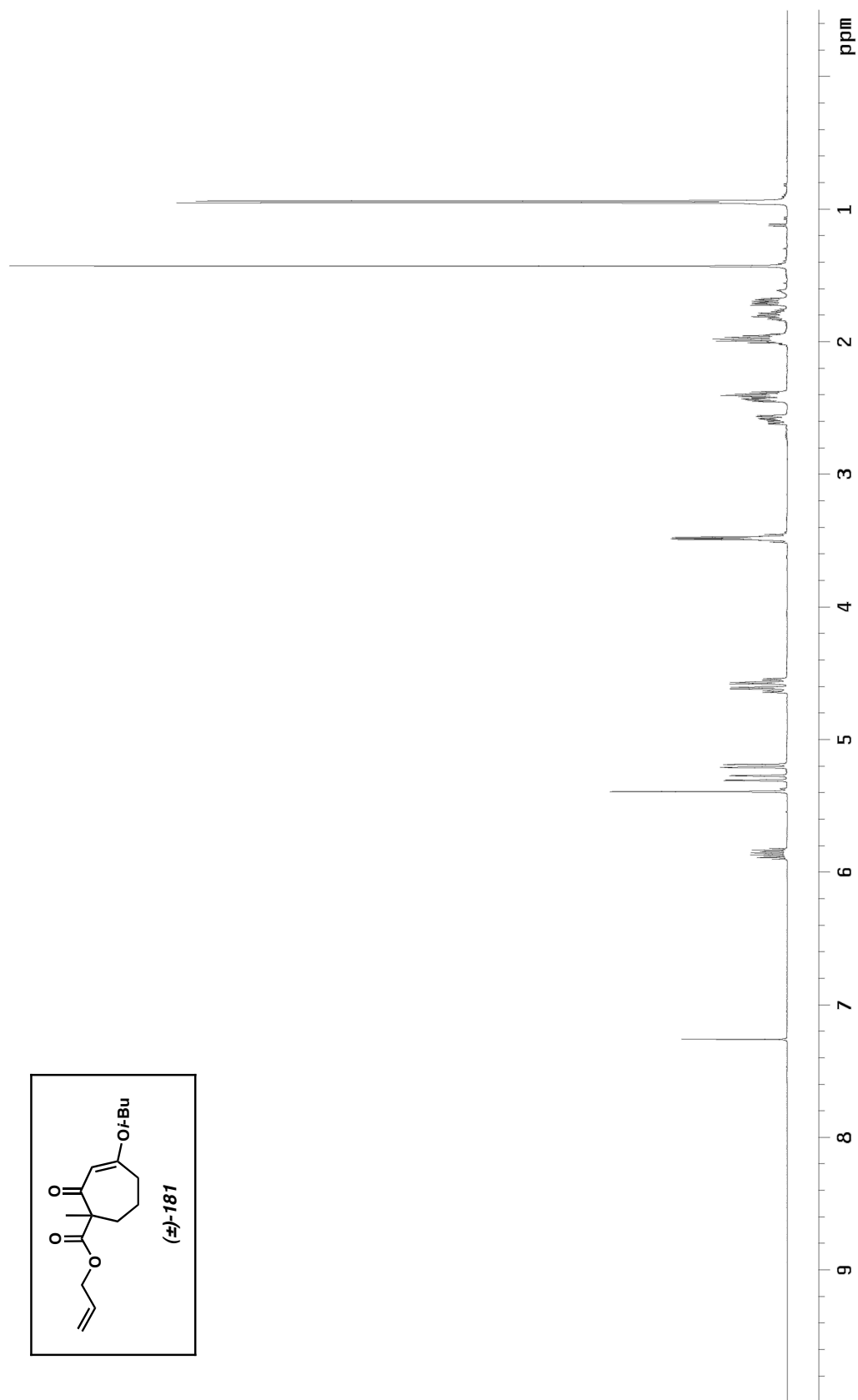


Figure A2.6. ¹³C NMR spectrum (75 MHz, CDCl₃) of **180**.

Figure A2.7. ^1H NMR spectrum (500 MHz, CDCl_3) of **181**.

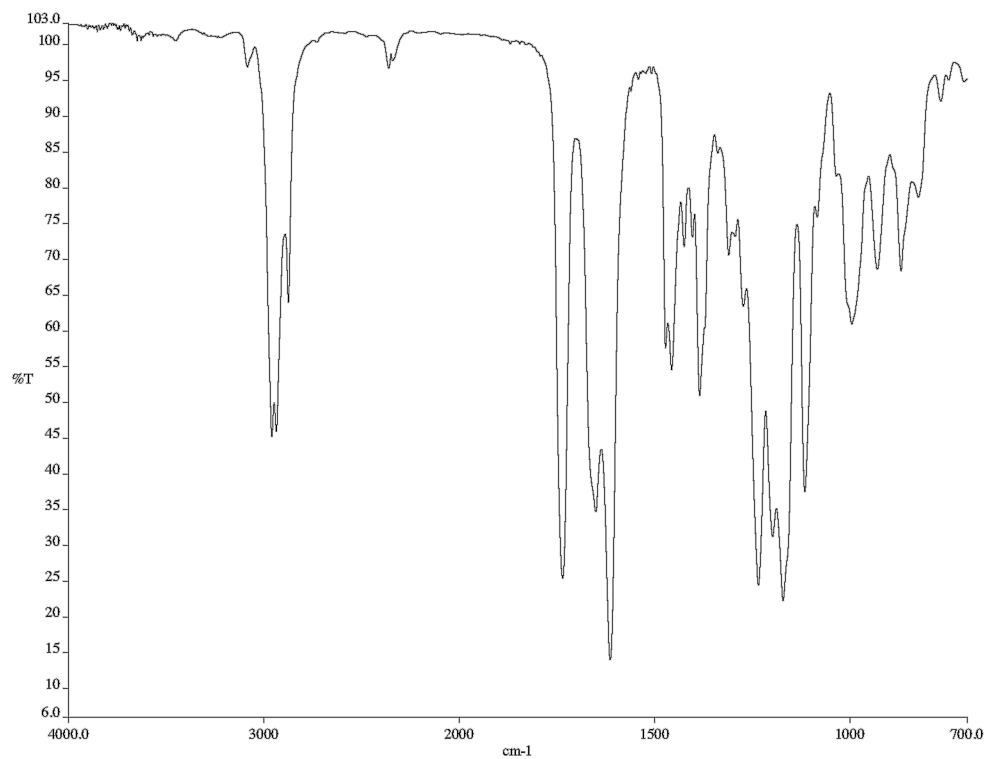


Figure A2.8. Infrared spectrum (neat film/NaCl) of **181**.

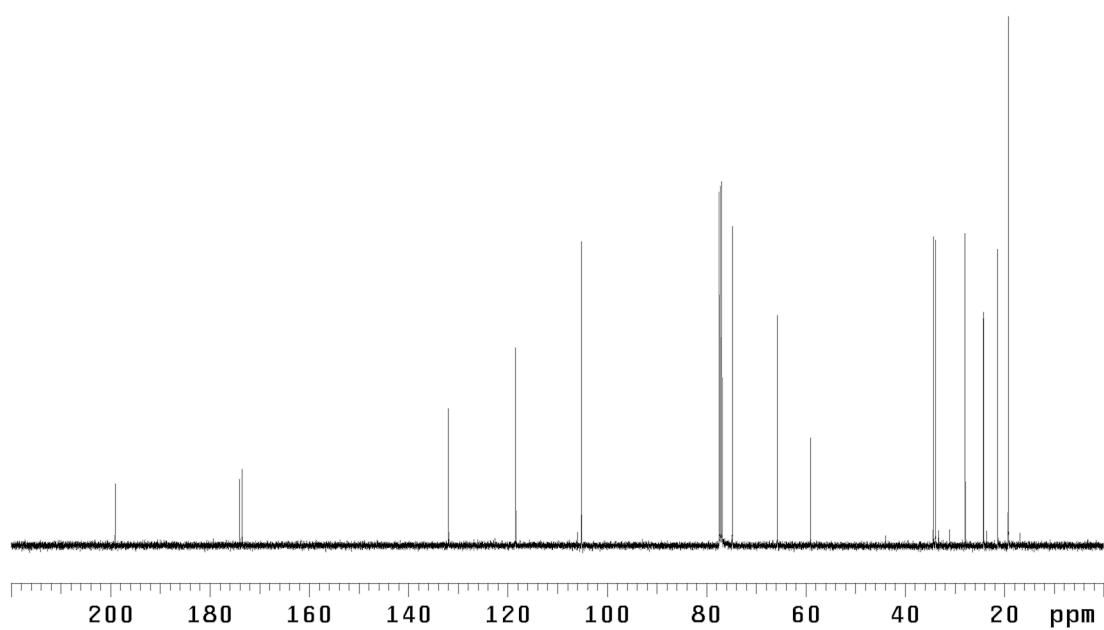
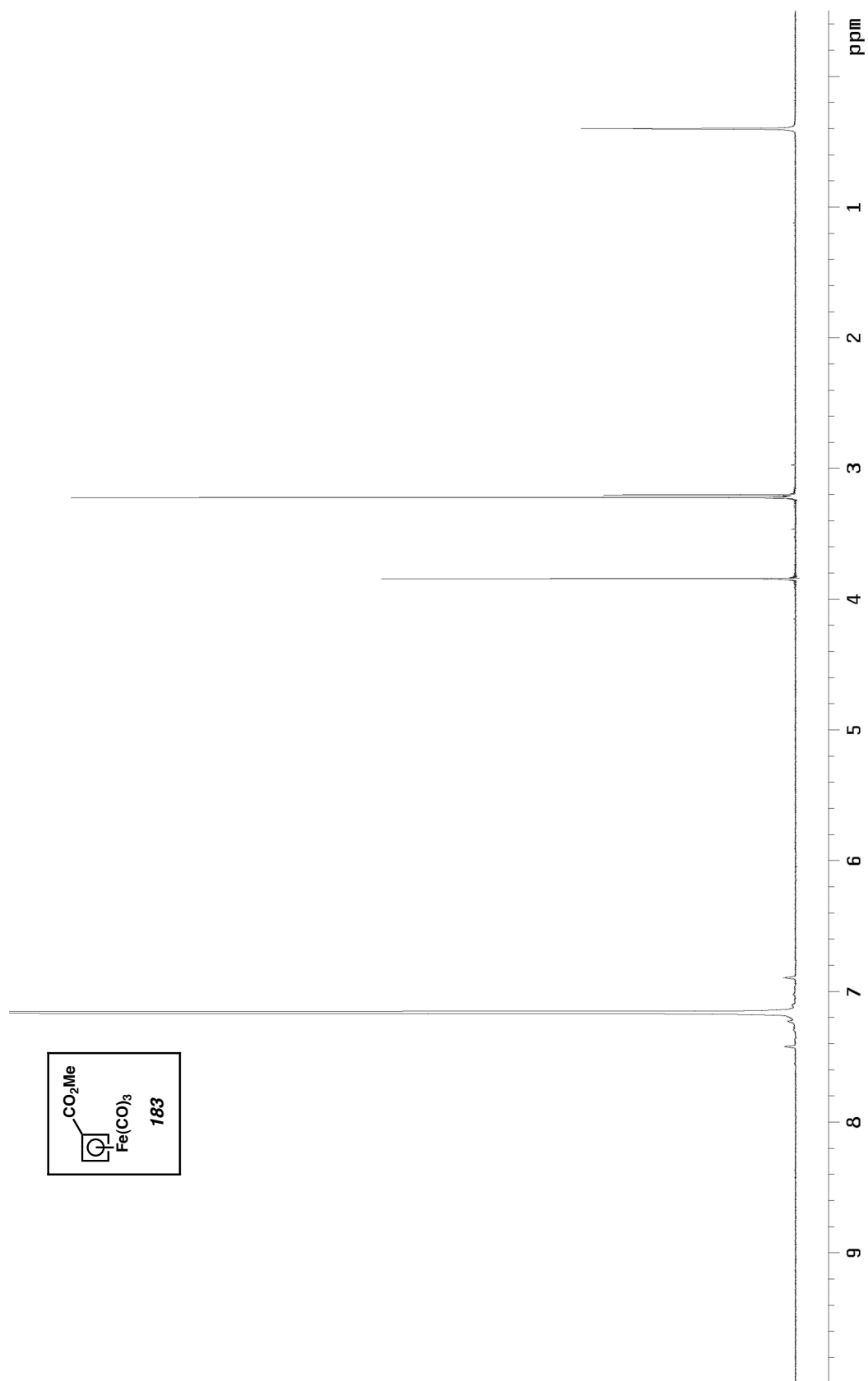
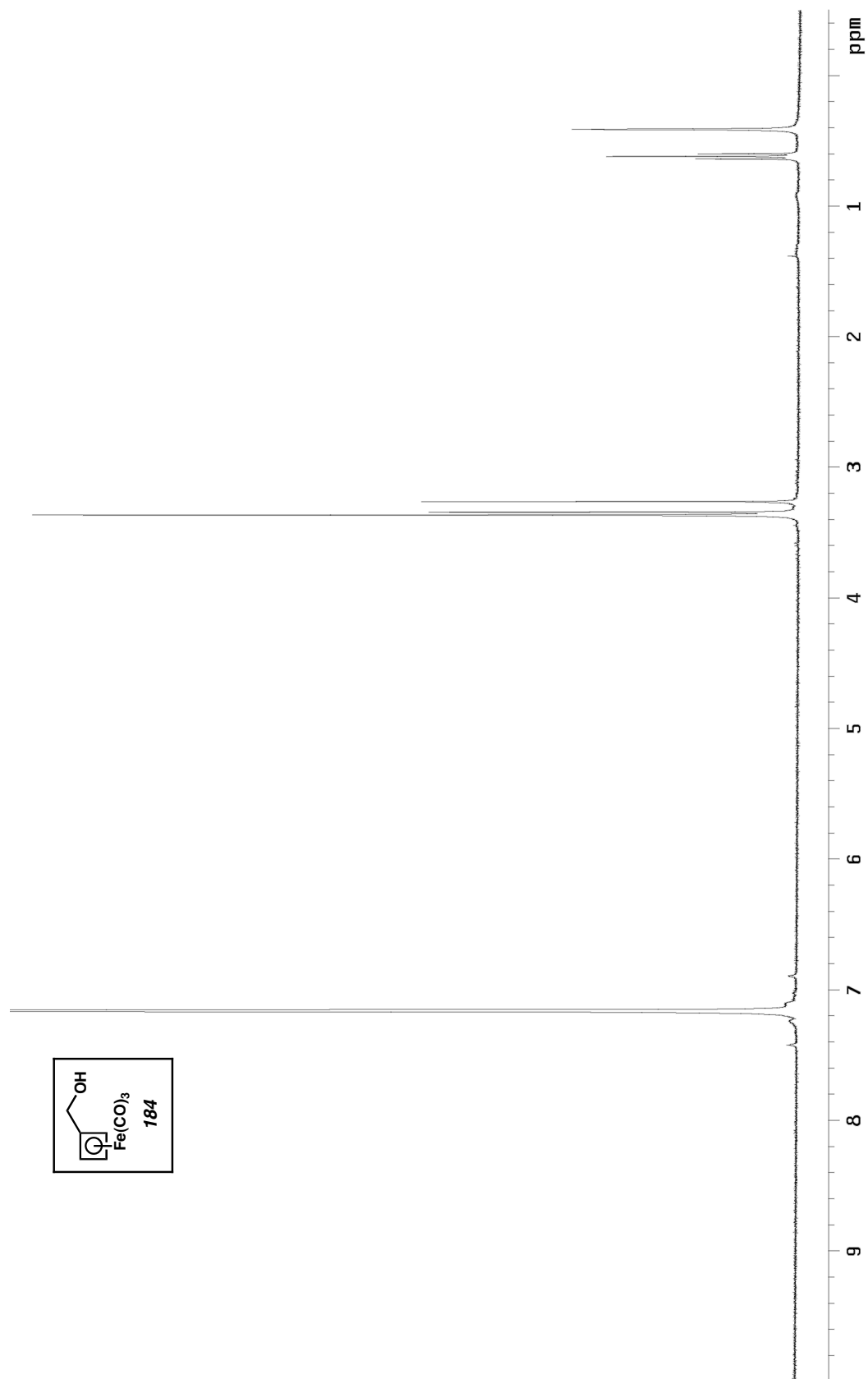


Figure A2.9. ¹³C NMR spectrum (126 MHz, CDCl₃) of **181**.

Figure A2.10. ^1H NMR spectrum (300 MHz, C_6D_6) of **183**.

Figure A2.11. ^1H NMR spectrum (300 MHz, C_6D_6) of **184**.

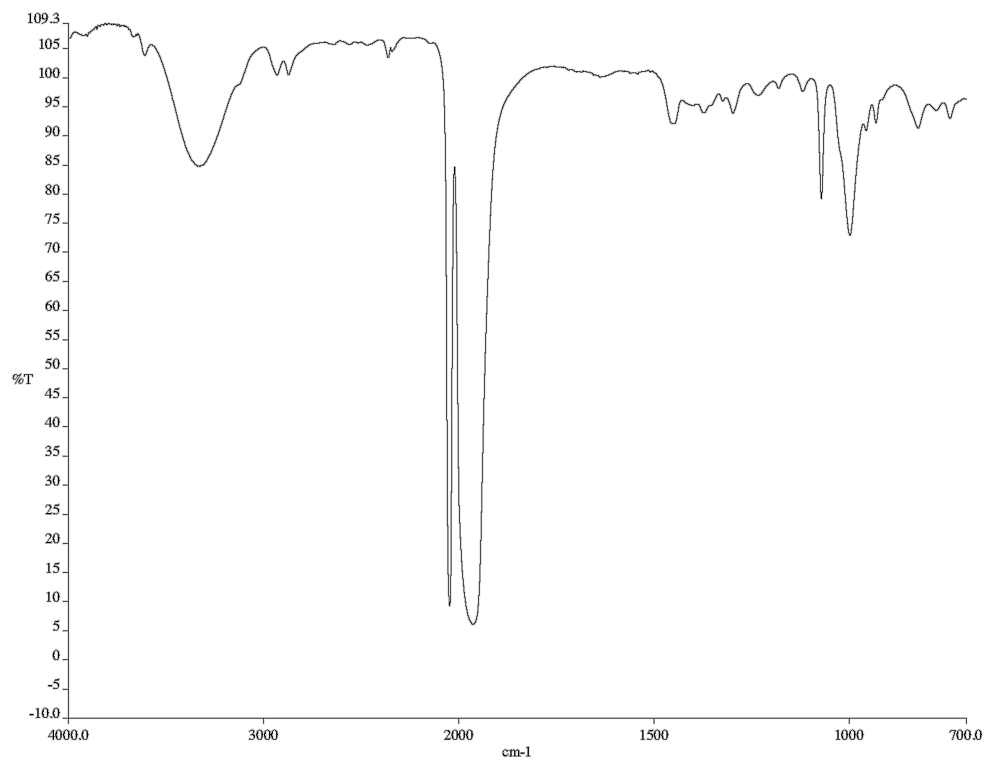


Figure A2.12. Infrared spectrum (neat film/NaCl) of **184**.

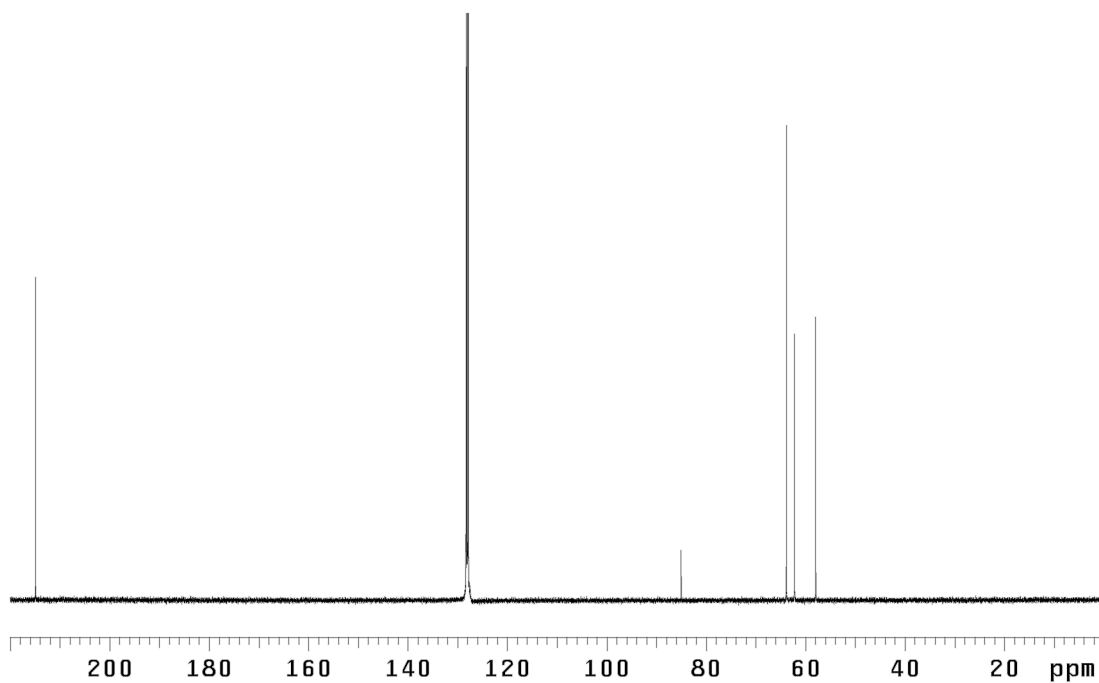
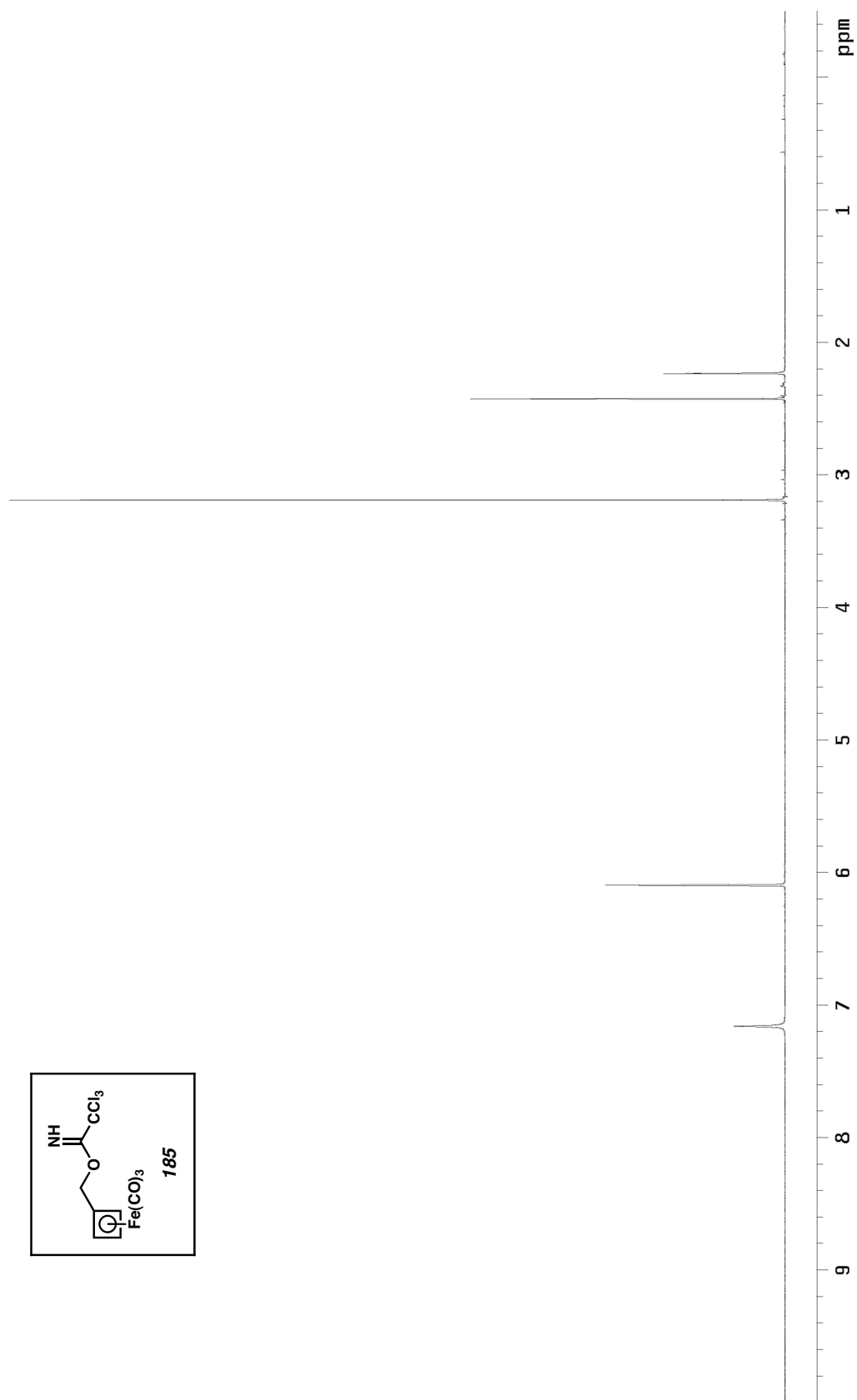


Figure A2.13. ¹³C NMR spectrum (126 MHz, C₆D₆) of **184**.

Figure A2.14. ^1H NMR spectrum (500 MHz, $\text{C}_6\text{D}_6\text{O}$) of **185**.

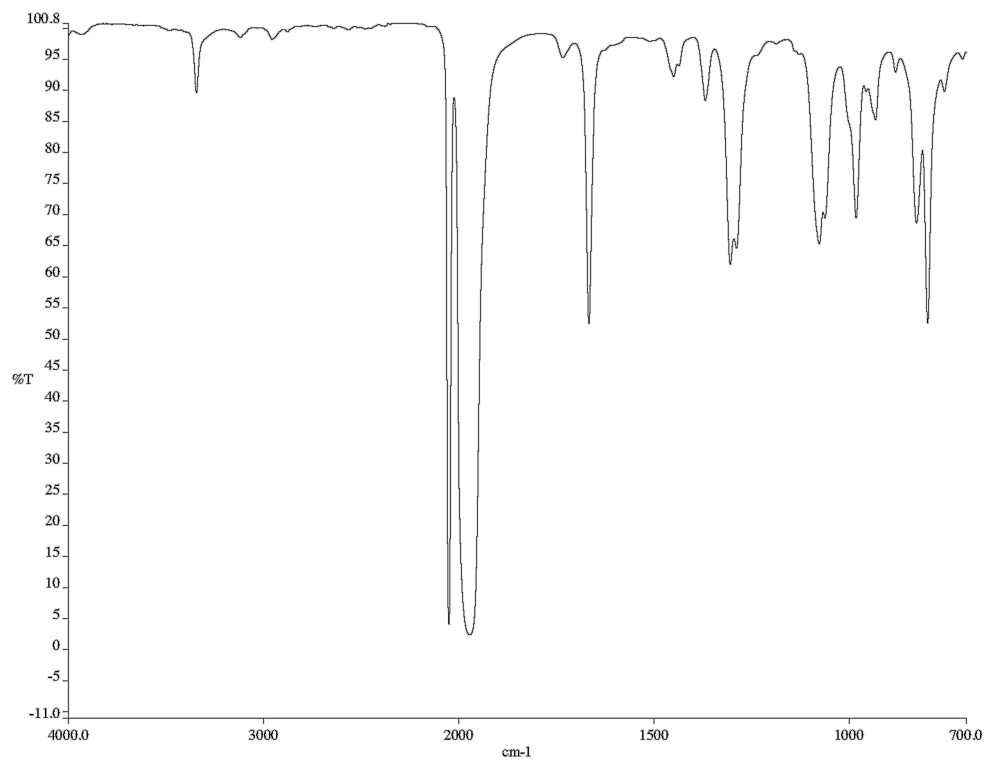


Figure A2.15. Infrared spectrum (neat film/NaCl) of **185**.

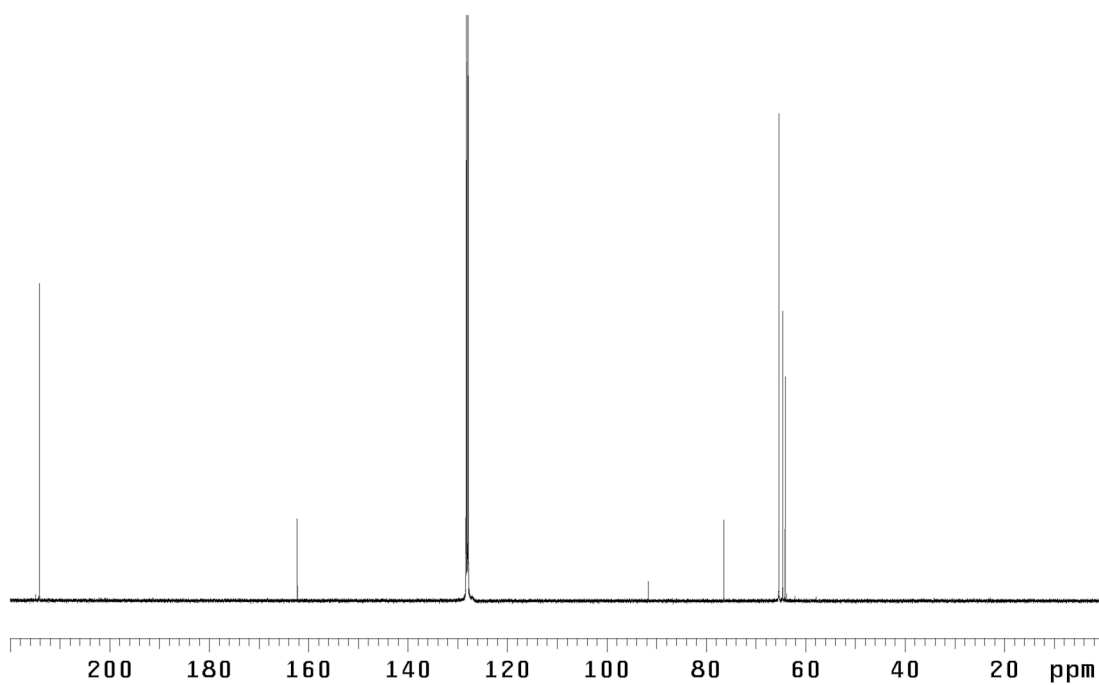
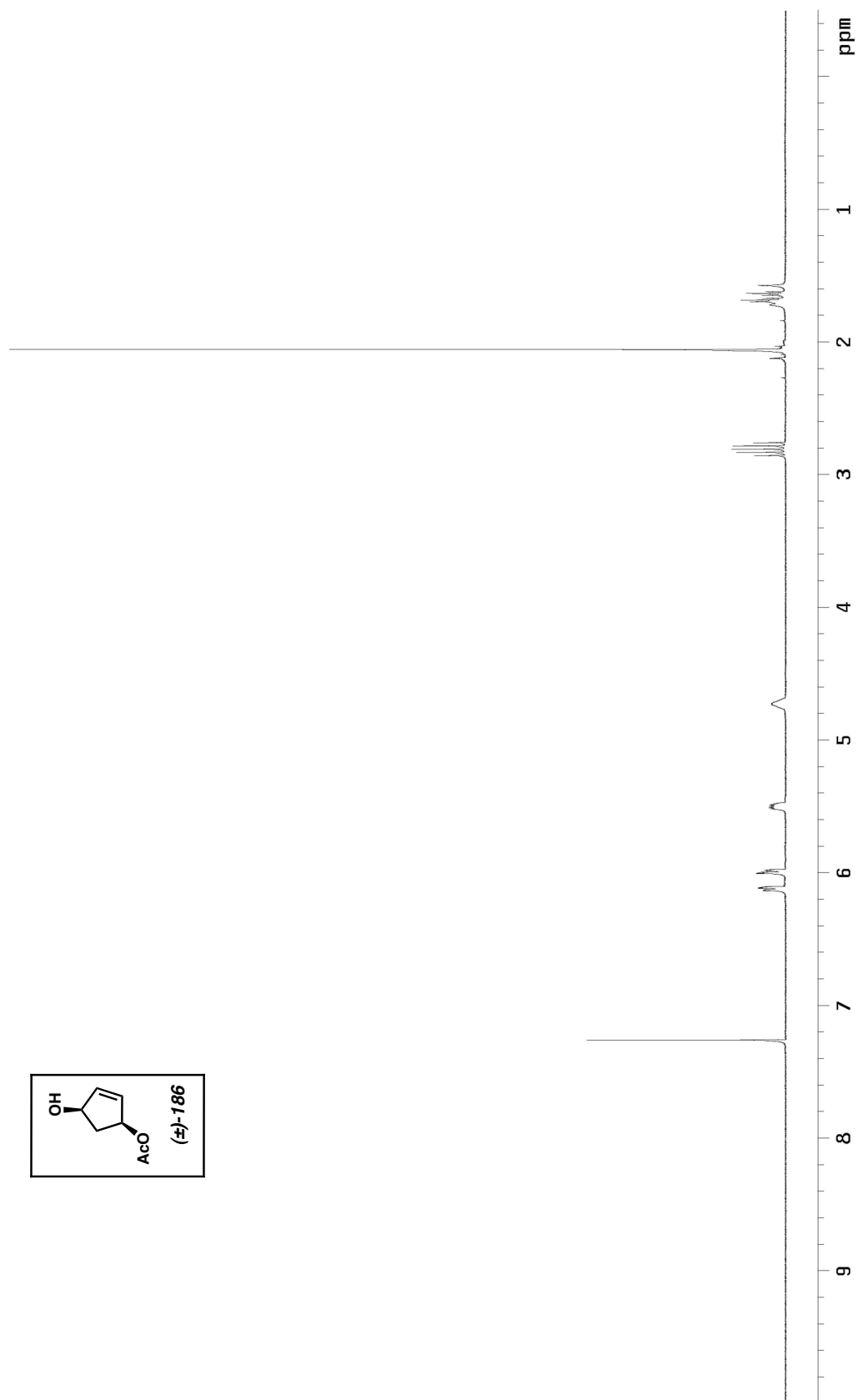
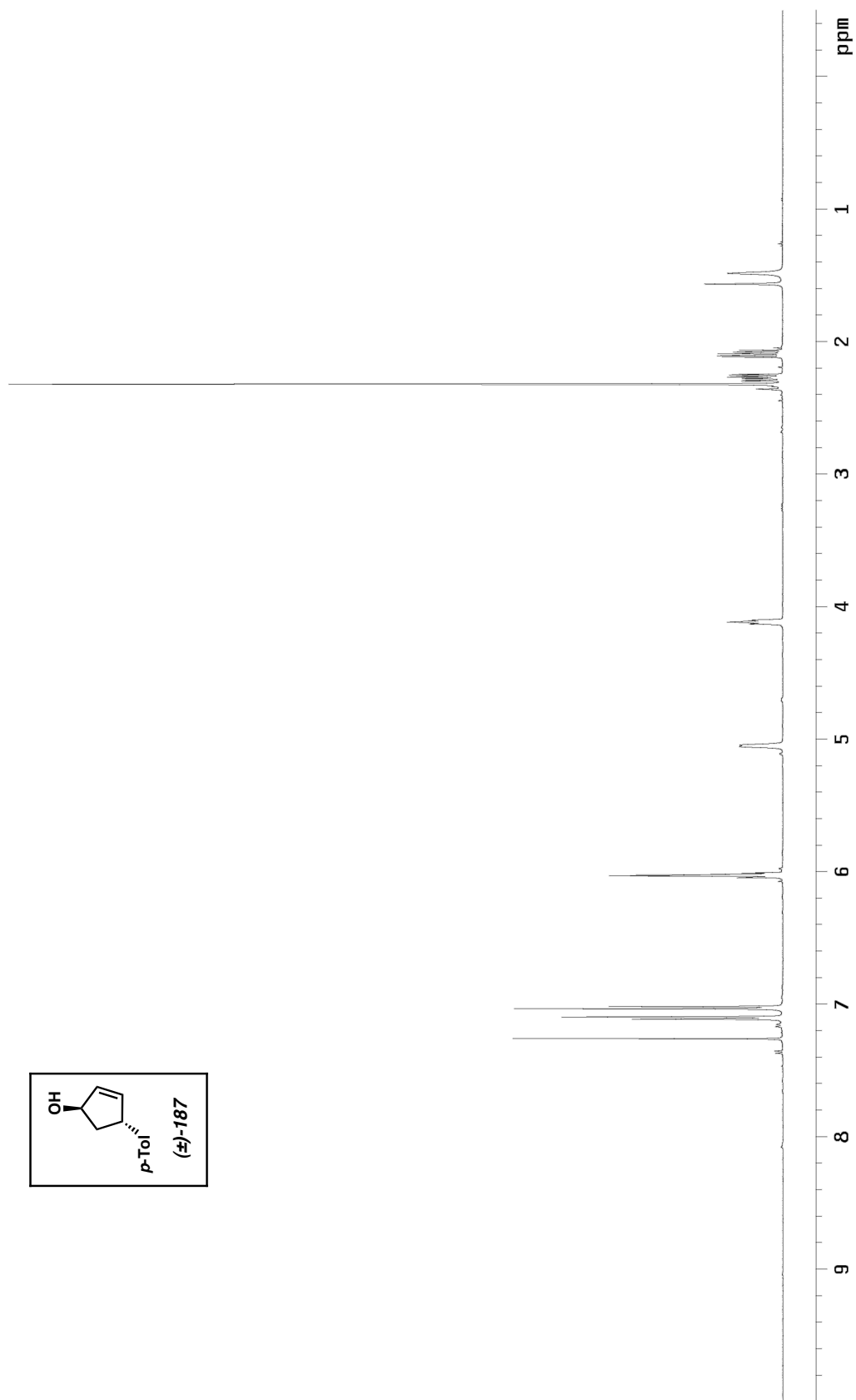
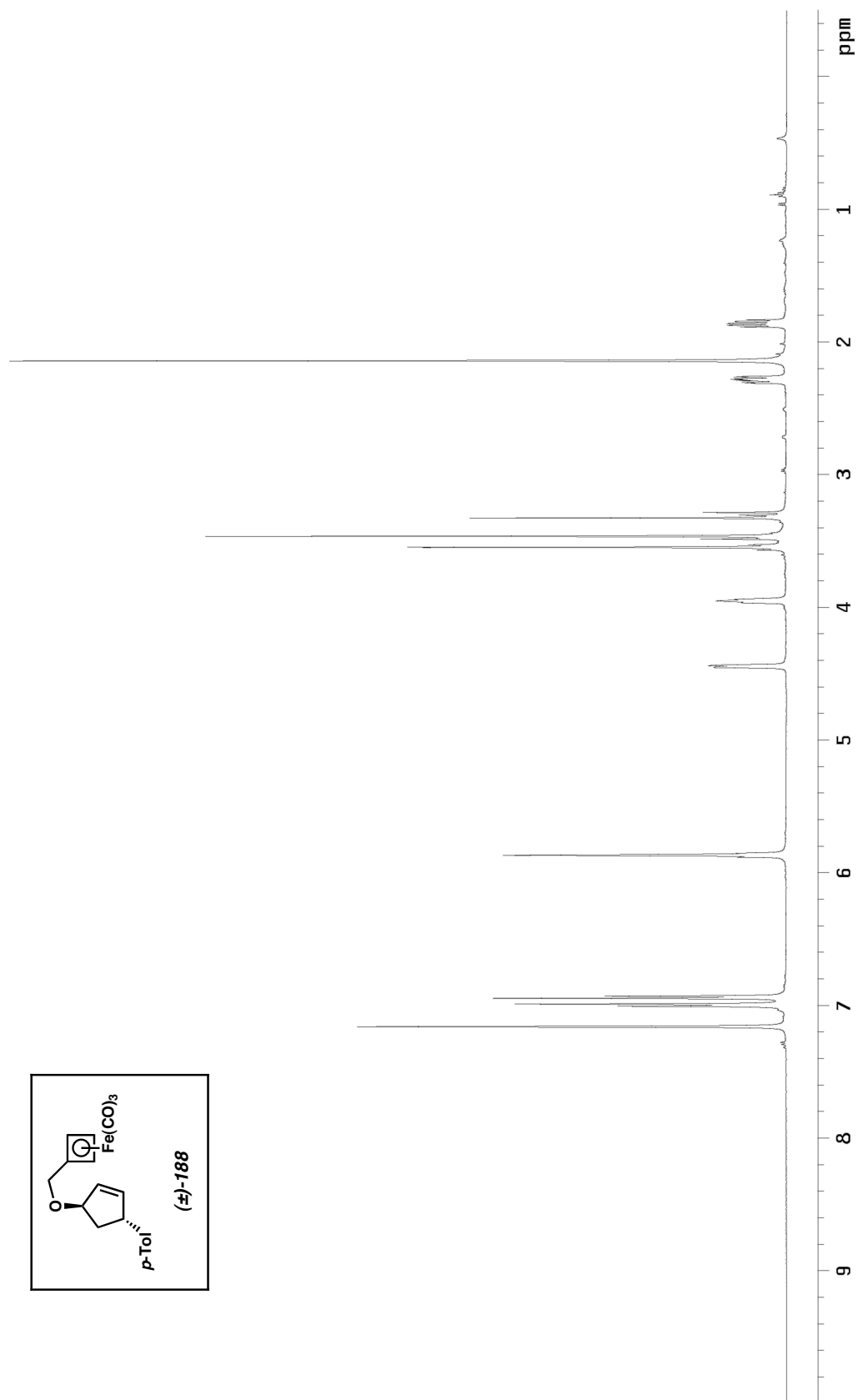


Figure A2.16. ¹³C NMR spectrum (126 MHz, C₆D₆) of **185**.

Figure A2.17. ^1H NMR spectrum (300 MHz, CDCl_3) of **186**.

Figure A2.18. ^1H NMR spectrum (500 MHz, CDCl_3) of **187**.

Figure A2.19. ^1H NMR spectrum (300 MHz, $\text{C}_6\text{D}_6\text{O}$) of **188**.

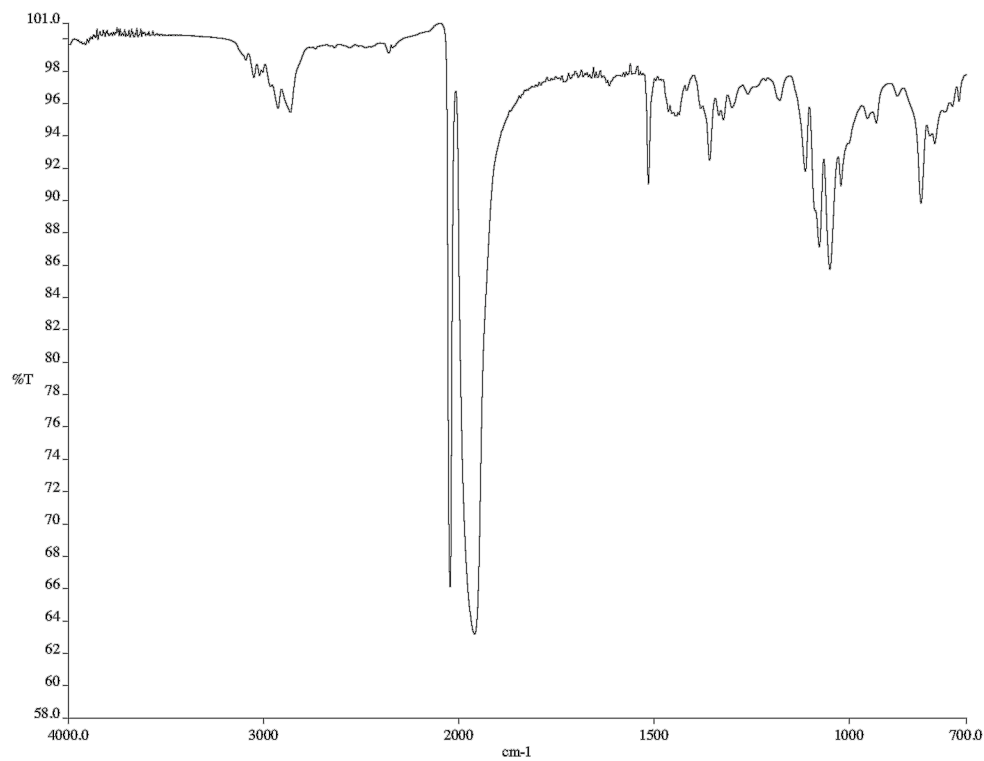


Figure A2.20. Infrared spectrum (neat film/NaCl) of **188**.

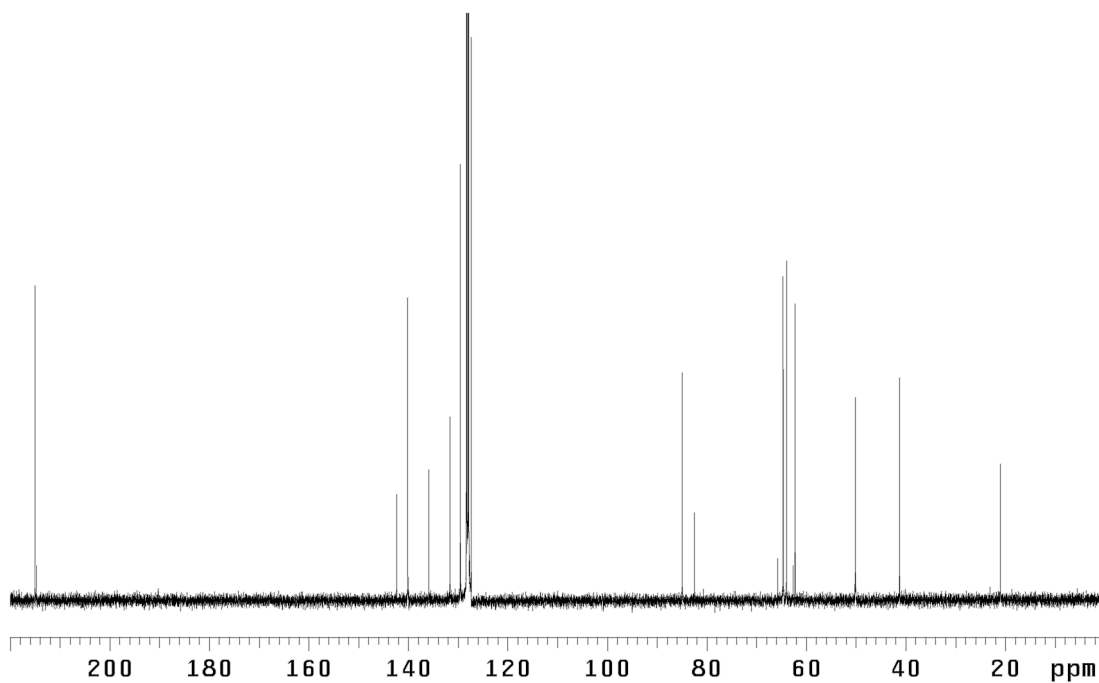
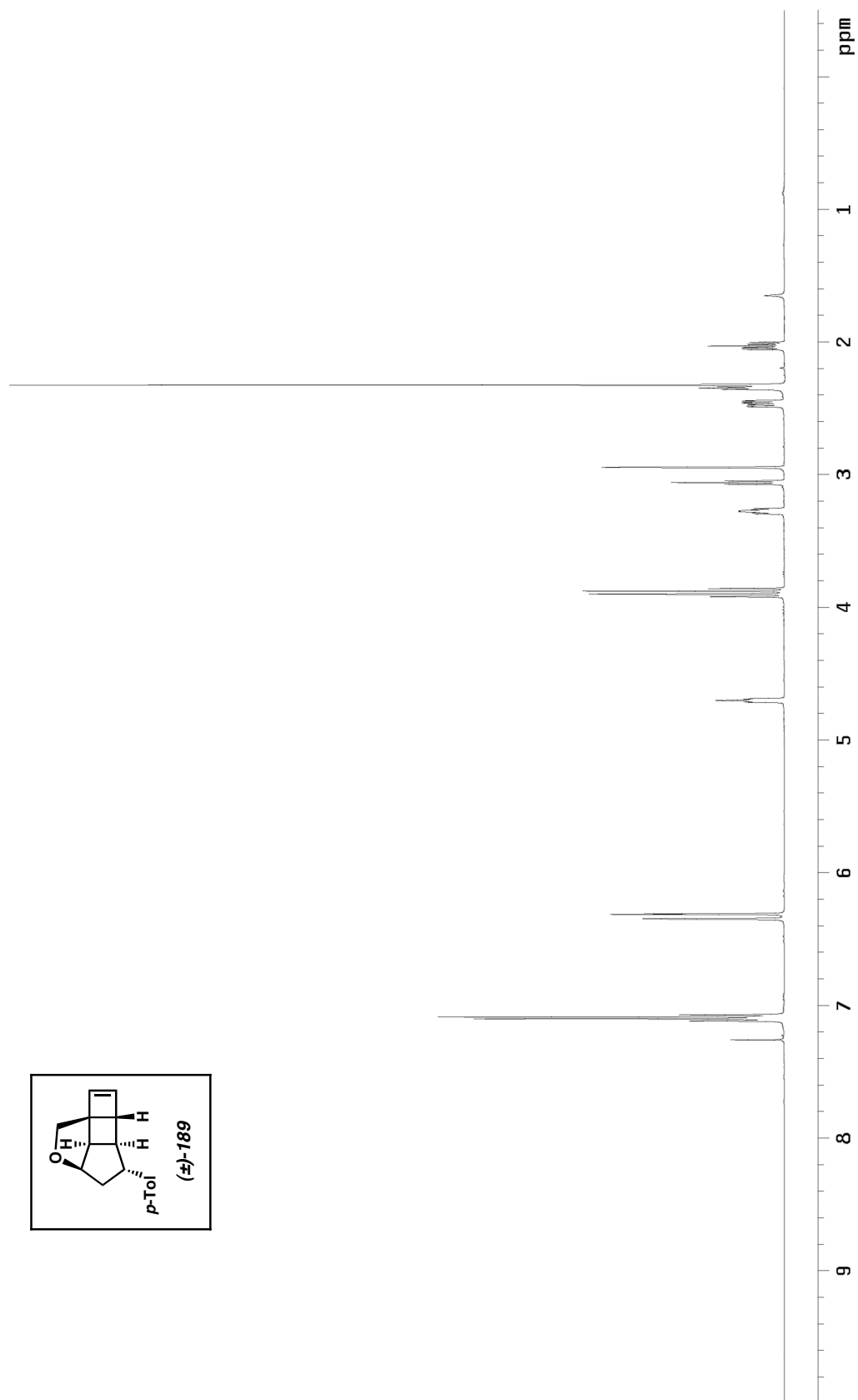


Figure A2.21. ^{13}C NMR spectrum (126 MHz, C_6D_6) of **188**.

Figure A2.22. ^1H NMR spectrum (500 MHz, CDCl_3) of **189**.

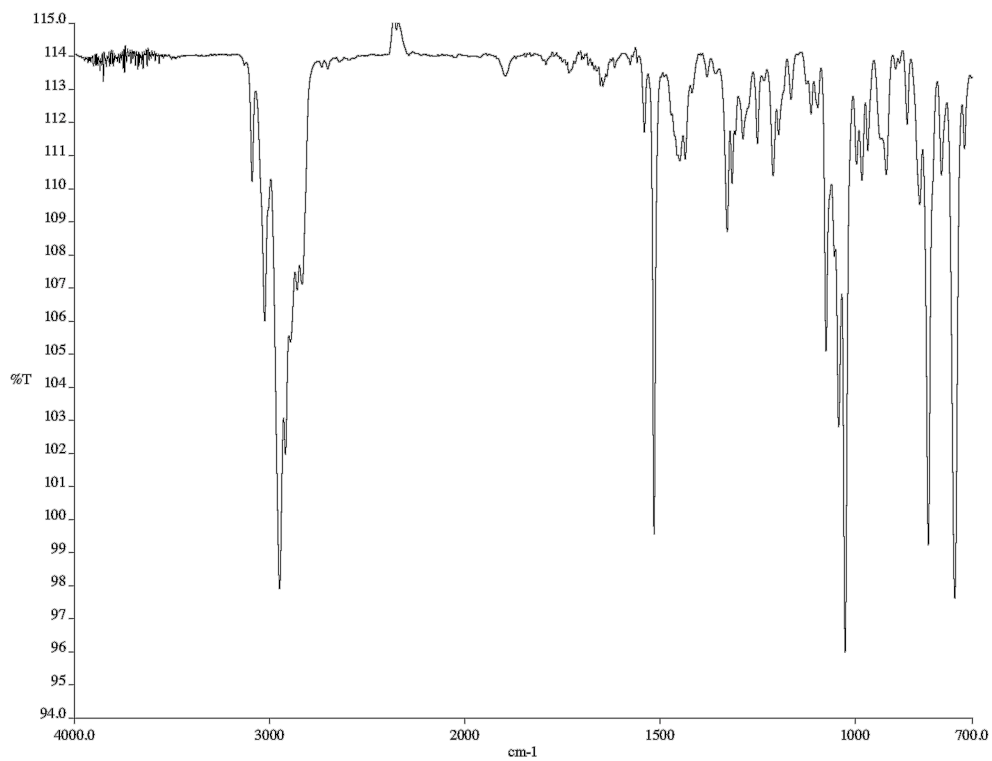


Figure A2.23. Infrared spectrum (neat film/NaCl) of **189**.

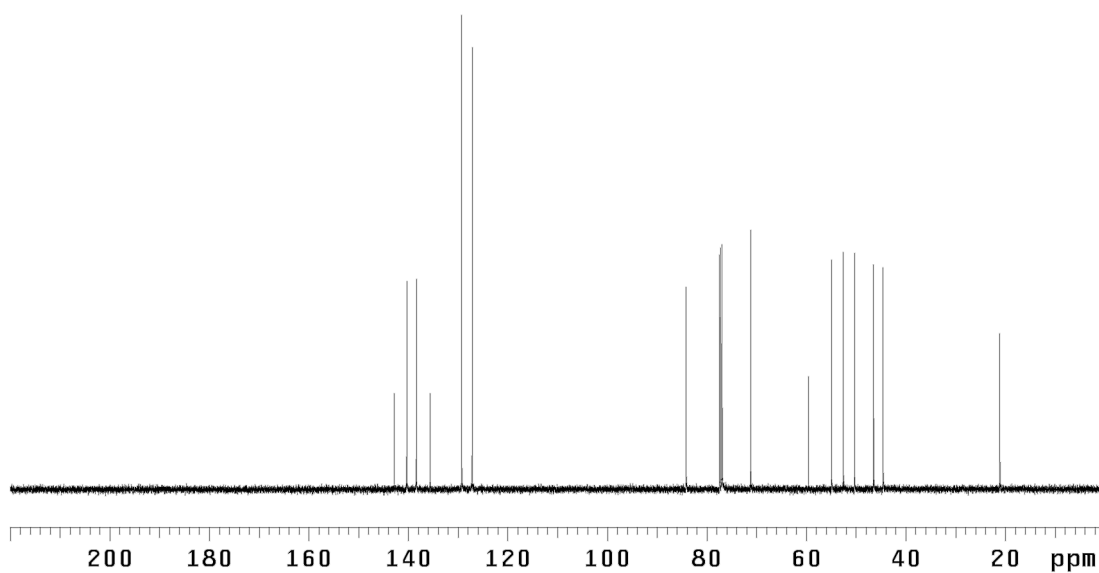
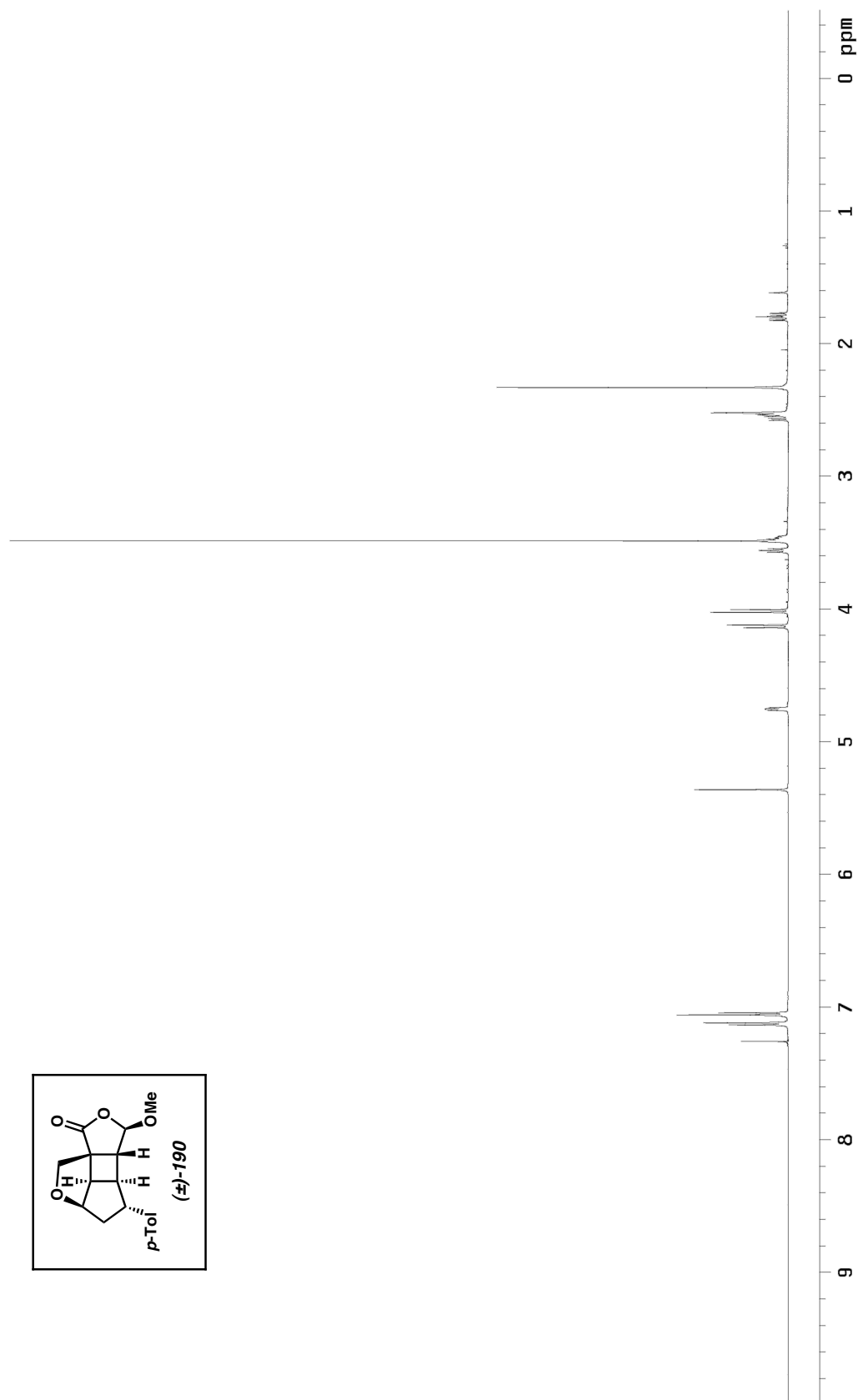


Figure A2.24. ¹³C NMR spectrum (126 MHz, CDCl₃) of **189**.

Figure A2.25. ^1H NMR spectrum (500 MHz, CDCl_3) of **190**.

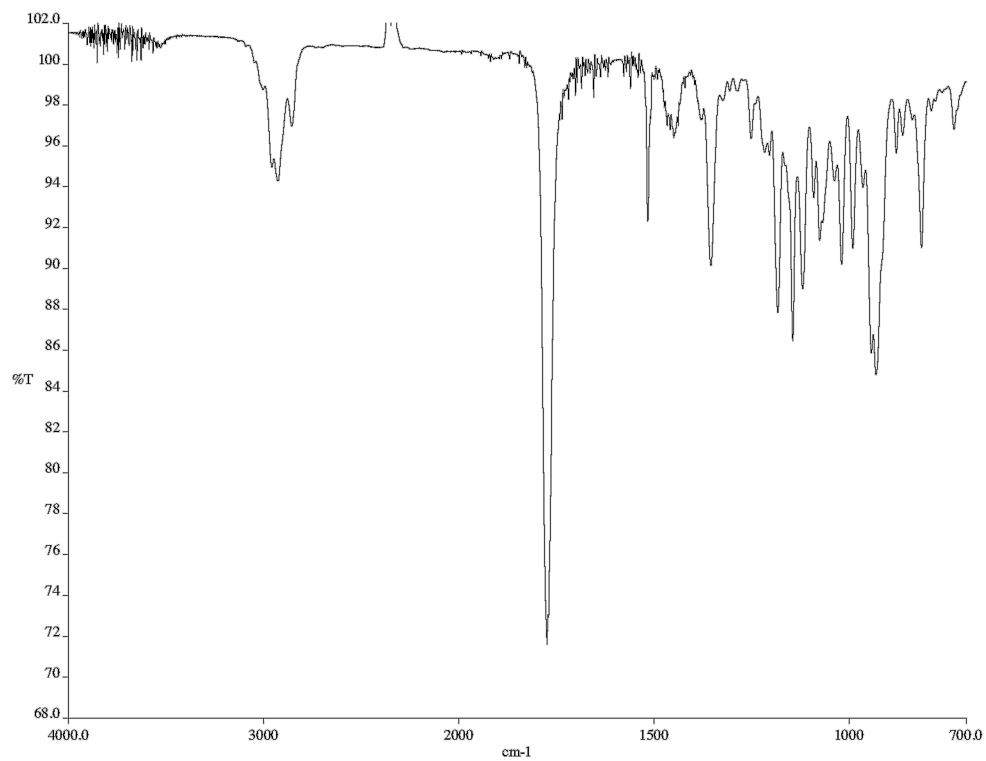


Figure A2.26. Infrared spectrum (neat film/NaCl) of **190**.

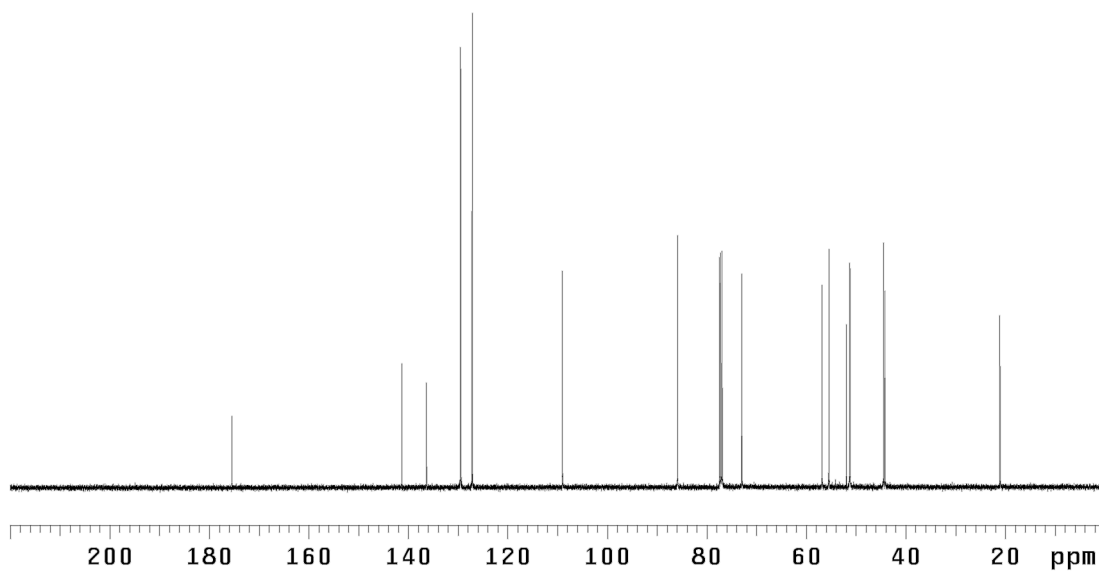
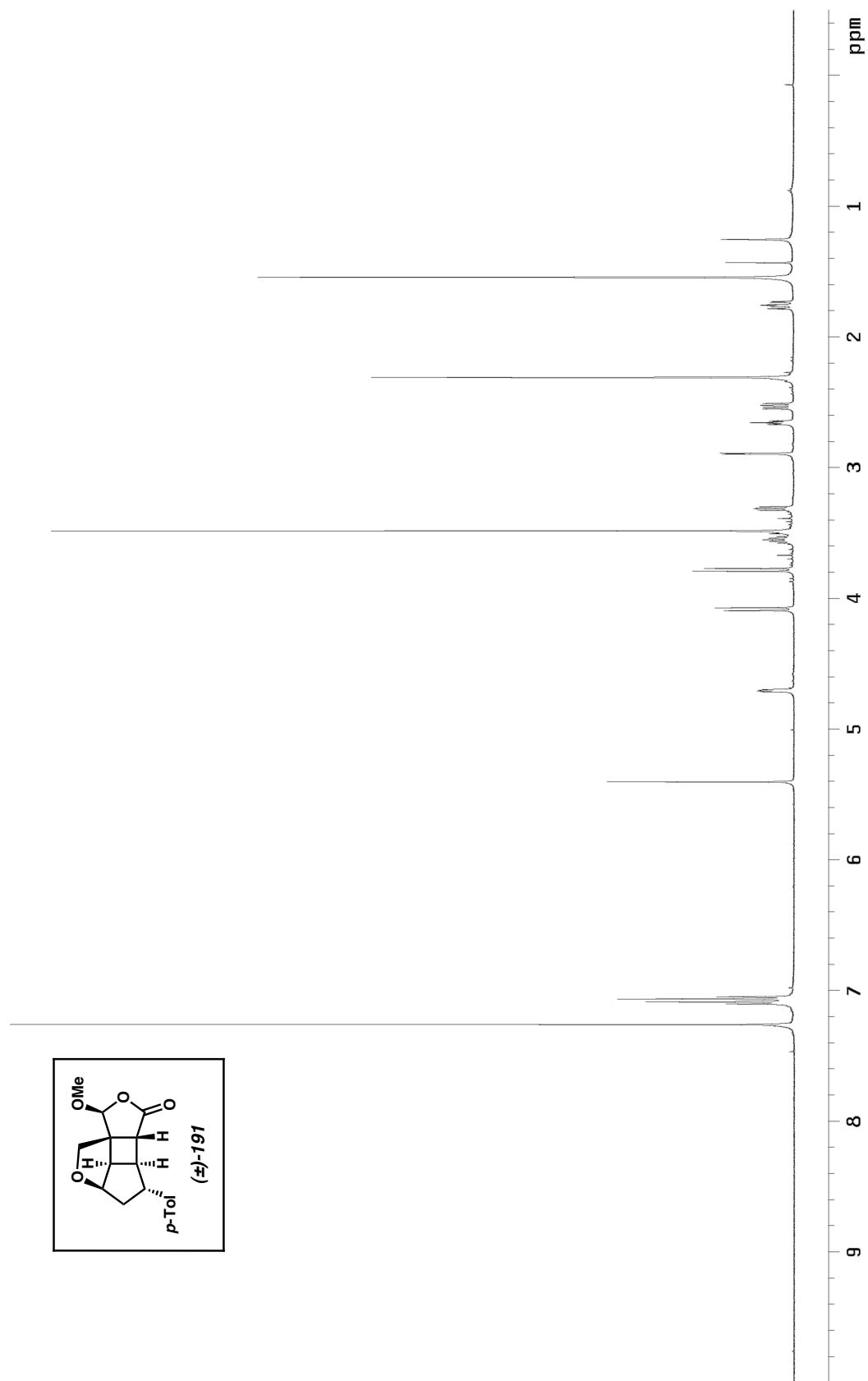


Figure A2.27. ¹³C NMR spectrum (126 MHz, CDCl₃) of **190**.

Figure A2.28. ^1H NMR spectrum (500 MHz, CDCl_3) of **191**.

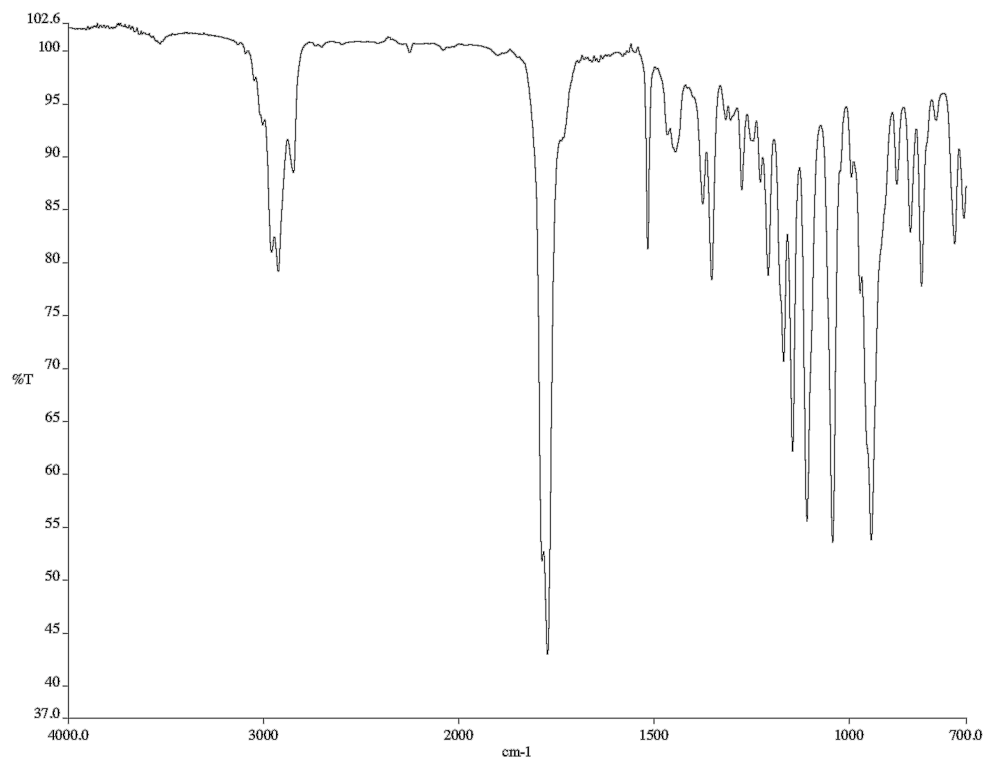


Figure A2.29. Infrared spectrum (neat film/NaCl) of **191**.

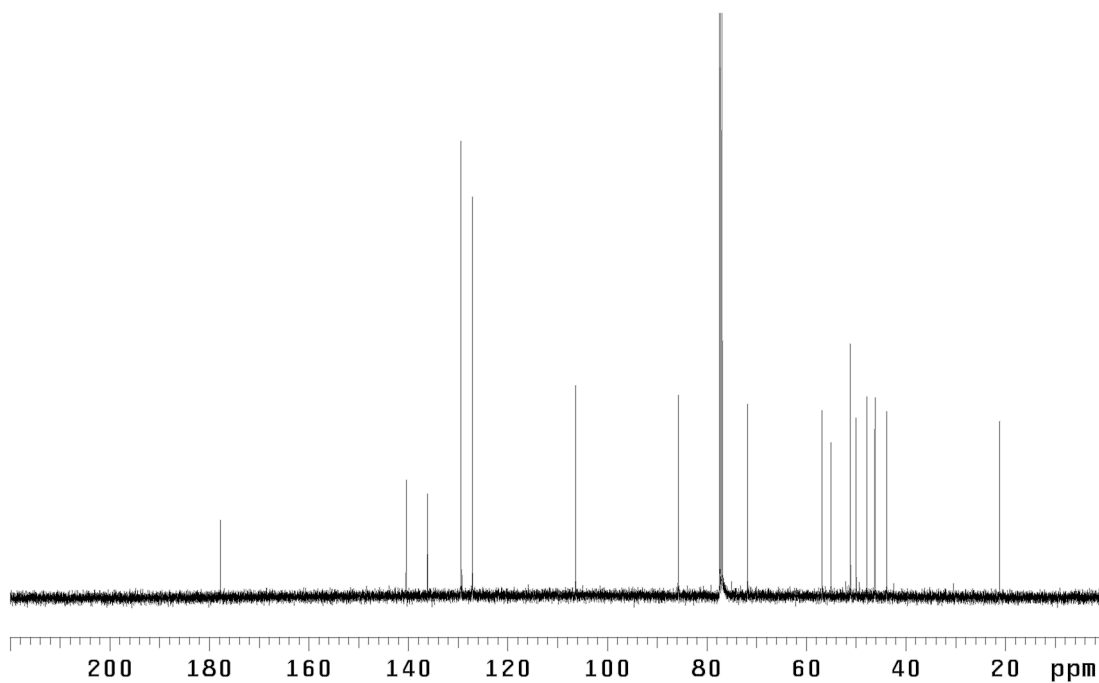
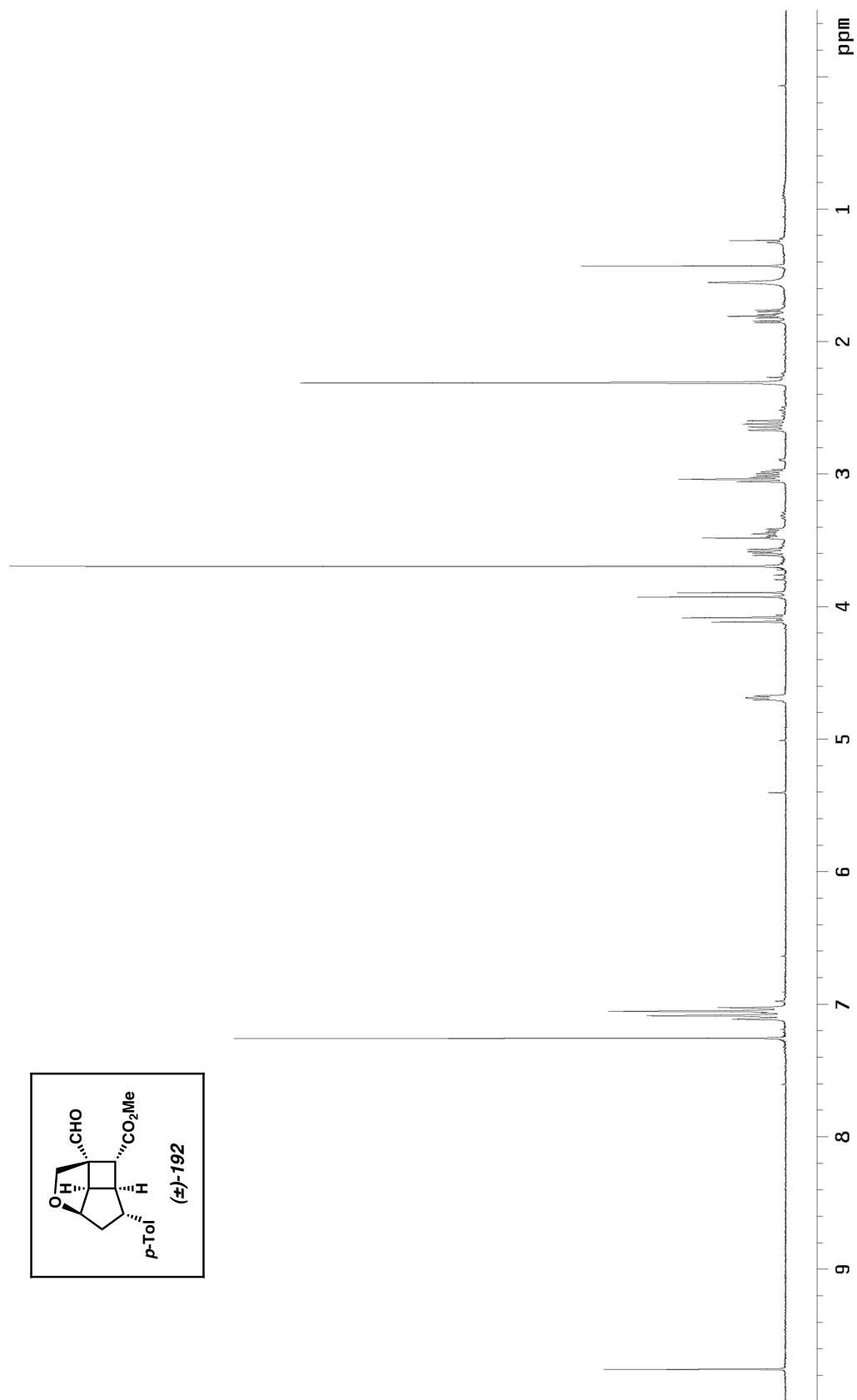
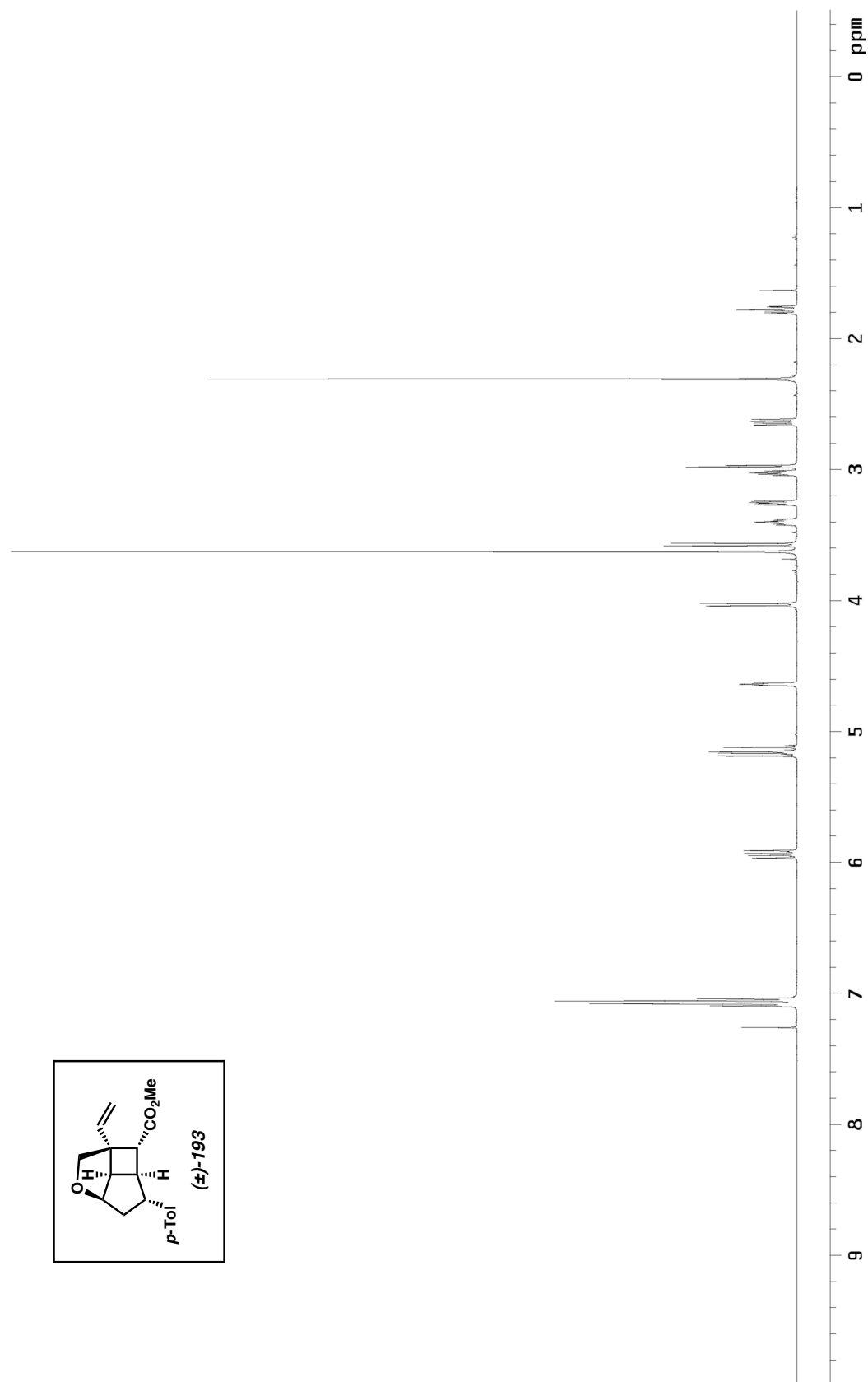


Figure A2.30. ^{13}C NMR spectrum (126 MHz, CDCl_3) of **191**.

Figure A2.31. ¹H NMR spectrum (300 MHz, CDCl₃) of **192**.

Figure A2.32. ^1H NMR spectrum (500 MHz, CDCl_3) of **193**.

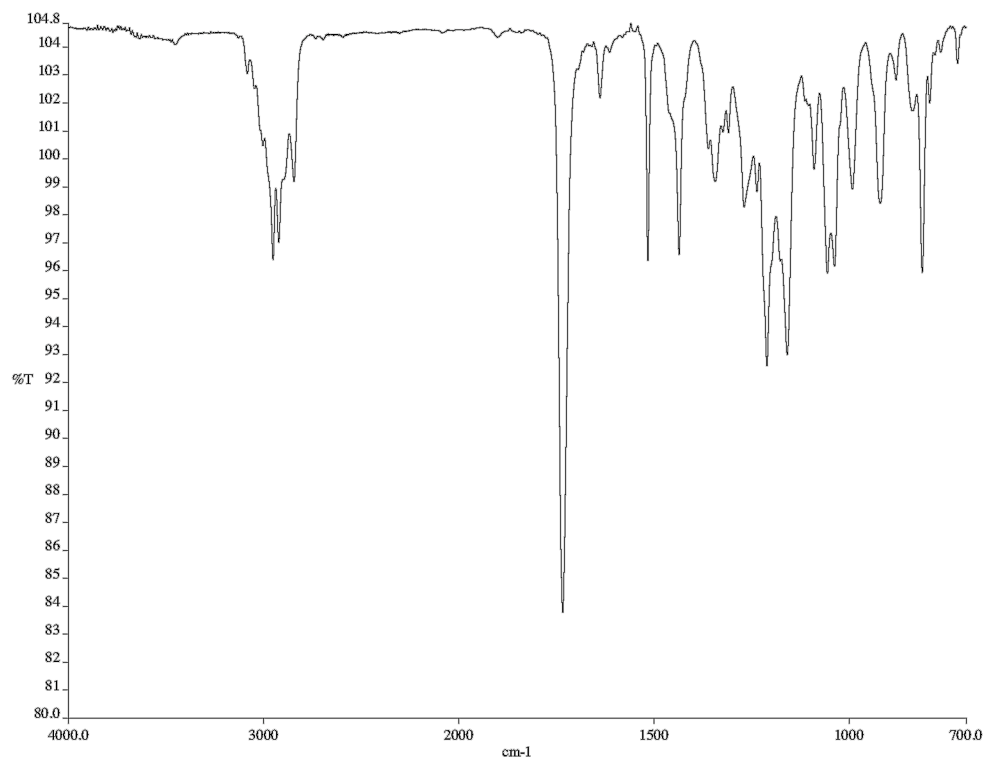


Figure A2.33. Infrared spectrum (neat film/NaCl) of **193**.

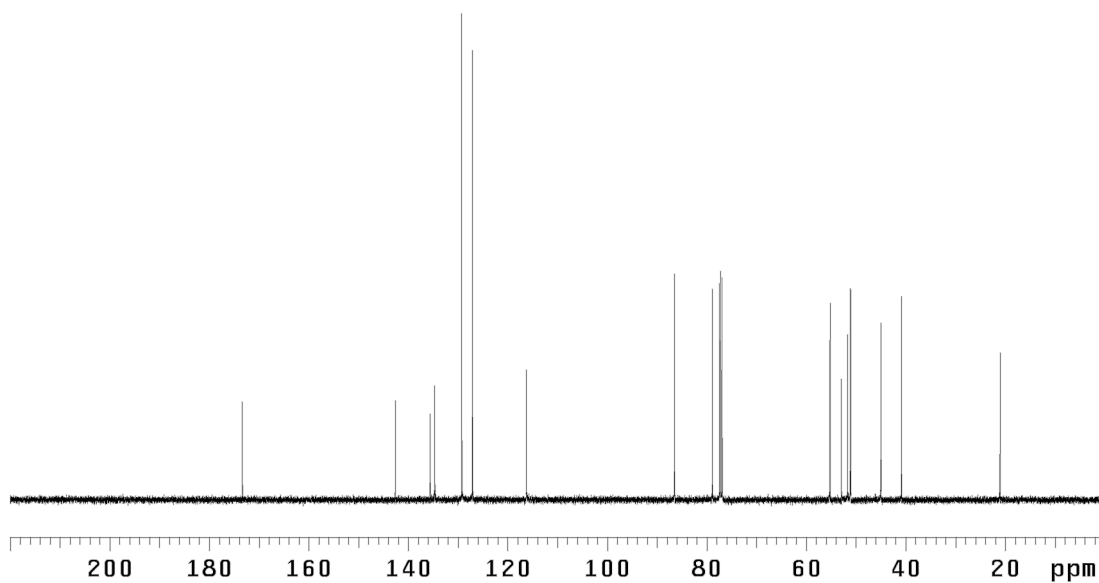
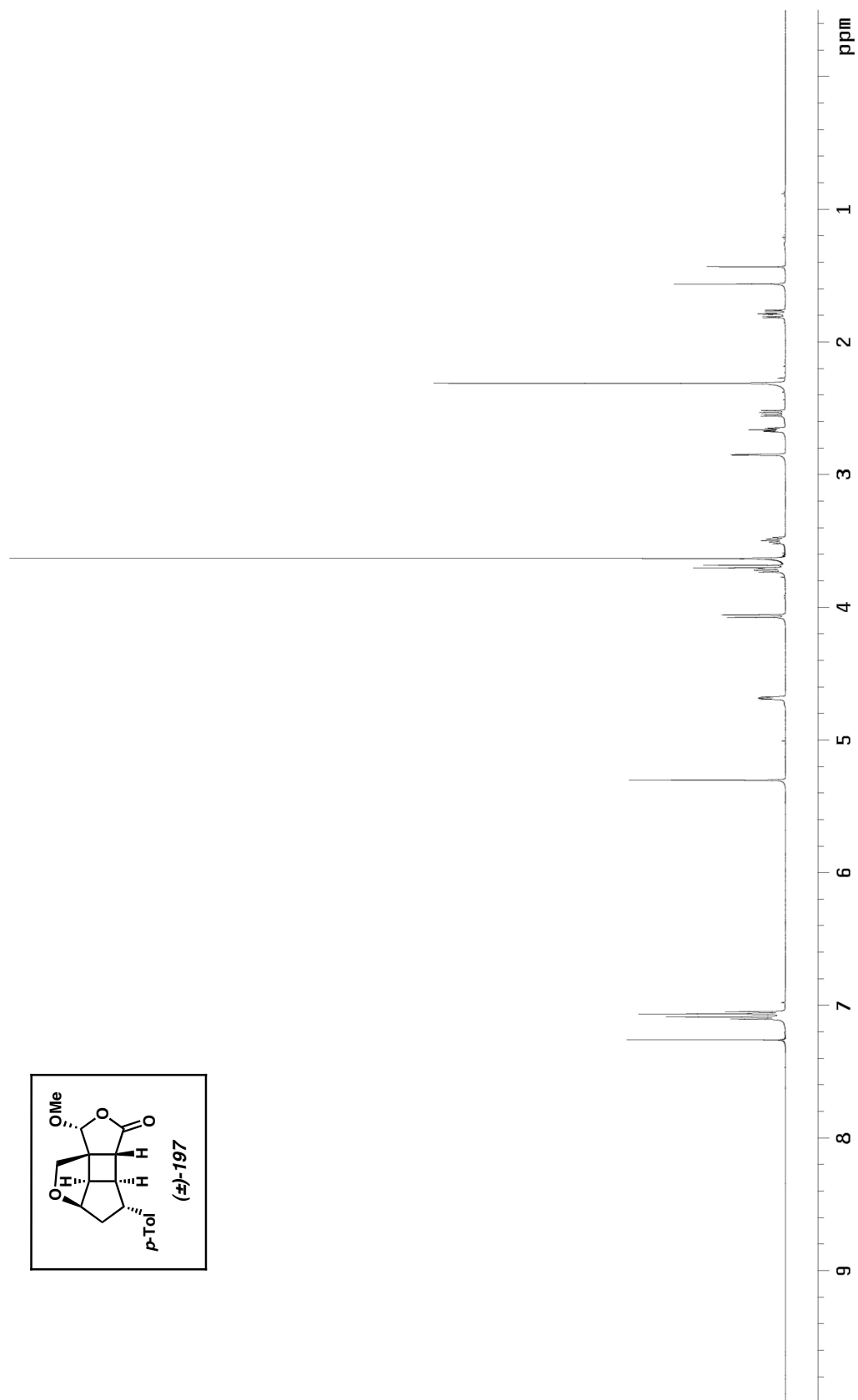


Figure A2.34. ¹³C NMR spectrum (126 MHz, CDCl₃) of **193**.

Figure A2.35. ¹H NMR spectrum (500 MHz, CDCl₃) of **197**.

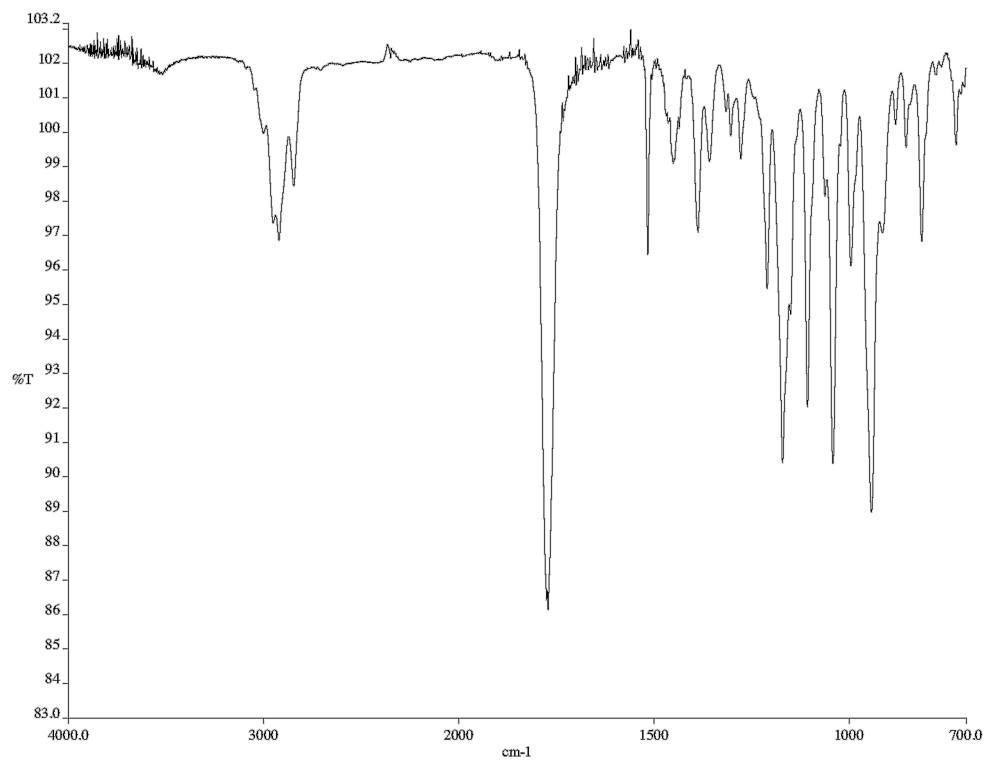


Figure A2.36. Infrared spectrum (neat film/NaCl) of **197**.

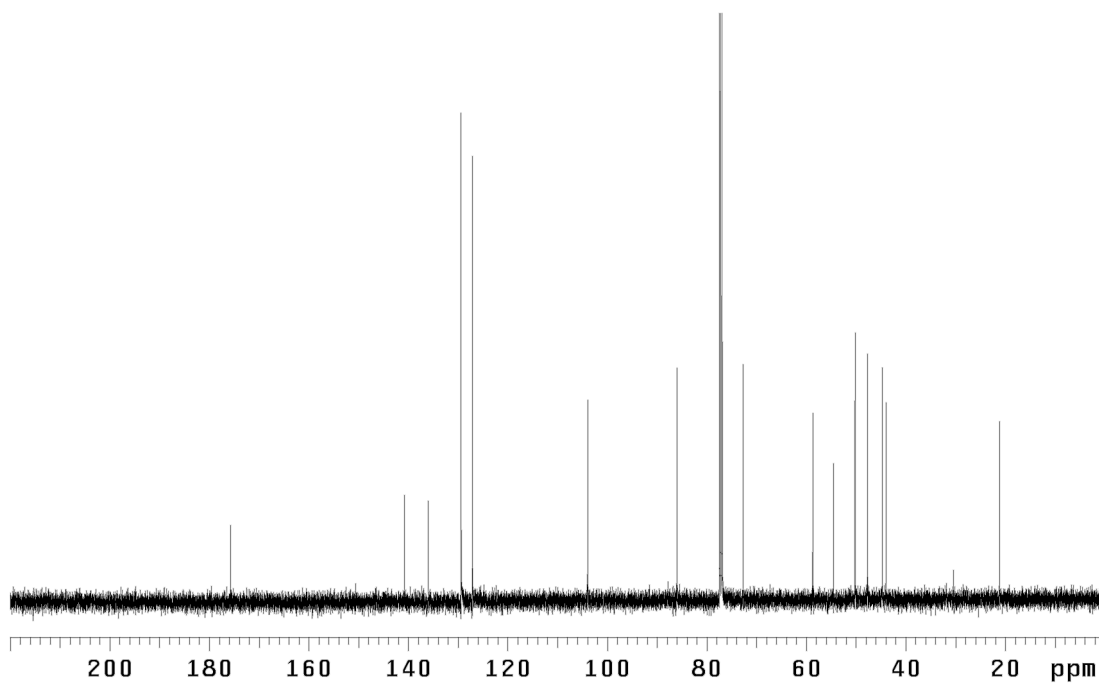
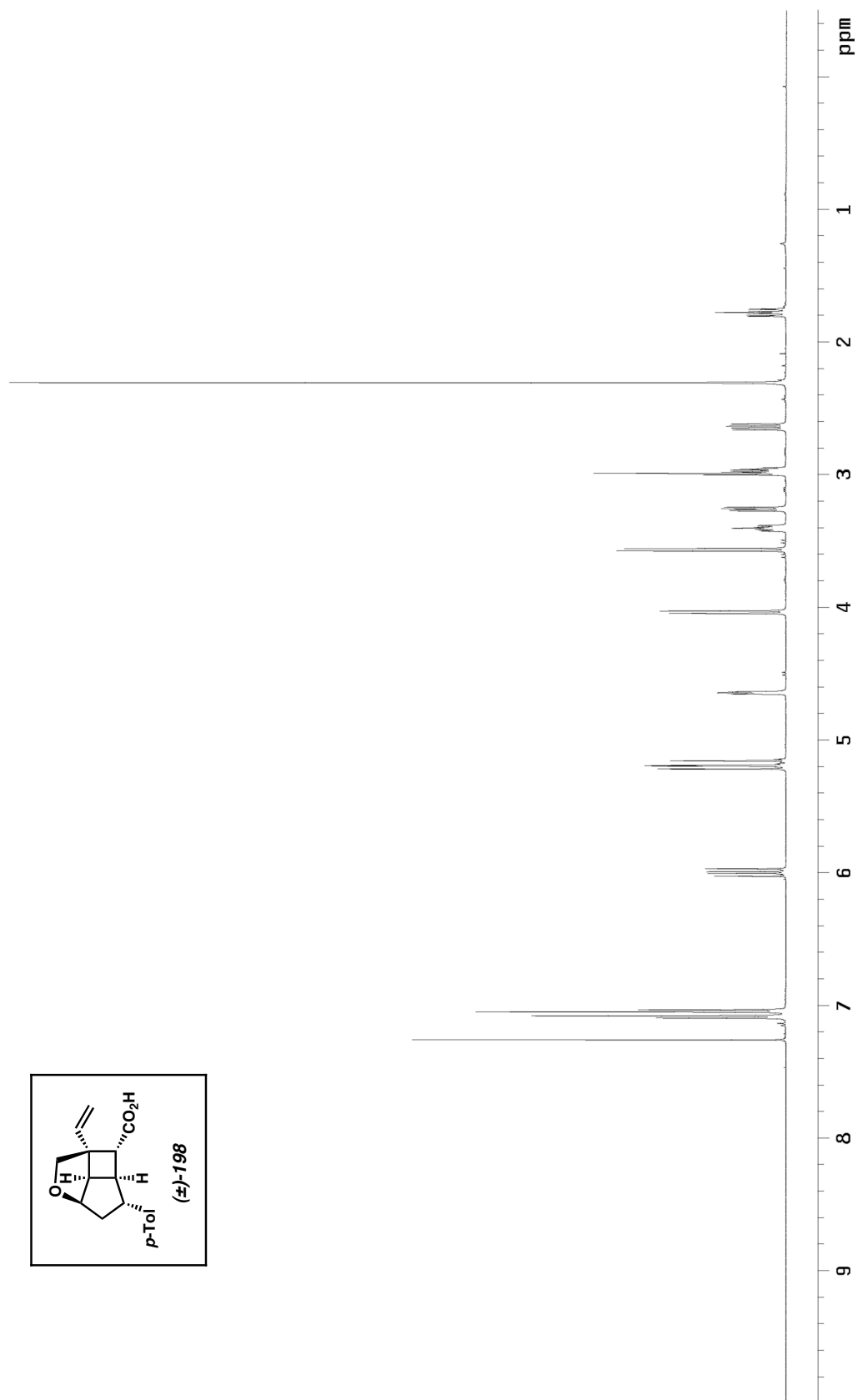


Figure A2.37. ¹³C NMR spectrum (126 MHz, CDCl₃) of **197**.

Figure A2.38. ^1H NMR spectrum (500 MHz, CDCl_3) of **198**.

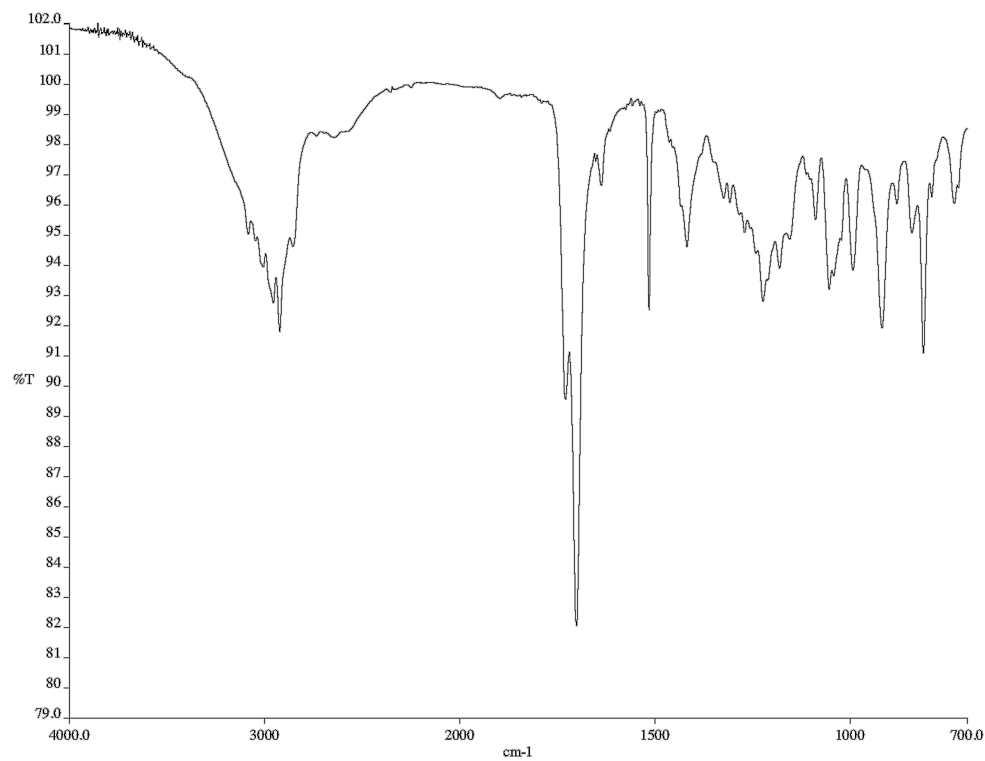


Figure A2.39. Infrared spectrum (neat film/NaCl) of **198**.

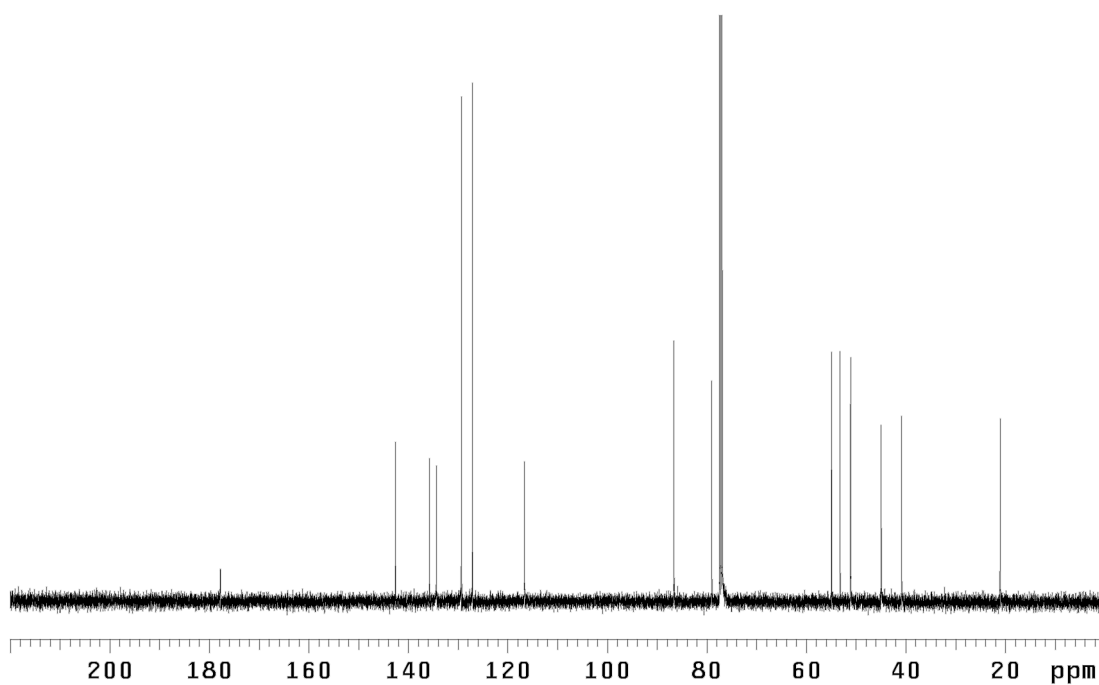


Figure A2.40. ¹³C NMR spectrum (126 MHz, CDCl₃) of **198**.

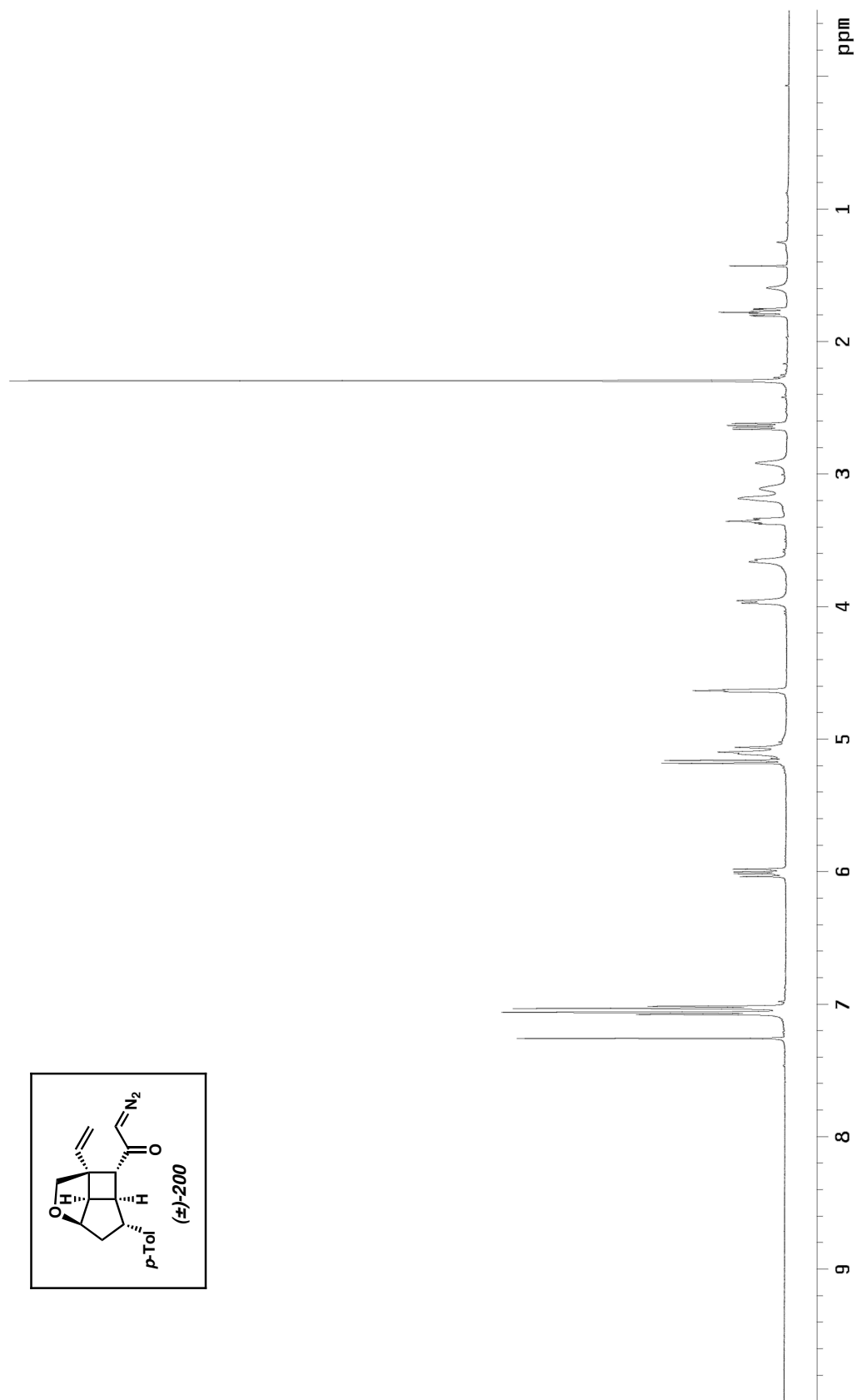


Figure A2.41. ^1H NMR spectrum (500 MHz, CDCl_3) of **200**.

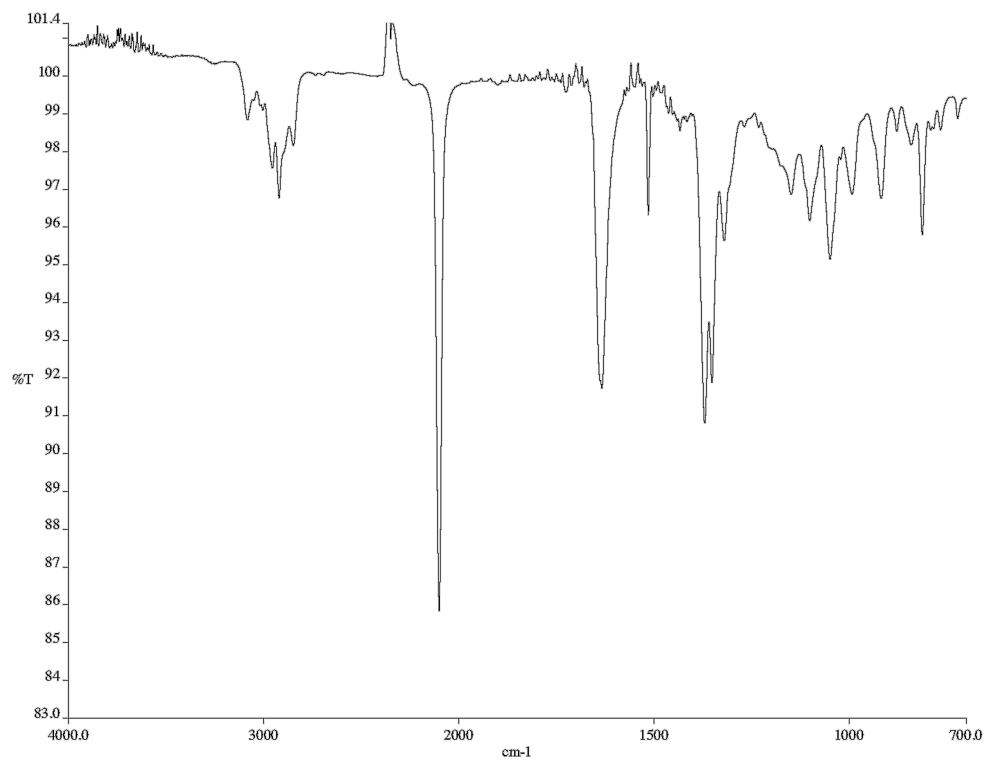


Figure A2.42. Infrared spectrum (neat film/NaCl) of **200**.

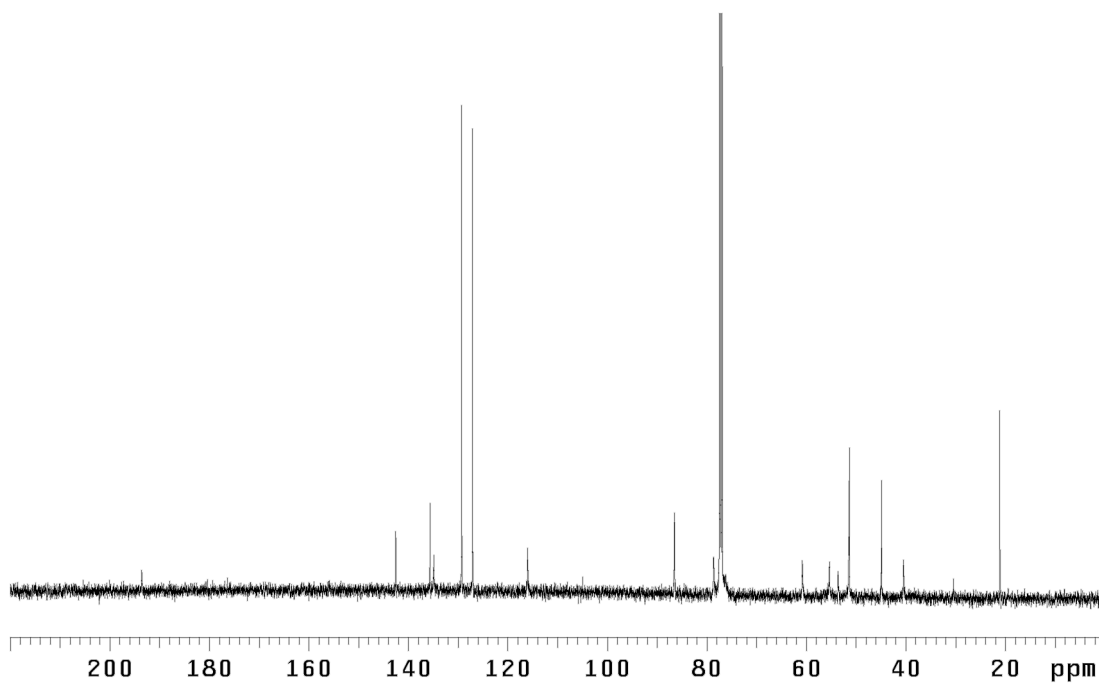
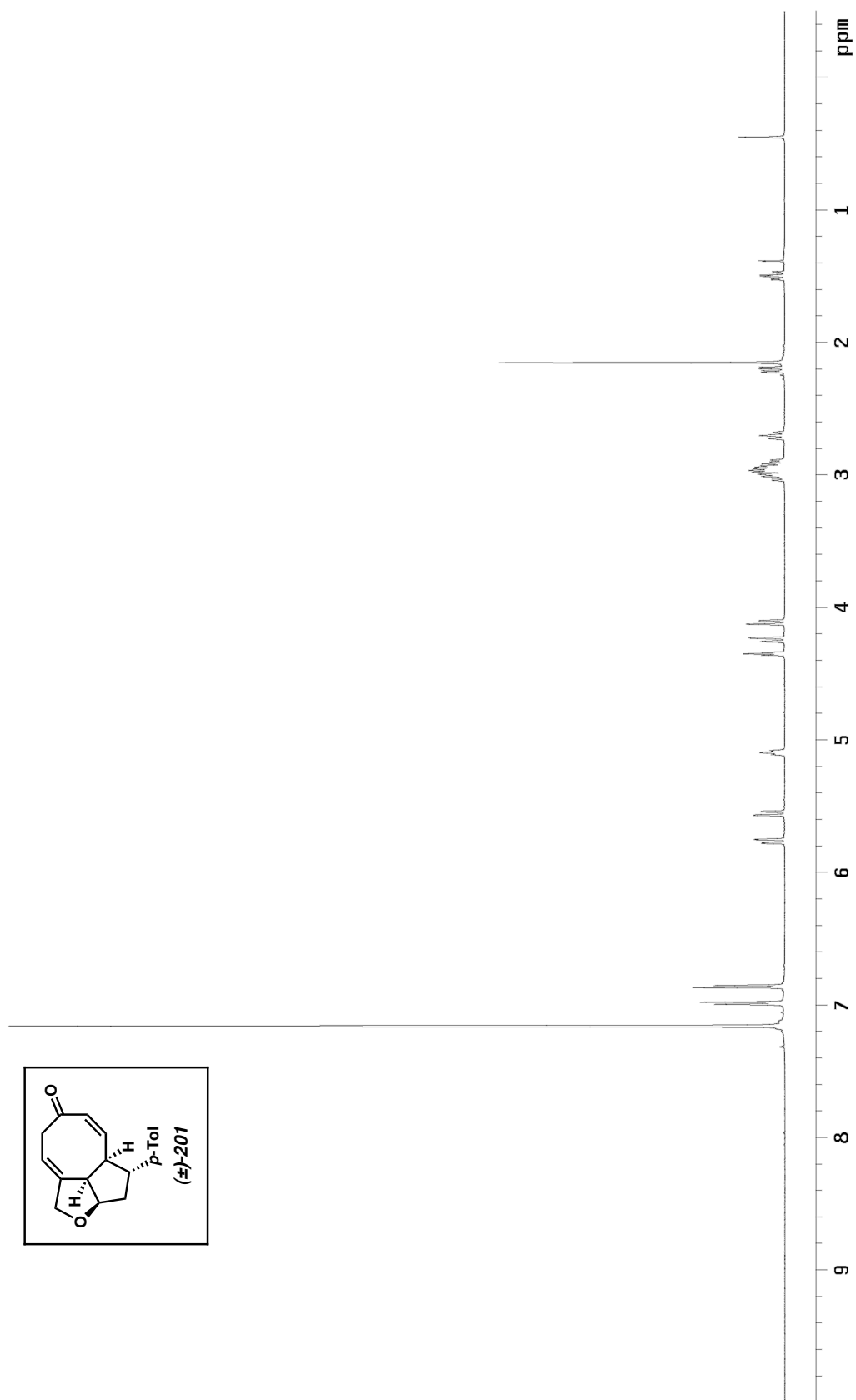
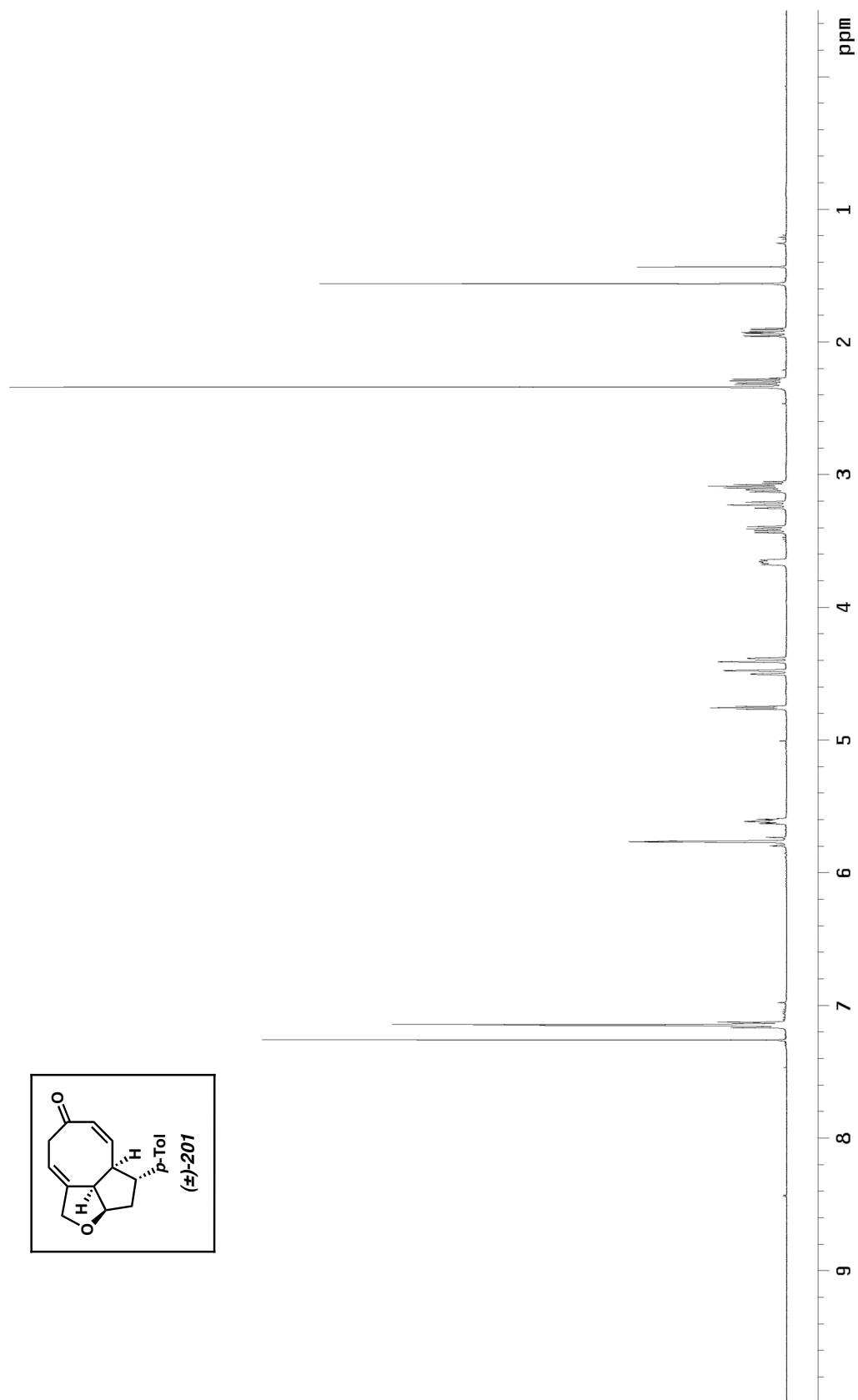


Figure A2.43. ^{13}C NMR spectrum (126 MHz, CDCl_3) of **200**.

Figure A2.44. ^1H NMR spectrum (500 MHz, $\text{C}_6\text{D}_6\text{O}$) of **201**.

Figure A2.45. ^1H NMR spectrum (500 MHz, CDCl_3) of **201**.

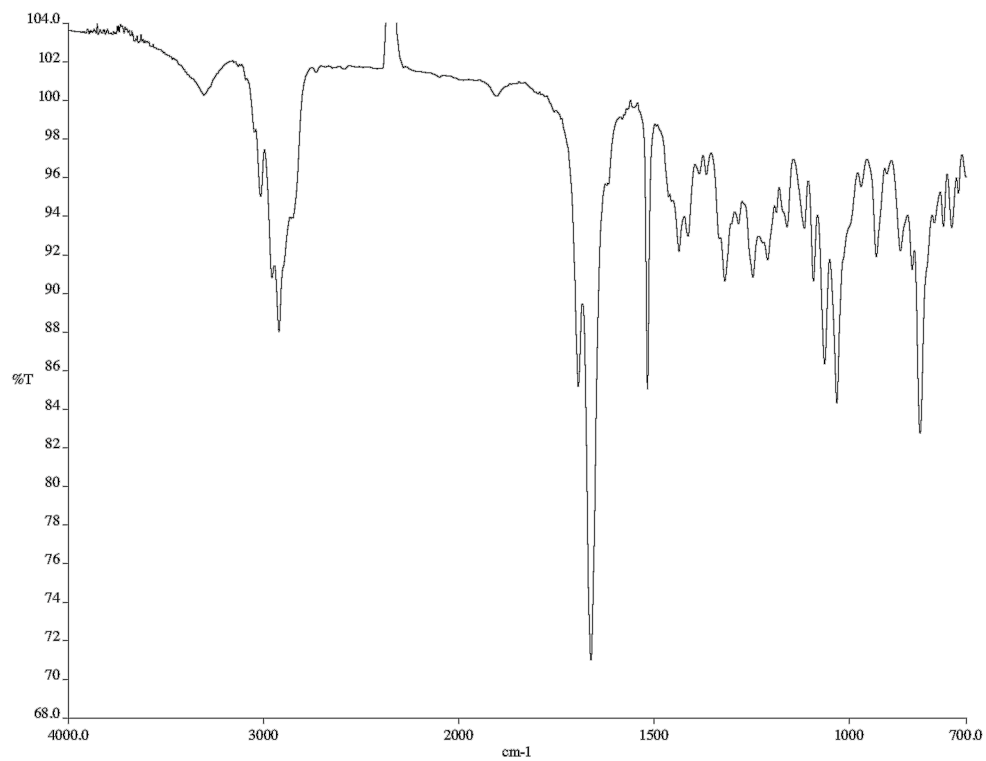


Figure A2.46. Infrared spectrum (neat film/NaCl) of **201**.

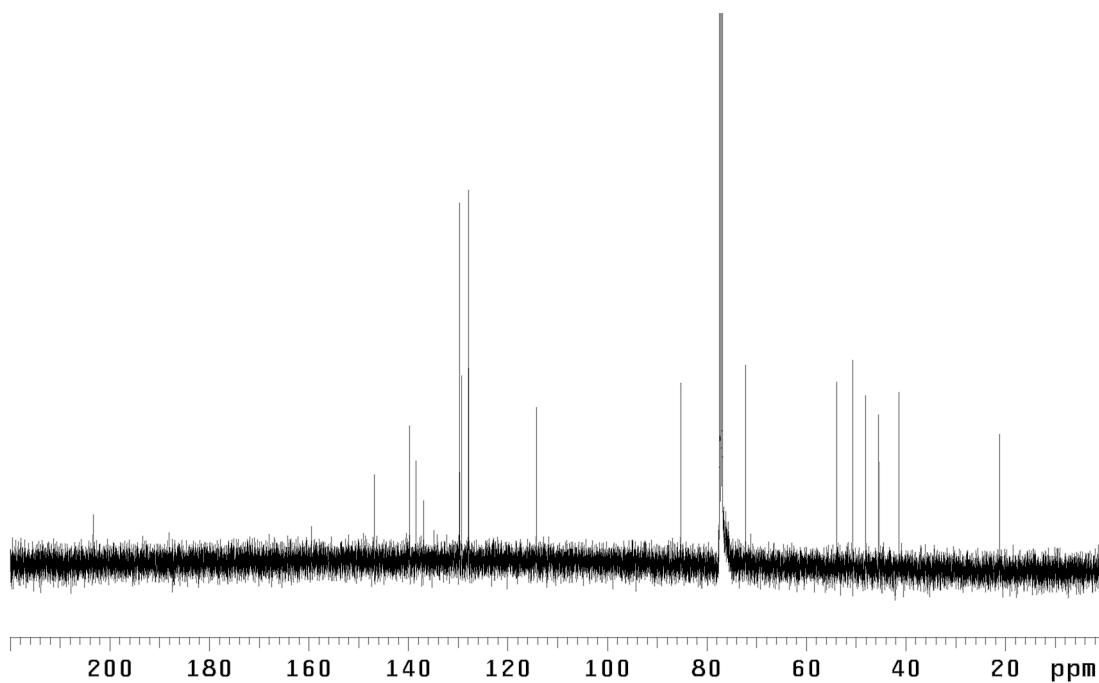
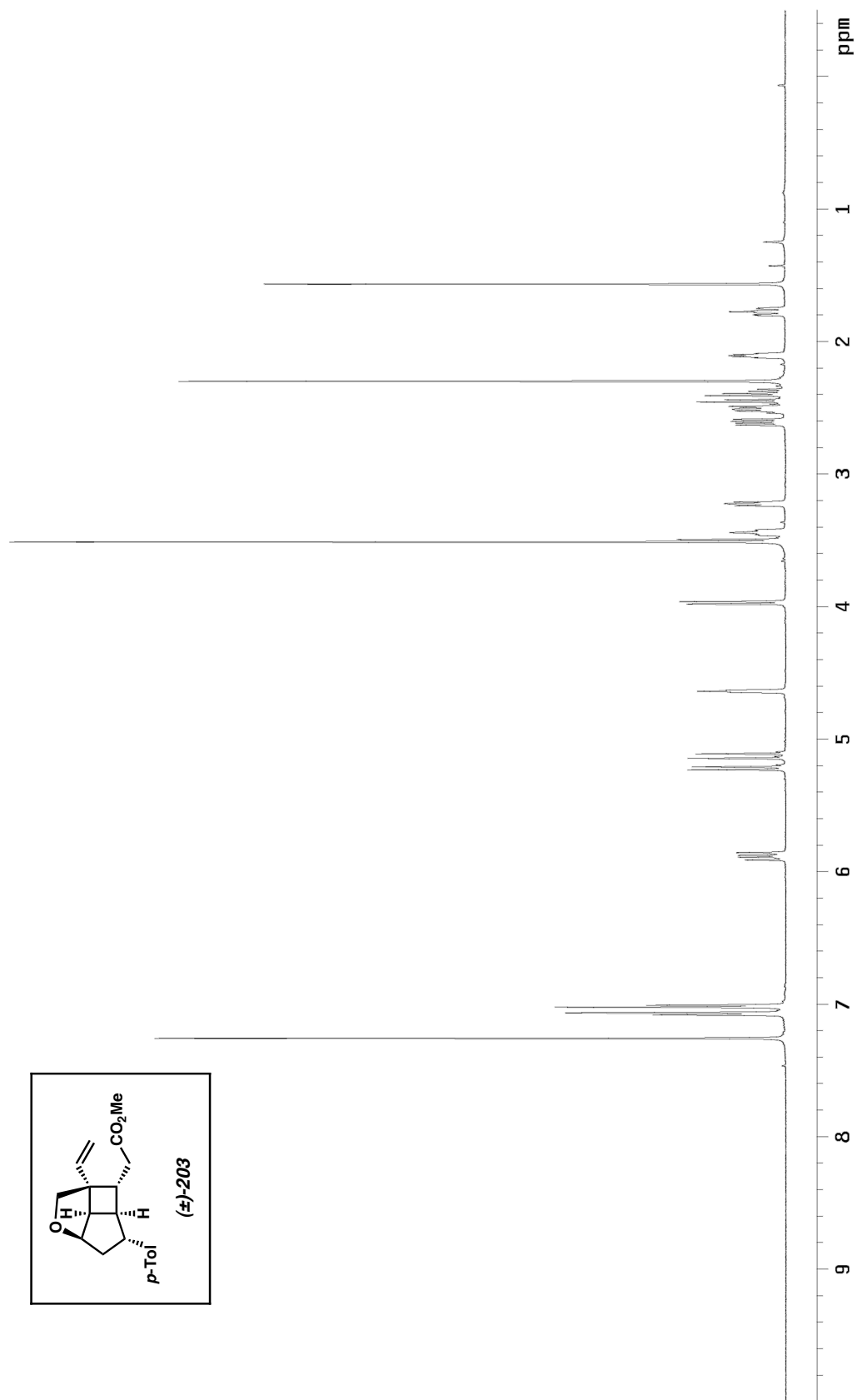


Figure A2.47. ¹³C NMR spectrum (126 MHz, CDCl₃) of **201**.

Figure A2.48. ^1H NMR spectrum (500 MHz, CDCl_3) of **203**.

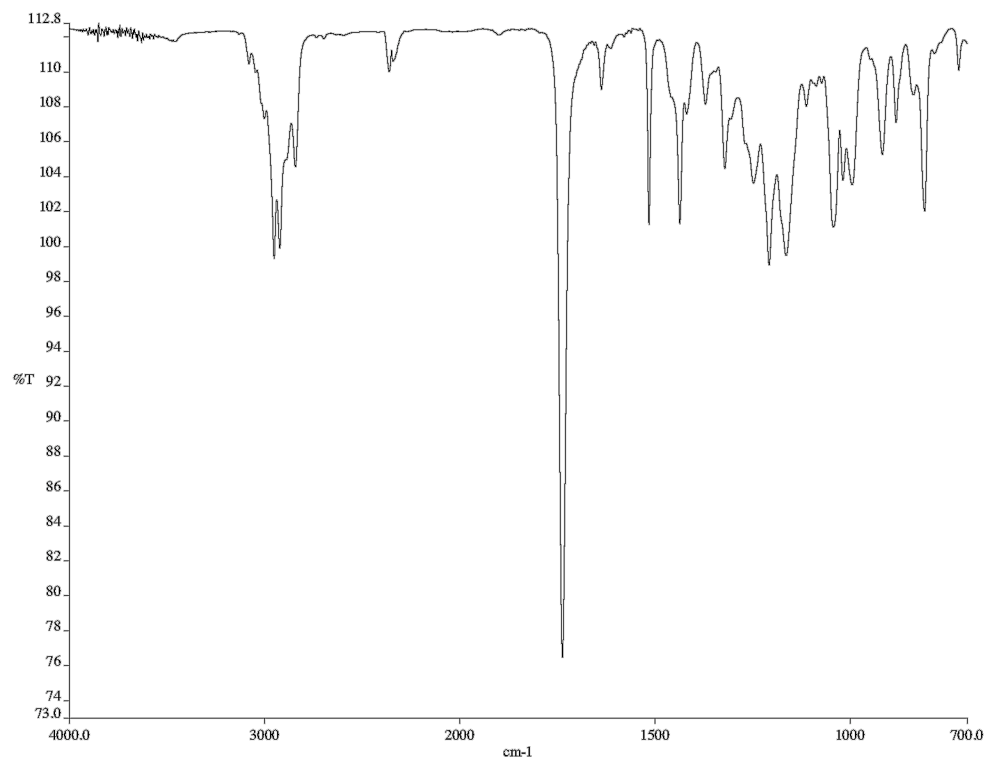


Figure A2.49. Infrared spectrum (neat film/NaCl) of **203**.

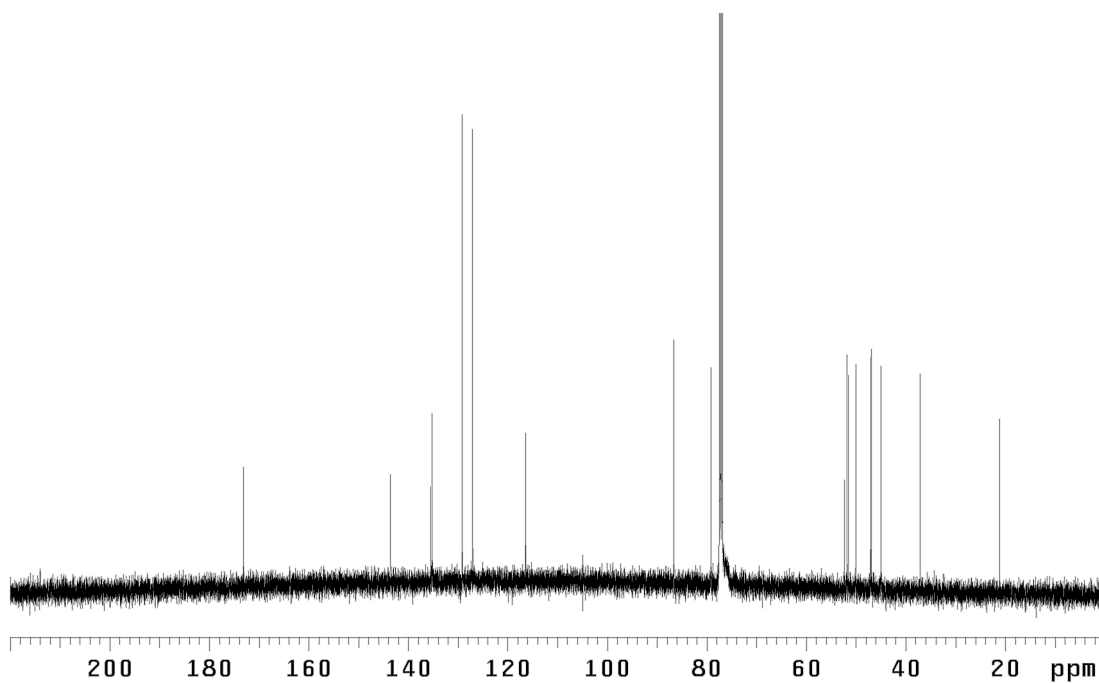
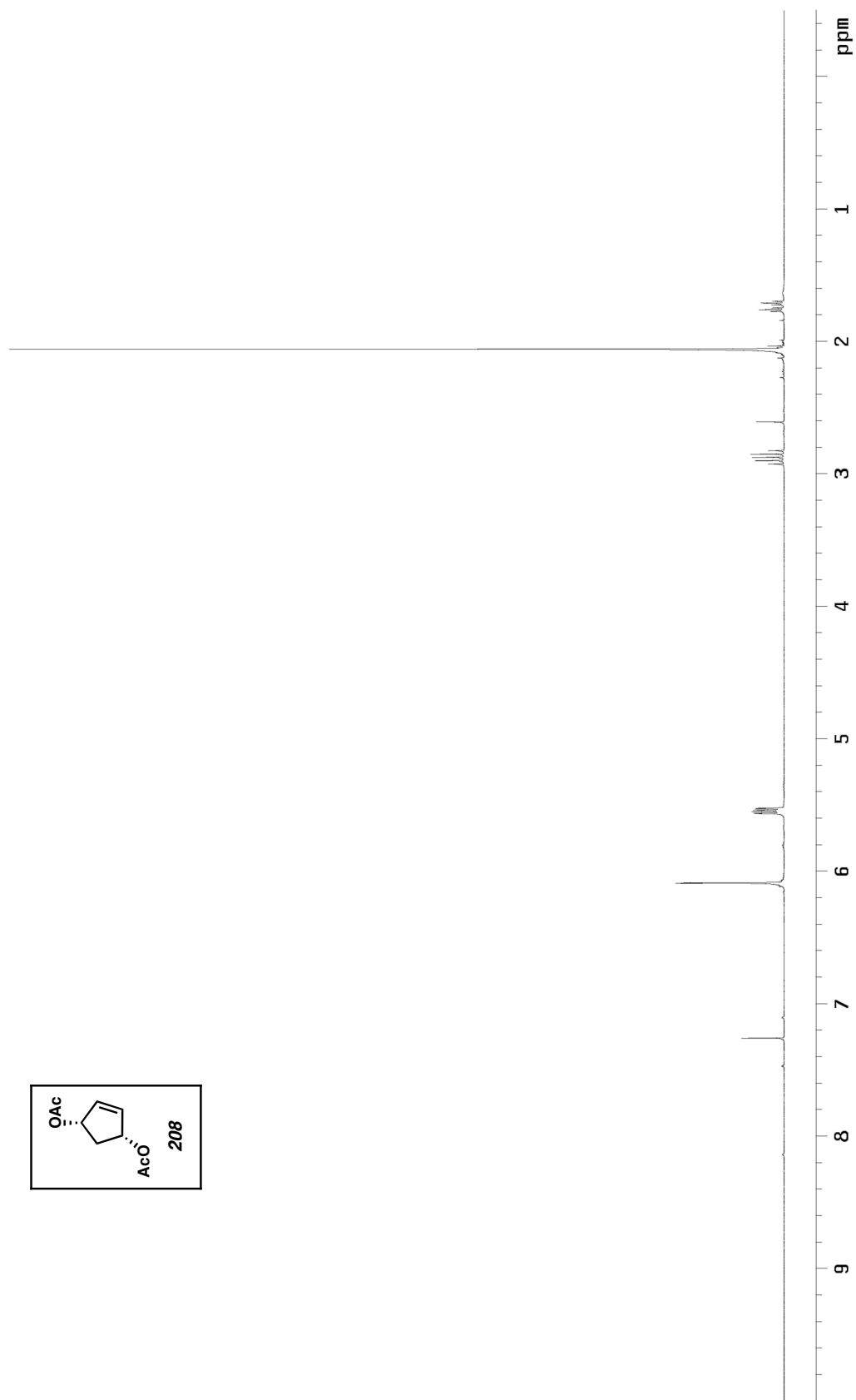
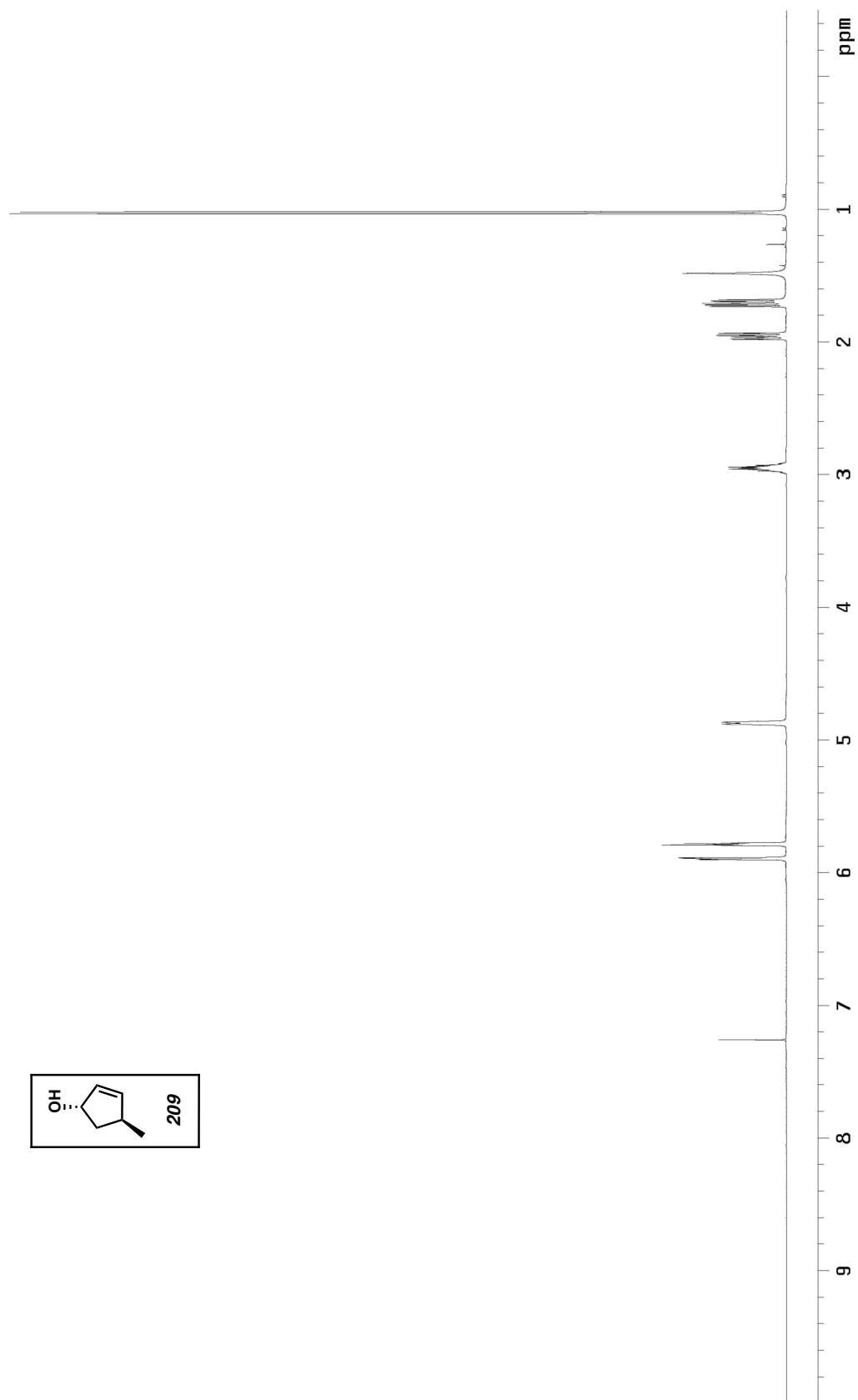


Figure A2.50. ¹³C NMR spectrum (126 MHz, CDCl₃) of **203**.

Figure A2.51. ^1H NMR spectrum (300 MHz, CDCl_3) of **208**.

Figure A2.52. ^1H NMR spectrum (500 MHz, CDCl_3) of **209**.

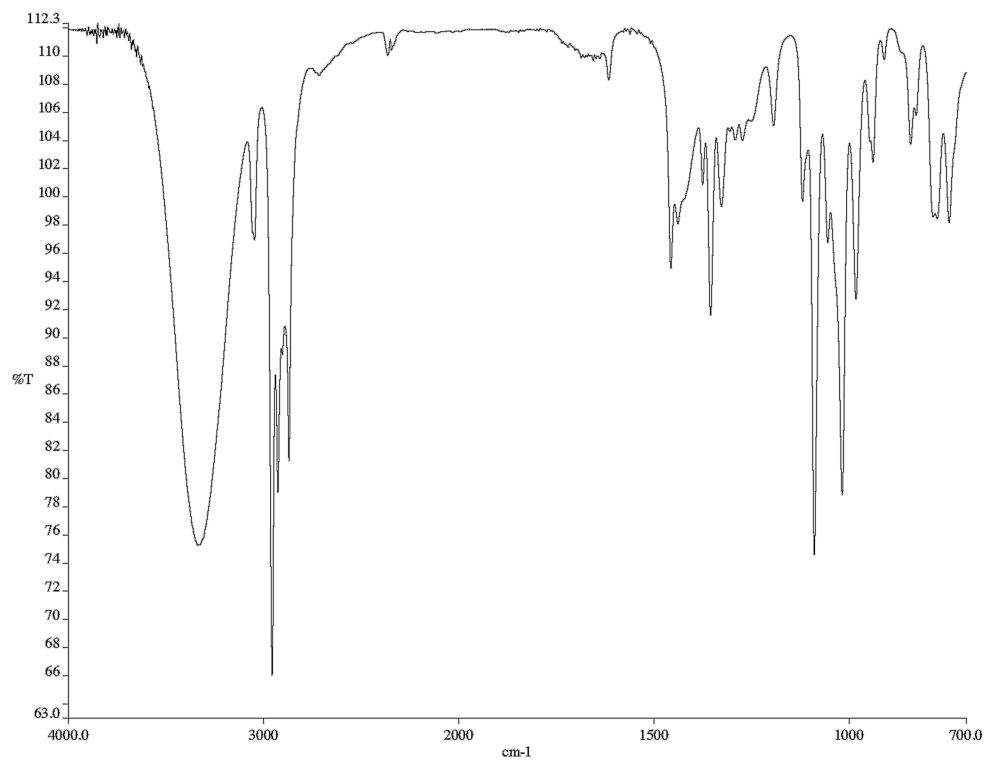


Figure A2.53. Infrared spectrum (neat film/NaCl) of **209**.

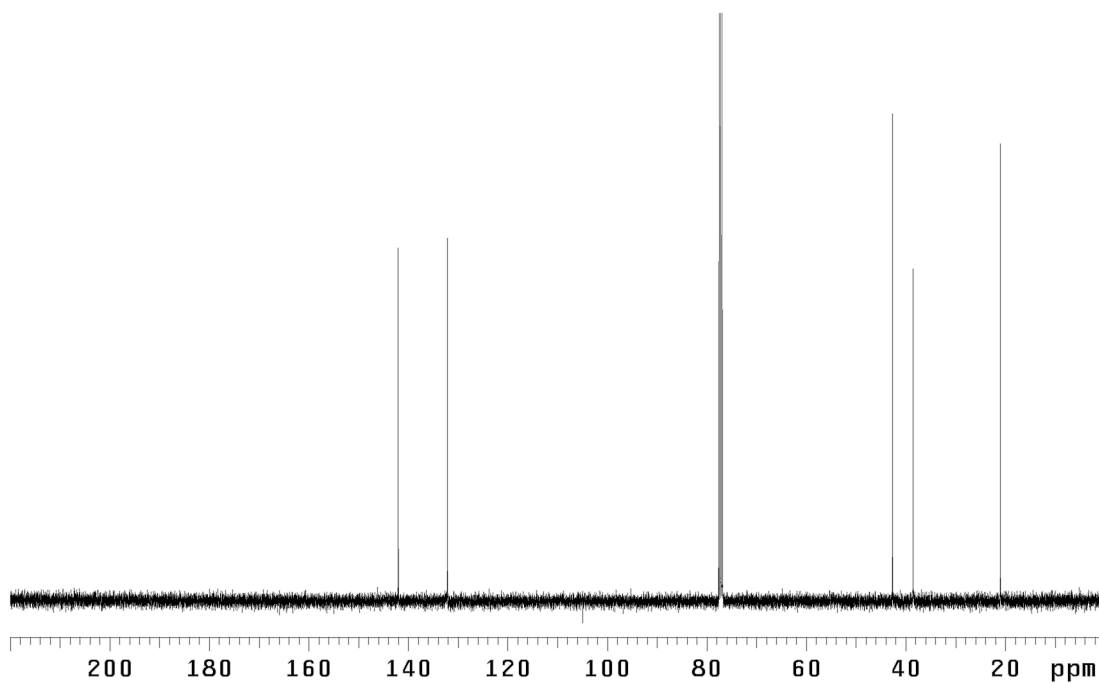
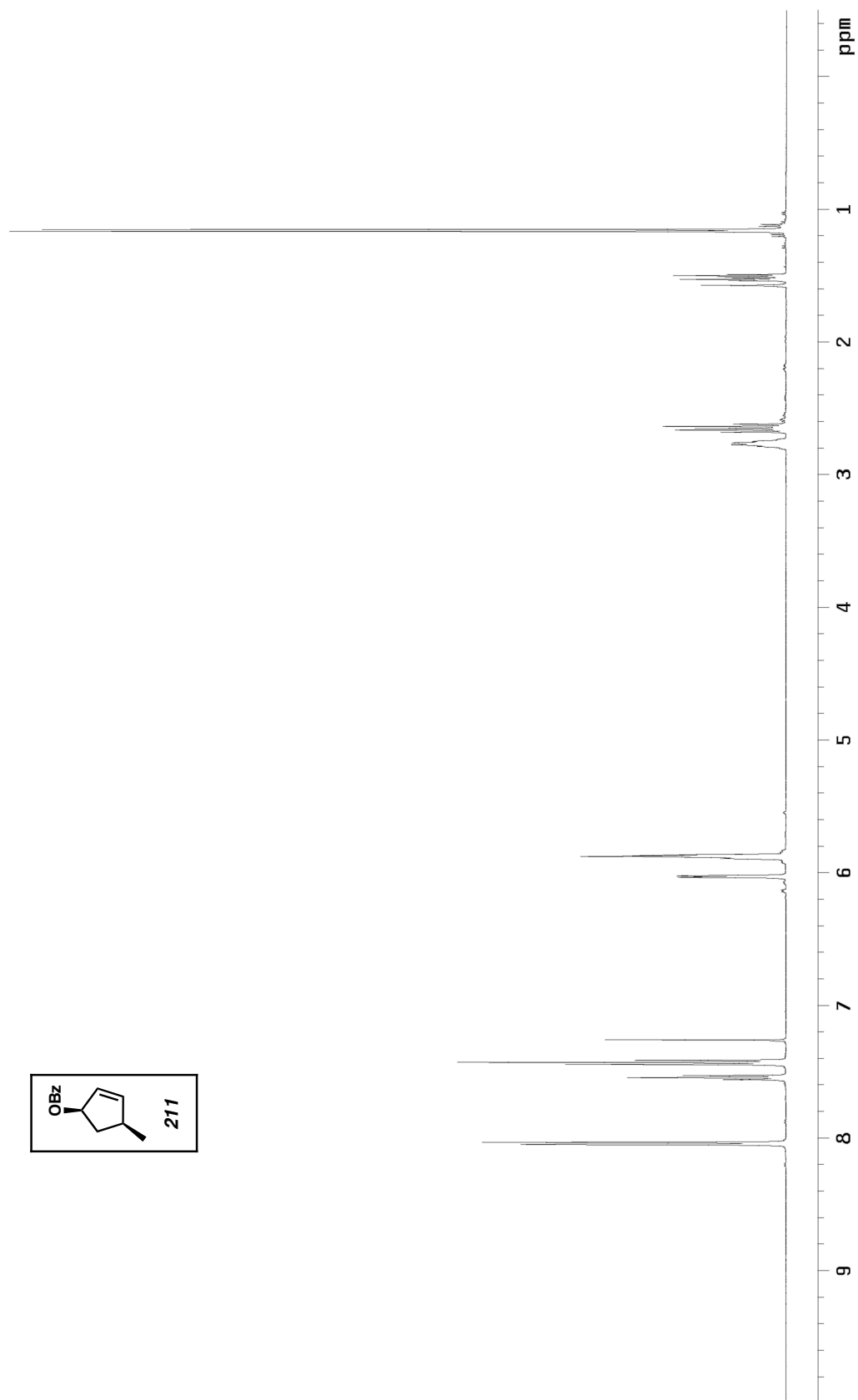


Figure A2.54. ¹³C NMR spectrum (126 MHz, CDCl₃) of **209**.

Figure A2.55. ^1H NMR spectrum (500 MHz, CDCl_3) of **211**.

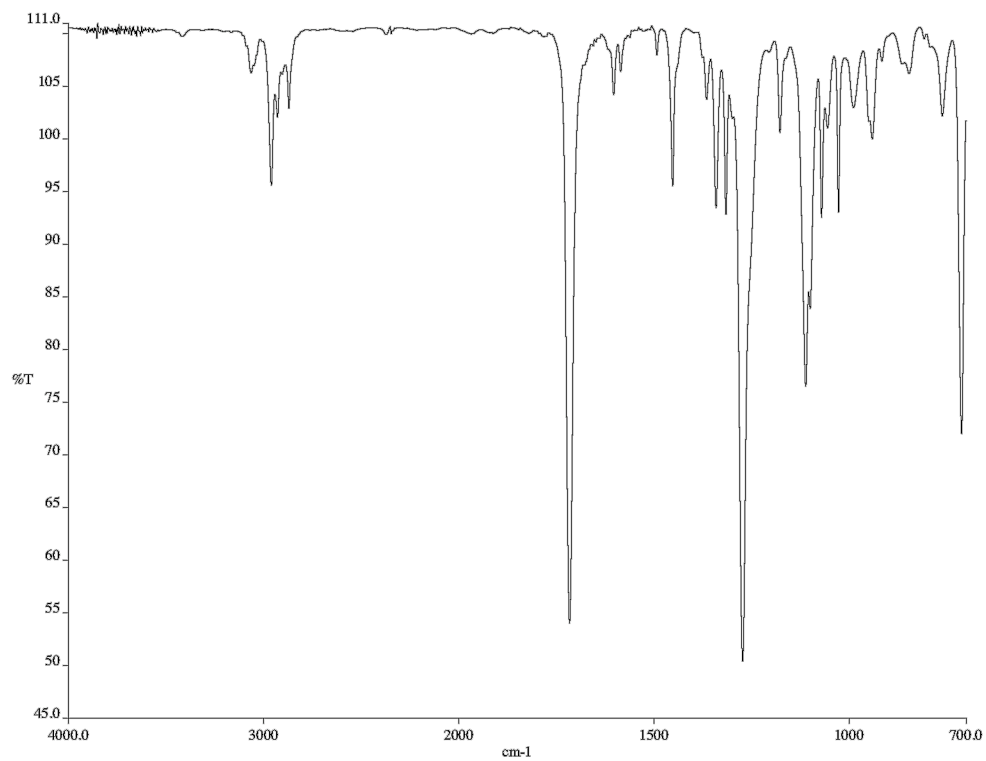


Figure A2.56. Infrared spectrum (neat film/NaCl) of **211**.

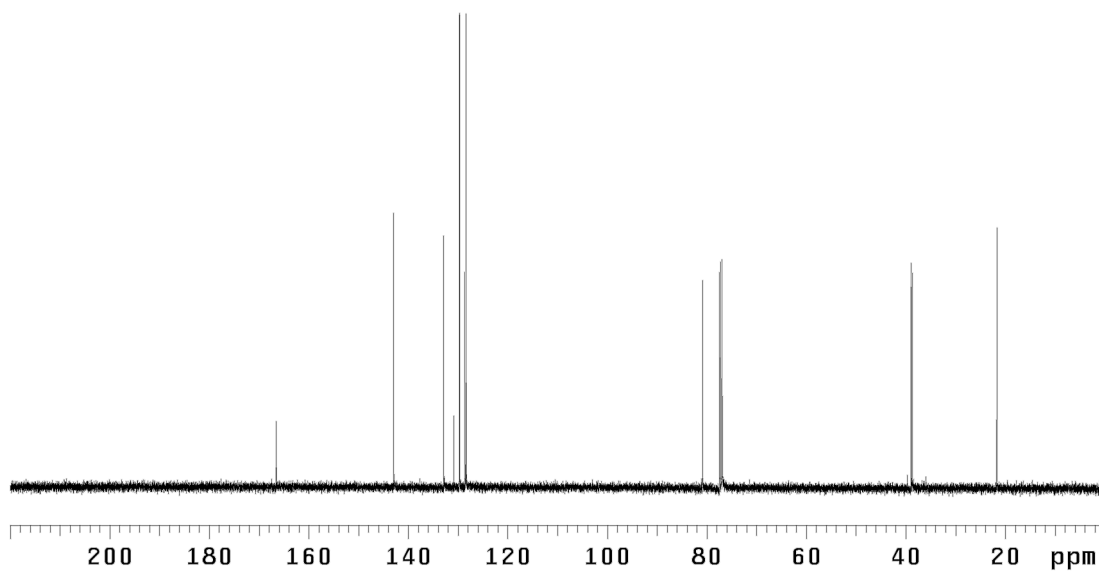
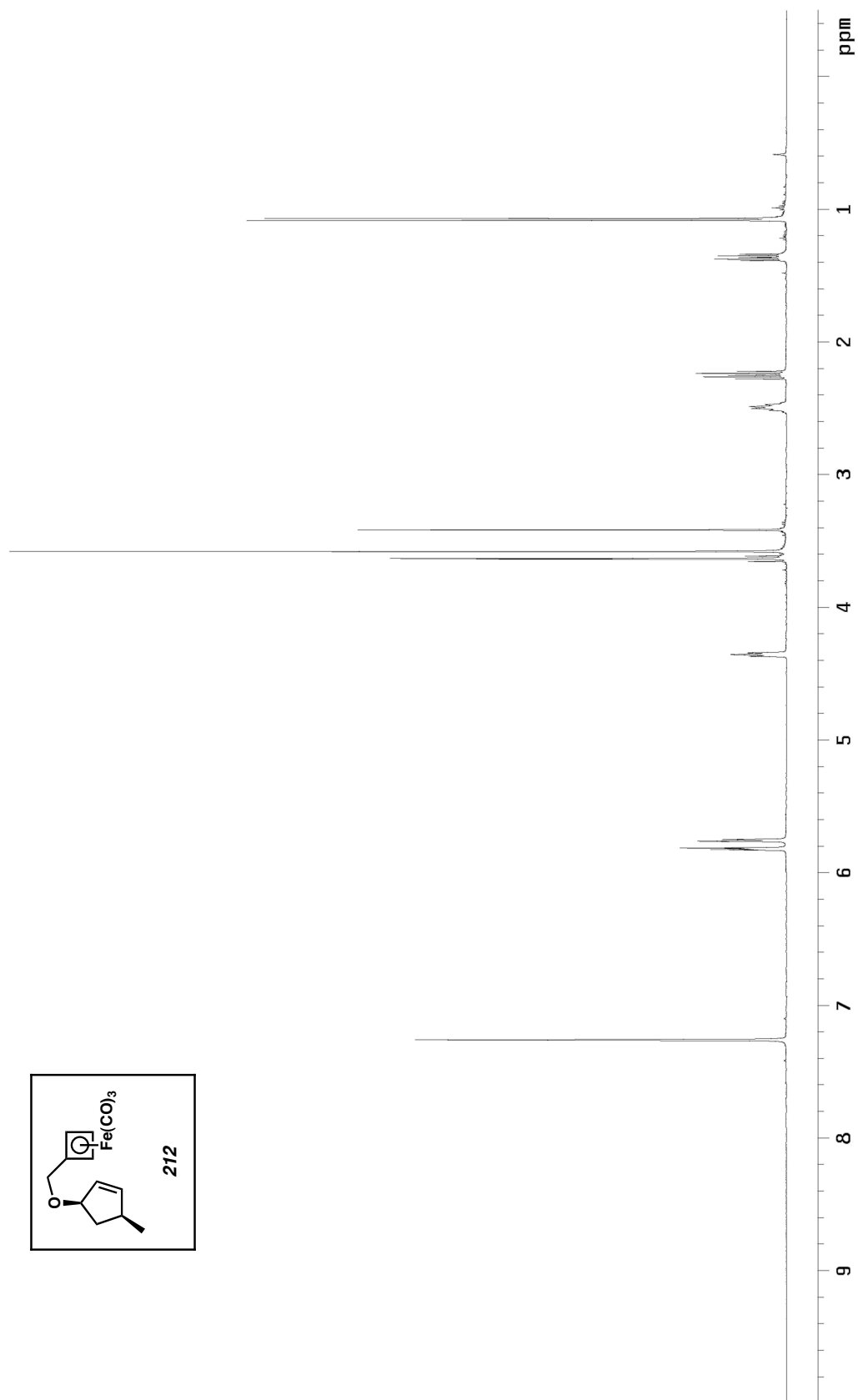


Figure A2.57. ¹³C NMR spectrum (126 MHz, CDCl₃) of **211**.

Figure A2.58. ^1H NMR spectrum (500 MHz, C_6D_6) of **212**.

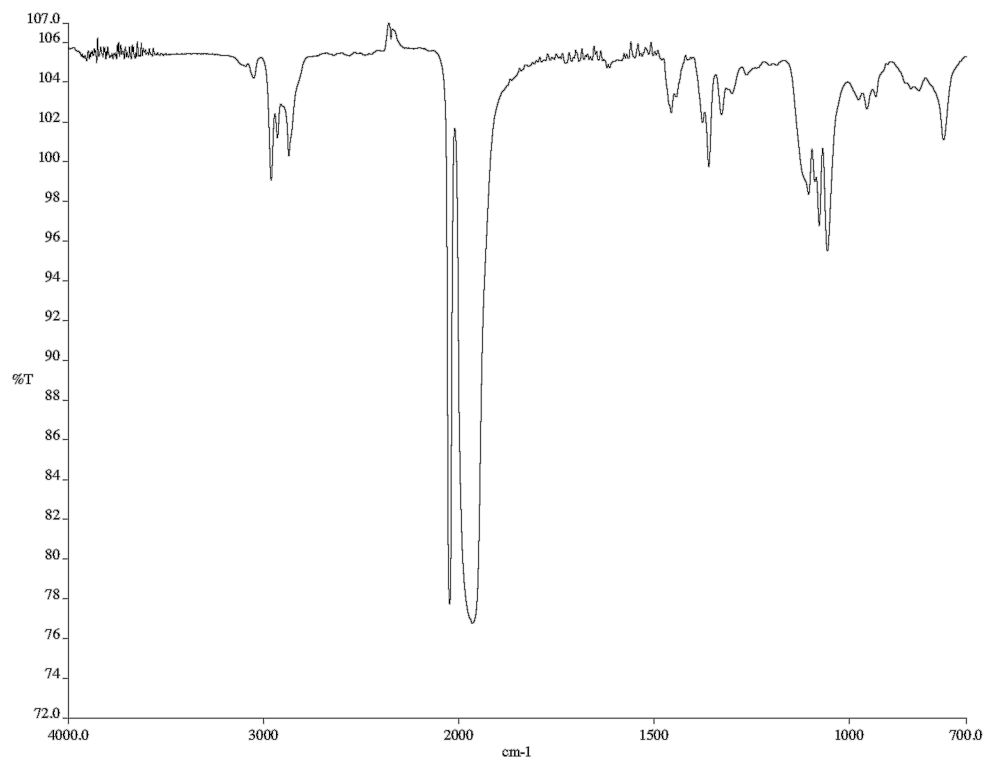


Figure A2.59. Infrared spectrum (neat film/NaCl) of **212**.

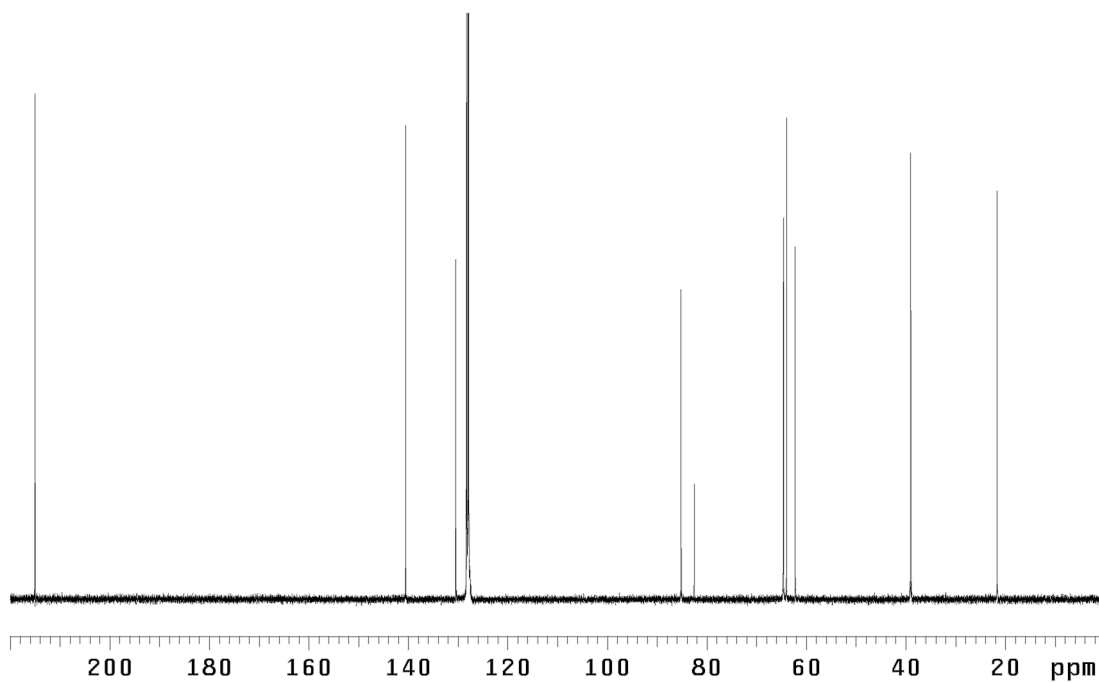
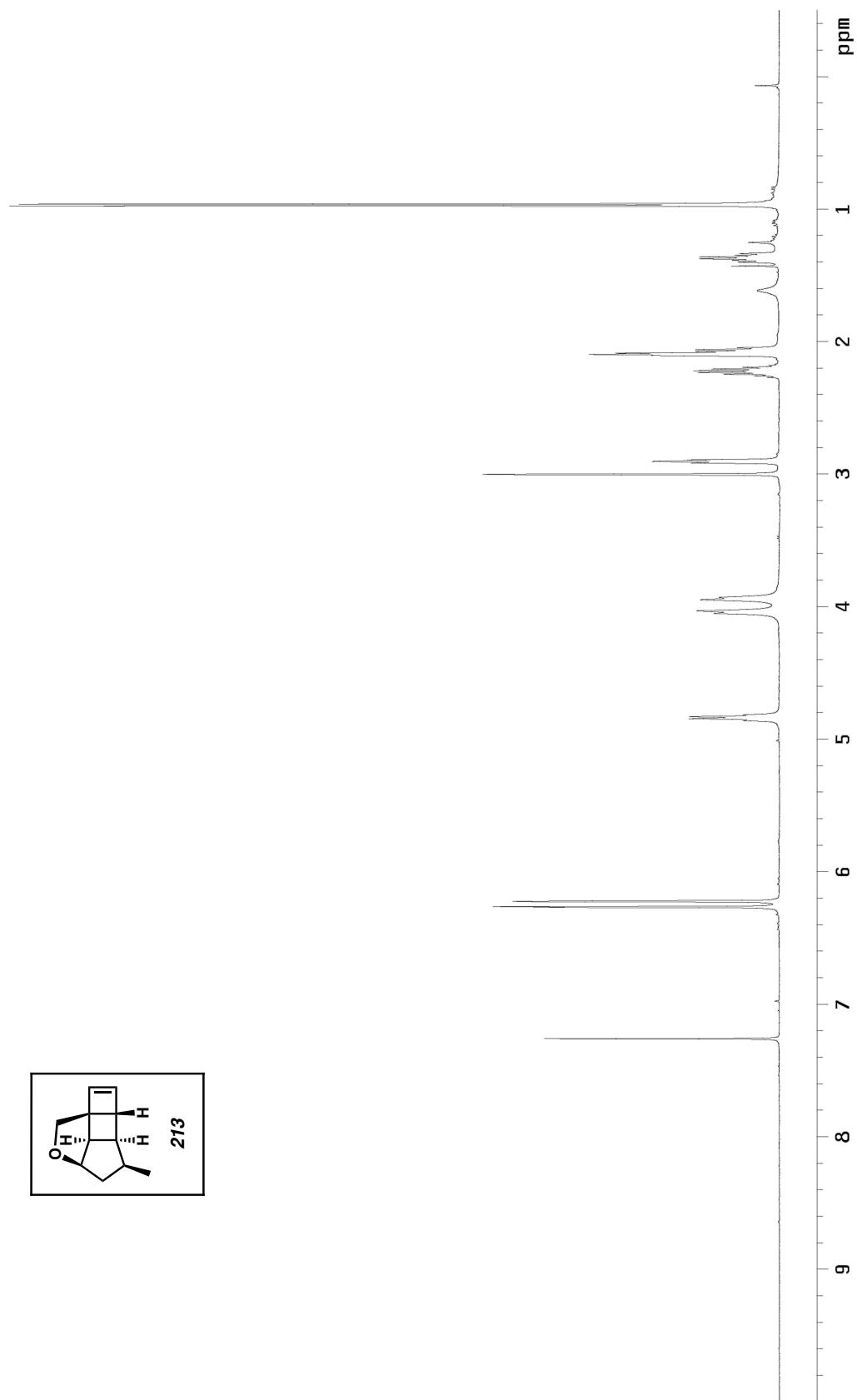


Figure A2.60. ¹³C NMR spectrum (126 MHz, CDCl₃) of **212**.

Figure A2.61. ^1H NMR spectrum (500 MHz, CDCl_3) of **213**.

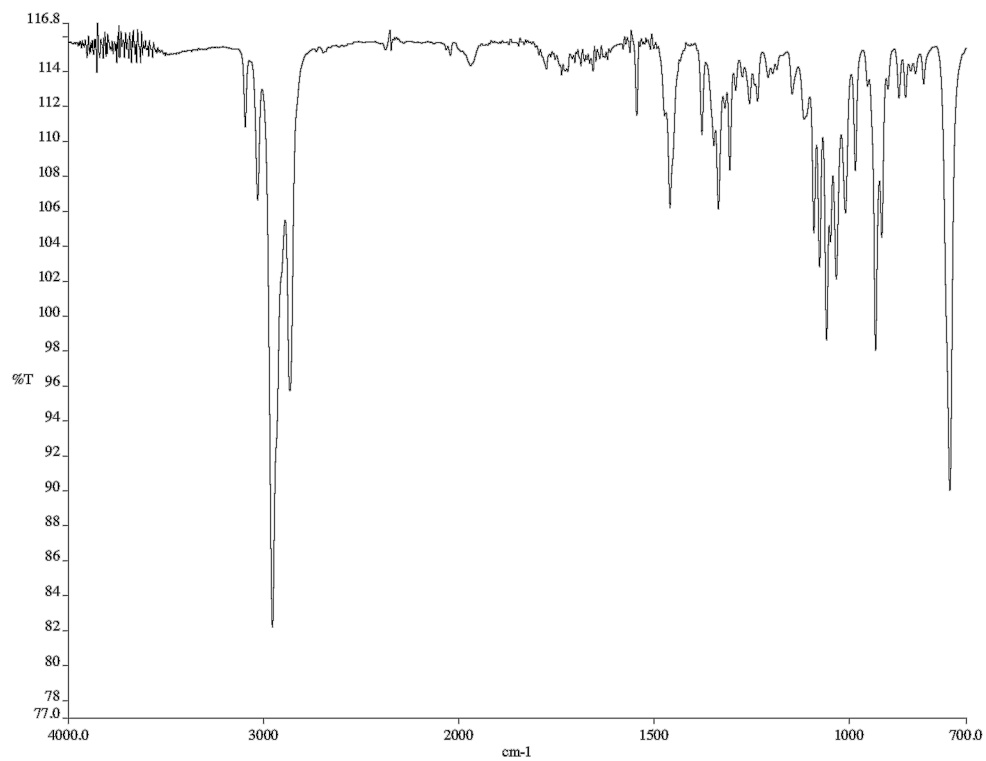


Figure A2.62. Infrared spectrum (neat film/NaCl) of **213**.

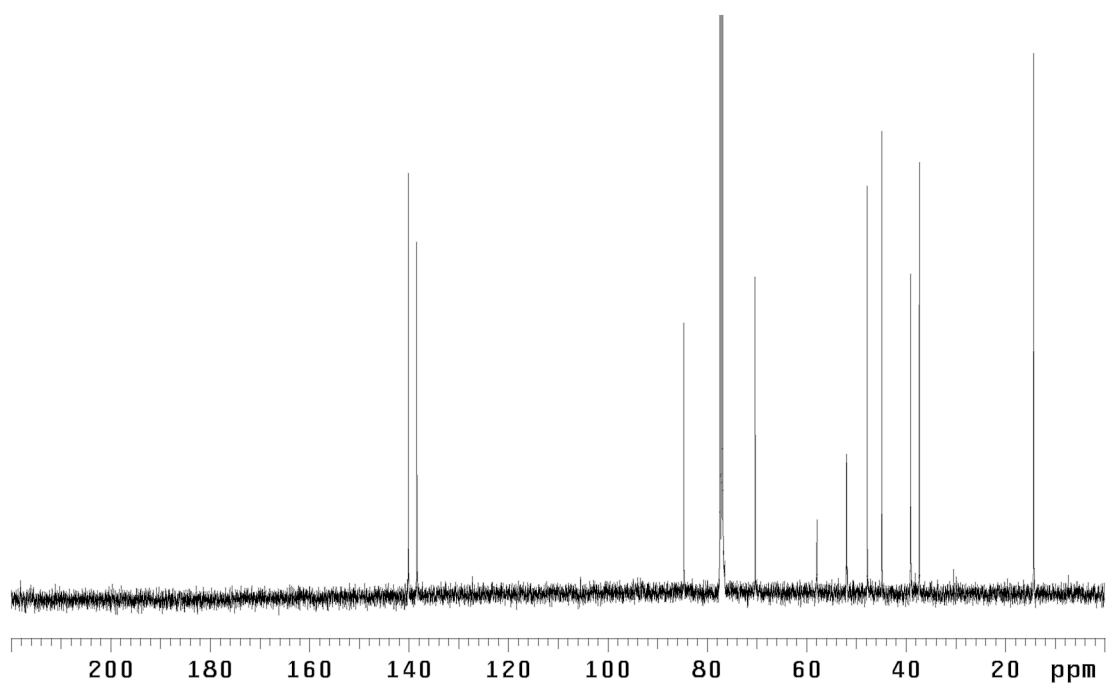
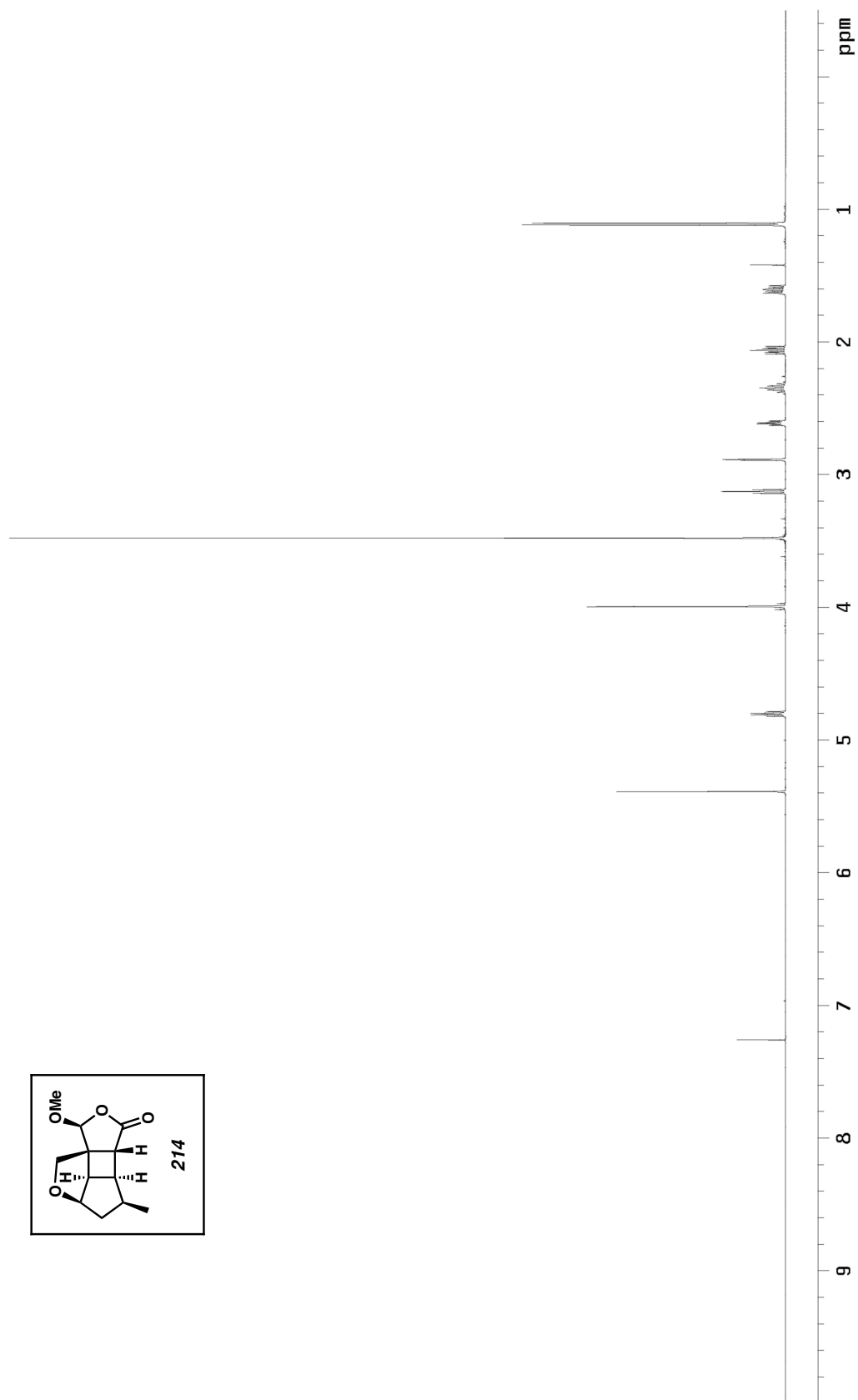


Figure A2.63. ¹³C NMR spectrum (126 MHz, CDCl₃) of **213**.

Figure A2.64. ^1H NMR spectrum (500 MHz, CDCl_3) of **214**.

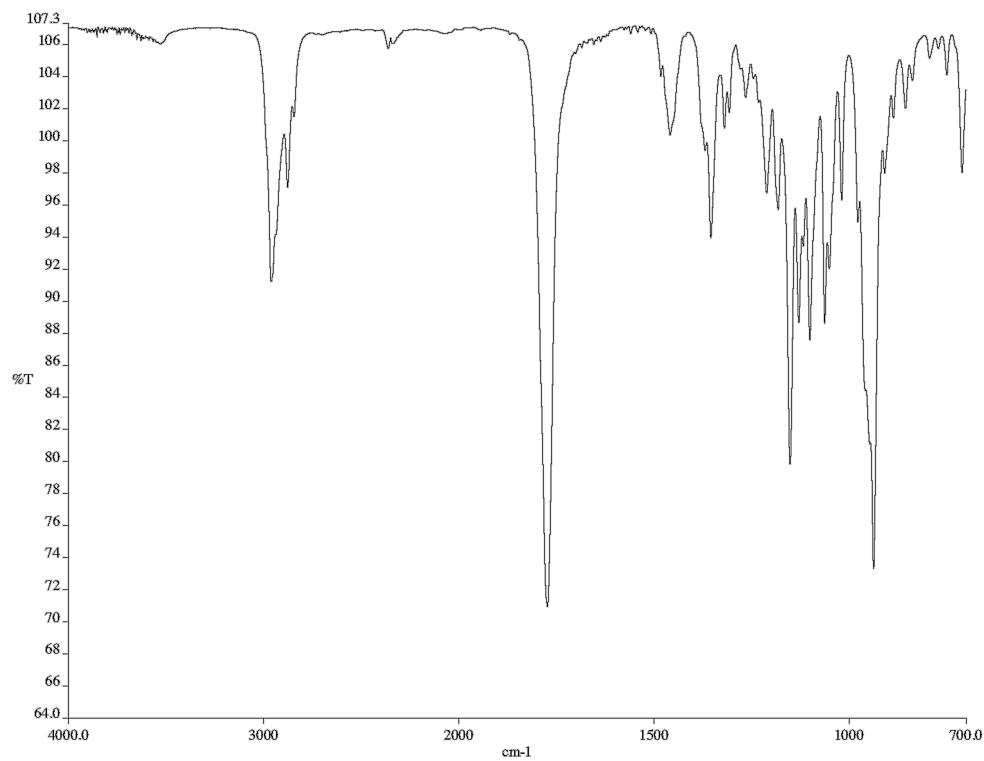


Figure A2.65. Infrared spectrum (neat film/NaCl) of **214**.

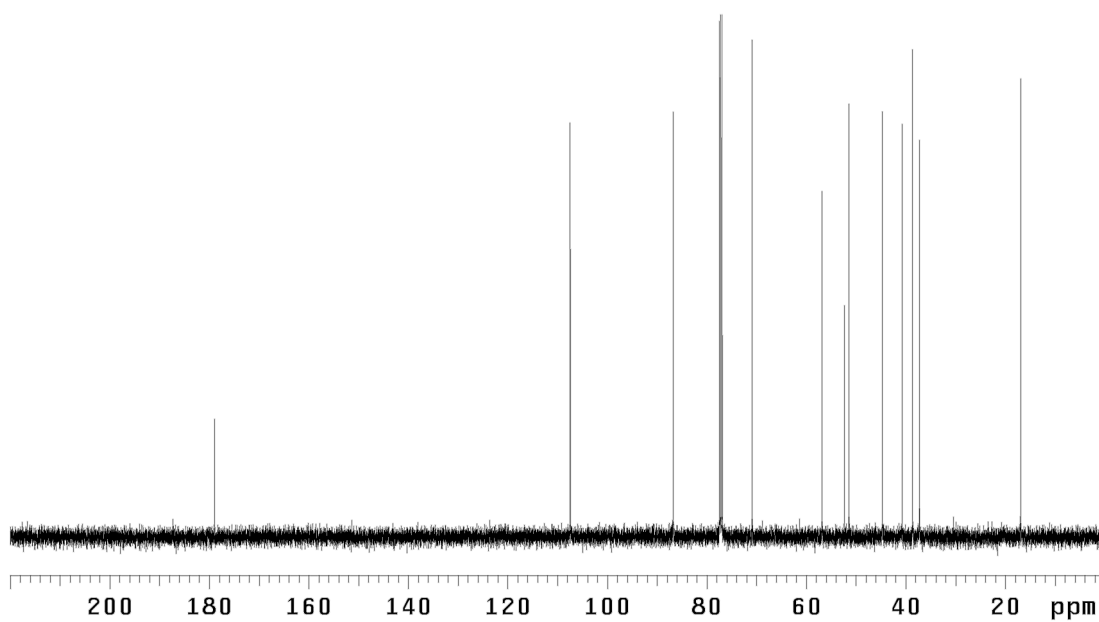
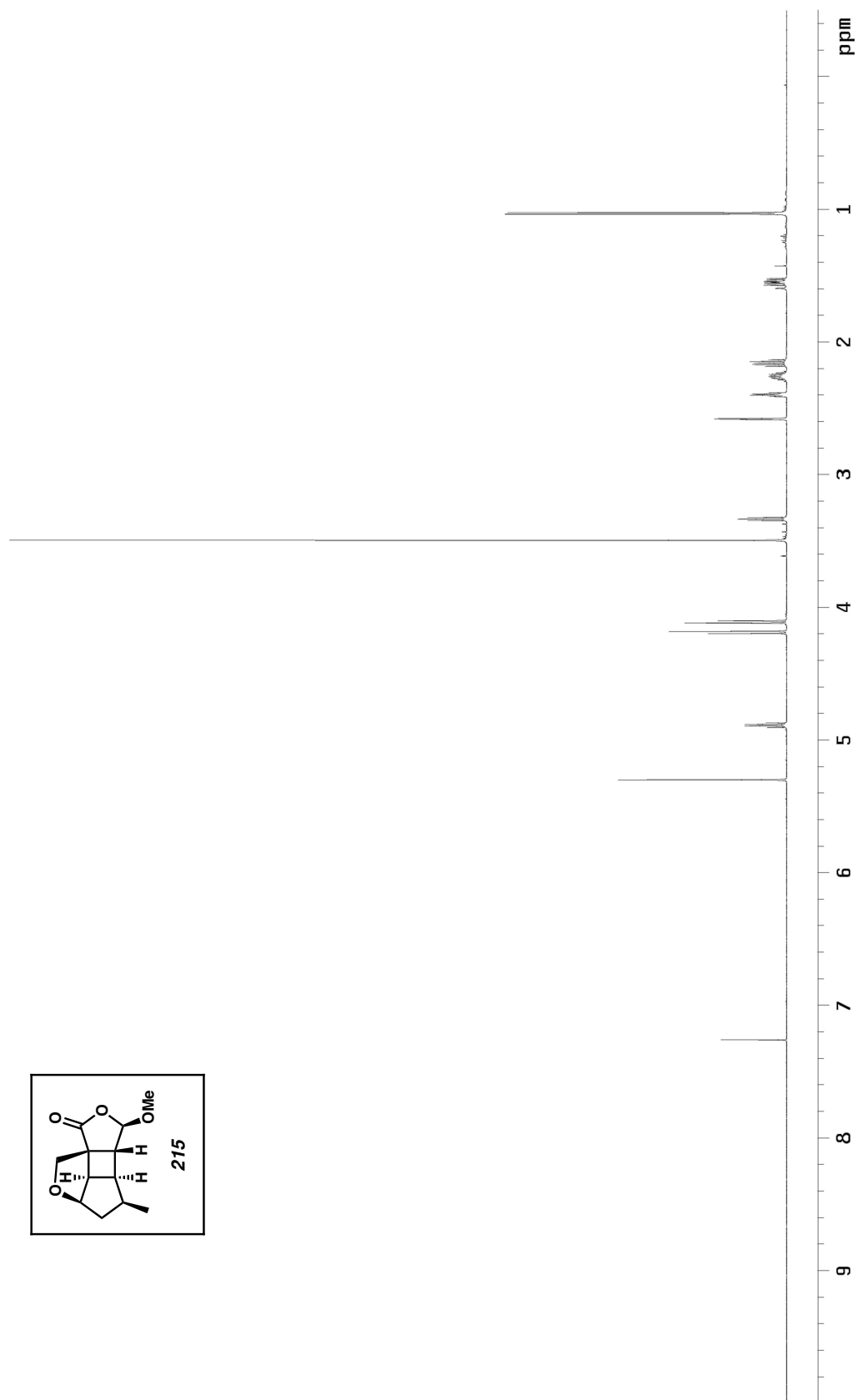


Figure A2.66. ¹³C NMR spectrum (126 MHz, CDCl₃) of **214**.

Figure A2.67. ^1H NMR spectrum (600 MHz, CDCl_3) of **215**.

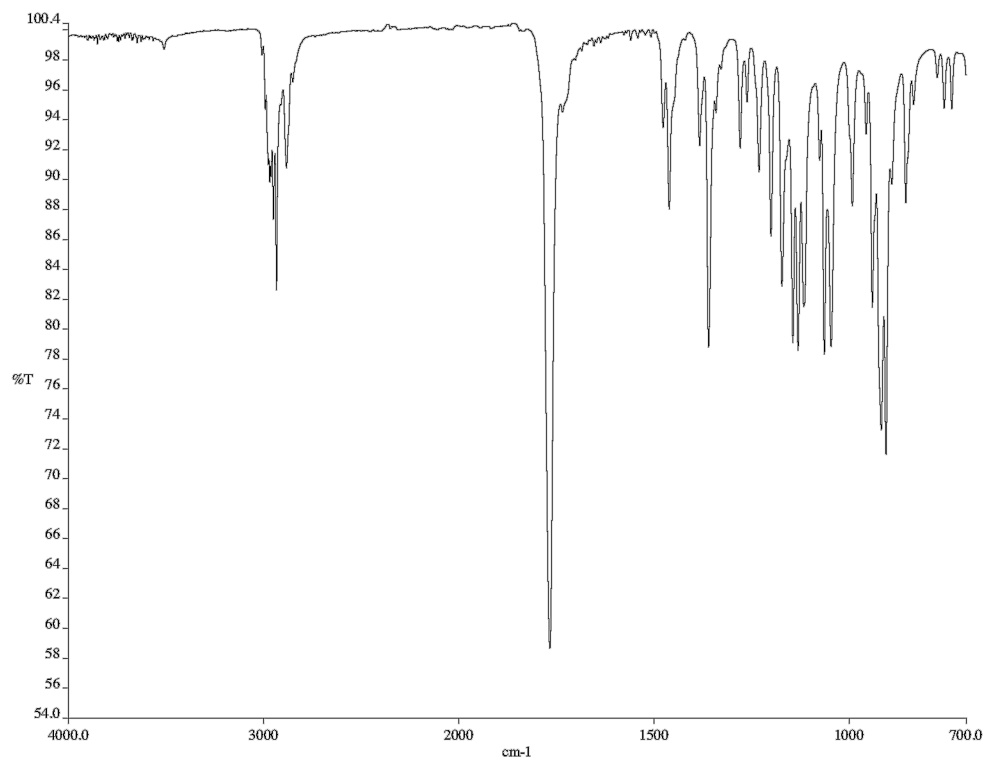


Figure A2.68. Infrared spectrum (neat film/NaCl) of **215**.

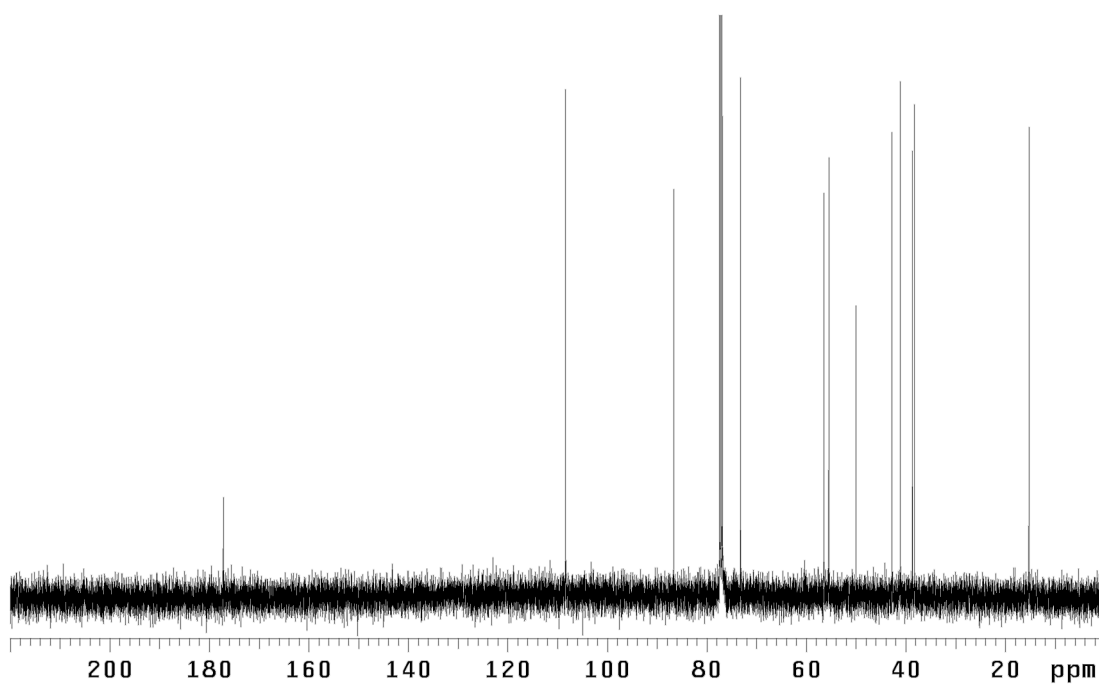
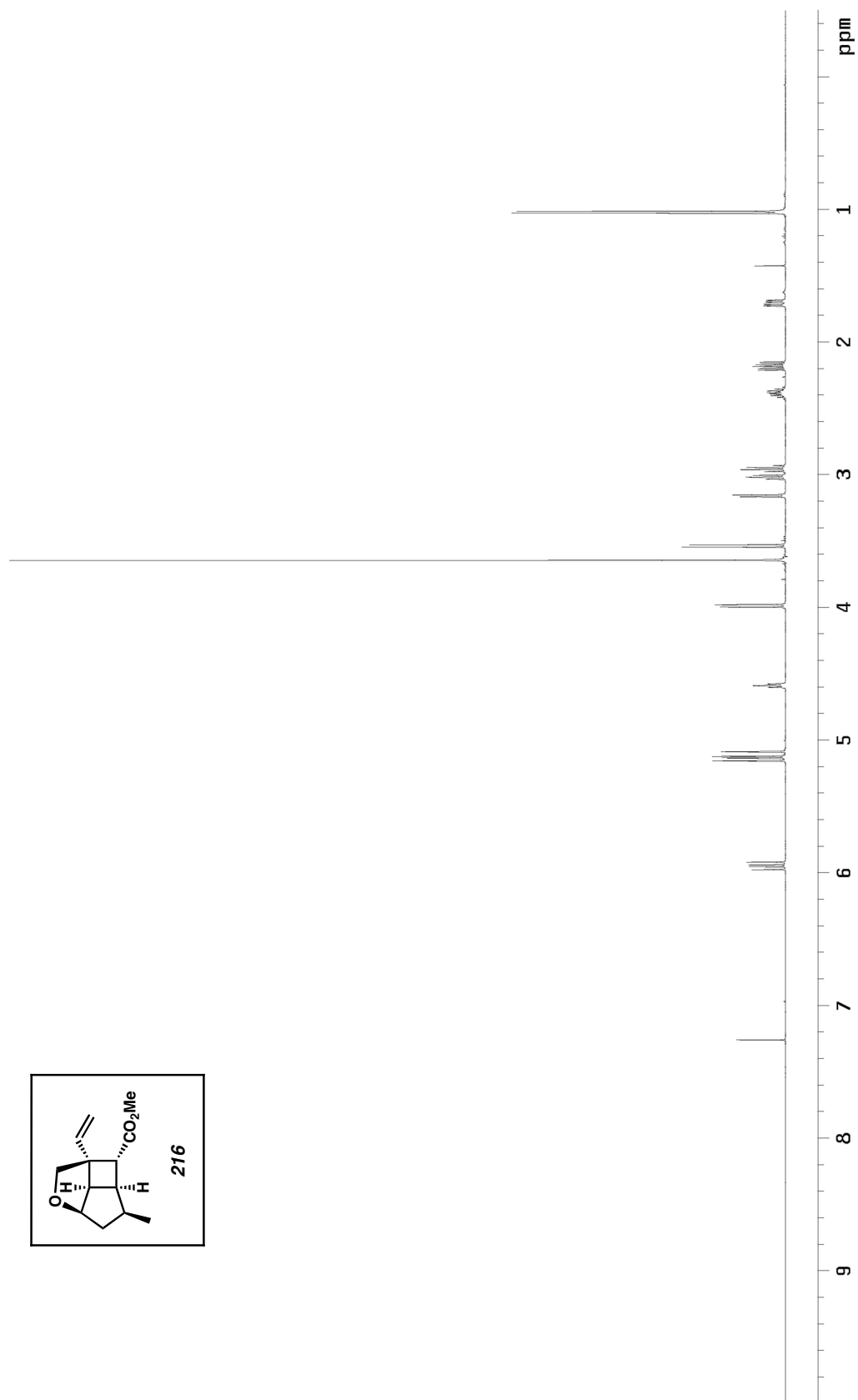


Figure A2.69. ¹³C NMR spectrum (126 MHz, CDCl₃) of **215**.

Figure A2.70. ^1H NMR spectrum (500 MHz, CDCl_3) of **216**.

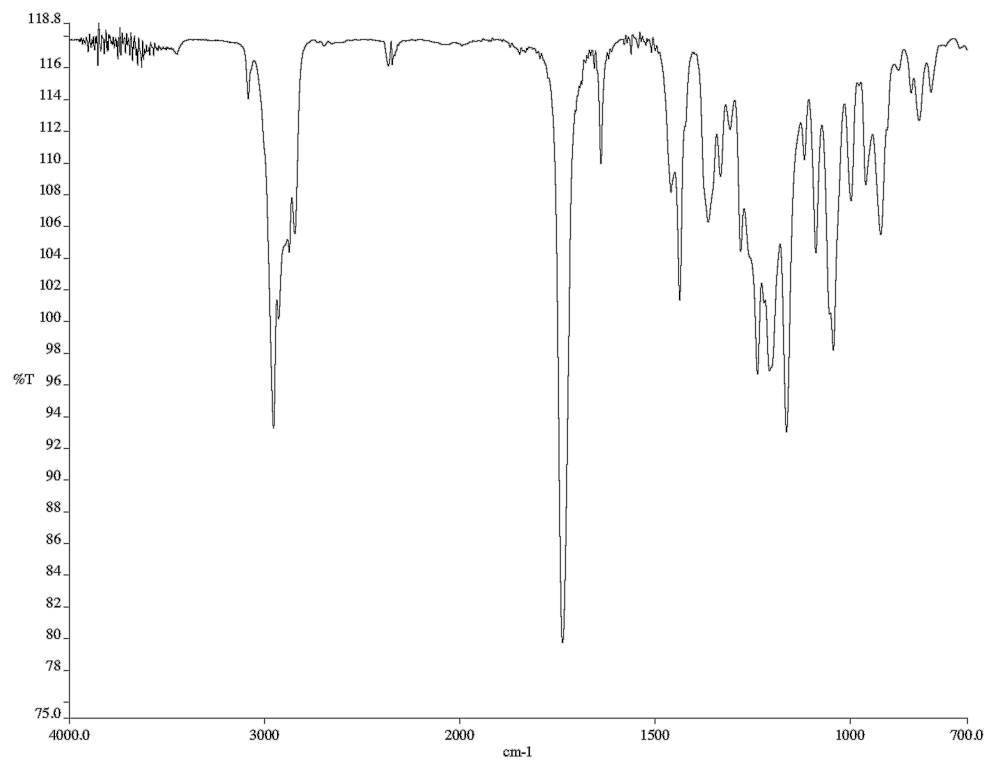


Figure A2.71. Infrared spectrum (neat film/NaCl) of **216**.

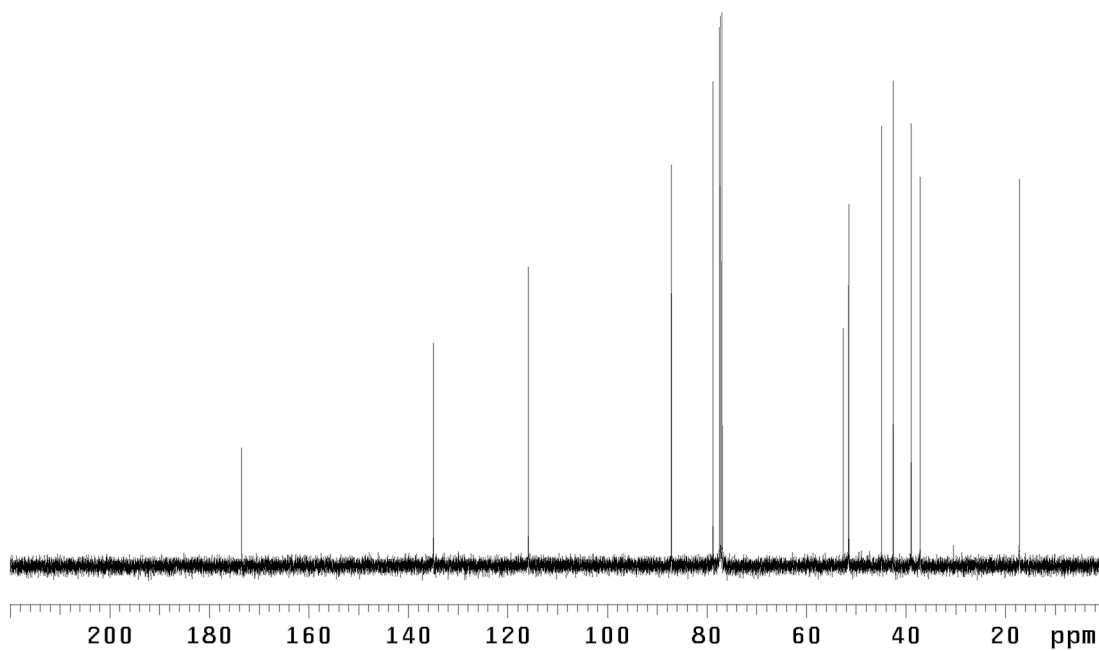
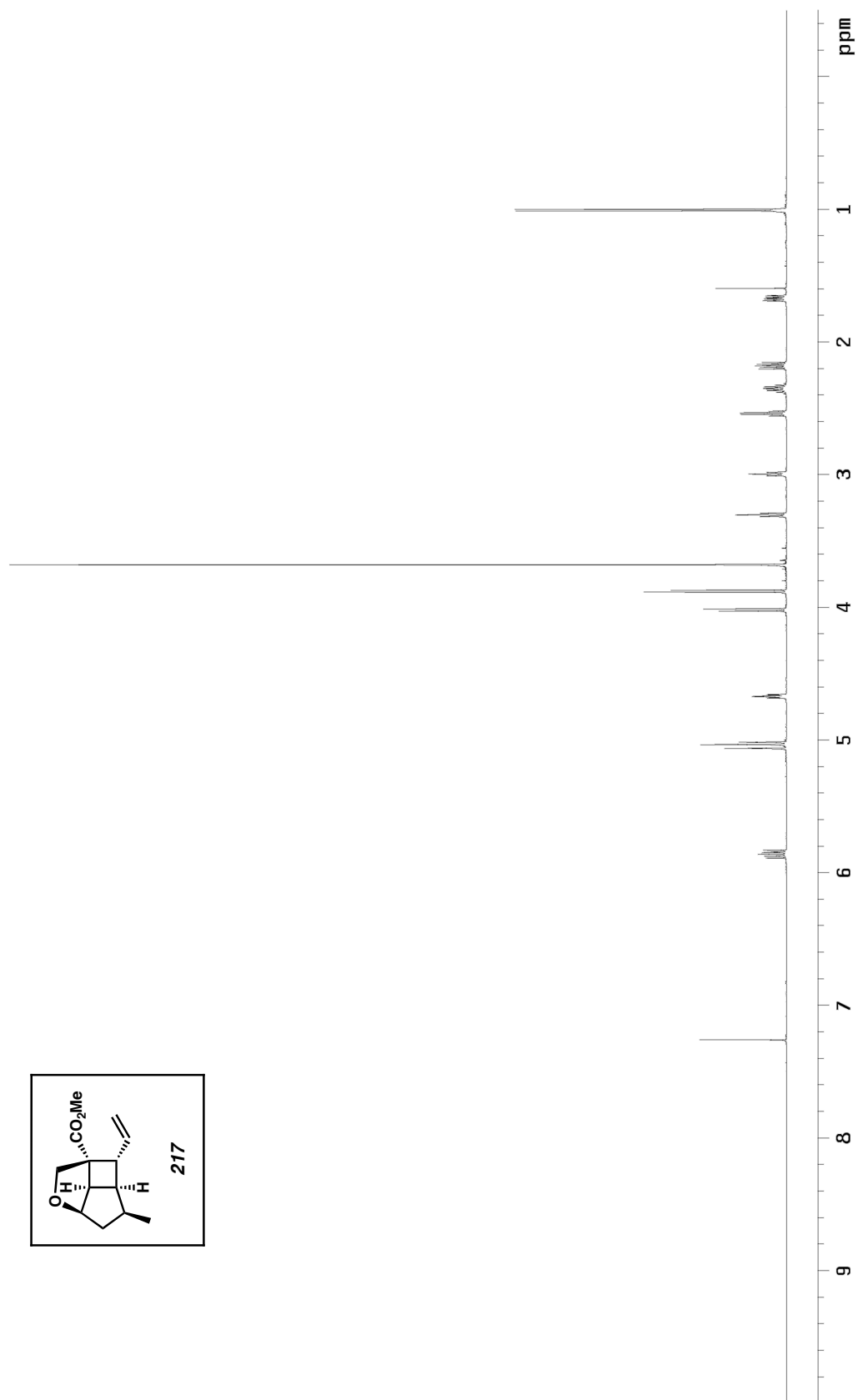


Figure A2.72. ¹³C NMR spectrum (126 MHz, CDCl₃) of **216**.

Figure A2.73. ^1H NMR spectrum (500 MHz, CDCl_3) of **217**.

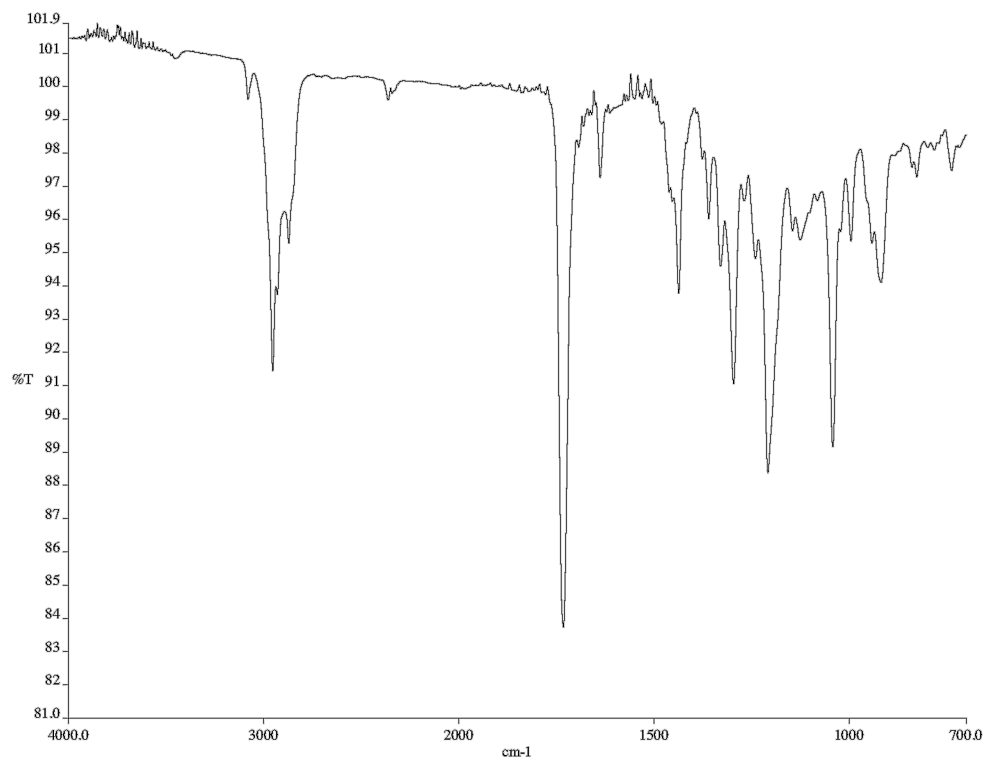


Figure A2.74. Infrared spectrum (neat film/NaCl) of **217**.

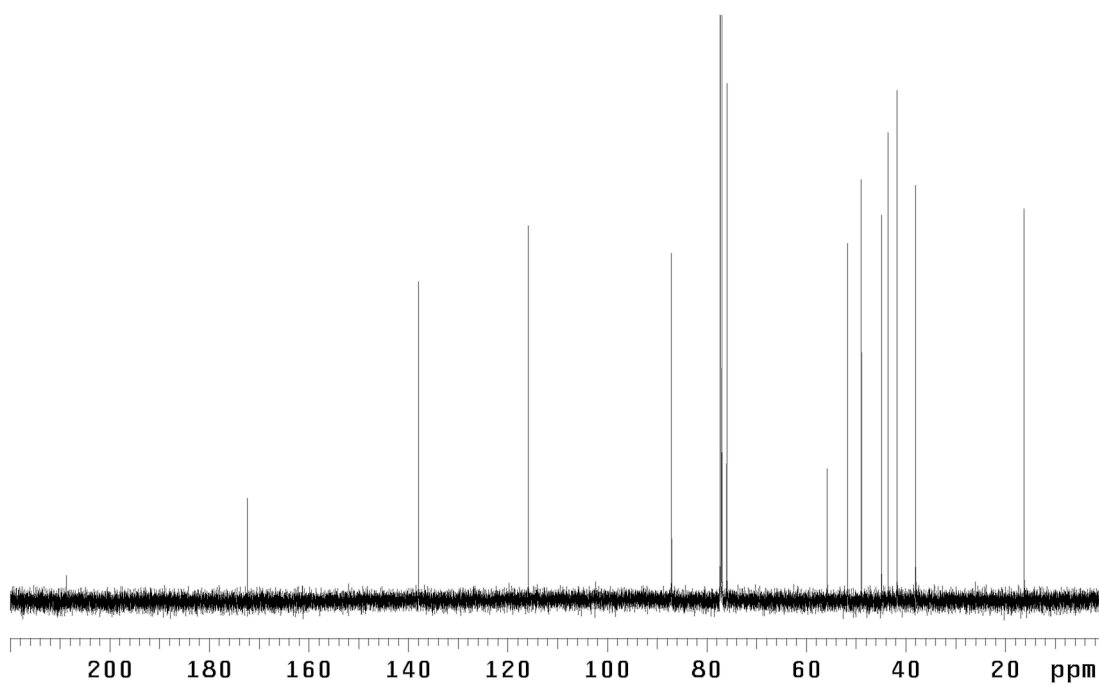
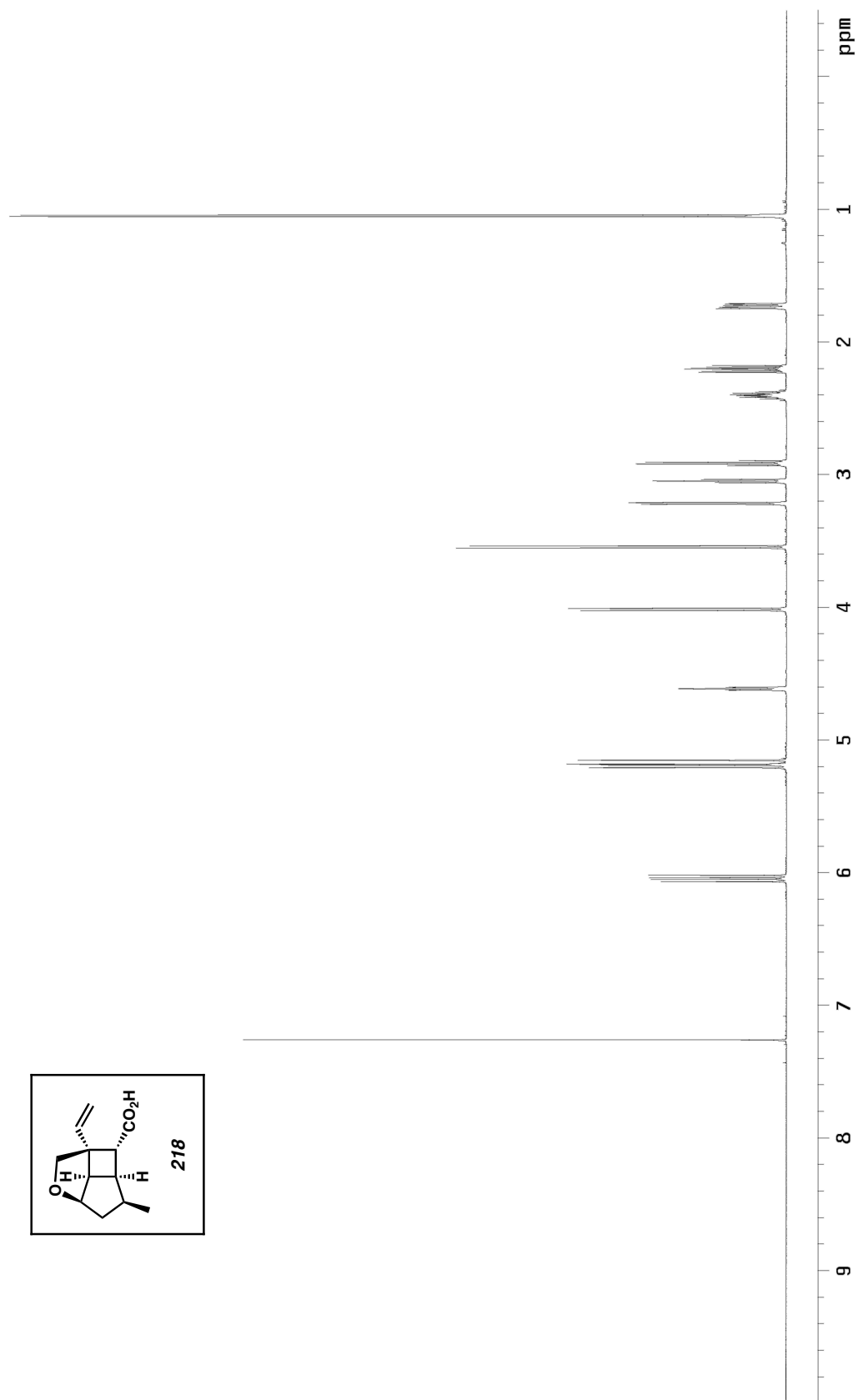


Figure A2.75. ¹³C NMR spectrum (126 MHz, CDCl₃) of **217**.

Figure A2.76. ^1H NMR spectrum (600 MHz, CDCl_3) of **218**.

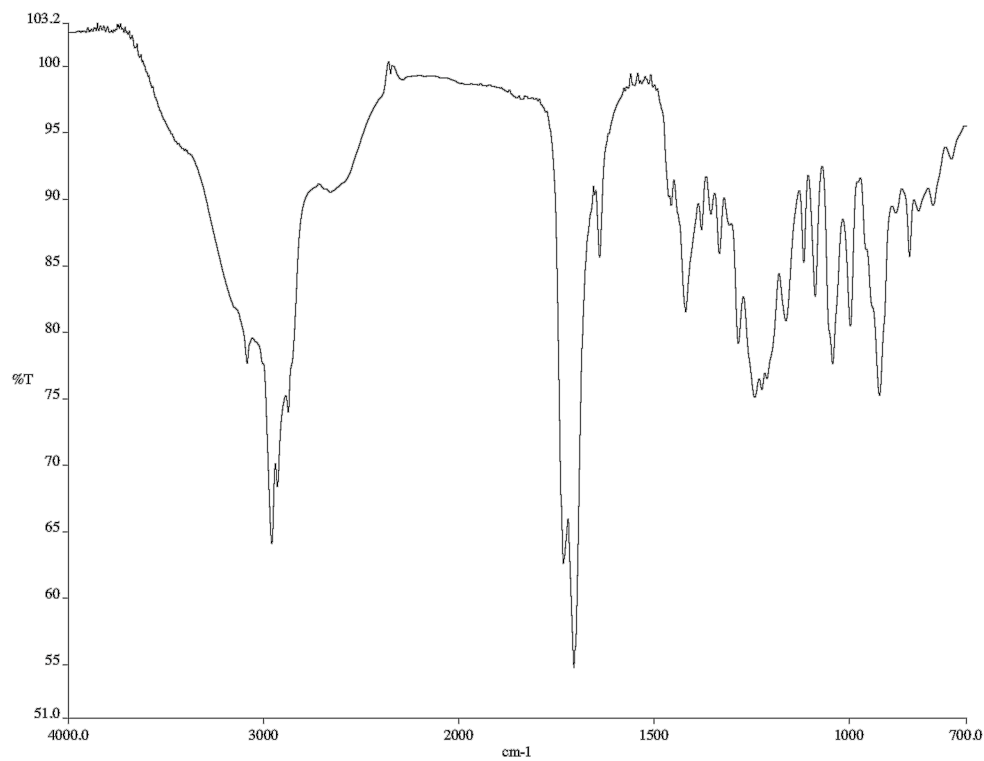


Figure A2.77. Infrared spectrum (neat film/NaCl) of **218**.

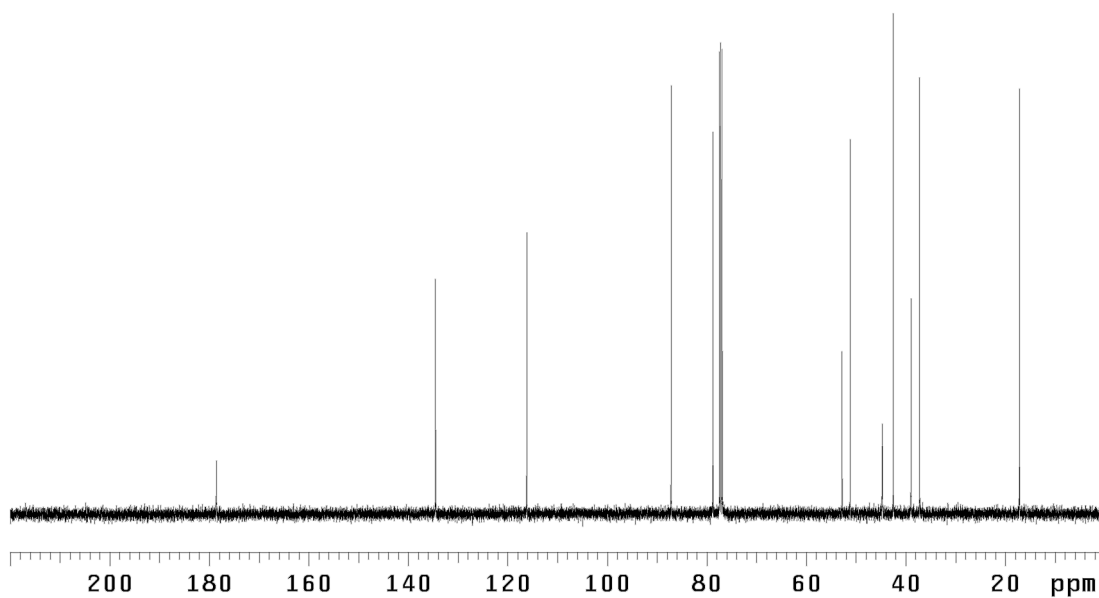
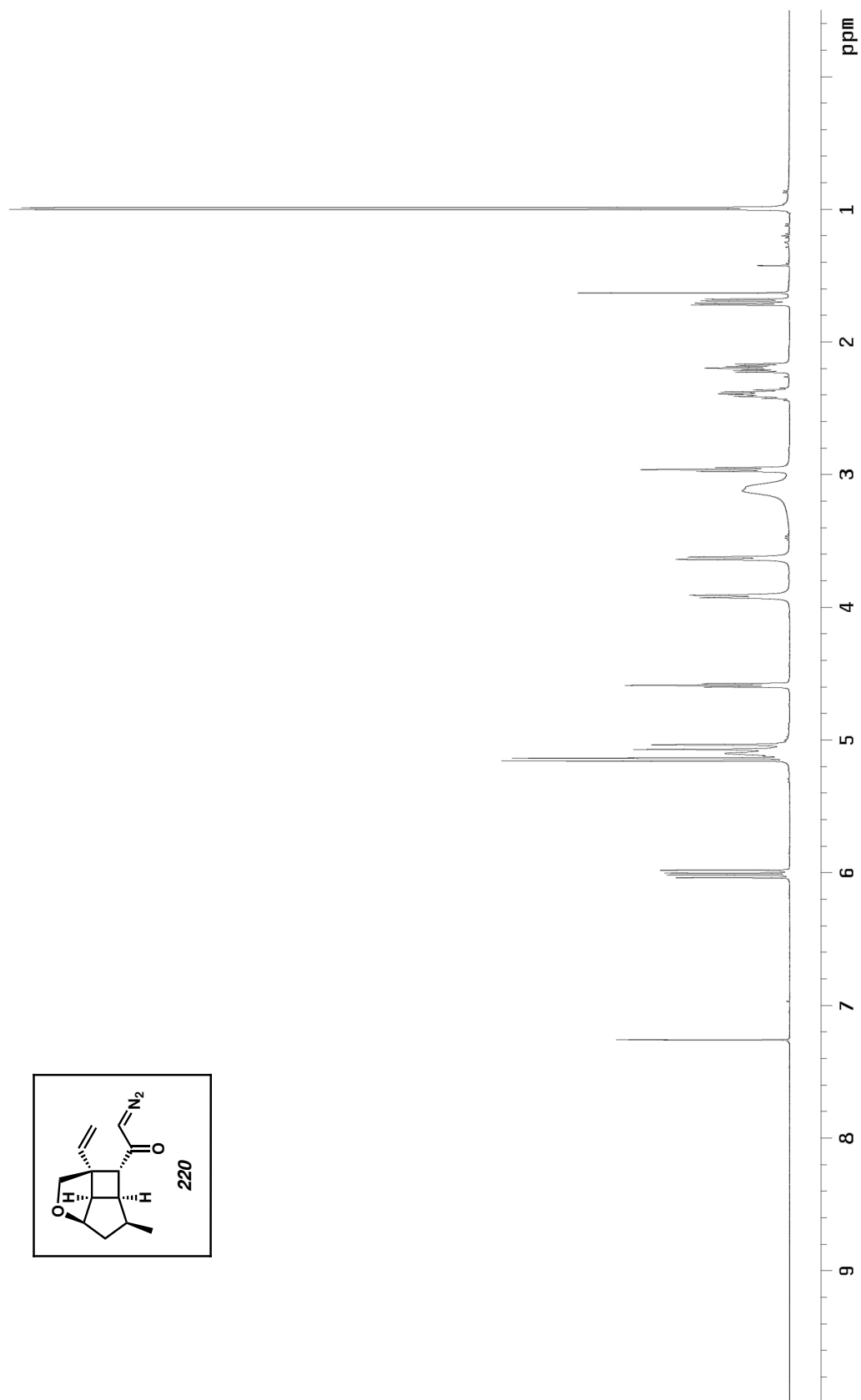


Figure A2.78. ¹³C NMR spectrum (126 MHz, CDCl₃) of **218**.

Figure A2.79. ^1H NMR spectrum (500 MHz, CDCl_3) of **220**.

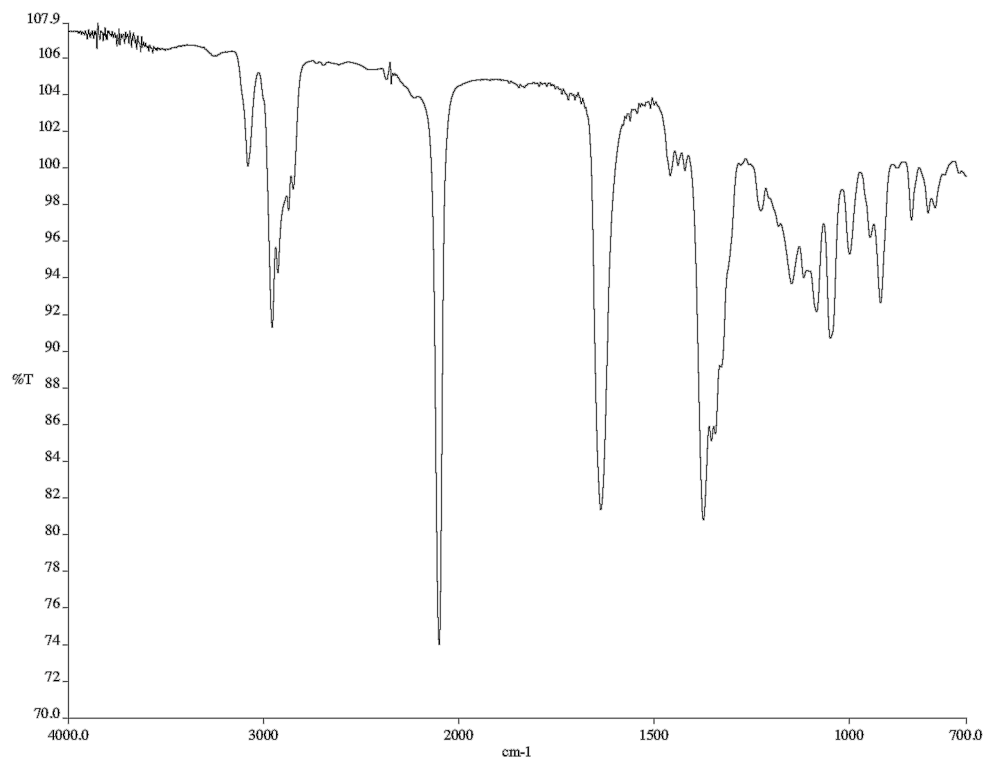


Figure A2.80. Infrared spectrum (neat film/NaCl) of **220**.

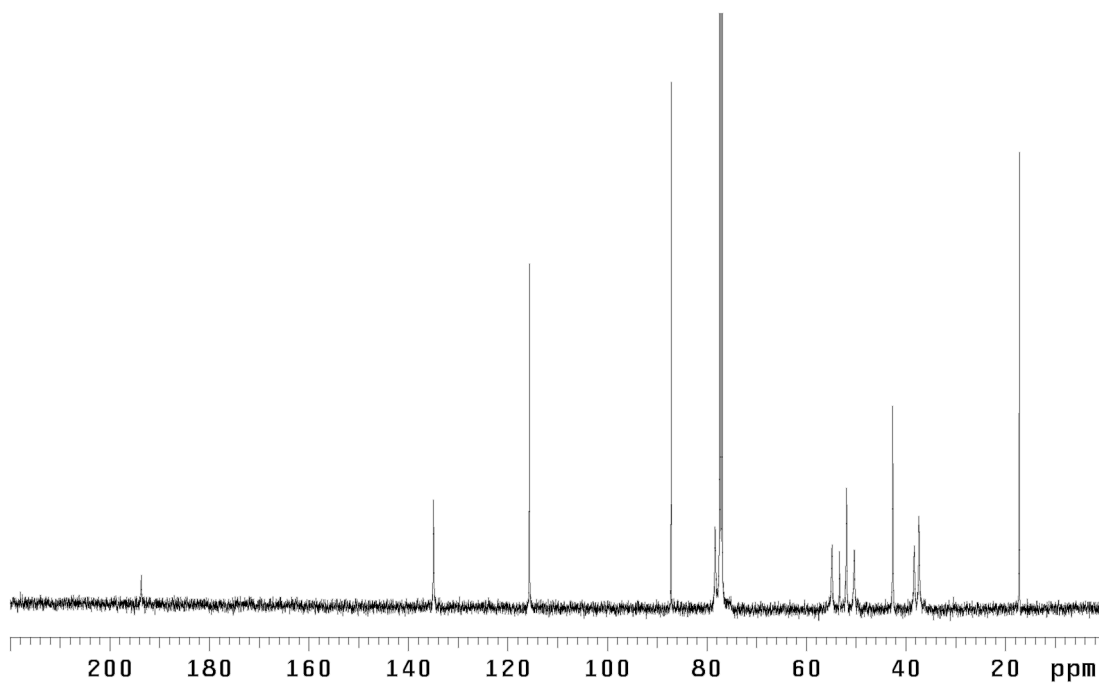
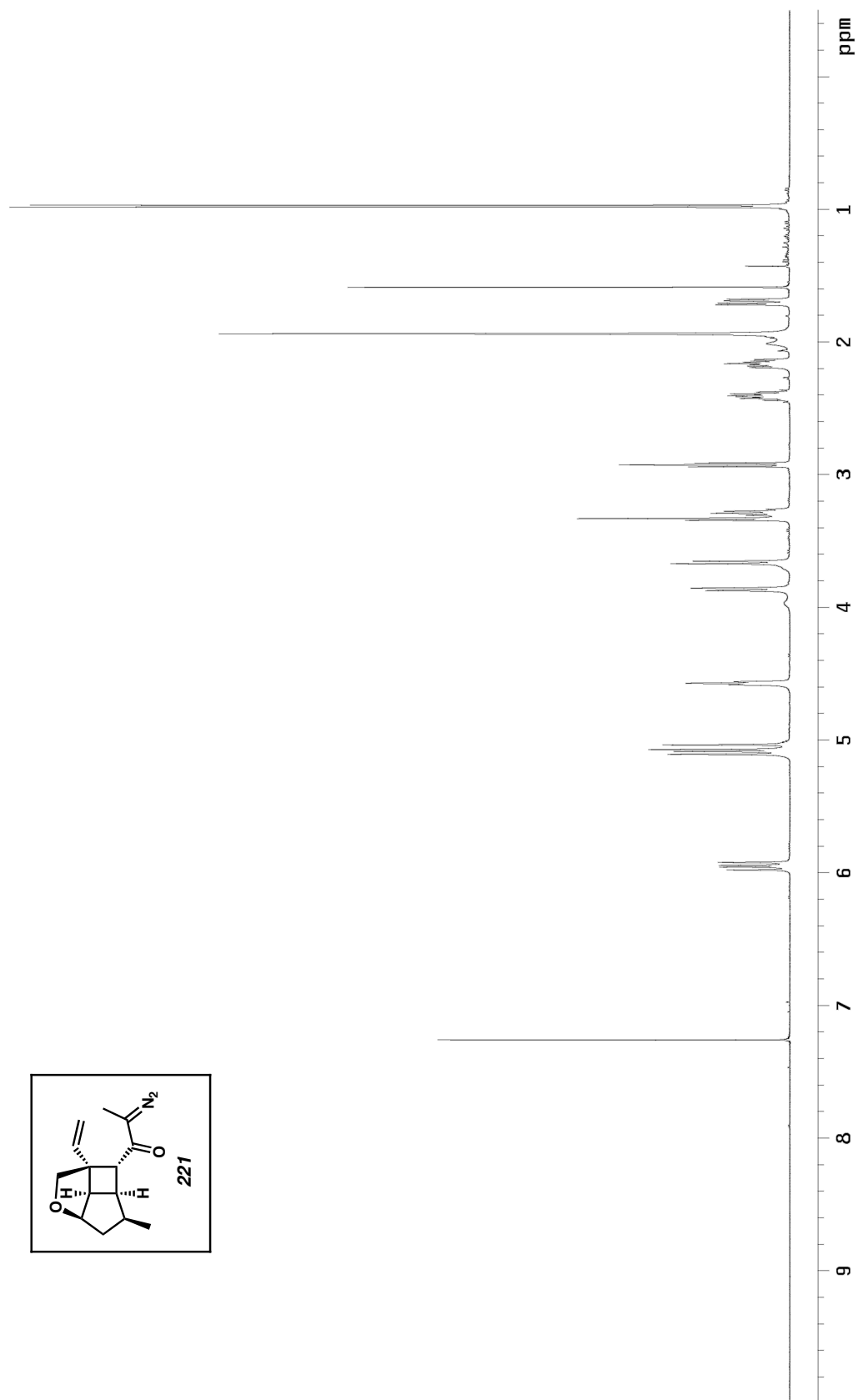


Figure A2.81. ¹³C NMR spectrum (126 MHz, CDCl₃) of **220**.

Figure A2.82. ^1H NMR spectrum (500 MHz, CDCl_3) of **221**.

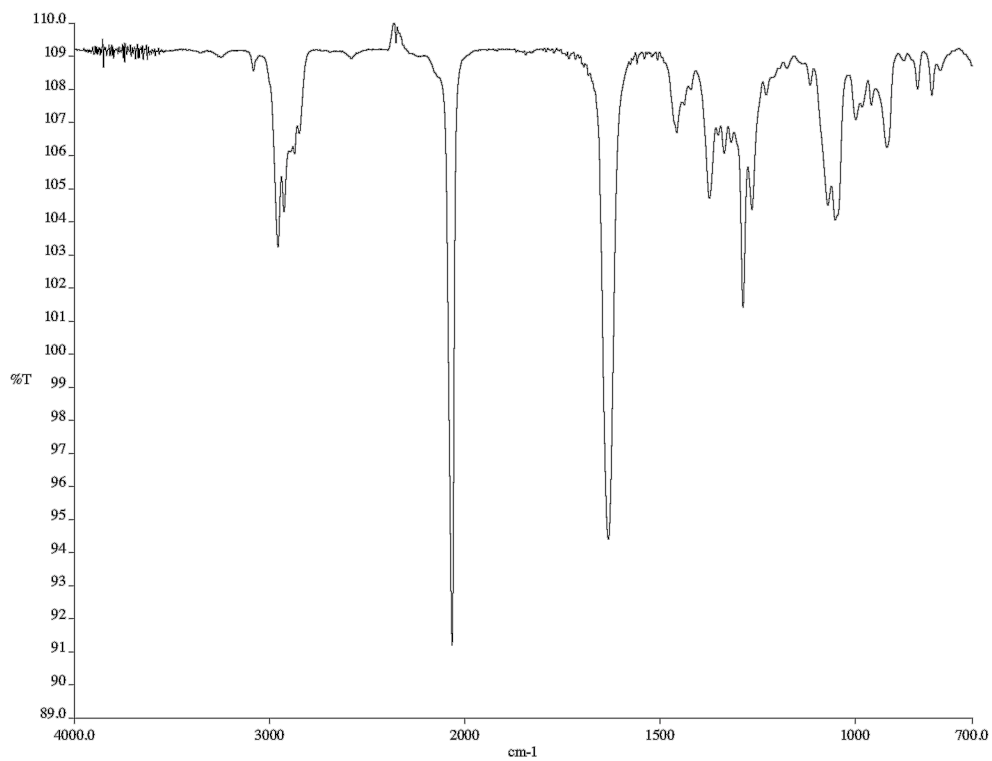


Figure A2.83. Infrared spectrum (neat film/NaCl) of **221**.

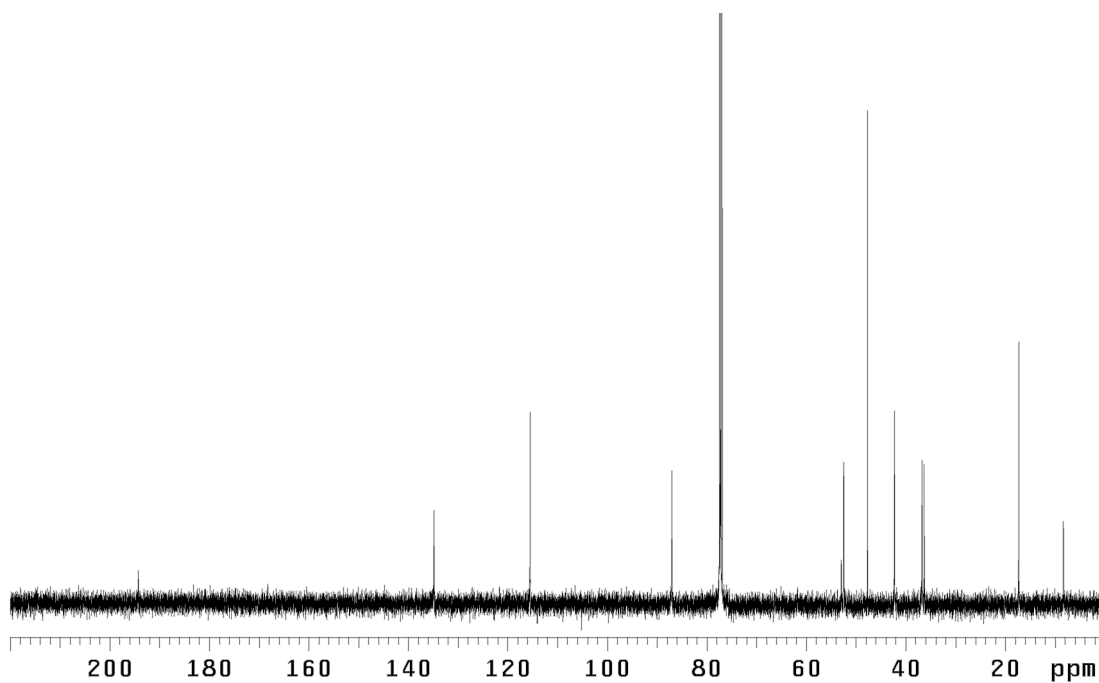
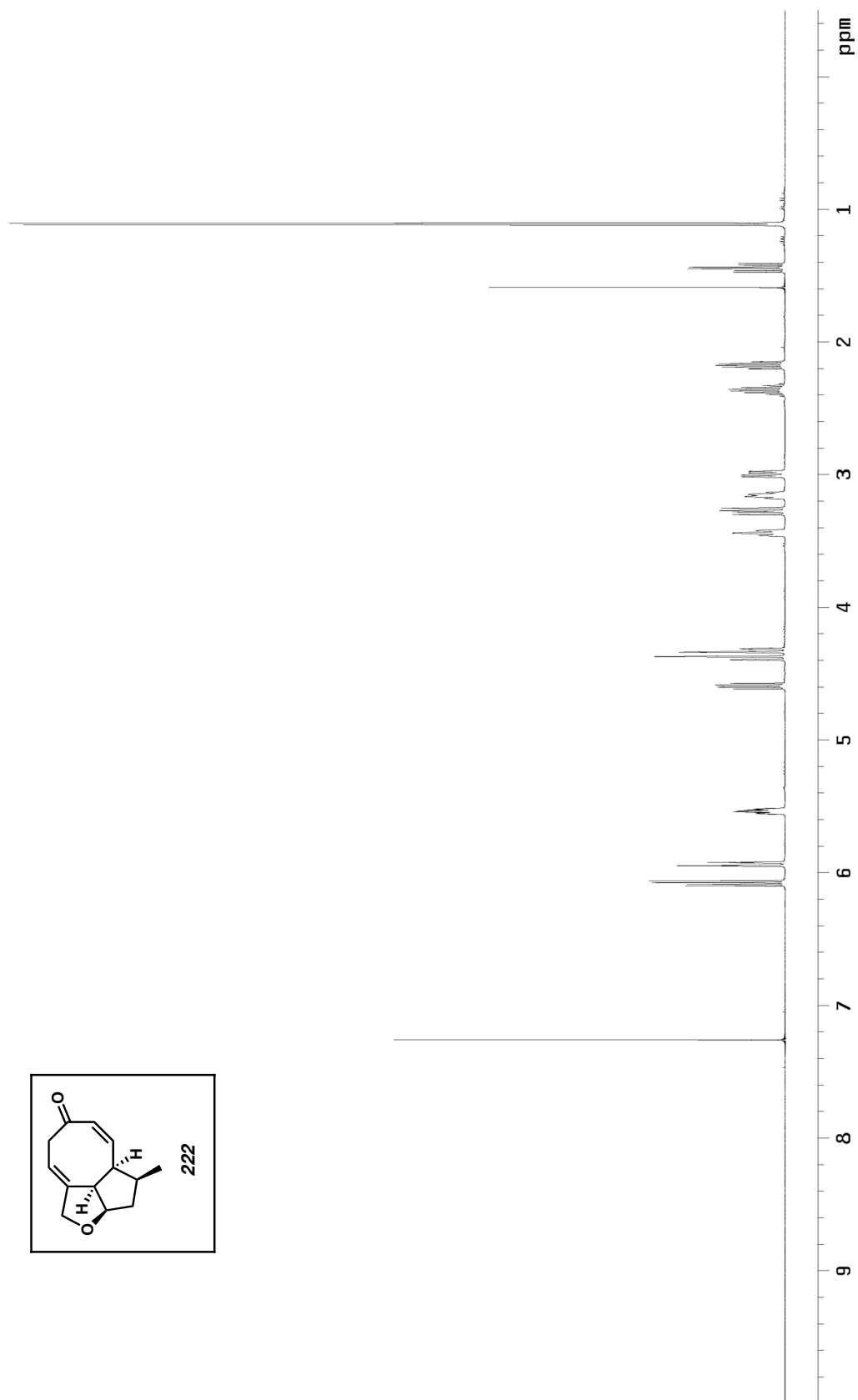


Figure A2.84. ¹³C NMR spectrum (126 MHz, CDCl₃) of **221**.

Figure A2.85. ^1H NMR spectrum (500 MHz, CDCl_3) of **222**.

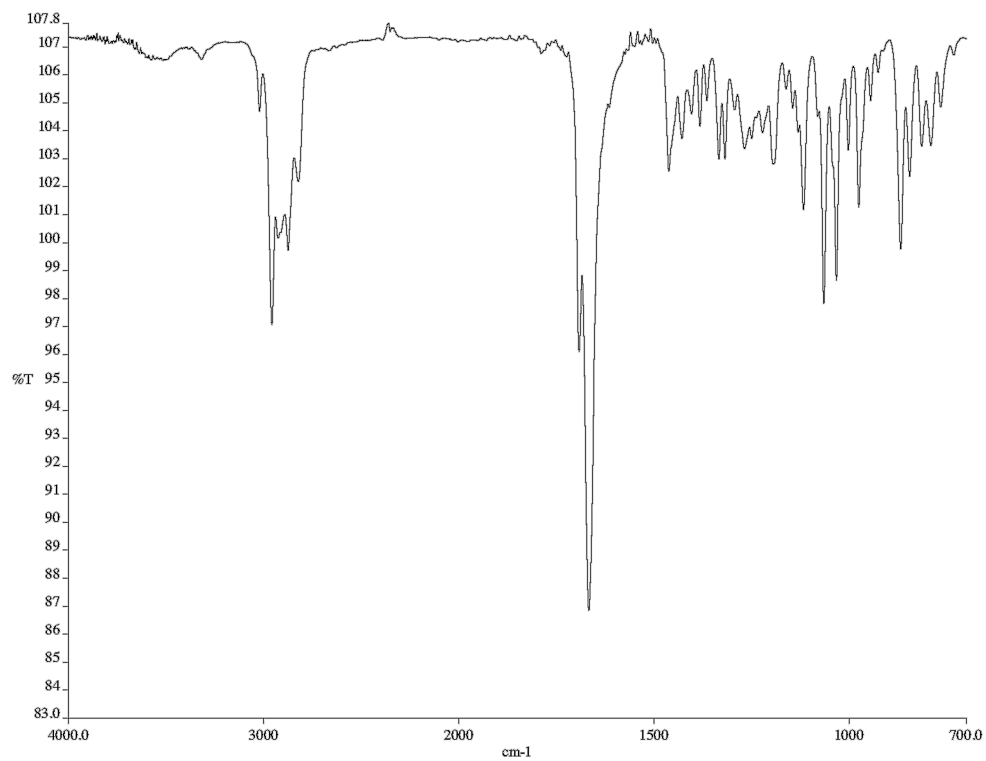


Figure A2.86. Infrared spectrum (neat film/NaCl) of **222**.

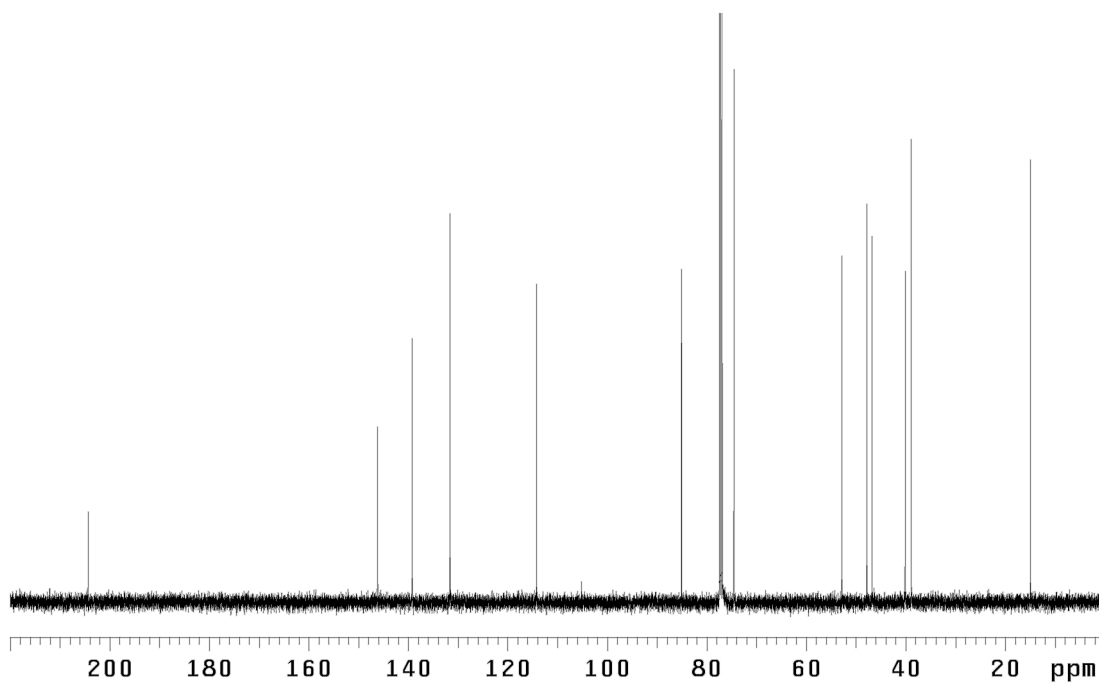
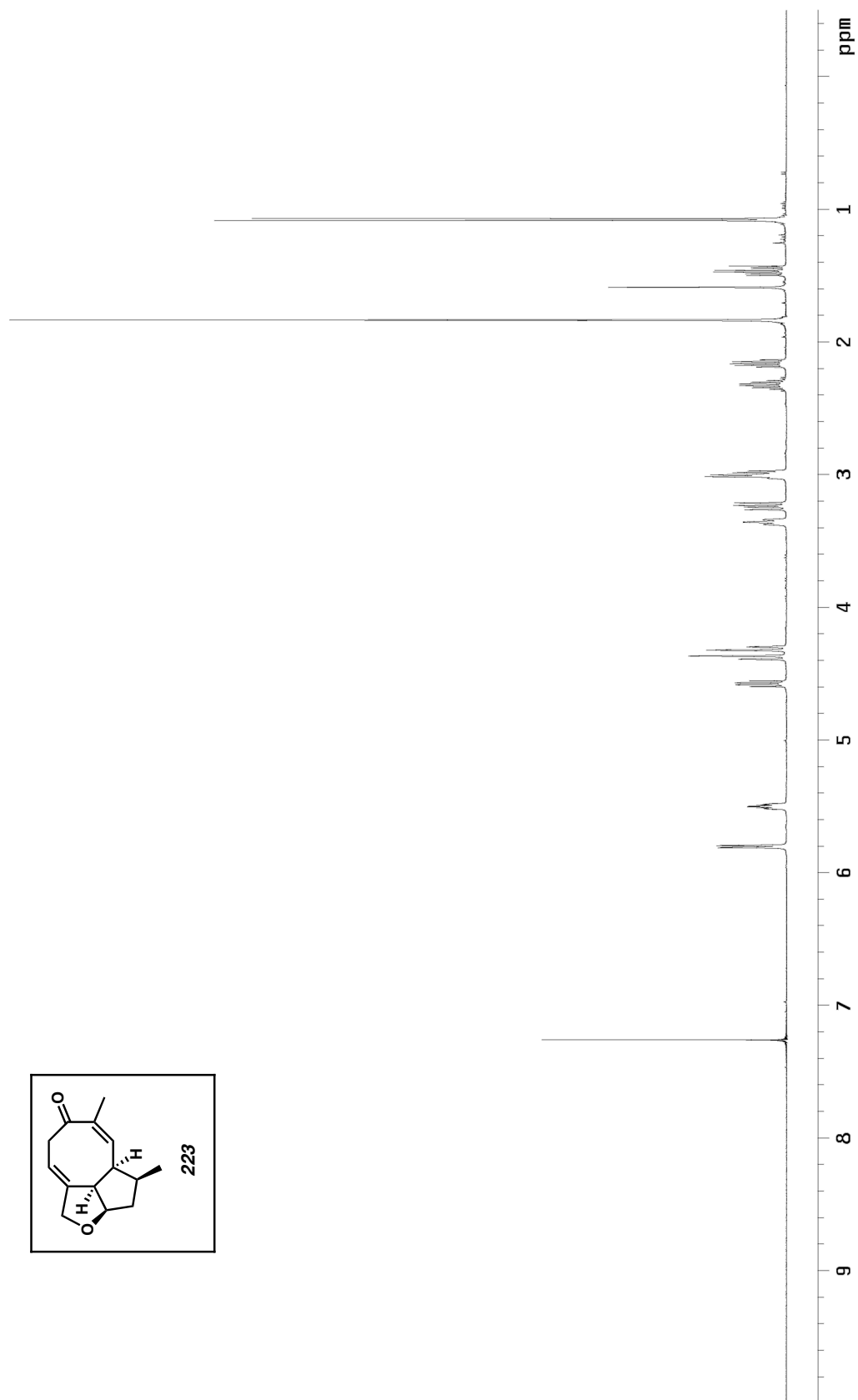


Figure A2.87. ¹³C NMR spectrum (126 MHz, CDCl₃) of **222**.

Figure A2.88. ^1H NMR spectrum (600 MHz, CDCl_3) of **223**.

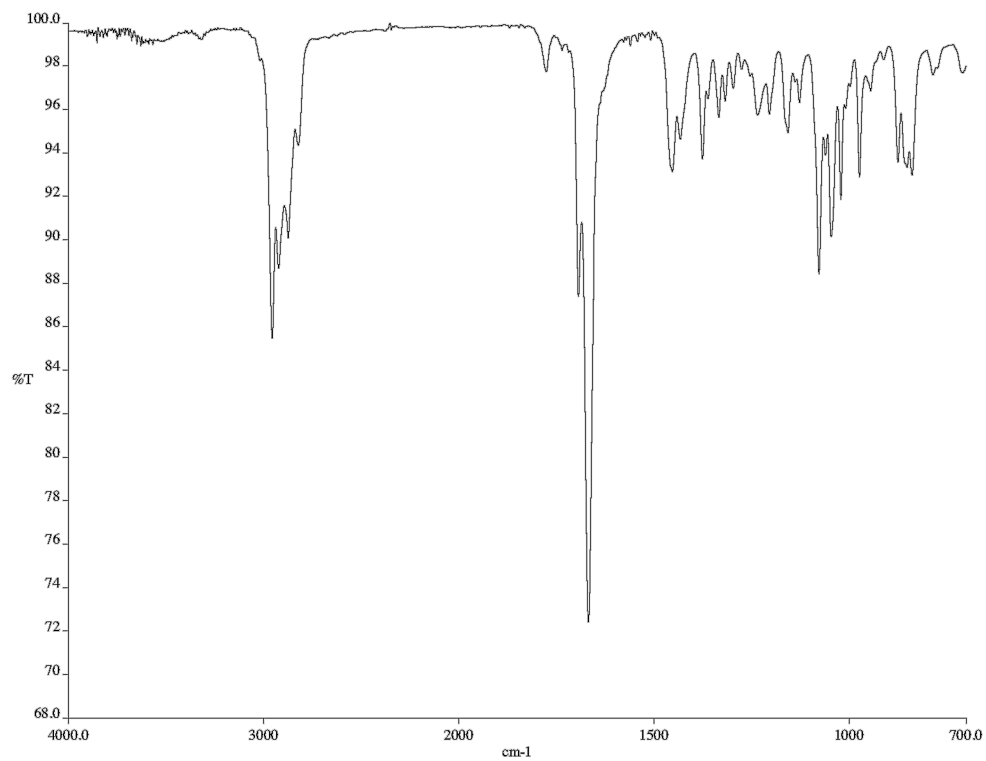


Figure A2.89. Infrared spectrum (neat film/NaCl) of **223**.

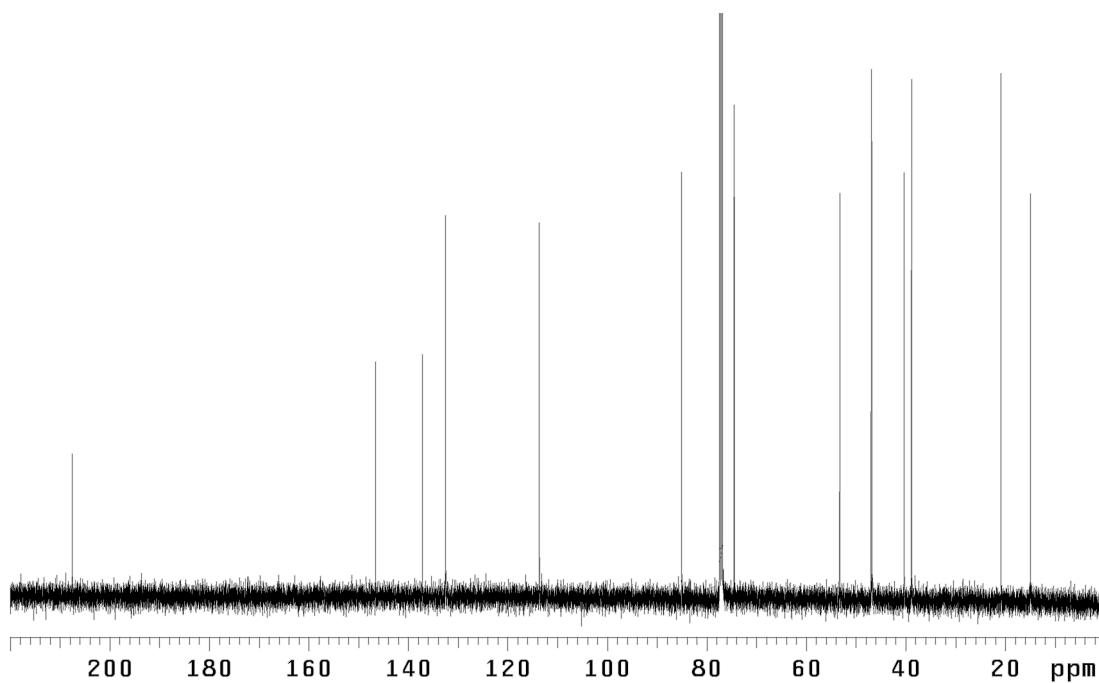
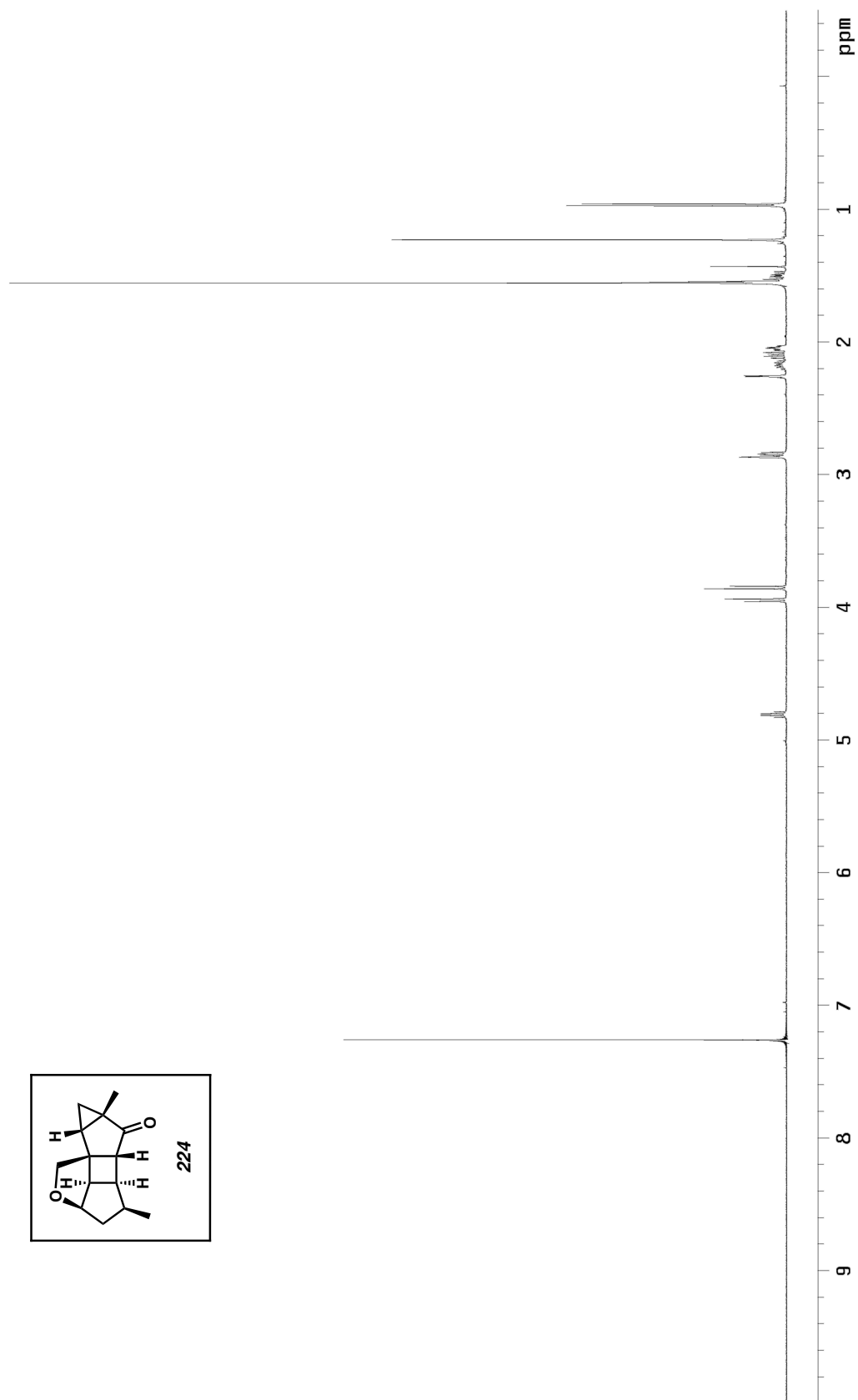


Figure A2.90. ¹³C NMR spectrum (126 MHz, CDCl₃) of **223**.

Figure A2.91. ^1H NMR spectrum (500 MHz, CDCl_3) of **224**.

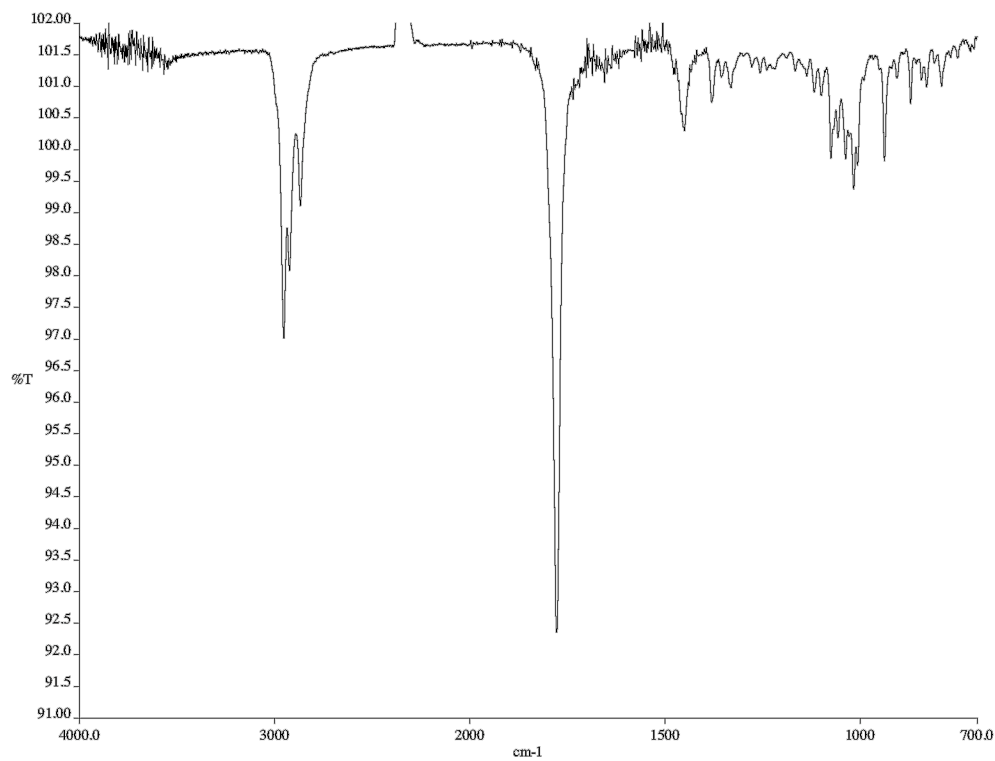


Figure A2.92. Infrared spectrum (neat film/NaCl) of **224**.

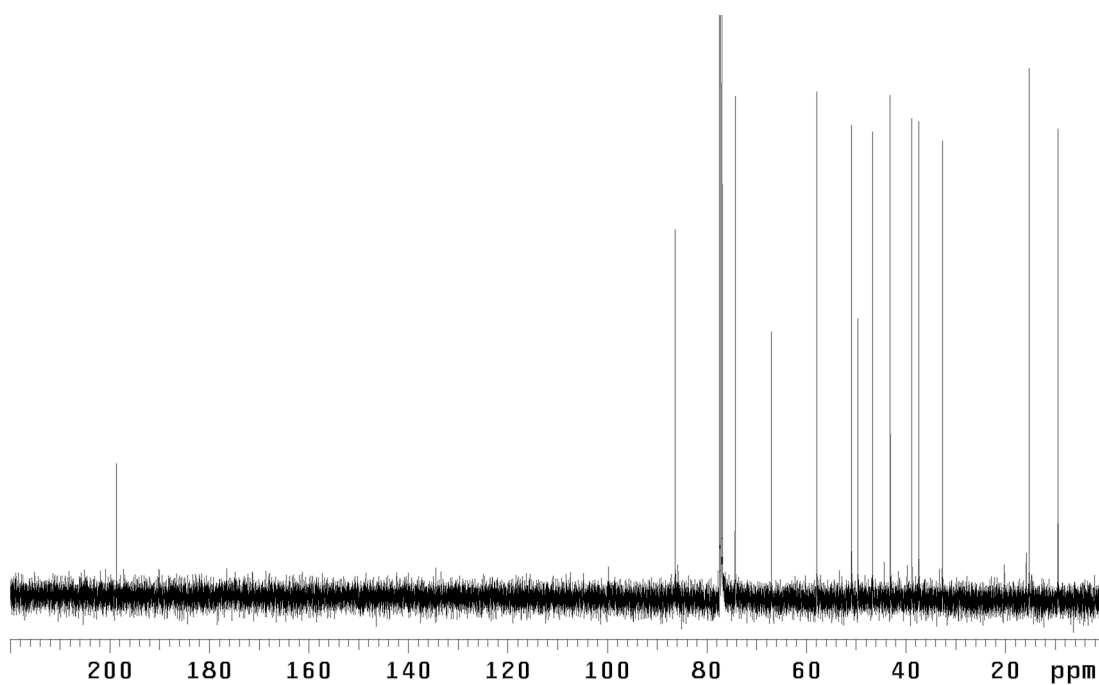
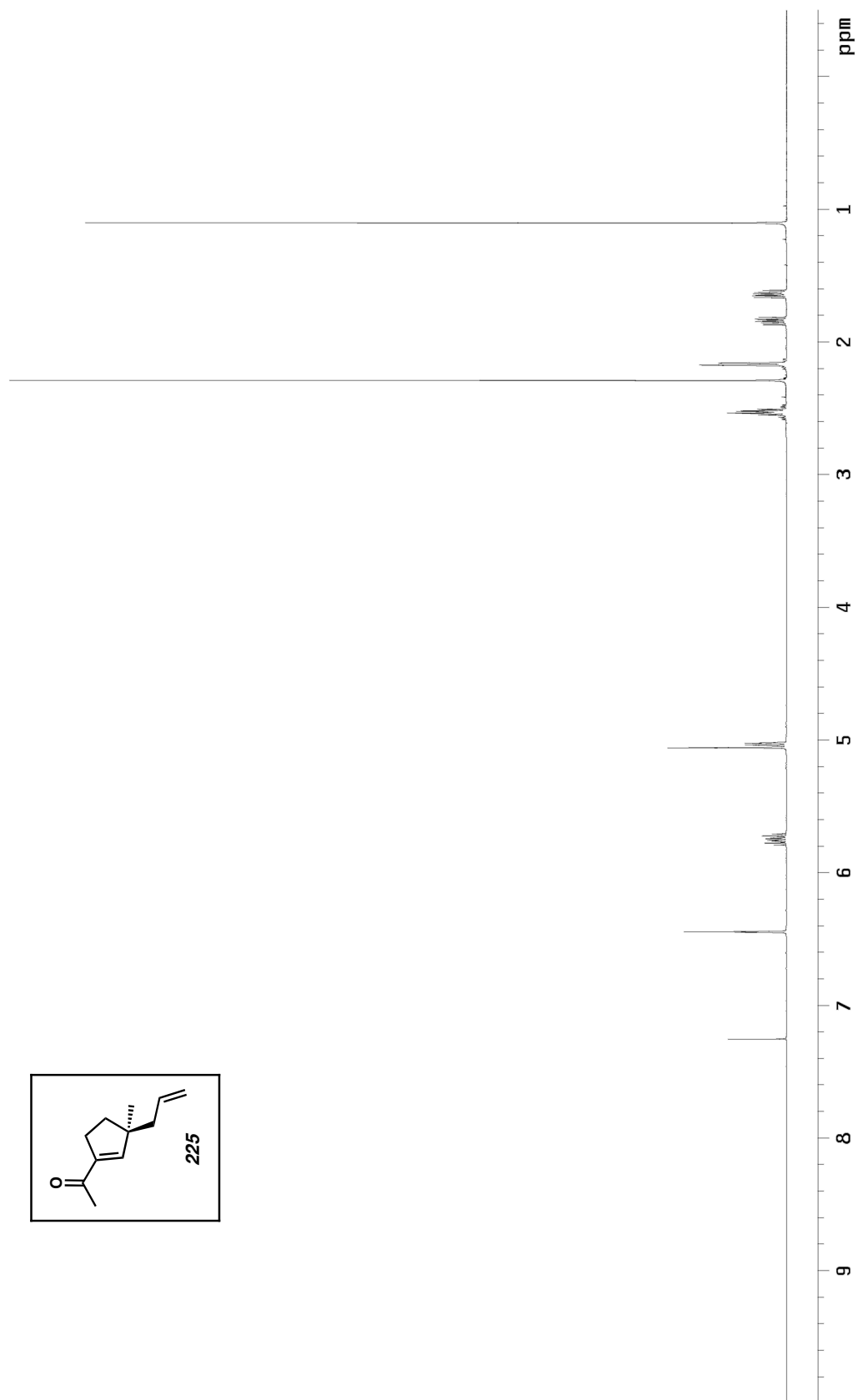


Figure A2.93. ¹³C NMR spectrum (126 MHz, CDCl₃) of **224**.

Figure A2.94. ^1H NMR spectrum (500 MHz, CDCl_3) of **225**.

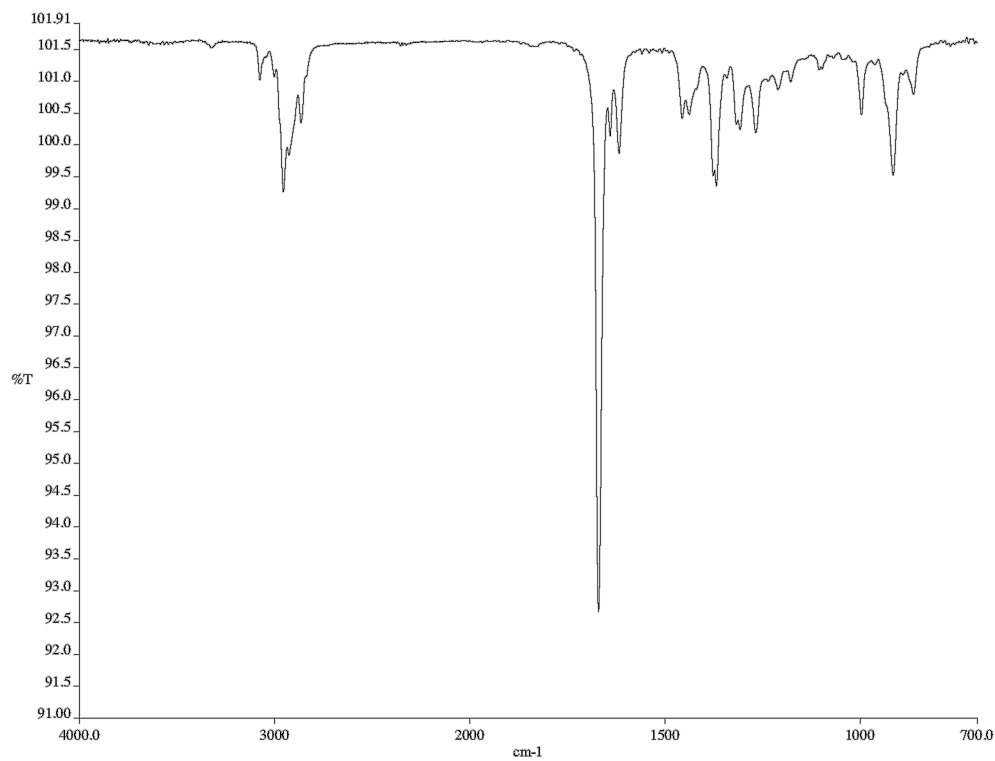


Figure A2.95. Infrared spectrum (neat film/NaCl) of **225**.

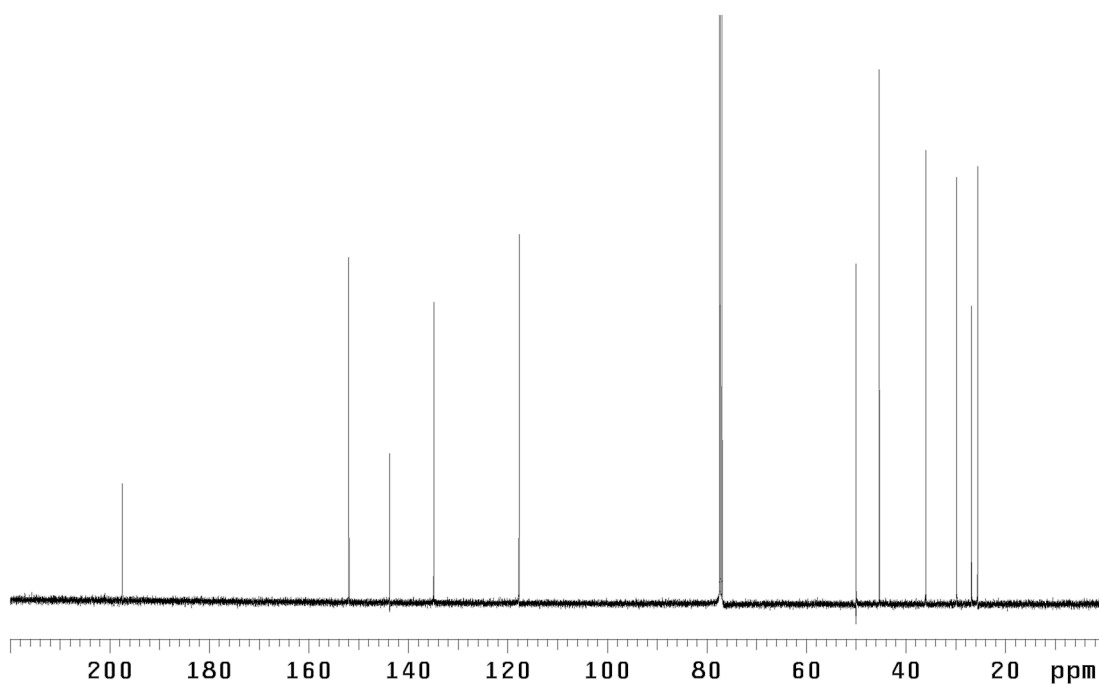
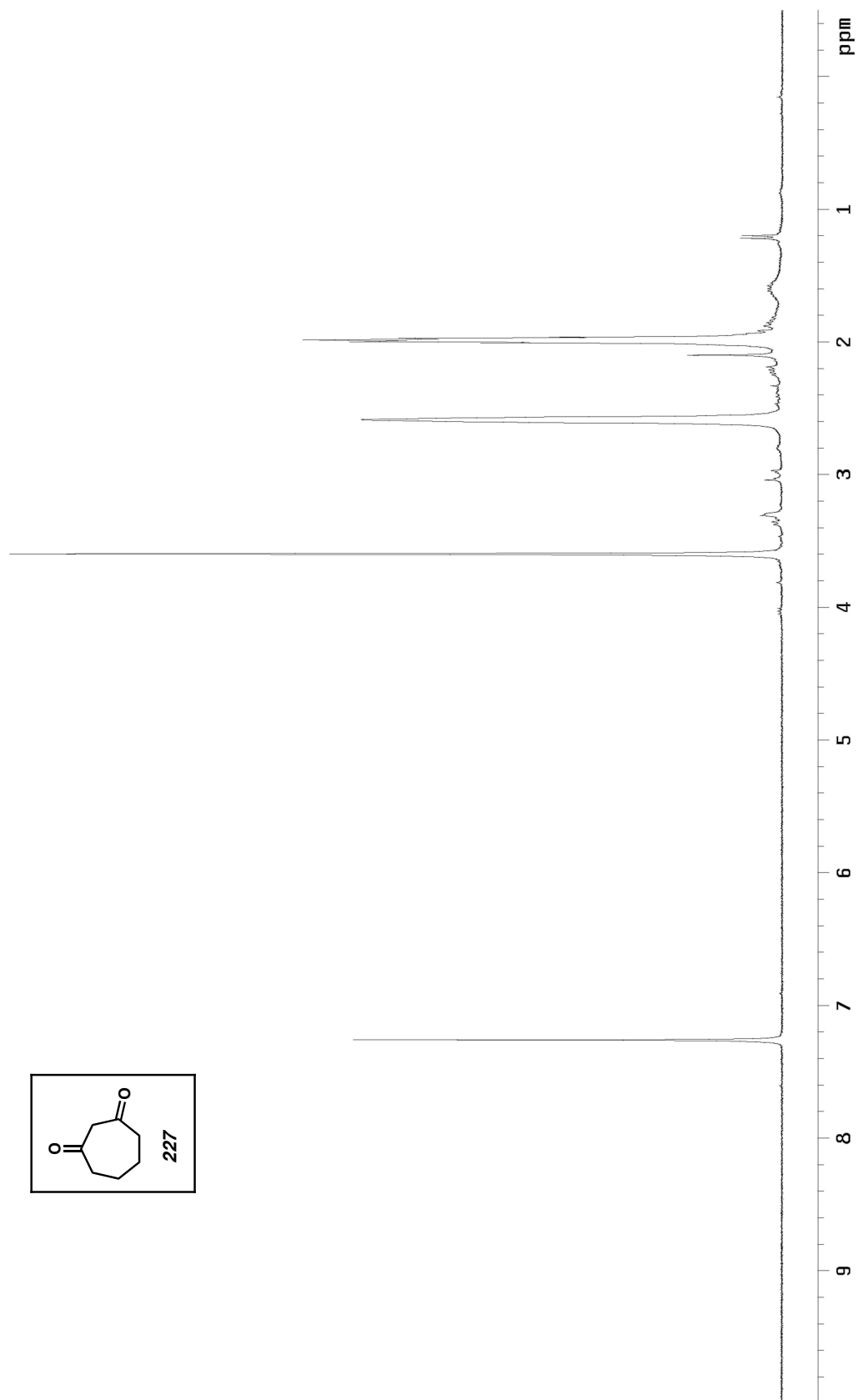
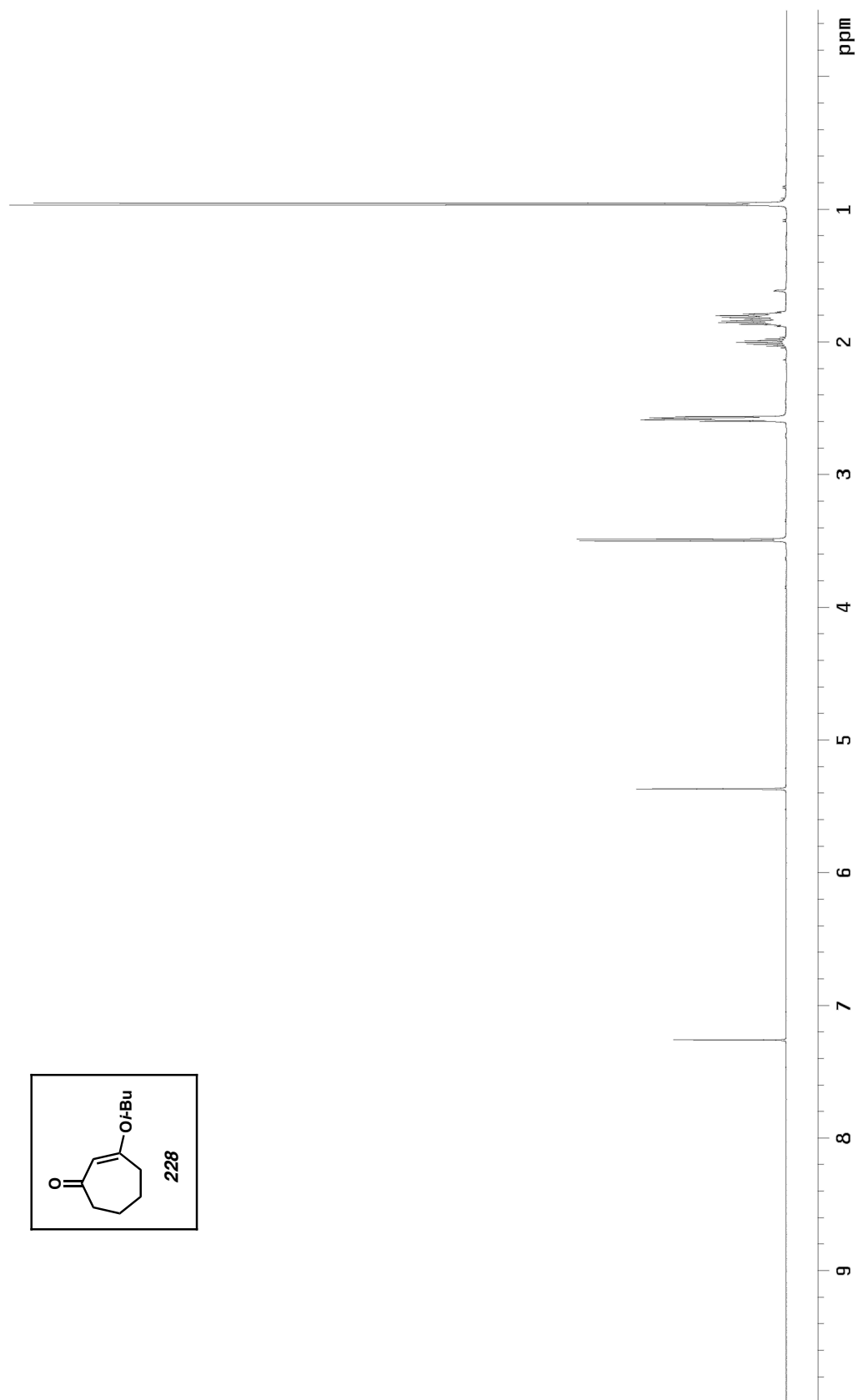


Figure A2.96. ¹³C NMR spectrum (126 MHz, CDCl₃) of **225**.

Figure A2.97. ^1H NMR spectrum (300 MHz, CDCl_3) of **227**.

Figure A2.98. ^1H NMR spectrum (500 MHz, CDCl_3) of **228**.

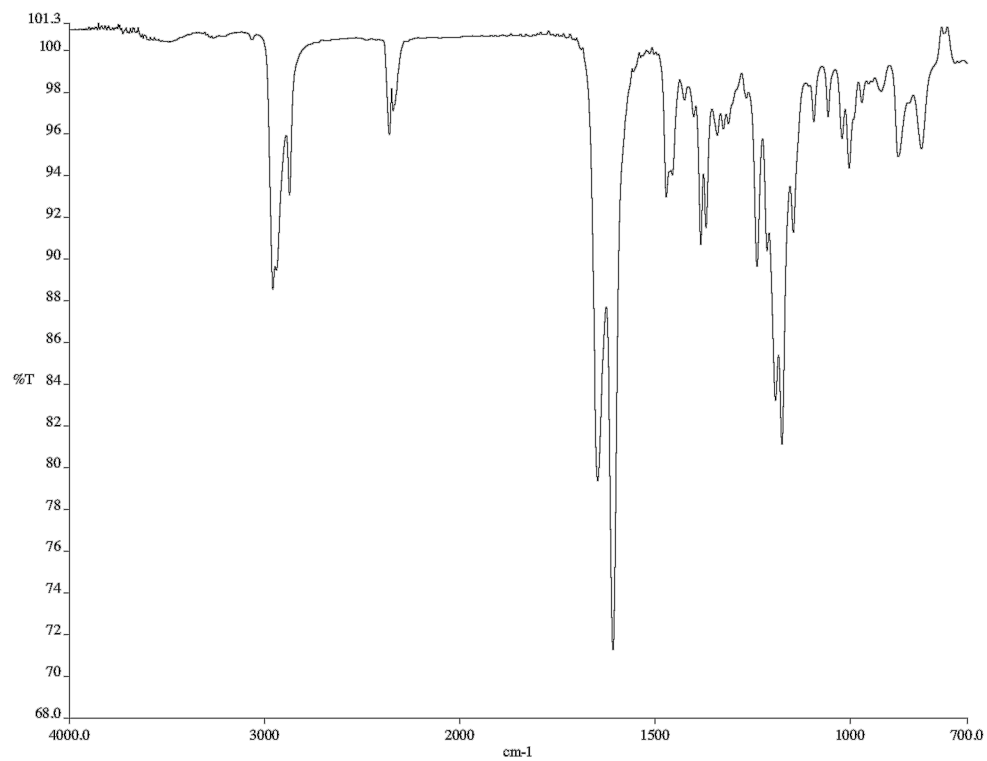


Figure A2.99. Infrared spectrum (neat film/NaCl) of **228**.

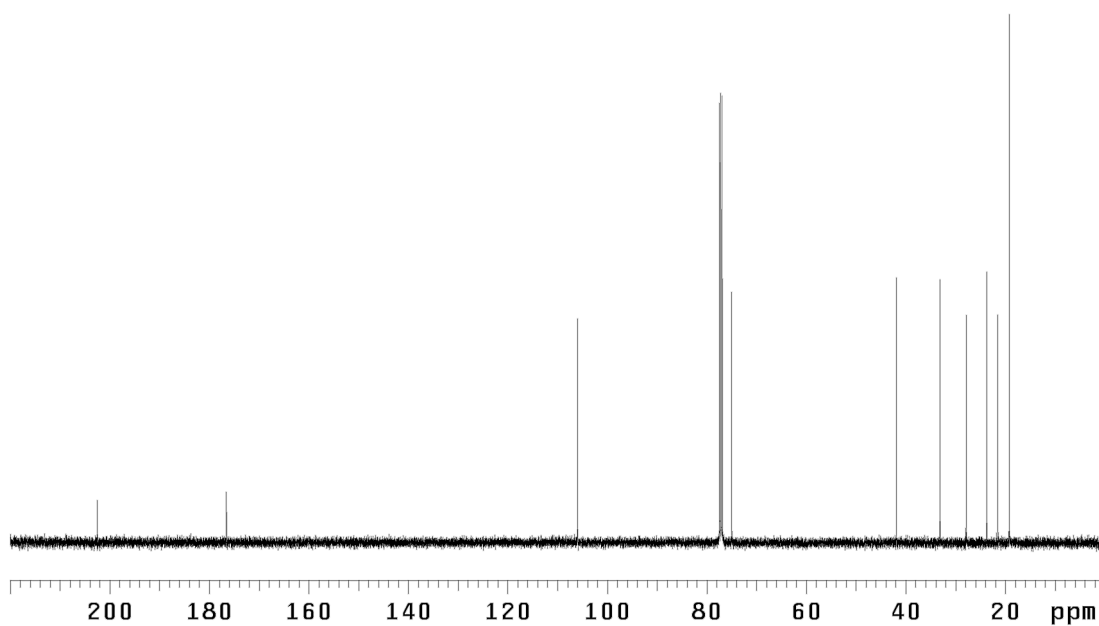
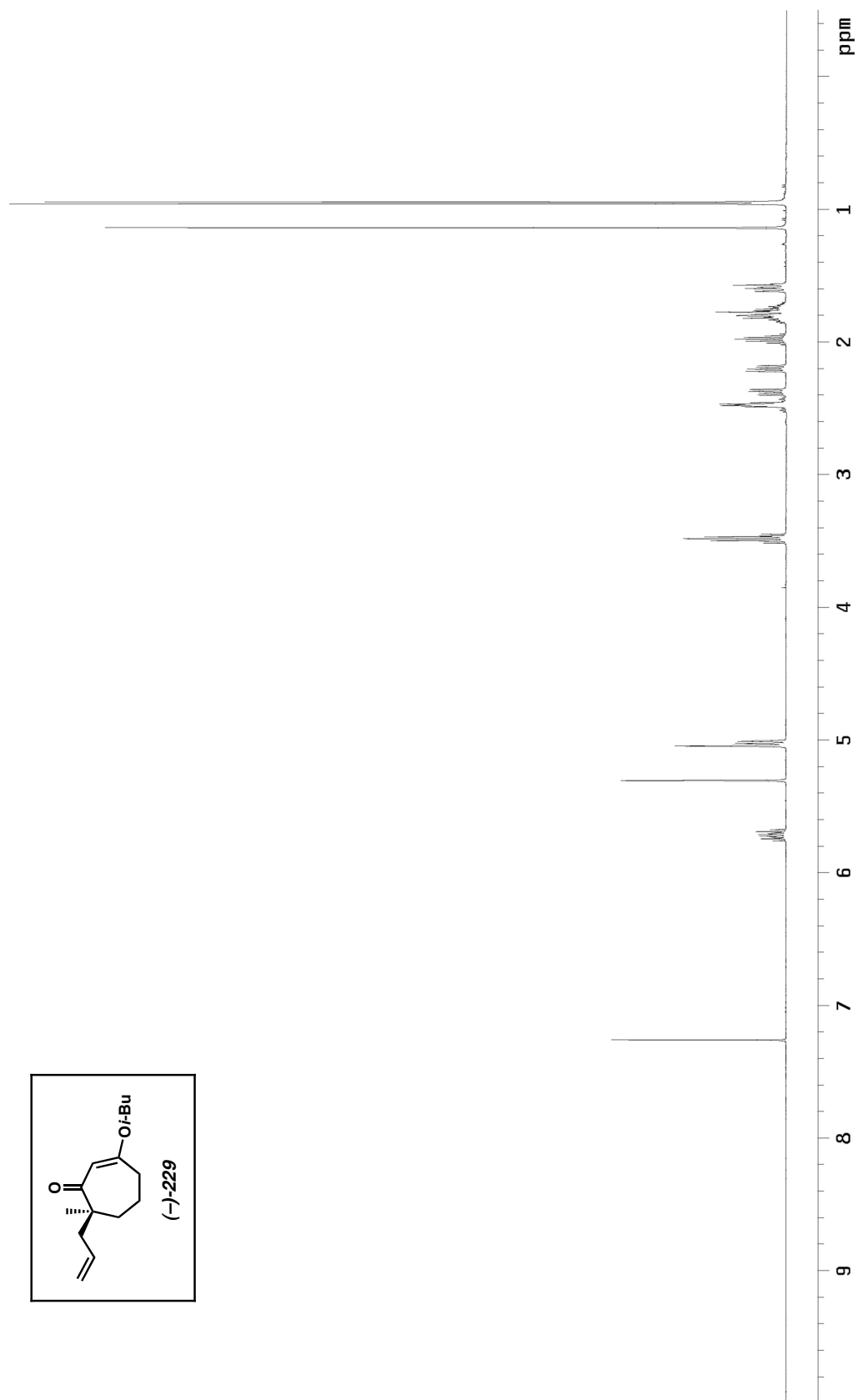


Figure A2.100. ¹³C NMR spectrum (126 MHz, CDCl₃) of **228**.

Figure A2.101. ¹H NMR spectrum (500 MHz, CDCl₃) of **229**.

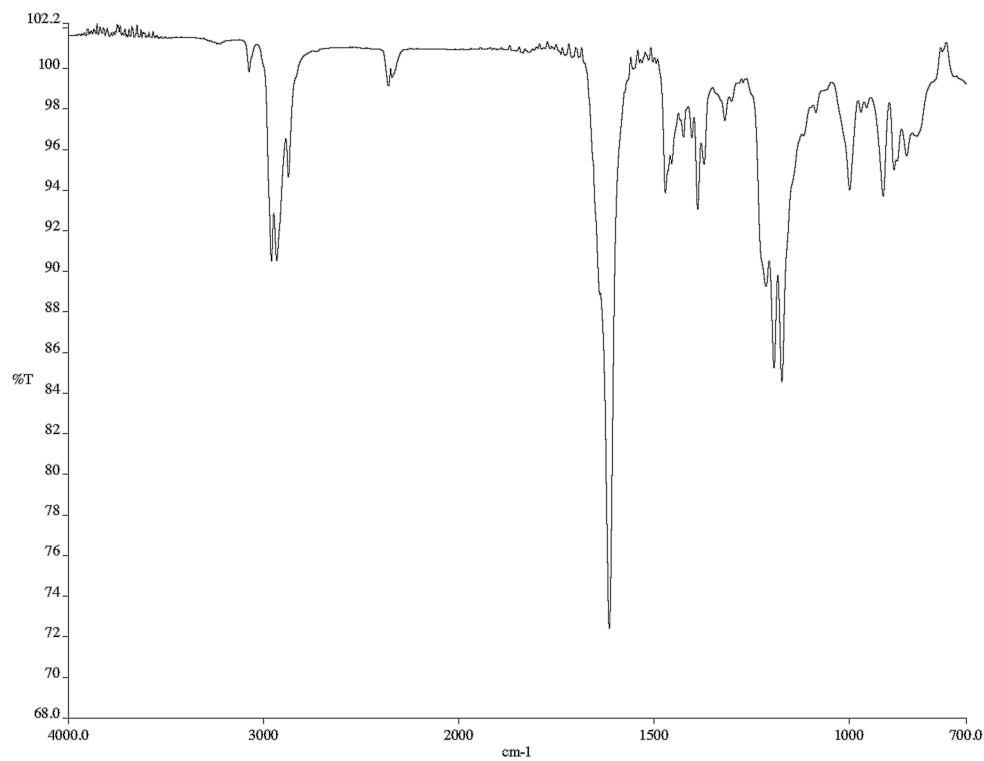


Figure A2.102. Infrared spectrum (neat film/NaCl) of **229**.

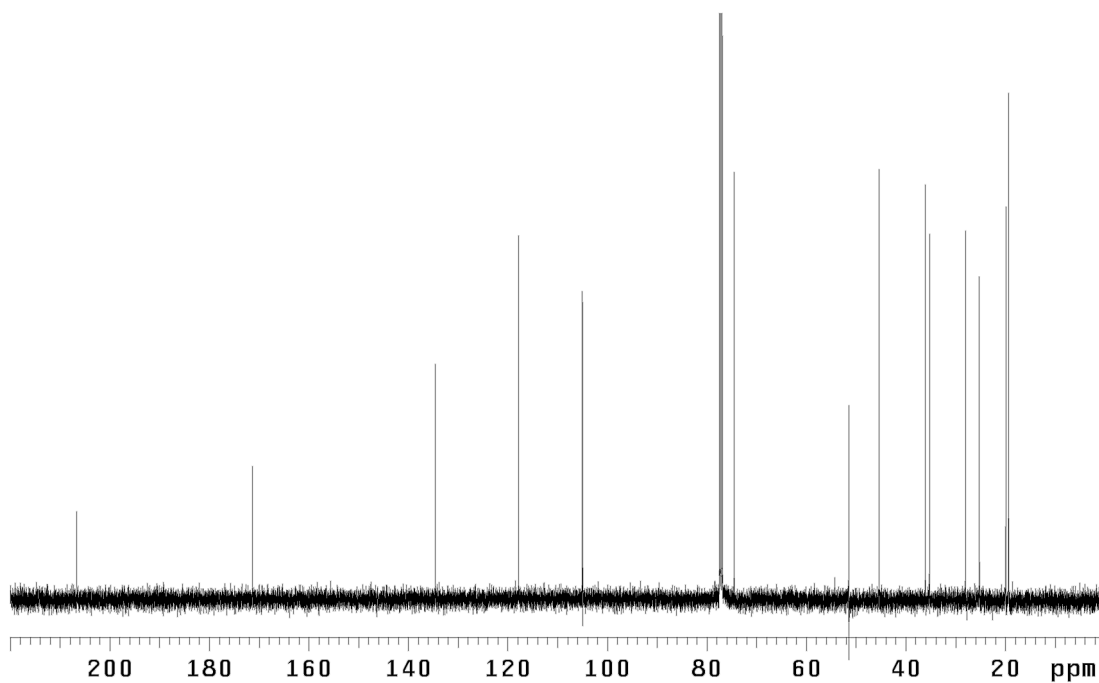
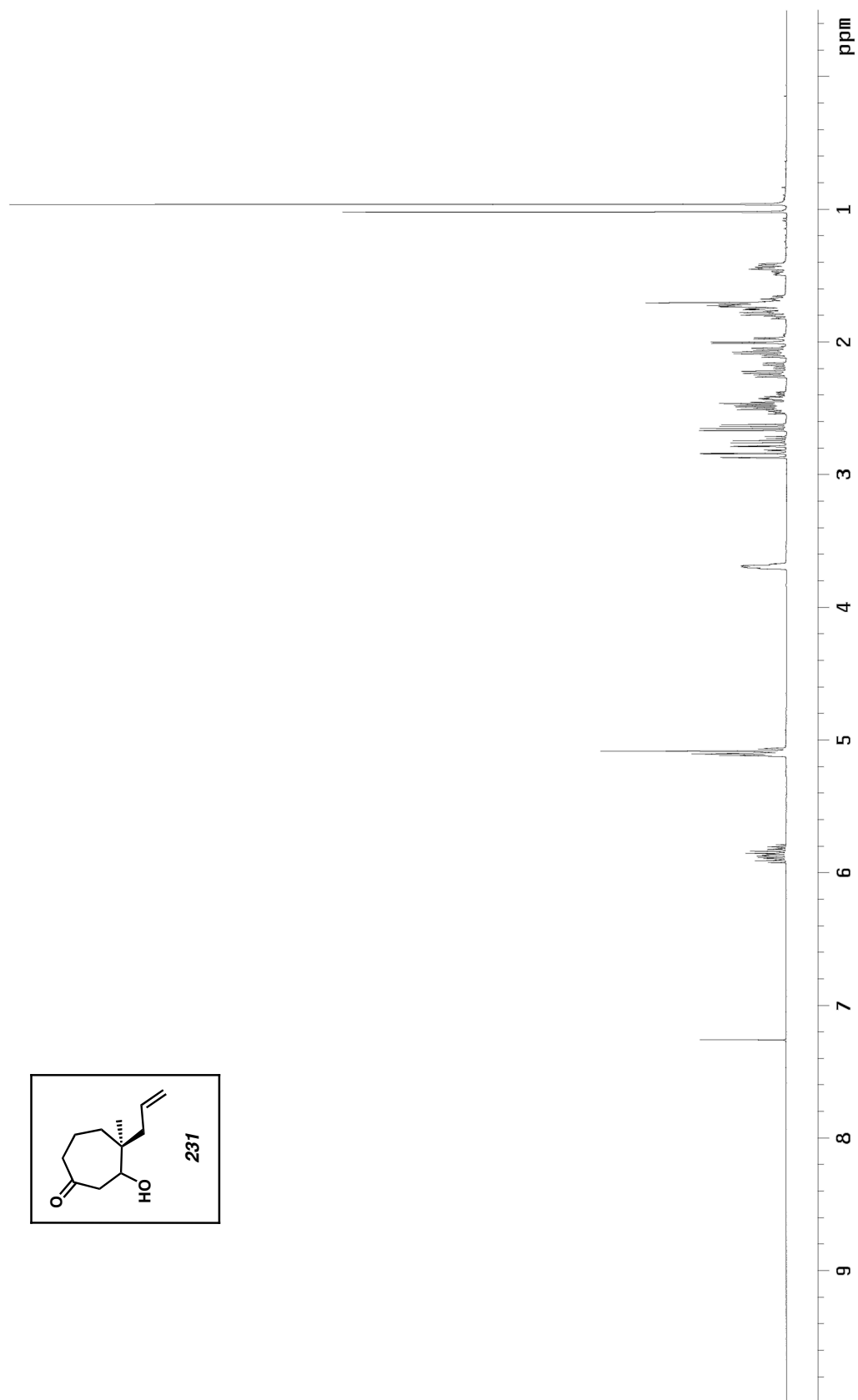


Figure A2.103. ¹³C NMR spectrum (126 MHz, CDCl₃) of **229**.

Figure A2.104. ^1H NMR spectrum (500 MHz, CDCl_3) of **231**.

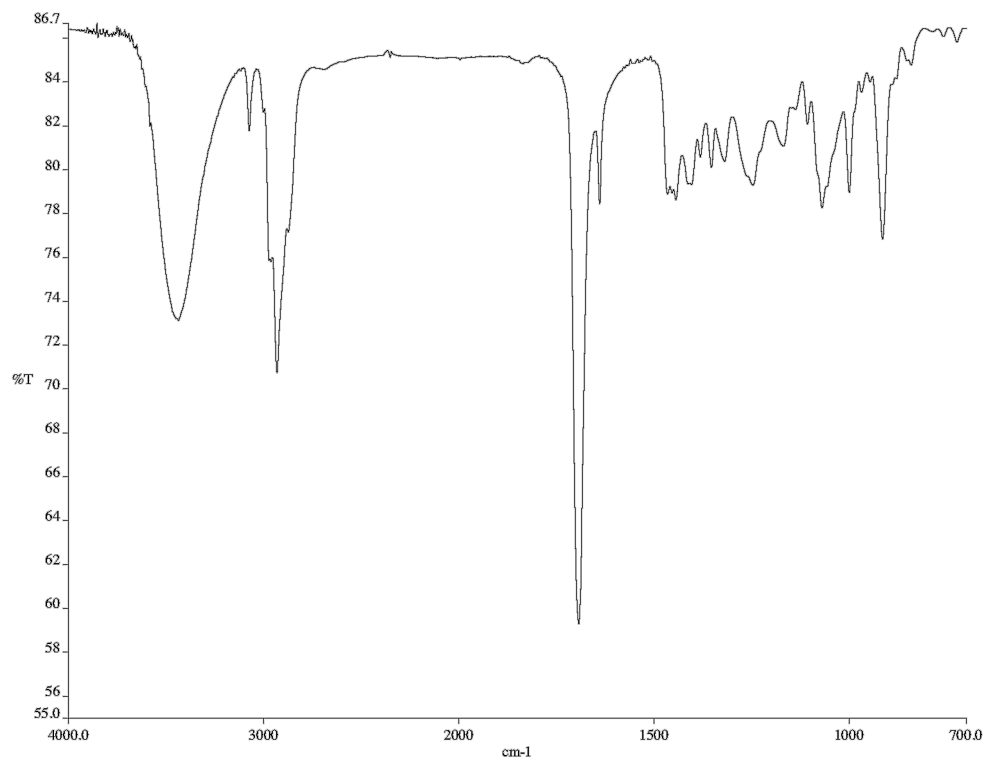


Figure A2.105. Infrared spectrum (neat film/NaCl) of **231**.

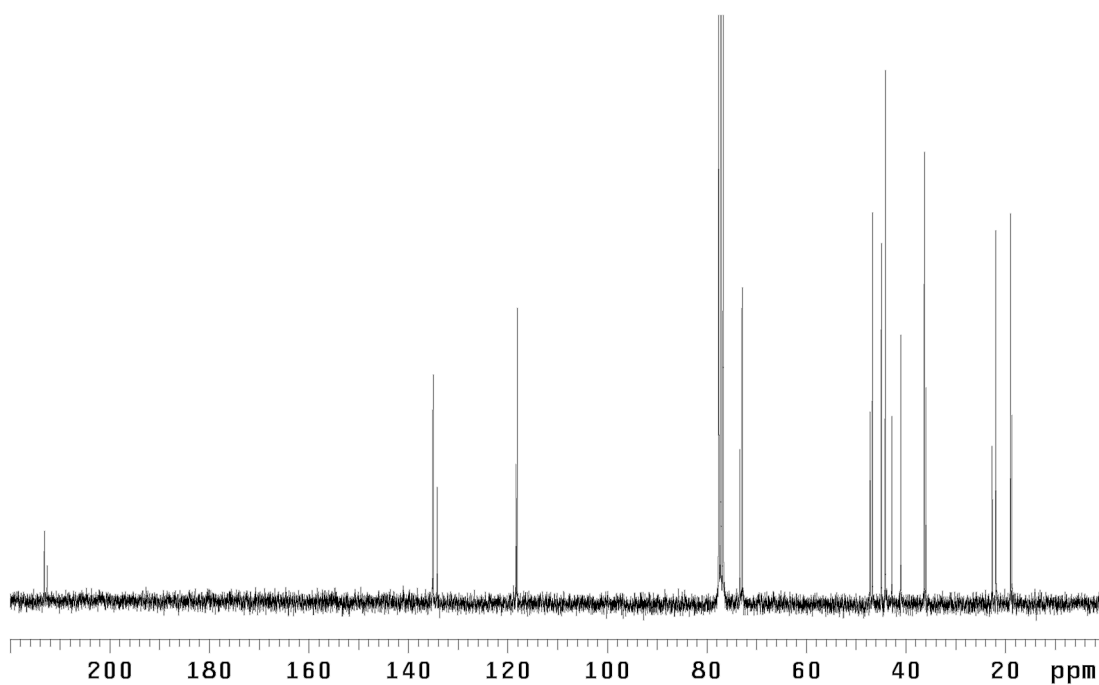
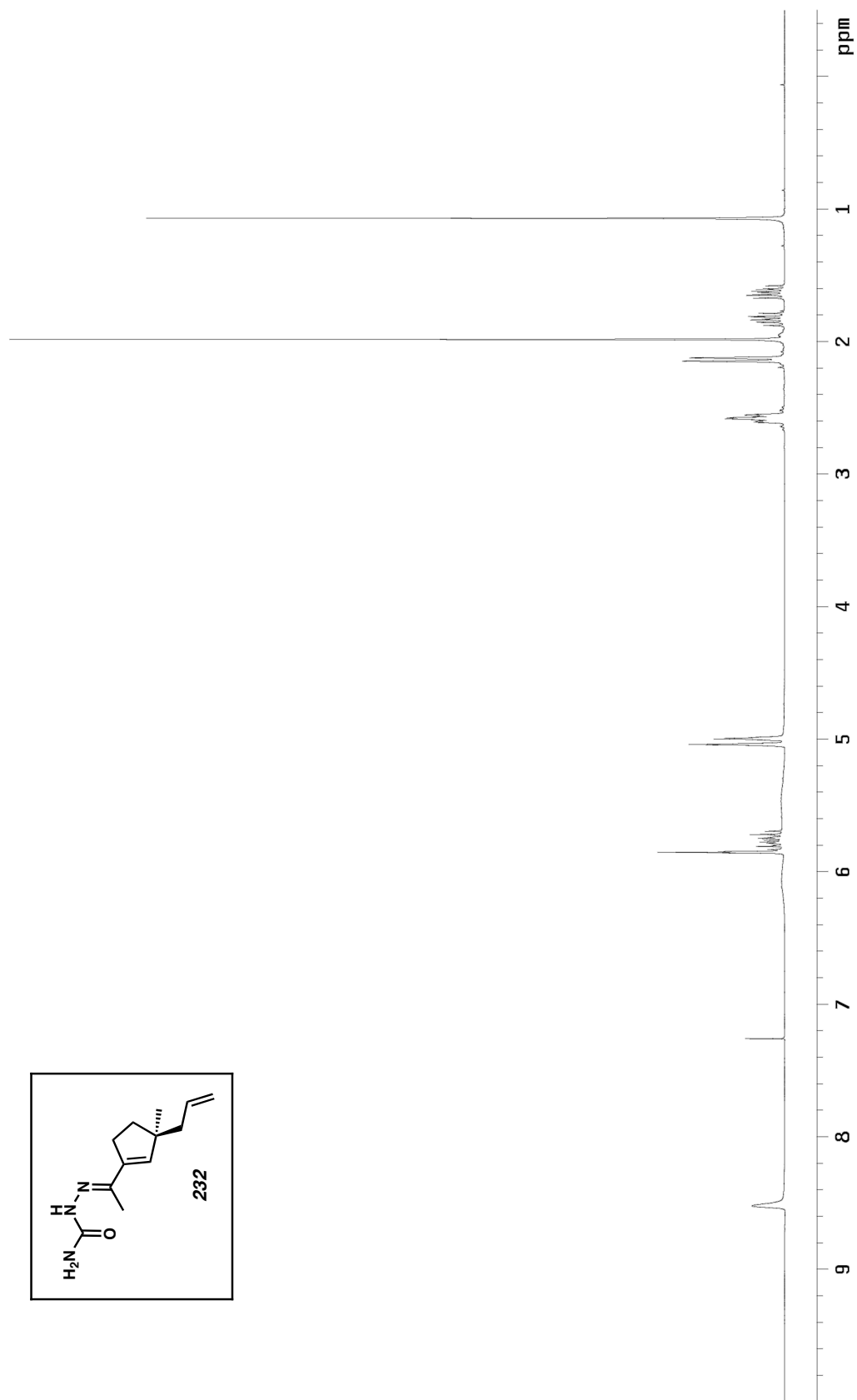


Figure A2.106. ¹³C NMR spectrum (75 MHz, CDCl₃) of **231**.

Figure A2.107. ^1H NMR spectrum (300 MHz, CDCl_3) of **232**.

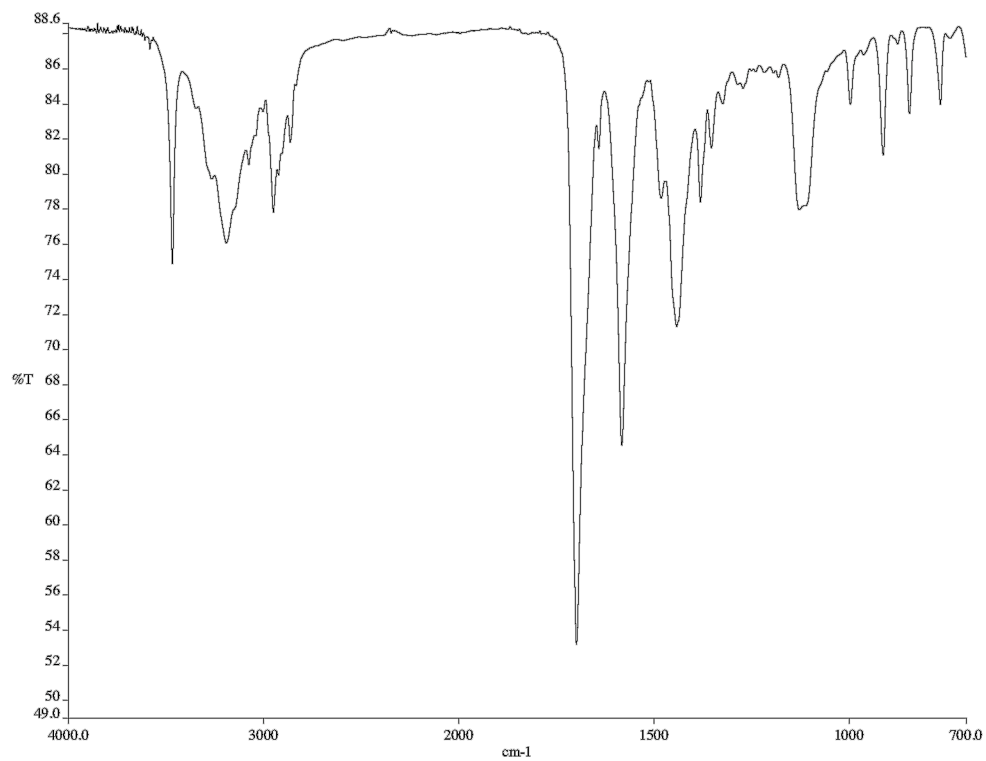


Figure A2.108. Infrared spectrum (neat film/NaCl) of **232**.

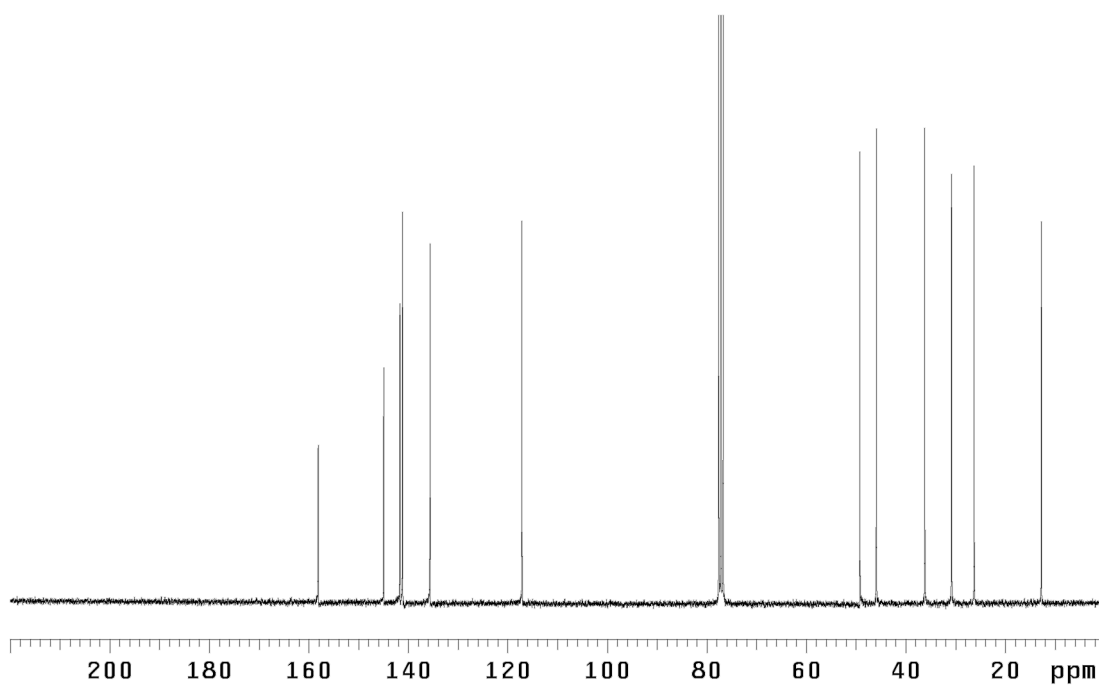
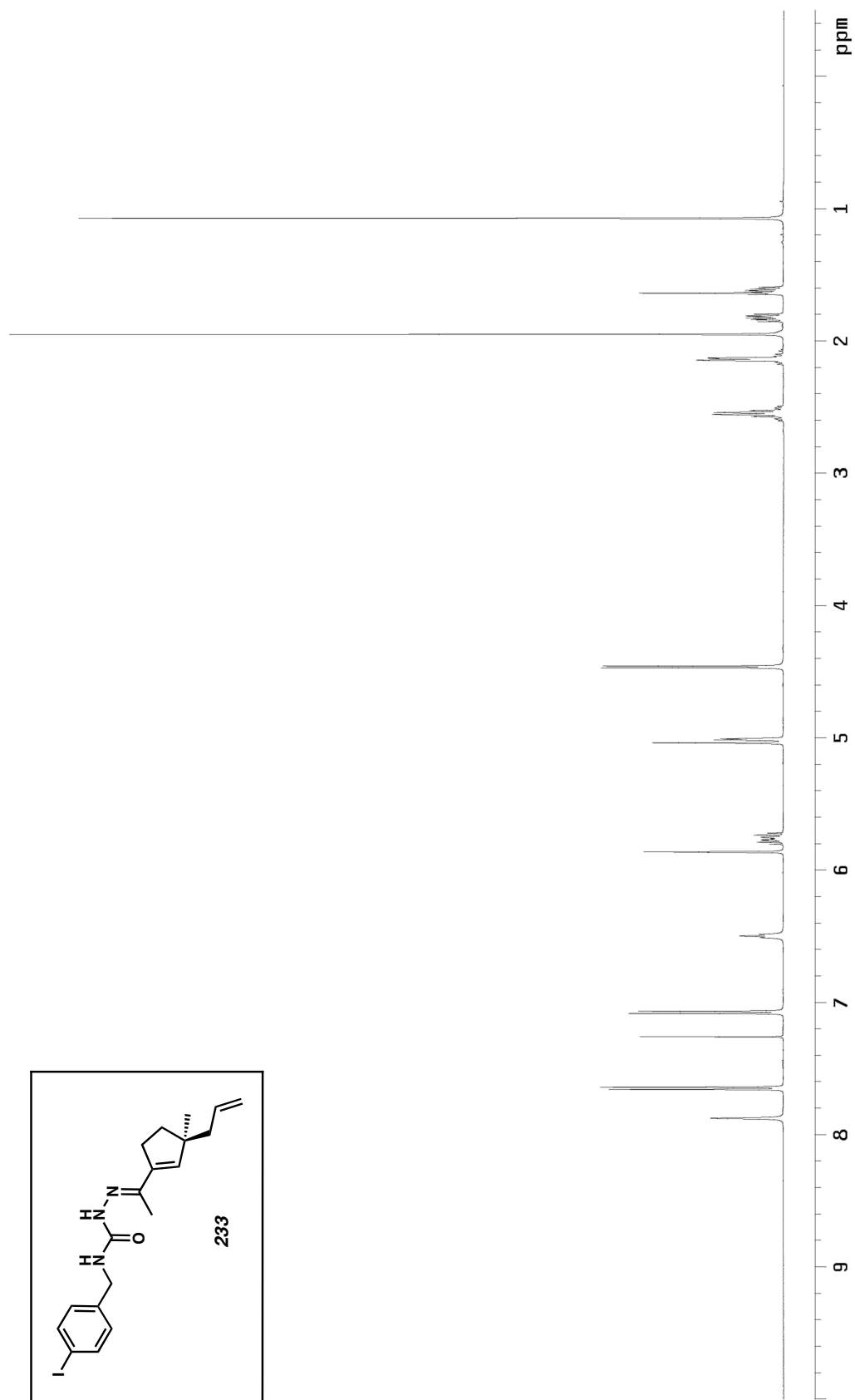


Figure A2.109. ¹³C NMR spectrum (75 MHz, CDCl₃) of **232**.

Figure A2.110. ^1H NMR spectrum (500 MHz, CDCl_3) of **233**.

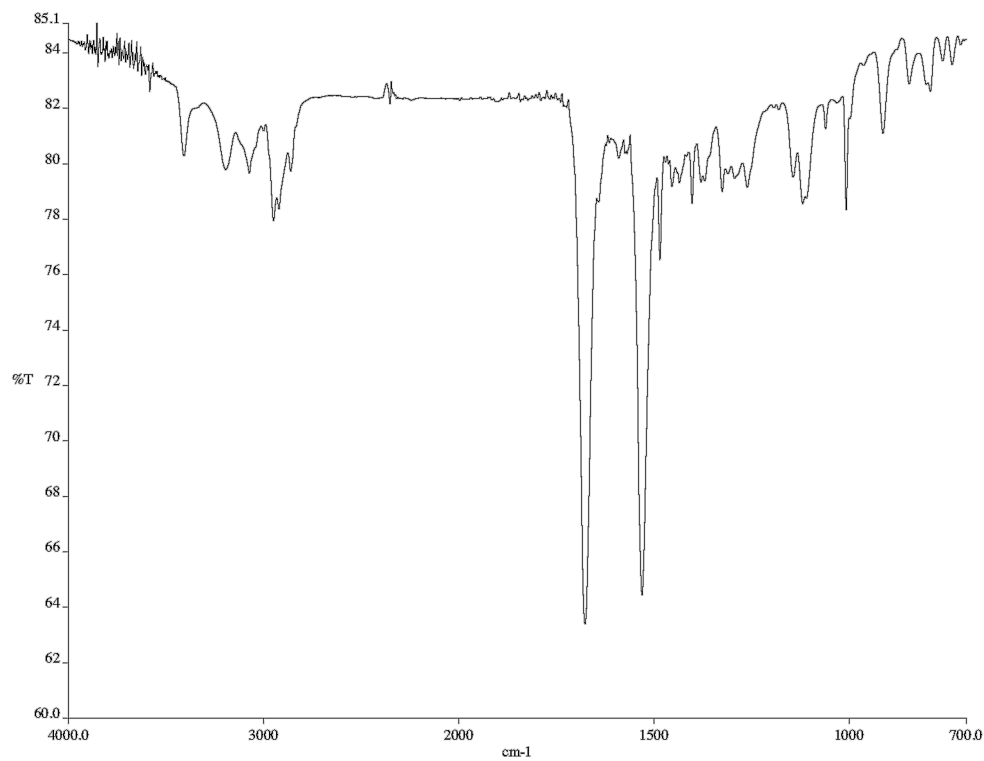


Figure A2.111. Infrared spectrum (neat film/NaCl) of **233**.

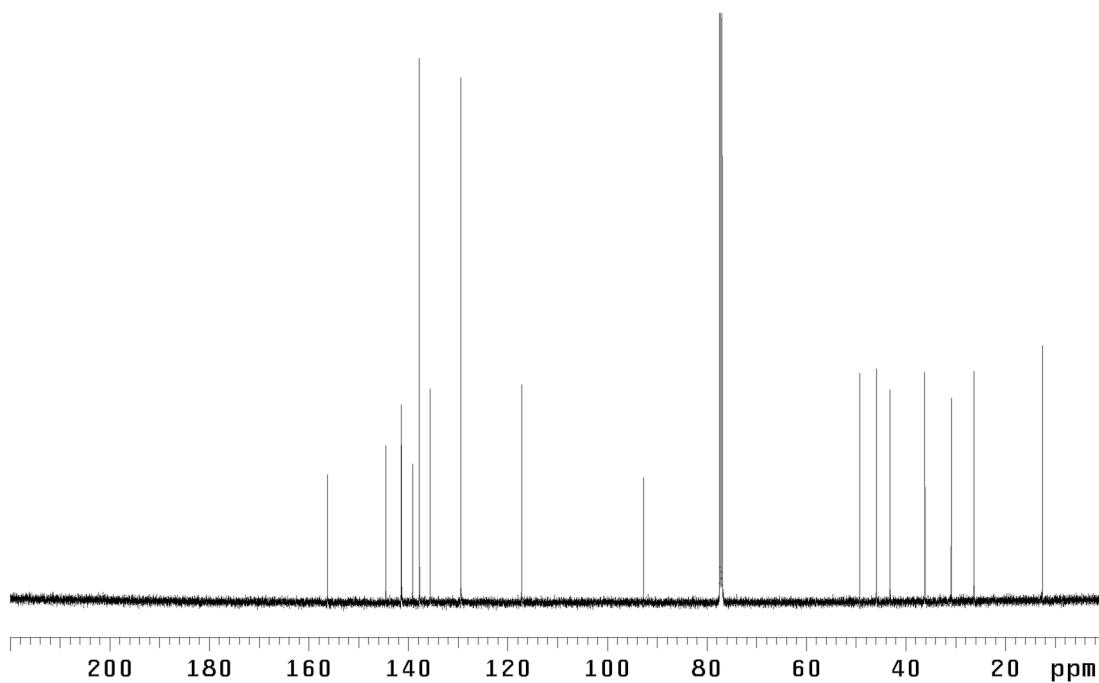
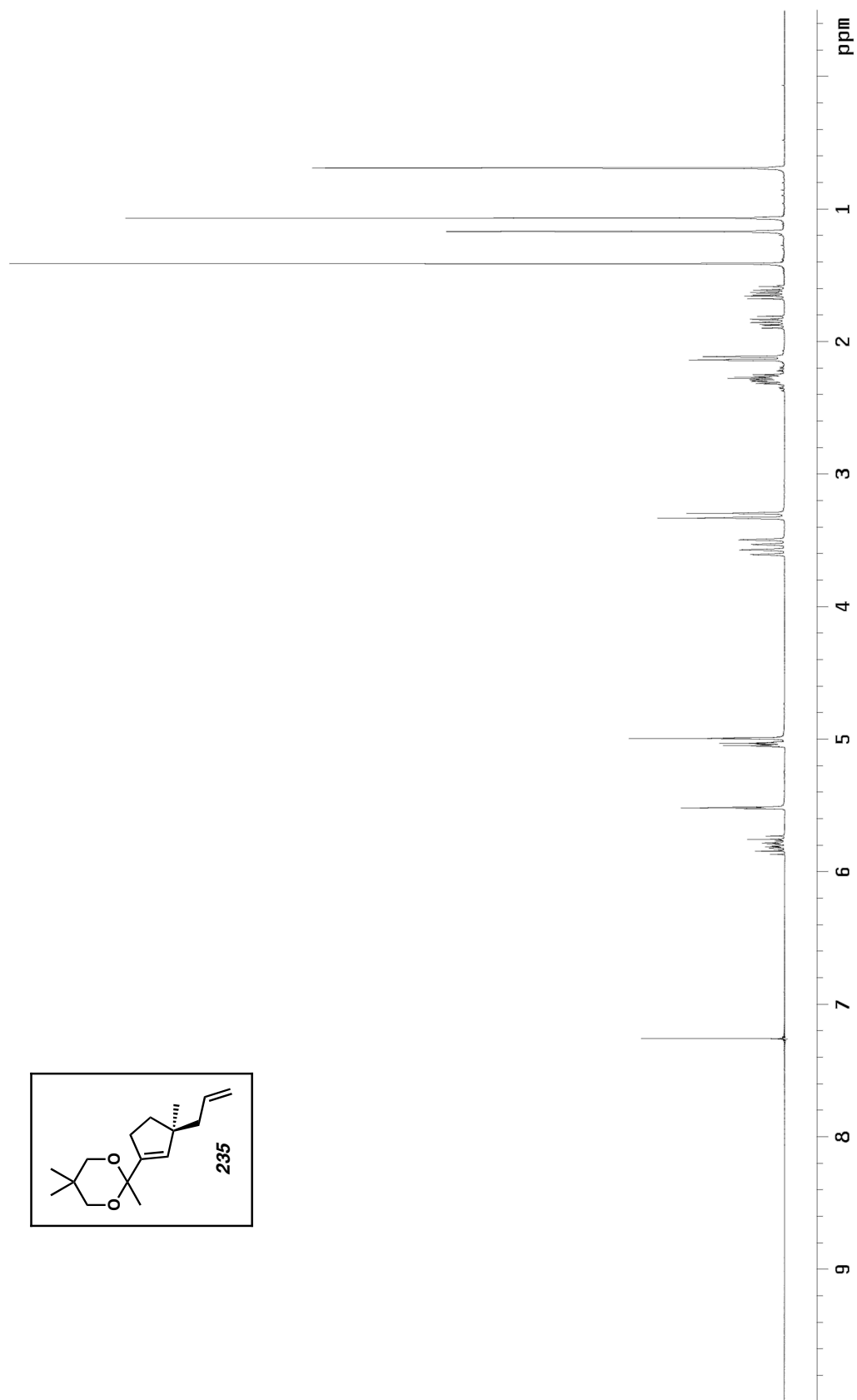


Figure A2.112. ¹³C NMR spectrum (126 MHz, CDCl₃) of **233**.

Figure A2.113. ^1H NMR spectrum (300 MHz, CDCl_3) of **235**.

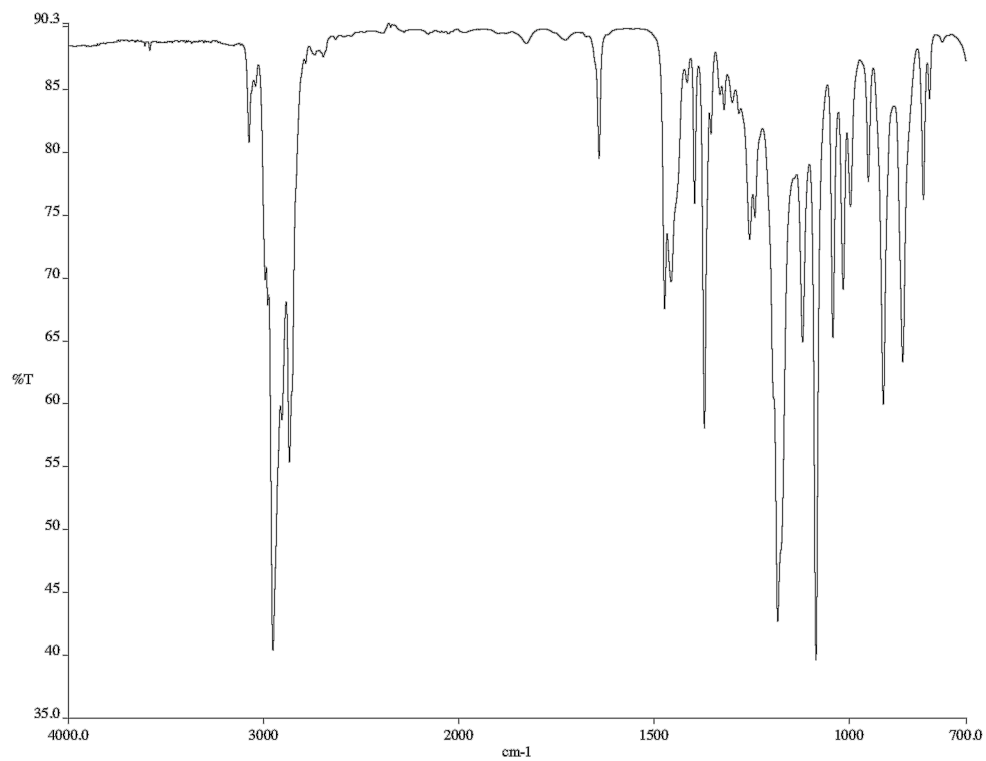


Figure A2.114. Infrared spectrum (neat film/NaCl) of **235**.

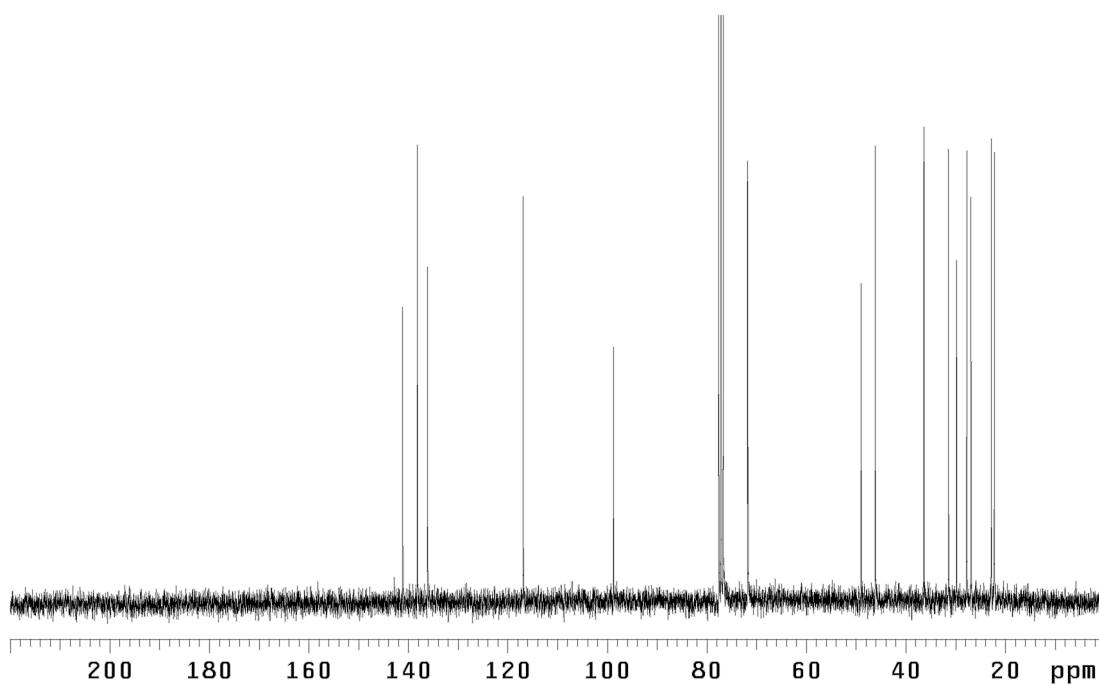
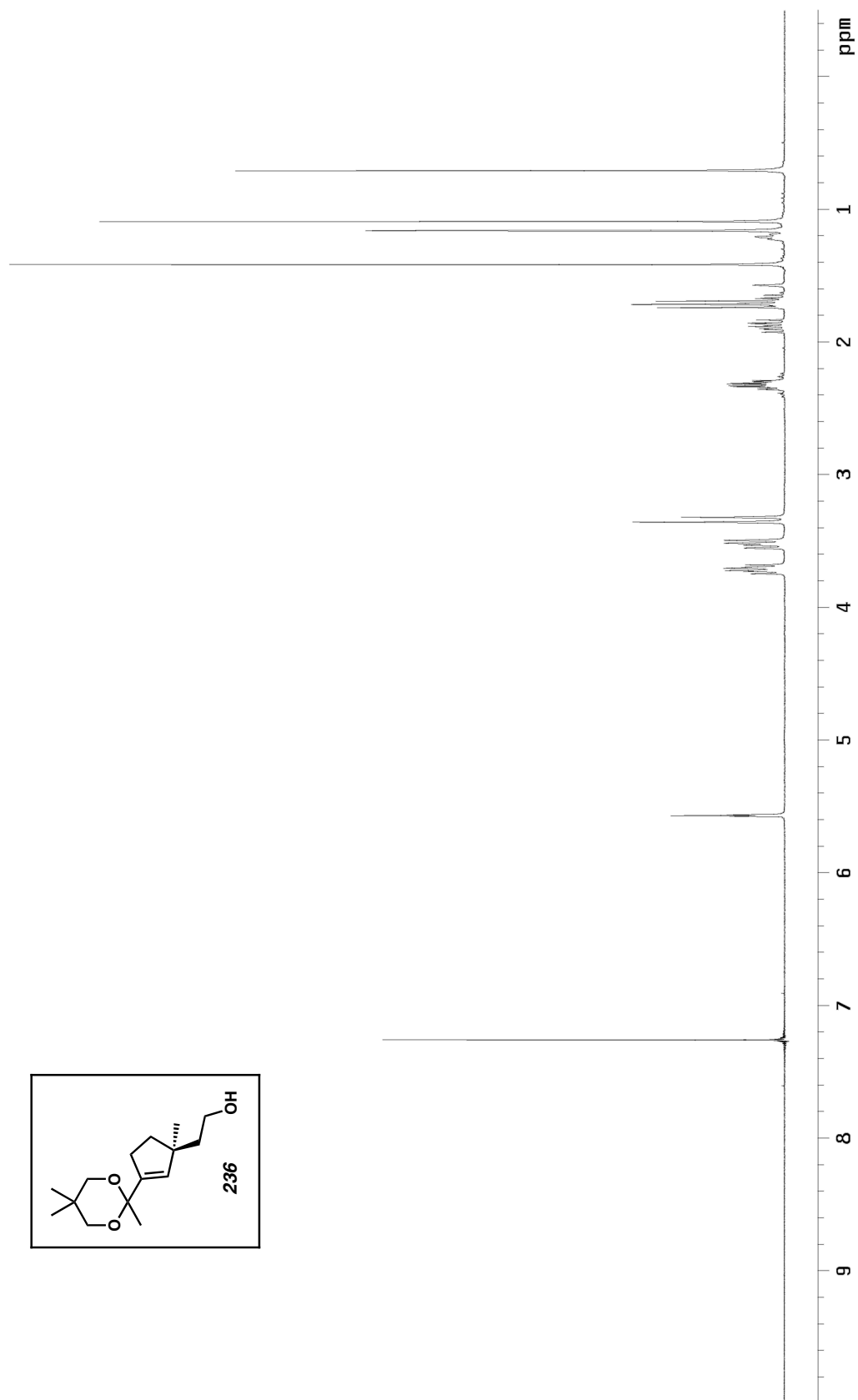


Figure A2.115. ¹³C NMR spectrum (75 MHz, CDCl₃) of **235**.

Figure A2.116. ^1H NMR spectrum (500 MHz, CDCl_3) of **236**.

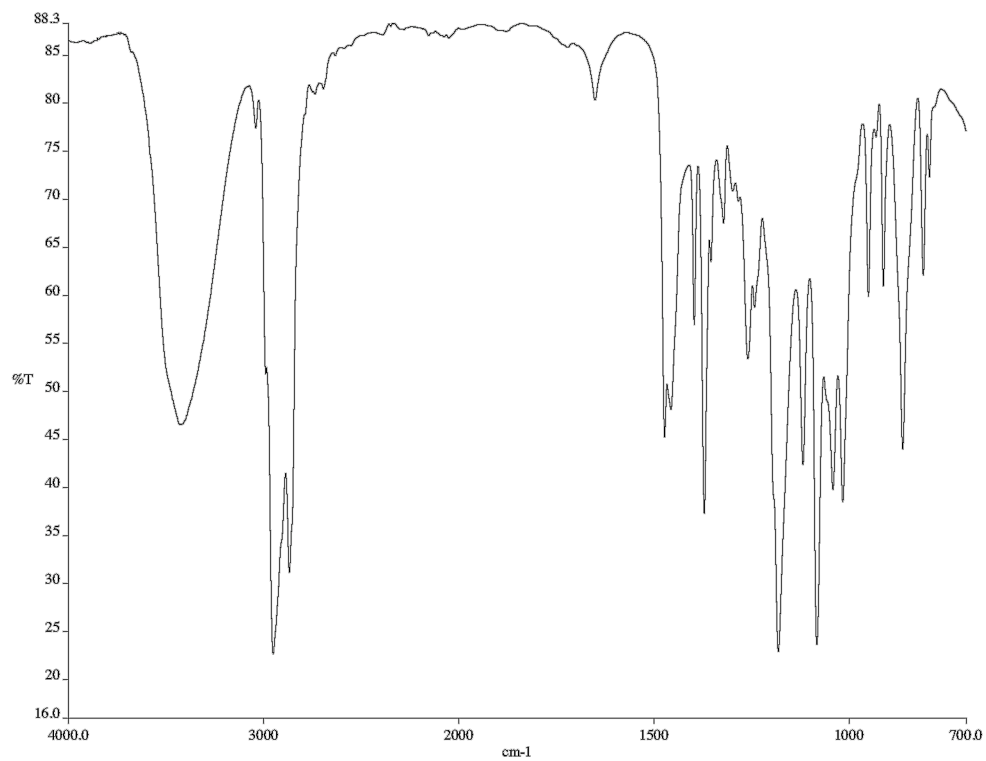


Figure A2.117. Infrared spectrum (neat film/NaCl) of **236**.

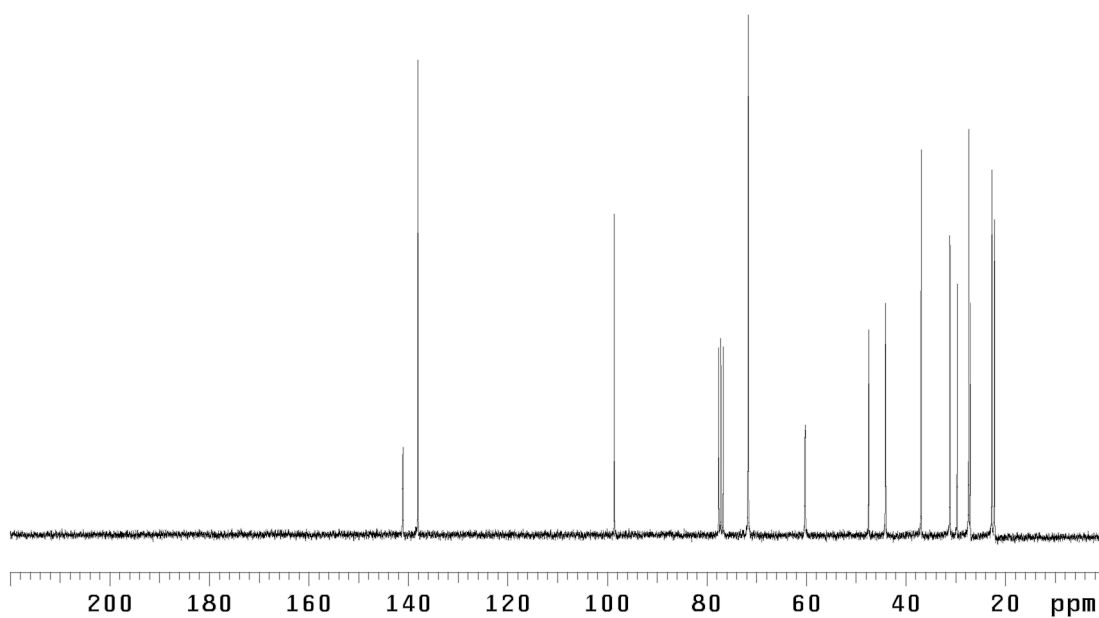
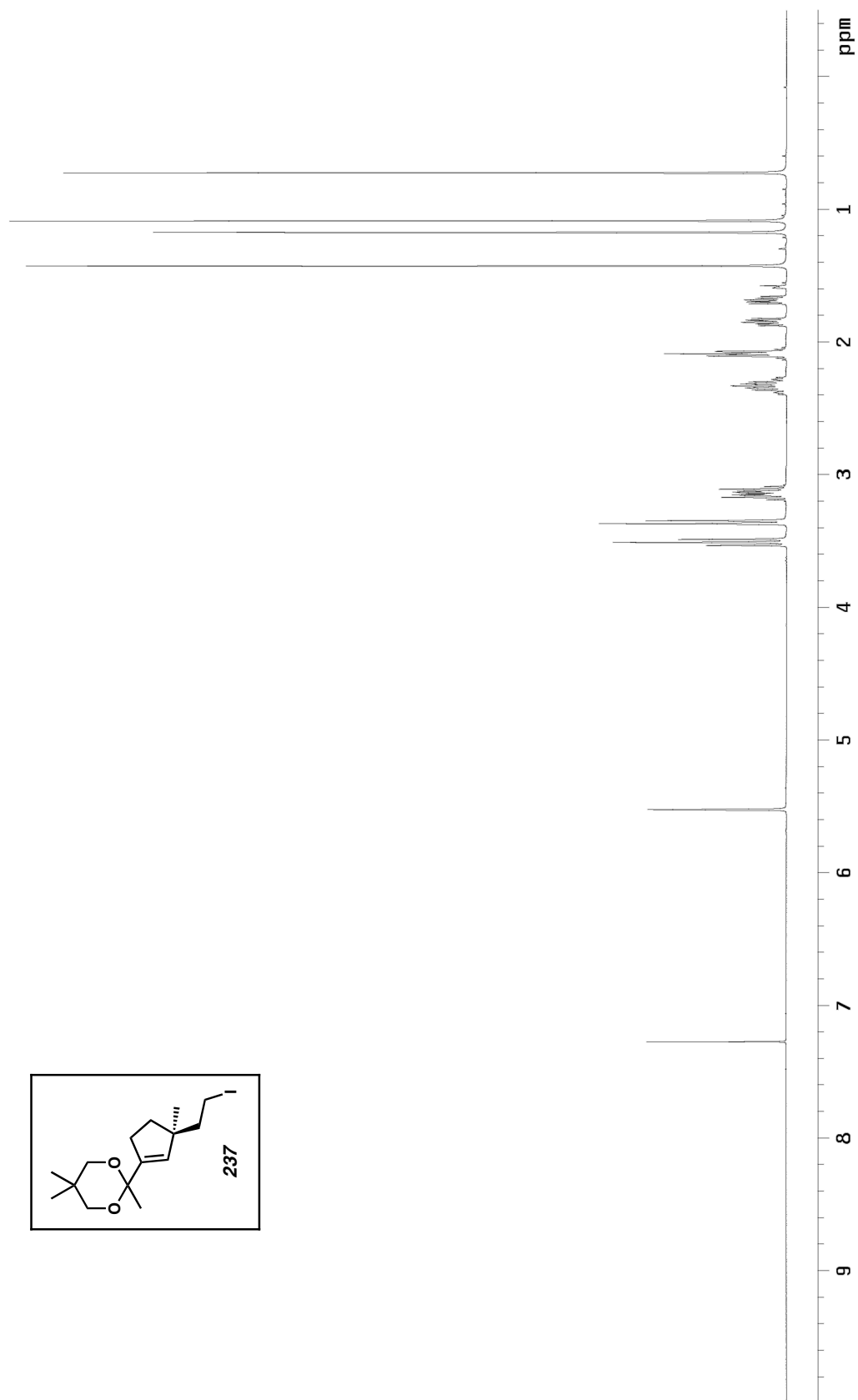


Figure A2.118. ¹³C NMR spectrum (75 MHz, CDCl₃) of **236**.

Figure A2.119. ^1H NMR spectrum (500 MHz, CDCl_3) of **237**.

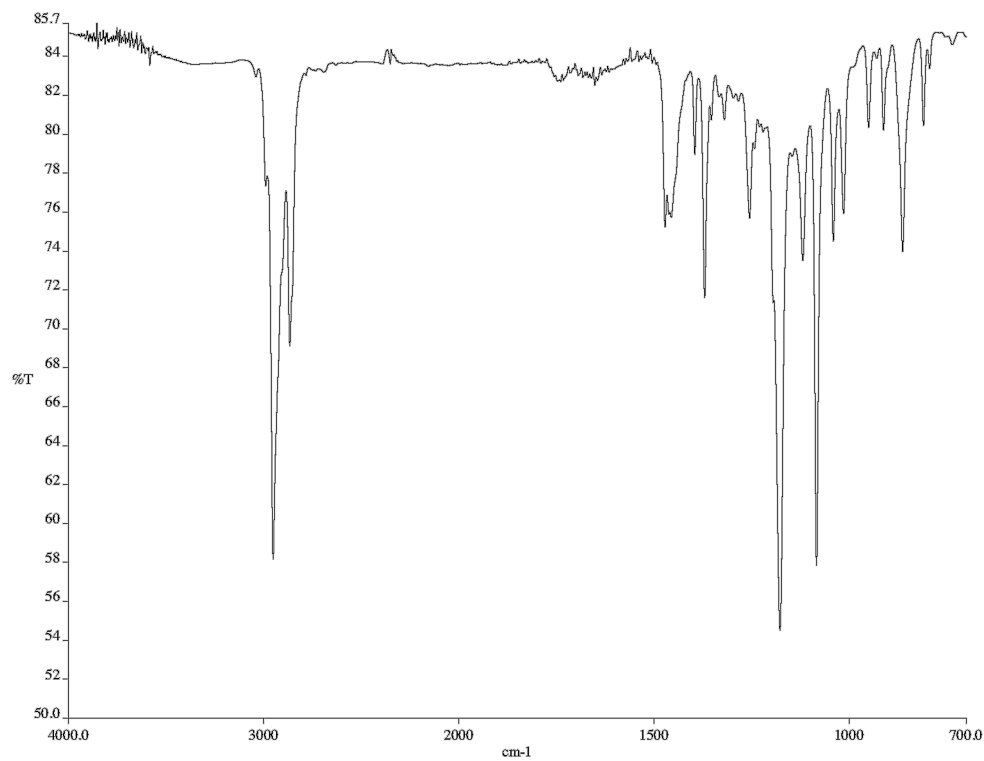


Figure A2.120. Infrared spectrum (neat film/NaCl) of **237**.

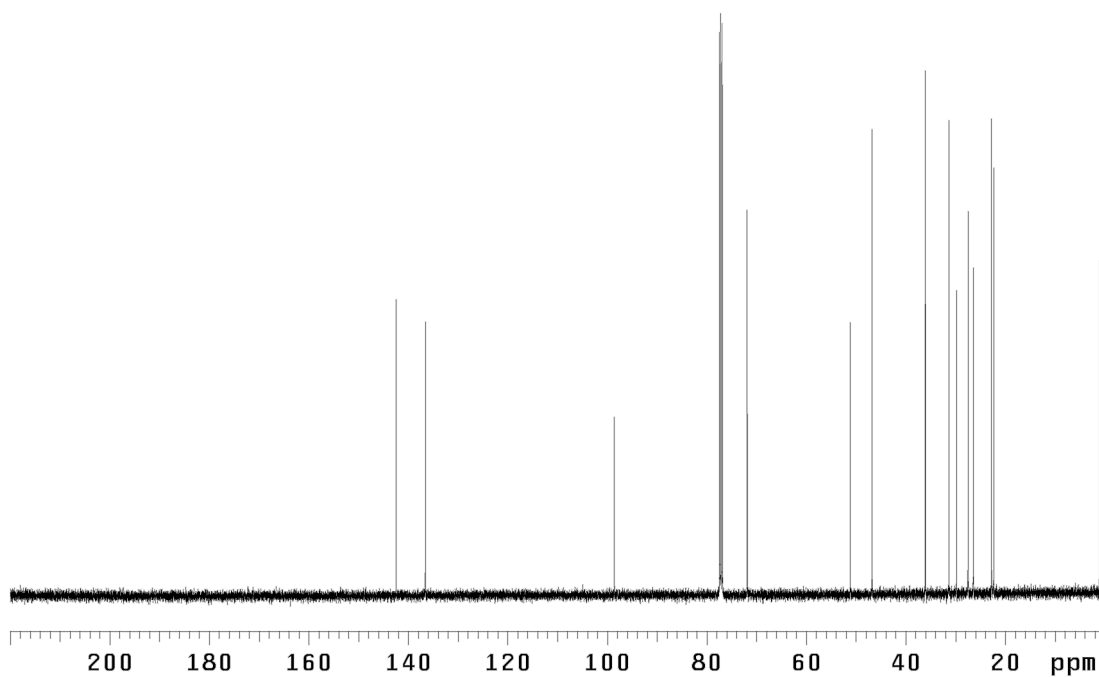
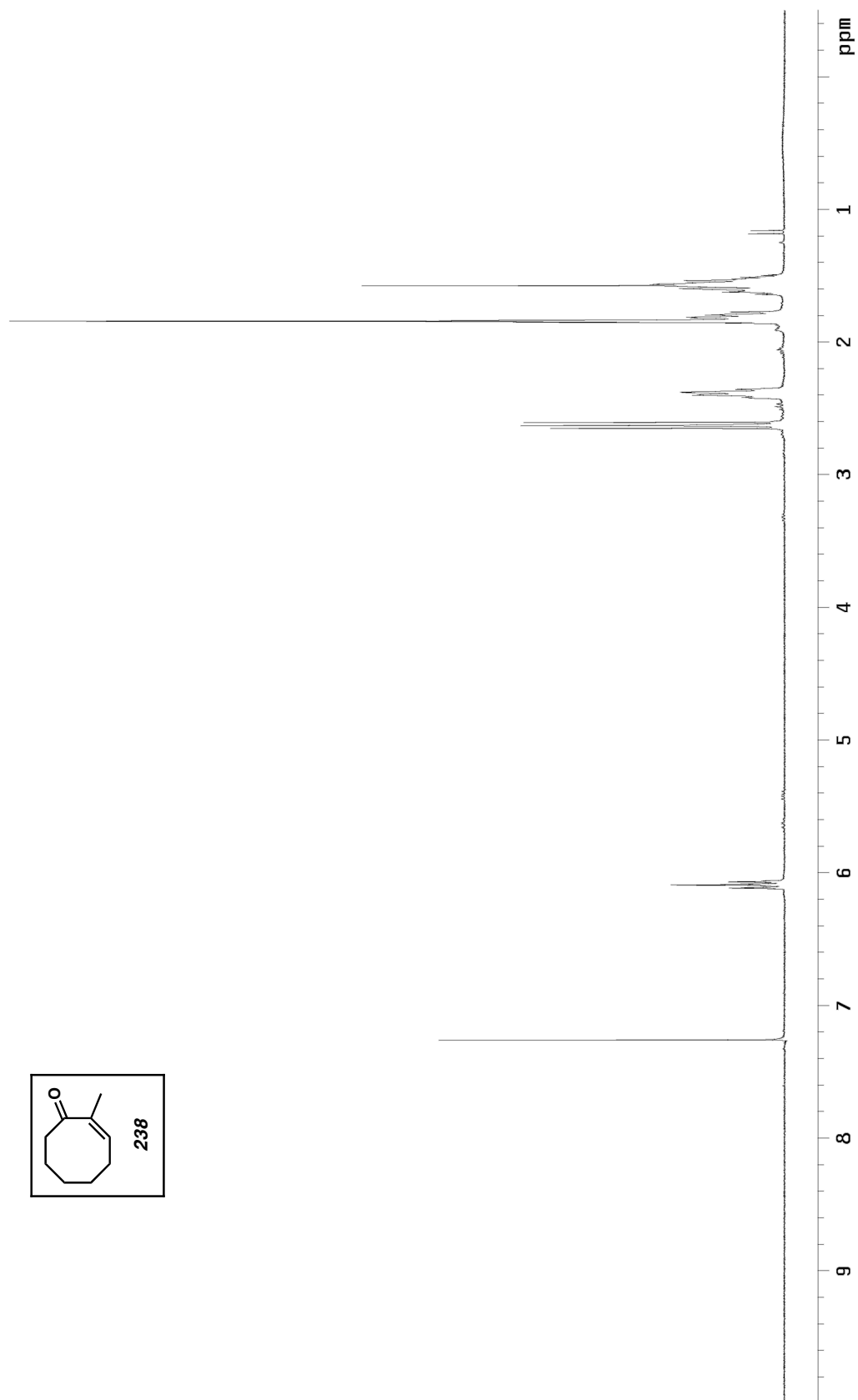


Figure A2.121. ¹³C NMR spectrum (126 MHz, CDCl₃) of **237**.

Figure A2.122. ^1H NMR spectrum (300 MHz, CDCl_3) of **238**.

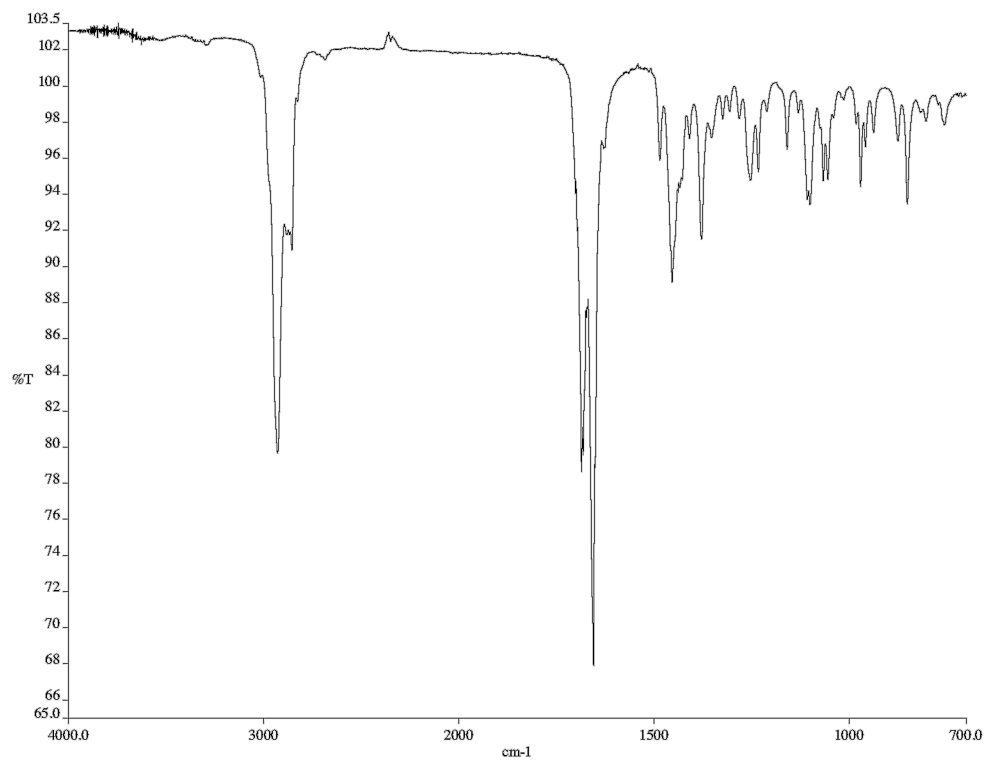


Figure A2.123. Infrared spectrum (neat film/NaCl) of **238**.

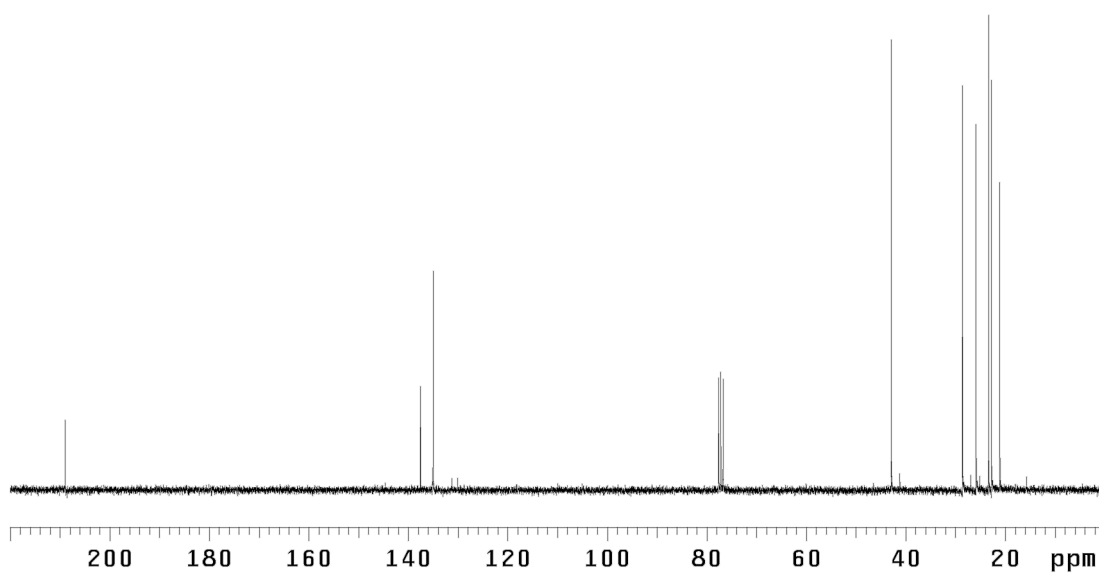
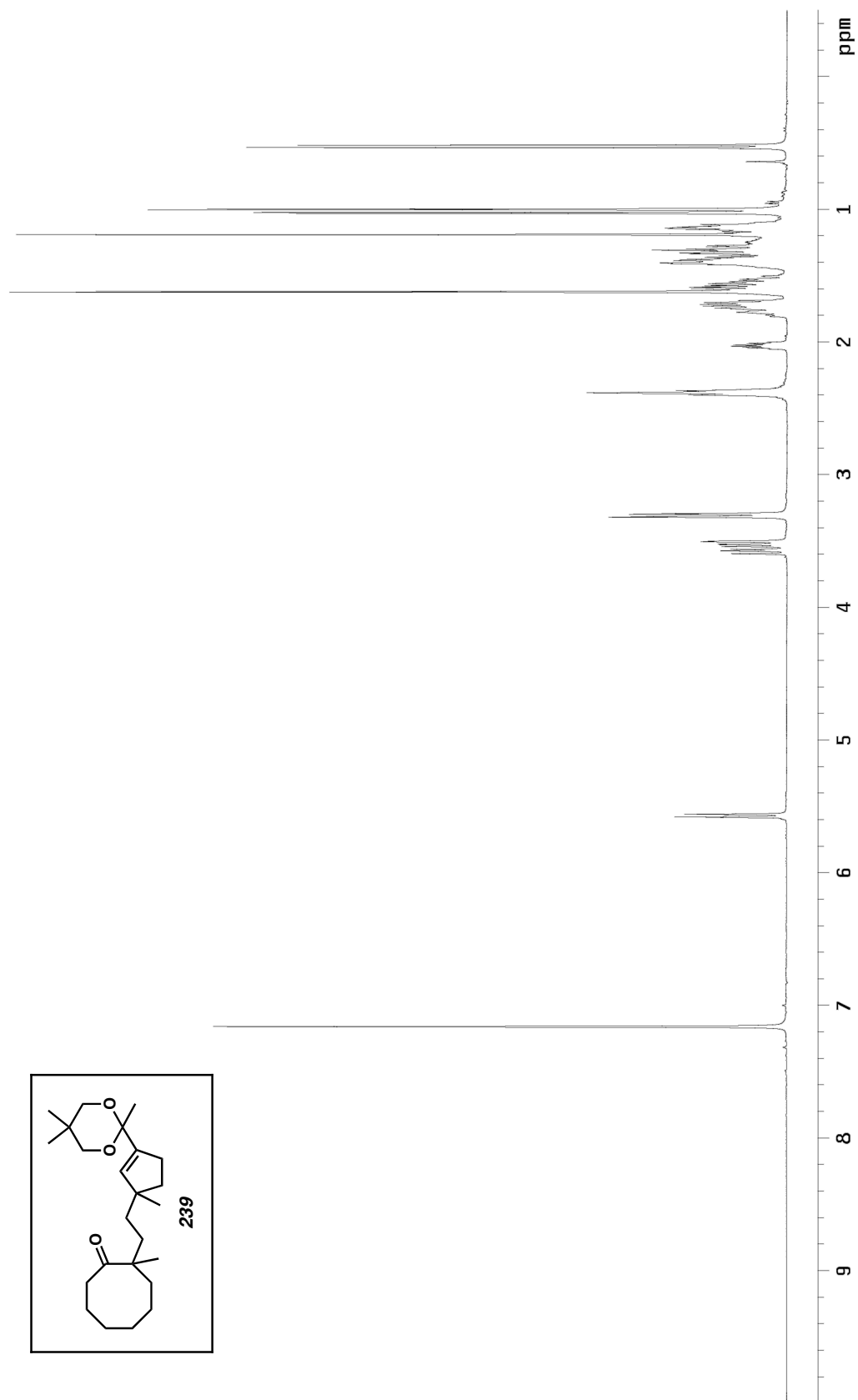


Figure A2.124. ¹³C NMR spectrum (75 MHz, CDCl₃) of **238**.

Figure A2.125. ^1H NMR spectrum (500 MHz, C_6D_6) of **239**.

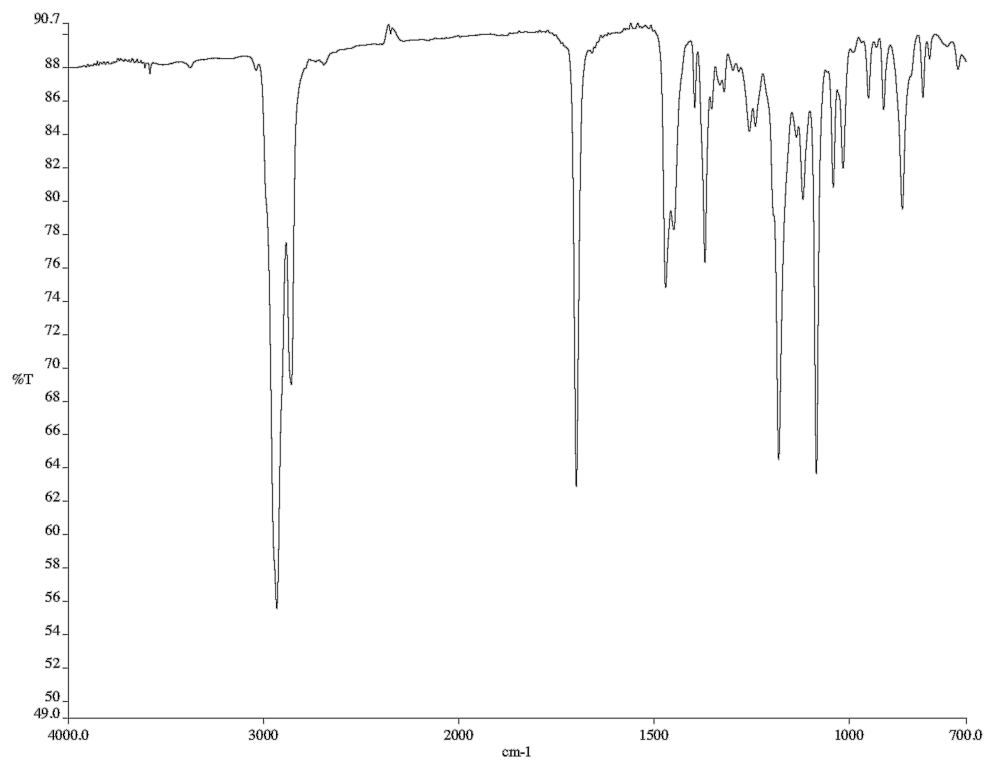


Figure A2.126. Infrared spectrum (neat film/NaCl) of **239**.

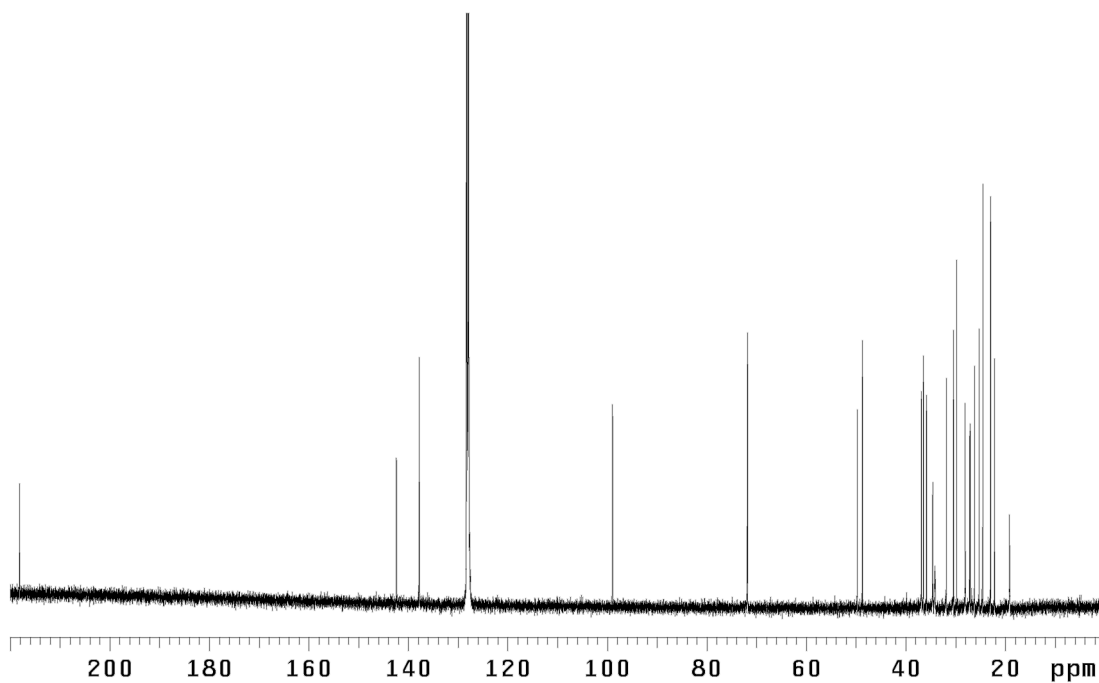
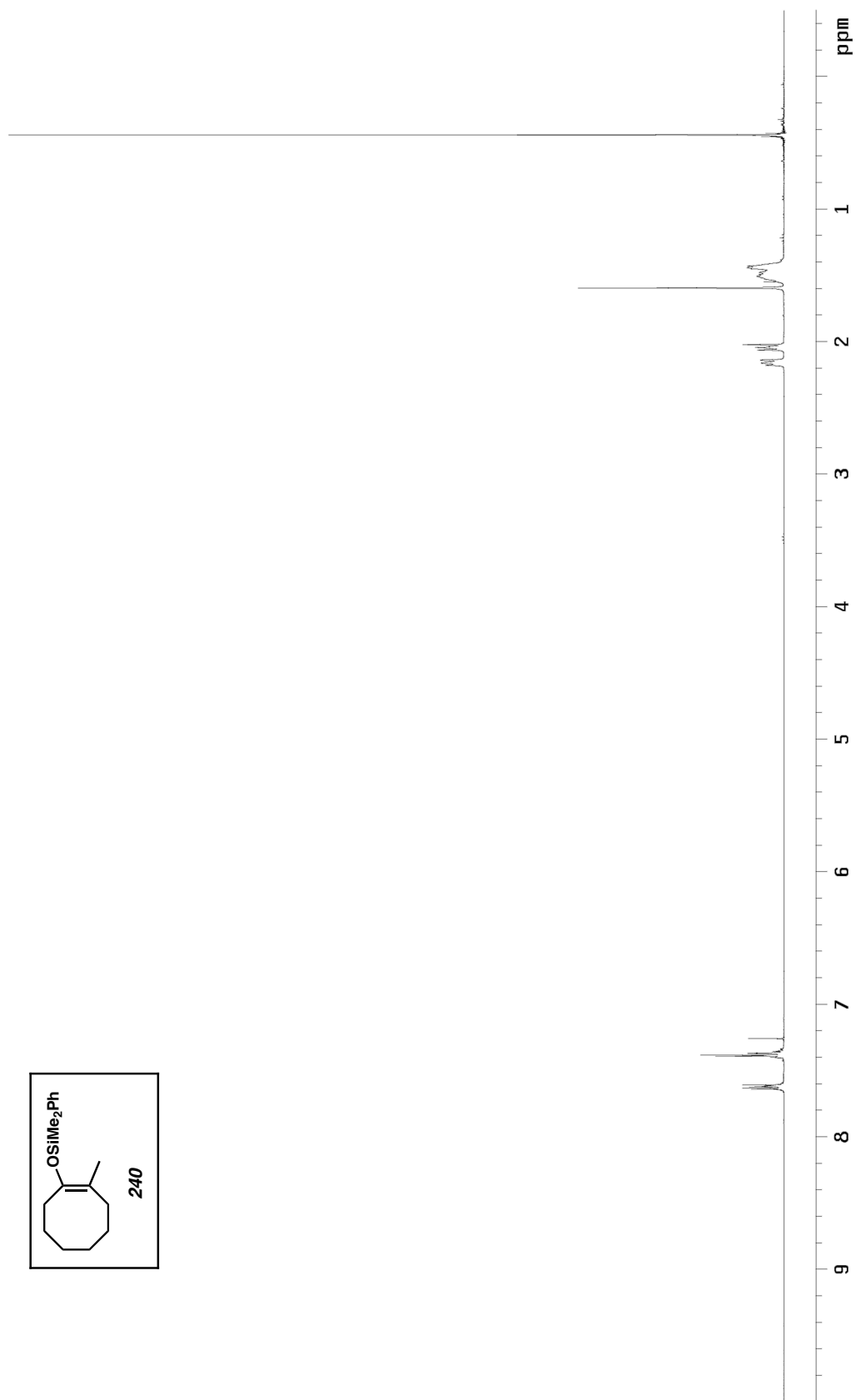


Figure A2.127. ¹³C NMR spectrum (126 MHz, C₆D₆) of **239**.

Figure A2.128. ^1H NMR spectrum (300 MHz, CDCl_3) of **240**.

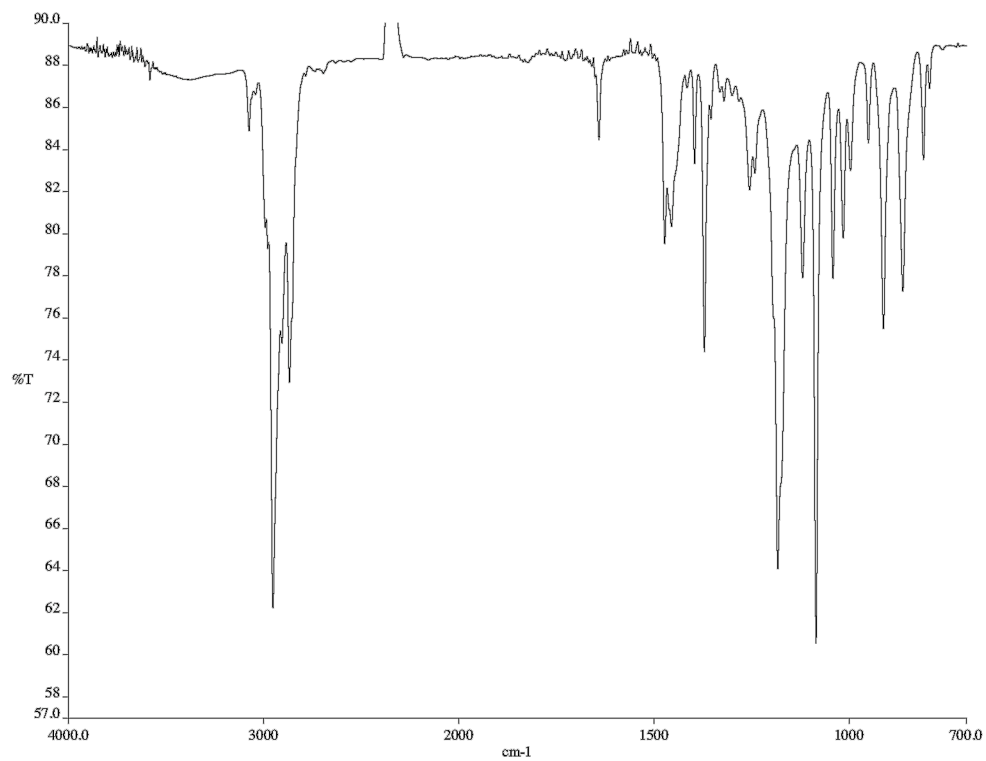


Figure A2.129. Infrared spectrum (neat film/NaCl) of **240**.

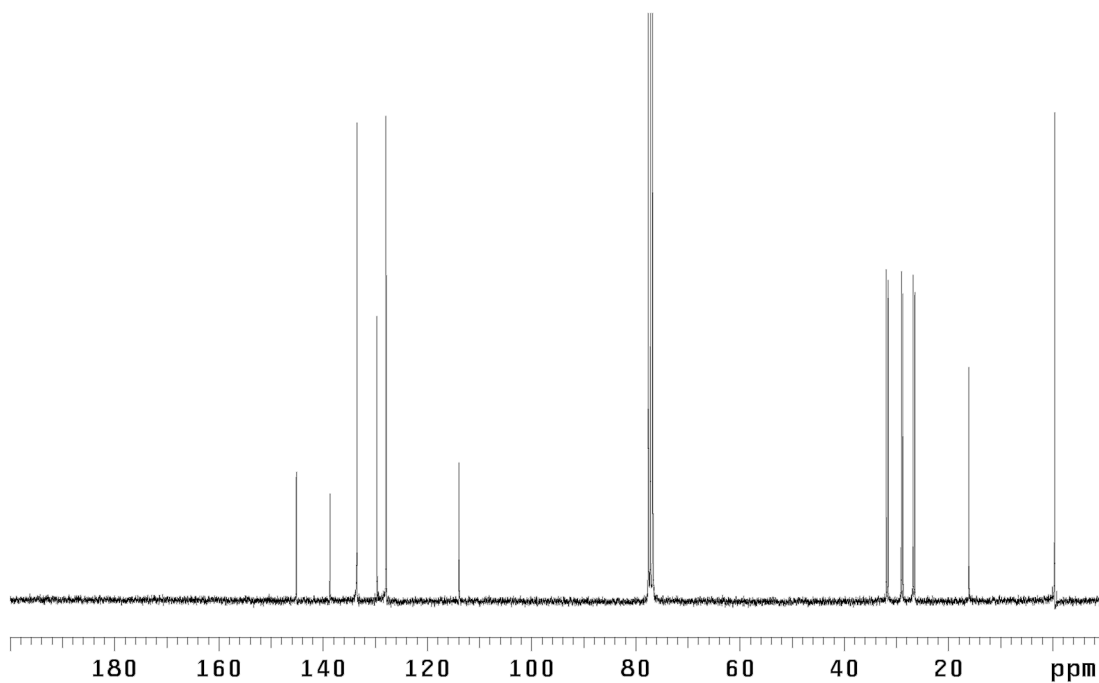
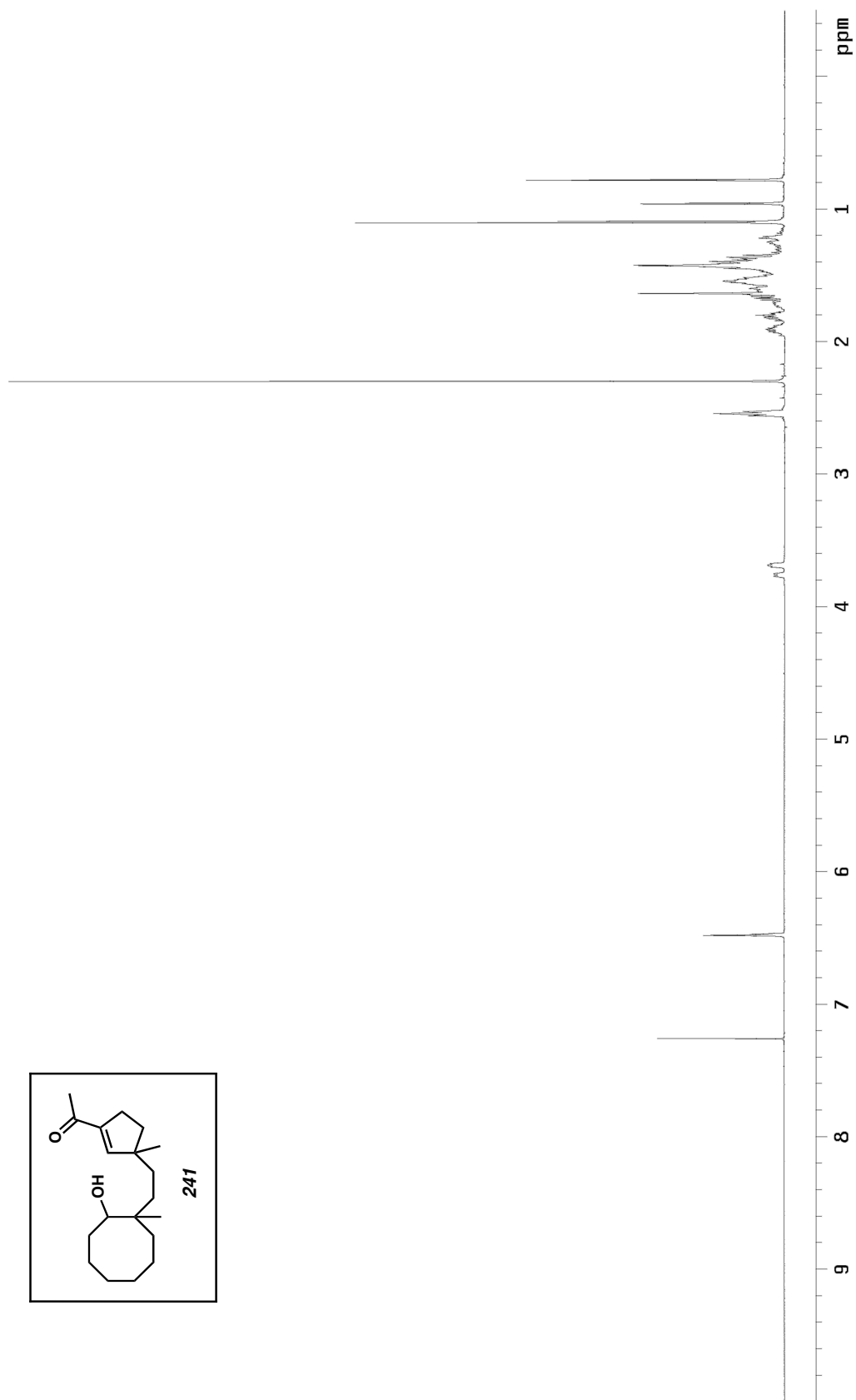


Figure A2.130. ^{13}C NMR spectrum (75 MHz, CDCl_3) of **240**.

Figure A2.131. ^1H NMR spectrum (500 MHz, CDCl_3) of **241**.

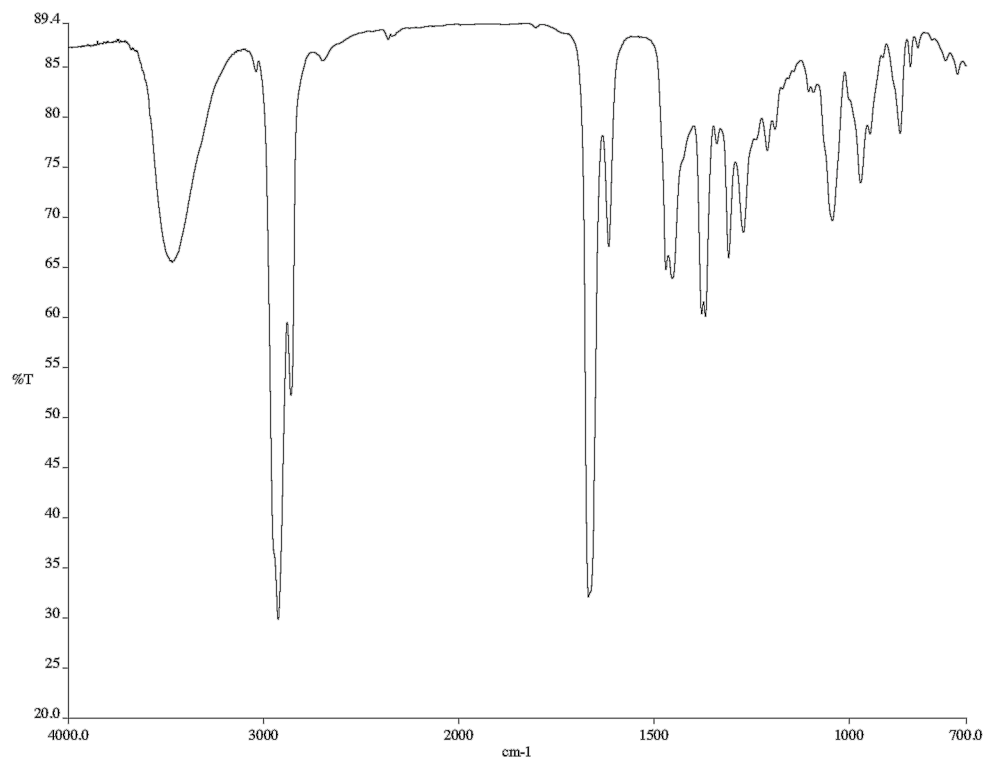


Figure A2.132. Infrared spectrum (neat film/NaCl) of **241**.

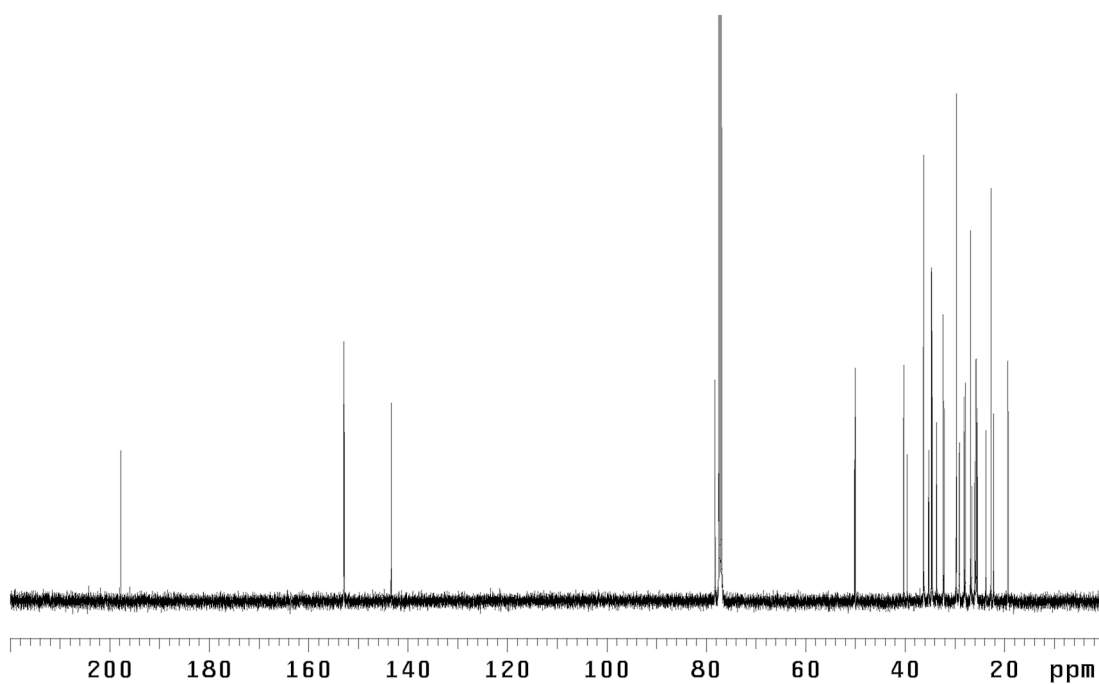
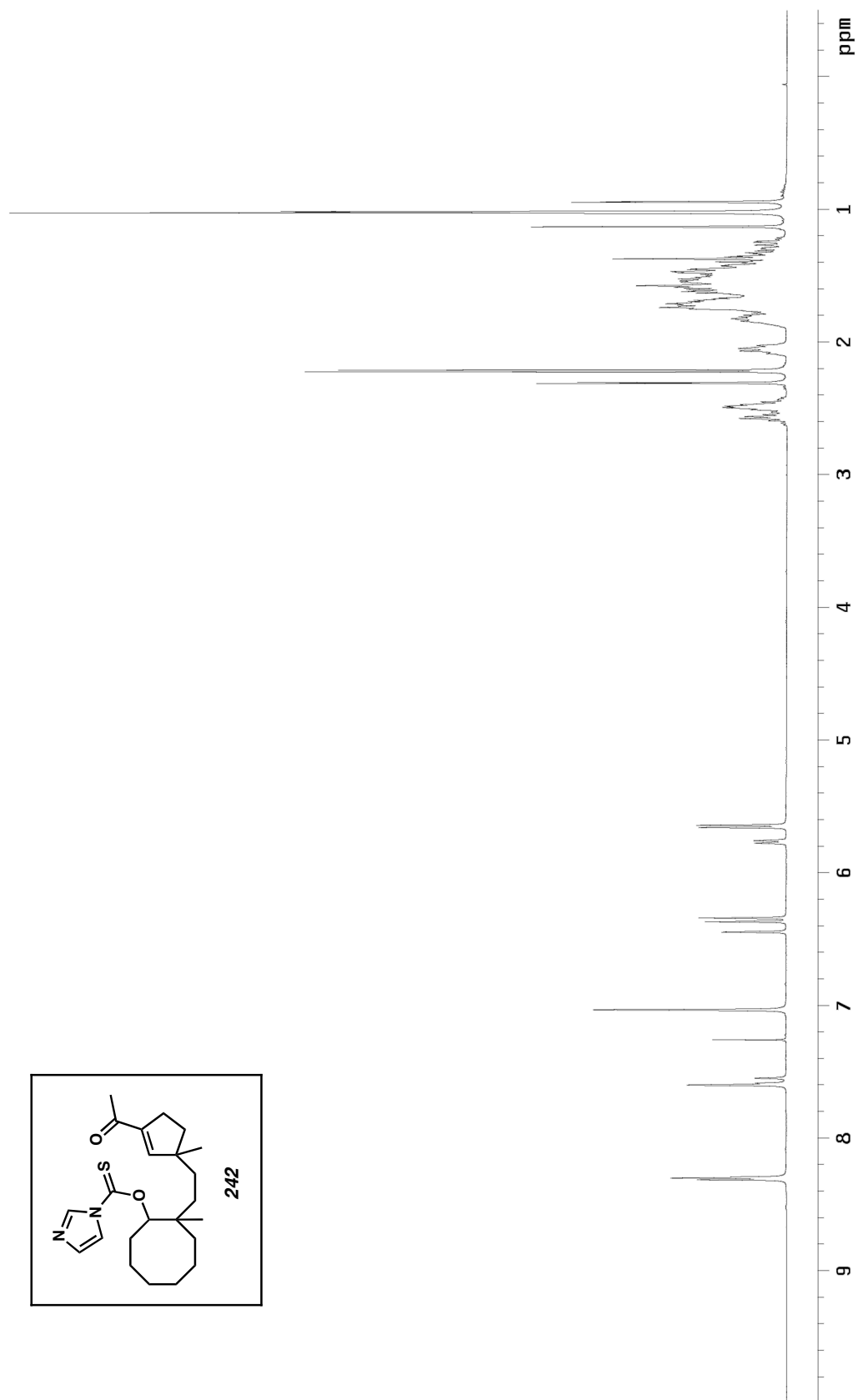


Figure A2.133. ¹³C NMR spectrum (126 MHz, CDCl₃) of **241**.

Figure A2.134. ^1H NMR spectrum (500 MHz, CDCl_3) of **242**.

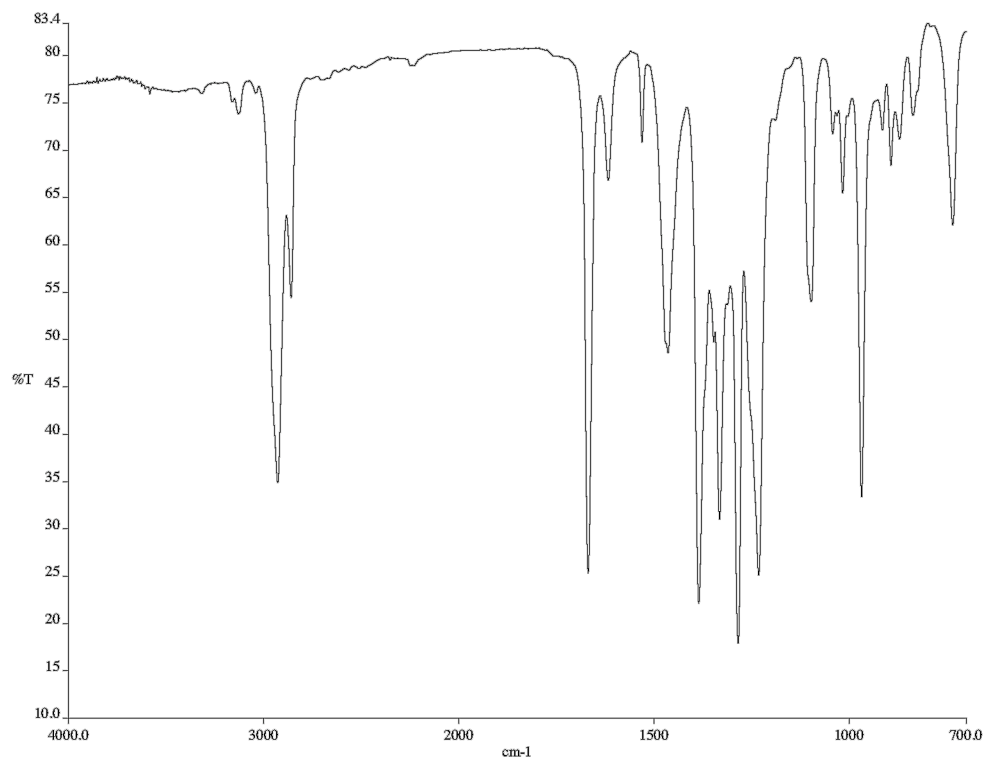


Figure A2.135. Infrared spectrum (neat film/NaCl) of **242**.

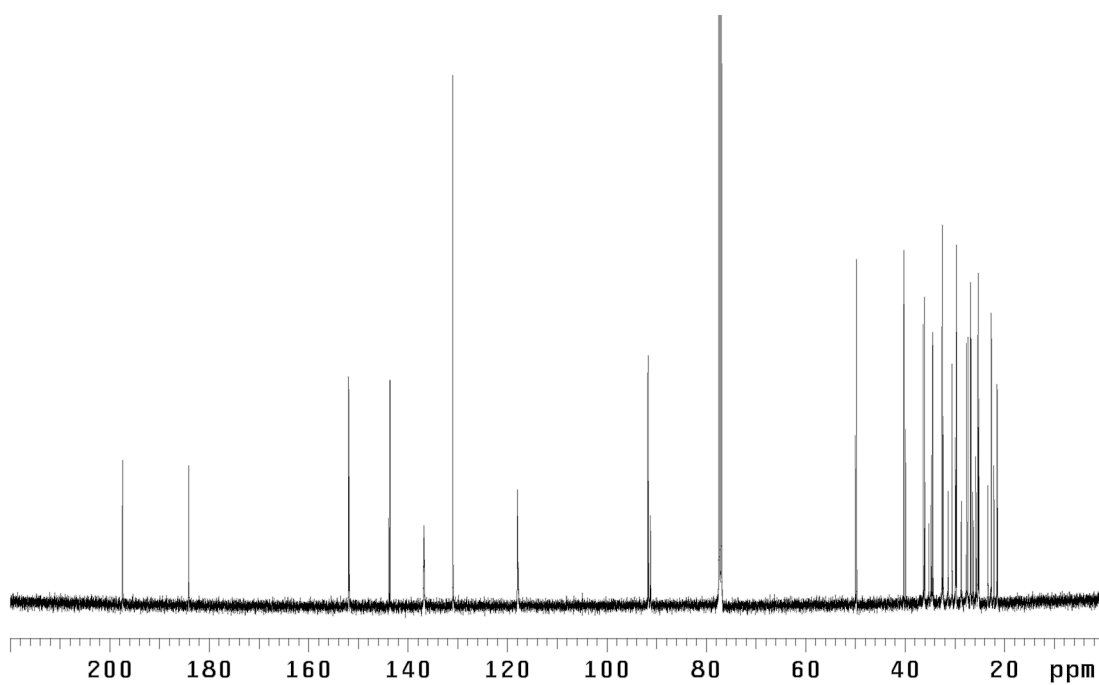


Figure A2.136. ¹³C NMR spectrum (126 MHz, CDCl₃) of **242**.

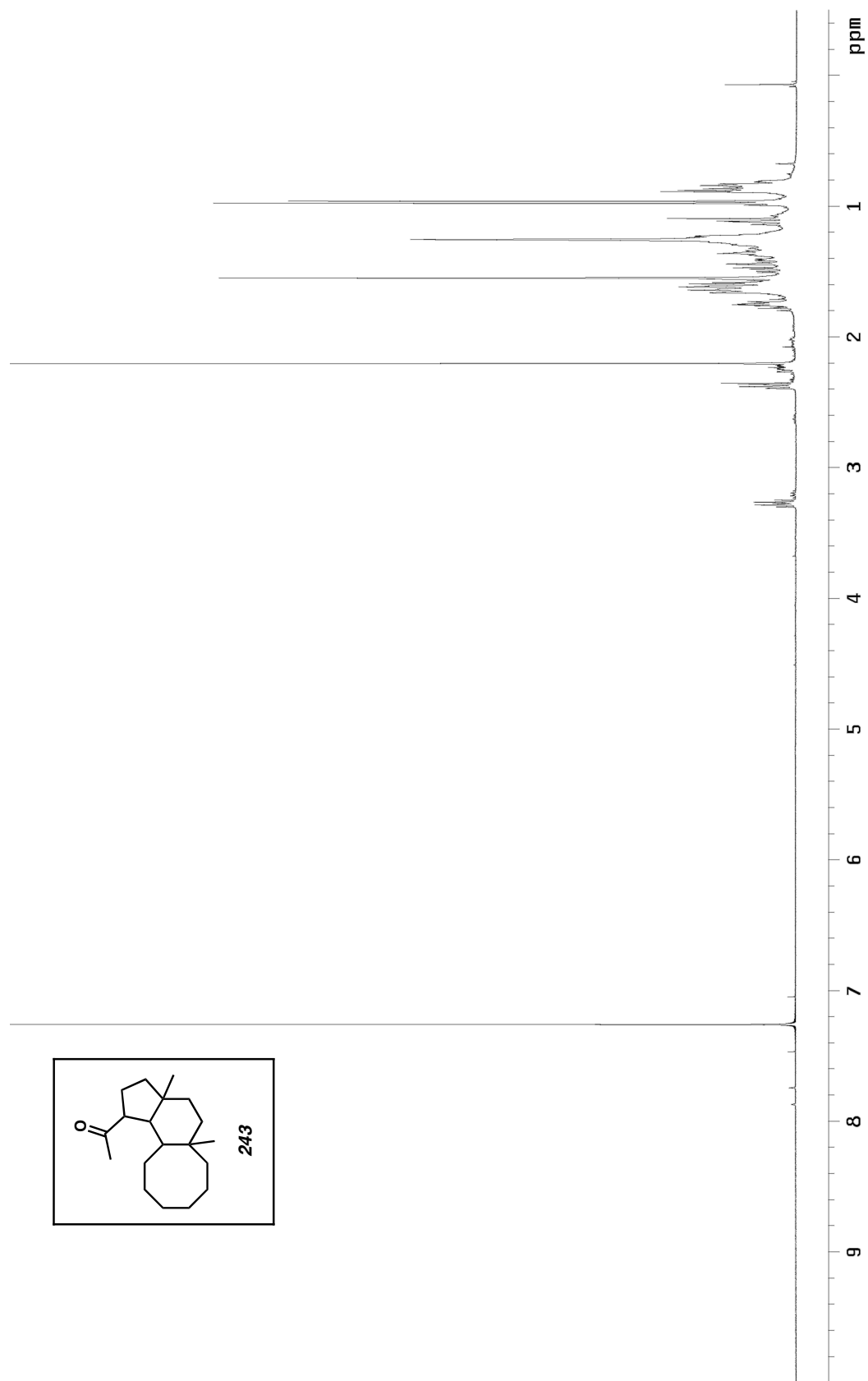


Figure A2.137. ^1H NMR spectrum (500 MHz, CDCl_3) of the major diastereomer of **243**.

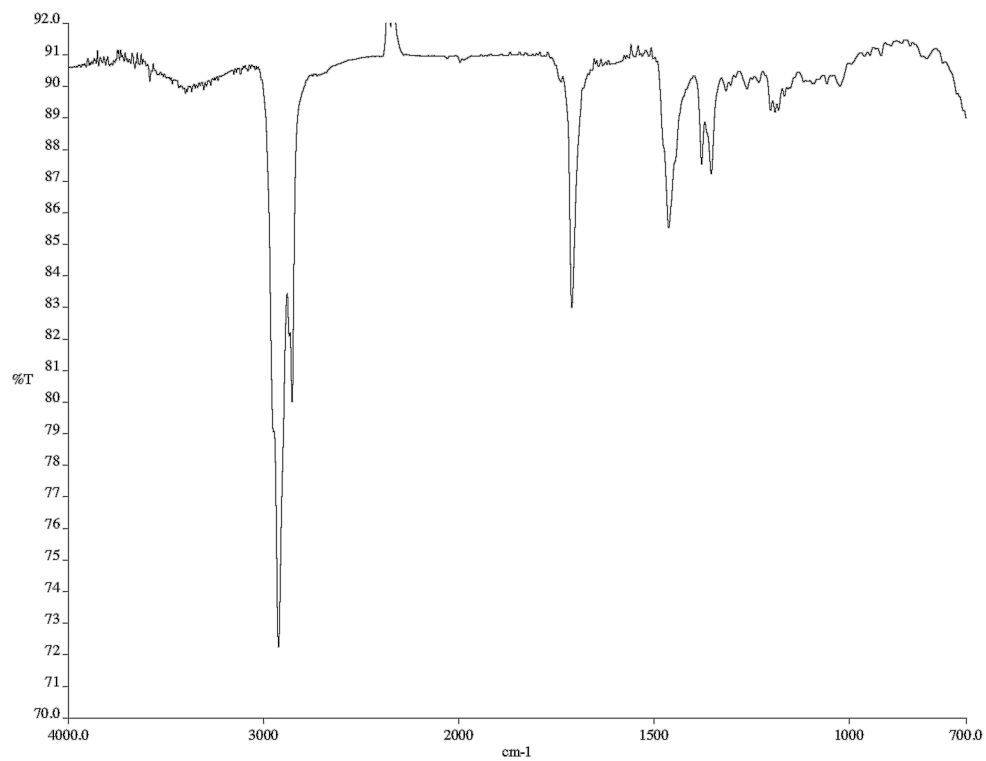


Figure A2.138. Infrared spectrum (neat film/NaCl) of the major diastereomer of **243**.

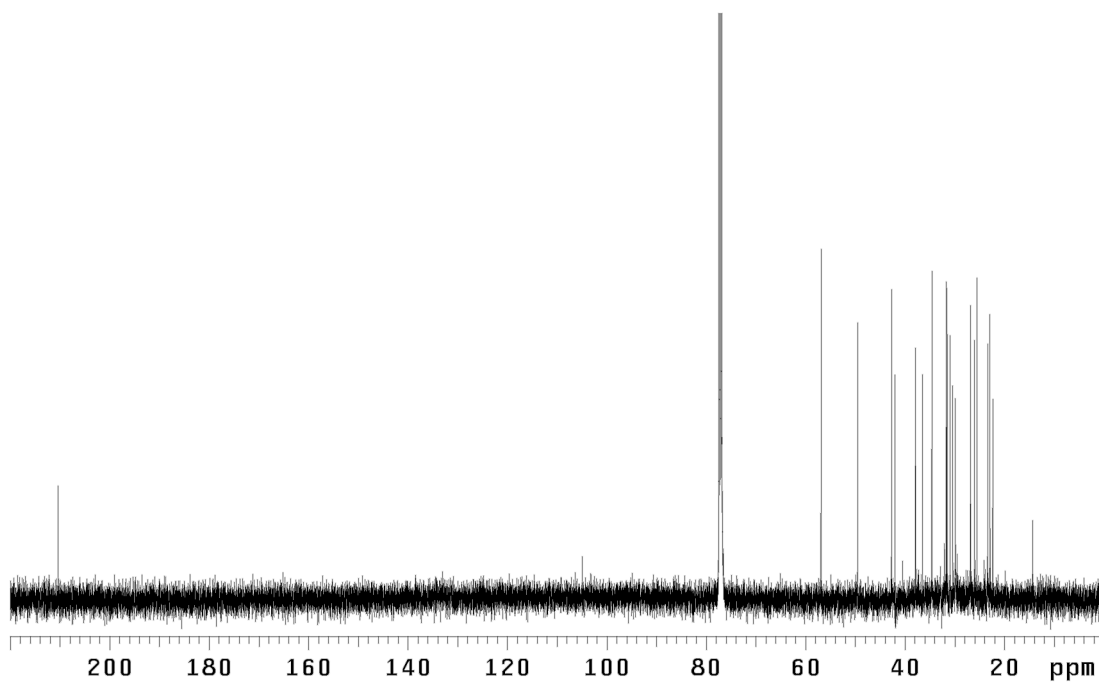


Figure A2.139. ¹³C NMR spectrum (126 MHz, CDCl₃) of the major diastereomer of **243**.

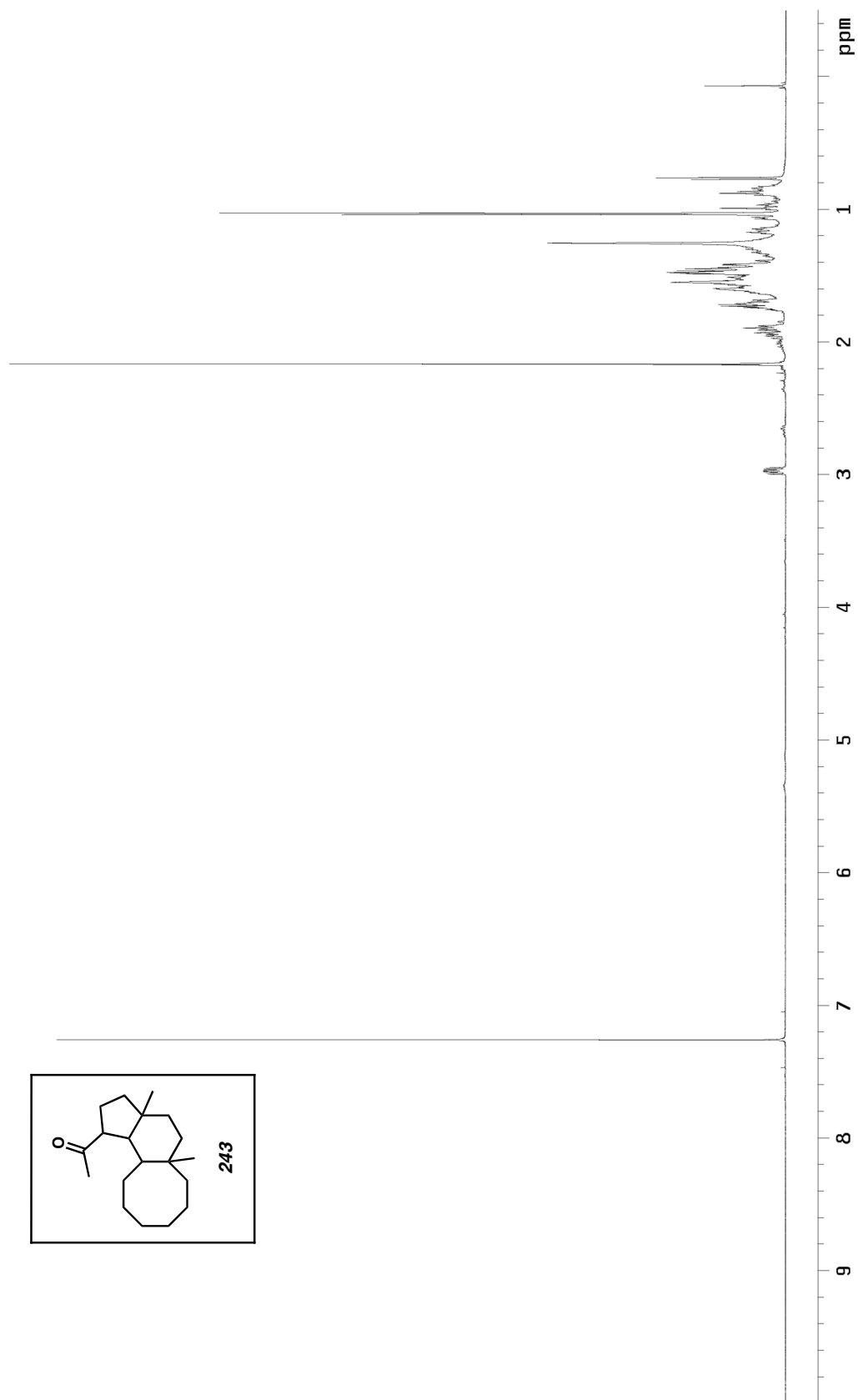


Figure A2.140. ^1H NMR spectrum (500 MHz, CDCl_3) of the minor diastereomer of **243**.

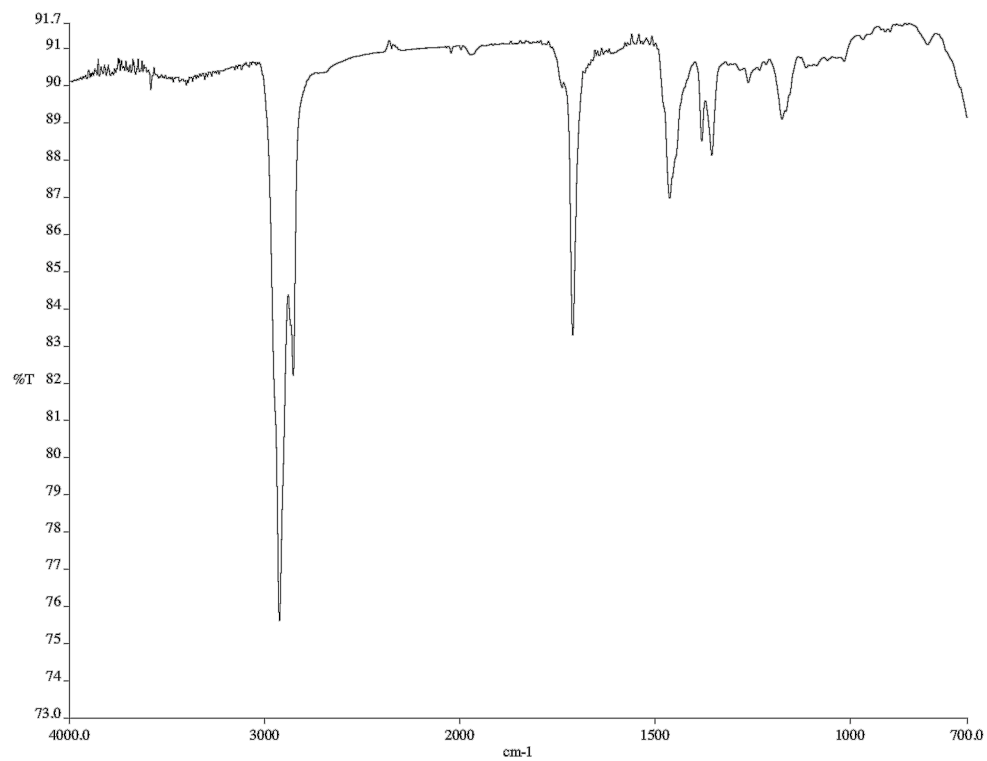


Figure A2.141. Infrared spectrum (neat film/NaCl) of the minor diastereomer of **243**.

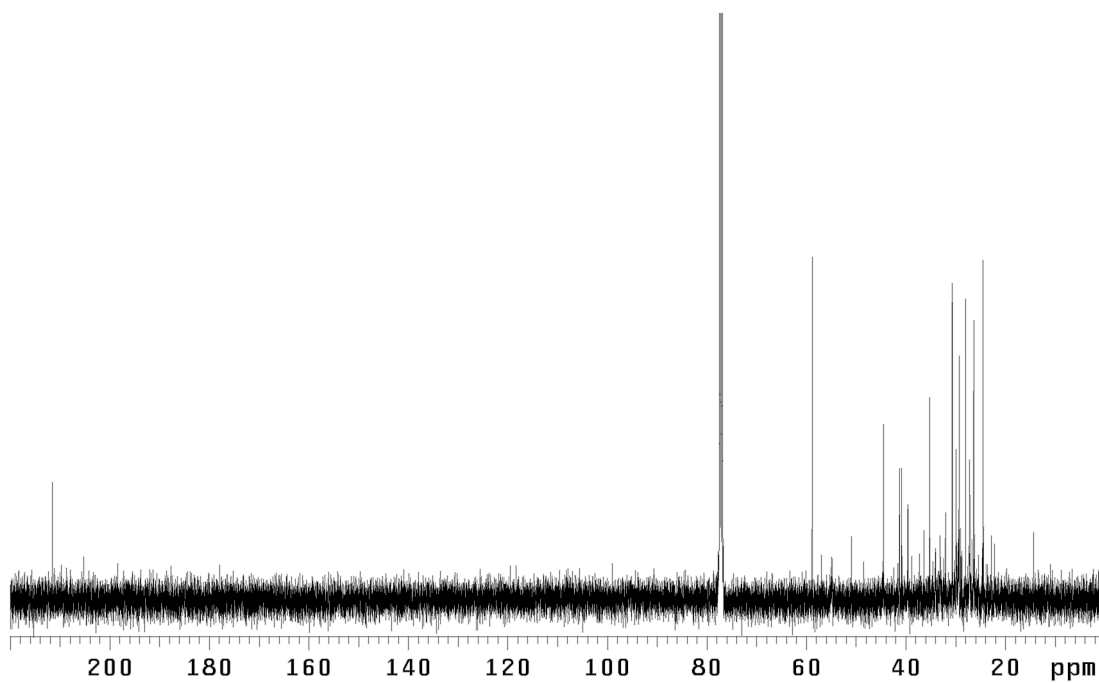
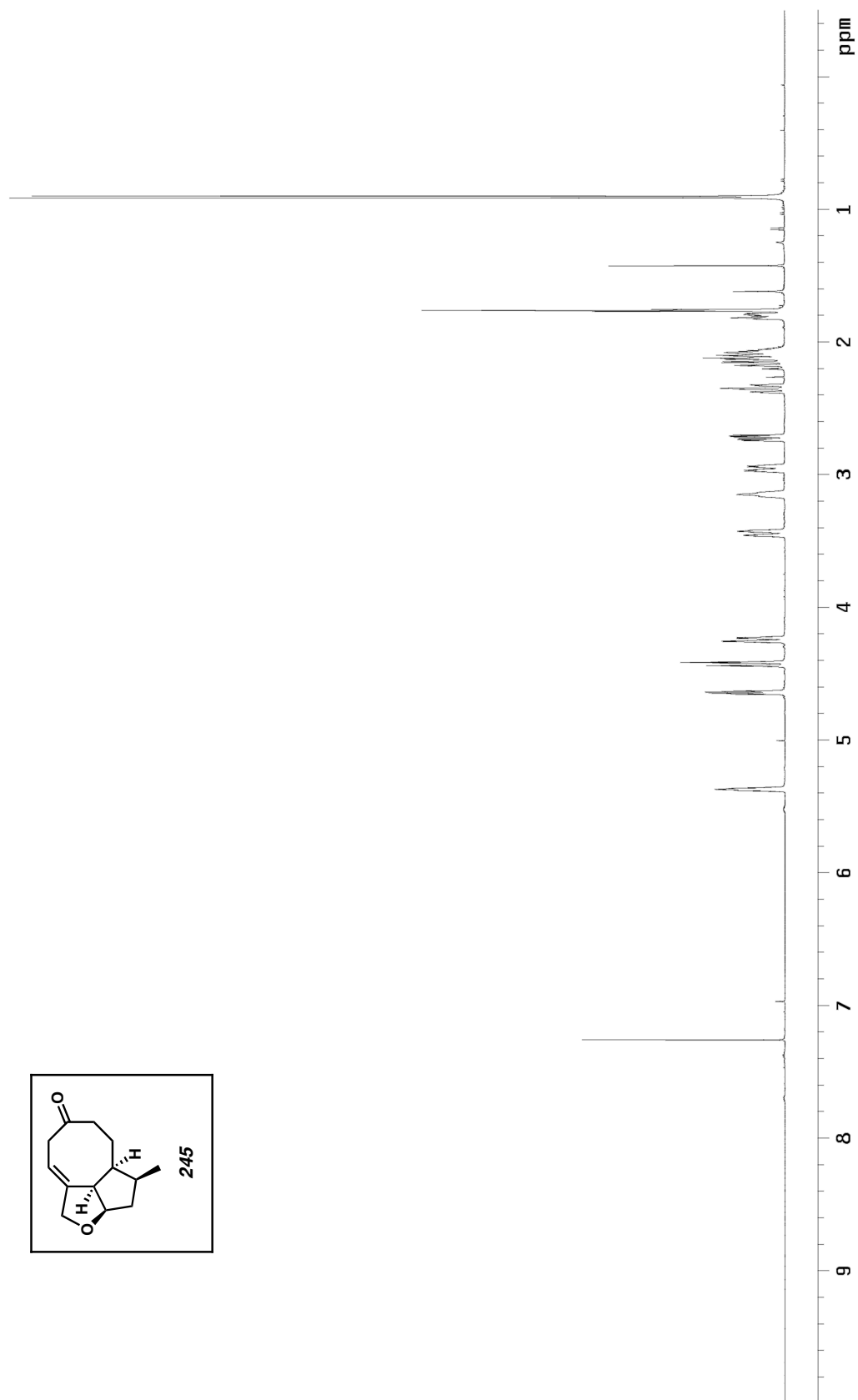


Figure A2.142. ¹³C NMR spectrum (neat film/NaCl) of the minor diastereomer of **243**.

Figure A2.143. ^1H NMR spectrum (500 MHz, CDCl_3) of **245**.

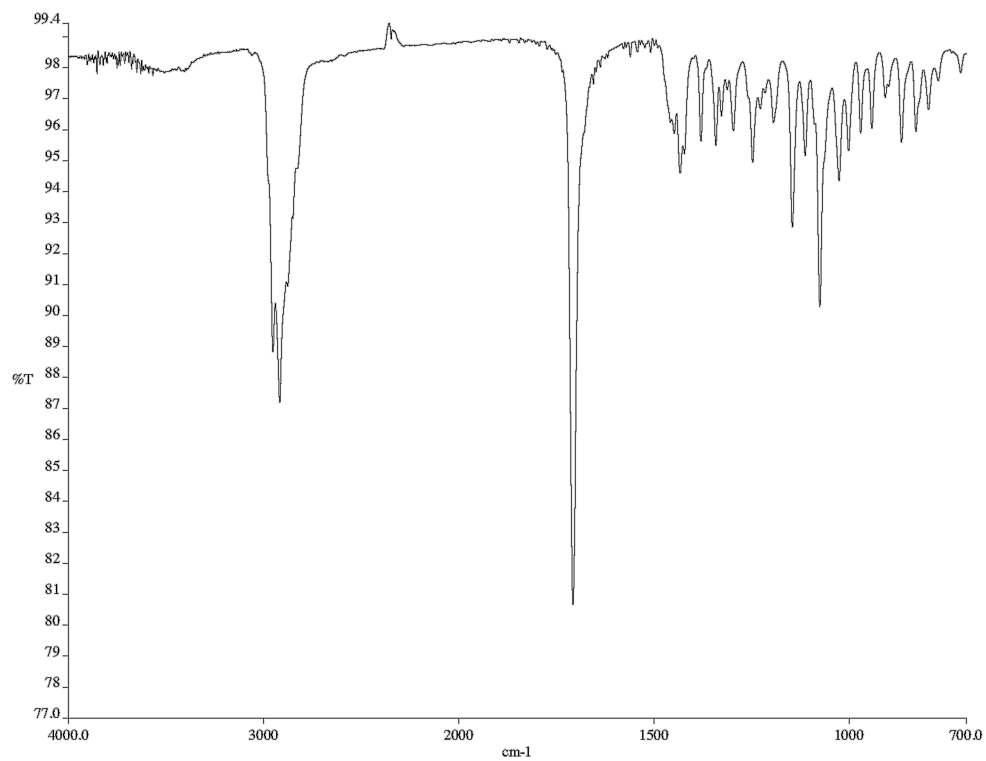


Figure A2.144. Infrared spectrum (neat film/NaCl) of **245**.

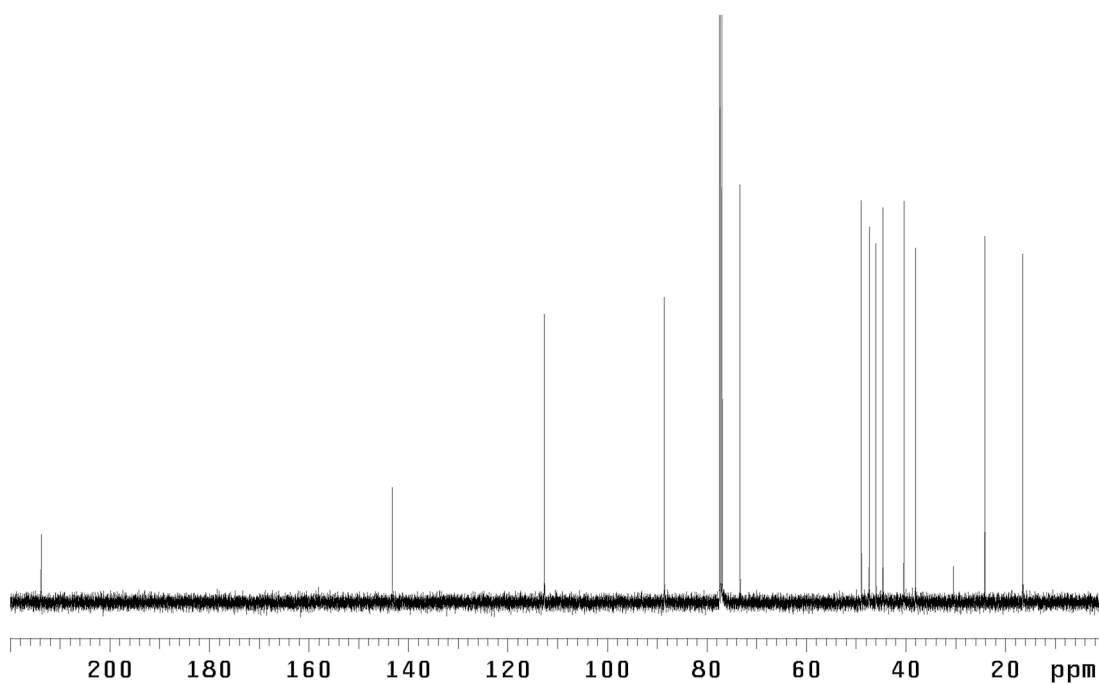
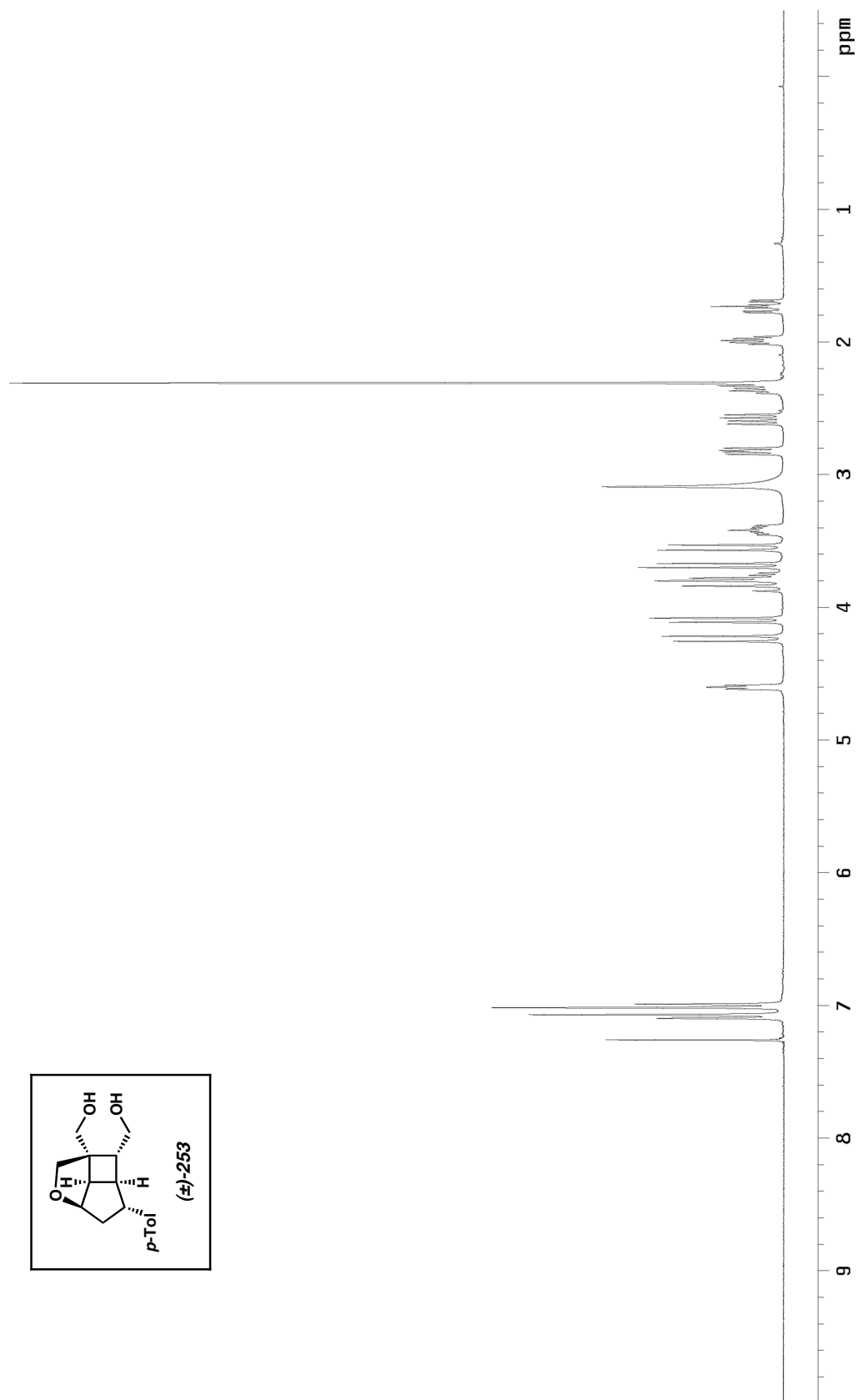


Figure A2.145. ¹³C NMR spectrum (126 MHz, CDCl₃) of **245**.

Figure A2.146. ^1H NMR spectrum (300 MHz, CDCl_3) of **253**.

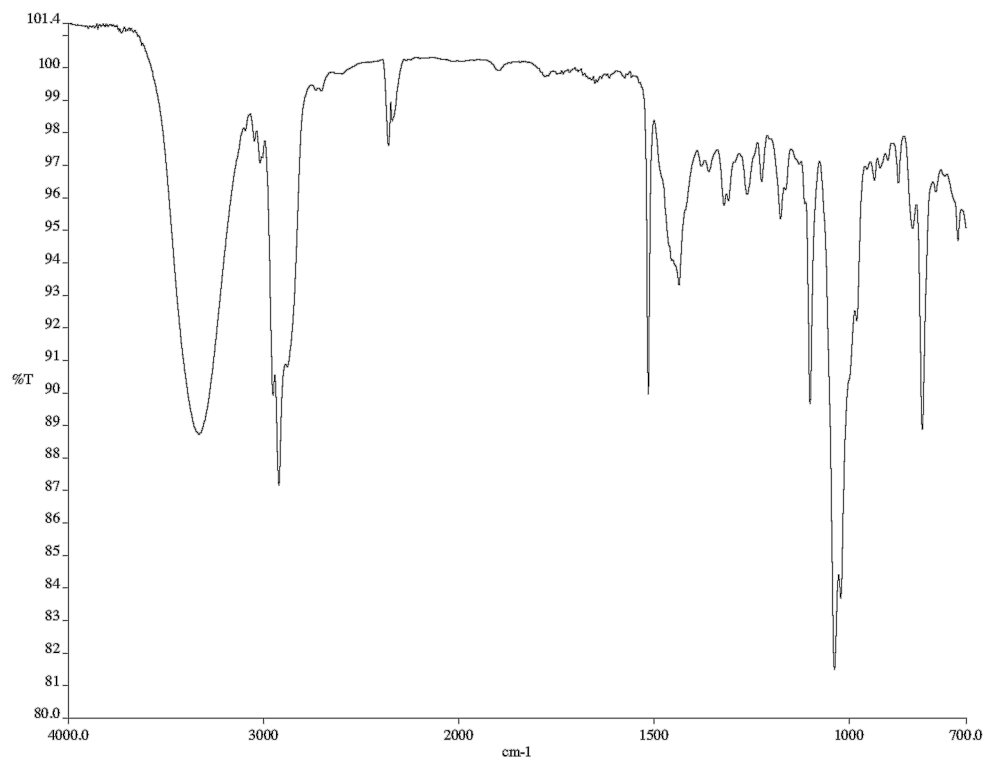


Figure A2.147. Infrared spectrum (neat film/NaCl) of **253**.

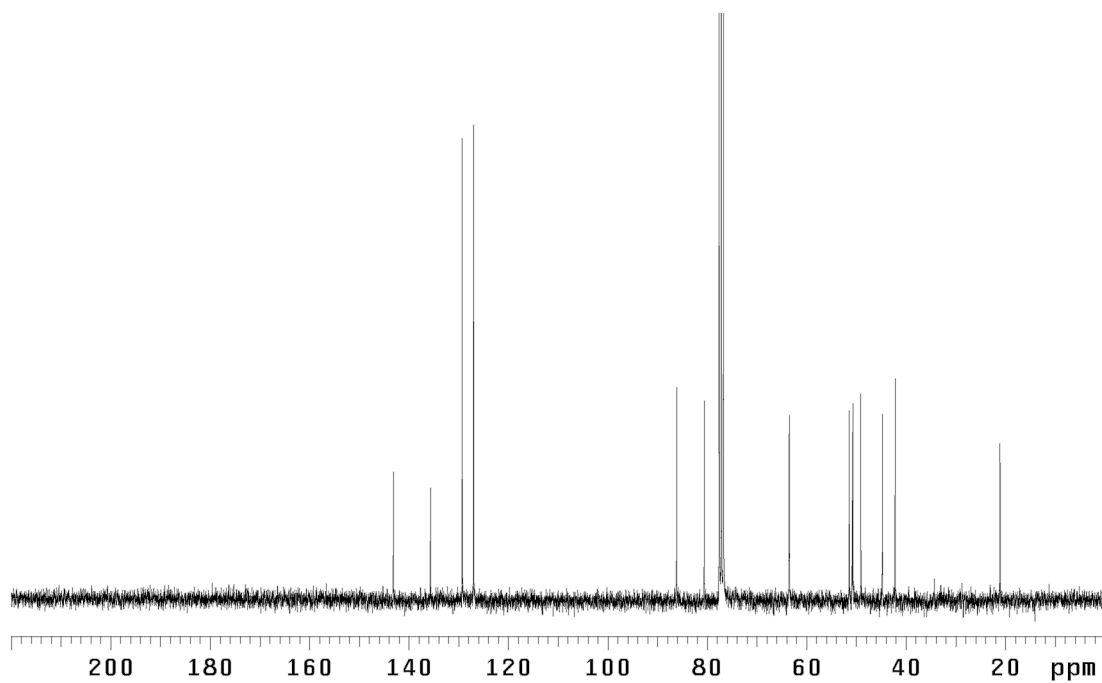
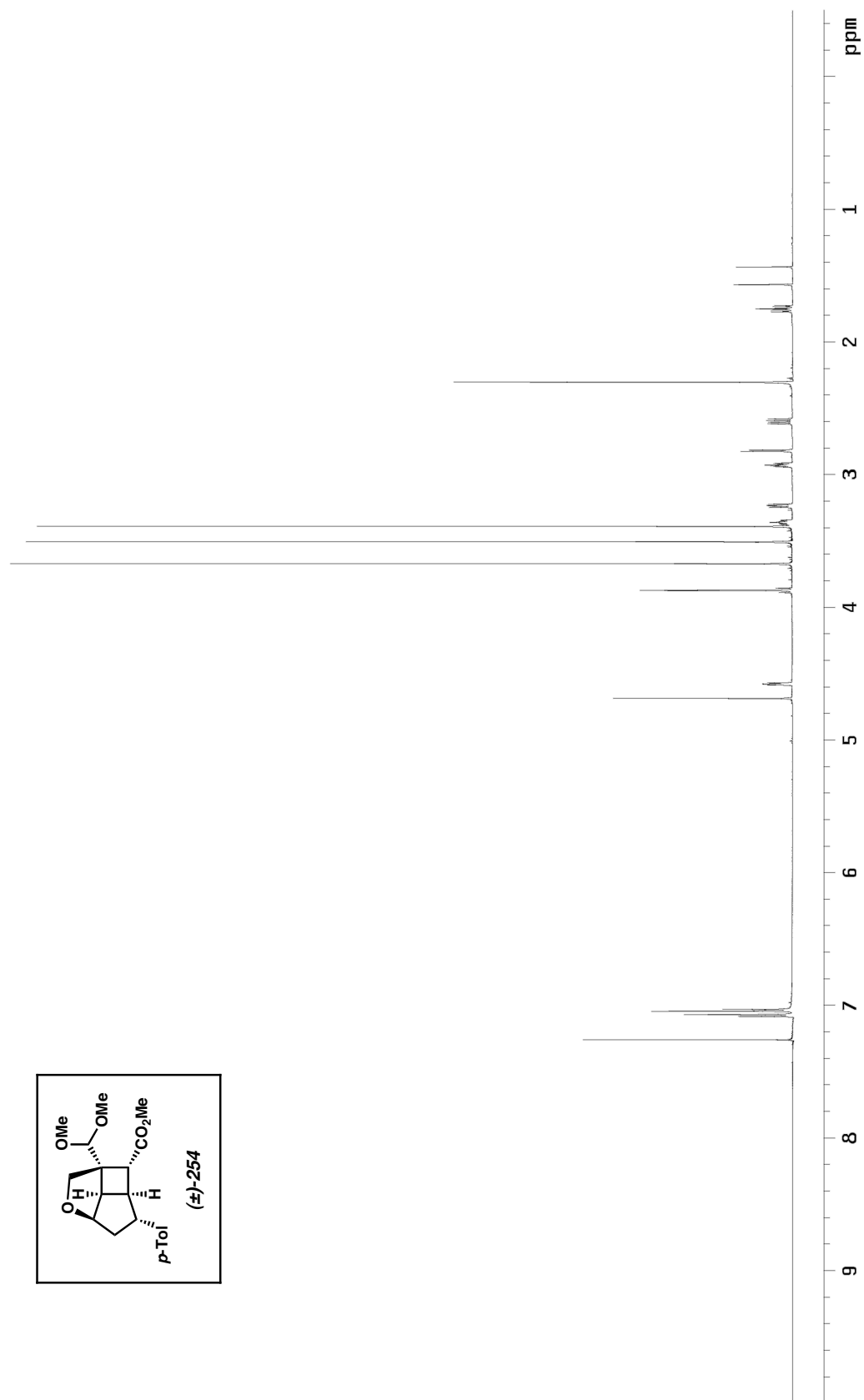


Figure A2.148. ^{13}C NMR spectrum (75 MHz, CDCl_3) of **253**.

Figure A2.149. ^1H NMR spectrum (600 MHz, CDCl_3) of **254**.

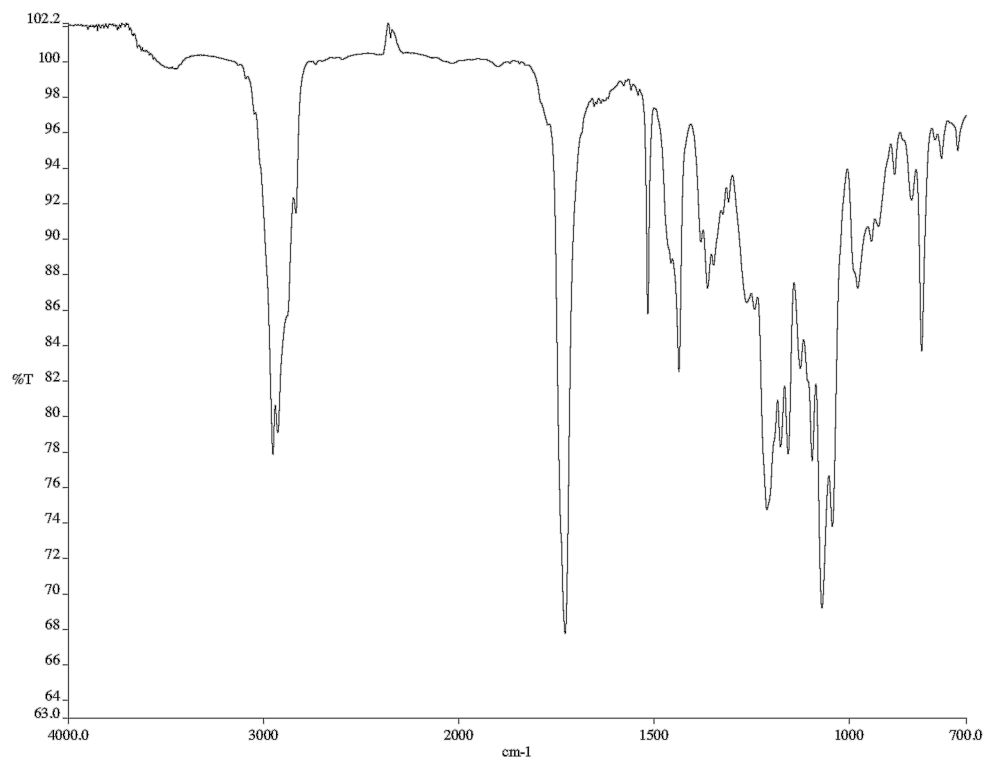


Figure A2.150. Infrared spectrum (neat film/NaCl) of **254**.

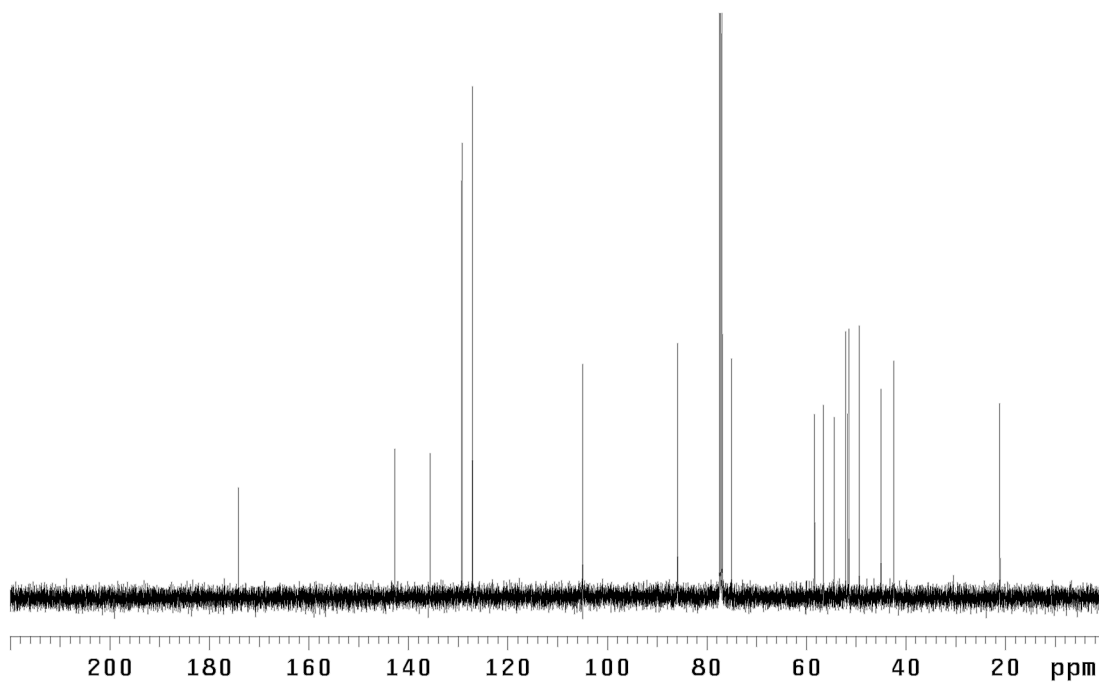
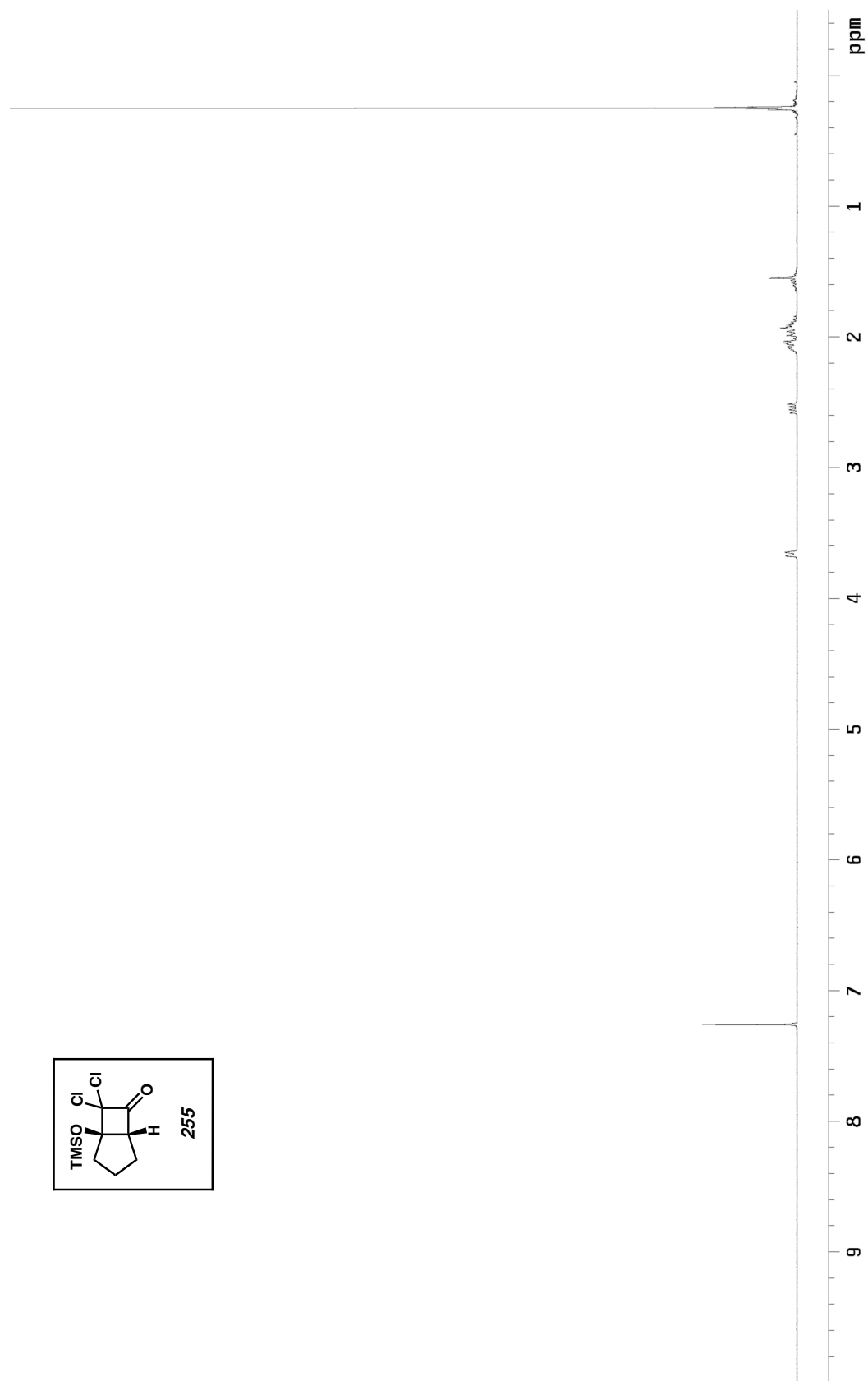
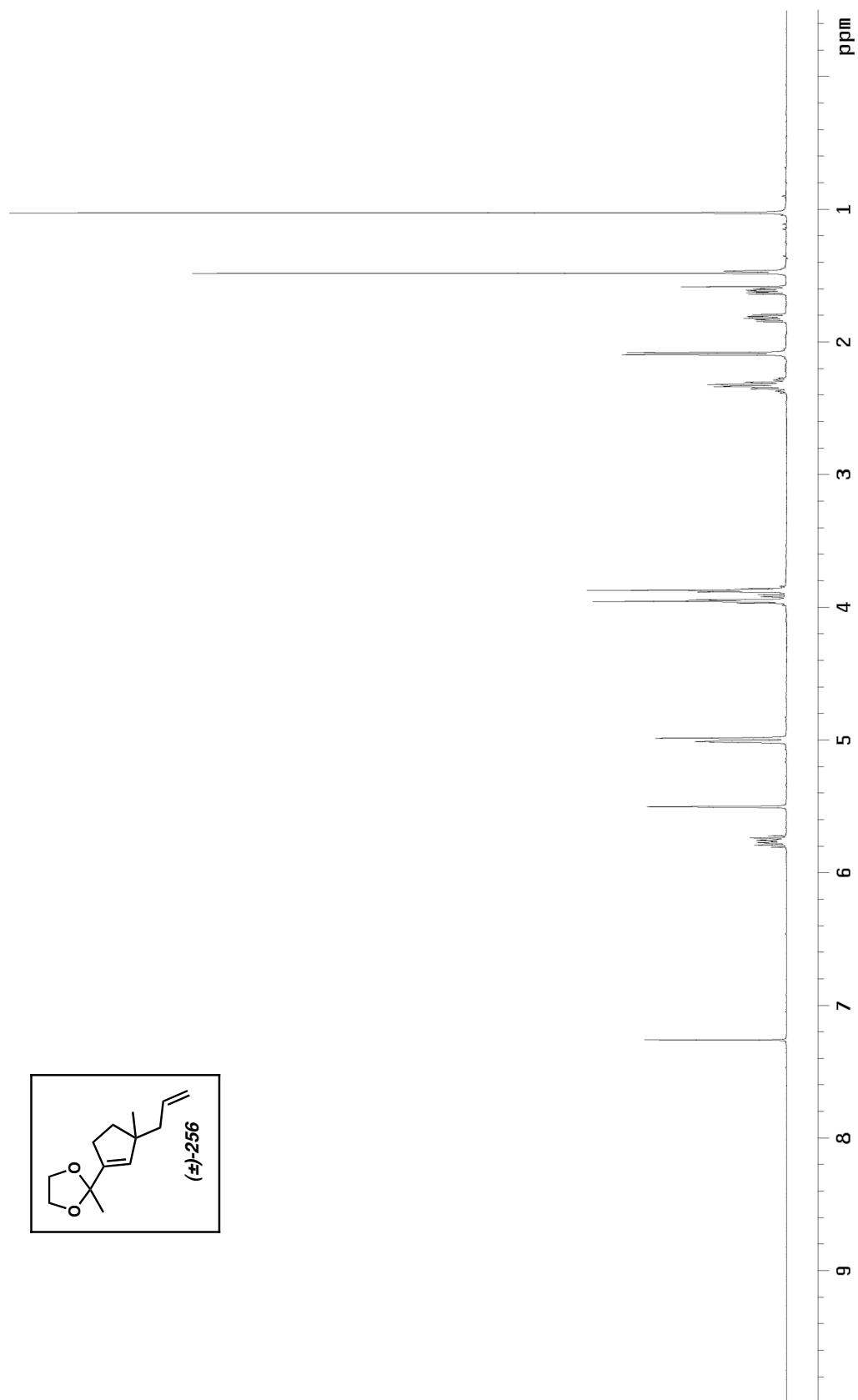


Figure A2.151. ¹³C NMR spectrum (126 MHz, CDCl₃) of **254**.

Figure A2.152. ^1H NMR spectrum (300 MHz, CDCl_3) of 255.

Figure A2.153. ^1H NMR spectrum (300 MHz, CDCl_3) of **256**.

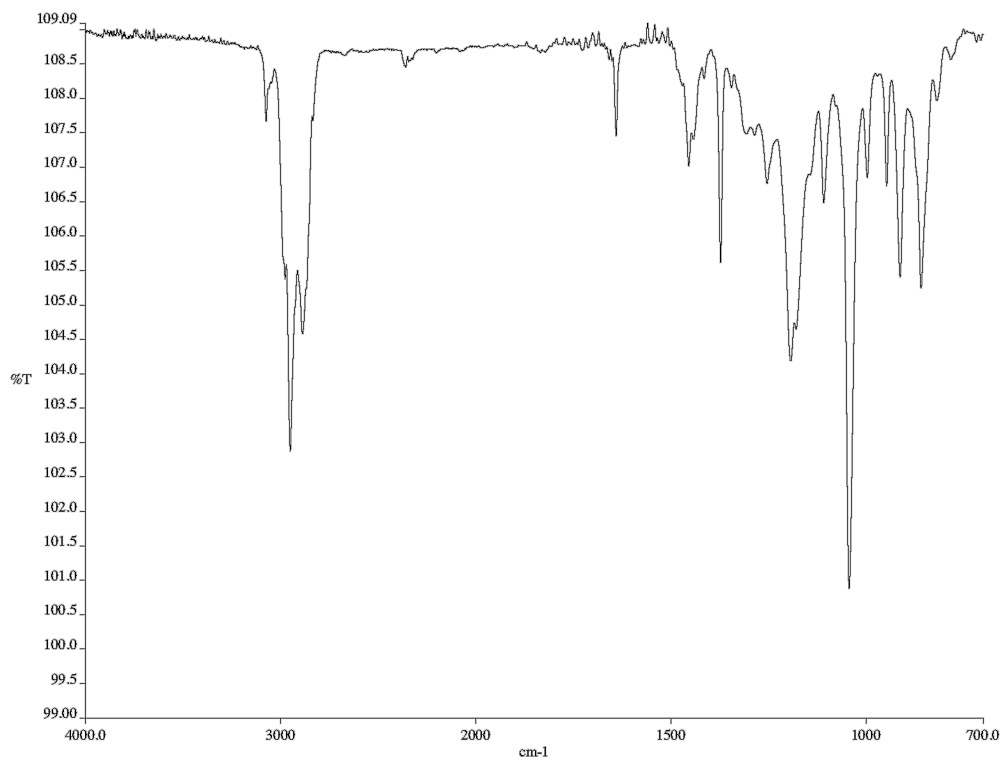


Figure A2.154. Infrared spectrum (neat film/NaCl) of **256**.

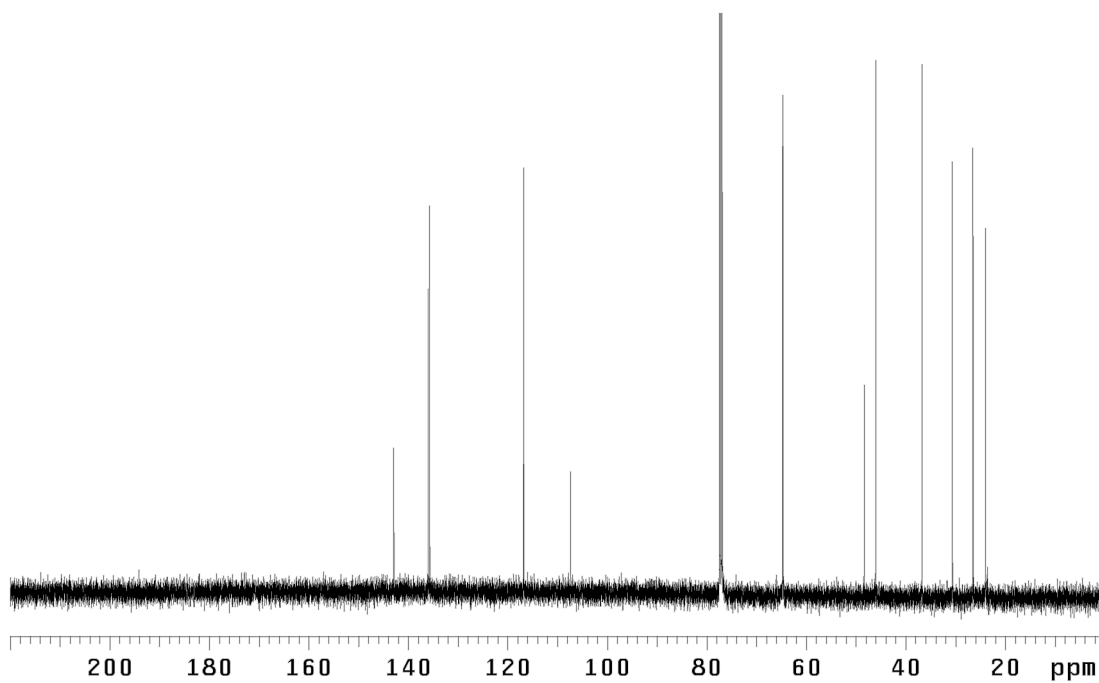


Figure A2.155. ¹³C NMR spectrum (126 MHz, CDCl₃) of **256**.

APPENDIX 3

X-Ray Crystallography Reports Relevant to Chapter 3: Progress toward the Asymmetric Total Synthesis of Variocolin

A3.1 CRYSTAL STRUCTURE ANALYSIS OF 215

Figure A3.1.1. Acetal **215** is shown with 50% probability ellipsoids. Crystallographic data have been deposited at the CCDC, 12 Union Road, Cambridge CB2 1EZ, UK, and copies can be obtained on request, free of charge, by quoting the publication citation and the deposition number 718289.

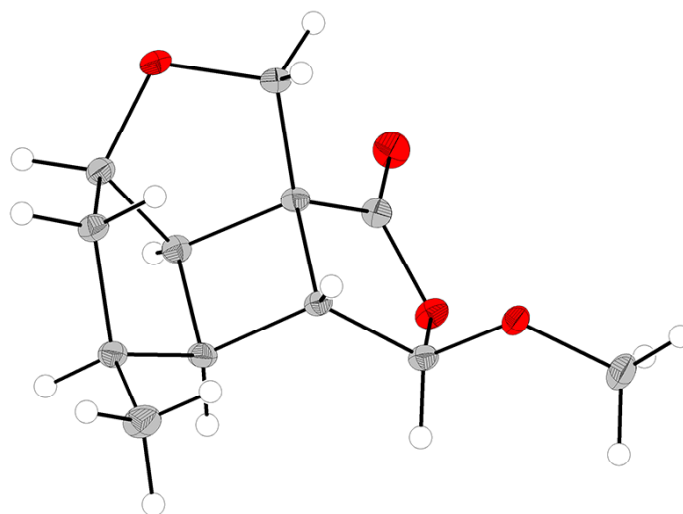


Table A3.1.1. Crystal data and structure refinement for **215** (CCDC 718289)

Empirical formula	C ₁₂ H ₁₆ O ₄
Formula weight	224.25
Crystallization solvent	Chloroform/dichloromethane/diethyl ether
Crystal habit	Block
Crystal size	0.30 x 0.28 x 0.20 mm ³
Crystal color	Colorless

Data Collection

Type of diffractometer	Bruker KAPPA APEX II
Wavelength	0.71073 Å MoK α
Data collection temperature	100(2) K
θ range for 9805 reflections used in lattice determination	3.31 to 34.80°
Unit cell dimensions	a = 6.3017(3) Å b = 11.7387(5) Å c = 14.4000(6) Å
Volume	1065.22(8) Å ³
Z	4
Crystal system	Orthorhombic
Space group	P2 ₁ 2 ₁ 2 ₁
Density (calculated)	1.398 Mg/m ³
F(000)	480
Data collection program	Bruker APEX2 v2.1-0
θ range for data collection	2.24 to 35.05°
Completeness to $\theta = 35.05^\circ$	97.3%
Index ranges	-10 ≤ h ≤ 10, -17 ≤ k ≤ 18, -23 ≤ l ≤ 22
Data collection scan type	ω scans; 13 settings
Data reduction program	Bruker SAINT-Plus v7.34A
Reflections collected	37096
Independent reflections	4514 [R _{int} = 0.1080]
Absorption coefficient	0.104 mm ⁻¹
Absorption correction	None
Max. and min. transmission	0.9794 and 0.9694

Table A3.1.1 (cont.)

Structure solution and Refinement

Structure solution program	SHELXS-97 (Sheldrick, 2008)
Primary solution method	Direct methods
Secondary solution method	Difference Fourier map
Hydrogen placement	Difference Fourier map
Structure refinement program	SHELXL-97 (Sheldrick, 2008)
Refinement method	Full matrix least-squares on F^2
Data / restraints / parameters	4514 / 0 / 209
Treatment of hydrogen atoms	Unrestrained
Goodness-of-fit on F^2	1.899
Final R indices [$I > 2\sigma(I)$, 4349 reflections]	$R1 = 0.0286$, $wR2 = 0.0740$
R indices (all data)	$R1 = 0.0301$, $wR2 = 0.0744$
Type of weighting scheme used	Sigma
Weighting scheme used	$w = 1/\sigma^2(Fo^2)$
Max shift/error	0.001
Average shift/error	0.000
Absolute structure determination	Not able to determine reliably
Absolute structure parameter	0.1(4)
Largest diff. peak and hole	0.339 and -0.290 e. \AA^{-3}

Special Refinement Details

Crystals were mounted on a glass fiber using Paratone oil then placed on the diffractometer under a nitrogen stream at 100 K.

Refinement of F^2 against ALL reflections. The weighted R-factor (wR) and goodness of fit (S) are based on F^2 , conventional R-factors (R) are based on F , with F set to zero for negative F^2 . The threshold expression of $F^2 > 2\sigma(F^2)$ is used only for calculating R-factors(gt) etc. and is not relevant to the choice of reflections for refinement. R-factors based on F^2 are statistically about twice as large as those based on F , and R-factors based on ALL data will be even larger.

All esds (except the esd in the dihedral angle between two l.s. planes) are estimated using the full covariance matrix. The cell esds are taken into account individually in the estimation of esds in distances,

angles and torsion angles; correlations between esds in cell parameters are only used when they are defined by crystal symmetry. An approximate (isotropic) treatment of cell esds is used for estimating esds involving l.s. planes.

Figure A3.1.2. Acetal **215**.

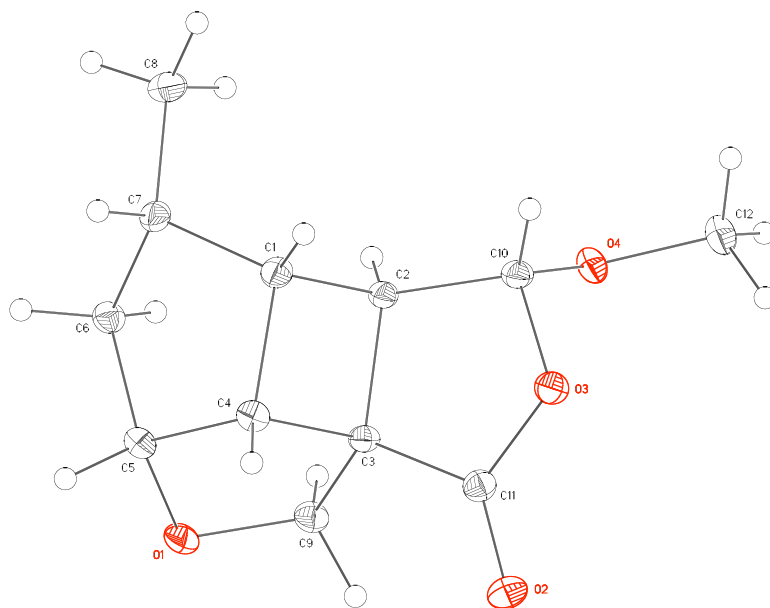


Table A3.1.2. Atomic coordinates ($\times 10^4$) and equivalent isotropic displacement parameters ($\text{\AA}^2 \times 10^3$) for acetal **215** (CCDC 718289). $U(\text{eq})$ is defined as the trace of the orthogonalized U^{ij} tensor

	x	y	z	U_{eq}
O(1)	3796(1)	867(1)	1413(1)	15(1)
O(2)	-1332(1)	-917(1)	2033(1)	18(1)
O(3)	-426(1)	-1149(1)	3528(1)	14(1)
O(4)	2465(1)	-2244(1)	3980(1)	14(1)
C(1)	2711(1)	953(1)	3797(1)	12(1)
C(2)	3032(1)	-331(1)	3582(1)	11(1)
C(3)	2043(1)	-173(1)	2600(1)	11(1)
C(4)	1818(1)	1127(1)	2799(1)	12(1)
C(5)	3644(1)	1607(1)	2205(1)	12(1)
C(6)	5609(1)	1592(1)	2839(1)	12(1)
C(7)	4740(1)	1674(1)	3834(1)	13(1)
C(8)	6340(1)	1339(1)	4579(1)	19(1)
C(9)	3337(1)	-276(1)	1708(1)	13(1)
C(10)	1560(1)	-1173(1)	4061(1)	12(1)
C(11)	-47(1)	-785(1)	2646(1)	13(1)
C(12)	1362(1)	-3130(1)	4468(1)	17(1)

Table A3.1.3. Bond lengths [\AA] and angles [$^\circ$] for acetal **215** (CCDC 718289)

O(1)-C(9)	1.4372(9)	C(3)-C(2)-H(2)	116.1(6)
O(1)-C(5)	1.4374(8)	C(11)-C(3)-C(9)	117.88(5)
O(2)-C(11)	1.2077(8)	C(11)-C(3)-C(2)	104.72(5)
O(3)-C(11)	1.3610(7)	C(9)-C(3)-C(2)	122.77(5)
O(3)-C(10)	1.4689(8)	C(11)-C(3)-C(4)	112.36(5)
O(4)-C(10)	1.3853(9)	C(9)-C(3)-C(4)	106.32(5)
O(4)-C(12)	1.4356(9)	C(2)-C(3)-C(4)	89.20(5)
C(1)-C(7)	1.5344(9)	C(5)-C(4)-C(1)	106.87(5)
C(1)-C(2)	1.5518(10)	C(5)-C(4)-C(3)	100.86(5)
C(1)-C(4)	1.5569(8)	C(1)-C(4)-C(3)	90.48(5)
C(1)-H(1)	0.942(11)	C(5)-C(4)-H(4)	113.5(6)
C(2)-C(10)	1.5213(9)	C(1)-C(4)-H(4)	123.1(6)
C(2)-C(3)	1.5565(8)	C(3)-C(4)-H(4)	118.0(7)
C(2)-H(2)	0.997(11)	O(1)-C(5)-C(6)	114.23(6)
C(3)-C(11)	1.5018(9)	O(1)-C(5)-C(4)	105.60(6)
C(3)-C(9)	1.5263(8)	C(6)-C(5)-C(4)	105.50(5)
C(3)-C(4)	1.5590(10)	O(1)-C(5)-H(5)	106.8(6)
C(4)-C(5)	1.5406(9)	C(6)-C(5)-H(5)	112.0(6)
C(4)-H(4)	0.962(10)	C(4)-C(5)-H(5)	112.7(6)
C(5)-C(6)	1.5385(9)	C(7)-C(6)-C(5)	105.43(5)
C(5)-H(5)	1.020(12)	C(7)-C(6)-H(6A)	110.2(6)
C(6)-C(7)	1.5370(8)	C(5)-C(6)-H(6A)	108.8(6)
C(6)-H(6A)	0.998(12)	C(7)-C(6)-H(6B)	111.8(6)
C(6)-H(6B)	0.957(11)	C(5)-C(6)-H(6B)	111.5(6)
C(7)-C(8)	1.5237(10)	H(6A)-C(6)-H(6B)	109.1(8)
C(7)-H(7)	0.960(14)	C(8)-C(7)-C(1)	115.71(6)
C(8)-H(8A)	1.004(13)	C(8)-C(7)-C(6)	113.83(6)
C(8)-H(8B)	0.934(15)	C(1)-C(7)-C(6)	103.23(5)
C(8)-H(8C)	0.985(15)	C(8)-C(7)-H(7)	108.4(7)
C(9)-H(9A)	0.919(12)	C(1)-C(7)-H(7)	106.3(7)
C(9)-H(9B)	0.973(11)	C(6)-C(7)-H(7)	108.9(7)
C(10)-H(10)	0.947(13)	C(7)-C(8)-H(8A)	112.1(8)
C(12)-H(12A)	0.977(13)	C(7)-C(8)-H(8B)	110.6(8)
C(12)-H(12B)	1.005(16)	H(8A)-C(8)-H(8B)	110.3(11)
C(12)-H(12C)	0.982(13)	C(7)-C(8)-H(8C)	111.7(7)
		H(8A)-C(8)-H(8C)	108.7(12)
		H(8B)-C(8)-H(8C)	103.0(11)
C(9)-O(1)-C(5)	108.46(4)	O(1)-C(9)-C(3)	106.39(5)
C(11)-O(3)-C(10)	110.14(5)	O(1)-C(9)-H(9A)	109.3(7)
C(10)-O(4)-C(12)	114.65(6)	C(3)-C(9)-H(9A)	111.9(7)
C(7)-C(1)-C(2)	115.74(6)	O(1)-C(9)-H(9B)	110.2(7)
C(7)-C(1)-C(4)	105.16(5)	C(3)-C(9)-H(9B)	111.9(7)
C(2)-C(1)-C(4)	89.45(5)	H(9A)-C(9)-H(9B)	107.2(10)
C(7)-C(1)-H(1)	113.3(8)	O(4)-C(10)-O(3)	108.92(5)
C(2)-C(1)-H(1)	114.1(8)	O(4)-C(10)-C(2)	107.47(5)
C(4)-C(1)-H(1)	116.8(7)	O(3)-C(10)-C(2)	105.66(5)
C(10)-C(2)-C(1)	117.45(5)	O(4)-C(10)-H(10)	114.1(8)
C(10)-C(2)-C(3)	104.21(5)	O(3)-C(10)-H(10)	103.9(8)
C(1)-C(2)-C(3)	90.76(5)	C(2)-C(10)-H(10)	116.2(8)
C(10)-C(2)-H(2)	109.7(6)	O(2)-C(11)-O(3)	121.58(6)
C(1)-C(2)-H(2)	116.9(7)		

Table A3.1.3 (cont.)

O(2)-C(11)-C(3)	128.11(6)	H(12A)-C(12)-H(12B)	114.0(11)
O(3)-C(11)-C(3)	110.21(5)	O(4)-C(12)-H(12C)	113.9(8)
O(4)-C(12)-H(12A)	112.8(8)	H(12A)-C(12)-H(12C)	103.4(11)
O(4)-C(12)-H(12B)	106.4(8)	H(12B)-C(12)-H(12C)	106.4(12)

Table A3.1.4. Anisotropic displacement parameters ($\text{\AA}^2 \times 10^4$) for acetal **215** (CCDC 718289). The anisotropic displacement factor exponent takes the form: $-2\pi^2 [h^2 a^{*2} U^{11} + \dots + 2 h k a^* b^* U^{12}]$

	U ¹¹	U ²²	U ³³	U ²³	U ¹³	U ¹²
O(1)	193(2)	161(2)	85(2)	11(2)	10(2)	-16(2)
O(2)	154(2)	213(3)	175(2)	3(2)	-58(2)	-25(2)
O(3)	104(2)	182(2)	129(2)	20(2)	0(2)	-20(2)
O(4)	156(2)	124(2)	128(2)	24(2)	24(2)	-6(2)
C(1)	128(3)	132(3)	98(2)	-18(2)	20(2)	-11(2)
C(2)	107(2)	125(3)	83(2)	3(2)	-1(2)	-12(2)
C(3)	101(2)	129(3)	86(2)	-2(2)	-5(2)	-1(2)
C(4)	112(2)	126(3)	115(2)	2(2)	4(2)	15(2)
C(5)	134(3)	126(3)	105(2)	14(2)	7(2)	5(2)
C(6)	116(3)	147(3)	110(2)	6(2)	12(2)	-8(2)
C(7)	138(3)	138(3)	103(2)	-12(2)	8(2)	-31(2)
C(8)	195(3)	242(4)	129(2)	6(2)	-40(2)	-61(3)
C(9)	156(3)	147(3)	94(2)	-8(2)	16(2)	-2(2)
C(10)	119(2)	139(3)	91(2)	0(2)	-2(2)	-10(2)
C(11)	119(3)	134(3)	127(2)	-5(2)	-1(2)	0(2)
C(12)	192(3)	160(3)	172(2)	49(2)	12(2)	-38(3)

Table A3.1.5. Hydrogen coordinates ($\times 10^4$) and isotropic displacement parameters ($\text{\AA}^2 \times 10^3$) for acetal **215** (CCDC 718289)

	x	y	z	U_{iso}
H(1)	1775(19)	1097(12)	4293(8)	21(3)
H(2)	4516(17)	-624(10)	3599(7)	11(2)
H(4)	471(15)	1482(10)	2675(7)	9(2)
H(5)	3332(18)	2403(11)	1957(8)	19(3)
H(6A)	6371(17)	854(10)	2751(7)	16(2)
H(6B)	6554(17)	2206(10)	2698(7)	13(2)
H(7)	4294(18)	2443(12)	3949(8)	22(3)
H(8A)	5740(20)	1409(13)	5221(9)	31(3)
H(8B)	7570(20)	1775(13)	4526(9)	31(3)
H(8C)	6860(20)	555(13)	4490(9)	30(3)
H(9A)	4588(18)	-661(10)	1802(7)	13(2)
H(9B)	2564(18)	-681(10)	1225(8)	20(3)
H(10)	1140(20)	-983(12)	4673(9)	25(3)
H(12A)	1180(20)	-2961(12)	5127(9)	31(3)
H(12B)	2160(20)	-3854(14)	4343(9)	34(3)
H(12C)	-90(20)	-3258(13)	4249(8)	28(3)

A3.2 CRYSTAL STRUCTURE ANALYSIS OF 233

Figure A3.2.1. Semicarbazone **233** is shown with 50% probability ellipsoids. Crystallographic data have been deposited at the CCDC, 12 Union Road, Cambridge CB2 1EZ, UK, and copies can be obtained on request, free of charge, by quoting the publication citation and the deposition number 686849.

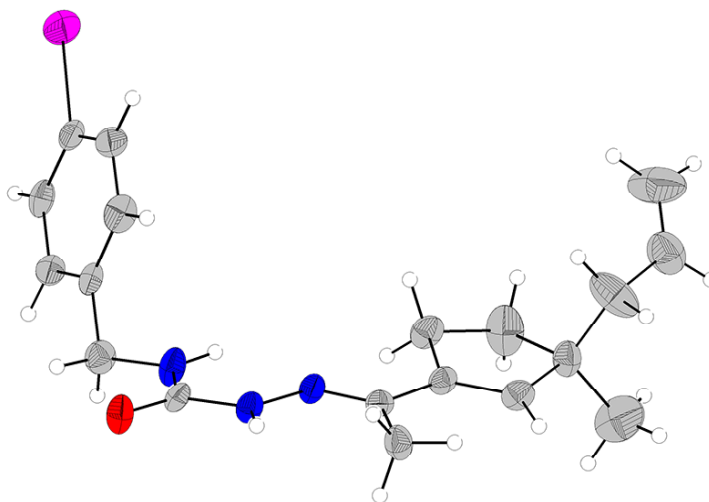


Table A3.2.1 Crystal data and structure refinement for **233** (CCDC 686849)

Empirical formula	C ₁₉ H ₂₄ N ₃ OI
Formula weight	437.31
Crystallization solvent	Dichloromethane/pentane
Crystal habit	Needle
Crystal size	0.28 x 0.11 x 0.07 mm ³
Crystal color	Colorless

Data Collection

Type of diffractometer	Bruker KAPPA APEX II
Wavelength	0.71073 Å MoK α
Data collection temperature	100(2) K

Table A3.2.1 (cont.)

θ range for 9911 reflections used in lattice determination	2.57 to 28.78°	
Unit cell dimensions	a = 17.160(4) Å b = 5.5921(14) Å c = 19.984(5) Å	β = 90.689(6)°
Volume	1917.6(8) Å ³	
Z	4	
Crystal system	Monoclinic	
Space group	P2 ₁	
Density (calculated)	1.515 Mg/m ³	
F(000)	880	
Data collection program	Bruker APEX2 v2.1-0	
θ range for data collection	1.55 to 29.84°	
Completeness to $\theta = 29.84^\circ$	88.9 %	
Index ranges	$-23 \leq h \leq 23, -7 \leq k \leq 7, -26 \leq l \leq 25$	
Data collection scan type	ω scans; 16 settings	
Data reduction program	Bruker SAINT-Plus v7.34A	
Reflections collected	8962	
Independent reflections	8962 [$R_{\text{int}} = 0.0000$]	
Absorption coefficient	1.680 mm ⁻¹	
Absorption correction	Semi-empirical from equivalents (TWNABS)	
Max. and min. transmission	0.7460 and 0.5010	

Structure solution and Refinement

Structure solution program	SHELXS-97 (Sheldrick, 2008)
Primary solution method	Direct methods
Secondary solution method	Difference Fourier map
Hydrogen placement	Geometric positions
Structure refinement program	SHELXL-97 (Sheldrick, 2008)
Refinement method	Full matrix least-squares on F ²
Data / restraints / parameters	8962 / 1 / 437
Treatment of hydrogen atoms	Riding
Goodness-of-fit on F ²	1.609
Final R indices [$I > 2\sigma(I)$, 7203 reflections]	R1 = 0.0409, wR2 = 0.0481
R indices (all data)	R1 = 0.0619, wR2 = 0.0493

Table A3.2.1 (cont.)

Type of weighting scheme used	Sigma
Weighting scheme used	$w=1/\sigma^2(Fo^2)$
Max shift/error	0.002
Average shift/error	0.000
Absolute structure determination	Anomalous differences
Absolute structure parameter	0.003(11)
Largest diff. peak and hole	0.807 and $-0.967 e.\text{\AA}^{-3}$

Special Refinement Details

The structure was refined as a single component, although the crystals were twins, using an HKLF4 format reflection file prepared with TWINABS (see below). The two orientations were separated using CELL_NOW as follows.

Rotated from first domain by 178.9 degrees about reciprocal axis $-0.032 \ 1.000 \ 0.104$ and real axis $-0.001 \ 1.000 \ 0.007$. Twin law to convert hkl from first to this domain (SHELXL TWIN matrix):

$$\begin{matrix} -1.000 & -0.065 & 0.016 \\ -0.003 & 0.998 & 0.014 \\ -0.022 & 0.207 & -0.999 \end{matrix}$$

From Saint integration; Twin Law, Sample 1 of 1 transforms $h1.1(1) \rightarrow h1.2(2)$

$$\begin{matrix} -0.99897 & -0.07583 & 0.01646 \\ -0.00750 & 0.99693 & 0.01538 \\ -0.02464 & 0.19596 & -0.99910 \end{matrix}$$

Twinabs;

PART 1 - Refinement of parameters to model systematic errors

18757 data (4443 unique) involve domain 1 only, mean I/sigma 13.7

18551 data (4364 unique) involve domain 2 only, mean I/sigma 7.1

10342 data (4106 unique) involve 2 domains, mean I/σ 19.2

HKLF 4 dataset constructed from all observations involving domains 1..2

8970 Corrected reflections written to file twin4.hkl

Reflections merged according to point-group 2

Minimum and maximum apparent transmission: 0.501007 0.745969

Additional spherical absorption correction applied with $\mu^*r = 0.2000$

Crystals were mounted on a glass fiber using Paratone oil then placed on the diffractometer under a nitrogen stream at 100 K.

Refinement of F^2 against ALL reflections. The weighted R-factor (wR) and goodness of fit (S) are based on F^2 , conventional R-factors (R) are based on F , with F set to zero for negative F^2 . The threshold expression of $F^2 > 2\sigma(F^2)$ is used only for calculating R-factors(gt) etc. and is not relevant to the choice of reflections for refinement. R-factors based on F^2 are statistically about twice as large as those based on F , and R-factors based on ALL data will be even larger.

All esds (except the esd in the dihedral angle between two l.s. planes) are estimated using the full covariance matrix. The cell esds are taken into account individually in the estimation of esds in distances, angles and torsion angles; correlations between esds in cell parameters are only used when they are defined by crystal symmetry. An approximate (isotropic) treatment of cell esds is used for estimating esds involving l.s. planes.

Table A3.2.2 (cont.)

C(11A)	4738(2)	3016(6)	3736(2)	25(1)
C(12A)	4902(2)	5012(5)	4229(2)	30(1)
C(13A)	4096(2)	6199(5)	4302(2)	34(1)
C(14A)	3501(2)	4222(5)	4130(2)	33(1)
C(15A)	3985(2)	2625(5)	3693(2)	32(1)
C(16A)	3271(2)	2838(6)	4771(2)	47(1)
C(17A)	2751(2)	5160(6)	3793(2)	36(1)
C(18A)	2864(2)	6198(6)	3116(2)	39(1)
C(19A)	2612(2)	8233(8)	2900(2)	51(1)
I(2)	5760(1)	351(1)	-1541(1)	52(1)
O(1B)	6661(1)	7118(3)	2275(1)	34(1)
N(1B)	7173(2)	4167(4)	1625(1)	34(1)
N(2B)	7955(2)	7040(4)	2098(1)	27(1)
N(3B)	8578(2)	5882(4)	1807(1)	26(1)
C(1B)	6496(2)	3858(5)	289(2)	33(1)
C(2B)	6341(2)	3322(8)	-374(2)	35(1)
C(3B)	5958(2)	1240(6)	-534(2)	29(1)
C(4B)	5742(2)	-303(6)	-40(2)	31(1)
C(5B)	5895(2)	235(6)	618(2)	28(1)
C(6B)	6287(2)	2329(5)	795(2)	26(1)
C(7B)	6454(2)	2863(6)	1519(2)	32(1)
C(8B)	7233(2)	6143(5)	2016(2)	25(1)
C(9B)	9266(2)	6619(5)	1925(2)	24(1)
C(10B)	9471(2)	8670(6)	2382(2)	33(1)
C(11B)	9892(2)	5325(6)	1586(2)	25(1)
C(12B)	9704(2)	3469(7)	1051(2)	34(1)
C(13B)	10499(2)	2401(6)	903(2)	54(1)
C(14B)	11131(2)	4019(5)	1204(2)	33(1)
C(15B)	10659(2)	5558(6)	1666(2)	30(1)
C(16B)	11736(3)	2543(7)	1600(2)	67(2)
C(17B)	11522(2)	5571(7)	690(2)	58(1)
C(18B)	12017(3)	4302(6)	194(2)	52(1)
C(19B)	11859(3)	3982(7)	-416(2)	77(2)

Table A3.2.3. Bond lengths [\AA] and angles [$^\circ$] for semicarbazone **233** (CCDC 686849)

I(1)-C(3A)	2.092(3)		
O(1A)-C(8A)	1.226(4)	C(8A)-N(1A)-C(7A)	120.7(3)
N(1A)-C(8A)	1.354(4)	C(8A)-N(2A)-N(3A)	119.8(3)
N(1A)-C(7A)	1.449(4)	C(9A)-N(3A)-N(2A)	118.6(3)
N(2A)-C(8A)	1.361(4)	C(2A)-C(1A)-C(6A)	122.1(3)
N(2A)-N(3A)	1.388(3)	C(1A)-C(2A)-C(3A)	119.6(3)
N(3A)-C(9A)	1.289(4)	C(2A)-C(3A)-C(4A)	119.8(3)
C(1A)-C(2A)	1.375(5)	C(2A)-C(3A)-I(1)	120.1(2)
C(1A)-C(6A)	1.386(4)	C(4A)-C(3A)-I(1)	119.9(2)
C(2A)-C(3A)	1.385(4)	C(5A)-C(4A)-C(3A)	119.7(3)
C(3A)-C(4A)	1.384(4)	C(4A)-C(5A)-C(6A)	121.7(3)
C(4A)-C(5A)	1.376(4)	C(1A)-C(6A)-C(5A)	117.2(3)
C(5A)-C(6A)	1.397(5)	C(1A)-C(6A)-C(7A)	122.8(3)
C(6A)-C(7A)	1.494(4)	C(5A)-C(6A)-C(7A)	120.1(3)
C(9A)-C(11A)	1.457(4)	N(1A)-C(7A)-C(6A)	115.0(3)
C(9A)-C(10A)	1.494(4)	O(1A)-C(8A)-N(1A)	123.1(3)
C(11A)-C(15A)	1.312(4)	O(1A)-C(8A)-N(2A)	121.2(3)
C(11A)-C(12A)	1.514(5)	N(1A)-C(8A)-N(2A)	115.8(3)
C(12A)-C(13A)	1.542(4)	N(3A)-C(9A)-C(11A)	116.2(3)
C(13A)-C(14A)	1.542(5)	N(3A)-C(9A)-C(10A)	123.9(3)
C(14A)-C(15A)	1.505(4)	C(11A)-C(9A)-C(10A)	119.8(3)
C(14A)-C(17A)	1.538(5)	C(15A)-C(11A)-C(9A)	127.4(3)
C(14A)-C(16A)	1.552(5)	C(15A)-C(11A)-C(12A)	109.9(3)
C(17A)-C(18A)	1.487(5)	C(9A)-C(11A)-C(12A)	122.6(3)
C(18A)-C(19A)	1.290(5)	C(11A)-C(12A)-C(13A)	102.6(3)
I(2)-C(3B)	2.096(3)	C(12A)-C(13A)-C(14A)	105.2(2)
O(1B)-C(8B)	1.242(4)	C(15A)-C(14A)-C(17A)	114.4(3)
N(1B)-C(8B)	1.356(4)	C(15A)-C(14A)-C(13A)	100.7(3)
N(1B)-C(7B)	1.447(4)	C(17A)-C(14A)-C(13A)	113.7(3)
N(2B)-C(8B)	1.346(4)	C(15A)-C(14A)-C(16A)	109.3(3)
N(2B)-N(3B)	1.383(3)	C(17A)-C(14A)-C(16A)	108.2(3)
N(3B)-C(9B)	1.270(4)	C(13A)-C(14A)-C(16A)	110.3(3)
C(1B)-C(6B)	1.376(4)	C(11A)-C(15A)-C(14A)	114.4(3)
C(1B)-C(2B)	1.380(5)	C(18A)-C(17A)-C(14A)	114.4(3)
C(2B)-C(3B)	1.373(5)	C(19A)-C(18A)-C(17A)	127.0(3)
C(3B)-C(4B)	1.366(4)	C(8B)-N(1B)-C(7B)	123.6(3)
C(4B)-C(5B)	1.372(4)	C(8B)-N(2B)-N(3B)	119.3(3)
C(5B)-C(6B)	1.394(5)	C(9B)-N(3B)-N(2B)	119.4(3)
C(6B)-C(7B)	1.501(5)	C(6B)-C(1B)-C(2B)	121.4(3)
C(9B)-C(11B)	1.467(4)	C(3B)-C(2B)-C(1B)	119.6(3)
C(9B)-C(10B)	1.504(4)	C(4B)-C(3B)-C(2B)	120.0(3)
C(11B)-C(15B)	1.330(4)	C(4B)-C(3B)-I(2)	120.1(3)
C(11B)-C(12B)	1.522(4)	C(2B)-C(3B)-I(2)	119.8(2)
C(12B)-C(13B)	1.521(5)	C(3B)-C(4B)-C(5B)	120.3(3)
C(13B)-C(14B)	1.530(5)	C(4B)-C(5B)-C(6B)	120.9(3)
C(14B)-C(15B)	1.505(4)	C(1B)-C(6B)-C(5B)	117.7(3)
C(14B)-C(17B)	1.509(5)	C(1B)-C(6B)-C(7B)	122.4(3)
C(14B)-C(16B)	1.537(6)	C(5B)-C(6B)-C(7B)	119.8(3)
C(17B)-C(18B)	1.493(5)	N(1B)-C(7B)-C(6B)	113.3(3)
C(18B)-C(19B)	1.260(5)	O(1B)-C(8B)-N(2B)	121.1(3)

Table A3.2.3 (cont.)

O(1B)-C(8B)-N(1B)	123.0(3)	C(12B)-C(13B)-C(14B)	108.9(3)
N(2B)-C(8B)-N(1B)	115.9(3)	C(15B)-C(14B)-C(17B)	109.6(3)
N(3B)-C(9B)-C(11B)	116.0(3)	C(15B)-C(14B)-C(13B)	101.3(3)
N(3B)-C(9B)-C(10B)	124.7(3)	C(17B)-C(14B)-C(13B)	112.9(3)
C(11B)-C(9B)-C(10B)	119.3(3)	C(15B)-C(14B)-C(16B)	110.9(3)
C(15B)-C(11B)-C(9B)	128.7(3)	C(17B)-C(14B)-C(16B)	110.8(3)
C(15B)-C(11B)-C(12B)	110.6(3)	C(13B)-C(14B)-C(16B)	110.9(3)
C(9B)-C(11B)-C(12B)	120.7(3)	C(11B)-C(15B)-C(14B)	114.2(3)
C(13B)-C(12B)-C(11B)	102.9(3)	C(18B)-C(17B)-C(14B)	116.1(3)
		C(19B)-C(18B)-C(17B)	126.3(5)

Table A3.2.4. Anisotropic displacement parameters ($\text{\AA}^2 \times 10^4$) for semicarbazone **233** (CCDC 686849). The anisotropic displacement factor exponent takes the form: $-2\pi^2 [h^2 a^{*2} U^{11} + \dots + 2 h k a^* b^* U^{12}]$

	U ¹¹	U ²²	U ³³	U ²³	U ¹³	U ¹²
I(1)	340(2)	433(1)	310(1)	1(1)	-116(1)	-2(1)
O(1A)	177(14)	294(13)	431(15)	-131(10)	-15(11)	35(10)
N(1A)	166(17)	377(19)	352(17)	-168(12)	3(13)	-6(12)
N(2A)	150(17)	315(15)	378(18)	-133(12)	-22(13)	22(12)
N(3A)	186(19)	310(15)	328(18)	-35(12)	-35(15)	38(13)
C(1A)	190(20)	176(16)	420(20)	13(15)	-22(18)	9(13)
C(2A)	250(20)	237(18)	320(20)	88(15)	-7(16)	-4(16)
C(3A)	170(20)	261(17)	270(20)	-18(14)	-7(16)	69(14)
C(4A)	180(20)	200(20)	310(20)	-23(14)	-29(15)	-13(14)
C(5A)	240(20)	201(19)	275(19)	26(16)	5(15)	34(16)
C(6A)	171(19)	195(18)	269(19)	-26(14)	-8(15)	64(14)
C(7A)	260(20)	280(18)	330(20)	-40(17)	-16(16)	-38(18)
C(8A)	200(20)	257(18)	260(20)	-33(14)	-61(17)	19(16)
C(9A)	200(20)	231(17)	330(20)	-9(14)	-9(18)	-26(15)
C(10A)	200(20)	410(20)	430(20)	-69(17)	3(18)	-44(17)
C(11A)	190(20)	240(20)	330(20)	21(16)	-31(15)	-26(17)
C(12A)	250(20)	283(18)	360(20)	-23(16)	-60(16)	-30(16)
C(13A)	260(20)	305(19)	440(20)	-99(15)	-50(18)	42(16)
C(14A)	190(20)	305(19)	490(30)	-7(15)	9(19)	19(15)
C(15A)	260(20)	240(20)	460(20)	-48(14)	-26(19)	-18(15)
C(16A)	360(30)	500(30)	540(30)	114(18)	30(20)	88(19)
C(17A)	250(20)	390(20)	450(20)	-34(18)	9(18)	40(20)
C(18A)	270(20)	480(20)	420(30)	-75(18)	-70(20)	77(18)
C(19A)	410(30)	600(20)	510(20)	40(20)	-88(19)	120(30)
I(2)	431(2)	791(2)	333(2)	-69(1)	-57(1)	-30(2)
O(1B)	227(16)	346(12)	447(16)	-105(10)	2(13)	9(11)
N(1B)	220(19)	350(17)	440(20)	-151(12)	-38(16)	9(12)
N(2B)	230(20)	301(15)	272(17)	-106(12)	-29(14)	3(13)
N(3B)	208(18)	309(16)	277(16)	-57(12)	-23(14)	26(14)
C(1B)	340(30)	190(20)	470(30)	-9(15)	-50(20)	-62(15)
C(2B)	310(20)	404(19)	350(20)	130(20)	-22(16)	20(20)
C(3B)	190(20)	370(20)	310(20)	-17(16)	-51(17)	17(16)
C(4B)	200(20)	270(20)	450(30)	-58(16)	-50(18)	-39(15)
C(5B)	270(20)	236(18)	340(20)	71(16)	-20(16)	-10(17)
C(6B)	170(20)	246(18)	350(20)	8(15)	-46(17)	-2(14)
C(7B)	300(20)	310(20)	360(20)	-12(15)	-23(17)	-59(16)
C(8B)	200(20)	282(19)	270(20)	-34(14)	-76(16)	-6(16)
C(9B)	250(20)	257(18)	220(20)	11(14)	2(17)	11(16)
C(10B)	260(20)	400(20)	330(20)	-104(16)	37(16)	-60(18)
C(11B)	250(20)	241(17)	253(19)	-25(16)	-45(15)	-52(18)
C(12B)	340(20)	341(18)	330(20)	-105(19)	-60(16)	10(20)
C(13B)	450(30)	450(20)	730(30)	-310(20)	70(30)	-4(19)
C(14B)	250(20)	350(20)	390(20)	-54(15)	20(19)	25(15)

Table A3.2.4 (cont.)

C(15B)	340(20)	290(18)	266(19)	-75(16)	-25(16)	33(18)
C(16B)	720(40)	680(30)	610(30)	-170(20)	-50(30)	380(30)
C(17B)	840(30)	400(20)	510(30)	-150(20)	330(20)	-90(20)
C(18B)	500(30)	540(30)	520(30)	-104(19)	110(30)	-49(19)
C(19B)	1060(50)	830(40)	420(30)	40(20)	60(30)	500(30)

Table A3.2.5. Hydrogen bonds for semicarbazone **233** (CCDC 686849) [\AA and $^\circ$]

D-H...A	d(D-H)	d(H...A)	d(D...A)	\angle (DHA)
N(2A)-H(2A)...O(1B)#1	0.88	2.13	2.972(3)	159.7
N(2B)-H(2B)...O(1A)#2	0.88	2.04	2.895(3)	163.1

Symmetry transformations used to generate equivalent atoms:

#1 $x, y-1, z$

#2 $x, y+1, z$

CHAPTER 4

Enantioselective Allylic Alkylations of Vinylogous β -Ketoester Derivatives: Total Synthesis of (+)-Carissone[†]

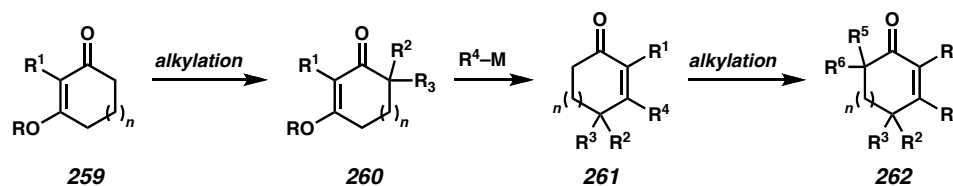
4.1 INTRODUCTION

Cyclic, unsaturated ketones possessing γ -substitution (e.g., **261**) are highly useful intermediates for applications in complex molecule synthesis (Figure 4.1.1).¹ Such γ -substituted enone moieties are typically accessed via transformations of masked, cyclic 1,3-dicarbonyl compounds made popular by Stork and Danheiser.² These so-called vinylogous esters (e.g., **259**) enable the regioselective functionalization of the ring, and are amenable to the preparation of numerous compounds possessing an array of substitution. A principle challenge to accessing members of this substrate class is the stereoselective construction of a quaternary stereocenter at the γ -position of the enone.³ Although methods for the asymmetric introduction of this moiety exist,⁴ we envisioned

[†] Studies toward the synthesis of (+)-carissone were performed primarily by Samantha R. Levine as a Marcella R. Bonsall Summer Undergraduate Research Fellow and partially sponsored by the Dalton Fund. Portions of this work were also conducted in collaboration with Krastina V. Petrova and Justin T. Mohr. These works have been published. See: (a) Levine, S. R.; Krout, M. R.; Stoltz, B. M. *Org. Lett.* **2009**, *11*, 289–292. (b) Petrova, K. V.; Mohr, J. T.; Stoltz, B. M. *Org. Lett.* **2009**, *11*, 293–295.

an enantioselective approach that harnesses the palladium-catalyzed alkylation methodology that has recently been developed in our laboratory.⁵ Herein, we detail our investigations of this important class of substrates and uncover a complex interplay between reaction selectivity and substrate structure and electronics.

Figure 4.1.1. Representative transformations of vinylogous esters.

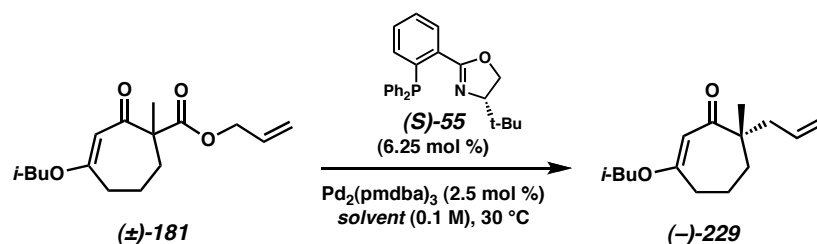


4.2 ENANTIOSELECTIVE DECARBOXYLATIVE ALKYLATIONS OF VINYLOGOUS β -KETOESTER DERIVATIVES

Our explorations of the asymmetric alkylation of vinylogous esters focused on the application of racemic β -ketoester derivatives. These substrates offer a practical advantage over enol carbonate and silyl enol ether substrates due to their ease of preparation and purification, as well as increased stability as enolate precursors.⁶ The design of methods directed toward the preparation and functionalization of seven-membered rings en route to the synthesis of natural products is an ongoing area of research in our laboratory,⁷ and thus our asymmetric alkylation studies initiated with the seven-membered ring vinylogous ester substrate class.

4.2.1 EFFECT OF SOLVENT

The optimization of the decarboxylative alkylation of vinylogous ester derivatives centered on vinylogous β -ketoester (\pm)-**181** (Table 4.2.1). Exposure of this substrate to our typical reaction conditions employing a palladium(0) catalyst and (*S*)-*t*-Bu-PHOX ((*S*)-**55**) in THF at 30 °C smoothly generated α -quaternary ketone **229** in 94% yield and 84% ee (entry 1). While this substrate class exhibited good reactivity, the selectivity provided by ligand **55** was lower than anticipated. Previous studies in our laboratory have established a minor role of solvent for selectivity of the asymmetric alkylation reactions,^{5a} although in certain circumstances solvent can have a notable effect on selectivity.^{5c} Accordingly, a survey of common reaction solvents revealed similar yields of ketone **229** with a distinct enhancement in selectivity. The use of ethereal solvents provided a modest increase in enantioselectivity, with conditions in Et₂O producing **229** in 86% ee (entries 2–5). Substitution with aromatic solvents benzene and toluene enabled a more substantial improvement in selectivity, with up to 88% ee in toluene (entries 6 and 7). Our results indicate that alkylations of substrates such as **181** are readily influenced by solvent, and thus it is a necessary variable for future vinylogous β -ketoester studies.

Table 4.2.1. Solvent screen for the Pd-catalyzed alkylation of vinylogous β -ketoester (\pm)-**181**

entry ^a	solvent	yield (%) ^b	ee (%) ^c
1	THF	94	84
2	1,4-dioxane	86	84
3	2-methyl THF	75	85
4	TBME	88	85
5	Et ₂ O	93	86
6	benzene	84	86
7	toluene	91	88

^a pmdba = bis(4-methoxybenzylidene)acetone.

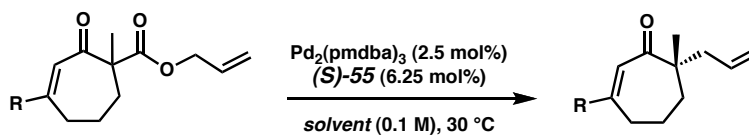
^b Isolated yield. ^c Enantiomeric excess determined by chiral HPLC.

4.2.2 EFFECT OF SUBSTRATE SUBSTITUTION

In addition to the optimization of solvent for the alkylation selectivity, we also examined the identity of the vinylogous moiety. The vinylogous ester substrate class contrasts most other substrates that we have examined in that they allow structural variations while maintaining similar functional reactivity for subsequent transformations. For example, the vinylogous ester **259** depicted in Figure 4.1.1 could possess OR where R = Me, Et, and *i*-Bu, and all three substrates would be unique, yet could function in a similar manner for each subsequent transformation, ultimately providing the same product at the end of the reaction sequence (i.e., **261**). This significant feature greatly expands the substrate potential for the transformation and allows the examination of the role of electronics toward reactivity and selectivity.

In our studies of vinylogous β -ketoester derivatives, we observed that substitution of the R group with ether derivative **263** furnished quaternary ketone **264** in similar selectivity (cf. entries 1–3, Table 4.2.2). Modification of the ether group to an acyl functionality facilitated the construction of ketones **266** and **268** with enhanced selectivity (88 and 90% ee, respectively), with benzoate **268** providing the best results (entries 4–6). The use of a thiophenyl-derived vinylogous ester **269** produced a similar result, affording vinylogous thioester **270** in 89% ee (entry 7). This limited data set demonstrates that reducing the electron density of the vinylogous moiety results in a marked improvement in selectivity and facilitates an increase in the reaction rate.⁸ We can rationalize the electronic role of substitution and reaction rate as a decrease in the energy required for the cleavage of a C–C bond in the decarboxylation event.⁹ However, the influence on selectivity is complex. As we descend down each entry in Table 4.2.2, the resulting enolate pK_a is distinctly reduced, suggesting that the electronics of the palladium–enolate complex impact the reaction such that an electron-deficient complex enhances selectivity,¹⁰ although the exact correlation is difficult to discern.¹¹ Nonetheless, the versatile nature of this substrate class holds the potential for interesting applications.

Table 4.2.2. Variation of the vinylogous functional group for improved stereoselectivity



entry	R	substrate	product	solvent	yield (%) ^a	ee (%) ^b
1	<i>i</i> -BuO	181	229	THF	94	84
2	<i>i</i> -BuO	181	229	Et ₂ O	93	86
3	CH ₃ OCH ₂ O	263	264	THF	79	85
4	<i>t</i> -BuCO ₂	265	266	THF	68	87
5	<i>t</i> -BuCO ₂	265	266	Et ₂ O	84	88
6	PhCO ₂	267	268	THF	85	90
7 ^c	PhS	269	270	Et ₂ O	86	89

^a Isolated yield. ^b Enantiomeric excess determined by chiral HPLC. ^c Using Pd(dmdba)₂ at 25 °C.

4.2.3 EXTENSIONS TO SIX-MEMBERED RINGS

The established viability of seven-membered vinylogous β -ketoester substrates for our asymmetric alkylation method encouraged the extension to six-membered derivatives. Application of the six-membered analog **271** with our standard conditions required an increase in reaction temperature to 50 °C to achieve complete conversion to ketone **272**, although with a noticeable decrease in selectivity to 83% ee (entry 1, Table 4.2.3). Solvent identity displays a key role for six-membered substrates, as the use of toluene for the production of **272** increased the selectivity to 86% ee (entry 2). Moreover, substitution at the α -position of the β -ketoester to an ethyl group afforded ketone **274** in 86% ee (entry 3).¹² Examination of substrates that possess substitution α to the vinylogous moiety afforded strikingly different results. Substrate reactivity for the production of vinylogous ester **275** was exceedingly slow at 50 °C, and an increase to 80 °C facilitated complete conversion to **276** with a modest 75% ee (entries 4 and 5).

However, the utilization of a vinylogous thioester **277** enabled complete conversion at 50 °C to α -quaternary vinylogous thioester **278** in a remarkable 92% ee, with an absence of solvent influence (entries 6 and 7).

Table 4.2.3. Six-membered vinylogous β -ketoester substrates

entry	product	R ³	substrate	product	solvent	yield (%)	ee (%)
1		Me	271	272	THF	80	83
2		Me	271	272	toluene	79	86
3 ^a		Et	273	274	THF	82	86
4 ^b			275	276	toluene	19	79
5 ^c			275	276	toluene	86	75
6			277	278	toluene	86	92
7			277	278	THF	88	92

^a Reaction performed using 5 mol % Pd(dmdba)₂. ^b β -ketoester starting material was isolated in 69% yield. ^c At 80 °C.

In general, substrates that possess a six-membered ring require additional energy to break the C–C bond in the decarboxylation event of the β -ketoester compared to seven-membered rings, resulting in increased reaction temperatures and times (see the subsection 4.3.3.1).¹³ A comparison of substrates **271** and **275** underscores the difference in reactivity and selectivity resulting from the addition of a methyl group to the α -position (cf. entries 2 and 4). Moreover, adjusting the electronics of the vinylogous moiety exhibits a large impact on selectivity (cf. entries 4 and 6). Taken together, these

seemingly trivial substrate changes have a significant impact on reactivity and selectivity, making it difficult to delineate reaction trends.

4.2.4 **FUTURE STUDIES OF VINYLOGOUS β -KETOESTER SUBSTRATES**

Our preliminary asymmetric alkylation studies of vinylogous β -ketoester substrates have displayed a range of selectivities and reactivities, indicating a complex role of substrate structure and electronics of the vinylogous moiety. Future efforts for this class of substrates will expand on substrate substitution for both seven and six-membered rings to examine the generality of the transformation. In addition to the increase in number of substrates, a thorough investigation encompassing solvent variation and substrate electronics could enable the development of predictive tools for general use. Furthermore, the utility of enol carbonate vinylogous ester derivatives and ligands possessing variable electronic properties are viable options for challenging substrates.¹⁰ The elaboration of the various vinylogous products obtained from the asymmetric alkylation reaction into useful intermediates is of importance for the utility of this class of molecules. Importantly, the reactivities and selectivities observed for the vinylogous ester derivatives provide access to a variety of enantioenriched α -quaternary enones using Stork–Danheiser chemistry and provide a firm precedent for future studies.

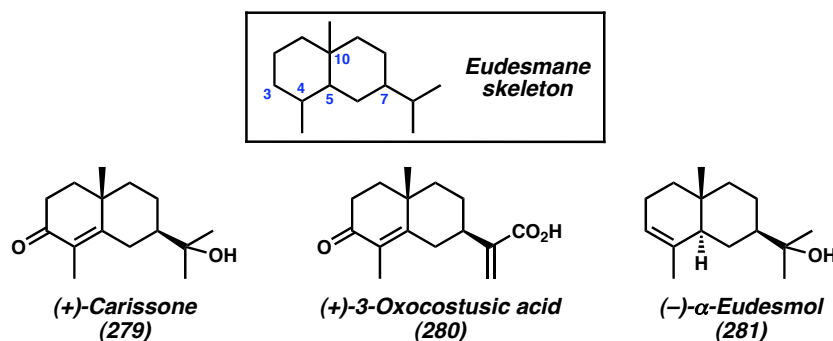
4.3 CATALYTIC ENANTIOSELECTIVE APPROACH TO THE EUDESMANE SESQUITERPENOIDS

The production of highly enantioenriched materials from the enantioselective alkylation of vinylogous β -ketoester derivatives enables their use for various applications. Specifically, we sought to harness this transformation as the key enantioselective reaction in a multistep synthesis. Here we detail our efforts to utilize the asymmetric alkylation of vinylogous β -ketoester derivatives toward a general approach to the eudesmane sesquiterpenoids.

4.3.1 BACKGROUND OF THE EUDESMANE SESQUITERPENOIDS

The flowering plants of the family Asteraceae (Compositae) have many historical uses, including rubber, medicines, edible oils and vegetables, and pesticides.¹⁴ Among these floras are a large number of species abundant in structurally diverse sesquiterpenoids, particularly ones that contain the eudesmane skeleton (Figure 4.3.1). Over 1000 eudesmanes have been identified from these sources with their structures diverging based on oxygenation and oxidation patterns within the carbon framework.

Figure 4.3.1. Representative eudesmane sesquiterpenoids.

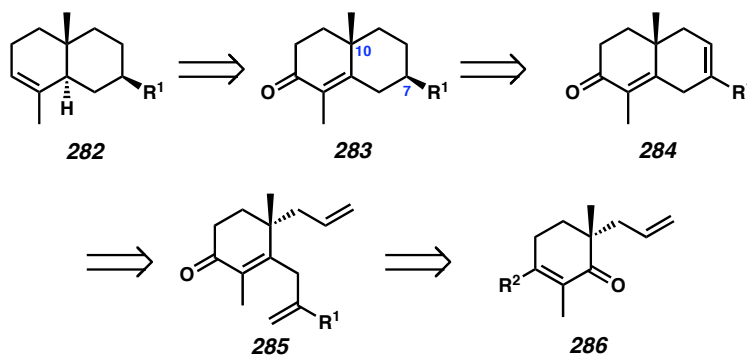


This ever-growing¹⁵ class of important secondary metabolites possesses a wide range of biological properties including plant growth inhibition, insect antifeedant, antibacterial, antifungal, and antitumor activities. Representative eudesmanes comprise antibacterial agents (+)-carissone (**279**)¹⁶ and (+)-3-oxocostusic acid (**280**),¹⁷ as well as P/Q-type calcium channel blocker (-)- α -eudesmol (**281**)¹⁸ (Figure 4.3.1). These examples typify common structural motifs within this class of sesquiterpenoids, primarily the C(10) all-carbon quaternary stereocenter and stereogenic C(7) substituent. The structural similarities and interesting biology associated with this class of molecules has stimulated several synthetic efforts, most of which employ semisynthetic or chiral pool strategies.^{19,20,21} To date, no catalytic asymmetric approach toward these eudesmanes has been developed. Herein, we report an approach²² that incorporates our recent method for the catalytic asymmetric formation of enantioenriched all-carbon quaternary stereocenters into a general synthetic strategy for this class of sesquiterpenoids.

4.3.2 RETROSYNTHETIC ANALYSIS OF THE EUDESMANE CARBOCYCLIC CORE

In devising a strategy to access the eudesmanes, we simplified our target structure to enone **283**, which has been utilized in the preparation of structures such as **282**^{19c} and embodies many features present in various family members (cf. **283** and **279**, **280**) (Scheme 4.3.1). We envisioned that the stereochemistry of the C(7) substituent could arise by means of the diastereoselective hydrogenation of a substituted cyclohexene (i.e., **284**), the stereochemical outcome of which would be controlled by the C(10) quaternary stereocenter. This cyclohexene could be obtained from a ring-closing metathesis of triolefin **285**, which would be derived from an appropriately substituted α -quaternary ketone (i.e., **286**). Thus, we sought to develop an efficient and selective preparation of the C(10) quaternary stereocenter³ as the key control element in our synthetic approach toward the eudesmanes.

Scheme 4.3.1. Retrosynthetic analysis of the eudesmanes



4.3.3 TOTAL SYNTHESIS OF (+)-CARISSONE

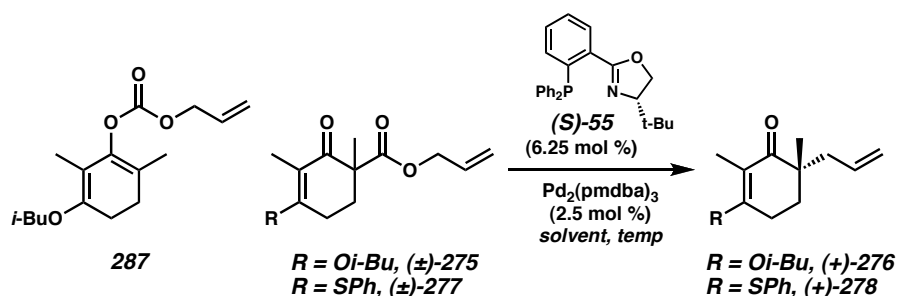
4.3.3.1 Pd-CATALYZED ENANTIOSELECTIVE ALKYLATION OF VINYLOGOUS ESTER DERIVATIVES

The enantioselective alkylation of ketone enolates is an area of intense investigation in our laboratory.⁵ This method has resulted in the preparation of a wide range of carbonyl compounds with adjacent quaternary stereocenters with high levels of selectivity and excellent yields, some of which have proved valuable in synthetic endeavors.^{7e,10b,23} The application of α -quaternary ketones such as **286** for the devised strategy would require a carbonyl transposition (i.e., **286** \rightarrow **285**), and we therefore chose to exploit the unique properties of vinylogous esters (i.e., **286** where $R^2 = OR$) pioneered by Stork and Danheiser² for this purpose.

Our initial studies for the asymmetric generation of quaternary stereocenters utilizing vinylogous ester derivatives focused on enol carbonates due to preliminary investigations^{4a,10b} that have demonstrated successes for similar substrates. Exposure of allyl enol carbonate **287** to typical reaction conditions consisting of a palladium(0) catalyst and ligand (*S*)-**55**²⁴ in toluene generated vinylogous ester (+)-**276**, albeit in variable yield and selectivity (Table 4.3.1, entry 1). Unfortunately, the instability of **287** impeded further studies, as these results were highly dependent on the composition of this enol carbonate.²⁵ Given the range of substrate possibilities for this transformation,^{5d} we next focused on racemic β -ketoester (\pm)-**275**. Surprisingly, this substrate proved only modestly reactive at 50 °C, producing ketone **276** in 19% yield and 79% ee (entry 2).²⁶ Increasing the reaction temperature to 80 °C enabled complete conversion to ketone **276**, although with slightly reduced selectivity (entry 3). As the lack of reactivity seemed to

be a major complication with this substrate, we considered vinylogous thioesters (i.e., (\pm)-**277**) for their reported activation properties.^{4a} Indeed, racemic β -ketoester (\pm)-**277** did prove more reactive and produced ketone (+)-**278** at 50 °C in good yield and 92% ee (entry 4). A screen of solvents revealed that benzene (entry 5) and ethereal solvents (entries 6 and 7) provided similar selectivities to toluene.

Table 4.3.1. Asymmetric allylation of vinylogous ester derivatives



entry	substrate	solvent	T (°C)	product	yield ^a (%)	ee ^b (%)
1	287	toluene	25	276	22–61	84–88
2	275	toluene	50	276	19 ^c	79
3	275	toluene	80	276	86	75
4	277	toluene	50	278	86	92
5	277	benzene	50	278	61 ^d	92
6	277	THF	50	278	88	92
7	277	1,4-dioxane	50	278	90	91

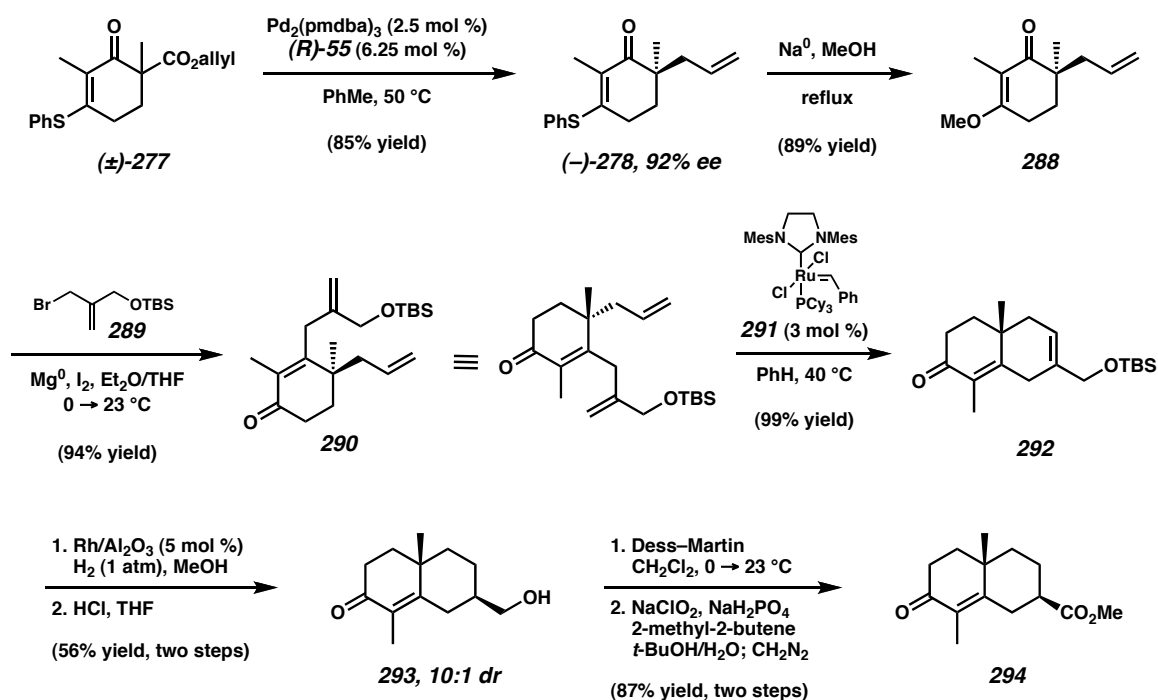
^a Isolated yields. ^b Enantiomeric excess determined by chiral HPLC or SFC. ^c β -Ketoester (\pm)-**275** was recovered in 69% yield. ^d β -Ketoester (\pm)-**277** was recovered in 26% yield.

4.3.3.2 PREPARATION OF THE BICYCLIC CORE

With optimal conditions for the preparation of **278**, we sought to demonstrate the feasibility of using this ketone for the total synthesis of (+)-carissone (**279**). Accordingly, racemic β -ketoester (\pm)-**277** was transformed to (–)-**278** in 85% yield²⁷ and 92% ee using ligand (*R*)-**55** to correlate with the natural antipode of **279** (Scheme 4.3.2). Subsequent

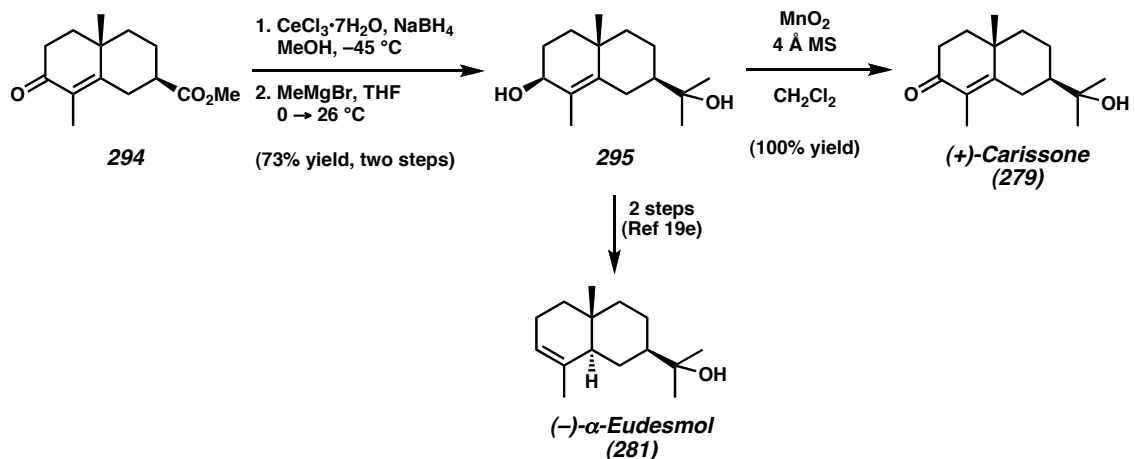
conversion of vinylogous thioester **278** into vinylogous ester **288** was achieved with sodium methoxide in refluxing methanol. Exposure of the resulting vinylogous ester to the substituted allylmagnesium bromide generated from **289**²⁸ provided enone **290** in 94% yield. We were encouraged by the success of allylmagnesium bromide additions to vinylogous ester **288** and investigated similar reactions of various organometallic reagents with vinylogous thioester **278**; however, several conditions afforded intractable mixtures with no desired products.²⁹ Nonetheless, ring-closing metathesis of enone **290** using Grubbs' catalyst **291**³⁰ efficiently prepared the desired substrate (i.e., **292**) for the diastereoselective hydrogenation. Gratifyingly, the heterogeneous hydrogenation of **292** utilizing Rh/Al₂O₃ catalyst³¹ in methanol and subsequent TBS cleavage provided alcohol **293** in good overall yield with excellent diastereoselectivity.³² This notable transformation generates alcohol **293** with the C(10) and C(7) stereocenters in the desired syn configuration required for **279**. Conversion of alcohol **293** to ester **294** was achieved by a two-step process involving Dess–Martin oxidation,³³ followed by chlorite oxidation³⁴ with diazomethane workup.

Scheme 4.3.2. Enantioselective synthesis of the eudesmane bicyclic core



4.3.3.3 COMPLETION OF (+)-CARISSONE AND A FORMAL SYNTHESIS OF (-)- α -EUDESMOL

The availability of ester **294** in the desired configuration enabled preparation of (+)-carissone (**279**) in short order. Diastereoselective reduction of the enone carbonyl under Luche conditions,³⁵ followed by treatment of the resulting alcohol with methylmagnesium bromide^{21f} provided diol **295**^{19a} in 73% yield (Scheme 4.3.3). The preparation of this diol intersects Aoyama's synthesis (-)- α -eudesmol (**281**)^{19c} and represents a formal total synthesis. Furthermore, facile allylic oxidation with manganese dioxide gave (+)-carissone (**279**) having spectroscopic data (¹H NMR, ¹³C NMR, IR, HRMS, optical rotation) identical to those reported for natural **279**.

Scheme 4.3.3. End game for (+)-carissone (**279**) and the formal synthesis of (-)- α -eudesmol (**281**)

4.4 CONCLUSION

In summary, we have described the palladium-catalyzed asymmetric alkylation of various vinylogous β -ketoester substrates to provide access to enantioenriched α -quaternary ketones in high yields. Our studies revealed a significant influence of solvent, substrate structure, and electronics on the reactivity and selectivity of the transformation. Importantly, the incorporation of electron-withdrawing groups on the vinylogous moiety increases reaction rates and enhances selectivities over traditional vinylogous esters. We have demonstrated the utility of the resulting α -quaternary products in a general synthetic approach for the total synthesis of the eudesmane sesquiterpenoids. Fundamental to this strategy is the use of the resulting C(10) quaternary stereocenter to control the C(7) stereochemistry via a diastereoselective hydrogenation, providing a highly selective and efficient route to the antibacterial agent (+)-carissone (**279**). Studies to understand the interplay between substrate reactivity and selectivity for the asymmetric alkylation of vinylogous ester derivatives, as well as the

use of the resulting enantioenriched products in the synthesis of other bioactive natural substances, are currently underway.

4.5 EXPERIMENTAL SECTION

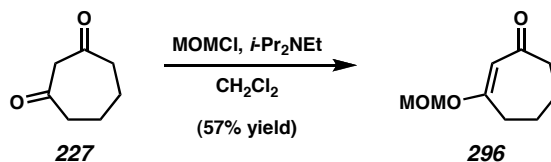
4.5.1 MATERIALS AND METHODS

Unless otherwise stated, reactions were performed in flame-dried glassware under an argon or nitrogen atmosphere using dry, deoxygenated solvents. Solvents were dried by passage through an activated alumina column under argon. All the starting materials were purchased from commercial sources and used as received, unless otherwise stated. Liquids and solutions were transferred via syringe or positive-pressure cannulation. Brine solutions refer to saturated aqueous sodium chloride solutions. TMEDA was distilled from sodium under nitrogen prior to use. Benzenethiol was distilled under nitrogen prior to use. For data regarding the conversion of (\pm)-**181** to ($-$)-**229**, see Chapter 3 of this thesis. Previously reported methods were used to prepare (*S*)-*t*-BuPHOX ((*S*)-**55**) and (*R*)-*t*-BuPHOX ((*R*)-**55**),³⁶ as well as Pd₂(pmdba)₃.³⁷ Grubbs' catalyst **291** was a generous gift from Materia, Inc. Rhodium was purchased from Strem as a 1 wt % loading on alumina powder in reduced form. Diazomethane (**199**) was freshly prepared from Diazald as a solution in Et₂O. Manganese dioxide was purchased from Aldrich in activated form, ~85%, <5 μ m, and used as received. Reaction temperatures were controlled by an IKAmag temperature modulator. Thin-layer chromatography (TLC) was performed using E. Merck silica gel 60 F254 precoated plates (0.25 mm) and visualized by UV fluorescence quenching, anisaldehyde, or KMnO₄ staining. SiliCycle SiliaFlash P60 Academic Silica Gel (particle size 40–63 μ m; pore diameter 60 Å) was used for flash chromatography. Analytical chiral HPLC was performed with an Agilent 1100 Series HPLC utilizing Chiralpak AD and OD-H columns

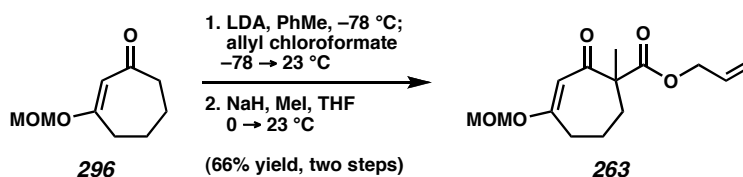
(4.6 mm x 25 cm) obtained from Daicel Chemical Industries, Ltd. with 1 mL/min flow rate and visualization at 254 nm. Analytical chiral supercritical fluid chromatography was performed with a Berger Analytix SFC (Thar Technologies) utilizing a Chiralpak AD-H column (4.6 mm x 25 cm) obtained from Daicel Chemical Industries, Ltd. with 2 mL/min flow rate at 30 °C and visualization at 244 nm. Optical rotations were measured with a Jasco P-1010 polarimeter at 589 nm in spectrophotometric grade solvents. ^1H and ^{13}C NMR spectra were recorded on a Varian Mercury 300 (at 300 MHz and 75 MHz respectively) or a Varian Inova 500 (at 500 MHz and 126 MHz, respectively), and are reported relative to Me_4Si (δ 0.0 ppm).³⁸ Data for ^1H NMR spectra are reported as follows: chemical shift (δ ppm) (multiplicity, coupling constant (Hz), integration). Multiplicity and qualifier abbreviations are as follows: s = singlet, d = doublet, t = triplet, q = quartet, m = multiplet, comp = complex, br = broad, app = apparent. IR spectra were recorded on a Perkin Elmer Paragon 1000 spectrometer and are reported in frequency of absorption (cm^{-1}). Melting points are uncorrected. High-resolution mass spectra were obtained from the Caltech Mass Spectral Facility

4.5.2 PREPARATIVE PROCEDURES

4.5.2.1 ASYMMETRIC ALKYLATION OF VINYLOGOUS β -KETOESTER DERIVATIVES



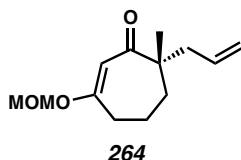
Vinylogous ester 296. To a solution of dione **227** (574.6 mg, 4.55 mmol, 1.0 equiv) in CH₂Cl₂ (22.8 ml, 0.2 M) was added MOM-Cl (381 μ L, 5.01 mmol, 1.1 equiv) followed by *i*-Pr₂NEt (873 μ L, 5.01 mmol, 1.1 equiv). After 12 h the reaction was diluted with CH₂Cl₂ (25 mL), washed with 1 N HCl, sat aq NaHCO₃, brine, dried over MgSO₄, filtered, and concentrated in vacuo. The crude material was purified by flash chromatography on SiO₂ (4:1 \rightarrow 2:1 hexanes/EtOAc) to give **296** (441.9 mg, 2.596 mmol, 57% yield) as a pale yellow oil. $R_f = 0.16$ (2:1 hexanes/EtOAc); ¹H NMR (300 MHz, CDCl₃) δ 5.50 (s, 1H), 4.97 (s, 2H), 3.43 (s, 3H), 2.59–2.55 (comp m, 4H), 1.90–1.74 (comp m, 4H); ¹³C NMR (75 MHz, CDCl₃) δ 202.4, 173.8, 108.0, 94.2, 57.0, 42.0, 32.9, 23.8, 21.4; IR (Neat Film NaCl) 2942, 1645, 1611, 1454, 1376, 1215, 1153, 1071, 972, 924 cm⁻¹; HRMS (FAB+) m/z calc'd for C₉H₁₅O₃ [M + H]⁺: 171.1021, found 171.1055.



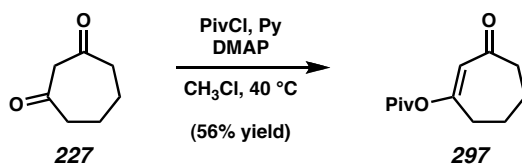
Vinylogous β -ketoester 263. To a solution of *i*-Pr₂NH (764 μ L, 5.45 mmol, 2.1 equiv) in PhMe (18 mL) cooled to -78 °C was added a solution of *n*-BuLi (2.09 mL of a 2.55 M solution in hexane, 5.32 mmol, 2.05 equiv). The flask was placed in a 0 °C cooling bath for 10 min, cooled back down to -78 °C, and to this was added a solution of vinylogous ester **296** (441.9 mg, 2.60 mmol, 1.0 equiv) in PhMe (2 mL, wash with extra 2 mL). After 30 min, allyl chloroformate (290 μ L, 2.73 mmol, 1.05 equiv) was added dropwise and the bath was removed. The reaction was quenched with 1 N KHSO₄ (15 mL) after stirring at room temperature for 30 min, the layers were separated, and the aq was extracted with CH₂Cl₂ (3 x 15 mL). The combined organics were washed with brine, dried over MgSO₄, filtered, and concentrated in vacuo.

The resulting crude oil was dissolved in THF (5.2 mL, 0.5 M) and cooled to 0 °C in an ice bath. To this was added NaH (124.6 mg, 3.12 mmol, 1.2 equiv) in one portion, and after 30 min, MeI (485 μ L, 7.79 mmol, 3.0 equiv) was added and the cooling bath was removed. After 4 h, the reaction was quenched with 50% sat. aq NH₄Cl (15 mL) and diluted with Et₂O (15 mL), the layers were separated, and the aq was extracted with Et₂O (3 x 15 mL). The combined organics were washed with brine, dried over Na₂SO₄, filtered, and concentrated in vacuo. The crude was purified by flash chromatography on SiO₂ (6:1 \rightarrow 3:1 \rightarrow 2:1 hexanes/EtOAc) to afford vinylogous β -ketoester **263** (459.6 mg, 1.71 mmol, 66% yield over two steps) as a colorless oil. $R_f = 0.22$ (4:1 hexanes/EtOAc); ¹H NMR (300 MHz, CDCl₃) δ 5.87 (dddd, $J = 17.2, 10.4, 5.6, 5.6$ Hz, 1H), 5.57 (d, $J = 1.1$ Hz, 1H), 5.29 (app dq, $J = 17.2, 1.6$ Hz, 1H), 5.21 (app dq, $J = 10.4, 1.3$ Hz, 1H), 4.99 (d, $J = 6.1$ Hz, 1H), 4.96 (d, $J = 6.1$ Hz, 1H), 4.66–4.52 (comp m, 2H), 3.43 (s, 3H), 2.61 (dddd, $J = 18.1, 9.8, 4.1, 1.2$ Hz, 1H), 2.48–2.38 (comp m, 2H), 2.06–1.92 (m, 1H), 1.87–

1.64 (comp m, 2H), 1.43 (s, 3H); IR (Neat Film NaCl) 2938, 1734, 1649, 1617, 1454, 1423, 1379, 1234, 1147, 1114, 1069, 966, 926, 861 cm^{-1} ; HRMS (FAB+) m/z calc'd for $\text{C}_{14}\text{H}_{21}\text{O}_5$ $[\text{M} + \text{H}]^+$: 269.1389, found 269.1381.

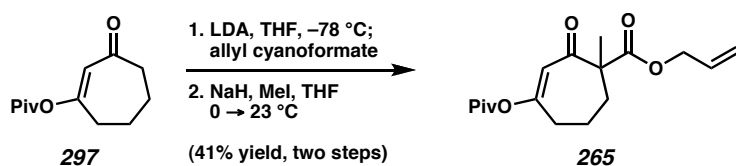


Vinylogous ester 264. A typical asymmetric alkylation reaction was run on 28.6 mg (0.100 mmol) of **263** at 30 °C in THF (0.1 M) for 9 h using (*S*)-**55** and $\text{Pd}_2(\text{pmdba})_3$. The crude material was purified by flash chromatography on SiO_2 (6:1 hexanes/EtOAc, PhMe load) to provide **264** (17.8 mg, 0.0794 mmol, 79% yield) as a pale yellow oil. $R_f = 0.31$ (1:1 hexanes/EtOAc); IR (Neat Film NaCl) 2934, 1620, 1454, 1389, 1216, 1148, 1067, 992, 957, 924, 879 cm^{-1} . HPLC conditions: 0.5% EtOH in hexanes, OD-H column, t_R (min): major = 12.69, minor = 13.59.



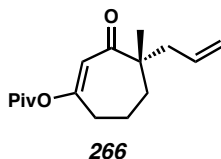
Vinylogous pivalate 297. To a solution of diketone **227** (229.7 mg, 1.82 mmol, 1.0 equiv) dissolved in CHCl_3 (9.1 mL, 0.2 M) was added pyridine (147 μL , 1.82 mmol, 1.0 equiv), PivCl (247 μL , 2.00 mmol, 1.1 equiv), and DMAP (44.5 mg, 0.364 mmol, 0.2 equiv), and the resulting solution was placed in a 40 °C oil bath. After 24 h, the reaction was diluted with CH_2Cl_2 (10 mL), washed with 1 N HCl (10 mL), then sat. aq NaHCO_3 (10 mL), dried over MgSO_4 , filtered, and concentrated in vacuo. The crude oil was

purified by flash chromatography on SiO₂ (9:1 → 6:1 hexanes/EtOAc, PhMe load) to give **297** (213.2 mg, 1.01 mmol, 56% yield) as a colorless oil. $R_f = 0.23$ (6:1 hexanes/EtOAc); ¹H NMR (300 MHz, CDCl₃) δ 5.80–5.79 (m, 1H), 2.64 (dd, $J = 7.0, 5.4$ Hz, 2H), 2.58 (dd, $J = 6.7, 5.5$ Hz, 2H), 1.97–1.81 (comp m, 4H), 1.24 (s, 9H); ¹³C NMR (75 MHz, CDCl₃) δ 201.7, 176.3, 167.5, 122.1, 43.2, 39.1, 33.4, 27.0, 24.4, 21.7; IR (Neat Film NaCl) 2974, 2938, 2873, 1749, 1667, 1650, 1481, 1458, 1369, 1275, 1114 cm⁻¹; HRMS (EI+) m/z calc'd for C₁₂H₁₈O₃ [M]⁺: 210.1256, found 210.1253.



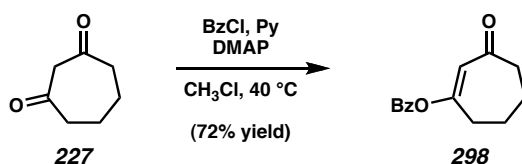
Vinylogous β -ketoester 265. To a solution of *i*-Pr₂NH (333 μ L, 2.38 mmol, 1.2 equiv) in THF (8 mL) at 0 °C was added a solution of *n*-BuLi (890 μ L of a 2.45 M solution in hexane, 2.18 mmol, 1.1 equiv). After 30 min, the solution was cooled to -78 °C and a solution of vinylogous pivalate **297** (416.5 mg, 1.98 mmol, 1.0 equiv) in THF (2 mL) was added dropwise via cannula transfer. After 1 h at -78 °C, allyl cyanoformate (237 μ L, 2.18 mmol, 1.1 equiv) was added. After 30 min the reaction was quenched with 50% sat. aq NH₄Cl (10 mL) and warmed to room temperature. The layers were separated and the aq layer was extracted with Et₂O (3 x 15 mL), the combined organics were washed with brine (10 mL), dried over MgSO₄, filtered, and concentrated in vacuo. The crude material was purified by flash chromatography on SiO₂ (9:1 → 3:1 hexanes/Et₂O) to provide the desired acylated intermediate (274.0 mg, 0.93 mmol, 47% yield).

The resulting intermediate was dissolved in THF (4.7 mL, 0.2 M) and cooled to 0 °C, at which point NaH (44.7 mg, 1.12 mmol, 1.2 equiv) was added in one portion. After 20 min, MeI (173 μ L, 2.79 mmol, 3.0 equiv) was added and the cooling bath was removed. The reaction was quenched with 50% sat. aq NH_4Cl after 10 h, diluted with Et_2O (10 mL), the layers were separated and the aq layer was extracted with Et_2O (3 x 10 mL). The combined organics were washed with brine, dried over MgSO_4 , filtered, and concentrated to a crude oil. Purification by flash chromatography on SiO_2 (9:1 \rightarrow 6:1 hexanes/ Et_2O) provided vinylogous β -ketoester **265** (253.2, 0.821 mmol, 41% yield over two steps) as a colorless oil. $R_f = 0.34$ (3:1 hexanes/ Et_2O); ^1H NMR (300 MHz, CDCl_3) δ 5.87 (dddd, $J = 17.2, 10.4, 5.7, 5.7$ Hz, 1H), 5.83 (d, $J = 1.0$ Hz, 1H), 5.29 (app dq, $J = 17.2, 1.5$ Hz, 1H), 5.21 (app dq, $J = 10.4, 1.3$ Hz, 1H), 4.62 (app dt, $J = 5.6, 1.4$ Hz, 2H), 2.61 (dddd, $J = 18.6, 8.7, 4.3, 1.4$ Hz, 1H), 2.50–2.39 (comp m, 2H), 2.07–1.94 (m, 1H), 1.91–1.81 (m, 1H), 1.76 (ddd, $J = 11.0, 7.6, 2.9$ Hz, 1H), 1.43 (s, 3H), 1.24 (s, 9H); ^{13}C NMR (75 MHz, CDCl_3) δ 198.9, 176.1, 173.2, 164.6, 131.8, 121.0, 118.5, 66.1, 66.0, 60.0, 39.2, 34.0, 33.7, 27.0, 23.5, 21.6, 15.4; IR (Neat Film NaCl) 2977, 2934, 1746, 1685, 1650, 1454, 1379, 1274, 1233, 1180, 1103, 1027, 980, 909 cm^{-1} ; HRMS (FAB+) m/z calc'd for $\text{C}_{17}\text{H}_{25}\text{O}_5$ $[\text{M} + \text{H}]^+$: 309.1702, found 309.1619.

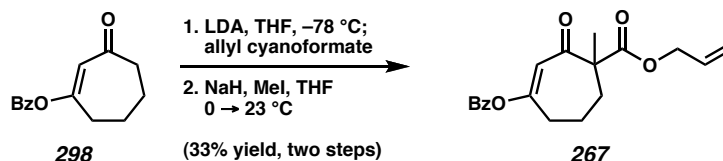


Vinylogous pivalate 266. A typical asymmetric alkylation reaction was run on 42.0 mg (0.136 mmol) of **265** at 30 °C in Et_2O (0.1 M) for 2 h using (*S*)-**55** and $\text{Pd}_2(\text{pmdba})_3$. The crude material was purified by preparative TLC on SiO_2 (3:1

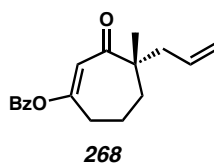
hexanes/Et₂O) to provide **266** (30.2 mg, 0.114 mmol, 84% yield) as a pale yellow oil. $R_f = 0.34$ (1:1 hexanes/EtOAc); ¹H NMR (300 MHz, CDCl₃) δ 5.72–5.71 (m, 1H), 5.70 (dddd, $J = 16.6, 10.5, 7.4, 7.4$ Hz, 1H), 5.08–5.06 (m, 1H), 5.05–5.06 (m, 1H), 5.05–5.00 (m, 1H), 2.49 (dd, $J = 6.3, 5.3$ Hz, 2H), 2.30 (app qd, $J = 13.7, 7.4$ Hz, 2H), 1.92–1.61 (comp m, 4H), 1.25 (s, 9H), 1.15 (s, 3H); ¹³C NMR (75 MHz, CDCl₃) δ 206.2, 176.4, 162.7, 133.8, 120.6, 118.4, 52.5, 44.6, 39.2, 34.9, 34.8, 27.1, 24.3, 20.0; IR (Neat Film NaCl) 2976, 2936, 2873, 1749, 1656, 1480, 1461, 1379, 1276, 1105, 914 cm⁻¹. HPLC conditions: 0.25% *i*-PrOH in hexanes, OD-H column, t_R (min): major = 10.24, minor = 11.73.



Vinylogous benzoate 298. Prepared in the exact manner as vinylogous pivalate **297** using 220.5 mg (1.75 mmol) of diketone **227**. The crude material was purified by flash chromatography on SiO₂ (6:1 \rightarrow 4:1 hexanes/EtOAc, PhMe load) to provide **298** (291.8 mg, 1.27 mmol, 72% yield) as a pale yellow oil. $R_f = 0.26$ (4:1 hexanes/EtOAc); ¹H NMR (300 MHz, CDCl₃) δ 8.08–8.05 (comp m, 2H), 7.66–7.60 (m, 1H), 7.51–7.46 (comp m, 2H), 5.99 (s, 1H), 2.77–2.69 (comp m, 4H), 2.05–1.87 (comp m, 4H); ¹³C NMR (75 MHz, CDCl₃) δ 201.7, 167.4, 164.3, 134.0, 130.2, 129.8, 128.8, 122.6, 43.3, 33.5, 24.5, 21.8; IR (Neat Film NaCl) 3064, 2941, 2870, 1733, 1663, 1652, 1601, 1452, 1315, 1262, 1202, 1176, 1112, 1090, 1052, 1024, 878, 855, 708, 524 cm⁻¹; HRMS (EI+) m/z calc'd for C₁₄H₁₄O₃ [M]⁺: 230.0943, found 230.0940.

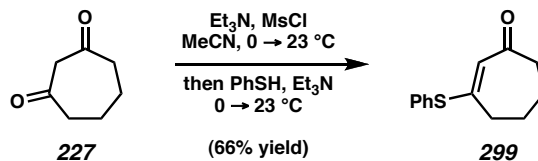


Vinylogous β -ketoester 267. Prepared in the exact manner as vinylogous β -ketoester **265**. Purified by flash chromatography on SiO_2 (9:1 \rightarrow 6:1 hexanes/EtOAc) to afford **267** (229.6 mg, 0.699 mmol, 33% yield over two steps) as a pale yellow oil. $R_f = 0.37$ (4:1 hexanes/EtOAc); $^1\text{H NMR}$ (300 MHz, CDCl_3) δ 8.06–8.03 (comp m, 2H), 7.64–7.58 (m, 1H), 7.49–7.44 (comp m, 4H), 6.01 (d, $J = 6.0$ Hz, 1H), 5.90 (dddd, $J = 17.0, 10.6, 5.7, 5.7$ Hz, 1H), 5.31 (app dq, $J = 17.2, 1.4$ Hz, 1H), 5.22 (ddd, $J = 10.4, 2.3, 1.2$ Hz, 1H), 4.65 (app dt, $J = 5.7, 1.3$ Hz, 2H), 2.77 (dddd, $J = 18.6, 8.9, 4.1, 1.4$ Hz, 1H), 2.65–2.47 (comp m, 2H), 2.13–2.01 (m, 1H), 1.97–1.76 (m, 1H), 1.81 (ddd, $J = 14.3, 7.6, 3.5$ Hz, 1H), 1.47 (s, 3H); $^{13}\text{C NMR}$ (75 MHz, CDCl_3) δ 198.8, 173.2, 164.3, 164.1, 133.9, 131.8, 130.2, 129.0, 128.7, 121.4, 118.6, 66.1, 60.0, 34.1, 33.9, 23.4, 21.8; HRMS (FAB+) m/z calc'd for $\text{C}_{19}\text{H}_{21}\text{O}_5$ [$\text{M} + \text{H}$] $^+$: 329.1389, found 329.1378.



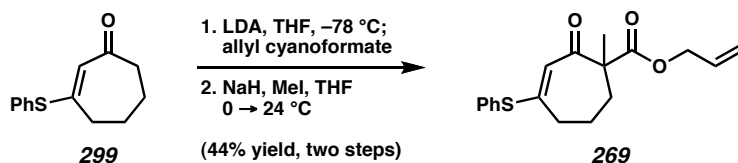
Vinylogous benzoate 268. A typical asymmetric alkylation reaction was run on 39.5 mg (0.120 mmol) of **267** at 30 $^\circ\text{C}$ in THF (0.1 M) for 8 h (overnight) using (*S*)-**55** and $\text{Pd}_2(\text{pmdba})_3$. The crude material was purified by preparative TLC on SiO_2 (4:1 hexanes/EtOAc) to provide **268** (2.1 mg, 0.102 mmol, 85% yield) as a colorless oil. $R_f = 0.47$ (4:1 hexanes/EtOAc); $^1\text{H NMR}$ (300 MHz, CDCl_3) δ 8.08–8.04 (comp m, 2H), 7.64–7.59 (m, 1H), 7.51–7.45 (comp m, 2H), 5.90 (app t, $J = 1.1$ Hz, 1H), 5.74 (dddd, $J =$

16.3, 10.8, 7.4, 7.4, 1H), 5.10–5.09 (m, 1H), 5.07–5.03 (m, 1H), 2.68–2.63 (comp m, 2H), 2.34 (app qt, $J = 13.8, 1.1$ Hz, 2H), 1.99–1.67 (comp m, 4H), 1.19 (s, 3H). HPLC conditions: 2% *i*-PrOH in hexanes, OD-H column, t_R (min): major = 10.86, minor = 12.39.



Vinylogous thioester 299. To a solution of dione **227** (1.3727 g, 10.88 mmol, 1.0 equiv) in MeCN (12.1 mL, 0.9 M) cooled to 0 °C was added Et₃N (1.70 mL, 12.2 mmol, 1.12 equiv) and MsCl (884 μ L, 11.4 mmol, 1.05 equiv). The reaction was slowly warmed to 23 °C over 1 h, then cooled to 0 °C and Et₃N (1.70 mL, 12.2 mmol, 1.12 equiv) followed by freshly distilled PhSH (1.15 mL, 11.21 mmol, 1.03 equiv) were added. The reaction was slowly warmed to 23 °C overnight. When starting material was consumed, the reaction was quenched with sat. aq Na₂CO₃ (30 mL), extracted with Et₂O (3 x 50 mL), the organics were dried over MgSO₄, filtered, and concentrated under reduced pressure to a yellow oil. The crude oil was purified by flash chromatography on SiO₂ (3:1 \rightarrow 1:1 hexanes/Et₂O) to afford **299** as a pale yellow solid (1.5617 g, 7.154 mmol, 66% yield). $R_f = 0.31$ (1:1 hexanes/Et₂O); mp = 73–75 °C; ¹H NMR (500 MHz, CDCl₃) δ 7.48–7.46 (comp m, 2H), 7.43–7.40 (comp m, 3H), 5.48 (s, 1H), 2.65 (dd, $J = 6.1, 6.1$ Hz, 2H), 2.55 (dd, $J = 6.3, 6.3$ Hz, 2H), 1.93–1.88 (comp m, 2H), 1.84–1.79 (comp m, 2H); ¹³C NMR (125 MHz, CDCl₃) δ 200.6, 163.5, 163.4, 135.6, 130.2, 130.0, 129.7, 124.3, 41.4, 33.0, 24.9, 21.0; IR (Neat Film NaCl) 3058, 2939, 2866, 1648. 1586,

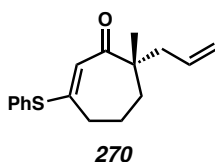
1475, 1440, 1267, 1190, 1016, 750, 691 cm^{-1} ; HRMS (EI+) m/z calc'd for $\text{C}_{13}\text{H}_{14}\text{OS}$ $[\text{M}]^+$: 218.0765, found 218.0758.



Vinylogous β -ketoester 269. To a solution of *i*-Pr₂NH (590 μL , 4.21 mmol, 1.3 equiv) in THF (14 mL) at 0 $^\circ\text{C}$ was added a solution of *n*-BuLi (1.56 mL of a 2.5 M solution in hexane, 3.89 mmol, 1.2 equiv). After 30 min, the solution was cooled to $-78\text{ }^\circ\text{C}$ and a solution of vinylogous thioester **299** (707.5 mg, 3.24 mmol, 1.0 equiv) in THF (2.2 mL) was added dropwise via cannula transfer. After 1 h at $-78\text{ }^\circ\text{C}$, allyl cyanoformate (389 μL , 3.56 mmol, 1.1 equiv) was added. After 2 h the reaction was quenched with 50% sat. aq NH_4Cl (5 mL) and warmed to room temperature. The layers were separated and the aq layer was extracted with Et_2O (3 x 10 mL), the combined organics were washed with brine (10 mL), dried over MgSO_4 , filtered, and concentrated in vacuo.

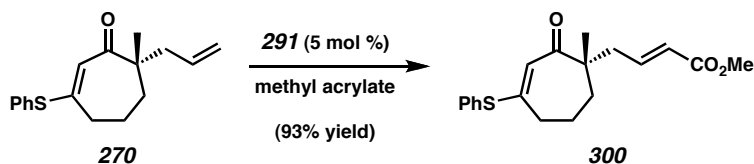
The resulting crude oil was dissolved in THF (4.7 mL) and cooled to 0 $^\circ\text{C}$, at which point NaH (149 mg, 3.73 mmol, 1.15 equiv) was added in two portions. After 20 min, MeI (605 μL , 9.72 mmol, 3 equiv) was added and the cooling bath was removed. The reaction was quenched with 50% sat. aq NH_4Cl after 11 h, diluted with Et_2O (10 mL), the layers were separated and the aq layer was extracted with Et_2O (3 x 10 mL). The combined organics were washed with brine, dried over MgSO_4 , filtered, and concentrated to a crude yellow oil. Purification by flash chromatography on SiO_2 (6:1 \rightarrow 3:1 hexanes/ Et_2O) provided vinylogous β -ketoester **269** (0.3426 g, 1.08 mmol, 34% yield

over two steps) as a pale yellow oil. $R_f = 0.25$ (3:1 hexanes/Et₂O); ¹H NMR (500 MHz, CDCl₃) δ 7.46–7.38 (comp m, 5H), 5.86 (dddd, $J = 10.5, 5.6, 5.6, 0.7$ Hz, 1H), 5.56 (d, $J = 1.5$ Hz, 1H), 5.29 (dddd, $J = 17.1, 1.5, 1.5, 1.5$ Hz, 1H), 5.23 (dddd, $J = 10.5, 1.2, 1.2, 1.2$ Hz, 1H), 4.60 (dddd, $J = 19.5, 5.9, 1.5, 1.5$ Hz, 2H), 2.67 (dddd, $J = 17.6, 10.3, 3.7, 1.7$ Hz, 1H), 2.50–2.43 (comp m, 2H), 2.08–1.98 (m, 1H), 1.86–1.77 (m, 1H), 1.68 (ddd, $J = 14.2, 6.4, 5.4$ Hz, 1H), 1.38 (s, 3H); ¹³C NMR (125 MHz, CDCl₃) δ 197.6, 173.6, 159.5, 135.6, 131.8, 130.1, 129.9, 123.8, 118.7, 66.0, 58.8, 34.2, 33.7, 23.9, 23.8; IR (Neat Film NaCl) 3060, 2982, 2935, 1735, 1650, 1593, 1440, 1230, 1178, 1113, 980, 750, 692 cm⁻¹; HRMS (EI+) m/z calc'd for C₁₈H₂₀O₃S [M]⁺: 316.1133, found 316.1119.

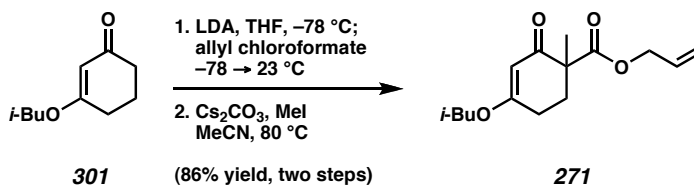


Vinylogous thioester 270. A typical asymmetric alkylation reaction was run on 78.2 mg (0.287 mmol) of **269** at 25 °C in Et₂O (0.1 M) for 5 h using (*S*)-**55** and Pd(dmdba)₂. The crude material was purified by flash chromatography on SiO₂ (15:1 → 9:1 hexanes/Et₂O, PhMe load) to provide **270** (67.1 mg, 0.246 mmol, 86% yield) as a pale yellow oil. $R_f = 0.46$ (3:1 hexanes/Et₂O); ¹H NMR (500 MHz, CDCl₃) δ 7.49–7.46 (comp m, 2H), 7.42–7.38 (comp m, 3H), 5.66 (dddd, $J = 16.8, 10.1, 7.3, 7.3$ Hz, 1H), 5.54 (s, 1H), 5.04–4.98 (comp m, 2H), 2.59–2.48 (m, 2H), 2.29 (dd, $J = 13.7, 7.3$ Hz, 1H), 2.20 (dd, $J = 13.7, 7.6$ Hz, 1H), 1.93–1.77 (comp m, 2H), 1.64–1.58 (m, 1H), 1.09 (s, 3H); ¹³C NMR (125 MHz, CDCl₃) δ 206.0, 155.7, 135.5, 134.2, 130.4, 129.8, 129.8, 124.0, 118.1, 51.3, 44.6, 36.3, 35.2, 24.3, 22.5; IR (Neat Film NaCl) 3074, 2931, 2865, 1650, 1597, 1474, 1440, 1197, 916, 749, 691 cm⁻¹; HRMS (EI+) m/z calc'd for C₁₇H₂₀SO

[M]⁺: 272.1235, found 272.1243; [α]_D^{24.8} -86.35° (*c* 0.905, CH₂Cl₂, 89% ee). HPLC conditions: see derivative **300**.



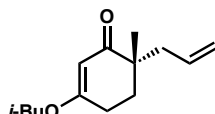
Acrylate 300. To a solution of vinylogous thioester **270** (19.4 mg, 0.0712 mmol, 1.0 equiv) was added methyl acrylate (128 μ L, 0.142 mmol, 20 equiv), followed by Grubbs' catalyst **291** (3.1 mg, 0.0036 mmol, 0.05 equiv) and CH₂Cl₂ (100 μ L). The vial was flushed with argon, capped, and immersed in a 40 °C oil bath overnight. After 10 h, the reaction was concentrated under reduced pressure and purified by preparative TLC on SiO₂ (3:1 hexanes/Et₂O) to give acrylate **300** (21.9 mg, 0.0663 mmol, 93% yield) as a pale yellow oil. *R*_f = 0.19 (3:1 hexanes/Et₂O); ¹H NMR (500 MHz, CDCl₃) δ 7.50–7.40 (comp m, 5H), 6.84 (ddd, *J* = 15.7, 8.0, 8.0 Hz, 1H), 5.81 (ddd, *J* = 15.4, 1.3, 1.3 Hz, 1H), 5.51 (s, 1H), 3.72 (s, 3H), 2.56 (dd, *J* = 7.0, 5.0 Hz, 2H), 2.46 (ddd, *J* = 13.8, 7.4, 1.3 Hz, 1H), 2.33 (ddd, *J* = 13.8, 7.4, 1.3 Hz, 1H), 1.90–1.75 (comp m, 3H), 1.69–1.61 (m, 1H), 1.14 (s, 3H); ¹³C NMR (125 MHz, CDCl₃) δ 204.7, 166.7, 157.0, 145.3, 135.6, 130.1, 130.0, 129.9, 124.0, 123.3, 51.6, 51.3, 42.8, 36.3, 35.3, 24.8, 22.5; IR (Neat Film NaCl) 3057, 2934, 1723, 1654, 1597, 1439, 1272, 1197, 1113, 986, 751, 692 cm⁻¹; HRMS (EI+) *m/z* calc'd for C₁₉H₂₂O₃S [M]⁺: 330.1290, found 330.1293; [α]_D^{25.1} -58.79° (*c* 0.355, CH₂Cl₂, 89% ee). HPLC conditions: 3% EtOH in hexanes, AD column, *t*_R (min): major = 22.3, minor = 18.7.



Vinylogous β -ketoester 271. To a solution of *i*-Pr₂NH (854 μ L, 6.09 mmol, 2.05 equiv) in PhMe (20 mL) cooled to -78 °C was added a solution of *n*-BuLi (2.32 mL of a 2.56 M solution in hexane, 5.94 mmol, 2.0 equiv). The flask was placed in a 0 °C cooling bath for 10 min, cooled back down to -78 °C, and to this was added a solution of vinylogous ester **301**³⁹ (500 mg, 2.97 mmol, 1.0 equiv) in PhMe (3 mL, wash with extra 1 mL). After 30 min, allyl chloroformate (332 μ L, 3.12 mmol, 1.05 equiv) was added dropwise and the bath was removed. The reaction was quenched with 1 N KHSO₄ (15 mL) after stirring at room temperature for 30 min, the layers were separated, and the aq was extracted with Et₂O (2 x 10 mL). The combined organics were washed with brine, dried over MgSO₄, filtered, and concentrated in vacuo.

The resulting crude oil was dissolved in MeCN (12 mL, 0.25 M), and to this was added Cs₂CO₃ (1.160 g, 3.56 mmol, 1.2 equiv) and MeI (555 μ L, 8.90 mmol, 3.0 equiv). The reaction was placed in an 80 °C oil bath and stirred vigorously, and after 17 h the contents were warmed to room temperature. The reaction was diluted with EtOAc (25 mL), dried over MgSO₄, filtered, and concentrated to a crude oil. Purification by flash chromatography on SiO₂ (6:1 \rightarrow 2:1 \rightarrow 1:2 hexanes/Et₂O) to afford vinylogous β -ketoester **271** (679.8 mg, 2.55 mmol, 86% yield over two steps) as a colorless oil. R_f = 0.53 (2:1 hexanes/EtOAc); ¹H NMR (300 MHz, CDCl₃) δ 5.94–5.81 (m, 1H), 5.36 (s, 3H), 5.29 (app dq, J = 17.2, 1.6, 1H), 5.20 (app dq, J = 10.5, 1.3 Hz, 1H), 4.61 (ddd, J = 5.5, 2.9, 1.5 Hz, 2H), 3.60 (d, J = 6.5 Hz, 2H), 2.65–2.35 (comp m, 4H), 2.01 (septuplet,

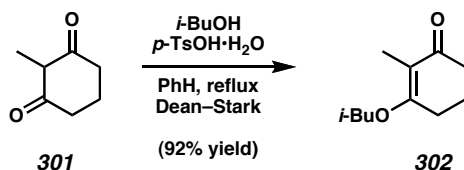
$J = 6.8$ Hz, 1H), 1.88 (ddd, $J = 13.0, 8.0, 4.8$ Hz, 1H), 1.42 (s, 3H), 0.97 (d, $J = 6.7$ Hz, 6H); ^{13}C NMR (75 MHz, CDCl_3) δ 196.7, 176.9, 172.7, 131.9, 118.2, 101.8, 75.0, 65.7, 52.5, 31.8, 27.8, 26.5, 20.7, 19.2; HRMS (FAB+) m/z calc'd for $\text{C}_{15}\text{H}_{23}\text{O}_4$ $[\text{M} + \text{H}]^+$: 267.1596, found 267.1594.



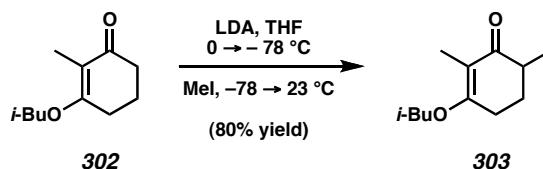
272

Vinylogous ester 272. A typical asymmetric alkylation reaction was run on 26.6 mg (0.100 mmol) of **271** at 50 °C in PhMe (0.1 M) for 33 h using (*S*)-**55** and $\text{Pd}(\text{dmdba})_2$. The crude material was purified by flash chromatography on SiO_2 (9:1 \rightarrow 6:1 hexanes/EtOAc) to provide **272** (17.5 mg, 078.7 μmol , 79% yield) as a colorless oil. $R_f = 0.37$ (6:1 hexanes/EtOAc); ^1H NMR (300 MHz, CDCl_3) δ 5.81–5.68 (m, 1H), 5.25 (s, 1H), 5.08 (s, 1H), 5.05–5.02 (m, 1H), 3.58 (d, $J = 3.5$ Hz, 2H), 2.42 (t, $J = 6.4$ Hz, 2H), 2.36 (dd, $J = 13.6, 7.7$ Hz, 1H), 2.18 (dd, $J = 13.6, 7.7$ Hz, 1H), 2.02 (septuplet, $J = 6.7$ Hz, 1H), 1.92 (app dt, $J = 13.4, 6.2$ Hz, 1H), 1.70 (app dt, $J = 13.5, 6.2$ Hz, 1H), 1.08 (s, 3H), 0.97 (d, $J = 6.7$ Hz, 6H); ^{13}C NMR (75 MHz, CDCl_3) δ 203.7, 176.2, 134.5, 118.0, 101.4, 74.8, 43.3, 41.7, 31.9, 27.9, 26.1, 22.3, 19.2; IR (Neat Film NaCl) 2962, 2932, 2875, 1654, 1611, 1384, 1368, 1239, 1194, 1178, 996, 912, 840 cm^{-1} ; HRMS (FAB+) m/z calc'd for $\text{C}_{14}\text{H}_{23}\text{O}_2$ $[\text{M} + \text{H}]^+$: 223.1698, found 223.1706. HPLC conditions: 5% *i*-PrOH, OD-H column, t_R (min): major = 5.75, minor = 6.40.

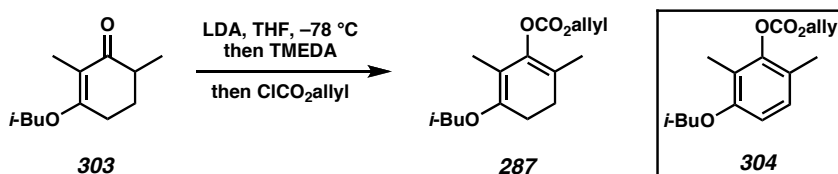
4.5.2.2 ENANTIOSELECTIVE TOTAL SYNTHESIS OF (+)-CARISSONE



Vinylogous ester 302.⁴⁰ Diketone **301** (3.000 g, 23.78 mmol, 1.0 equiv) was partially dissolved in PhH (42.5 mL, 0.56 M), and *i*-BuOH (12.75 mL, 137.9 mmol, 5.8 equiv) and *p*-TsOH \cdot H₂O (226 mg, 1.19 mmol, 0.05 equiv) were added with vigorous stirring. A Dean–Stark adapter and a water-cooled condenser were attached to the flask and the contents were warmed to reflux in a 104 °C oil bath. Upon consumption of **301** by TLC analysis (ca. 3.5 h), the reaction was cooled to ambient temperature, diluted with Et₂O (50 mL), and poured into saturated aq NaHCO₃ (20 mL). The layers were separated and the aq layer was extracted with Et₂O (3 x 15 mL). The organics were combined, washed with brine, dried over Na₂SO₄, filtered, and concentrated in vacuo to afford a pale brown oil. To this oil was added PhMe (ca. 10 mL) followed by further concentration in vacuo. Purification by bulb-to-bulb distillation yielded vinylogous ester **302** (3.988 g, 21.88 mmol, 92% yield) as a clear, colorless oil. $R_f = 0.48$ (2:1 EtOAc/hexanes); bp = 135–140 °C at 0.8 torr; ¹H NMR (300 MHz, CDCl₃) δ 3.76 (d, $J = 6.5$ Hz, 2H), 2.54 (ddd, $J = 6.1, 1.5, 1.5$ Hz, 2H), 2.34 (t, $J = 7.1$ Hz, 2H), 2.08–1.90 (comp m, 3H), 1.72 (app t, $J = 1.5$ Hz, 3H), 0.99 (d, $J = 6.7$ Hz, 6H). All other spectral data are consistent with reported values.



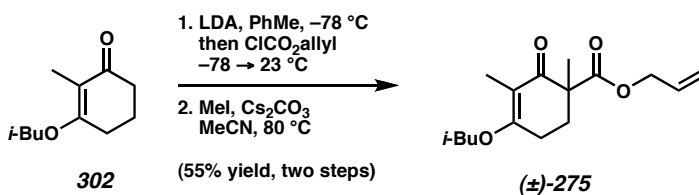
Methyl vinylogous ester 303.⁴⁰ To a solution of *i*-Pr₂NH (1.12 mL, 7.99 mmol, 1.9 equiv) in THF (26 mL, 0.15 M) at 0 °C was added dropwise a solution of *n*-BuLi (2.55 M in hexanes, 3.06 mL, 7.80 mmol, 1.85 equiv). After 15 min, a solution of vinylogous ester **302** (765.2 mg, 4.198 mmol, 1.0 equiv) in THF (2.0 mL) was added dropwise via cannula transfer. The resulting solution was cooled to -78 °C and stirred for 45 min, to which a solution of MeI (485 μ L, 7.80 mmol, 1.85 equiv) in THF (5.0 mL) was added over 30 min via positive-pressure cannula transfer. The cooling bath was allowed to expire over ca. 4 h and the reaction was quenched with brine (15 mL), the phases were separated, and the aq layer was extracted with hexanes (3 x 25 mL). The combined organics were washed with brine, dried over MgSO₄, filtered, and concentrated in vacuo to a yellow oil. Purification by flash chromatography (4:1 \rightarrow 2:1 hexanes/Et₂O) afforded methyl vinylogous ester **303** (659 mg, 3.36 mmol, 80% yield) as a pale yellow oil. R_f = 0.48 (2:1 hexanes/EtOAc); ¹H NMR (300 MHz, CDCl₃) δ 3.73 (ddd, J = 15.6, 9.2, 6.5 Hz, 2H), 2.61 (ddd, J = 17.3, 5.3, 1.2 Hz, 1H), 2.55–2.44 (m, 1H), 2.35–2.19 (m, 1H), 2.06 (app dq, J = 8.3, 4.8 Hz, 1H), 1.98 (app septet, J = 6.6 Hz, 1H), 1.71 (dd, J = 1.6, 1.6 Hz, 3H), 1.73–1.60 (m, 1H), 1.14 (d, J = 6.9 Hz, 3H), 0.99 (d, J = 6.7 Hz, 6H). All other spectral data are consistent with reported values.



Enol carbonate 287. To a solution of *i*-Pr₂NH (1.56 mL, 11.15 mmol, 1.2 equiv) in THF (85 mL, 0.11 M) at 0 °C was added a solution of *n*-BuLi (2.55 M in hexanes, 4.0 mL, 10.22 mmol, 1.1 equiv) dropwise. The reaction mixture was allowed to stir for 30 min and then cooled to -78 °C. A solution of ketone **303** (1.824 g, 9.29 mmol, 1.0 equiv) in THF (10 mL) was added dropwise via cannula and stirred for 1 h. TMEDA (1.67 mL, 11.15 mmol, 1.2 equiv) was then added via syringe and the resulting solution stirred for 75 min. To this solution was added allyl chloroformate (1.08 mL, 10.13 mmol, 1.09 equiv) via syringe and the reaction mixture was stirred at -78 °C for an additional hour. The reaction was quenched with saturated aq NaHCO₃ (40 mL) and H₂O (40 mL), and the flask was transferred to a 23 °C water bath and allowed to equilibrate. The phases were separated and the aqueous was extracted with Et₂O (2 x 200 mL). The combined organics were washed with brine, dried over MgSO₄, and concentrated in vacuo to afford enol carbonate **287** as a yellow oil (2.472 g); ¹H NMR analysis shows **287** is the major product with other impurities present. *R_f* = unstable to SiO₂; ¹H NMR (500 MHz, CDCl₃) δ 5.97 (dddd, *J* = 16.4, 10.8, 5.8, 5.8 Hz, 1H), 5.42 (app d, *J* = 17.2 Hz, 1H), 5.33 (app d, *J* = 10.4 Hz, 1H), 4.72 (dd, *J* = 5.7, 0.8 Hz, 2H), 3.86 (d, *J* = 6.7 Hz, 2H), 2.85 (app t, *J* = 7.9 Hz, 2H), 2.52 (app t, *J* = 7.9 Hz, 2H), 2.19 (s, 3H), 1.92 (app septuplet, *J* = 6.7 Hz, 1H), 1.82 (s, 3H), 0.93 (d, *J* = 6.7 Hz, 6H); IR (Neat Film NaCl) 2963, 1760, 1736, 1699, 1361, 1248, 1170, 990 cm⁻¹; HRMS (FAB+) *m/z* calc'd for C₁₃H₁₉O₄ [M - C₃H₅]⁺: 239.1283, found 239.1273.

This material was unstable to various purification attempts (distillation or flash chromatography using silica gel or Florisil) and storage. Aromatic carbonate **304** was identified as a colorless oil from this complex mixture. *R_f* = 0.51 (4:1 hexanes/EtOAc);

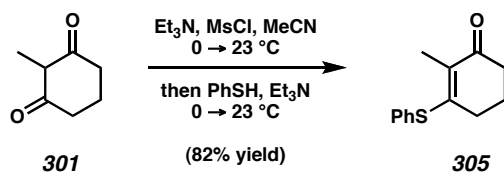
^1H NMR (500 MHz, CDCl_3) δ 6.97 (d, $J = 8.4$ Hz, 1H), 6.65 (d, $J = 8.4$ Hz, 1H), 6.00 (dddd, $J = 17.1, 10.5, 5.7, 5.7$ Hz, 1H), 5.43 (dddd, $J = 17.2, 1.4, 1.4, 1.4$ Hz, 1H), 5.33 (dddd, $J = 10.5, 1.2, 1.2, 1.2$ Hz, 1H), 4.75 (app dt, $J = 5.8, 1.3$ Hz, 2H), 3.70 (d, $J = 6.4$ Hz, 2H), 2.14 (s, 3H), 2.09 (s, 3H), 2.09 (app septuplet, $J = 6.6$ Hz, 1H), 1.03 (d, $J = 6.7$ Hz, 6H); ^{13}C NMR (126 MHz, CDCl_3) δ 156.3, 153.0, 148.7, 131.4, 127.7, 121.8, 119.5, 119.4, 109.1, 74.9, 69.2, 28.6, 19.5, 15.7, 9.2; IR (Neat Film NaCl) 2960, 2874, 1762, 1620, 1494, 1470, 1365, 1244, 1202, 1172, 1115, 1048, 799 cm^{-1} ; HRMS (FAB+) m/z calc'd for $\text{C}_{16}\text{H}_{22}\text{O}_4$ $[\text{M}]^+$: 278.1518, found 278.1517.



β -Ketoester (\pm)-275. To a -78°C solution of $i\text{-Pr}_2\text{NH}$ (425 μL , 3.03 mmol, 1.9 equiv) in PhMe (10 mL) was added dropwise $n\text{-BuLi}$ (2.55 M in hexanes, 1.16 mL, 2.96 mmol, 1.85 equiv). The reaction vessel was placed in an ice/water bath and allowed to stir for 10 min, and then cooled to -78°C . A solution of vinylogous ester **302** (291 mg, 1.60 mmol, 1.0 equiv) in PhMe (1.4 mL) was added dropwise via cannula to the reaction vessel, and the resulting solution was allowed to stir for 30 min. Allyl chloroformate (173 μL , 1.63 mmol, 1.02 equiv) was added dropwise, and the reaction vessel was allowed to warm to 23°C over 1 h. After stirring for 4 h, the reaction was slowly quenched with aq KHSO_4 (1 N, 4 mL) and the resulting biphasic mixture was allowed to stir for 10 min. The phases were separated, and the aq phase was extracted with Et_2O (2 x 10 mL). The combined organic extracts were washed with brine (10 mL),

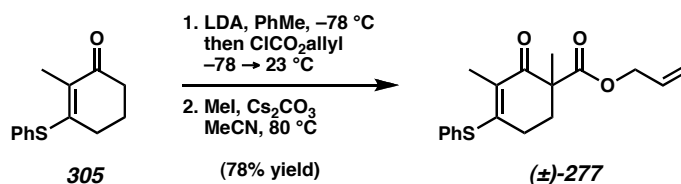
dried over MgSO_4 , filtered, and concentrated in vacuo. The isolated crude yellow oil was used in the next step without further purification.

The resulting crude yellow oil was dissolved in MeCN (5.9 mL, 0.27 M), and Cs_2CO_3 (603 mg, 1.85 mmol, 1.16 equiv), and MeI (276 μL , 4.44 mmol, 2.8 equiv) were added. A water-cooled condenser was attached to the flask and the resulting suspension was warmed to reflux in an 80 °C oil bath with vigorous stirring. After 10 h, the reaction was cooled to room temperature and diluted with EtOAc (25 mL). The organics were dried with MgSO_4 , filtered, and the solvent was evaporated in vacuo. Purification by flash chromatography (15:1 \rightarrow 9:1 \rightarrow 4:1 hexanes/EtOAc) afforded β -ketoester (\pm)-**275** as pale yellow oil (246 mg, 55% yield over two steps). $R_f = 0.27$ (2:1 hexanes/EtOAc); ^1H NMR (500 MHz, CDCl_3) δ 5.82 (dddd, $J = 17.2, 10.7, 5.4, 5.4$ Hz, 1H), 5.22 (dddd, $J = 17.2, 1.6, 1.6, 1.6$ Hz, 1H), 5.15 (dddd, $J = 10.5, 1.2, 1.2, 1.2$ Hz, 1H), 4.56 (dddd, $J = 13.5, 5.4, 1.5, 1.5$ Hz, 2H), 3.72 (ddd, $J = 9.2, 6.6, 3.2$ Hz, 2H), 2.69–2.62 (m, 1H), 2.53–2.44 (comp m, 2H), 1.95 (app septuplet, $J = 6.6$ Hz, 1H), 1.85–1.80 (m, 1H), 1.70 (dd, $J = 1.5, 1.5$ Hz, 3H), 1.36 (s, 3H), 0.95 (dd, $J = 6.7, 0.8$ Hz, 6H); ^{13}C NMR (126 MHz, CDCl_3) δ 195.8, 172.6, 170.3, 131.9, 117.8, 113.8, 73.9, 65.5, 51.6, 31.2, 28.8, 23.0, 20.8, 19.1, 19.0, 8.0; IR (Neat Film NaCl) 2961, 2935, 2875, 1733, 1649, 1618, 1460, 1382, 1354, 1237, 1176, 1103, 983 cm^{-1} ; HRMS (FAB+) m/z calc'd for $\text{C}_{16}\text{H}_{25}\text{O}_4$ $[\text{M} + \text{H}]^+$: 281.1753, found 281.1740.



Vinylogous Thioester 305.^{4a} To a solution of diketone **301** (2.500 g, 19.82 mmol,

1.0 equiv) in MeCN (22.0 mL, 0.9 M) was added Et₃N (3.1 mL, 22.2 mmol, 1.12 equiv) and the solution was allowed to stir for 5 min, then cooled to 0 °C. Methanesulfonyl chloride (1.63 mL, 21.0 mmol, 1.06 equiv) was added, and the reaction was warmed to 23 °C over 2 h. Stirring was continued for 5 h, at which point the reaction was cooled to 0 °C. Triethylamine (3.1 mL, 22.2 mmol, 1.12 equiv) was added, followed by benzenethiol (2.1 mL, 20.4 mmol, 1.03 equiv). The reaction was allowed to warm to 23 °C over 2 h and stirring was continued for 9 h. Saturated aq Na₂CO₃ (35 mL) was added, the phases were separated, and the aq phase was extracted with Et₂O (3 x 60 mL). The combined organic extracts were dried over Na₂SO₄, filtered, and the solvent was evaporated in vacuo. Purification by flash chromatography (4:1 → 2:1 hexanes/Et₂O) afforded vinylogous thioester **305** as a white crystalline solid (3.565 g, 16.33 mmol, 82% yield). $R_f = 0.34$ (1:1 hexanes/Et₂O); mp = 85 °C; ¹H NMR (500 MHz, CDCl₃) δ 7.51–7.49 (m, 2H), 7.44–7.37 (comp m, 3H), 2.38 (t, $J = 6.5$ Hz, 2H), 2.18 (tq, $J = 6.5, 2.0$ Hz, 2H), 1.97 (t, $J = 2.0$ Hz, 3H), 1.87 (app pentuplet, $J = 6.0$ Hz, 2H). All other spectral data are consistent with reported values.

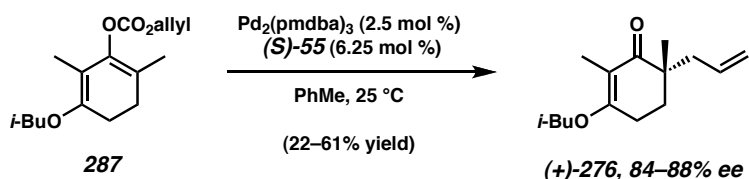


β -Ketoester (±)-277. To a -78 °C solution of *i*-Pr₂NH (2.63 mL, 18.78 mmol, 2.00 equiv) in PhMe (70 mL) was added dropwise *n*-BuLi (2.53 M in hexanes, 7.24 mL, 2.00 equiv). The reaction vessel was warmed to 0 °C, allowed to stir for 10 min, and cooled to -78 °C. A solution of vinylogous thioester **305** (2.00 g, 9.16 mmol, 1.00 equiv) in PhMe

(15 mL) was added dropwise via cannula to the reaction vessel, and the resulting solution was allowed to stir for 30 min. Allyl chloroformate (1.02 mL, 9.62 mmol, 1.05 equiv) was added dropwise and the reaction vessel was allowed to warm to 23 °C over 1 h. Stirring was continued for 4 h, at which point aq KHSO₄ (1 N, 70 ml) was slowly added and the resulting solution was allowed to stir for 10 min. The phases were separated, and the aq phase was extracted with Et₂O (3 x 30 mL). The combined organic extracts were washed with brine (1 x 30 mL), dried over Na₂SO₄, filtered, and concentrated in vacuo. The isolated crude yellow oil was used in the next step without further purification.

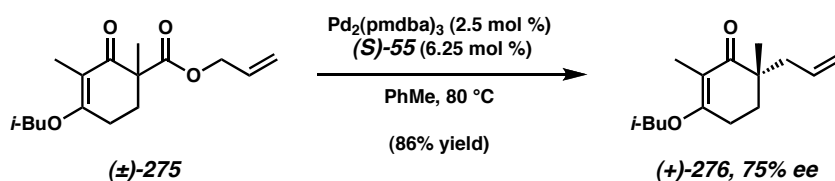
To a solution of the crude yellow oil (3.32 g) in CH₃CN (40 mL) in a flask with an attached reflux condenser was added cesium carbonate (4.48 g, 13.74 mmol, 1.50 equiv) and MeI (1.71 mL, 27.48 mmol, 3.00 equiv). The resulting suspension was refluxed at 80 °C for 5 h, at which point additional MeI (1.00 mL, 16.06 mmol, 1.75 equiv) was added. The reaction was refluxed at 80 °C for 2 h, cooled to room temperature, filtered through Celite (EtOAc eluent), dried over Na₂SO₄, filtered, and the solvent was evaporated in vacuo. Purification by flash chromatography (18% EtOAc in hexanes) afforded β -ketoester (\pm)-**277** as a colorless oil that solidifies to a white solid over time or in a -20 °C freezer (2.26 g, 7.14 mmol, 78% yield over two steps). $R_f = 0.35$ (30% EtOAc in hexanes); mp 34 °C; ¹H NMR (300 MHz, CDCl₃) δ 7.51–7.35 (comp m, 5H), 5.87 (app ddt, $J = 10.5, 17.1, 5.4$ Hz, 1H), 5.27 (app ddt, $J = 17.1, 1.7, 1.8$ Hz, 1H), 5.22 (app ddt, $J = 9.9, 1.7, 1.2$ Hz, 1H), 4.65 (dddd, $J = 1.5, 1.8, 5.7, 13.5$ Hz, 1H), 4.55 (dddd, $J = 1.5, 1.8, 5.7, 13.5$ Hz, 1H), 2.41–2.32 (m, 1H), 2.30–2.21 (m, 1H), 2.16–2.06 (1H), 2.00 (t, $J = 1.8$ Hz, 3H), 1.78 (ddd, $J = 4.5, 8.1, 13.2$ Hz, 1H), 1.38 (s, 3H); ¹³C NMR (75 MHz, CDCl₃) δ 193.0, 172.6, 156.7, 135.6, 131.9, 129.7, 129.5, 128.9, 118.1, 65.7,

52.3, 33.1, 27.4, 20.7, 12.9; IR (Neat Film NaCl) 2936, 1733, 1656, 1580, 1314, 1254, 1238, 1174, 985, 752, 693 cm^{-1} ; HRMS (FAB+) m/z calc'd for $\text{C}_{18}\text{H}_{20}\text{O}_3\text{S}$ $[\text{M} + \text{H}]^+$: 317.1211, found 317.1211.

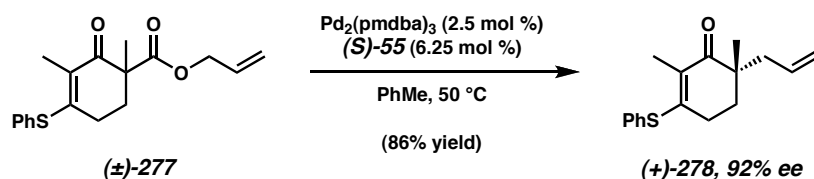


Ketone (+)-276 from enol carbonate 287. A 1-dram vial containing a stir bar was charged with $\text{Pd}_2(\text{pmdba})_3$ (4.9 mg, 0.0045 mmol, 0.025 equiv) and $(S)\text{-55}$ (4.4 mg, 0.0112 mmol, 0.0625 equiv), sealed with a septum, and the atmosphere was purged by three evacuate/purge cycles. To this was added PhMe (0.9 mL) and the ligation reaction was stirred for 30 min in a 25 °C oil bath, upon which time a solution of enol carbonate **287** (50.2 mg, 0.179 mmol, 1.0 equiv) in PhMe (0.9 mL, 0.1 M total) was added via cannula. After 21.5 h the reaction was diluted with Et_2O (2 mL), filtered through a SiO_2 plug, and concentrated in vacuo. The filtrate was purified by flash chromatography on SiO_2 (15:1 \rightarrow 4:1 hexanes/ EtOAc) to afford ketone **276** as a pale yellow oil (22–61% yield, 84–88% ee). $R_f = 0.49$ (4:1 hexanes/ EtOAc); ^1H NMR (500 MHz, CDCl_3) δ 5.73 (dddd, $J = 16.6, 10.6, 7.4, 7.4$ Hz, 1H), 5.06–5.04 (m, 1H), 5.04–5.01 (m, 1H), 3.74 (dd, $J = 9.7, 6.7$ Hz, 2H), 2.59–2.47 (comp m, 2H), 2.33 (dd, $J = 13.7, 7.2$ Hz, 1H), 2.16 (dddd, $J = 13.7, 7.6, 1.0, 1.0$ Hz, 1H), 1.98 (app septuplet, $J = 6.6$ Hz, 1H), 1.90 (ddd, $J = 13.3, 7.2, 5.7$ Hz, 1H), 1.72–1.67 (m, 1H), 1.70 (dd, $J = 1.6, 1.6$ Hz, 3H), 1.06 (s, 3H), 0.99 (d, $J = 6.7$ Hz, 6H); ^{13}C NMR (126 MHz, CDCl_3) δ 202.7, 169.5, 134.8, 117.8, 113.3, 73.8, 42.5, 41.9, 31.5, 29.0, 22.5, 22.4, 19.2, 8.0; IR (Neat Film NaCl) 3076, 2962, 2931, 1622,

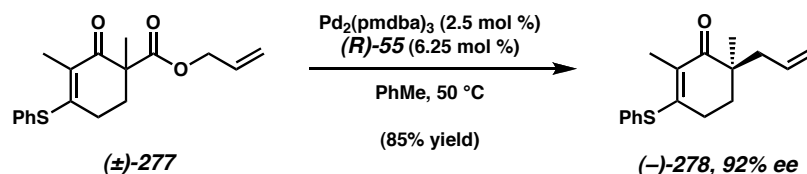
1463, 1381, 1355, 1229, 1113, 1002, 915 cm^{-1} ; HRMS (EI+) m/z calc'd for $\text{C}_{15}\text{H}_{24}\text{O}_2$ $[\text{M}]^+$: 236.1776, found 236.1771; $[\alpha]_{\text{D}}^{21.2}$ $+13.2^\circ$ (c 0.20, CH_2Cl_2 , 88% ee). SFC conditions: 5% *i*-PrOH, AD column, t_{R} (min): major = 5.18, minor = 6.02.



Ketone (+)-276 from β -ketoester (\pm)-275. A 2-dram vial containing a stir bar was charged with $\text{Pd}_2(\text{pmdba})_3$ (10.6 mg, 0.00968 mmol, 0.025 equiv) and $(S)\text{-55}$ (9.4 mg, 0.0242 mmol, 0.0625 equiv). This was connected to a 1-dram vial containing a stir bar and β -ketoester (\pm)-**275** (108.6 mg, 0.387 mmol, 1.0 equiv) via a cannula, and PhMe (3.9 mL, 0.1 M) was added to the vial containing the Pd/L and immediately immersed in liquid N_2 . The vials were rigorously degassed by three freeze-pump-thaw cycles and warmed to 23°C . After ligation for 30 min (purple \rightarrow orange color change), the catalyst solution was transferred to the substrate via cannula and immersed in an 80°C oil bath, at which point the reaction immediately turned yellow in color. After 23 h the reaction was cooled to ambient temperature, diluted with Et_2O (4 mL), and filtered through a small SiO_2 plug. The filtrate was concentrated and purified by flash chromatography as above to afford ketone **276** as a colorless oil (78.5 mg, 0.332 mmol, 86% yield, 75% ee).

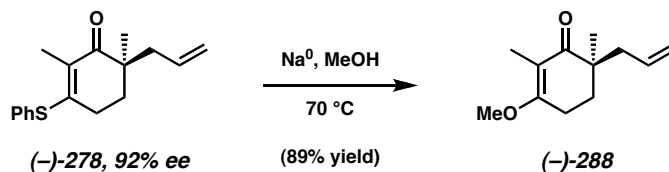


Ketone (+)-278 from β -ketoester (\pm)-277. The reaction was performed exactly as described for enol carbonate **287** using β -ketoester (\pm)-**277** (41.8 mg, 0.132 mmol, 1.0 equiv). After complexation of the metal for 30 min at 25 °C, a solution of the substrate was added and the reaction was warmed to 50 °C in an oil bath. After 23 h, the reaction was cooled to room temperature, diluted with Et₂O, and filtered through a SiO₂ plug. The filtrate was concentrated and purified by flash chromatography (15:1 \rightarrow 9:1 hexanes/EtOAc) to afford ketone **278** as a colorless oil (31.0 mg, 0.114 mmol, 86% yield, 92% ee). $R_f = 0.35$ (9:1 hexanes/EtOAc); ¹H NMR (300 MHz, CDCl₃) δ 7.52–7.48 (m, 2H), 7.43–7.35 (comp m, 3H), 5.68 (dddd, $J = 16.6, 10.4, 7.6, 7.6$ Hz, 1H), 5.03 (dddd, $J = 9.9, 2.4, 0.9, 0.6$ Hz, 1H), 5.01 (dddd, $J = 17.4, 2.4, 1.5, 1.2$ Hz, 1H), 2.32 (app ddt, $J = 13.8, 7.2, 1.2$ Hz), 2.19–2.10 (comp m, 3H), 1.96 (app t, $J = 1.8$ Hz, 3H), 1.81 (ddd, 13.5, 6.4, 6.4 Hz, 1H), 1.66–1.56 (m, 1H), 1.04 (s, 3H); ¹³C NMR (75 MHz, CDCl₃) δ 199.5, 155.6, 135.6, 134.4, 130.3, 129.6, 129.5, 128.8, 118.2, 43.1, 41.7, 33.1, 26.9, 22.3, 12.9; IR (Neat Film NaCl) 3074, 2964, 2929, 1652, 1582, 1440, 1339, 1287, 1228 cm⁻¹; HRMS (FAB+) m/z calc'd for C₁₇H₂₀OS [M + H]⁺: 273.1313, found 273.1317; [α]_D^{19.0} +56.7° (c 1.36, CH₂Cl₂, 92% ee). HPLC conditions: 4% EtOH in hexanes, AD column, t_R (min): major = 7.24, minor = 9.48.



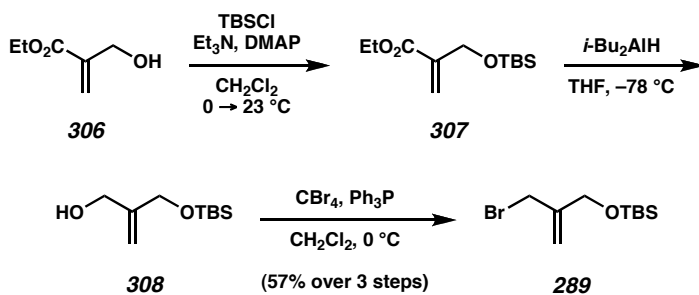
Scale up of ketone (-)-278 from β -ketoester (\pm)-277. In a glove box, a flask containing a stir bar was charged with Pd₂(pmdba)₃ (493.1 mg, 0.045 mmol, 0.025 equiv)

and ligand (*R*)-**55** (435.9 mg, 1.125 mmol, 0.0625 equiv). The solids were dissolved in PhMe (150 mL) and stirred for 45 min (purple \rightarrow orange color change). To this was added a solution of β -ketoester (\pm)-**277** (5.6956 g, 18.00 mmol, 1.0 equiv) in PhMe (30 mL, 0.1 M total). The flask was transferred out of the glove box, placed under an argon atmosphere and warmed in a 50 °C oil bath (orange \rightarrow yellow color change). After 66 h, the reaction was cooled to room temperature and concentrated in vacuo. Purification by flash chromatography (as above, dry load onto SiO₂) afforded ketone ($-$)-**278** as a pale yellow oil (4.184 g, 15.36 mmol, 85% yield, 92% ee) and recovered β -ketoester (\pm)-**277** (500.5 mg, 1.582 mmol, 9% yield). $[\alpha]_D^{25.4} -57.4^\circ$ (*c* 1.00, CH₂Cl₂, 92% ee).



Methoxy vinylogous ester ($-$)-288**.** To a 3-neck flask equipped with water-cooled reflux condenser charged with dry MeOH (33.7 mL, 0.26 M) at 0 °C was added hexanes-washed Na⁰ (1.047 g, 45.5 mmol, 5.2 equiv), after which the bath was removed. The contents were stirred at 23 °C until all Na⁰ was dissolved. A solution of ketone **278** (2.3991 g, 8.81 mmol, 1.0 equiv) in MeOH (10 mL) was added dropwise via cannula to the generated NaOMe and the resulting solution was heated in an oil bath at 70 °C. Upon consumption of **278** by TLC analysis (4:1 hexanes/EtOAc), the reaction mixture was cooled to ambient temperature and transferred to a separate flask with Et₂O and concentrated in vacuo to a thick yellow slurry. This was dissolved in saturated aq NaHCO₃ (150 mL), stirred for ca. 20 min, and extracted with Et₂O (3 x 100 mL). The

organics were dried over Na_2SO_4 , filtered, and concentrated in vacuo to a yellow oil. Purification by flash chromatography (15:1 \rightarrow 6:1 hexanes/EtOAc) afforded ketone (–)-**288** as a colorless oil that solidifies in a $-20\text{ }^\circ\text{C}$ freezer to an off-white semisolid (1.5241 g, 7.845 mmol, 89% yield). $R_f = 0.40$ (4:1 hexanes-EtOAc); $^1\text{H NMR}$ (500 MHz, CDCl_3) δ 5.74 (dddd, $J = 16.8, 10.5, 7.5, 7.5$ Hz, 1H), 5.07–5.05 (m, 1H), 5.05–5.02 (m, 1H), 3.80 (s, 3H), 2.62–2.49 (comp m, 2H), 2.33 (dd, $J = 13.7, 7.2$ Hz, 1H), 2.17 (dddd, $J = 13.8, 7.6, 1.0, 1.0$ Hz, 1H), 1.92 (ddd, $J = 13.4, 7.2, 5.8$ Hz, 1H), 1.72 (ddd, $J = 13.4, 6.7, 5.6$ Hz, 1H), 1.68 (dd, $J = 1.6, 1.6$ Hz, 3H), 1.06 (s, 3H); $^{13}\text{C NMR}$ (126 MHz, CDCl_3) δ 202.6, 169.6, 134.8, 117.9, 113.2, 55.0, 42.5, 41.9, 31.4, 22.4, 21.8, 7.9; IR (Neat Film NaCl) 2929, 1620, 1461, 1375, 1356, 1234, 1154, 1116, 999, 916 cm^{-1} ; HRMS (EI+) m/z calc'd for $\text{C}_{12}\text{H}_{18}\text{O}_2$ $[\text{M}]^+$: 194.1307, found 194.1310; $[\alpha]_{\text{D}}^{22.9} -10.6^\circ$ (c 1.26, CH_2Cl_2 , 92% ee).



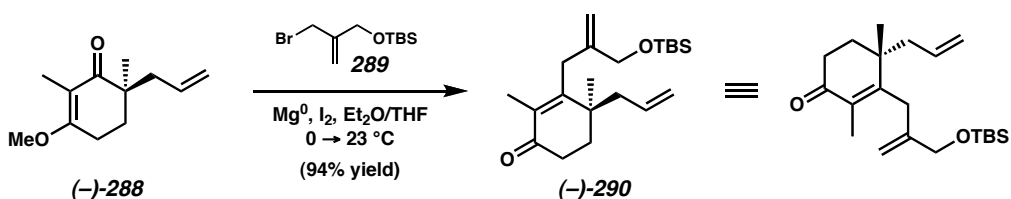
TBS-acrylate 307.⁴¹ To a solution of α -hydroxymethylacrylate **306**⁴² (4.7012 g, 36.19 mmol, 1.0 equiv) and TBSCl (6.00 g, 39.8 mmol, 1.1 equiv) in CH_2Cl_2 (72 mL, 0.5 M) at $0\text{ }^\circ\text{C}$ was added Et_3N (15.1 mL, 108.6 mmol, 3.0 equiv) and DMAP (442 mg, 3.62 mmol, 0.1 equiv). The reaction was allowed to stir for 30 min, at which point the cooling bath was removed and the contents warmed to $23\text{ }^\circ\text{C}$ and stirred overnight. The reaction mixture was filtered into a separatory funnel and washed with 1N HCl (70 mL),

saturated aq NaHCO₃ (100 mL), and brine (100 mL). The organics were dried over MgSO₄, filtered, and concentrated in vacuo to afford TBS-acrylate **307** as a colorless oil (8.806 g). The material was used in the next step without purification. $R_f = 0.63$ (6:1 hexanes/EtOAc); ¹H NMR (300 MHz, CDCl₃) δ 6.25 (dd, $J = 2.0, 2.0$ Hz, 1H), 5.90 (dd, $J = 2.0, 2.0$ Hz, 1H), 4.37 (dd, $J = 2.1, 2.1$ Hz, 2H), 4.21 (q, $J = 7.1$ Hz, 2H), 1.30 (t, $J = 7.1$ Hz, 3H), 0.92 (s, 9H), 0.08 (s, 6H).

Allylic alcohol 308.⁴¹ To a solution of crude TBS-acrylate **307** (8.806 g, 36.03 mmol, 1.0 equiv) in THF (144 mL, 0.25 M) cooled to -78 °C was added dropwise *i*-Bu₂AlH (neat, 14.1 mL, 79.3 mmol, 2.2 equiv) over 15 min. The resulting solution was stirred at -78 °C until complete consumption by TLC analysis (4:1 hexanes/EtOAc), at which point the excess *i*-Bu₂AlH was quenched with dry EtOAc (4 mL). The resulting solution was stirred for 10 min at -78 °C, then warmed to 0 °C and aged for 30 min. A solution of Rochelle's salt (75 mL, 1 M) was then added slowly with vigorous stirring. The cooling bath was removed and the contents were vigorously stirred until two homogeneous layers appeared (several hours). The phases were separated and the aq layer was extracted with Et₂O (3 x 75 mL), the combined organics were washed with brine (2 x 100 mL), dried over MgSO₄, filtered, and concentrated in vacuo to afford **308** as a cloudy colorless oil (7.29 g). The crude material was used in the next reaction without purification. $R_f = 0.19$ (4:1 hexanes/EtOAc); ¹H NMR (300 MHz, CDCl₃) δ 5.10 (s, 1H), 5.08 (s, 1H), 4.24 (s, 2H), 4.17 (d, $J = 5.5$ Hz, 2H), 1.95 (t, $J = 6.0$ Hz, 1H), 0.91 (s, 9H), 0.09 (s, 6H).

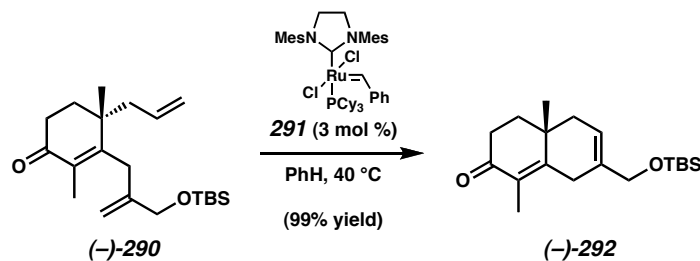
Allylic bromide 289.²⁸ To a solution of crude allylic alcohol **308** (7.29 g, 36.04 mmol, 1.0 equiv) in CH₂Cl₂ (120 mL, 0.3 M) cooled to 0 °C was added CBr₄ (17.942,

54.1 mmol, 1.5 equiv) and PPh_3 (11.331 g, 43.2 mmol, 1.2 equiv). The reaction mixture was stirred at 0 °C until consumption by TLC analysis (4:1 hexanes/EtOAc; required ca. 30 min). The reaction was then quenched slowly with saturated aq NaHCO_3 (40 mL) and warmed to ambient temperature while stirring. The phases were separated and the aq layer was extracted with EtOAc (3 x 50 mL). The combined organics were washed with brine, dried over MgSO_4 , filtered, and concentrated in vacuo to afford a yellow oil containing a Ph_3PO precipitate. This material was dry loaded on SiO_2 and purified by flash chromatography (24:1 \rightarrow 15:1 \rightarrow 3:1 hexanes/ Et_2O). Fractions containing the desired product were repurified by flash chromatography on SiO_2 (49:1 \rightarrow 24:1 hexanes/acetone) to afford allylic bromide **289** as a pale yellow oil (5.4251 g, 20.45 mmol, 57% yield over 3 steps). $R_f = 0.48$ (24:1 hexanes/ Et_2O); ^1H NMR (300 MHz, CDCl_3) δ 5.26–5.25 (m, 1H), 5.23 (ddd, $J = 1.4, 1.4, 1.4$ Hz, 1H), 4.27 (dd, $J = 1.4, 1.4$ Hz, 2H), 4.01 (s, 2H), 0.92 (s, 9H), 0.10 (s, 6H). All other spectral data are consistent with reported values.

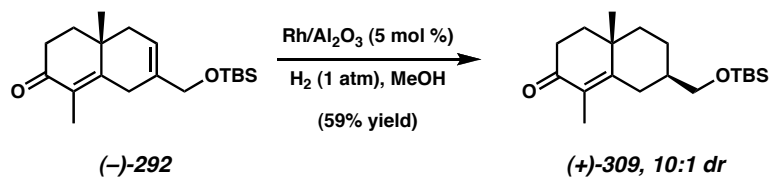


Triolefin (-)-290. To a flask containing Mg^0 turnings (125.4 mg, 5.16 mmol, 3.0 equiv) was added Et_2O (30 mL) and a chip of I_2 . The contents were stirred for 25 min at 23 °C and then cooled to 0 °C. A solution of allylic bromide **289** (1.141 g, 4.30 mmol, 2.5 equiv) in Et_2O (5 mL) was transferred via cannula to the $\text{Mg}/\text{Et}_2\text{O}$ and stirred for 30 min at 0 °C, then warmed to 23 °C over 30 min. A solution of ketone **288** (333.5 mg,

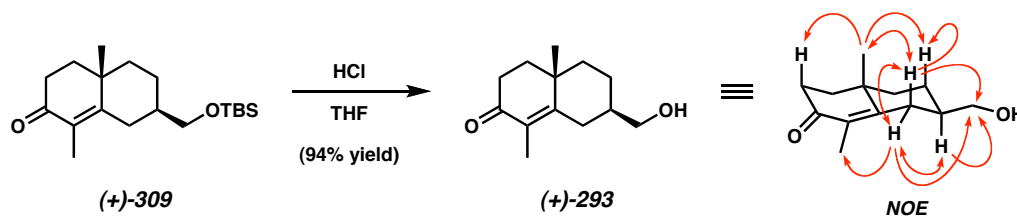
1.72 mmol, 1.0 equiv) in THF (5 mL) was transferred dropwise to the allylmagnesium bromide via cannula, followed by washings to total 35 mL of THF. Upon consumption of ketone **288** by TLC analysis (4:1 hexanes/EtOAc), the reaction was quenched slowly with aq ammonium chloride (50 mL) and stirred until complete dissolution of Mg^0 . The phases were separated and the aq phase was extracted with EtOAc (3 x 50 mL). The combined organics were washed with brine, dried over MgSO_4 , filtered, and concentrated to a pale yellow oil. Purification by flash chromatography (9:1 \rightarrow 4:1 hexanes/ Et_2O , dry load onto SiO_2) afforded the desired triolefin **290** as a colorless oil (563.4 mg, 1.616 mmol, 94% yield). $R_f = 0.62$ (4:1 hexanes/EtOAc); ^1H NMR (500 MHz, C_6D_6) δ 5.54 (dddd, $J = 17.6, 10.3, 7.3, 7.3$ Hz, 1H), 5.06 (dd, $J = 3.2, 1.7$ Hz, 1H), 4.97 (ddd, $J = 10.3, 2.2, 1.2$ Hz, 1H), 4.92 (dddd, $J = 16.9, 2.4, 1.2, 1.2$ Hz, 1H), 4.56 (d, $J = 1.2$ Hz, 2H), 3.95 (s, 2H), 2.75 (dd, $J = 17.1, 17.1$ Hz, 2H), 2.36 (dddd, $J = 17.1, 17.1, 10.3, 5.1$ Hz, 1H), 2.33 (dddd, $J = 17.1, 17.1, 7.1, 5.4$ Hz, 1H), 2.01 (dddd, $J = 13.9, 13.9, 13.9, 7.6$ Hz, 2H), 1.89 (s, 3H), 1.60 (ddd, 13.4, 6.8, 5.1 Hz, 1H), 1.41 (ddd, 13.4, 10.0, 5.1 Hz, 1H), 0.98 (s, 9H), 0.87 (s, 3H), 0.06 (s, 6H); ^{13}C NMR (126 MHz, C_6D_6) δ 196.6, 158.9, 144.4, 134.5, 134.3, 118.0, 110.3, 67.1, 43.2, 39.2, 34.2, 33.9, 33.2, 26.1, 23.9, 18.5, 12.5, -5.2; IR (Neat Film NaCl) 3078, 2930, 2857, 1668, 1610, 1463, 1337, 1081, 1005, 912, 836, 776 cm^{-1} ; HRMS (EI+) m/z calc'd for $\text{C}_{21}\text{H}_{36}\text{O}_2\text{Si}$ $[\text{M}]^+$: 348.2485, found 348.2499; $[\alpha]_D^{21.0} -37.3^\circ$ (c 1.11, CH_2Cl_2 , 92% ee).



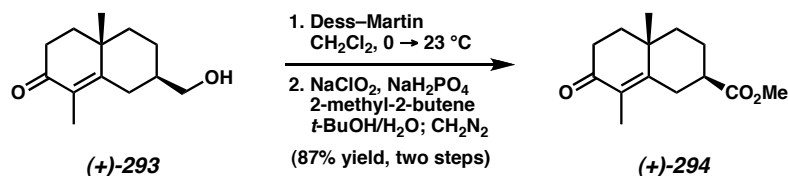
Cyclohexene (-)-292. Trioletin **290** (280.1 mg, 0.804 mmol, 1.0 equiv) was dissolved in PhH (16 mL, 0.05 M) and sparged with N_2 for 15 min. Grubbs' catalyst **291** (20.5 mg, 0.0241 mmol, 0.03 equiv) was added to the solution and the flask was placed in a 40 °C oil bath. Upon consumption by TLC analysis (3:1 hexanes/ Et_2O), the reaction was cooled to ambient temperature and ethyl vinyl ether (8 mL) was added to the solution. After stirring for ca. 30 min the solution was concentrated in vacuo. Purification via flash chromatography (9:1 \rightarrow 4:1 hexanes/ Et_2O) afforded cyclohexane **292** as a colorless oil (256.3 mg, 0.800 mmol, 99% yield). $R_f = 0.30$ (3:1 hexanes/ Et_2O); ^1H NMR (500 MHz, C_6D_6) δ 5.58 (dddd, $J = 5.4, 1.5, 1.5, 1.5$ Hz, 1H), 3.93 (d, $J = 1.2$ Hz, 1H), 2.86 (d, $J = 22.0$ Hz, 1H), 2.60 (d, $J = 21.7$ Hz, 1H), 2.32–2.29 (comp m, 2H), 1.87 (d, $J = 1.2$ Hz, 3H), 1.83 (dd, $J = 16.9, 2.0$ Hz, 1H), 1.61 (dd, $J = 16.9, 6.1$ Hz, 1H), 1.45–1.35 (comp m, 2H), 0.99 (s, 9H), 0.85 (s, 3H), 0.08 (s, 3H), 0.07 (s, 3H); ^{13}C NMR (126 MHz, C_6D_6) δ 196.4, 157.4, 135.1, 129.5, 119.5, 66.7, 39.6, 36.4, 35.1, 34.3, 29.7, 26.1, 24.0, 18.6, 11.2, -5.1, -5.2; IR (Neat Film NaCl) 2929, 2857, 1668, 1615, 1463, 1305, 1257, 1158, 1086, 1048, 837, 776 cm^{-1} ; HRMS (EI+) m/z calc'd for $\text{C}_{19}\text{H}_{31}\text{O}_2\text{Si}$ $[\text{M} + \text{H} - \text{H}_2]^+$: 319.2093, found 319.2096; $[\alpha]_{\text{D}}^{21.2} -9.4^\circ$ (c 0.60, CH_2Cl_2 , 92% ee).



Enone (+)-309. Cyclohexene **292** (25.0 mg, 78.0 μmol , 1.0 equiv) was dissolved in MeOH (3.1 mL, 25 mM) and Rh/Al₂O₃ catalyst (40.1 mg, 3.90 μmol , 0.05 equiv) was added with vigorous stirring. The vial was placed under an atmosphere of hydrogen via a balloon and stirred at 26 °C. Upon consumption by TLC (3:1 hexanes/Et₂O, developed thrice), the solids were filtered over Celite washing with EtOAc and concentrated in vacuo. Purification via flash chromatography (9:1 hexanes/Et₂O) afforded the desired enone **309** as a colorless oil (14.8 mg, 45.9 μmol , 59% yield, 10:1 dr). $R_f = 0.36$ (3:1 hexanes/Et₂O, developed twice); ¹H NMR (500 MHz, C₆D₆, major diastereomer) δ 3.33 (ddd, $J = 14.0, 9.8, 5.1$ Hz, 2H), 2.63 (ddd, $J = 14.7, 1.7, 1.7$ Hz, 1H), 2.38–2.26 (comp m, 2H), 1.96 (s, 3H), 1.68 (dd, $J = 13.7, 13.7$ Hz, 1H), 1.44 (ddd, $J = 13.4, 13.4, 3.7$ Hz, 1H), 1.42–1.39 (m, 1H), 1.31–1.23 (comp m, 2H), 1.08 (ddd, $J = 14.2, 14.2, 3.6$ Hz, 1H), 0.99 (s, 9H), 0.84 (s, 3H), 0.06 (s, 6H); ¹³C NMR (126 MHz, C₆D₆) δ 197.0, 160.0, 129.2, 68.1, 41.6, 41.5, 37.7, 36.0, 34.1, 30.9, 26.1, 24.7, 22.2, 18.5, 11.2, –5.2 (2C); IR (Neat Film NaCl) 2928, 2857, 1668, 1612, 1472, 1256, 1098, 838, 776 cm⁻¹; HRMS (FAB+) m/z calc'd for C₁₉H₃₅O₂Si [M + H]⁺: 323.2406, found 323.2402; $[\alpha]_D^{21.4} +73.0^\circ$ (c 0.53, CH₂Cl₂, 92% ee).



Alcohol (+)-293. Enone **309** (40.3 mg, 0.125 mmol, 1.0 equiv) was dissolved in THF (2.5 mL, 50 mM) and aq 1 N HCl (1.0 mL) was added with vigorous stirring. Upon consumption by TLC (2:1 hexanes/EtOAc), brine was added, the layers were separated, and the aq layer was extracted with Et₂O (3 x 4 mL). The combined organics were washed with saturated aq NaHCO₃, this aq was back extracted with Et₂O (2 x 5 mL), the organics were dried over MgSO₄, filtered, and concentrated in vacuo. Purification via flash chromatography (2:1 → 1:1 hexanes/EtOAc) afforded alcohol **293** as a colorless oil (24.5 mg, 0.118 mmol, 94% yield, 10:1 dr). $R_f = 0.37$ (1:1 hexanes/EtOAc); ¹H NMR (500 MHz, C₆D₆, major diastereomer) δ 3.12 (d, $J = 5.5$ Hz, 2H), 2.52 (ddd, $J = 14.6, 1.9, 1.9$ Hz, 1H), 2.37–2.24 (comp m, 2H), 1.92 (dd, $J = 1.3, 1.3$ Hz, 3H), 1.52 (ddd, $J = 13.1, 13.1, 3.1$ Hz, 1H), 1.43 (ddd, $J = 13.4, 13.4, 5.3$ Hz, 1H), 1.36–1.33 (m, 1H), 1.29–1.21 (comp m, 3H), 1.17–1.09 (m, 1H), 1.03 (ddd, $J = 12.9, 12.9, 3.3$ Hz, 1H), 0.79 (s, 3H), 0.74 (br s, 1H); ¹³C NMR (126 MHz, C₆D₆) δ 197.2, 160.1, 129.1, 67.7, 41.5, 41.4, 37.7, 35.9, 34.1, 30.8, 24.6, 22.2, 11.3; IR (Neat Film NaCl) 3418 (br), 2924, 1660, 1652, 1608, 1453, 1352, 1150, 1083, 1013 cm⁻¹; HRMS (EI+) m/z calc'd for C₁₃H₂₀O₂ [M]⁺: 208.1463, found 208.1463; $[\alpha]_D^{23} +120.9^\circ$ (c 0.35, CH₂Cl₂, 92% ee).

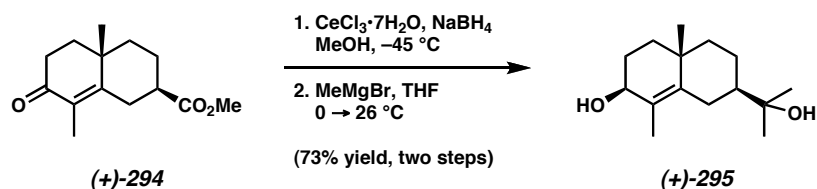


Ester (+)-294. To a solution of alcohol **293** (24.5 mg, 0.118 mmol, 1.0 equiv) in CH₂Cl₂ (2.4 mL, 50 mM) at 0 °C was added Dess–Martin periodinane (69.8 mg, 0.165 mmol, 1.4 equiv), and after 5 min the bath was removed and the reaction was

stirred at room temperature. Upon completion by TLC analysis (2:1 hexanes/EtOAc), the reaction was diluted with 1:1 hexanes/Et₂O (4 mL) and filtered through a small silica gel plug. Heptanes (5 mL) were added and the filtrate was concentrated in vacuo to a white solid. Purification by filtration through a silica gel plug (3:1 → 1:1 hexanes/Et₂O) afforded a colorless oil (22.3 mg) that was used in the next step.

The resulting material was dissolved in *t*-BuOH (1.7 mL), to which 2-methyl-2-butene (85 μ L, 0.80 mmol, 7.4 equiv) was added with stirring. To this was added a solution of NaH₂PO₄•H₂O (103 mg, 0.746 mmol, 6.9 equiv) and NaClO₂ (89.9 mg, 0.995 mmol, 9.2 equiv) in water (850 μ L) over ca. 5 min. Upon consumption by TLC analysis (1:1 hexanes/EtOAc), the *t*-BuOH was removed on a rotovap, water (2 mL) was added to this slurry, and 1 N HCl was added dropwise until pH < 3. The resulting aq layer was extracted with Et₂O (4 x 4 mL), a stir bar was added and the extract was cooled in an ice/water bath. A fresh solution of CH₂N₂ in Et₂O (5 mL) was added and the bath was allowed to expire. After the solution was colorless it was dried over MgSO₄, filtered, and concentrated in vacuo. Purification via flash chromatography (3:1 → 2:1 hexanes/Et₂O) afforded ester **294** as a colorless oil that solidifies to a white solid over time or in a -20 °C freezer (24.4 mg, 0.103 mmol, 87% yield over two steps). The diastereomers are separable by flash chromatography with 3:1 hexanes/Et₂O. R_f = 0.59 (1:1 hexanes/EtOAc); mp = 46–48 °C; ¹H NMR (500 MHz, C₆D₆, major diastereomer) δ 3.38 (s, 3H), 2.83–2.76 (m, 1H), 2.30–2.09 (comp m, 4H), 1.82 (m, 3H), 1.66–1.62 (comp m, 2H), 1.32 (ddd, J = 13.6, 13.6, 4.9 Hz, 1H), 1.17 (ddd, J = 13.2, 3.9, 3.9 Hz, 1H), 1.12 (ddd, J = 13.5, 2.8, 2.8 Hz, 1H), 0.91–0.85 (m, 1H), 0.72 (s, 3H); ¹³C NMR (126 MHz, C₆D₆) δ 196.8, 174.7, 157.7, 129.9, 51.3, 43.5, 40.9, 37.4, 35.4, 34.0, 29.9,

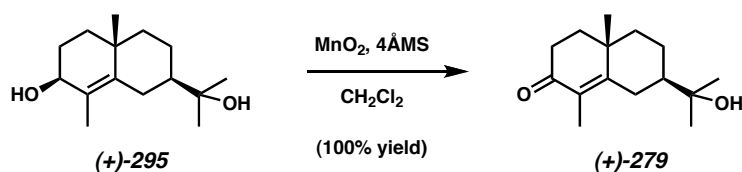
24.7, 21.9, 11.2; IR (Neat Film NaCl) 2949, 1733, 1668, 1613, 1435, 1350, 1301, 1256, 1190, 1173, 1024, 914 cm^{-1} ; HRMS (FAB+) m/z calc'd for $\text{C}_{14}\text{H}_{21}\text{O}_3$ $[\text{M} + \text{H}]^+$: 237.1491, found 237.1493; $[\alpha]_{\text{D}}^{20.4} +64.0^\circ$ (c 0.56, CH_2Cl_2 , 92% ee).



Diol (+)-295.^{19a,c} To a solution of ester **294** (10.1 mg, 42.7 μmol , 1.0 equiv) in MeOH (1.7 mL, 25 mM) was added $\text{CeCl}_3 \cdot 7\text{H}_2\text{O}$ (47.8 mg, 128 μmol , 3.0 equiv), followed by cooling to ca. -45°C in a MeCN/ $\text{CO}_2(\text{s})$ bath. Solid NaBH_4 (3.2 mg, 85.5 μmol , 2.0 equiv) was added, and upon consumption by TLC analysis (1:1 hexanes/EtOAc), acetone (5 drops) was added, followed by brine (1 mL) and EtOAc (1 mL). The suspension was warmed to room temperature, the aq layer was extracted with EtOAc (2 x 4 mL), dried over MgSO_4 , filtered, and concentrated in vacuo to a colorless film (9.1 mg). This material was used directly in the following reaction.

To a solution of the crude material in THF (1.5 mL, 25 mM) at 0°C was added a solution of MeMgBr (71 μL , 2.7 M in THF, 191 μmol , 5 equiv) and the bath was removed after 5 min. Upon consumption by TLC analysis (1:1 hexanes/EtOAc), the reaction was cooled in an ice/water bath, and MeOH (200 μL), brine (1 mL), saturated aq NH_4Cl (1 mL), and EtOAc (2 mL) were added. The aq layer was extracted with EtOAc (2 x 4 mL), dried over MgSO_4 , filtered, and concentrated in vacuo. Purification via flash chromatography (2:1 hexanes/EtOAc) afforded diol **295** as a colorless film that solidifies over time to an off-white solid (7.4 mg, 31.0 μmol , 73% yield over two steps, >20:1 dr).

$R_f = 0.30$ (1:1 hexanes/EtOAc); mp = 123–126 °C; $^1\text{H NMR}$ (500 MHz, CDCl_3) δ 4.03 (app t, $J = 6.6$ Hz, 1H), 2.60 (app dt, $J = 13.5, 2.8$ Hz, 1H), 1.94–1.88 (m, 1H), 1.73 (s, 3H), 1.71–1.23 (comp m, 11H), 1.21 (s, 6H), 1.08 (s, 3H); $^{13}\text{C NMR}$ (126 MHz, CDCl_3) δ 139.7, 126.9, 72.9, 71.7, 50.7, 41.7, 36.2, 35.3, 29.0, 27.4, 27.0, 26.9, 24.8, 23.2, 15.2; IR (Neat Film NaCl) 3366 (br), 2934, 2863, 1455, 1374, 1277, 1138, 1076, 1014, 922, 734 cm^{-1} ; HRMS (FAB+) m/z calc'd for $\text{C}_{15}\text{H}_{26}\text{O}_2$ $[\text{M}]^+$: 238.1933, found 238.1921; $[\alpha]_D^{21.6} +21.6^\circ$ (c 0.34, MeOH, 92% ee).



(+)-Carissone (279).^{19e} To a solution of diol **295** (3.1 mg, 13.0 μmol , 1.0 equiv) in CH_2Cl_2 (520 μL , 25 mM) was added oven-dried 4 Å MS (15 mg), followed by MnO_2 (13.3 mg, 130 μmol , 10 equiv). Upon consumption by TLC (1:1 hexanes/EtOAc), the reaction was diluted with Et_2O (2 mL) and filtered through a small plug of silica gel, washing with Et_2O . This was concentrated in vacuo to afford (+)-carrissone (**279**) as a colorless film (3.1 mg, 131 μmol , 100% yield). $R_f = 0.34$ (1:1 hexanes/EtOAc); $^1\text{H NMR}$ (500 MHz, CDCl_3) δ 2.86 (app dt, $J = 14.4, 2.6$ Hz, 1H), 2.51 (ddd, $J = 16.9, 13.3, 6.4$ Hz, 1H), 2.39 (app dt, $J = 16.8, 3.8$ Hz, 1H), 1.90 (app t, $J = 13.9$ Hz, 1H), 1.82–1.69 (comp m, 4H), 1.78 (s, 3H), 1.55–1.36 (comp m, 3H), 1.26 (s, 3H), 1.25 (s, 3H), 1.20 (s, 3H); $^{13}\text{C NMR}$ (126 MHz, CDCl_3) δ 199.1, 162.6, 128.8, 72.4, 49.6, 41.9, 37.3, 35.8, 33.7, 28.7, 27.5, 26.7, 22.5, 22.4, 10.9; IR (Neat Film NaCl) 3448 (br), 2970, 2935, 1652, 1608, 1452, 1353, 1300, 1212, 1189, 1149, 1014, 918, 817 cm^{-1} ; HRMS (FAB+) m/z

calc'd for $C_{15}H_{25}O_2$ $[M + H]^+$: 237.1855, found 237.1844; $[\alpha]_D^{23.1} +119.6^\circ$ (*c* 0.31, $CHCl_3$, 92% ee); lit. $[\alpha]_D^{22} +138.7^\circ$ (*c* 0.163, $CHCl_3$).

4.6 NOTES AND REFERENCES

- (1) For representative examples in natural product total synthesis, see: (a) Varseev, G. N.; Maier, M. E. *Angew. Chem., Int. Ed.* **2009**, *48*, –3685–3688. (b) Zhao, Y.; Zhou, Y.; Liang, L.; Yang, X.; Du, F.; Li, L.; Zhang, H. *Org. Lett.* **2009**, *11*, 555–558. (c) McGrath, N. A.; Lee, C. A.; Araki, H.; Brichacek, M.; Njardarson, J. T. *Angew. Chem., Int. Ed.* **2008**, *47*, 9450–9453. (d) Bisai, A.; West, S. P.; Sarpong, R. *J. Am. Chem. Soc.* **2008**, *130*, 7222–7223. (e) Iimura, S.; Overman, L. E.; Paulini, R.; Zakarian, A. *J. Am. Chem. Soc.* **2006**, *128*, 13095–13101. (f) Miyaoka, H.; Kajiwara, Y.; Hara, Y.; Yamada, Y. *J. Org. Chem.* **2001**, *66*, 1429–1435. (g) Kwon, O.; Su, D.-S.; Meng, D.; Deng, W.; D’Amico, D. C.; Danishefsky, S. J. *Angew. Chem., Int. Ed.* **1998**, *37*, 1877–1880. (h) Smith, A. B., III.; Nolen, E. G., Jr.; Shirai, R.; Blase, F. R.; Ohta, M.; Chida, N.; Hartz, R. A.; Fitch, D. M.; Clark, W. M.; Sprengeler, P. A. *J. Org. Chem.* **1995**, *60*, 7837–7848.
- (2) Stork, G.; Danheiser, R. L. *J. Org. Chem.* **1973**, *38*, 1775–1776.
- (3) For reviews of the synthesis of quaternary stereocenters, see: (a) Cozzi, P. G.; Hilgraf, R.; Zimmermann, N. *Eur. J. Org. Chem.* **2007**, *36*, 5969–5994. (b) Trost, B. M.; Jiang, C. *Synthesis* **2006**, 369–396. (c) *Quaternary Stereocenters: Challenges and Solutions for Organic Synthesis*, Christoffers, J., Baro, A., Eds.; Wiley: Weinheim, 2005. (d) Douglas, C. J.; Overman, L. E. *Proc. Natl. Acad. Sci. U.S.A.* **2004**, *101*, 5363–5367. (e) Denissova, I.; Barriault, L. *Tetrahedron* **2003**, *59*, 10105–10146.
- (4) (a) Trost, B. M.; Bream, R. N.; Xu, J. *Angew. Chem., Int. Ed.* **2006**, *45*, 3109–3112. (b) Meyers, A. I.; Hanreich, R.; Wanner, K. T. *J. Am. Chem. Soc.* **1985**,

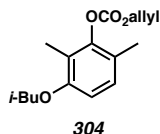
- 107, 7776–7778. (c) Miyaoka, H.; Kajiwara, Y.; Hara, M.; Suma, A.; Yamada, Y. *Tetrahedron: Asymmetry* **1999**, *10*, 3189–3196.
- (5) (a) Behenna, D. C.; Stoltz, B. M. *J. Am. Chem. Soc.* **2004**, *126*, 15044–15055. (b) Mohr, J. T.; Behenna, D. C.; Harned, A. M.; Stoltz, B. M. *Angew. Chem., Int. Ed.* **2005**, *44*, 6924–6927. (c) Seto, M.; Roizen, J. L.; Stoltz, B. M. *Angew. Chem., Int. Ed.* **2008**, *47*, 6873–6876. (d) For a review of the development of the enantioselective Tsuji allylation in our lab and others, see: Mohr, J. T.; Stoltz, B. M. *Chem.—Asian J.* **2007**, *2*, 1476–1491.
- (6) Difficulties for the selective preparation of enol carbonate vinylogous ester derivatives have been noted. See Ref 4a.
- (7) (a) Sarpong, R.; Su, J. T.; Stoltz, B. M. *J. Am. Chem. Soc.* **2003**, *125*, 13624–13625. (b) Tambar, U. K.; Stoltz, B. M. *J. Am. Chem. Soc.* **2005**, *127*, 5340–5341. (c) Tambar, U. K.; Ebner, D. C.; Stoltz, B. M. *J. Am. Chem. Soc.* **2006**, *128*, 11752–11753. (d) Liu, Q.; Ferreira, E. M.; Stoltz, B. M. *J. Org. Chem.* **2007**, *72*, 7352–7358. (e) Enquist, J. A., Jr.; Stoltz, B. M. *Nature* **2008**, *453*, 1228–1231. (f) Krishnan, S.; Bagdanoff, J. T.; Ebner, D. C.; Ramtohl, Y. K.; Tambar, U. K.; Stoltz, B. M. *J. Am. Chem. Soc.* **2008**, *130*, 13745–13754.
- (8) Qualitatively, the reaction rates for the electron deficient acyl substrates are faster than the traditional vinylogous esters. For example, substrates **181** and **263** require 10–16 h to reach complete conversion, whereas substrates **265**, **267**, and **269** reach full conversion in 2–4 h.
- (9) We have recently obtained spectroscopic and crystallographic evidence indicating that a Pd- β -keto carboxylate complex is the resting state of the catalytic cycle for

- β -ketoester substrates. See: Sherden, N. H.; Behenna, D. C.; Virgil, S. C.; Stoltz, B. M. *Angew. Chem., Int. Ed.* **2009**, *48*, 6840–6843.
- (10) (a) Tani, K.; Behenna, D. C.; McFadden, R. M.; Stoltz, B. M. *Org. Lett.* **2007**, *9*, 2529–2531. (b) White, D. E.; Stewart, I. C.; Grubbs, R. H.; Stoltz, B. M. *J. Am. Chem. Soc.* **2008**, *130*, 810–811.
- (11) Asymmetric alkylation reactions that feature stabilized enolates typically proceed with excellent conversion and low enantioselectivity, further complicating the interpretation of the influence of enolate pK_a for this transformation.
- (12) McFadden, R. M. Applications of Palladium-Catalyzed Enantioselective Decarboxylative Alkylation in Natural Products Total Synthesis. Ph.D. Thesis, California Institute of Technology, Pasadena, CA, December 2007.
- (13) Six-membered vinylogous esters exhibit better overlap of the vinylogous moiety with the carbonyl compared to seven-membered vinylogous esters, increasing the strength of the C–C bond and requiring higher reaction temperatures for the rate-limiting decarboxylation. See: Ragan, J. A.; Murry, J. A.; Castaldi, M. J.; Conrad, A. K.; Jones, B. P.; Li, B.; Makowski, T. W.; McDermott, R.; Sitter, B. J.; White, T. D.; Young, G. R. *Org. Process Res. Dev.* **2001**, *5*, 498–507.
- (14) For a comprehensive review of the eudesmane sesquiterpenoids of the Asteraceae family, see: Wu, Q.-X.; Shi, Y.-P.; Jia, Z.-J. *Nat. Prod. Rep.* **2006**, *23*, 699–734.
- (15) (a) Fraga, B. M. *Nat. Prod. Rep.* **2006**, *23*, 943–972. (b) Fraga, B. M. *Nat. Prod. Rep.* **2007**, *24*, 1350–1381. (c) Fraga, B. M. *Nat. Prod. Rep.* **2008**, *25*, 1180–1209.

- (16) For the isolation and biological activity of (+)-carissone, see: (a) Mohr, K.; Schindler, O.; Reichstein, T. *Helv. Chim. Acta.* **1954**, *37*, 462–471. (b) Joshi, D. V.; Boyce, S. F. *J. Org. Chem.* **1957**, *22*, 95–97. (c) Achenbach, H.; Waibel, R.; Addae-Mensah, I. *Phytochemistry* **1985**, *24*, 2325–2328. (d) Lindsay, E. A.; Berry, Y.; Jamie, J. F.; Bremner, J. B. *Phytochemistry* **2000**, *55*, 403–406.
- (17) For the isolation and biological activity of (+)-3-oxocostusic acid, see: (a) Bohlmann, F.; Jakupovic, J.; Lonitz, M. *Chem. Ber.* **1977**, *110*, 301–314. (b) Khanina, M. A.; Kulyyasov, A. T.; Bagryanskaya, I. Y.; Gatilov, Y. V.; Adekenov, S. M.; Raldugin, V. A. *Chem. Nat. Compd.* **1998**, *34*, 145–147. (c) Al-Dabbas, M. M.; Hashinaga, F.; Abdelgaleil, S. A. M.; Suganuma, T.; Akiyama, K.; Hayashi, H. *J. Ethnopharmacol.* **2005**, *97*, 237–240. (d) Mohamed, A. E.-H., Ahmed, A. A.; Wollenweber, E.; Bohm, B.; Asakawa, Y. *Chem. Pharm. Bull.* **2006**, *54*, 152–155.
- (18) For the isolation and biological activity of α -eudesmol, see: (a) McQuillin, F. J.; Parrack, J. D. *J. Chem. Soc.* **1956**, 2973–2978. (b) Asakura, K.; Kanemasa, T.; Minagawa, K.; Kagawa, K.; Ninomiya, M. *Brain Res.* **1999**, *823*, 169–176. (c) Toyota, M.; Yonehara, Y.; Horibe, I.; Minagawa, K.; Asakawa, Y. *Phytochemistry* **1999**, *52*, 689–694. (d) Asakura, K.; Kanemasa, T.; Minagawa, K.; Kagawa, K.; Yagami, T.; Nakajima, M.; Ninomiya, M. *Brain Res.* **2000**, *873*, 94–101.
- (19) For syntheses of carissone, see: (a) Pinder, A. R.; Williams, R. A. *J. Chem. Soc.* **1963**, 2773–2778. (b) Sathe, V. M.; Rao, A. S. *Indian J. Chem.* **1971**, *9*, 95–97. (c) Kutney, J. P.; Singh, A. K. *Can. J. Chem.* **1982**, *60*, 1842–1846. (d) Wang,

- C.-C. *J. Nat. Prod.* **1996**, *59*, 409–411. (e) Aoyama, Y.; Araki, Y.; Konoike, T. *Synlett* **2001**, *9*, 1452–1454.
- (20) For syntheses of 3-oxocostusic acid, see: (a) Ceccherelli, P.; Curini, M.; Marcotullio, M. C.; Rosati, O. *Tetrahedron Lett.* **1990**, *31*, 3071–3074. (b) Xiong, Z.; Yang, J.; Li, Y. *Tetrahedron: Asymmetry* **1996**, *7*, 2607–2612.
- (21) For syntheses of α -eudesmol, see: (a) Humber, D. C.; Pinder, A. R.; Williams, R. *A. J. Chem. Soc.* **1967**, 2335–2340. (b) Taber, D. F.; Saleh, S. A. *Tetrahedron Lett.* **1982**, *23*, 2361–2364. (c) Schwartz, M. A.; Willbrand, A. M. *J. Org. Chem.* **1985**, *50*, 1359–1365. (d) Chou, T.-S.; Lee, S.-J.; Yao, N.-K. *Tetrahedron* **1989**, *45*, 4113–4124. (e) Frey, B.; Hünig, S.; Koch, M.; Reissig, H.-U. *Synlett* **1991**, 854–856. (f) Frey, B.; Schnaubelt, J.; Reißig, H.-U. *Eur. J. Org. Chem.* **1999**, 1385–1393.
- (22) For a review of enantioselective methodologies inspired by target-directed synthesis, see: Mohr, J. T.; Krout, M. R.; Stoltz, B. M. *Nature* **2008**, *455*, 323–332.
- (23) (a) McFadden, R. M.; Stoltz, B. M. *J. Am. Chem. Soc.* **2006**, *128*, 7738–7739. (b) Behenna, D. C.; Stockdill, J. L.; Stoltz, B. M. *Angew. Chem., Int. Ed.* **2007**, *46*, 4077–4080.
- (24) For the development of phosphinoxazoline (PHOX) ligands, see: (a) Helmchen, G.; Pfaltz, A. *Acc. Chem. Res.* **2000**, *33*, 336–345. (b) Williams, J. M. J. *Synlett* **1996**, 705–710.

- (25) Enol carbonate **287** was unstable to air, forming complex reaction mixtures that substantially affected yields and selectivities for the alkylation. Aromatic carbonate **304** was identified from this mixture. See supporting information for more details.



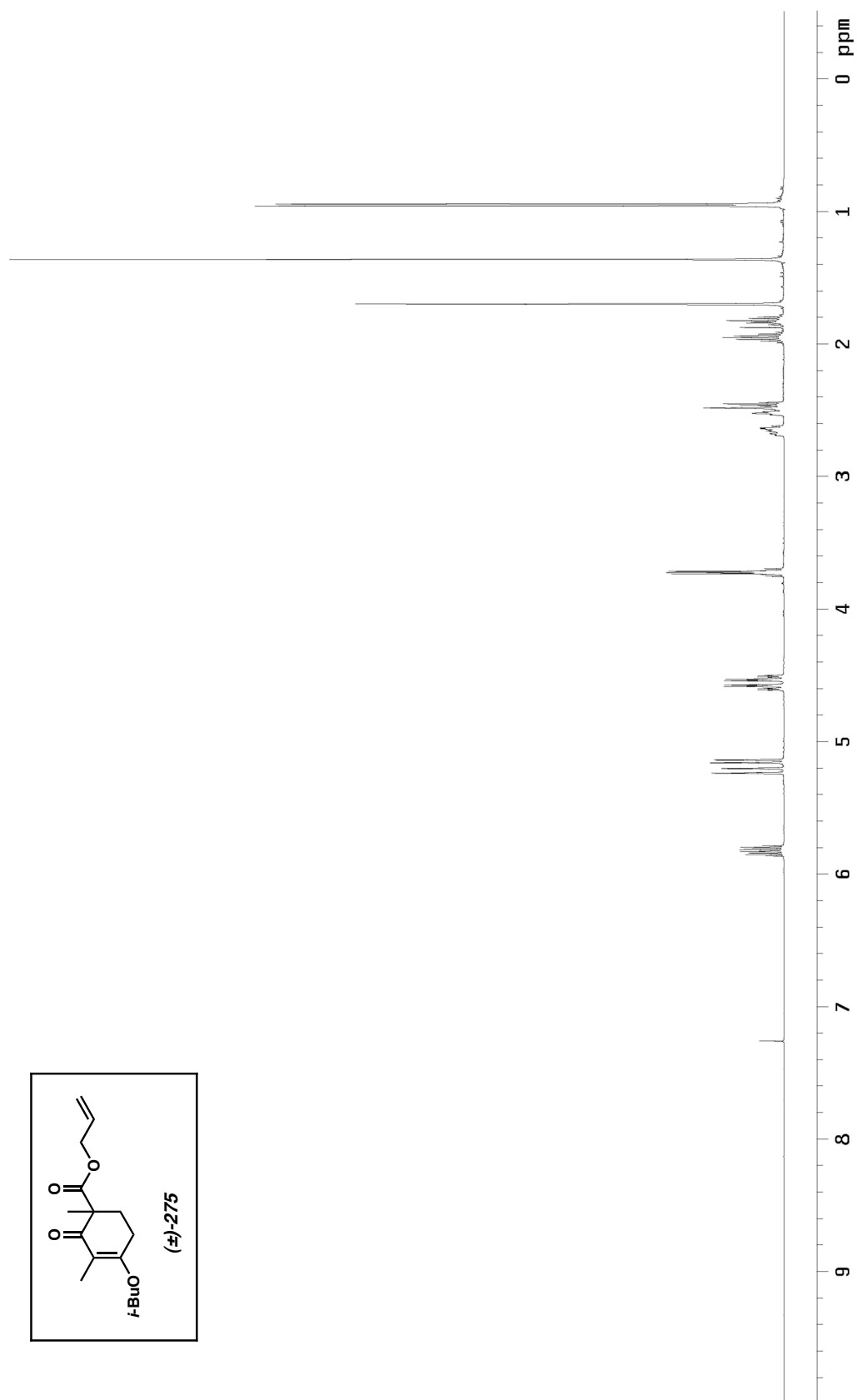
- (26) The reactivity of vinylogous β -ketoester (\pm)-**275** contrasts significantly with that of related derivative (\pm)-**271**. See the subsection 4.2.3.
- (27) β -ketoester (\pm)-**275** was recovered in 9% yield.
- (28) Breit, B.; Breuninger, D. *J. Am. Chem. Soc.* **2004**, *126*, 10244–10245.
- (29) Studies employing allylmagnesium bromide generated from **289**, MeLi, or MeMgBr nucleophiles were unsuccessful. Difficulties with these types of additions into vinylogous thioesters have been noted. See ref 4a.
- (30) Scholl, M.; Ding, S.; Lee, C. W.; Grubbs, R. H. *Org. Lett.* **1999**, *1*, 953–956.
- (31) A variety of homogeneous and heterogeneous catalysts were screened for the hydrogenation of **292**. Of those that were reactive, most promoted undesired reactivity, including enone reduction and further decomposition. Rh/Al₂O₃ proved to be a mild catalyst at 1 atm H₂ in MeOH for this substrate.
- (32) The stereochemistry of **293** was initially verified using NOE correlations. See the subsection 4.5.2.2 for details.
- (33) Dess, D. B.; Martin, J. C. *J. Org. Chem.* **1983**, *48*, 4155–4156.

- (34) (a) Lindgren, B. O.; Nilsson, T. *Acta Chem. Scand.* **1973**, *27*, 888–890.
(b) Kraus, G. A.; Roth, B. *J. Org. Chem.* **1980**, *45*, 4825–4830. (c) Bal, B. S.; Childers, W. E.; Pinnick, H. W. *Tetrahedron* **1981**, *37*, 2091–2096.
- (35) Luche, J. L.; Gemal, A. L. *J. Am. Chem. Soc.* **1979**, *101*, 5848–5849.
- (36) Krout, M. R.; Mohr, J. T.; Stoltz, B. M. *Org. Synth.* **2009**, *86*, 181–193.
- (37) Ukai, T.; Kawazura, H.; Ishii, Y.; Bonnet, J. J.; Ibers, J. A. *J. Organomet. Chem.* **1974**, *65*, 253–266.
- (38) Gottlieb, H. E.; Kotlyar, V.; Nudelman, A. *J. Org. Chem.* **1997**, *62*, 7512–7515.
- (39) Gulías, M.; Rodríguez, J. R.; Castedo, L.; Mascareñas, J. L. *Org. Lett.* **2003**, *5*, 1975–1977.
- (40) Paquette, L. A.; Sauer, D. R.; Cleary, D. G.; Kinsella, M. A.; Blackwell, C. M.; Anderson, L. G. *J. Am. Chem. Soc.* **1992**, *114*, 7375–7387.
- (41) Danishefsky, S. J.; Mantlo, N. *J. Am. Chem. Soc.* **1988**, *110*, 8129–8133.
- (42) Villieras, J.; Rambaud, M. *Organic Syntheses*; Wiley & Sons: New York, 1993; Collect. Vol. VIII, pp 265–267.

APPENDIX 4

Spectra Relevant to Chapter 4:

*Enantioselective Allylic Alkylations of Vinylogous
 β -Ketoester Derivatives: Total Synthesis of (+)-Carissone*

Figure A4.1. ¹H NMR spectrum (500 MHz, CDCl₃) of 275.

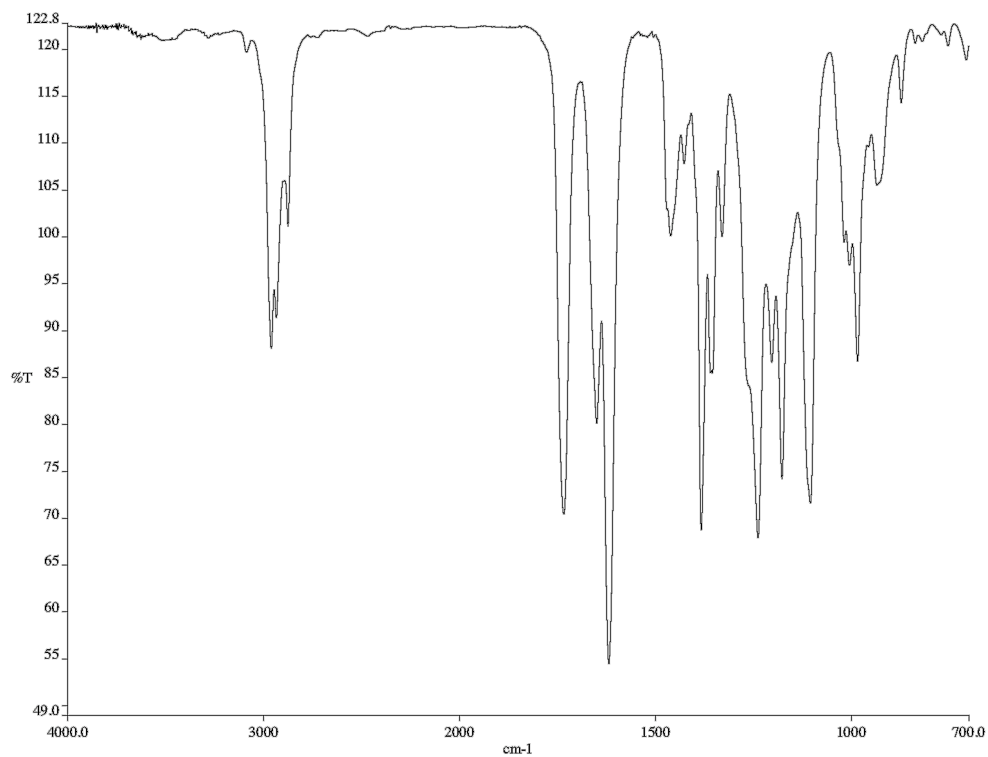


Figure A4.2. Infrared spectrum (neat film/NaCl) of **275**.

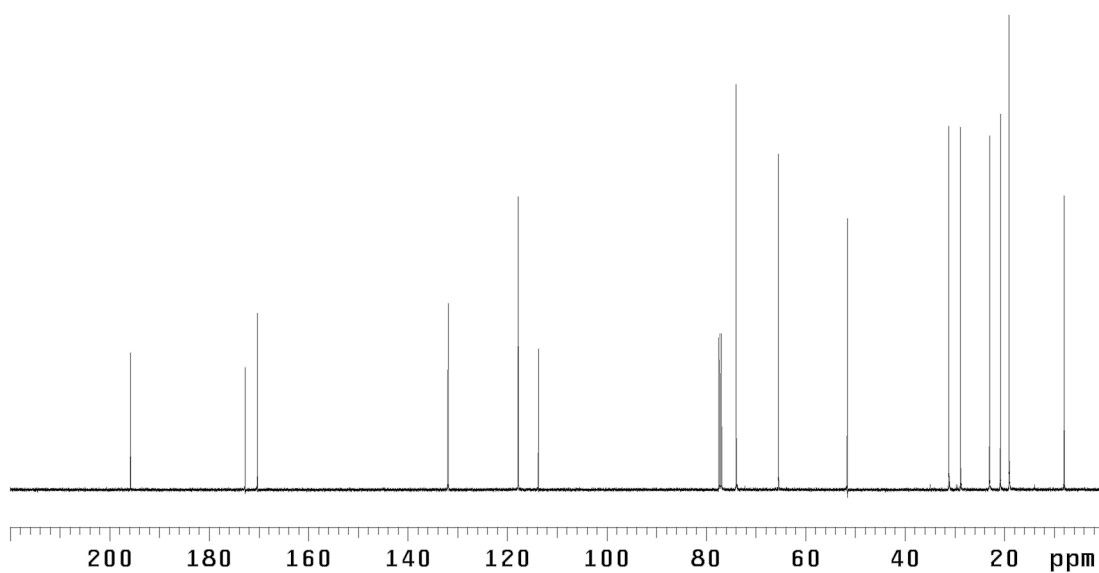
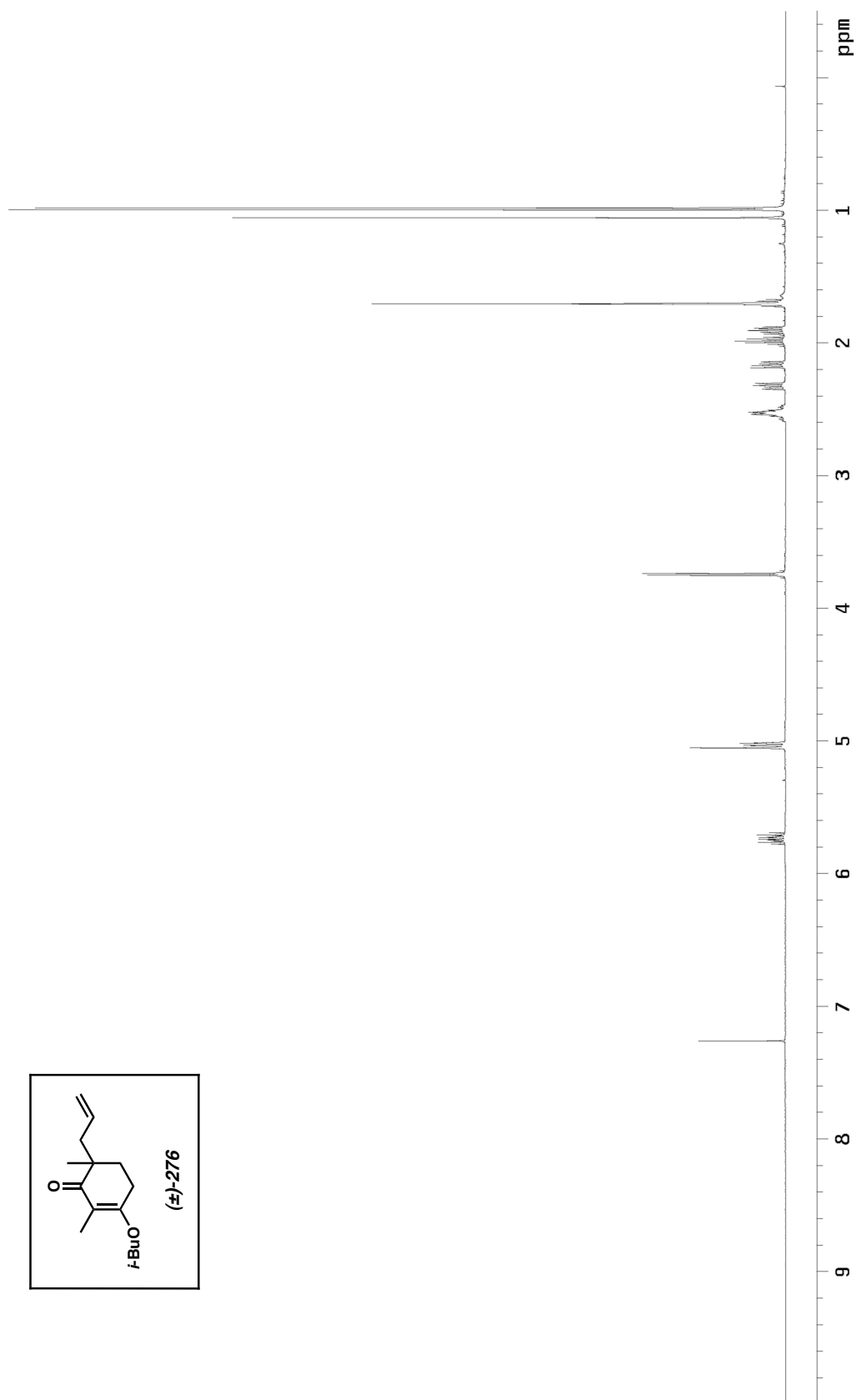


Figure A4.3. ¹³C NMR spectrum (126 MHz, CDCl₃) of **275**.

Figure A4.4. ^1H NMR spectrum (500 MHz, CDCl_3) of **276**.

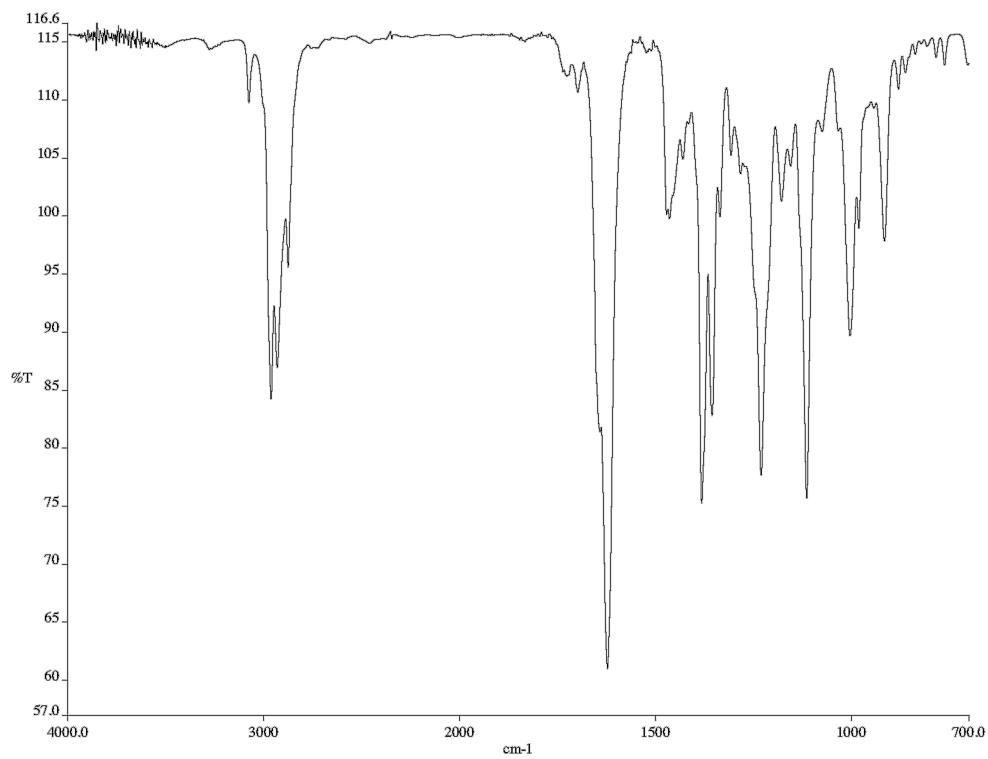


Figure A4.5. Infrared spectrum (neat film/NaCl) of **276**.

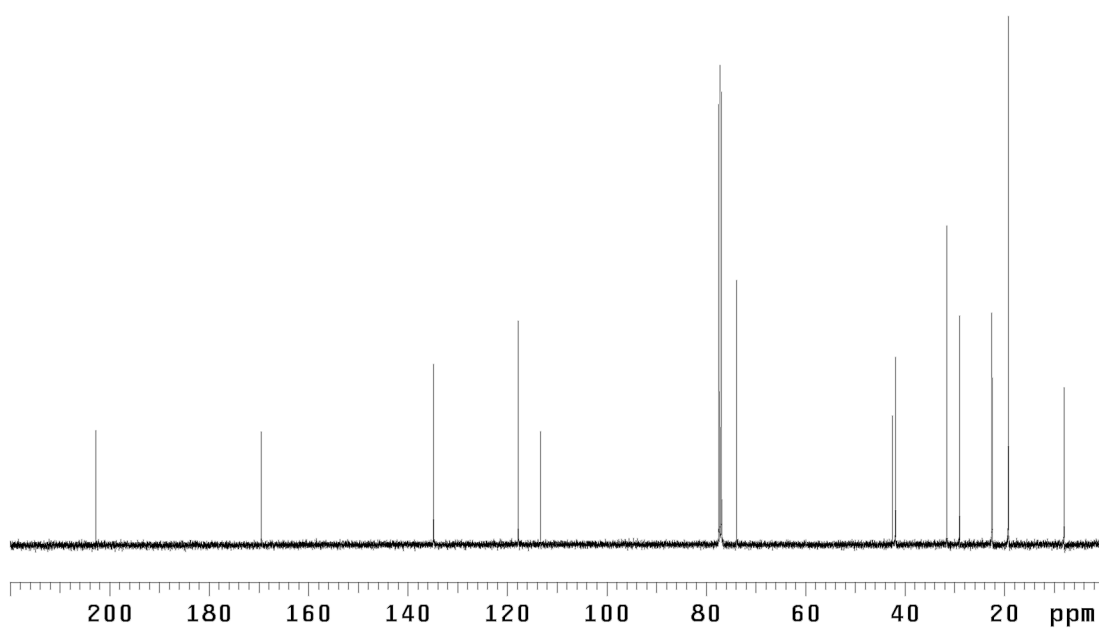
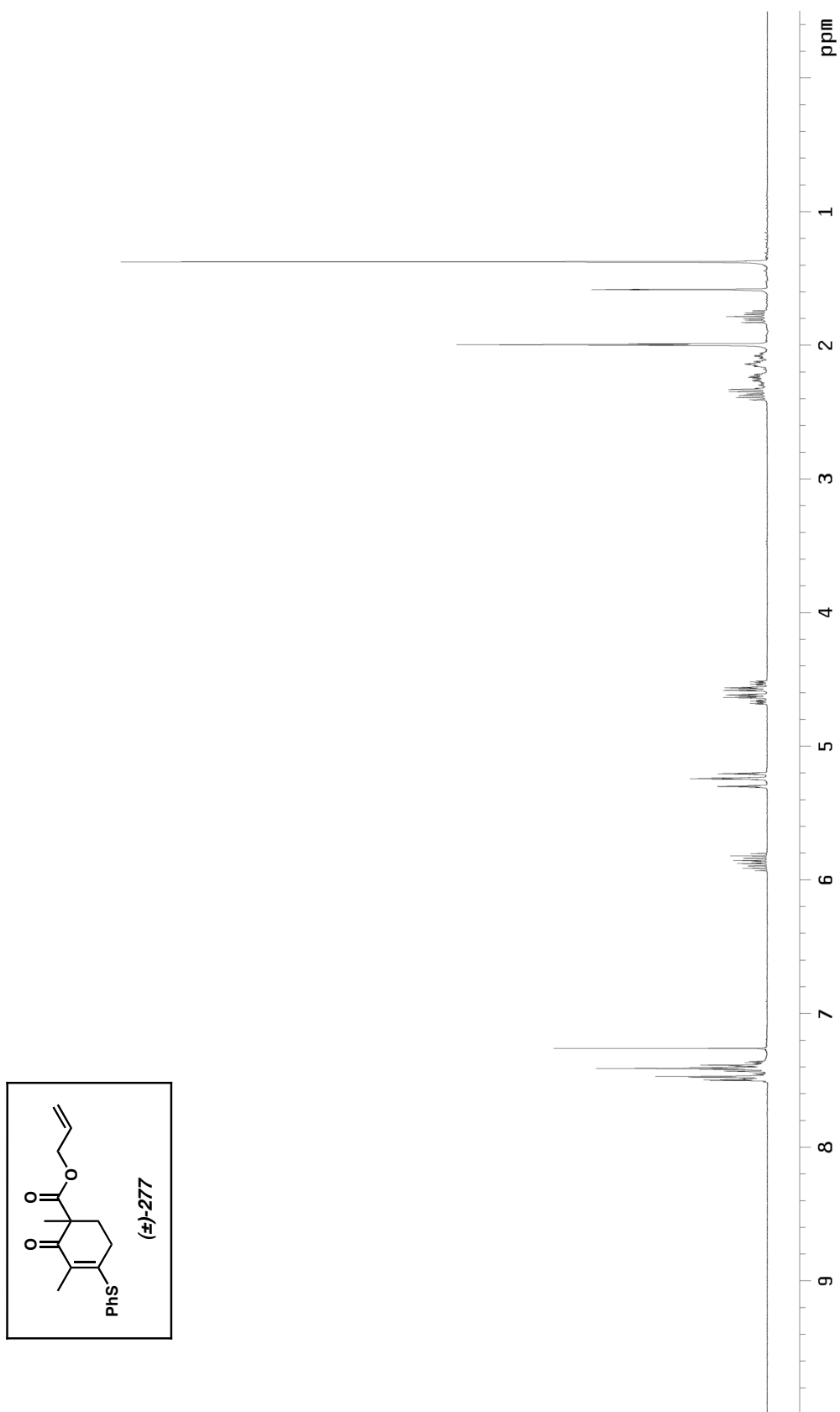


Figure A4.6. ¹³C NMR spectrum (126 MHz, CDCl₃) of **276**.

Figure A4.7. ^1H NMR spectrum (300 MHz, CDCl_3) of **277**.

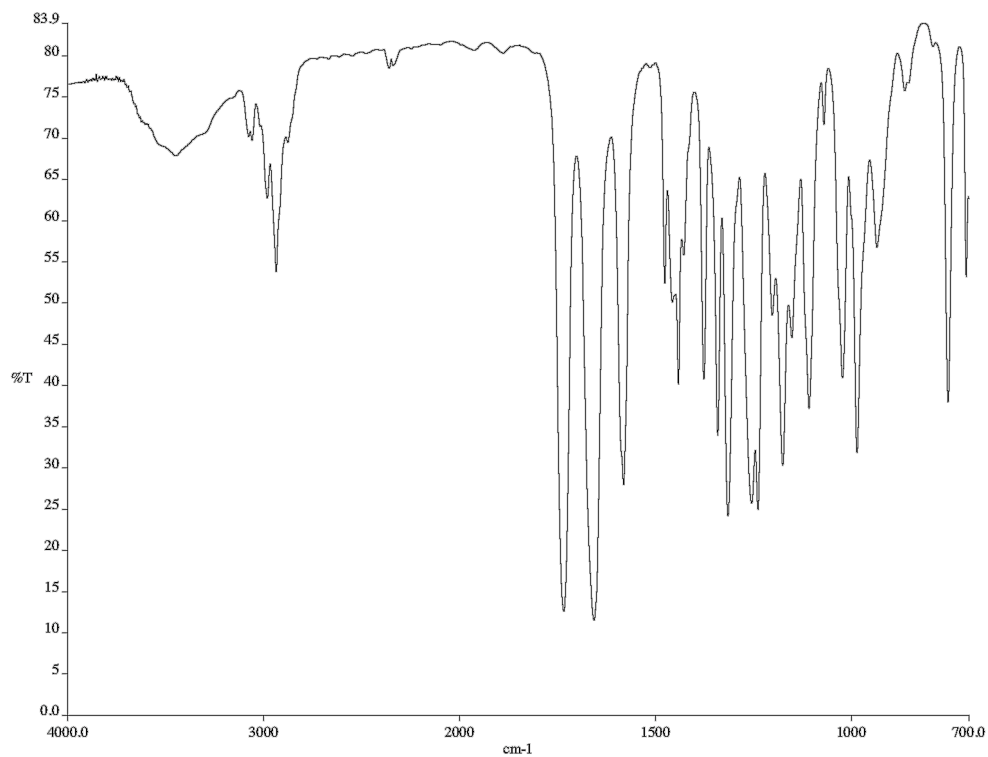


Figure A4.8. Infrared spectrum (neat film/NaCl) of **277**.

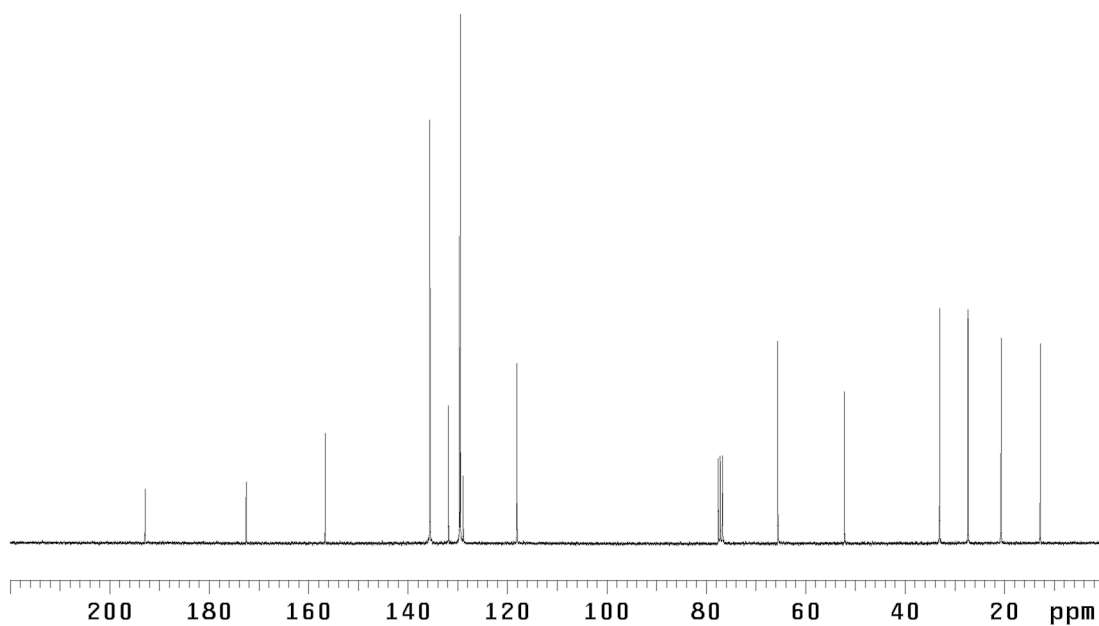
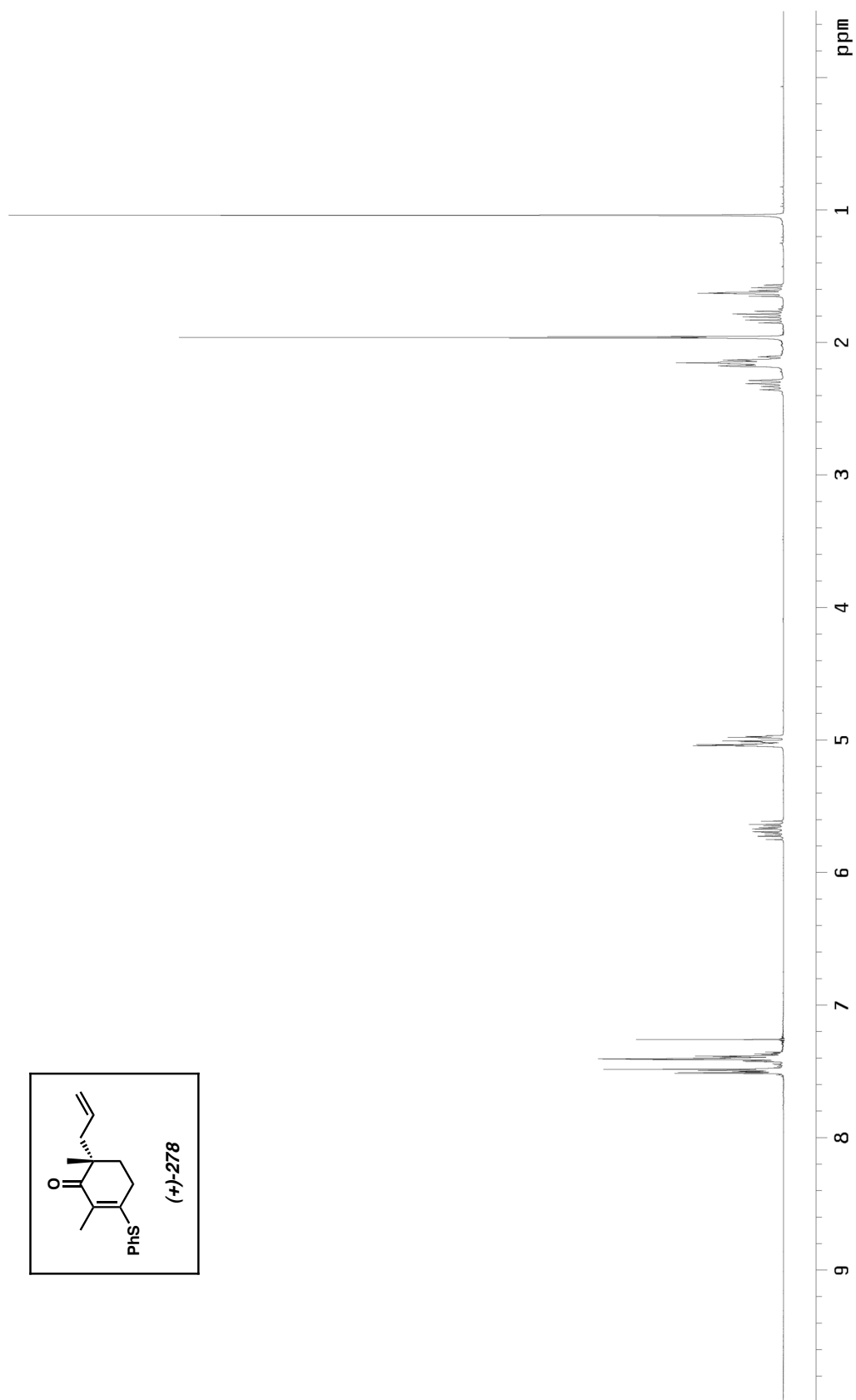


Figure A4.9. ¹³C NMR spectrum (75 MHz, CDCl₃) of **277**.

Figure A4.10. ^1H NMR spectrum (300 MHz, CDCl_3) of **278**.

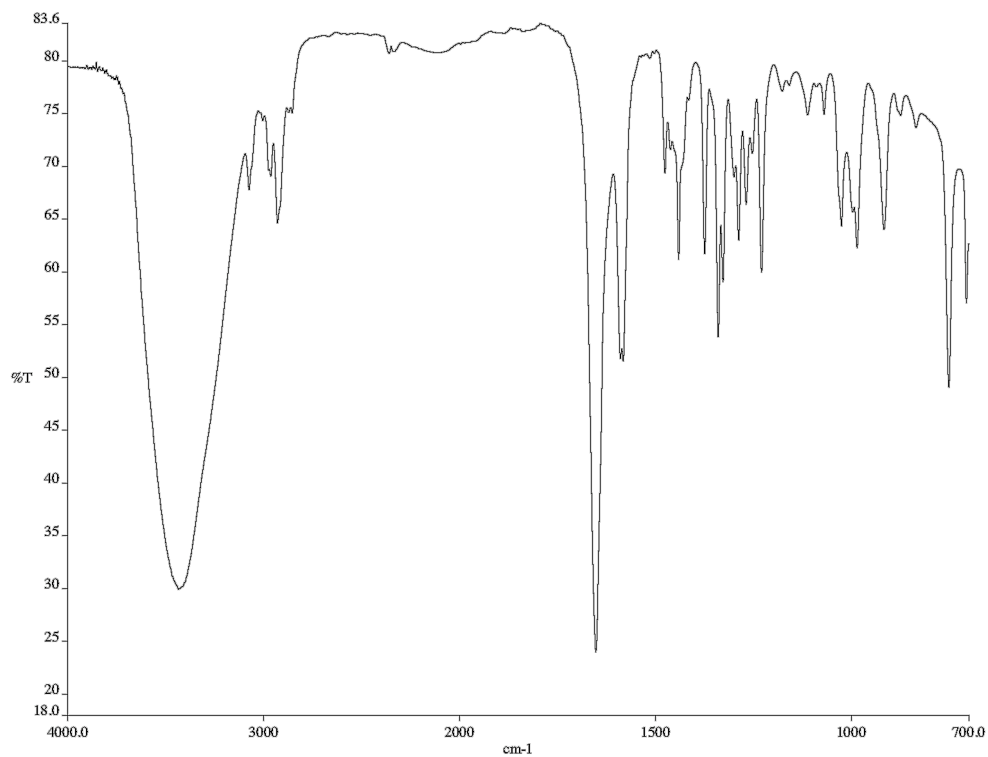


Figure A4.11. Infrared spectrum (neat film/NaCl) of **278**.

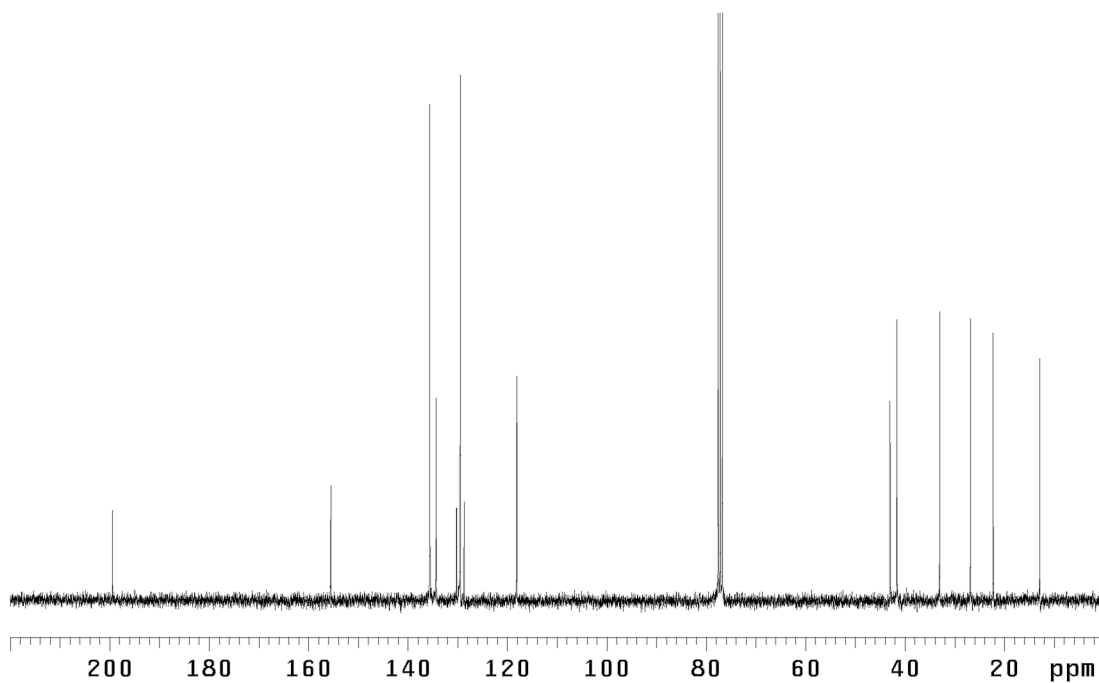
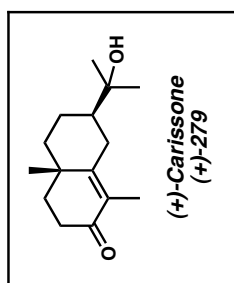
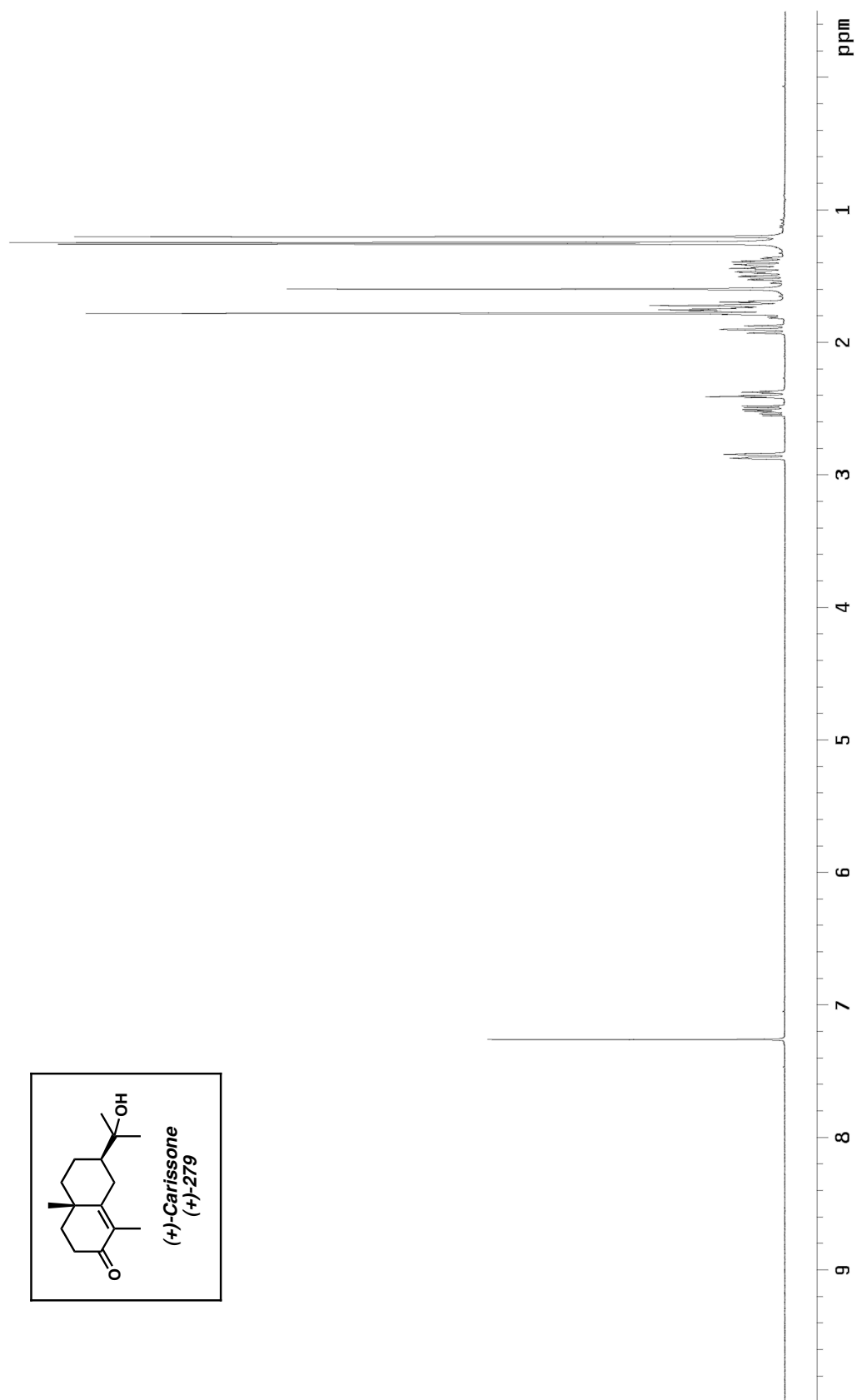


Figure A4.12. ¹³C NMR spectrum (75 MHz, CDCl₃) of **278**.

Figure A4.13. ¹H NMR spectrum (500 MHz, CDCl₃) of (+)-carissone (279).

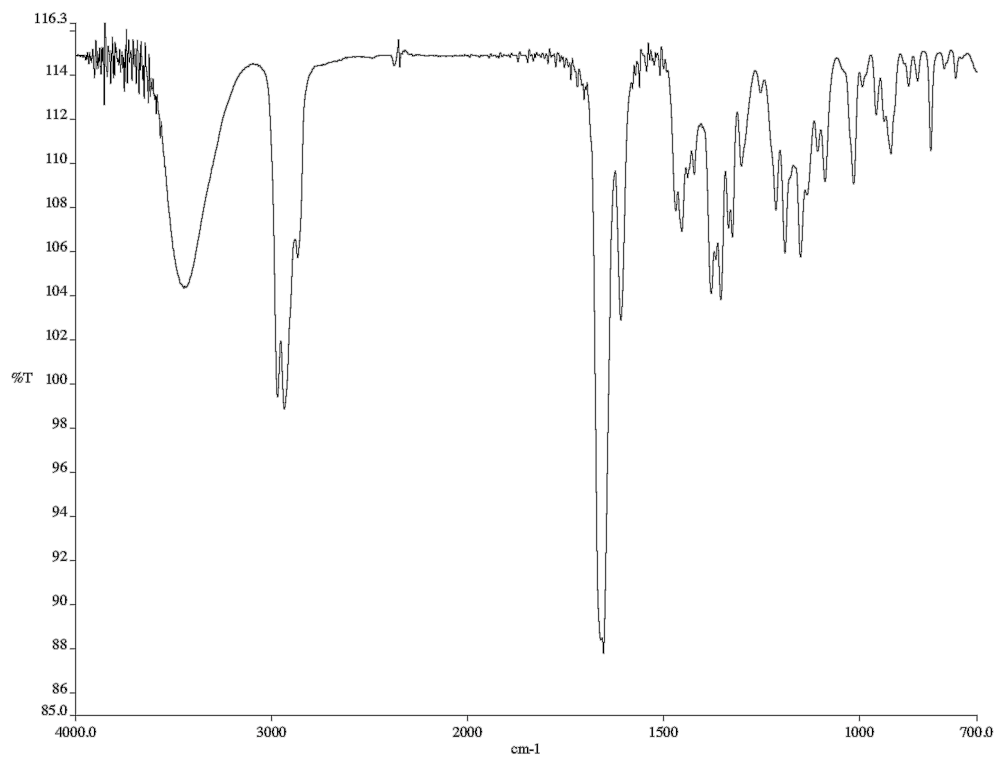


Figure A4.14. Infrared spectrum (neat film/NaCl) of (+)-carissone (**279**).

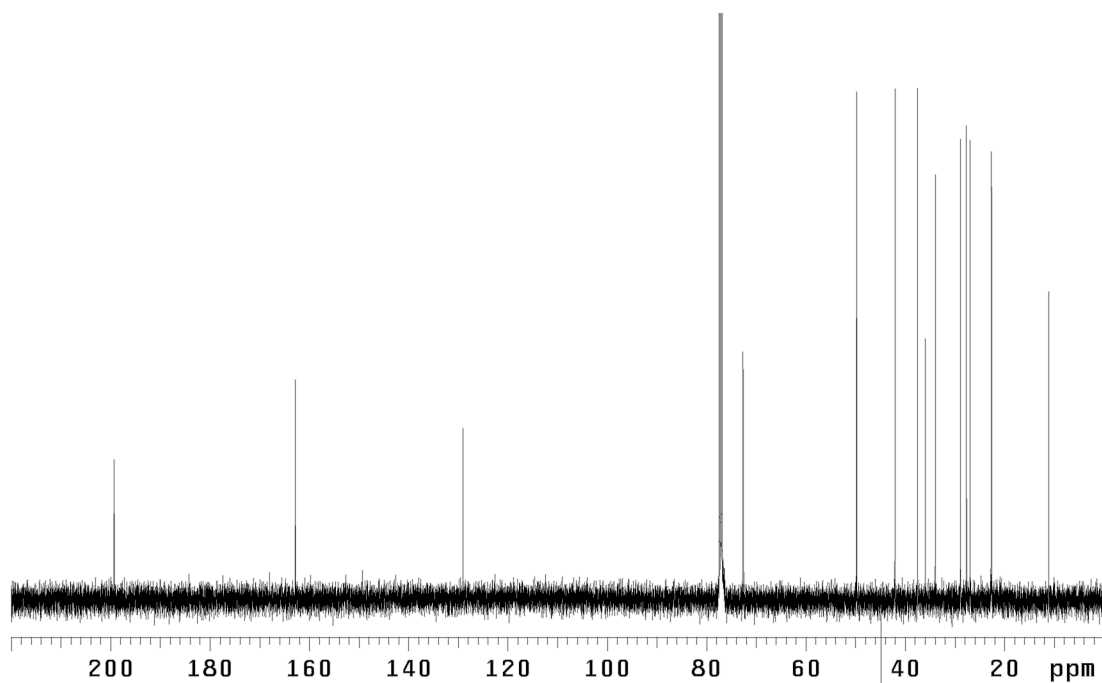
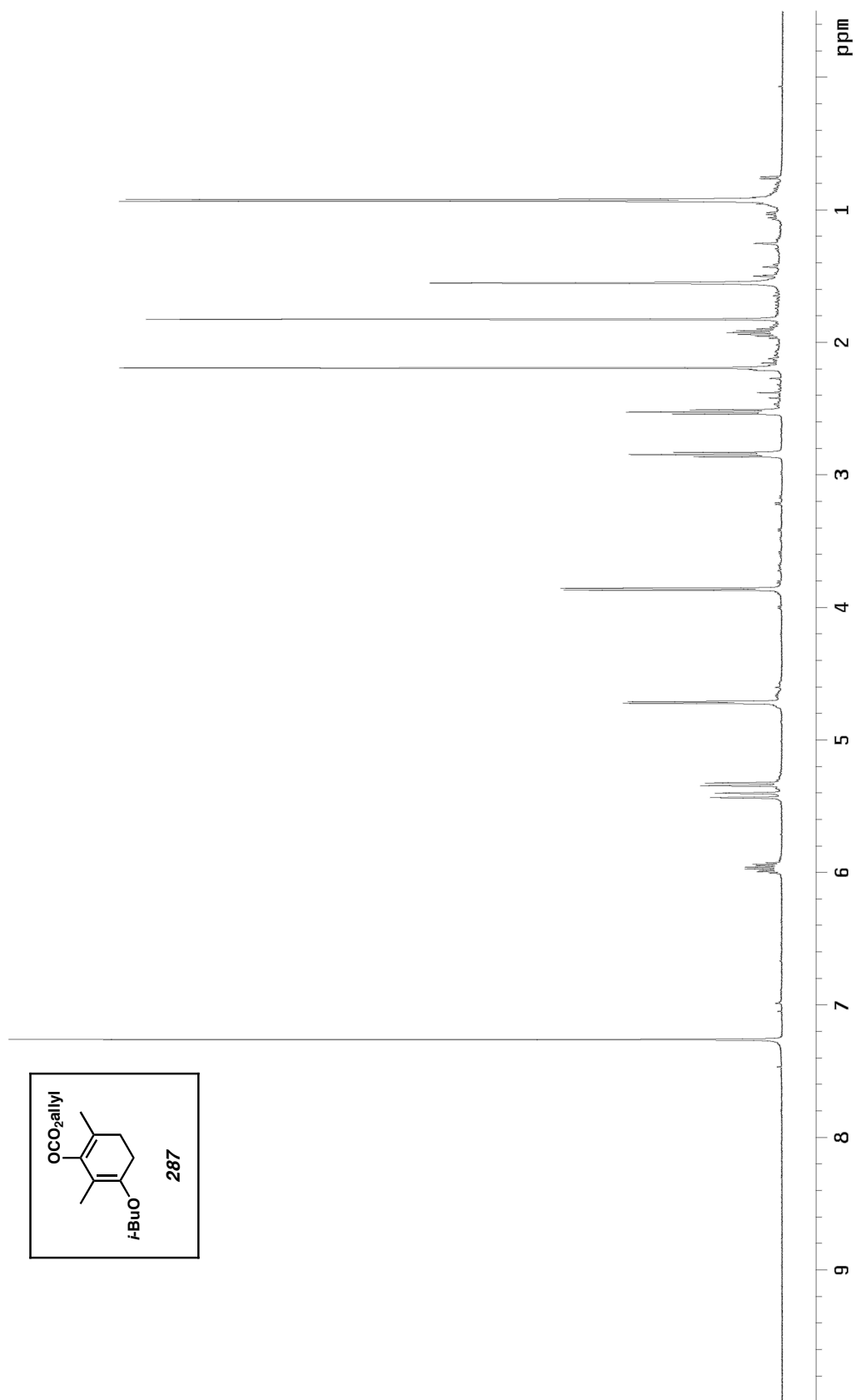
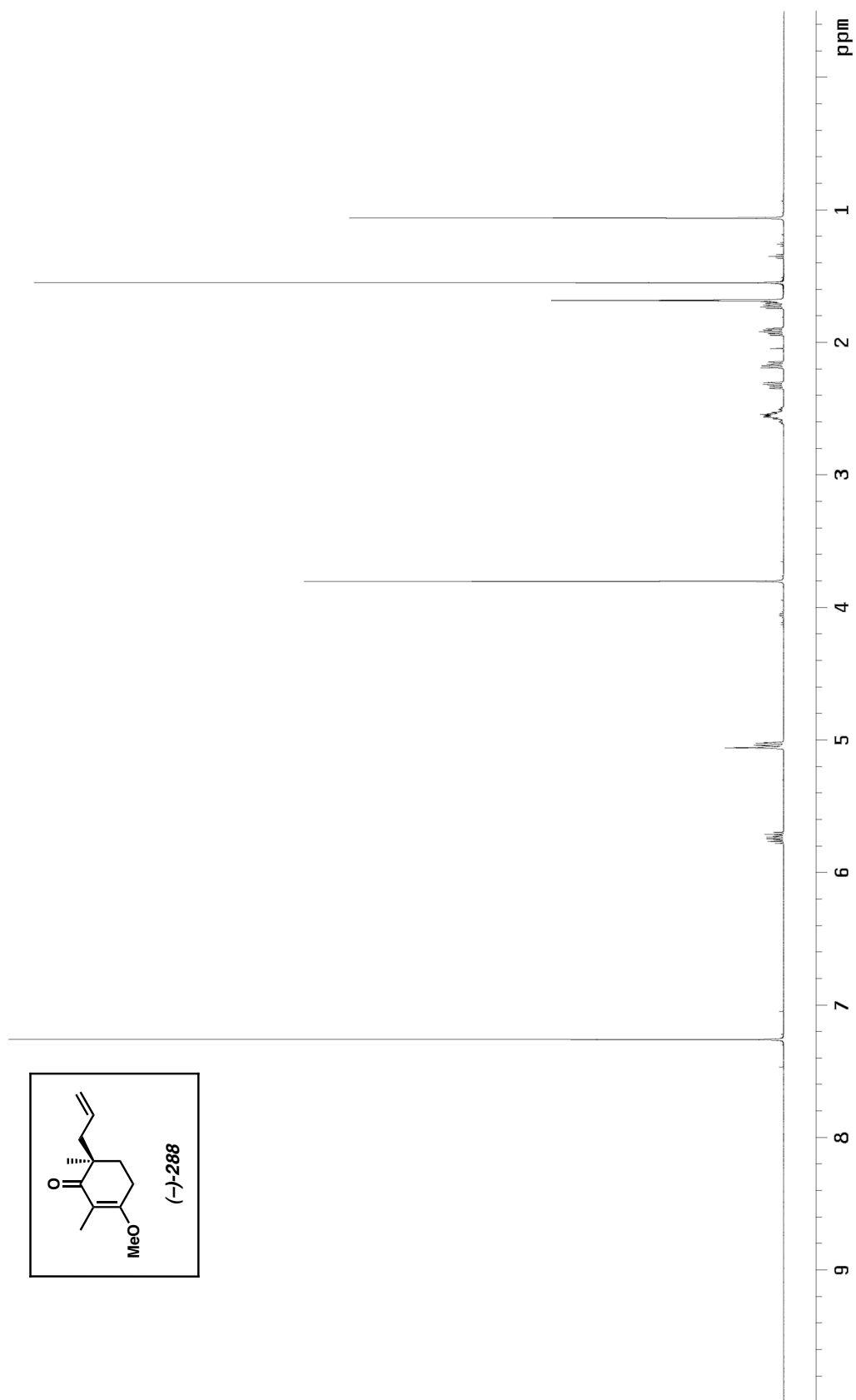


Figure A4.15. ¹³C NMR spectrum (126 MHz, CDCl₃) of (+)-carissone (**279**).

Figure A4.16. ^1H NMR spectrum (500 MHz, CDCl_3) of **287**.

Figure A4.17. ^1H NMR spectrum (500 MHz, CDCl_3) of **288**.

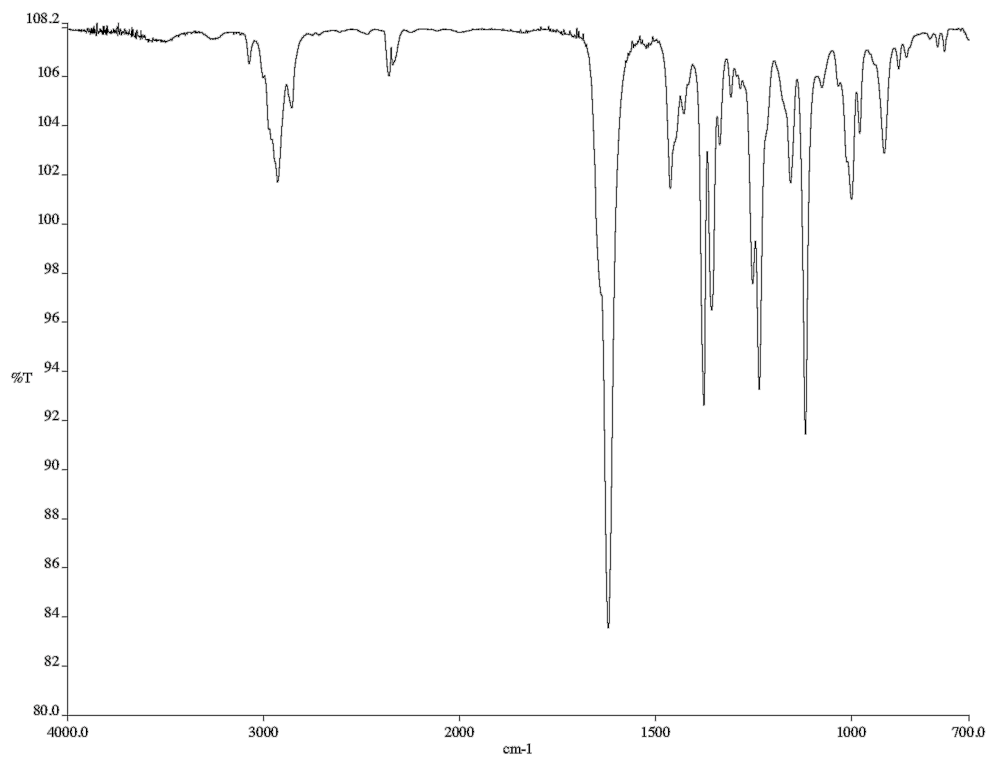


Figure A4.18. Infrared spectrum (neat film/NaCl) of **288**.

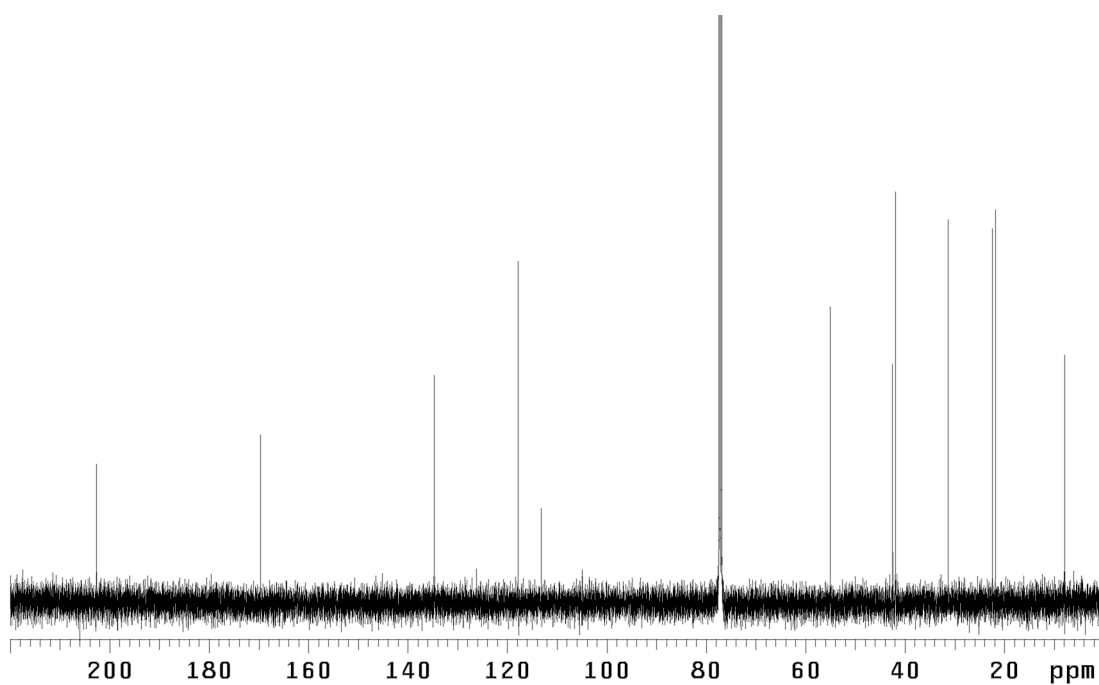
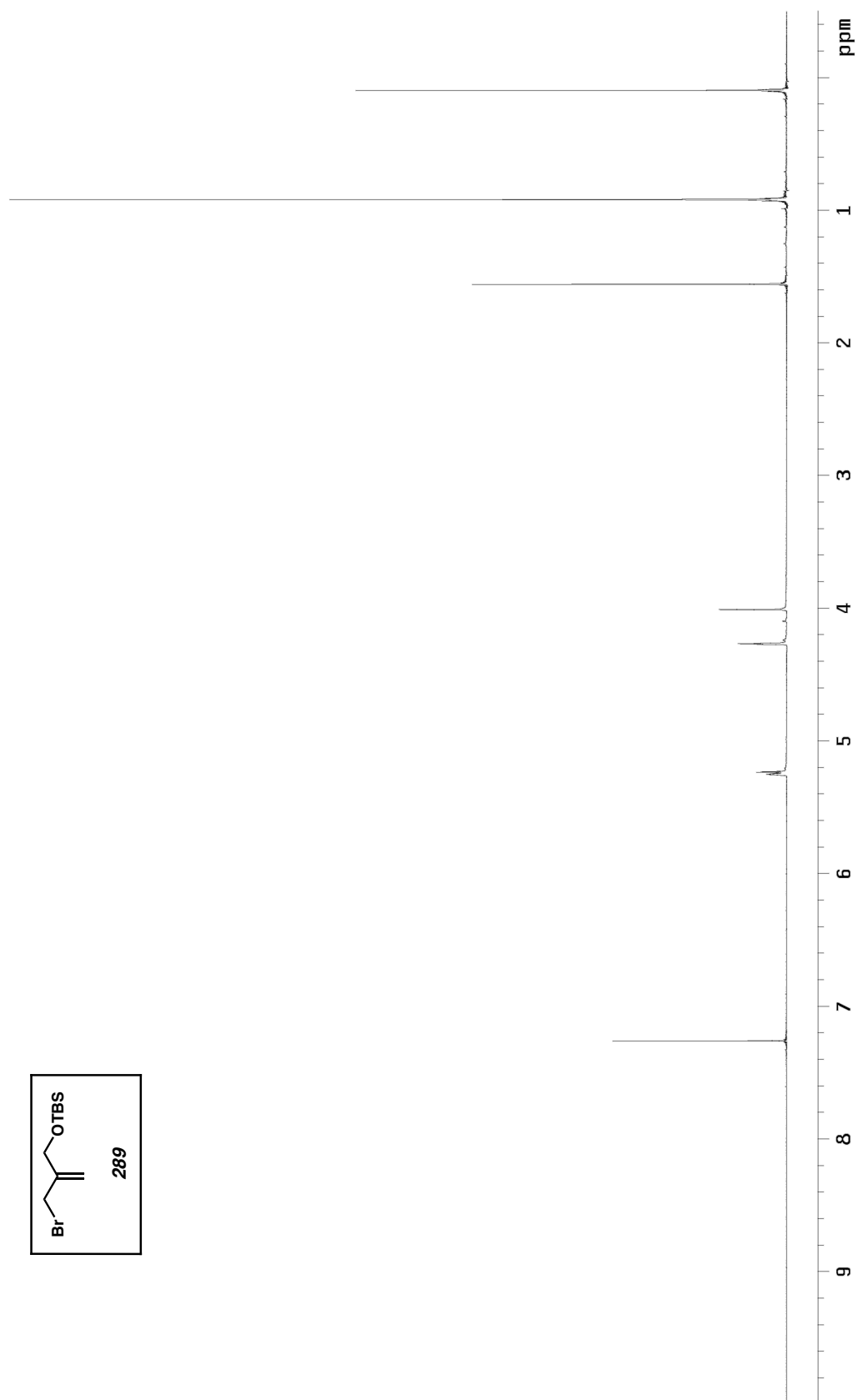
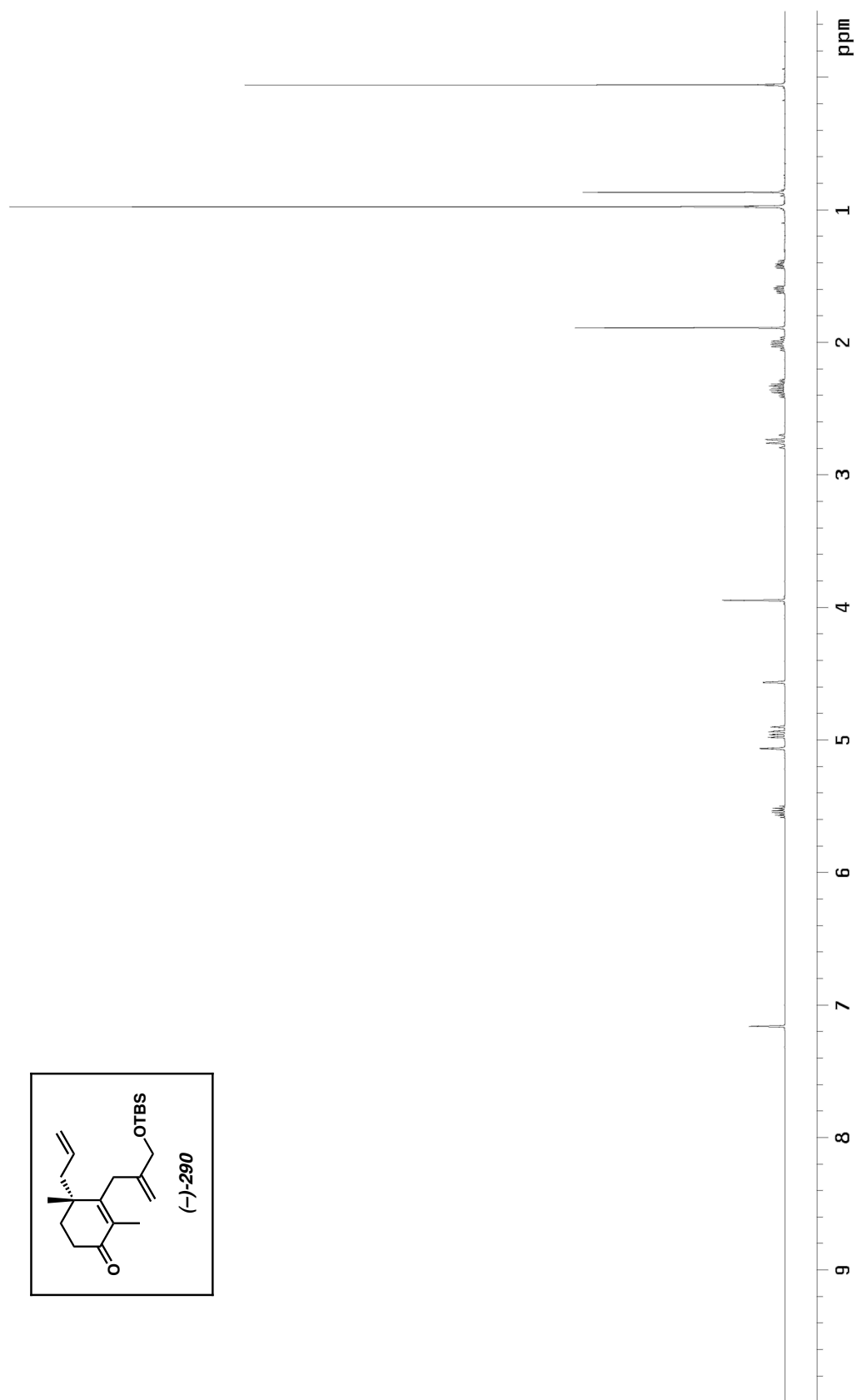


Figure A4.19. ¹³C NMR spectrum (126 MHz, CDCl₃) of **288**.

Figure A4.20. ^1H NMR spectrum (300 MHz, CDCl_3) of **289**.

Figure A4.2.1. ^1H NMR spectrum (500 MHz, C_6D_6) of **290**.

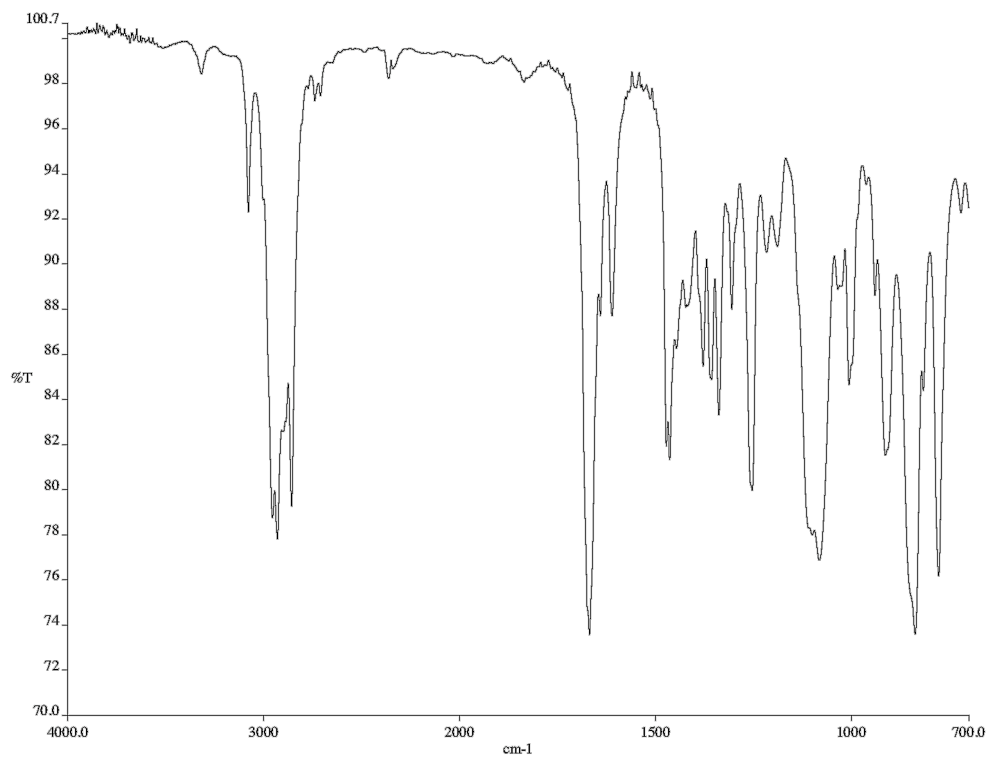


Figure A4.22. Infrared spectrum (neat film/NaCl) of **290**.

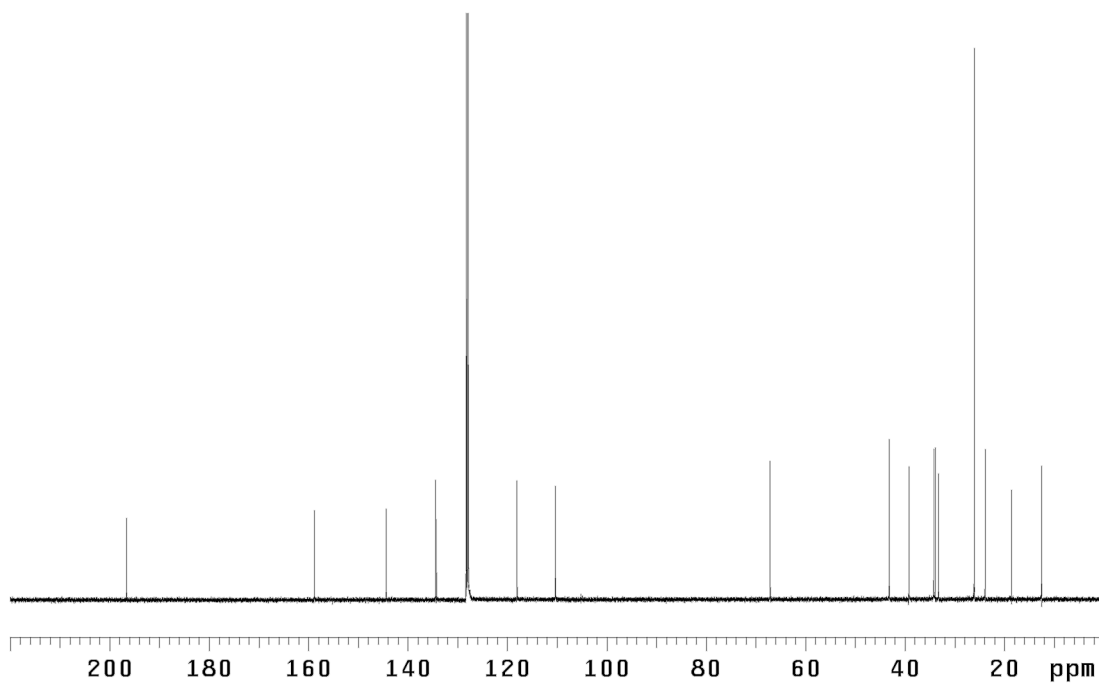
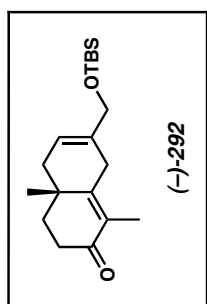
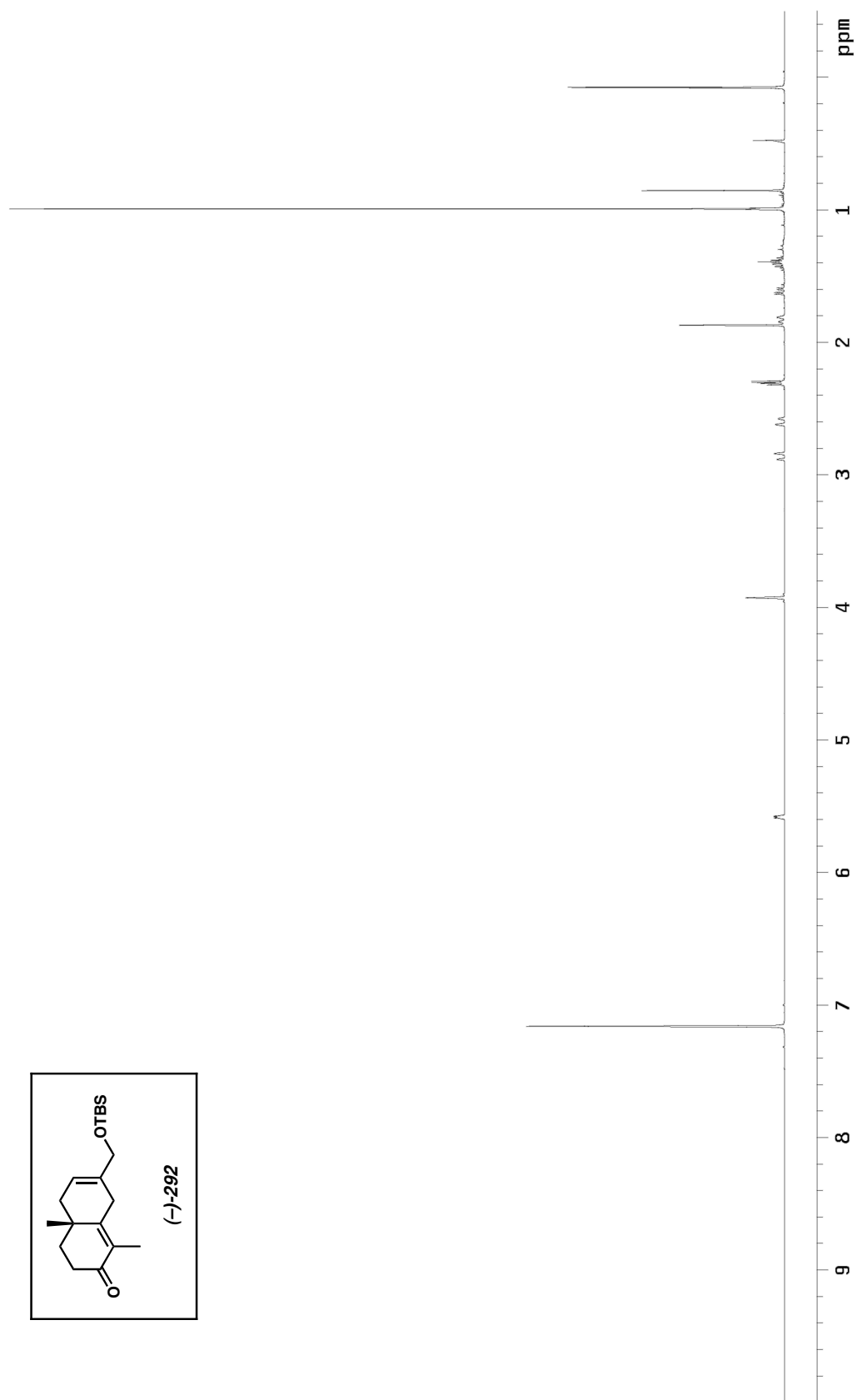


Figure A4.23. ¹³C NMR spectrum (126 MHz, C₆D₆) of **290**.

Figure A4.24. ^1H NMR spectrum (500 MHz, $\text{C}_6\text{D}_6\text{O}$) of **292**.

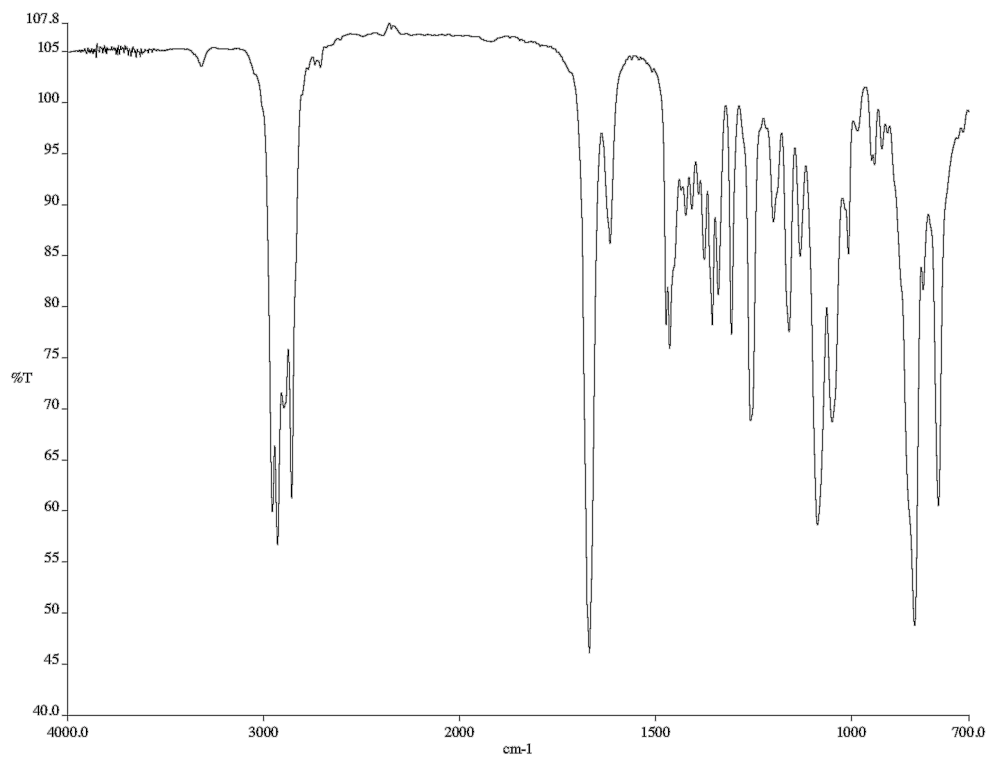


Figure A4.25. Infrared spectrum (neat film/NaCl) of **292**.

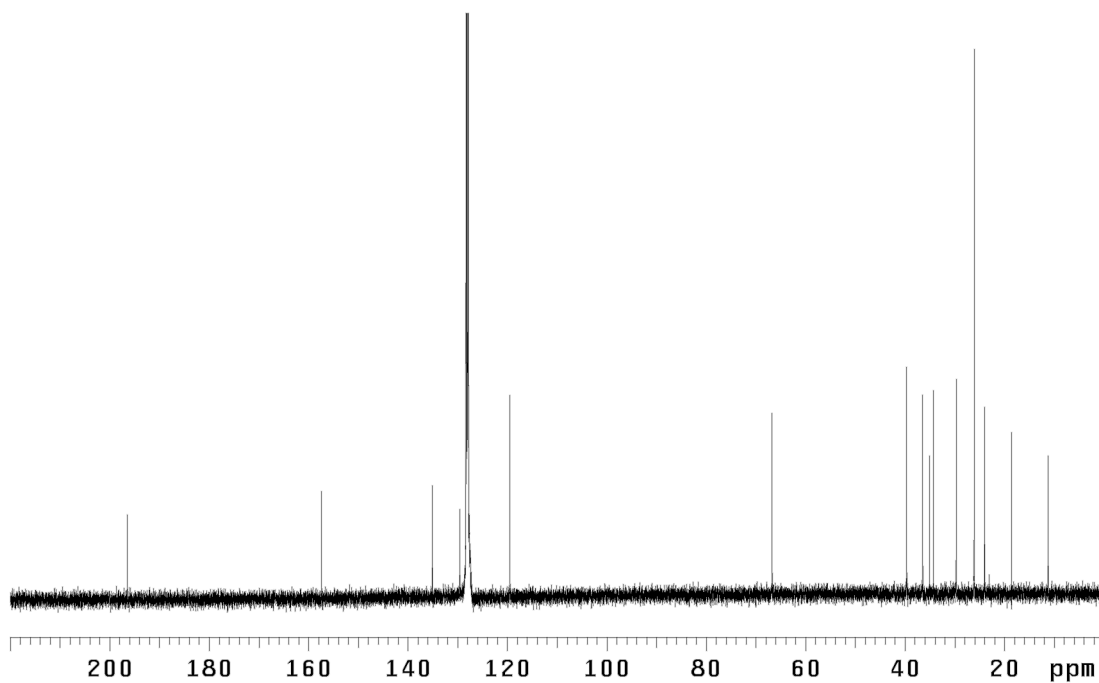
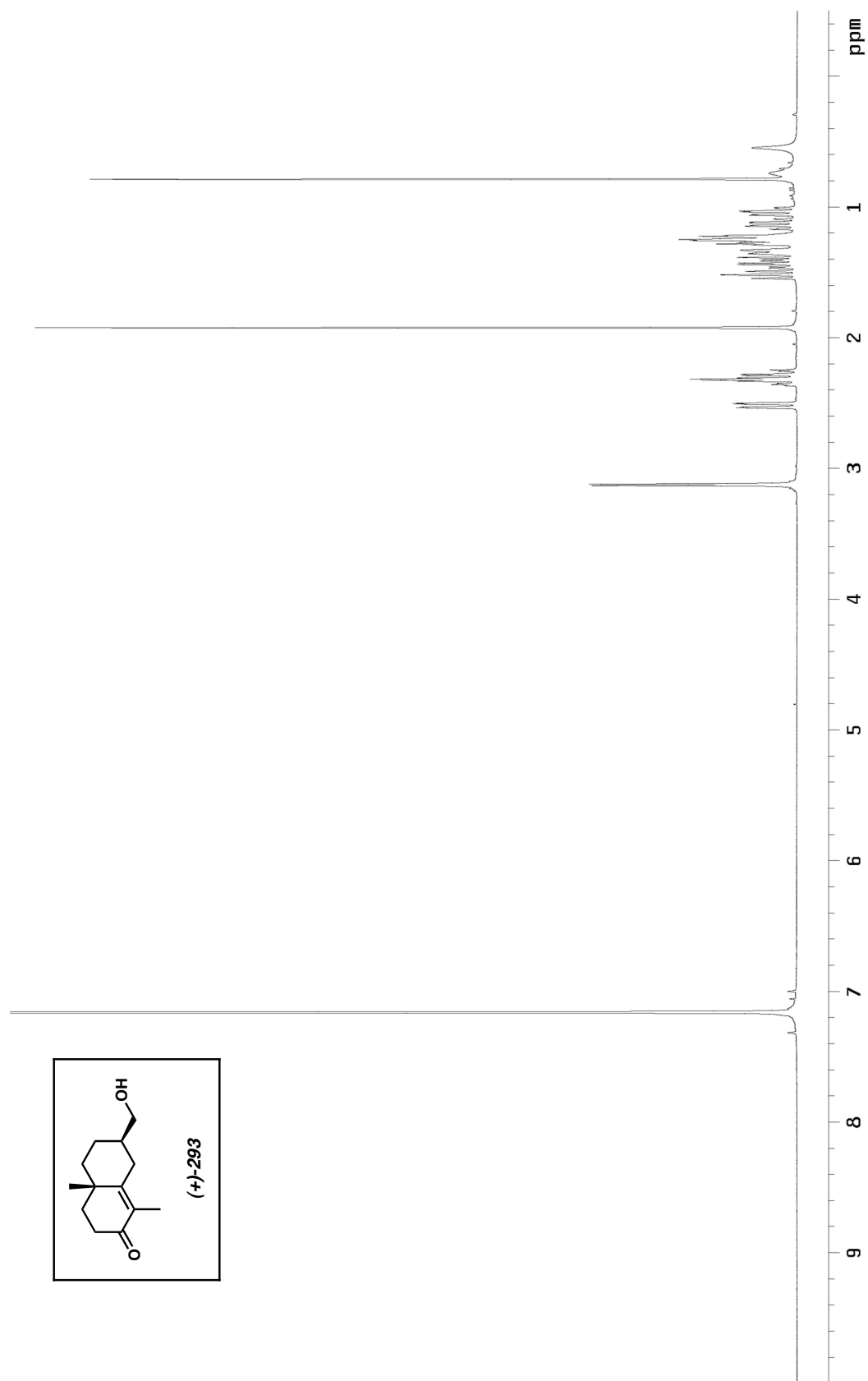


Figure A4.26. ¹³C NMR spectrum (126 MHz, C₆D₆) of **292**.

Figure A4.27. ^1H NMR spectrum (500 MHz, C_6D_6) of **293**.

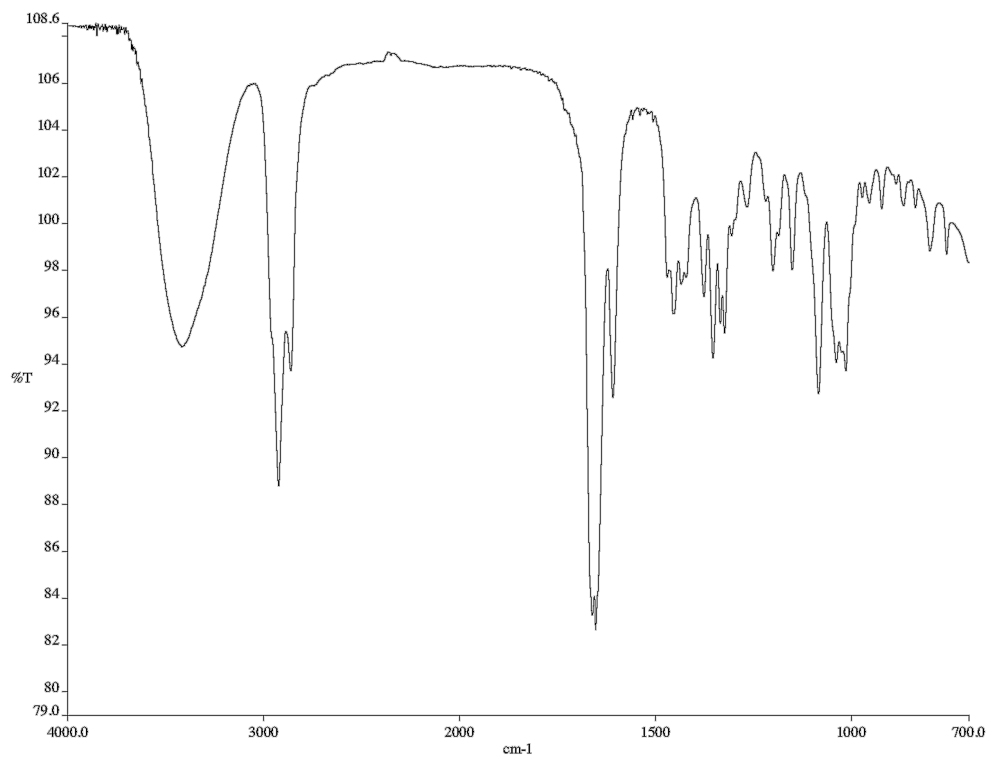


Figure A4.28. Infrared spectrum (neat film/NaCl) of **293**.

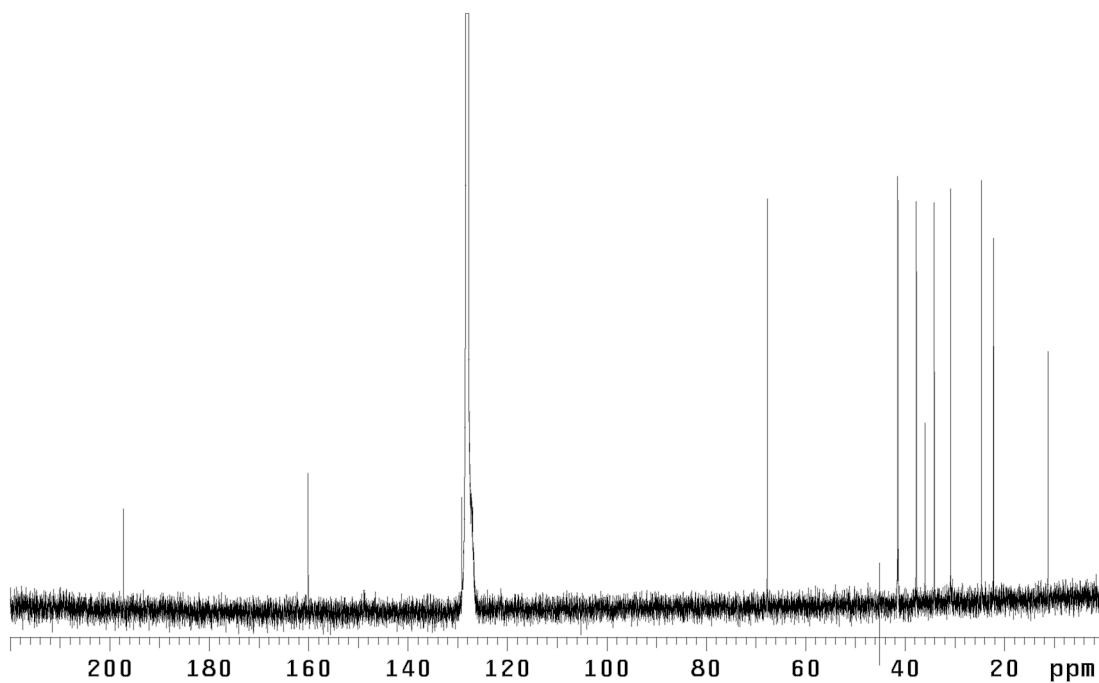
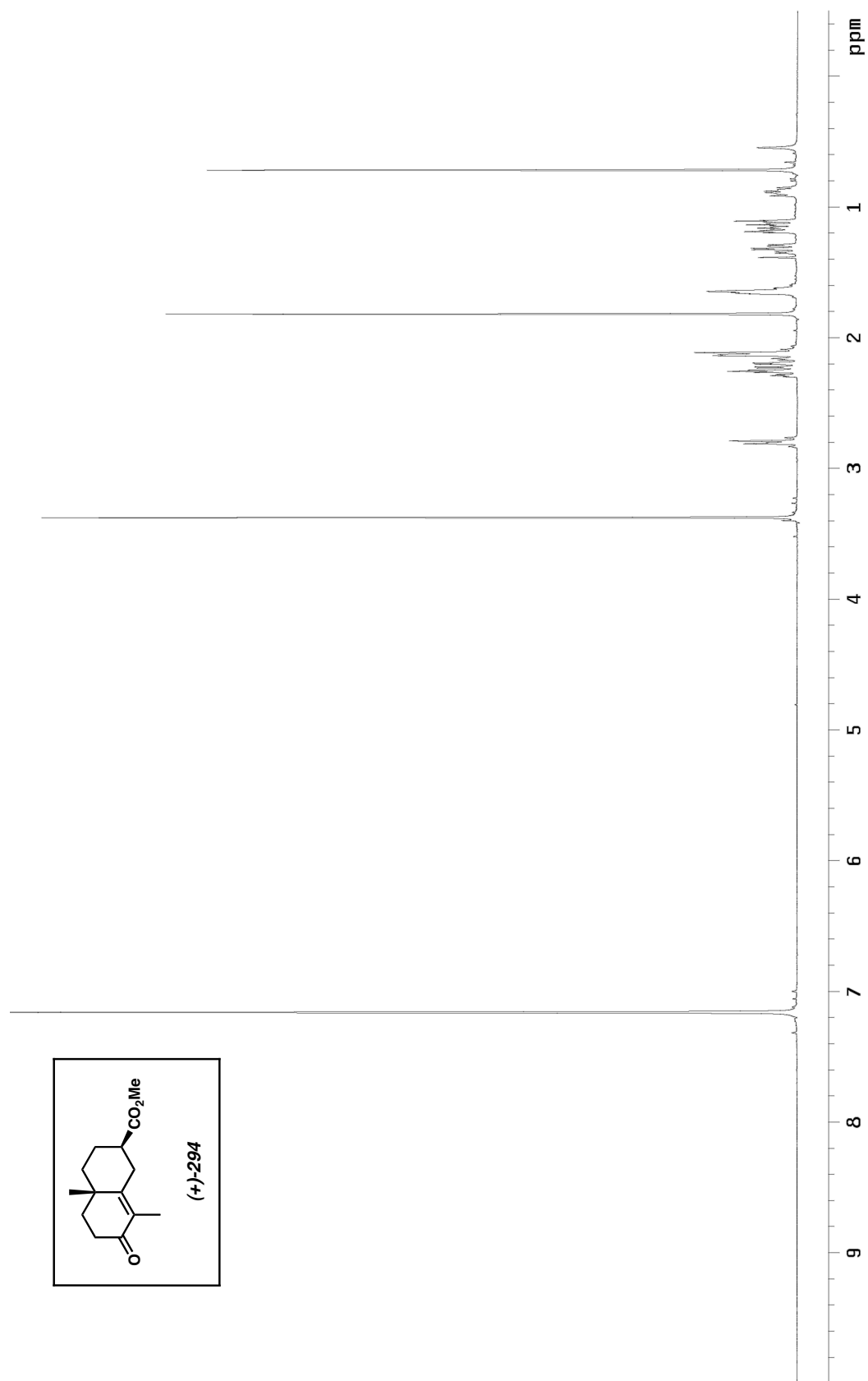


Figure A4.29. ¹³C NMR spectrum (126 MHz, C₆D₆) of **293**.

Figure A4.30. ^1H NMR spectrum (500 MHz, $\text{C}_6\text{D}_6\text{O}$) of **294**.

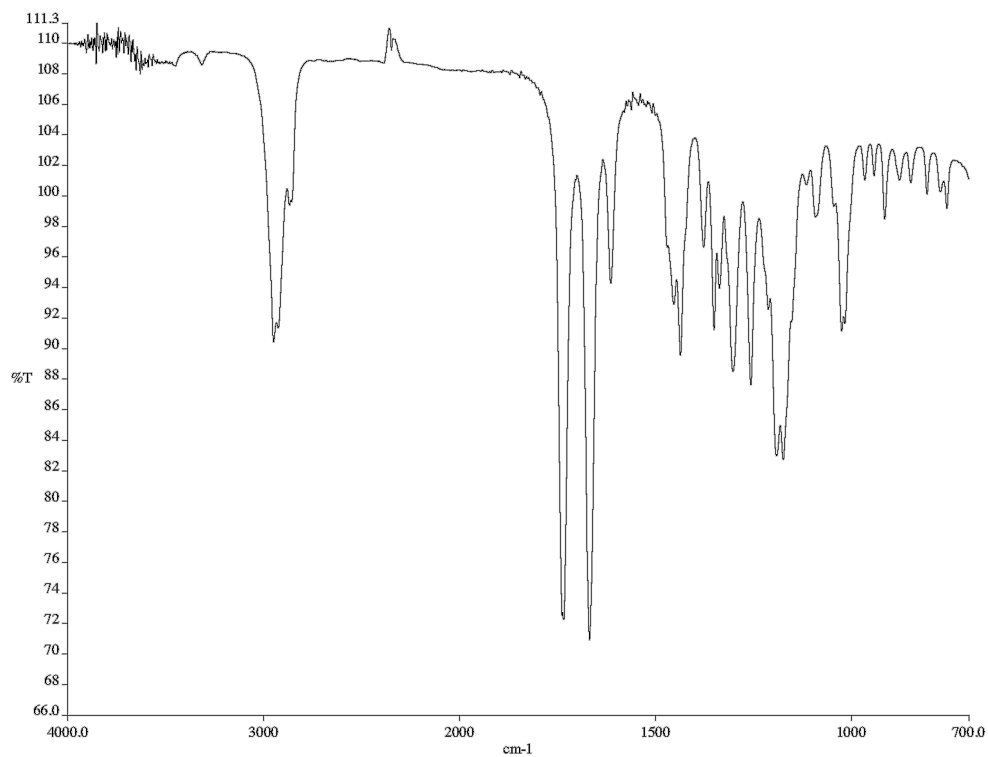


Figure A4.31. Infrared spectrum (neat film/NaCl) of **294**.

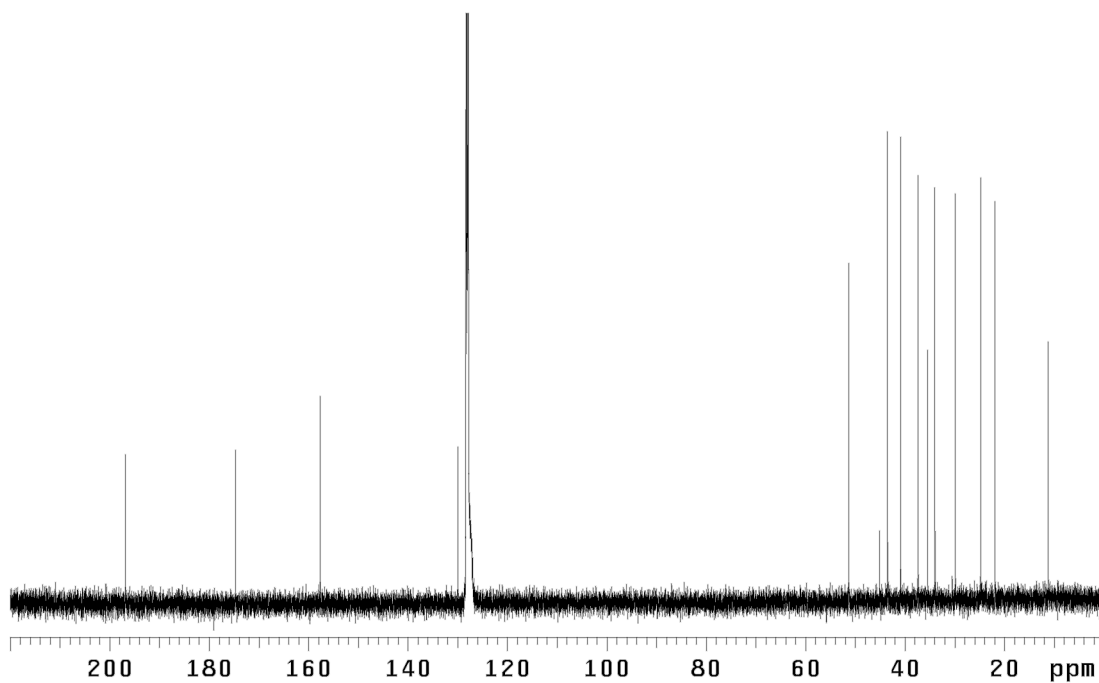


Figure A4.32. ¹³C NMR spectrum (126 MHz, C₆D₆) of **294**.

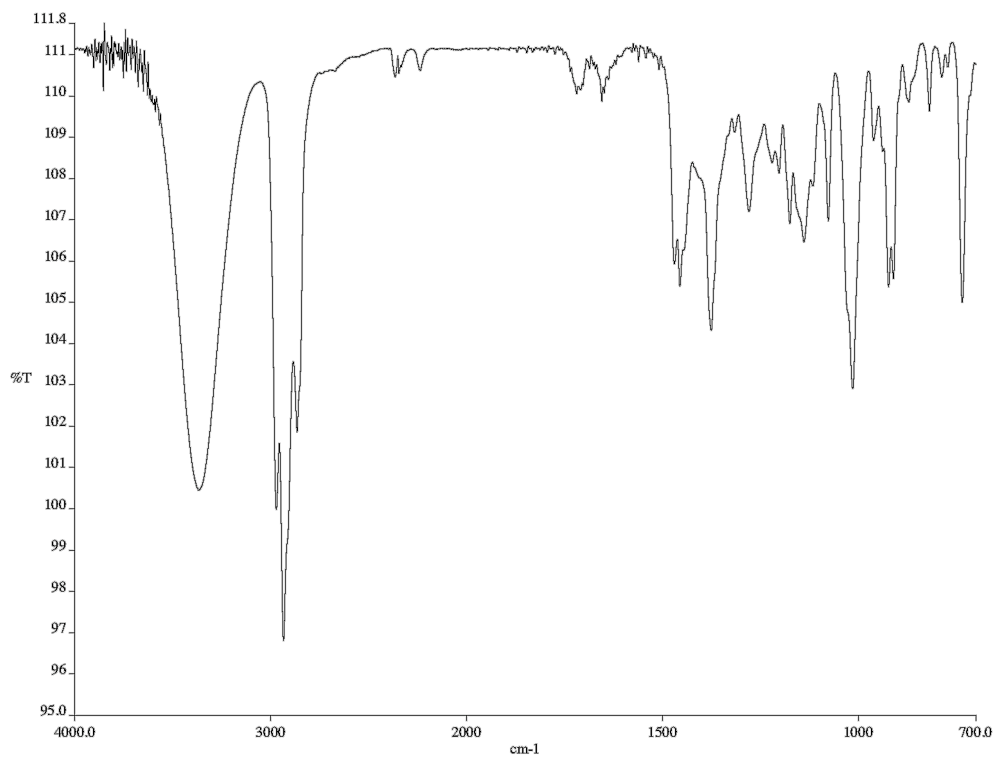


Figure A4.34. Infrared spectrum (neat film/NaCl) of **295**.

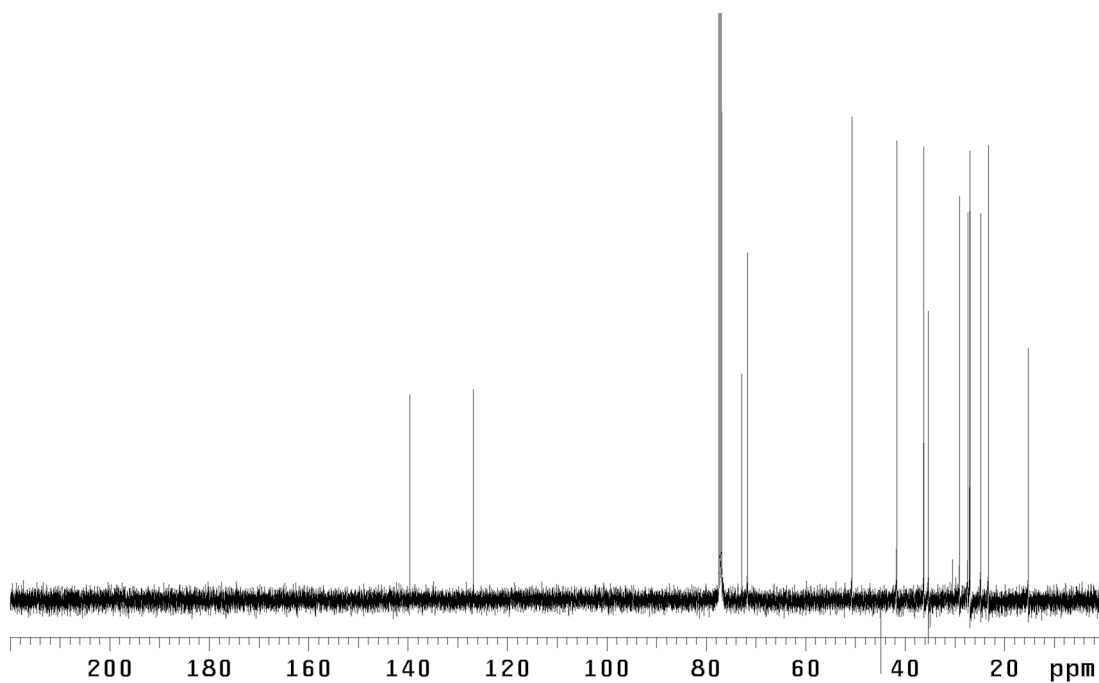
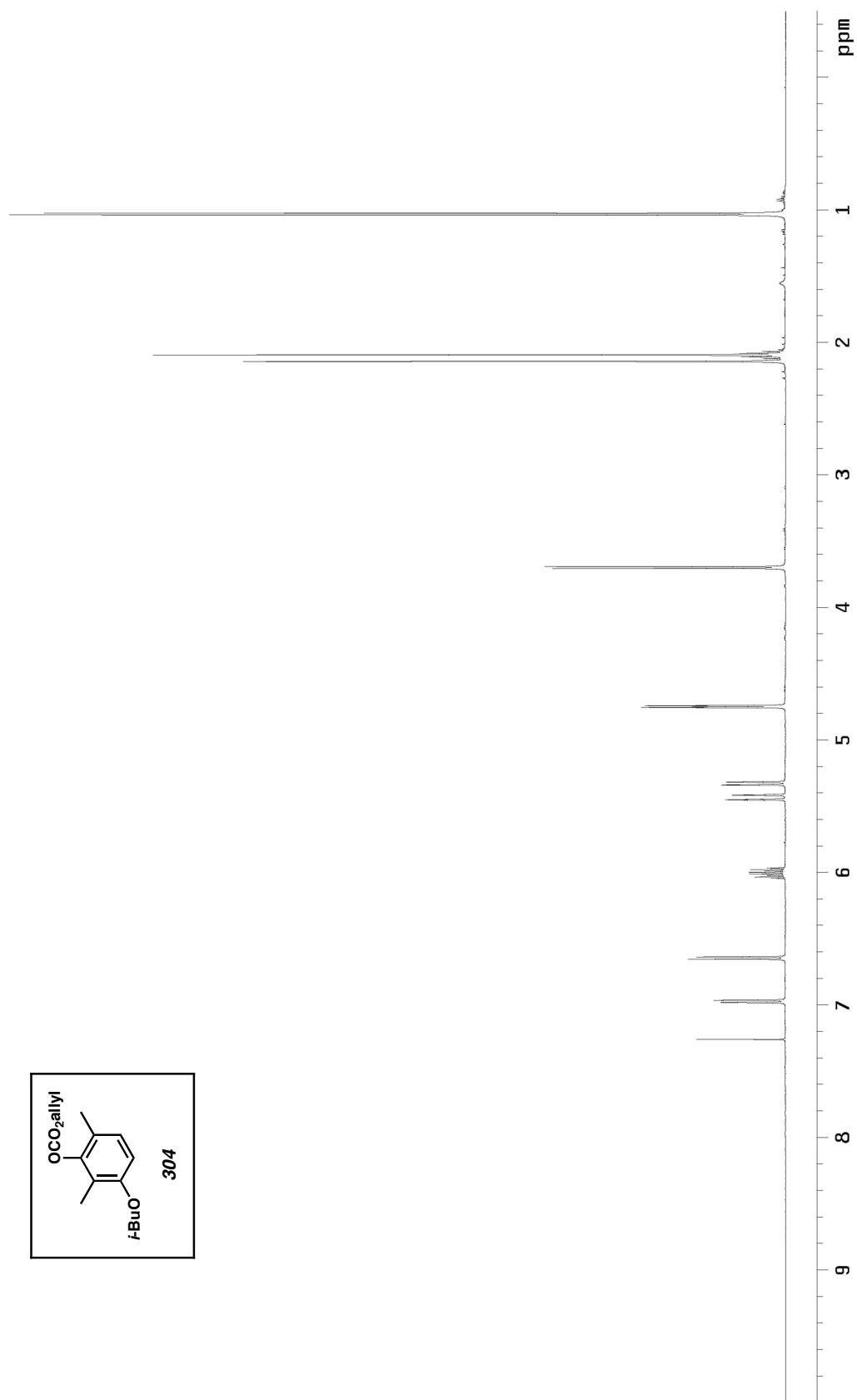


Figure A4.35. ¹³C NMR spectrum (126 MHz, CDCl₃) of **295**.

Figure A4.36. ^1H NMR spectrum (500 MHz, CDCl_3) of **304**.

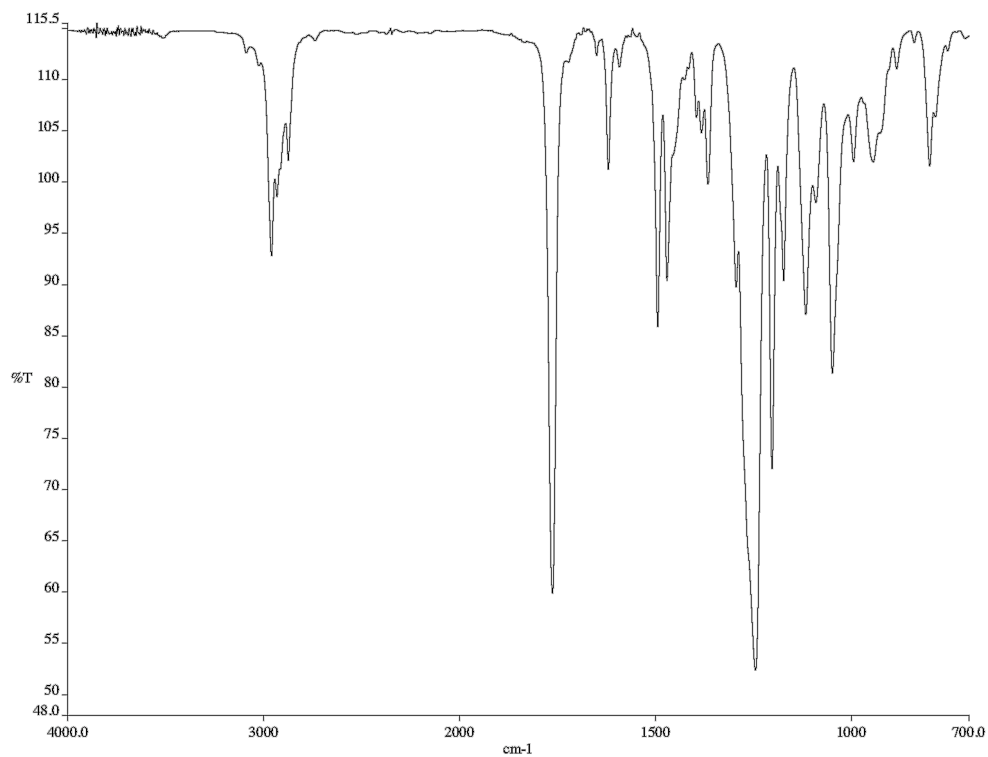


Figure A4.37. Infrared spectrum (neat film/NaCl) of **304**.

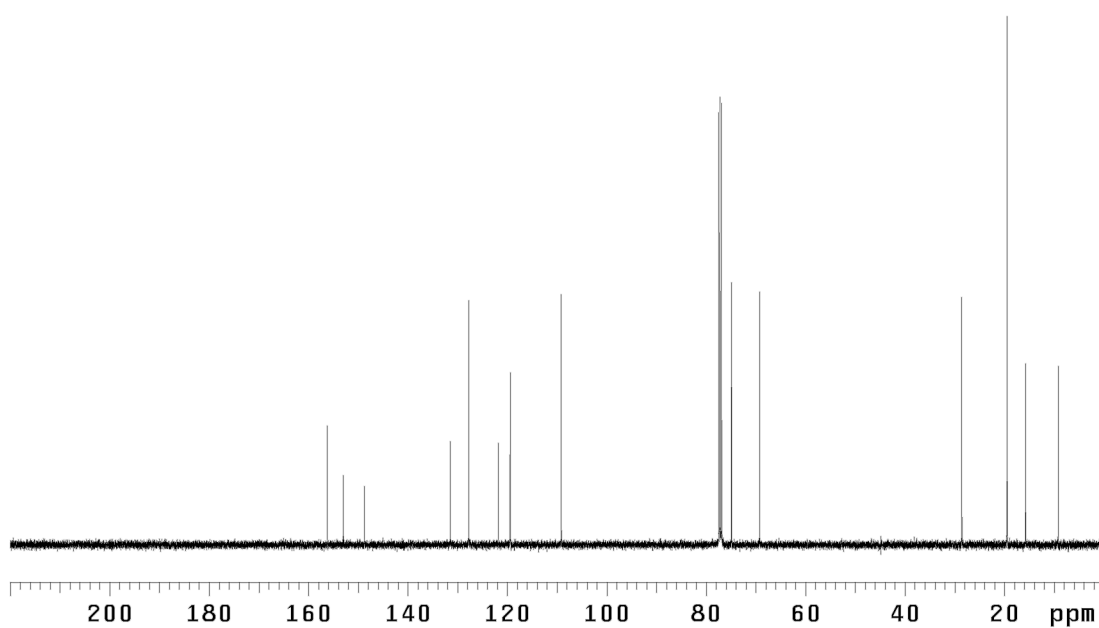
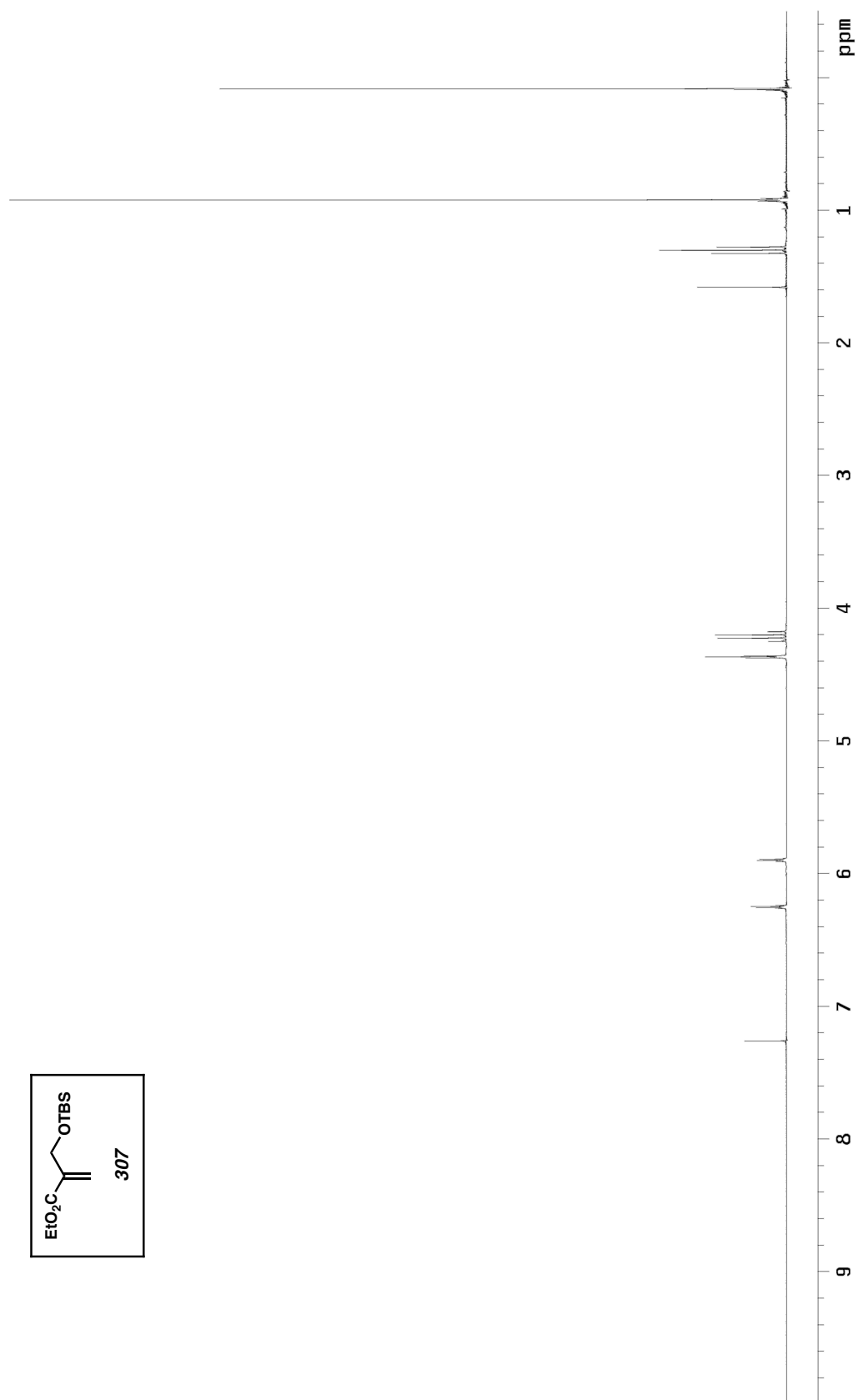
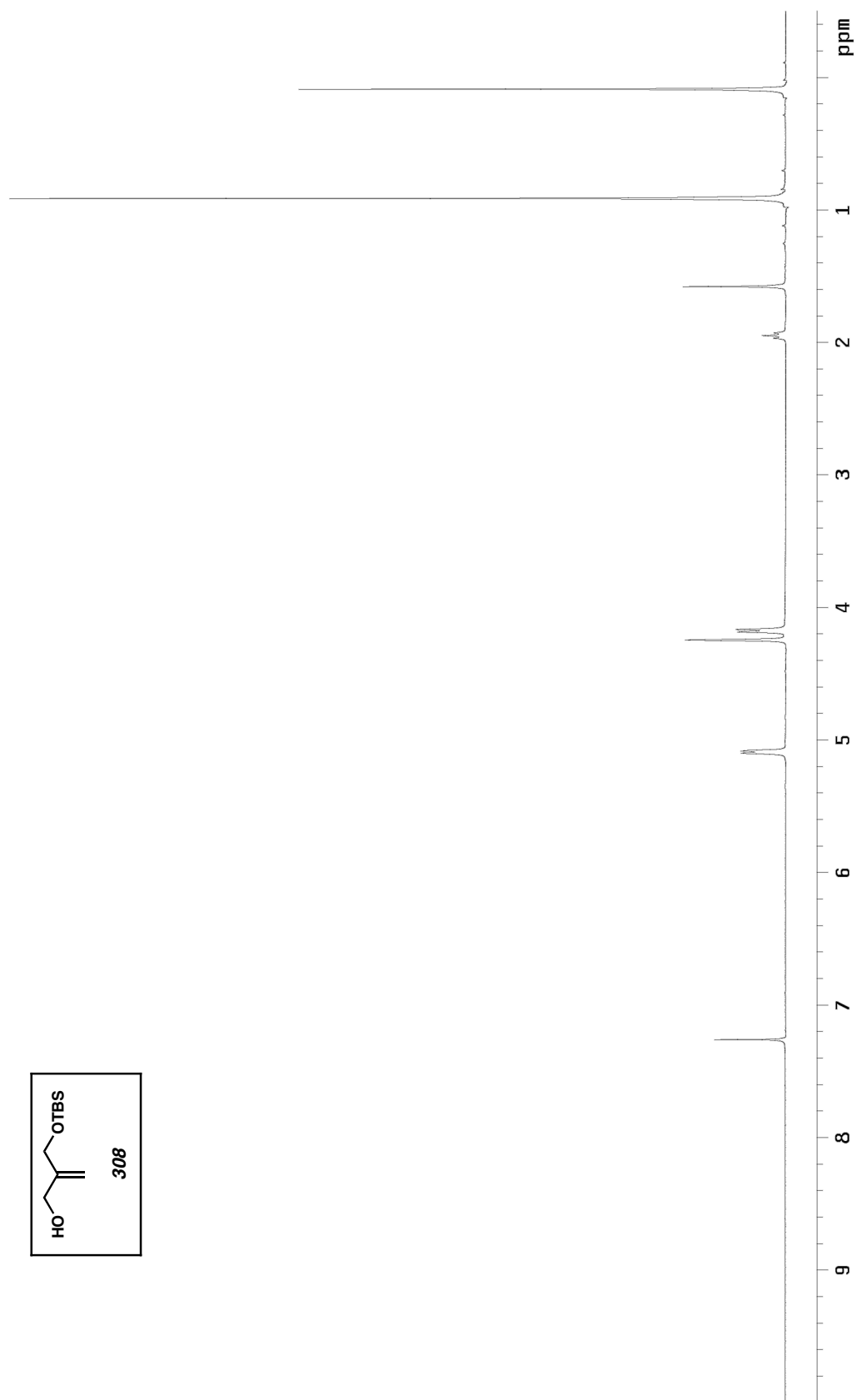
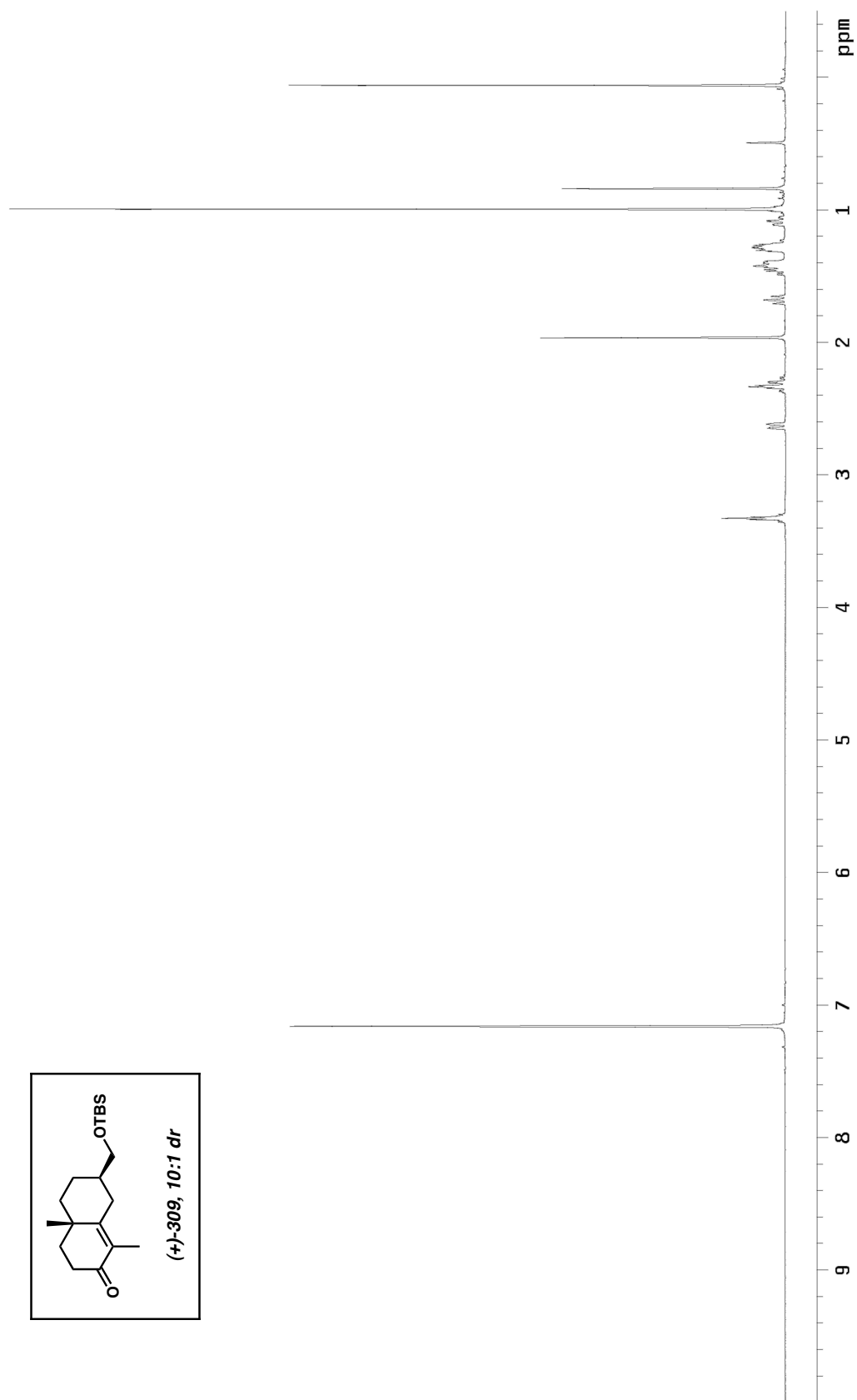


Figure A4.38. ¹³C NMR spectrum (126 MHz, CDCl₃) of **304**.

Figure A4.39. ^1H NMR spectrum (300 MHz, CDCl_3) of **307**.

Figure A4.40. ^1H NMR spectrum (300 MHz, CDCl_3) of **308**.

Figure A4.41. ¹H NMR spectrum (500 MHz, C₆D₆) of the major diastereomer of **309**.

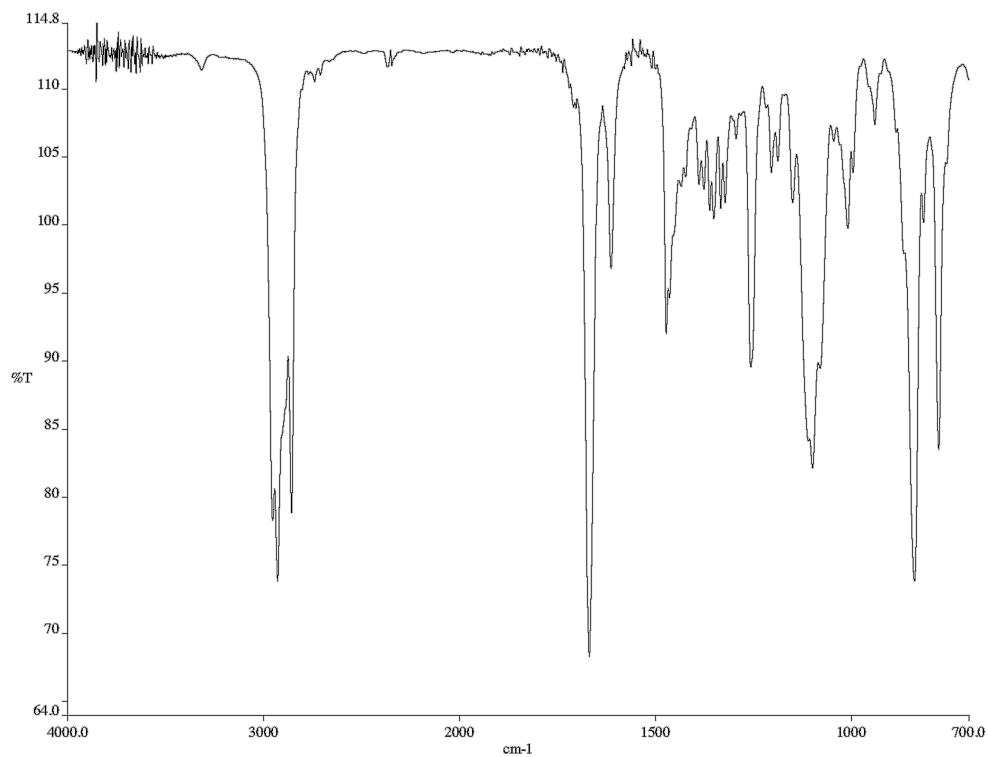


Figure A4.42. Infrared spectrum (neat film/NaCl) of the major diastereomer of **309**.

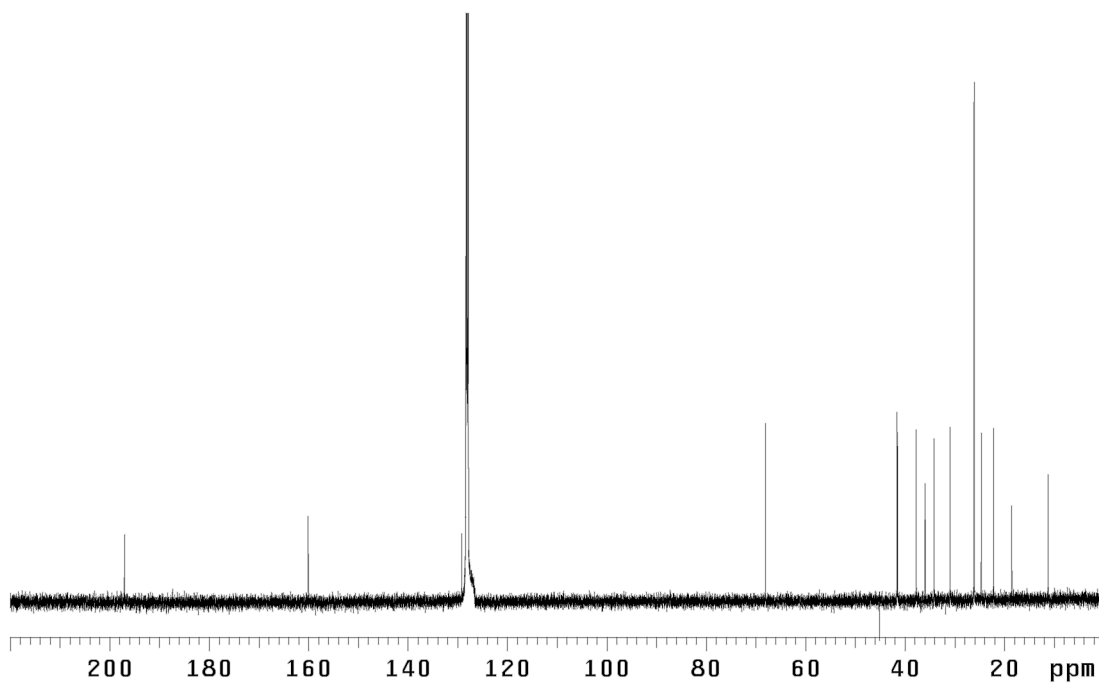


Figure A4.43. ¹³C NMR spectrum (126 MHz, C₆D₆) of the major diastereomer of **309**.

CHAPTER 5

Synthesis, Structural Analysis, and Gas-Phase Studies of 2-Quinuclidonium Tetrafluoroborate[†]

5.1 INTRODUCTION AND BACKGROUND

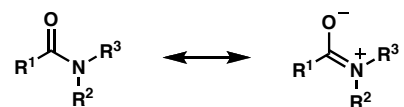
5.1.1 THE AMIDE LINKAGE

The amide bond is one of the most fundamental motifs in biology and chemistry as it plays the essential role of linking functionality between amino acids in peptides. Extensive studies over the past century have delineated the unique properties of this indispensable functional group.¹ Typical amides exhibit remarkable stability, with half-lives in aqueous solution exceeding hundreds of years.² This stability is in part due to resonance stabilization between the π -orbitals of the O–C–N linkage (Figure 5.1.1).^{1,3} The significant contribution of this resonance structure also gives rise to a planar

[†] This work was performed in collaboration with Tony Ly, a graduate student in laboratory of Prof. Ryan Julian at the University of California, Riverside, Don K. Pham, a summer NSF REU fellow in the Julian group, Dr. Kousuke Tani, a postdoctoral scholar in the Stoltz group, and Dr. Ryan R. Julian, assistant Prof. of Chemistry at the University of California, Riverside. These works have been published. See: (a) Ly, T.; Krout, M.; Pham, D. K.; Tani, K.; Stoltz, B. M.; Julian, R. R. *J. Am. Chem. Soc.* **2007**, *129*, 1864–1865. (b) Tani, K.; Stoltz, B. M. *Nature* **2006**, *441*, 731–734.

geometry about the peptide bond, as demonstrated by a high C–N rotational barrier (~20 kcal/mol) and the propensity for protonation at oxygen over nitrogen.^{1,4}

Figure 5.1.1. Resonance stabilization of a typical amide.



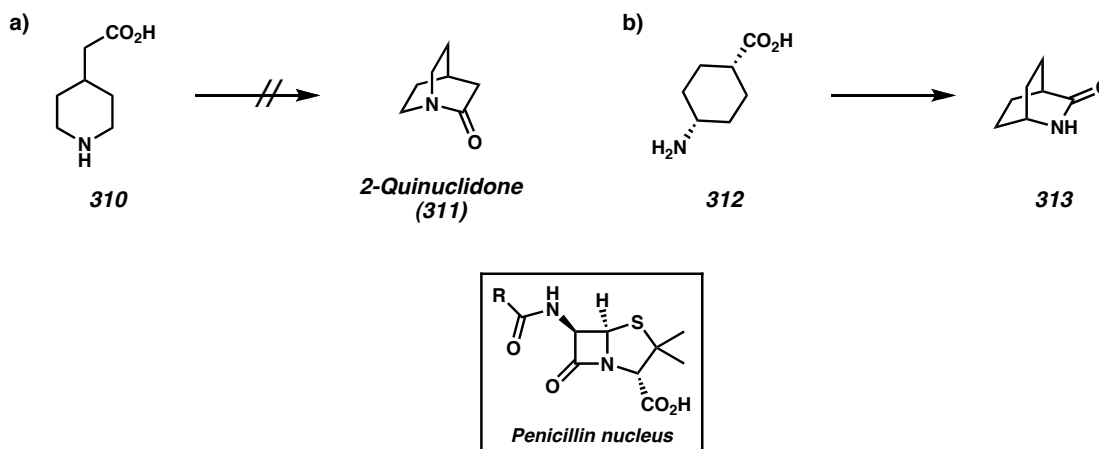
Disruption of the preferred planar geometry dramatically changes the stability and reactivity of the amide functionality. Nonplanar distortions typically lead to increased nitrogen basicity, pyramidalization of nitrogen, increased hydrolytic lability, and selective reactivity of electrophiles with nitrogen.^{1,5,6} Though more rare than standard amides, twisted amides are critical design elements in peptide hydrolysis,⁷ antibiotic efficacy of β -lactams,¹ and protein folding, with importance in autoimmunosuppression.⁸

5.1.2 2-QUINUCLIDONE

The intriguing qualities of these twisted amides were first recognized in 1938 when one of the simplest families was introduced—molecules containing the 1-azabicyclo[2.2.2]octan-2-one system, the quintessential member being 2-quinuclidone (**311**).⁹ In this original report, Lukeš surmised that the most effective way to obtain an amide in twisted conformation is to constrain the nitrogen at the bridgehead of a bicyclic system. Following the report of these “anti-Bredt” lactams,¹⁰ Woodward became interested in the properties of 2-quinuclidone as it related to studies toward quinine (~1941) and later in the context of the structural elucidation of penicillin.¹¹ The

Woodward laboratory's inability to synthesize **311** from amino acid **310** was attributed to the unstable nature of this amide bond (Figure 5.1.2a), and was supported by the ease of the construction of constitutional isomer **313** from **312** (Figure 5.1.2b).^{11a} These observations were of significance to the penicillins, as they indicated that their characteristic reactivity arises not only from ring strain of the β -lactam, but also as a result of nonplanar amide distortions in the fused bicycle.

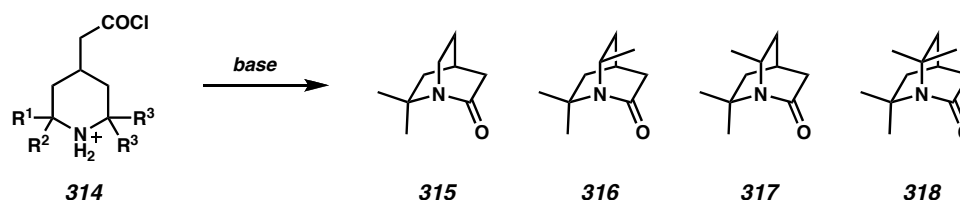
Figure 5.1.2. a) Woodward's failed synthesis of **311** from amino acid **310**. b) Facile amide bond formation to afford constitutional isomer **313**.



Subsequent studies toward 2-quinuclidone included a report by Yakhontov¹² that claimed to have synthesized **311** using the Woodward approach for amide bond formation. The formation of the strained bicyclic lactam proceeded surprisingly with an aqueous workup, with the reported product (**311**) characterized only by elemental analysis for nitrogen. A later study by Pracejus¹³ failed to isolate **311** by the method of Yakhontov, calling the original synthesis into question. However, the preparation of a variety of methyl-substituted 2-quinuclidone derivatives (**315–318**) using the amino acid

cyclization approach supported the notion that the original Yakhontov synthesis was flawed, at least in the isolation of **311** (Scheme 5.1.1).¹⁴

Scheme 5.1.1. Synthesis of methyl-substituted 2-quinuclidone derivatives



Although the definitive characterization and isolation of **311** has remained elusive despite its apparent simplicity,^{6c,15} this quintessential twisted amide has been the subject of computational investigations.^{4,16} Studies of this model amide are of particular interest to explore the significance of this distortion phenomenon to provide insights into a number of research areas.⁵ Owing to the colorful history^{11c,17} and challenges associated with the preparation, isolation, characterization of **311**, we pursued a synthesis using an alternative approach to the classic route for amide bond formation.

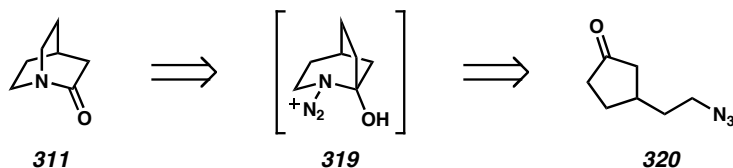
5.2 THE SYNTHESIS AND CHARACTERIZATION OF 2-QUINUCLIDONIUM TETRAFLUOROBORATE

In this section we describe our synthetic approach that has enabled the unambiguous preparation and characterization of the quintessential twisted amide 2-quinuclidone (**311**) as its HBF₄ salt. The studies presented in section 5.2 are a partial account of work performed by Dr. Kousuke Tani.¹⁸

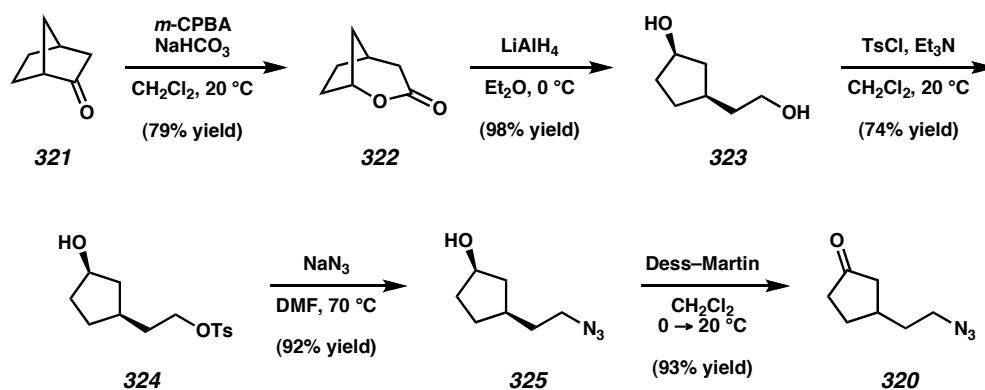
5.2.1 SYNTHESIS OF 2-QUINUCLIDONIUM VIA AN INTRAMOLECULAR SCHMIDT–AUBÉ CYCLIZATION

At the outset of these studies, a strategy was considered that refrained from the use of typical peptide coupling reagents to aid in purification of the likely reactive molecule. It was envisioned that reactions that harnessed the release of dinitrogen could impart significant driving force to assemble the strained bicyclic system. One such approach¹⁹ that met these criteria was the intramolecular Schmidt–Aubé cyclization of ketoazide **320**, which has seen wide use for the synthesis of N-substituted lactams since its initial discovery (Scheme 5.2.1).²⁰ Moreover, this method recently has been used for the preparation of other types of twisted lactams.²¹

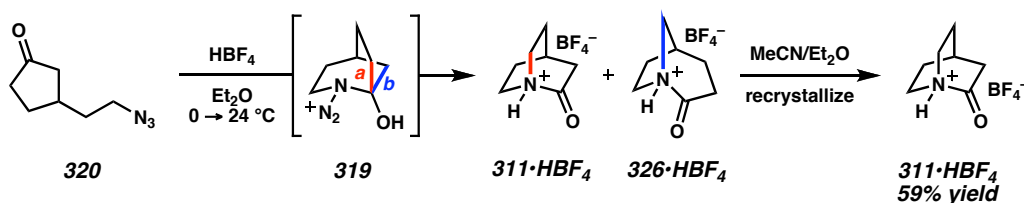
Scheme 5.2.1. Retrosynthetic analysis of 2-quinuclidone using the Schmidt–Aubé reaction



The preparation of ketoazide **320** was accomplished as shown in Scheme 5.2.2. Bayer–Villiger oxidation of norcamphor (**321**) provided bicyclic lactone **322** that was reduced with LiAlH_4 to generate *syn*-diol **323** in good yield. Selective tosylation of **323** and $\text{S}_{\text{N}}2$ displacement with sodium azide produced azide **325**. Alcohol oxidation using Dess–Martin periodinane afforded the requisite ketoazide **320**.

Scheme 5.2.2. Preparation of ketoazide **320**

Initial studies toward the intramolecular Schmidt–Aubé reaction of ketoazide **320** demonstrated that a selection of strong acids (e.g., TFA, TfOH, HBF₄, and Tf₂NH) produced a noticeable gas evolution with consumption of **320**. A survey of various acids and solvents established HBF₄ in Et₂O as the optimal conditions for the transformation of **320** into isomeric bicyclic lactams **311**•HBF₄ and **326**•HBF₄ (76:24, respectively).²² The observation of the two structural isomers **311**:**326** in ~3:1 ratio of indicated a moderately selective C–N migration of bond *a* from intermediate **319** to generate 2-quinuclidonium tetrafluoroborate (**311**•HBF₄) as a major reaction component, whereas minor product **326**•HBF₄ is derived from migration of bond *b* from **319**. The crystallinity of the crude lactams facilitated purification by selective recrystallization with MeCN/Et₂O to afford pure 2-quinuclidonium tetrafluoroborate (**311**•HBF₄) as colorless crystals.

Scheme 5.2.3. Synthesis of 2-quinuclidonium tetrafluoroborate (**311**•HBF₄)

5.2.2 CHARACTERIZATION, PROPERTIES, AND REACTIVITY

The structure of **311**•HBF₄ was unambiguously determined by spectroscopic evaluation. The carbonyl infrared absorption band for **311**•HBF₄ was observed at 1822 cm⁻¹ (KBr). This value compares well with the HCl salts of known [2.2.2]bicyclic lactams **316**¹³ and **318**^{14c} (1818 and 1811 cm⁻¹, respectively) and is more consistent with that of an acid chloride (1820–1750 cm⁻¹) or anhydride (1870–1770 cm⁻¹) than an amide (1690–1650 cm⁻¹).²³ Additionally, the ¹³C chemical shift of the carbonyl group was observed at δ 175.9 ppm (CD₃CN). Crystals suitable for X-ray analysis enabled the identification of all hydrogens from the electron density map. The structure depicted in Figure 5.2.1 shows that **311**•HBF₄ exists in the N-protonated form, which has been supported by calculations (see subsection 5.3.1) and highlights the twisted nature of the amide.

Figure 5.2.1. ORTEP drawing of **311**•HBF₄ (shown with 50% probability ellipsoids; BF₄ omitted for clarity).

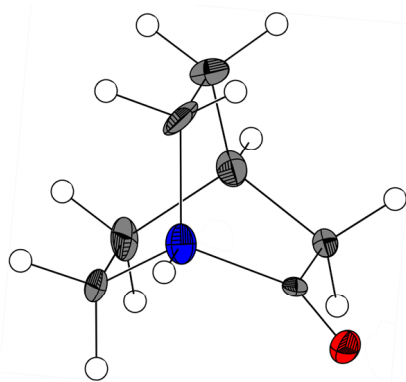


Table 5.2.1 summarizes selected bond lengths and distortion parameters obtained from the X-ray structure of **311**•HBF₄ and previously calculated structures. Two crystallographically independent molecules corresponding to **311**•HBF₄ were observed in the unit cell. The observed bond lengths for the N–C(O) were 1.526 and 1.484 Å while the C=O bond lengths were 1.192 and 1.168 Å. These distances are in good agreement to calculated values for N-protonated **311**•H⁺ and show a minimal decrease in the length of C=O bond while the N–C(O) bond is significantly longer than a typical amide (cf. formamide).^{4b,15c} Winkler and Dunitz have described distortion parameters for the quantitative evaluation of the twisting of an amide bond, and include the pyramidalization about the nitrogen (χ_N) and carbon (χ_C) atoms and the torsion about the C–N bond (τ).²⁴ For a representative planar amide (e.g., formamide), these parameters are all 0°. ²⁵ The structures of **311**•HBF₄ possessed a χ_N of 58.9 and 59.5°, while the τ was found to be 90.8 and 90.9°. These values compare well with nonplanar formamide and quantitatively establish the highly twisted nature of **311**•HBF₄.

Table 5.2.1. Comparison of structural parameters for **311**•HBF₄ and formamide

compound	bond length (Å)		distortion parameters (°) ^a		
	N–C(O)	C=O	χ_N	χ_C	τ
311 •HBF ₄ (X-ray)	1.526(5)	1.192(4)	59.5	0.2	90.9
	1.484(6)	1.168(6)	58.9	–2.4	90.8
311 (N-protonated, calc'd) ^b	1.504	1.167	57.6	0.0	89.9
311 (calc'd) ^b	1.433	1.183	55.6	0.0	90.0
formamide (planar, calc'd) ^{b,c}	1.349	1.193	0.0	0.0	0.0
formamide (perpendicular, calc'd) ^{b,c}	1.423	1.179	63.4	0.0	90.0

^a Ref 24. ^b Ref 4. ^c Ref 25.

The reactivity of 2-quinuclidonium tetrafluoroborate was investigated. **311**•HBF₄ is hypersensitive to hydrolysis, with a $t_{1/2} = <15$ s in neat D₂O, as well as unstable to manipulations in common nucleophilic solvents (e.g., DMSO, MeOH, pyridine). Furthermore, attempts to neutralize the salt of **311** with various bases lead to the formation of polymeric material, highlighting that the fortuitous protonation of **311** upon Schmidt–Aubé cyclization to **311**•HBF₄ was critical to avoid decomposition. These observations provide further support for the increased reactivity that results from nonplanar distortions of the amide bond.

5.3 GAS-PHASE STUDIES

To gain further insight into twisted amides we explored the gas-phase chemistry of **311**. In this section we present the first experimental results characterizing the basicity of **311**, which is found to be more basic than typical amides. In addition, we report an intriguing gas-phase dissociation as well as a second synthetic route to **311**•H⁺, which only occurs in the gas phase.

5.3.1 PROTON AFFINITY VIA THE EXTENDED KINETIC METHOD

The kinetic method, which relies on competitive fragmentation of proton-bound dimers, was employed to determine the proton affinity (PA) of **311** relative to a series of reference bases (shown in Figure 5.3.1) according to previously established methods.²⁶ Briefly, dimers were introduced into an LTQ linear ion trap mass spectrometer by electrospraying solutions of the tetrafluoroborate salt of **311** in dry acetonitrile and a

reference base. The noncovalently bound dimers were then subjected to collision-induced dissociation (CID) to determine the most basic site (which retains the proton more often). The results are shown in Figure 5.3.1. Analysis of the data yields a PA of 230.6 kcal/mol for **311** using the simple kinetic method. Application of the more rigorous extended kinetic method²⁷ yields a value of 230.4 kcal/mol, suggesting that entropic effects have a minimal impact on the measured PA. Calculations at the B3LYP 6-311++G** level of theory yield a PA of 225.7 kcal/mol. Previous calculations predicted a PA of 228.9 kcal/mol.⁴ Thus **311** is found to be very basic by theory and experiment. By comparison, typical amides have PAs in the range of 210–215 kcal/mol (Figure 5.3.2).²⁸ In terms of basicity, **311** behaves more like a secondary or tertiary amine owing to the lack of resonance within the amide. In addition, the site of protonation differs for twisted amides with protonation at the nitrogen being favored by ~21.5 kcal/mol according to our calculations.²⁹ In the process of collecting data to establish the PA of **311**, reference bases were found to separate into two groups. The less bulky bases give the data shown in Figure 5.3.1, which corresponds to dimers that are capable of hydrogen bonding to the nitrogen of **311**. The remaining reference bases are too bulky to access the nitrogen and presumably interact with the carbonyl oxygen of **311**.³⁰

Figure 5.3.1. Data from kinetic method experiments showing the relative PA versus natural log of the ratio of ion intensities minus protonation entropies.³¹ Three representative collision energies are shown for each reference base. The collinearity of all three lines indicates few entropic effects. The PA of **311** is determined to be 230.4 kcal/mol by the extended kinetic method.

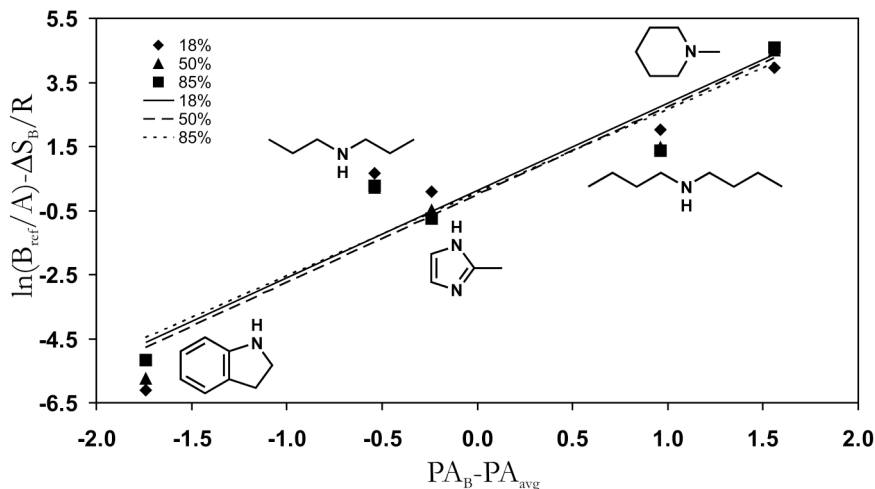
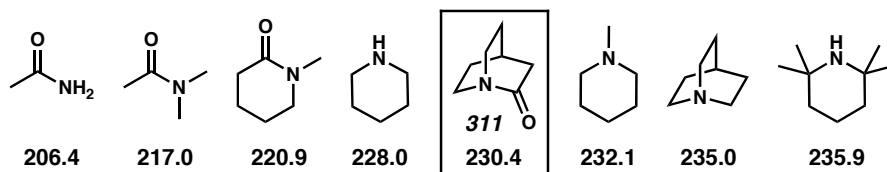


Figure 5.3.2. Representative amide and amine experimentally determined PAs (kcal/mol).

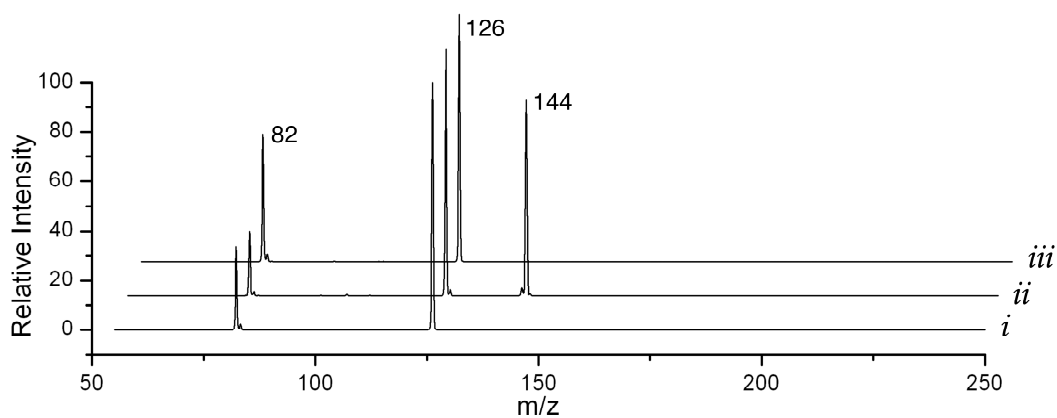


5.3.2 COLLISION-INDUCED DISSOCIATION PATHWAY

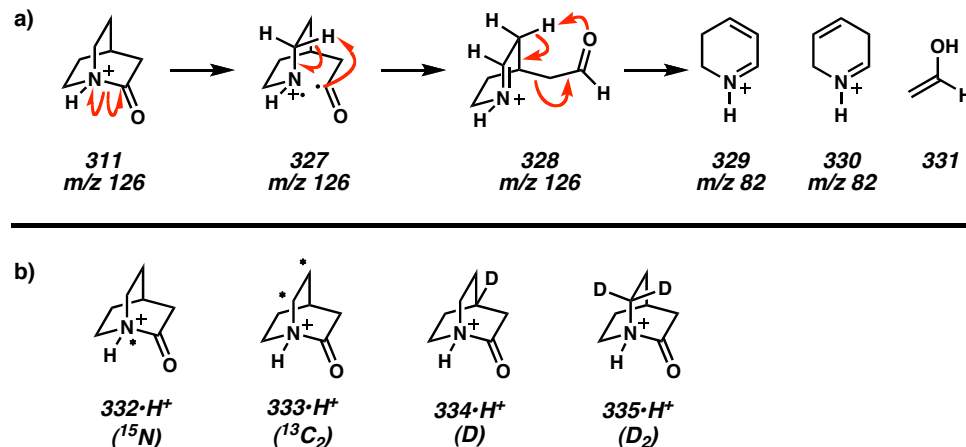
The gas-phase properties of 2-quinuclidone (**311**) were explored further by collision-induced dissociation (CID) experiments. The CID spectrum for **311**•H⁺ is shown in Figure 5.3.3i. Surprisingly, a single loss of 44 Da is the only major product that is observed, indicating that a single fragmentation pathway is energetically favored. Because of the bicyclic nature of **311**•H⁺, two covalent bonds must be broken en route to the observed fragmentation. A loss of 44 Da further requires at least one hydrogen

transfer. We propose the mechanism shown in Scheme 5.3.1a to account for the observed loss. Homolytic cleavage of the amide to bond to **327** leads to abstraction of one out of two equivalent hydrogens facing the radical (**327** → **328**). Two possible McLafferty-type³² rearrangements (one is shown in Scheme 5.3.1a) then lead to the second hydrogen transfer and the production of isomeric dihydropyridiniums **329** and **330** with the loss of ethenol (**331**). In order to verify this mechanism, a series of four compounds labeled with stable isotopes were prepared (**332–335**) (Scheme 5.3.1b).

Figure 5.3.3. i) CID spectrum of **311**•H⁺ ($m/z = 126$) with a single fragment being detected. ii) CID spectrum of **310**•H⁺ ($m/z = 144$). The loss of water generates **311**•H⁺, which simultaneously fragments. iii) MS³ CID spectrum of the reisolated peak at m/z 126 from spectrum ii confirming that **311**•H⁺ is generated by the loss of water.



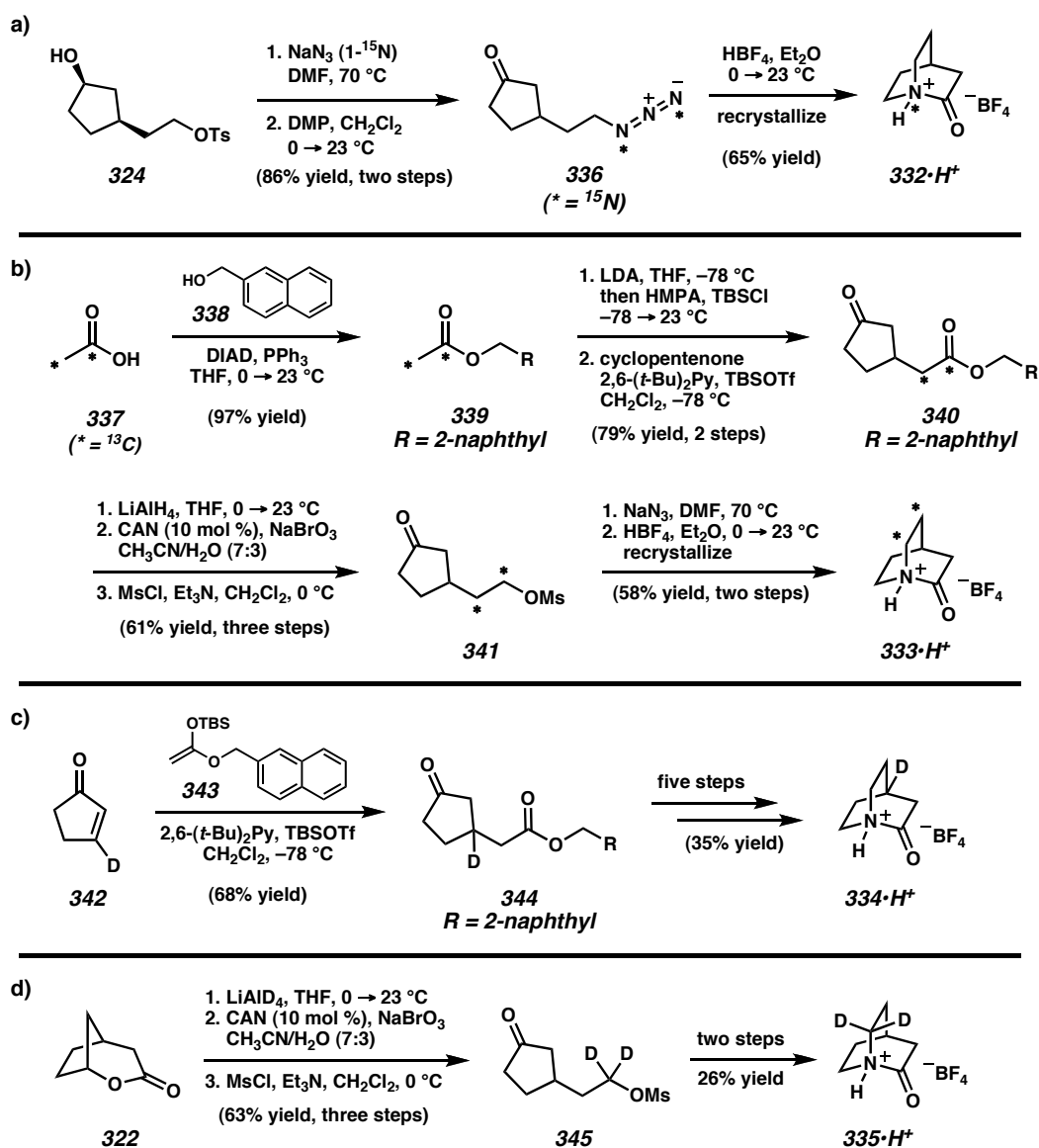
Scheme 5.3.1. a) Proposed CID fragmentation mechanism of **311**•H⁺. b) Isotopically labeled mechanistic probes



The synthesis of variously labeled derivatives of **311**•HBF₄ is shown in Scheme 5.3.2. Using a route identical to our original synthesis of **311**, substitution of monotosylate **324** with 1-¹⁵N-sodium azide and oxidation with Dess–Martin periodinane provided ketoazide **336**, which was subjected to the optimized Schmidt–Aubé conditions, and upon recrystallization, afforded ¹⁵N-labeled **332**•HBF₄ (Scheme 5.3.2a). The incorporation of ¹³C into **311** required a new approach starting from ¹³C₂-acetic acid (**337**). Accordingly, Mitsunobu substitution of alcohol **338** generated crystalline ester **339** (Scheme 5.3.2b). Enol silane generation and modified Mukaiyama–Michael addition to cyclopentenone employing buffered TBSOTf constructed ketoester **340** in 79% yield over two steps. Reduction of both carbonyls using LiAlH₄, chemoselective oxidation³³ of the secondary alcohol, and mesylation of the resulting primary alcohol yielded ketomesylate **341**. Typical azide substitution and cyclization then gave ¹³C₂-labeled **333**•HBF₄. A similar procedure using the conjugate addition with acceptor 3-*d*-cyclopentenone (**342**)³⁴ provided monodeuterated ketoester **344** that was transformed to D-labeled **334**•HBF₄.

over five steps (Scheme 5.3.2c). Reduction of lactone **322** with LiAlD_4 and two-step conversion to mesylate **345** enabled the preparation of D_2 -labeled **335**• HBF_4 (Scheme 5.3.2d).

Scheme 5.3.2. Synthetic route for the preparation of isotopically labeled mechanistic probes. a) ^{15}N -labeled **332**• HBF_4 ; b) $^{13}\text{C}_2$ -labeled **333**• HBF_4 ; c) D -labeled **334**• HBF_4 ; d) D_2 -labeled **335**• HBF_4



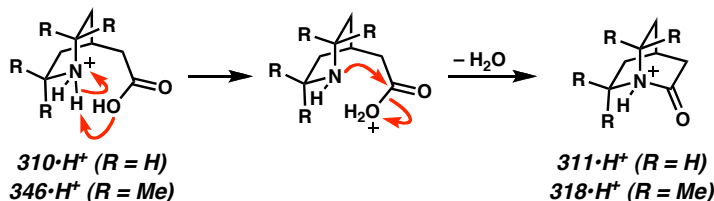
The preparation of various labeled derivatives enabled the verification of our proposed fragmentation mechanism. CID of **332**•H⁺ yields a single product that retains the ¹⁵N label as expected.³⁵ Similarly, **333**•H⁺ and **334**•H⁺ both fragment by yielding a single observable product with both ¹³C or deuterium labels retained, respectively, in agreement with our mechanism.³⁵ Additionally, fragmentation of **335**•H⁺ confirms that hydrogen transfer occurs.³⁵ In this case, two products are observed, with the difference between them being the loss of one or retention of two deuteriums. The loss of hydrogen is favored by a factor of 1.7, suggesting that isotope effects³⁶ may play a role in this reaction. Nevertheless, in each experiment the labeled atoms were lost or retained in agreement with the mechanism shown in Scheme 5.3.1a. As predicted, the amide bond is weakened by the lack of resonance stabilization and is the first bond to break upon collisional excitation.

5.3.3 GAS-PHASE SYNTHESIS OF 2-QUINUCLIDONIUM BY ELIMINATING WATER

Further insight into the chemistry of twisted amides can be obtained by synthesizing them in the absence of solvent. **311**•HBF₄ is observed to rapidly hydrolyze in the presence of water (see subsection 5.2.2), and attempts to drive the reverse reaction in solution have been unsuccessful.^{11a} Similarly, attempts to synthesize **311** with the acid chloride of **310** have met with frustration.¹³ Nevertheless, collisional excitation of the hydrolyzed derivative **310**•H⁺ in the gas phase yields quantitatively a product with the same mass as **311**•H⁺ as shown in Figure 5.3.3ii. Following reisolation and collisional cooling of this peak, the MS³ CID spectrum is identical to that obtained by fragmenting

311•H⁺ (compare Figure 5.3.3i and iii). Similarly, all isotopically labeled compounds react exclusively by eliminating water, followed by the same elimination that would be expected if **311•H⁺** were generated as the product.³⁵ Thus it is possible to selectively synthesize **311•H⁺** by eliminating water from **310**, as shown in Scheme 5.3.3, if the water can be rigorously removed from the reaction system. This is not a difficulty in the gas phase; however, the data in Figure 5.3.3ii also suggest that there is a high barrier to this process. Elimination of water to yield **311•H⁺** also results spontaneously in further fragmentation. As mentioned above, this requires the cleavage of two covalent bonds. Therefore, this reaction appears to be difficult in solution for two reasons: a high barrier to activation and back reactions with water.

Scheme 5.3.3. Gas-phase elimination of water to construct **311•H⁺** and **318•H⁺**

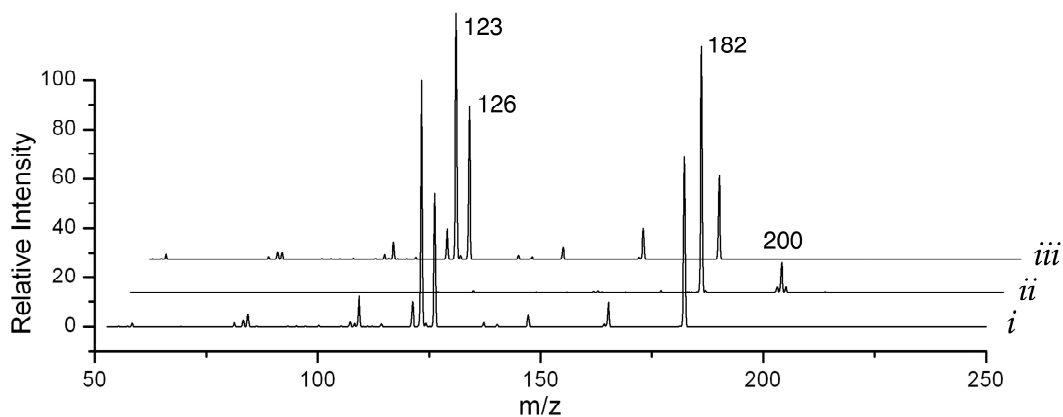


5.3.4 COMPARISON TO 6,6,7,7-TETRAMETHYL-2-QUINUCLIDONE

These results are further confirmed by examination of **318**, which has four additional methyl groups and can be generated from the acid chloride in solution.^{13,14d} CID of the hydrolyzed product **346•H⁺** yields exclusively **318•H⁺** without the accompanying loss of additional fragments. The synthesis is again confirmed by comparing fragmentation with the authentic molecule; comparison of Figure 5.3.4i with Figure 5.3.4iii reveals that even

very low abundance peaks are reproduced. In addition, the voltage amplitude required to carry out the dehydration of **346**•H⁺ (Scheme 5.3.3) is 20% lower in magnitude when compared to the voltage required for **310**•H⁺. Thus, the energy required to generate **318**•H⁺ by eliminating water is much lower, in agreement with the observed synthetic routes in solution. The gas-phase syntheses suggest that **318** is more nucleophilic than **311** and should therefore be more basic as well. Attempts to determine the PA of **318** experimentally by the kinetic method met with frustration. The steric hindrance of the additional methyl groups prevents access to the bridgehead nitrogen. However, theory can be used to estimate the proton affinity. The calculated PA for **318** at the B3LYP/6-311++G** level is 234.7 kcal/mol, which is significantly higher than that for **311** (230.4 kcal/mol) and supports the idea of enhanced nucleophilicity for **318**. The predicted increase in PA with increasing alkyl substitution is evident with the various piperidine derivatives depicted in Figure 5.3.2. However, **318** is also much more stable toward hydrolysis, indicating that stability does not share a simple relationship with basicity for twisted amides.^{14d}

Figure 5.3.4. i) CID spectrum of $318\bullet\text{H}^+$ ($m/z = 182$). ii) CID spectrum of $346\bullet\text{H}^+$ ($m/z = 200$). In this case, the synthesis proceeds cleanly without spontaneous fragmentation. iii) MS^3 CID spectrum showing that all fragment peaks are reproduced when the gas-phase product is compared to the bona-fide sample in spectrum i.



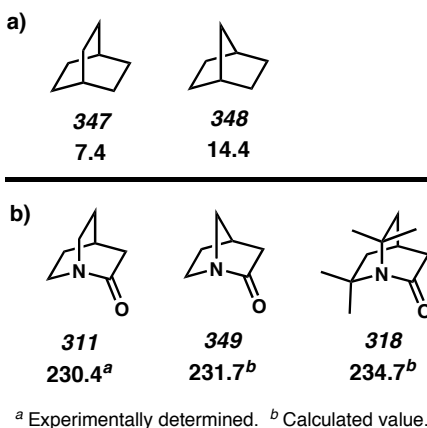
5.4 FUTURE STUDIES

The availability of 2-quinuclidone as its tetrafluoroborate salt ($311\bullet\text{HBF}_4$) has enabled the analysis of physical and chemical properties that were previously available only by theoretical calculations.⁴ However, experimentation can provide intriguing details and insights beyond what theory can explore as evidenced by subsections 5.3.2–5.3.4. Now that we have a powerful method for the construction of these unique twisted lactams, we can further assess their properties and combine experiment with theory to further the understanding of twisted amides. One particular area of interest is the relationship between the ring size of the bicyclic system and the resulting amide distortion.⁴

5.4.1 1-AZABICYCLO[2.2.1]HEPTAN-2-ONE

We envisioned 1-azabicyclo[2.2.1]heptan-2-one (**349**) in efforts to pursue a more strained derivative of the bridgehead bicyclic lactams (cf. **311**). By analogy, a comparison of ring strains in the parent bicyclic alkane systems reveals that the removal of a carbon from bicyclo[2.2.2]octane (**347**) to bicyclo[2.2.1]heptane (**348**) increases the ring strain from 7.4 to 14.1 kcal/mol, respectively (Figure 5.4.1a).³⁷ We have calculated the proton affinity of **349** to be 231.7 kcal/mol, which makes it slightly more basic than 2-quinuclidone (**311**) and less basic than tetramethyl derivative **318** (Figure 5.4.1b). This indicates that a predicted increase ring strain affects the nitrogen basicity, although ring strain does not necessarily correlate to an increase in basicity.^{4b,38} A detailed theoretical or experimental study of **349** could provide insights into this strained amide.

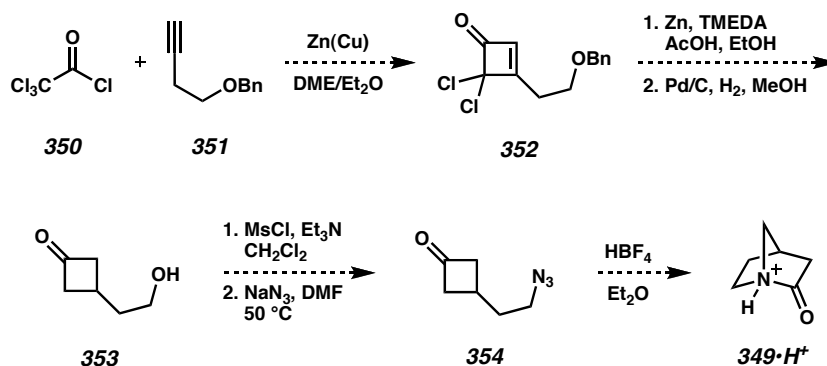
Figure 5.4.1. a) Comparison of strain energies of related bicyclic systems (kcal/mol).³⁷
b) Comparison of proton affinity values for select bicyclic twisted amides (kcal/mol).



A proposed synthetic route to **349** utilizing the Schmidt–Aubé cyclization is shown in Scheme 5.4.1. Intermolecular [2 + 2] cycloaddition³⁹ of dichloroketene generated from

350 and Zn(Cu) couple with alkyne **351**⁴⁰ should provide dichlorocyclobutenone **352**. Reductive dechlorination and olefin hydrogenation with benzyl cleavage could generate ketoalcohol **353**. Conversion to azide **354** over two steps and subsequent HBF₄-promoted intramolecular cyclization⁴¹ should construct **349**•H⁺. The devised synthetic route could enable rapid access to **349** for thorough experimental evaluation.

Scheme 5.4.1. Proposed synthesis of **349**•H⁺ employing the Schmidt–Aubé cyclization



5.4.2 1-AZABICYCLO[3.3.3]UNDECAN-2-ONE

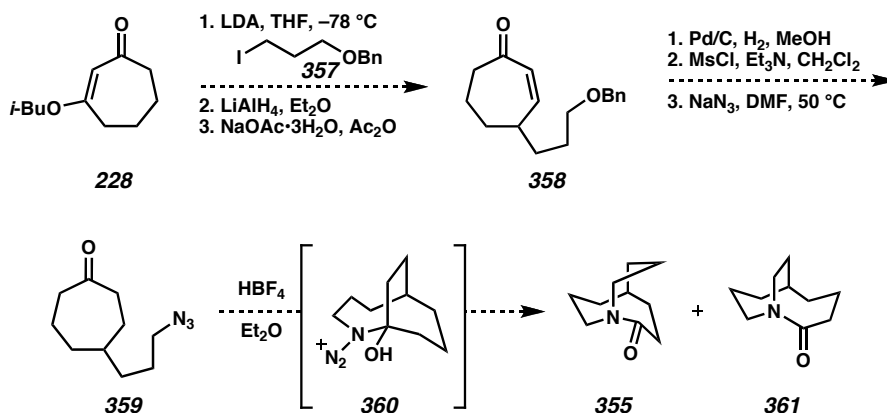
Another interesting example with regard to ring size is the theoretical molecule 1-azabicyclo[3.3.3]undecan-2-one (**355**). The parent amine (manxine, **356**) is extraordinary in that it exhibits a near coplanar geometry about the nitrogen in both neutral and protonated forms.⁴² Greenberg has calculated the PA of amide **355** and found that the bicyclo[3.3.3] system favors O-protonation over N-protonation by 3.5 kcal/mol,^{4b} suggesting that increase in ring size reduces strain and induces planarity of the nitrogen. As **355** approaches the geometric requirements for an unstrained amide linkage, it has the potential to form a hyperstable amide. The concept of hyperstability, as described by

Schleyer and co-workers for bridgehead olefins,⁴³ specifies that the strain energy in the enolized lactam is less than that of the parent lactam and could result in interesting reactivity of this larger bicyclic amide.

Figure 5.4.2. Bicyclo[3.3.3] bridgehead amide **355** and amine **356**.



A proposed synthesis of **355** is presented in Scheme 5.4.2. Enolization of vinylogous ester **228** and alkylation with iodide **357**,⁴⁴ followed by reductive carbonyl transposition could afford γ -substituted cycloheptenone **358**. Olefin hydrogenation with benzyl cleavage and two-step azide conversion would produce cyclization substrate **359**. Exposure to acidic conditions should facilitate carbonyl addition to intermediate **360** that can undergo a C–N migration in two possible ways to form desired **355** and isomer **361**. The planned route to **355** could provide material to support the evaluation of this intriguing amide.

Scheme 5.4.2. Proposed synthesis of **355** using the Schmidt–Aubé cyclization

5.5 CONCLUSION

In summary, we have achieved the first unambiguous synthesis, isolation, and X-ray characterization of the quintessential twisted amide 2-quinuclidone (**311**) as its HBF_4 salt. Our synthesis highlights the power of the Schmidt–Aubé reaction for the construction of highly strained amides. We have performed a thorough structural and chemical analysis of **311** and quantitatively established its highly twisted nature. Gas-phase investigations have assessed the basicity of **311** for the first time, revealing an intriguing dissociation mechanism and a second synthesis by eliminating water in the gas phase. Our results indicate that the gas-phase chemistry of these molecules closely reflects the properties observed in solution. Moreover, the studies herein demonstrate the importance of combining theory and experiment to further our understanding of this extraordinary class of compounds. Future studies on the role of ring size and the resulting effect on amide distortion and properties are proposed.

5.6 EXPERIMENTAL SECTION

5.6.1 MATERIALS AND METHODS

5.6.1.1 CHEMICAL SYNTHESIS

Unless stated otherwise, reactions were conducted in flame-dried glassware under an atmosphere of nitrogen using anhydrous solvents passed through activated alumina columns under argon. All commercially obtained reagents were used as received. Hexamethylphosphoramide was distilled from CaH_2 and stored in a Schlenk tube under argon. 3-*d*-cyclopentenone (**342**)³⁴ and 6,6,7,7-tetramethyl-2-quinuclidone (**318**)^{14d} were prepared by known methods. Labeled sodium azide (1-¹⁵N, 98 atom% ¹⁵N) and acetic acid (**337**, 1,2-¹³C₂, 99 atom% ¹³C) were purchased from Cambridge Isotope Laboratories. Lithium aluminum deuteride (98 atom% *d*) was purchased from Aldrich. Reaction temperatures were controlled using an IKAmag temperature modulator, and unless stated otherwise, reactions were performed at 23 °C. Thin-layer chromatography (TLC) was conducted with E. Merck silica gel 60 F254 pre-coated plates, (0.25 mm) and visualized using a combination of UV quenching and charring with *p*-anisaldehyde, ceric ammonium molybdate, or potassium permanganate stains. ICN silica gel (particle size 0.032–0.063 mm) was used for flash column chromatography. ¹H NMR spectra were recorded on a Varian Mercury 300 (at 300 MHz) or a Varian Inova 500 (at 500 MHz) and are reported relative to Me₄Si (δ 0.0).⁴⁵ Data for ¹H NMR spectra are reported as follows: chemical shift (δ ppm), multiplicity, coupling constant (Hz) and integration. ¹³C NMR spectra were recorded on a Varian Mercury 300 (at 75 MHz) or a Varian Inova 500 (at 126 MHz) and are reported relative to Me₄Si (δ 0.0).⁴⁵ Data for ¹³C NMR spectra are

reported in terms of chemical shift, multiplicity, and coupling constant. ^2H NMR spectra were recorded on a Varian Inova 500 (at 76 MHz) and are reported relative to Me_4Si (δ 0.0).⁴⁵ Data for ^2H NMR spectra are reported in terms of chemical shift and multiplicity. IR spectra were recorded on a Perkin Elmer Spectrum BXII spectrometer and are reported in terms of frequency of absorption (cm^{-1}). Melting points are uncorrected. High resolution mass spectra were obtained from the California Institute of Technology Mass Spectral Facility.

5.6.1.2 **EXTENDED KINETIC METHOD, GAS-PHASE SYNTHESIS, AND CALCULATIONS**

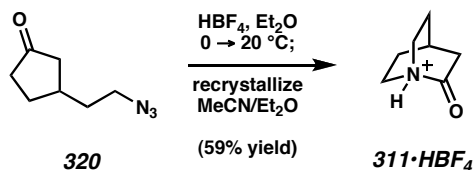
All mass spectra were obtained using an LTQ linear ion trap mass spectrometer (Thermo Electron, Waltham, MA) equipped with a standard electrospray ionization source. Voltages were optimized to maximize the [**311** + H^+ + B_{ref}] dimer peak intensities for kinetic method experiments. All reference bases were purchased from Sigma-Aldrich and were used without further purification.

To minimize hydrolysis of **311**• HBF_4 , samples containing 300 μM of **311** and reference base were prepared with dry acetonitrile unless otherwise noted and immediately infused into the electrospray source. The noncovalently bound dimers were then isolated and subjected to CID at normalized collision energies ranging from 18% to 85%. These percentages correspond to excitation voltage amplitudes of 0.00641 to 0.0303 V for a 100 m/z ion. To obtain tandem MS data, 30 μM solutions were prepared and analyzed as above under standard instrument tune conditions. Amino acid derivatives were prepared by either allowing a sample sufficient time to hydrolyze (ca.

30 min) or by addition of deionized water in molar excess.

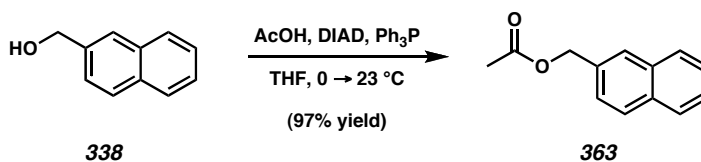
Proton affinities were calculated using hybrid density functional theory as implemented in Gaussian 03 Version 6.1 Revision D.01. Candidate structures were built using GaussView 3.0 and then submitted for optimization and vibrational frequency calculation at the B3LYP/6-31G* level. Total energies were calculated at the B3LYP/6-311++G** level. Total energies, zero point energies (ZPE), and thermal corrections were obtained from the optimization/frequency output. Zero point corrections were scaled by an empirical factor of 0.9877 as recommended by Andersson and Uvdal.⁴⁶ The basis set superposition error (BSSE) was calculated using the counterpoise (CP) method of Boys and Bernardi.⁴⁷

5.6.2 PREPARATIVE PROCEDURES

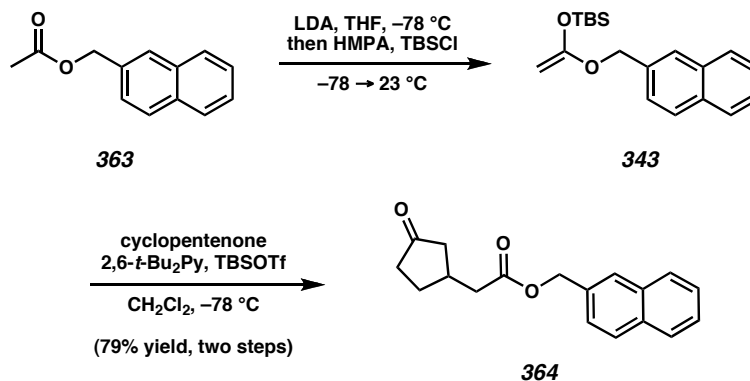


2-Quinuclidonium tetrafluoroborate (311·HBF₄). To a solution of **320** (356.5 mg, 2.33 mmol, 1.0 equiv) in Et₂O (4.7 mL, 0.5 M) at 0 °C was added an ethereal solution of HBF₄ (642 μL of a 54 wt % solution, 4.66 mmol, 2.0 equiv) at which time immediate gas evolution was observed. The cooling bath was removed and stirred at room temperature until gas evolution ceased (ca. 8 h) and TLC analysis confirmed consumption of **320**. The supernatant of the resulting suspension was removed by syringe and the remaining white solid was washed with Et₂O (3 x 3 mL) and dried in vacuo. This crude white solid was transferred into a glove box and purified by double recrystallization using slow diffusion of Et₂O into a MeCN solution of the crude. Specifically, the crude was dissolved in a minimal quantity of MeCN, filtered through a pipette with a small filter paper plug, and washed further with minimal MeCN. The resulting vial containing the MeCN solution of the crude was placed in a larger chamber, filled ~1/3 full with Et₂O, and the larger chamber was capped and placed in a -20 °C freezer. After 36–48 h, the chamber was equilibrated to ambient, the supernatant was decanted, and the resulting white solid was washed with excess Et₂O, and recrystallized using the same procedure. Isolation and drying of the resulting solid under vacuum afforded **311·HBF₄** (292.1 mg, 1.37 mmol, 59% yield) as white needles. Mp = 185–200 °C dec; ¹H NMR (300 MHz, CD₃CN) δ 8.02 (br, 1H), 3.85–3.60 (m, 4H), 2.99 (d, *J* = 3.0 Hz, 2H), 2.51 (septuplet, *J* =

3.0 Hz, 1H), 2.10–1.90 (m, 4H); ^{13}C NMR (75 MHz, CD_3CN) δ 175.9, 48.1, 40.1, 25.7, 22.7; IR (KBr) 3168, 2981, 1822, 1468, 1398, 1336, 1312, 948, 823, 799, 766, 716 cm^{-1} ; HRMS (FAB+) m/z calc'd for $\text{C}_7\text{H}_{12}\text{NO}$ [$\text{M} + \text{H}$] $^+$: 126.0919, found 126.0920.



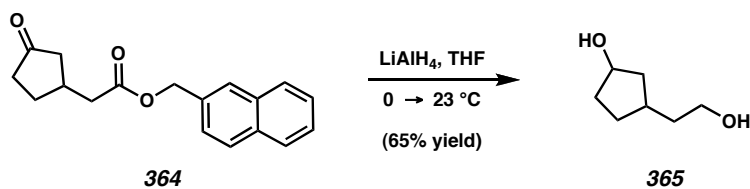
Naphthalen-2-ylmethyl acetate (363). Ph_3P (0.787 g, 3.0 mmol, 1.5 equiv) and alcohol **362** (0.475 g, 3.0 mmol, 1.5 equiv) were dissolved in THF (13.4 mL, 0.15 M). Acetic acid (114 μL , 2.0 mmol, 1.0 equiv) was added and the solution was cooled to 0 °C in an ice/water bath. DIAD (591 μL , 3.0 mmol, 1.5 equiv) dissolved in THF (1 mL) was added dropwise over 5 min via positive pressure cannulation. After 1 h, the reaction was quenched with 5 mL saturated NaHCO_3 , extracted with hexanes (3 x 20 mL), the organics were dried over MgSO_4 , filtered, and concentrated under reduced pressure to an off-white solid. The resulting crude material was purified by flash chromatography on SiO_2 (15:1 \rightarrow 9:1 hexanes/ Et_2O , PhMe loaded) to afford **363** (0.3830 g, 1.91 mmol, 96% yield) as a white solid. R_f = 0.28 (9:1 hexanes/ Et_2O); mp = 53–55 °C; ^1H NMR (300 MHz, CDCl_3) δ 7.89–7.85 (comp m, 4H), 7.53–7.47 (comp m, 3H), 5.30 (s, 2H), 2.16 (s, 3H); ^{13}C NMR (125 MHz, CDCl_3) δ 171.1, 133.5, 133.4, 133.3, 128.5, 128.1 (2C), 127.9, 127.5 (2C), 126.5, 126.4, 126.1, 66.6, 21.2; IR (Neat Film NaCl) 3055, 2953, 1736, 1378, 1364, 1248, 1030, 951, 896, 863, 822, 744, 480 cm^{-1} ; HRMS (EI+) m/z calc'd for $\text{C}_{13}\text{H}_{12}\text{O}_2$ [M] $^+$: 200.0837, found 200.0844.



Ketoester 364. To a cooled solution of *i*-Pr₂NH (341 μ L, 2.44 mmol, 1.15 equiv) in THF (2.12 mL, 1 M) at 0 $^\circ$ C was added *n*-BuLi (2.5 M in hexane) dropwise. After stirring for 15 min at 0 $^\circ$ C, the solution was cooled to -78 $^\circ$ C and a solution of acetate **363** (424.0 mg, 2.12 mmol, 1.0 equiv) in THF (1 mL) was added dropwise via positive pressure cannulation. After 15 min, HMPA (332 μ L, 1.91 mmol, 0.9 equiv), then TBSCl (351.0 mg, 2.33 mmol, 1.1 equiv) in THF (0.80 mL) were added and the cooling bath was removed. The reaction was warmed to ambient temperature and concentrated under reduced pressure. The resulting thick oil was dissolved in 9:1 hexanes/Et₂O (50 mL) and washed with distilled water (3 x 20 mL, pH \approx 7) and sat. brine. The organic layer was dried over MgSO₄, filtered, and concentrated under reduced pressure. The resulting yellow oil solidified after several hours under high vacuum to afford TBS-silylenol ether **343** (650.9 mg), which was used without further purification in the subsequent reaction. $R_f = \text{unstable to SiO}_2$.

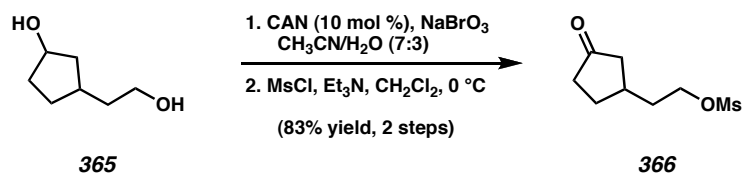
To a solution of **343** (1.2 equiv), cyclopentenone (145 μ L, 1.72 mmol, 1.0 equiv), and 2,6-di-*tert*-butylpyridine (465 μ L, 2.07 mmol, 1.2 equiv) in CH₂Cl₂ (20.7 mL, 0.1 M) cooled to -78 $^\circ$ C was added a solution of TBSOTf (475 μ L, 2.07 mmol, 1.2 equiv) in CH₂Cl₂ (2.1 mL) dropwise over 15 min. Following consumption of cyclopentenone by TLC analysis (ca. 15 min), the cooling bath was removed and the reaction was quenched

with 15 mL of 3% aq HCl. After stirring for 30 min the layers were separated and the aq layer was extracted with CH₂Cl₂ (3 x 25 mL), the organics dried over MgSO₄, filtered, and concentrated under reduced pressure to a yellow solid. The crude product was purified by flash chromatography on SiO₂ (9:1 → 4:1 → 3:1 hexanes/EtOAc, dry load) to afford ketoester **364** (385.4 mg, 1.37 mmol) as a light yellow oil. $R_f = 0.23$ (1:1 hexanes/Et₂O); ¹H NMR (300 MHz, CDCl₃) δ 7.87–7.82 (comp m, 4H), 7.53–7.49 (comp m, 2H), 7.45 (dd, $J = 8.5, 1.9$ Hz, 1H), 5.30 (s, 2H), 2.70–2.57 (m, 1H), 2.55 (d, $J = 1.1$ Hz, 1H), 2.53 (d, $J = 2.9$ Hz, 1H), 2.51–2.45 (m, 1H), 2.38–2.11 (comp m, 3H), 1.90 (ddd, $J = 18.1, 9.8, 1.1$ Hz, 1H), 1.66–1.51 (m, 1H); ¹³C NMR (75 MHz, CDCl₃) δ 218.4, 172.0, 133.3 (2C), 133.2, 128.6, 128.1, 127.9, 127.7, 126.5 (2C), 126.0, 66.7, 44.7, 39.9, 38.4, 33.6, 29.4; IR (Neat Film NaCl) 3049, 2956, 1737, 1271, 116, 817 cm⁻¹; HRMS (EI+) m/z calc'd for C₁₈H₁₈O₃ [M]⁺: 282.1256, found 282.1257.



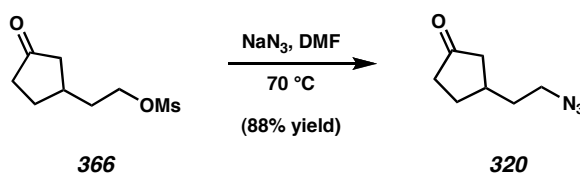
Diol 365. To a slurry of LiAlH₄ (74.3 mg, 1.96 mmol, 4.0 equiv) in THF (4.9 mL, 0.1M) at 0 °C was added ketoester **364** (138.1 mg, 0.498 mmol, 1.0 equiv) in 1.0 mL THF. The cooling bath was removed and the reaction was stirred for 2.5 h at ambient temperature. The reaction was then cooled to 0 °C and carefully quenched by slow addition of Na₂SO₄•10H₂O. When gas evolution had ceased, the flask was diluted up to 25 mL with EtOAc and stirred vigorously at ambient temperature for 2 h. The fine precipitate was then filtered through Celite, washing with excess EtOAc, and the

resulting filtrate was concentrated under reduced pressure to an off-white solid. This residue was purified by flash chromatography on SiO₂ (2:1 → 1:0 EtOAc/hexanes) to afford ~1:1 mixture of diastereomers of diol **365** (42.6 mg, 0.320 mmol, 65% yield) as a colorless oil. *R_f* = 0.15 (3:1 EtOAc/hexanes); ¹H NMR (500 MHz, CD₃OD) δ 4.26 (anti diastereomer, app dq, *J* = 8.4, 2.9 Hz, 0.47H), 4.21 (syn diastereomer, app pentet, *J* = 5.9 Hz, 0.53H), 3.56 (app t, *J* = 6.8 Hz, 2H), 2.20 (ddd, *J* = 16.4, 7.8, 7.8 Hz, 0.53H), 2.14 (ddd, *J* = 14.2, 7.6, 7.6 Hz, 0.53H), 1.98–1.90 (comp m, 1.5H), 1.81–1.72 (comp m, 1.5H), 1.65–1.60 (comp m, 1.5H), 1.59–1.51 (comp m, 1.5H), 1.44–1.31 (m, 1H), 1.19–1.12 (m, 1H); ¹³C NMR (125 MHz, CD₃OD) δ 74.1 (syn), 62.2, 62.1 (syn), 43.1, 42.9 (syn), 40.6 (syn), 40.1, 36.1 (syn), 35.8 (syn), 35.6, 35.2, 31.5, 31.2 (syn); IR (Neat Film NaCl) 3323 (br), 2931, 2864, 1434, 1344, 1052, 1013 cm⁻¹; HRMS (EI+) *m/z* calc'd for C₇H₁₄O₂ [M]⁺: 130.0994, found 130.0994.



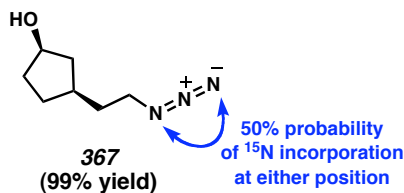
Ketomesylate 366.³³ To a solution of diol **365** (87.6 mg, 0.673 mmol, 1.0 equiv) in CH₃CN (2.8 mL, 0.167 M) in a vial was added CAN (36.9 mg, 0.673 mmol, 0.1 equiv), NaBrO₃ (101.5 mg, 0.673 mmol, 1.0 equiv), and distilled H₂O (1.2 mL) and vigorously stirred. Following consumption of diol **365** by TLC (ca. 6 h), the reaction was concentrated under reduced pressure. The resulting slurry was taken up in 10 mL H₂O, extracted with EtOAc (3 x 25 mL), dried over Na₂SO₄, filtered, and concentrated under reduced pressure to afford a crude yellow oil (85.5 mg).

The resulting crude material was dissolved in CH_2Cl_2 (1.35 mL, 0.5 M), cooled to 0 °C, and MsCl (77.4 μL , 1.0 mmol, 1.5 equiv) and Et_3N (167 μL , 1.2 mmol, 1.8 equiv) were added sequentially. After 5 min, the reaction was quenched with saturated aq NaHCO_3 (1 mL) and diluted up to 10 mL with CH_2Cl_2 . The biphasic solution was further diluted with sat. aq NaHCO_3 (2 mL) and sat. brine (2 mL), the layers were separated, and the aq layer was extracted with CH_2Cl_2 (3 x 10 mL). The combined organics were dried over MgSO_4 , filtered, and concentrated to a light yellow solid under reduced pressure. This residue was purified by flash chromatography on SiO_2 (2:1 \rightarrow 1:2 hexanes/ EtOAc , dry load) to afford ketomesylate **366** (115.4 mg, 0.560 mmol, 83% yield over two steps) as a colorless oil. $R_f = 0.31$ (3:1 EtOAc /hexanes); ^1H NMR (300 MHz, CDCl_3) δ 4.29 (app dt, $J = 6.4, 2.4, 2.4$ Hz, 2H), 3.02 (s, 3H), 2.51–2.42 (m, 1H), 2.40–2.12 (comp m, 4H), 1.95–1.89 (comp m, 2H), 1.84 (ddd, $J = 17.6, 7.7, 1.3$ Hz, 1H), 1.64–1.48 (m, 1H); ^{13}C NMR (75 MHz, CDCl_3) δ 218.3, 68.2, 44.8, 38.5, 37.6, 35.0, 33.8, 29.4; IR (Neat Film NaCl) 3023, 2935, 1737, 1350, 1173, 954 cm^{-1} ; HRMS (EI+) m/z calc'd for $\text{C}_8\text{H}_{14}\text{O}_4\text{S}$ $[\text{M}]^+$: 206.0613; found 206.0622.

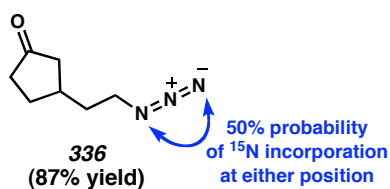


Ketoazide 320. To a solution of mesylate **366** (50.2 mg, 0.243 mmol, 1.0 equiv) in DMF (0.50 mL, 0.5 M) was added NaN_3 (17.4 mg, 0.268 mmol, 1.1 equiv), and the mixture was warmed to 70 °C until consumption of **366** by TLC. The reaction was cooled to 0 °C and stirred for 15 min, followed by dilution with Et_2O . The suspension was filtered through a plug of Celite with Et_2O , concentrated under reduced pressure, and purified by

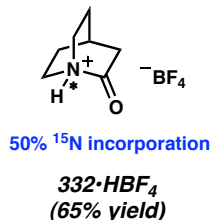
flash chromatography SiO_2 (6:1 \rightarrow 3:1 hexanes/ Et_2O , PhMe load) to afford ketoazide **320** (32.8 mg, 0.214 mmol, 88% yield) as a colorless oil. $R_f = 0.25$ (3:1 hexanes/ EtOAc); ^1H NMR (300 MHz, CDCl_3) δ 3.36 (t, $J = 7.1$ Hz, 2H), 2.50–2.10 (m, 5H), 1.90–1.70 (m, 3H), 1.54 (m, 1H). All other spectral data are consistent with reported values.



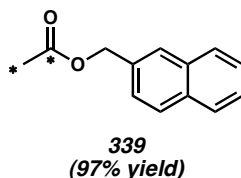
(^{15}N)-labeled azidoalcohol 367. Prepared by a known method using ($1\text{-}^{15}\text{N}$)- NaN_3 . The reaction was purified by flash chromatography on SiO_2 (3:1 \rightarrow 1:1 hexanes/ Et_2O , PhMe load) to afford ^{15}N -labeled azidoalcohol **367** (186.1 mg, 1.19 mmol, 99% yield) as colorless oil. $R_f = 0.14$ (1:1 hexanes/ Et_2O); IR (Neat Film NaCl) 3344, 2946, 2868, 2074, 1339, 1243 cm^{-1} ; HRMS (FAB+) m/z calc'd for $\text{C}_7\text{H}_{14}\text{N}_2\text{O}^{15}\text{N}$ [$\text{M} + \text{H}$] $^+$: 157.1107, found 157.1141. All other spectral data are consistent with reported values.



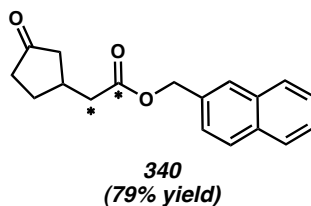
(^{15}N)-labeled ketoazide 336. Prepared by a known method. The reaction was purified by flash chromatography on SiO_2 (6:1 \rightarrow 3:1 hexanes/ Et_2O) to afford ketoazide **336** (155.5 mg, 1.00 mmol, 87% yield) as colorless oil. $R_f = 0.26$ (1:1 hexanes/ Et_2O); IR (Neat Film NaCl) 2931, 2873, 2076, 1740, 1242, 1160 cm^{-1} . All other spectral data are consistent with reported values.



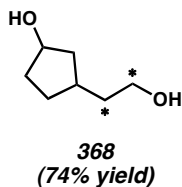
1-¹⁵N-2-quinuclidonium tetrafluoroborate (332•HBF₄). Prepared by a known method. The crude reaction precipitate was transferred to a glove box and recrystallized twice by slow diffusion of Et₂O into CH₃CN at -20 °C to afford **332•HBF₄** (127.7 mg, 0.598 mmol, 65% yield) as white needles. HRMS (FAB+) *m/z* calc'd for C₇H₁₂O¹⁵N [M + H]⁺: 127.0889, observed 127.0855; *m/z* calc'd for C₇H₁₂NO [M + H]⁺: 126.0919, observed 126.0915; relative peak ratio = 1:1.



¹³C₂-labeled acetate 339. Prepared as above to afford **339** (0.8326 g, 4.12 mmol, 97% yield) as an off-white solid. Mp = 54–56 °C; ¹H NMR (300 MHz, CDCl₃) δ 7.87–7.83 (comp m, 4H), 7.53–7.45 (comp m, 3H), 5.27 (d, *J*_{H-¹³C} = 3.2 Hz, 2H), 2.13 (dd, *J*_{H-¹³C} = 129.7, 6.9 Hz); ¹³C NMR (75 MHz, CDCl₃) δ 170.9 (d, *J*_{¹³C-¹³C} = 59.4 Hz), 21.1 (d, *J*_{¹³C-¹³C} = 59.2 Hz); IR (Neat Film NaCl) 3054, 2955, 1693, 1360, 1276, 1218, 1024, 970, 951, 897, 864, 823, 744 cm⁻¹; HRMS (EI+) *m/z* calc'd for C₁₁H₁₂O₂¹³C₂ [M]⁺: 202.0904, found 202.0913.

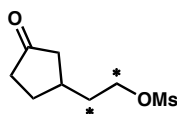


$^{13}\text{C}_2$ -labeled ketoester 340. Prepared as above to afford **340** (0.4204 g, 1.42 mmol, 79% yield) as a pale yellow oil. ^1H NMR (300 MHz, CDCl_3) δ 7.87–7.82 (comp m, 4H), 7.53–7.49 (comp m, 2H), 7.45 (dd, $J = 8.5, 1.6$ Hz, 1H), 5.30 (d, $J = 3.2$ Hz, 2H), 2.54 (dddd, $J_{\text{H-}^{13}\text{C}} = 129.2, 6.9$ Hz, $J = 10.9, 2.0$ Hz, 2H), 2.71–2.58 (m, 1H), 2.49 (ddd, $J = 16.8, 7.4$ Hz, $J_{\text{H-}^{13}\text{C}} = 1.3$ Hz, 1H), 2.28–2.11 (comp m, 3H), 1.96 (dddd, $J = 18.1, 10.4, 5.3$ Hz, $J_{\text{H-}^{13}\text{C}} = 1.3$ Hz, 1H), 1.67–1.50 (m, 1H); ^{13}C NMR (75 MHz, CDCl_3) δ 172.0 (d, $J_{^{13}\text{C}-^{13}\text{C}} = 57.2$ Hz), 39.9 (d, $J_{^{13}\text{C}-^{13}\text{C}} = 57.5$ Hz); IR (Neat Film NaCl) 3054, 2958, 1740, 1690, 1403, 1150, 1124, 818, 754 cm^{-1} ; HRMS (EI+) m/z calc'd for $\text{C}_{16}\text{H}_{18}\text{O}_3^{13}\text{C}_2$ $[\text{M}]^+$: 284.1323, found 284.1322. All other spectral data are consistent with reported values.



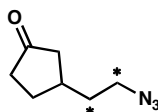
$^{13}\text{C}_2$ -labeled diol 368. Prepared as above to afford ~1:1 mixture of diastereomers of **368** (54.9 mg, 0.415 mmol, 74% yield) as a colorless oil. ^1H NMR (300 MHz, CD_3OD) δ 4.26 (dddd, $J = 5.6, 5.6, 2.9, 2.9$ Hz, 0.44H), 4.21 (dddd, $J = 4.8, 4.8, 4.8, 4.8, 0.56$ H), 3.56 (dddd, $J_{\text{H-}^{13}\text{C}} = 140.2, 6.9$ Hz, $J = 6.9, 2.4$ Hz, 2H), 2.18–2.09 (m, 1H), 2.0–1.7 (comp m, 3H), 1.65–1.49 (m, 1H), 1.46–1.28 (comp m, 2H), 1.23–1.09 (m, 1H); ^{13}C NMR (75 MHz, CD_3OD) δ 62.2 (d, $J_{^{13}\text{C}-^{13}\text{C}} = 37.3$ Hz, 0.44C), 62.1 (d, $J_{^{13}\text{C}-^{13}\text{C}} = 37.3$ Hz,

0.56C), 40.6 (d, $J_{13C-13C} = 37.3$ Hz, 0.56C), 40.1 (d, $J_{13C-13C} = 37.3$ Hz, 0.44C). All other spectral data are consistent with reported values.



341
(83% yield, two steps)

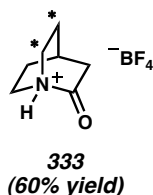
$^{13}C_2$ -labeled ketomesylate 341. Prepared as above to afford **341** (71.7 mg, 0.344 mmol, 83% yield over two steps) as a colorless oil. 1H NMR (300 MHz, $CDCl_3$) δ 4.30 (dddd, $J_{H-13C} = 149.4, 6.4$ Hz, $J = 6.4, 2.7$ Hz, 2H), 3.03 (s, 3H), 2.47 (ddd, $J = 17.8, 7.5$ Hz, $J_{H-13C} = 1.0$ Hz, 1H), 2.41–2.08 (comp m, 5H), 1.85 (dddd, $J = 17.8, 10.1, 5.1$ Hz, $J_{H-13C} = 1$ Hz, 1H), 1.74–1.66 (m, 1H), 1.63–1.52 (m, 1H); ^{13}C NMR (75 MHz, $CDCl_3$) δ 68.1 (d, $J_{13C-13C} = 37.9$ Hz), 35.0 (d, $J_{13C-13C} = 38.2$ Hz); HRMS (EI+) m/z calc'd for $C_6H_{14}SO_4^{13}C_2$ [M] $^+$: 208.0680, found 208.0688. All other spectral data are consistent with reported values.



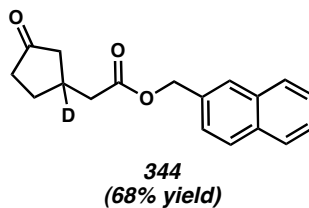
369
(96% yield)

$^{13}C_2$ -labeled ketoazide 369. Prepared as above to afford **369** (28.5 mg, 0.184 mmol, 96% yield) as a colorless oil. 1H NMR (300 MHz, $CDCl_3$) δ 3.36 (app ddt, $J_{H-13C} = 141.4, 6.9$ Hz, $J = 3.2$ Hz, 2H), 2.44 (dd, $J = 17.8, 8.0$ Hz, 1H), 2.37–2.11 (comp m, 4H), 2.00–1.91 (m, 1H), 1.83 (ddd, $J = 17.6, 9.8, 4.8$ Hz, 1H), 1.62–1.49 (comp m, 2H); ^{13}C NMR

(75 MHz, CDCl_3) δ 50.0 (d, $J_{13\text{C}-13\text{C}} = 36.8$ Hz), 34.6 (d, $J_{13\text{C}-13\text{C}} = 36.8$ Hz). All other spectral data are consistent with reported values.

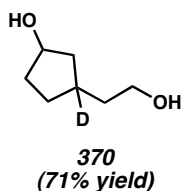


5,6- $^{13}\text{C}_2$ -2-quinuclidonium tetrafluoroborate (333•HBF₄). Prepared as above to afford **333•HBF₄** (36.5 mg, 0.170 mmol, 60% yield) as white needles. ^1H NMR (300 MHz, CD_3CN) δ 7.99 (br s, 1H), 3.69 (m, 2H), 3.69 (m, $J_{\text{H}-13\text{C}} = 150.4$ Hz, 2H), 2.97 (app d, $J = 5.4, 3.3$ Hz, 3H), 2.55–2.47 (m, 1H), 1.98 (m, 2H), 1.98 (m, $J_{\text{H}-13\text{C}} = 135.4$ Hz, 2H); ^{13}C NMR (75 MHz, CD_3CN) δ 47.9 (d, $J_{13\text{C}-13\text{C}} = 32.6$ Hz), 22.6 (d, $J_{13\text{C}-13\text{C}} = 32.6$ Hz); HRMS (FAB+) m/z calc'd for $\text{C}_5\text{H}_{12}\text{NO}^{13}\text{C}_2$ $[\text{M} + \text{H}]^+$: 128.0986, observed 128.0960.

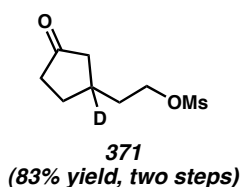


D-labeled ketoester 344. Prepared as above to afford **344** (0.3283 g, 1.15 mmol, 68% yield) as a pale yellow oil. ^1H NMR (300 MHz, CDCl_3) δ 7.87–7.82 (comp m, 4H), 7.53–7.49 (comp m, 2H), 7.45 (dd, $J = 8.5, 1.6$ Hz, 1H), 5.30 (s, 2H), 2.53 (dd, $J = 16.6, 16.6$ Hz, 2H), 2.48 (d, $J = 18.6$ Hz, 1H), 2.37–2.11 (comp m, 3H), 1.89 (d, $J = 18.6$ Hz, 1H), 1.64–1.51 (m, 1H); ^{13}C NMR (75 MHz, CDCl_3) δ 218.4, 172.0, 133.3 (2C), 128.6, 128.1, 127.9, 127.6, 126.5 (2C), 126.0, 66.7, 44.6, 39.7, 38.4, 33.2 (t, $J_{\text{CD}} = 20.2$ Hz),

29.2; ^2H NMR (76 MHz, CHCl_3) δ 2.66 (s); HRMS (EI+) m/z calc'd for $\text{C}_{18}\text{H}_{17}\text{O}_3^2\text{H} [\text{M}]^+$: 283.1319, found 283.1323. All other spectral data are consistent with reported values.

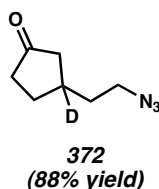


D-labeled diol 370. Prepared as above to afford ~1:1 mixture of diastereomers of **370** (46.0 mg, 0.351 mmol, 71% yield) as a colorless oil. ^1H NMR (300 MHz, CD_3OD) δ 4.26 (ddd, $J = 8.2, 3.5, 2.4$ Hz, 0.45H), 4.21 (ddd, $J = 11.3, 6.4, 6.4$ Hz, 0.55H), 3.56 (app t, $J = 6.9$ Hz, 2H), 2.13 (dd, $J = 13.3, 6.4$ Hz, 0.45H), 1.99–1.88 (m, 0.55H), 1.82–1.70 (comp m, 2H), 1.59 (dt, $J = 22.3, 6.9, 3\text{H}$), 1.44–1.30 (m, 1H), 1.14 (dd, $J = 12.0, 4.5$ Hz, 1H); ^{13}C NMR (75 MHz, CD_3OD) δ 74.1, 62.2, 62.1, 43.0, 42.7, 40.5, 40.0, 35.8, 35.6, 35.6 (t, $J_{\text{CD}} = 19.5$ Hz), 34.8 (t, $J_{\text{CD}} = 19.5$ Hz), 31.4, 31.1; ^2H NMR (76 MHz, CH_3OH) δ 2.14 (s), 1.87 (s). All other spectral data are consistent with reported values.

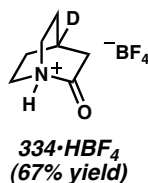


D-labeled ketomesylate 371. Prepared as above to afford **371** (60.3 mg, 0.291 mmol, 83% yield over two steps) as a colorless oil. ^1H NMR (300 MHz, CDCl_3) δ 4.30 (app dt, $J = 6.1, 2.7$ Hz, 2H), 3.03 (s, 3H), 2.46 (d, $J = 18.1$ Hz, 1H), 2.40–2.12 (comp m, 3H), 1.91 (app t, $J = 6.4$ Hz, 2H), 1.85 (d, $J = 18.6$ Hz, 1H), 1.61–1.50 (m, 1H); ^{13}C NMR (75 MHz, CDCl_3) δ 218.3, 68.1, 44.7, 38.5, 37.7, 34.9, 33.4 (t, $J_{\text{CD}} = 19.8$ Hz),

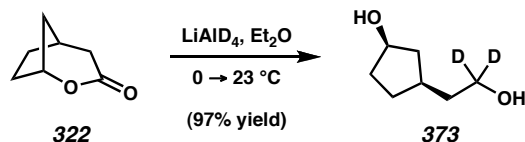
29.3; ^2H NMR (76 MHz, CHCl_3) δ 2.35 (s); HRMS (EI+) m/z calc'd for $\text{C}_8\text{H}_{13}\text{O}_4\text{S}^2\text{H}$ $[\text{M}]^+$: 207.0676, found 207.0673. All other spectral data are consistent with reported values.



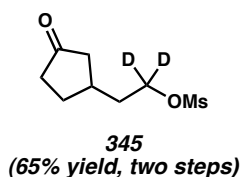
D-labeled ketoazide 372. Prepared as above to afford **372** (39.3 mg, 0.255 mmol, 88% yield) as a colorless oil. ^1H NMR (300 MHz, CDCl_3) δ 3.36 (ddd, $J = 6.8, 6.8, 2.9$ Hz, 2H), 2.43 (d, $J = 18.3$ Hz, 1H), 2.36–2.30 (m, 1H), 2.23–2.14 (comp m, 2H), 1.83 (d, $J = 18.1$ Hz, 1H), 1.74 (ddd, $J = 6.8, 6.8, 3.7$ Hz, 2H), 1.58–1.51 (m, 1H); ^{13}C NMR (125 MHz, CDCl_3) δ 218.6, 50.0, 44.8, 38.5, 34.6, 34.3 (t, $J_{\text{CD}} = 19.8$ Hz), 29.4; ^2H NMR (76 MHz, CHCl_3) δ 2.29 (s). All other spectral data are consistent with reported values.



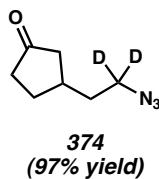
4-d-2-quinuclidonium tetrafluoroborate (334•HBF₄). Prepared as above to afford **334•HBF₄** (33.0 mg, 0.154 mmol, 67% yield) as white needles. ^1H NMR (300 MHz, CD_3CN) δ 7.95 (br s, 1H), 3.78–3.58 (m, 4H), 2.96 (s, 2H), 2.00–1.95 (m, 4H); ^2H NMR (76 MHz, CH_3CN) δ 2.49 (s); HRMS (FAB+) m/z calc'd for $\text{C}_7\text{H}_{11}\text{NO}^2\text{H} [\text{M} + \text{H}]^+$: 127.0982, observed 127.0943.



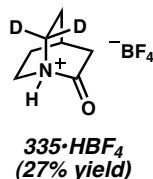
D₂-labeled *syn*-diol 373. Prepared by a known method using LiAlD₄. *syn*-Diol **373** isolated as a colorless oil (0.6317 g, 4.78 mmol, 97% yield) with >98% *d*-incorporation. ¹H NMR (300 MHz, CD₃OD) δ 4.21 (dddd, *J* = 5.8, 5.8, 5.8, 5.8 Hz, 1H), 2.14 (ddd, *J* = 13.6, 7.2, 7.2 Hz, 1H), 2.01–1.85 (m, 1H), 1.83–1.70 (comp m, 2H), 1.64–1.55 (comp m, 3H), 1.48–1.31 (m, 1H), 1.15 (dddd, *J* = 14.4, 9.6, 5.6, 0.5 Hz, 1H); ¹³C NMR (75 MHz, CD₃OD): δ 74.1, 61.4, 42.9, 40.4, 36.0, 35.8, 31.2; ²H NMR (76 MHz, CH₃OH) δ 3.51 (s); HRMS (EI+) *m/z* calc'd for C₇H₁₂O₂²H₂ [M]⁺: 132.1119, found 132.1113. All other spectral data are consistent with reported values.



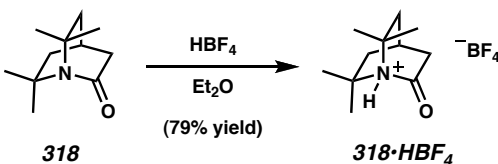
D₂-labeled ketomesylate 345. Prepared as above to afford **345** (0.3775 g, 1.81 mmol, 65% yield over two steps) as a colorless oil. ¹H NMR (300 MHz, CDCl₃) δ 3.01 (s, 3H), 2.49–2.40 (m, 1H), 2.39–2.10 (comp m, 4H), 1.89 (d, *J* = 6.9 Hz, 2H), 1.83 (ddd, *J* = 17.5, 7.4, 1.3 Hz, 1H), 1.63–1.47 (m, 1H); ¹³C NMR (75 MHz, CDCl₃) δ 218.3, 67.6 (pentet, *J*_{CD} = 22.7 Hz), 44.8, 38.4, 37.6, 34.7, 33.7, 29.4; ²H NMR (76 MHz, CHCl₃) δ 4.29 (s); HRMS (EI+) *m/z* calc'd for C₈H₁₂SO₄²H₂ [M]⁺: 208.0738, found 208.0741. All other spectral data are consistent with reported values.



D₂-labeled ketoazide 374. Prepared as above to afford **374** (143.6 mg, 0.925 mmol, 97% yield) as a colorless oil. ¹H NMR (300 MHz, CDCl₃) δ 2.48–2.39 (m, 1H), 2.37–2.11 (comp m, 4H), 1.83 (ddd, *J* = 17.6, 9.8, 1.3 Hz, 1H), 1.74 (d, *J* = 6.7 Hz, 2H), 1.61–1.50 (m, 1H); ¹³C NMR (75 MHz, CDCl₃) δ 218.6, 49.3 (pentet, *J*_{CD} = 21.7 Hz), 44.8, 38.5, 34.6, 34.4, 29.4; ²H NMR (76 MHz, CHCl₃) δ 3.32 (s). All other spectral data are consistent with reported values.



6,6-*d*₂-2-quinuclidonium tetrafluoroborate (335•HBF₄). Prepared as above to afford **335•HBF₄** (15.3 mg, 0.0712 mmol, 27% yield) as white needles. ¹H NMR (300 MHz, CD₃CN) δ 7.96 (br s, 1H), 3.77–3.58 (m, 2H), 2.97 (d, *J* = 3.2 Hz, 2H), 2.51 (app pentet, *J* = 3.2 Hz, 1H), 2.15 (m, 2H), 2.02–1.94 (m, 2H); ²H NMR (76 MHz, CH₃CN) δ 3.68 (s), 3.59 (s); HRMS (FAB+) *m/z* calc'd for C₇H₁₀NO²H₂ [M + H]⁺: 128.1044, observed 128.1042.

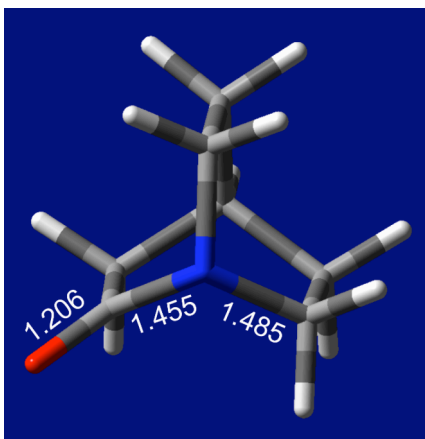


6,6,7,7-tetramethyl-2-quinuclidonium tetrafluoroborate (318•HBF₄). 6,6,7,7-tetramethyl-2-quinuclidone (**318**, 24.9 mg, 0.137 mmol, 1.0 equiv) was dissolved in Et₂O (1.0 mL, 0.14 M) and HBF₄ in Et₂O (54 wt % solution, 38 μL, 0.274 mmol, 2.0 equiv) was added in one portion. The reaction was stirred for 30 min and the precipitate was collected by filtration and dried under vacuum to afford **318•HBF₄** (31.6 mg, 0.117 mmol, 86% yield) as a tan solid. HRMS (FAB+) *m/z* calc'd for C₁₁H₂₀NO [M + H]⁺: 182.1545, observed 182.1552.

5.6.3 COMPUTATIONALLY OPTIMIZED STRUCTURES

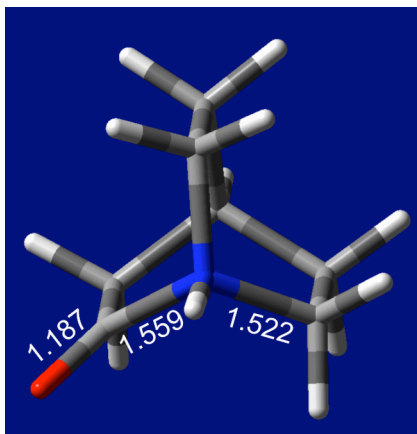
Bond lengths below are given in angstroms (Å). Structures were optimized at the B3LYP/6-31G* level. Total energies were then calculated at the B3LYP/6-311++G** level.

Figure 5.6.1. Optimized structure of 2-quinuclidone (**311**).



O=C–N–C dihedral angles: +121°, –121°

Total energy: –403.4361217 hartrees

Figure 5.6.2. Optimized structure of *N*-protonated 2-quinuclidone (**311**•H⁺).

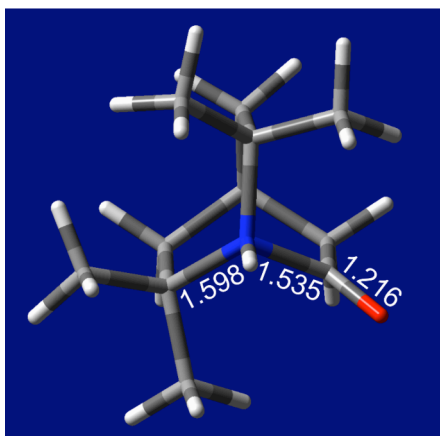
O=C–N–C dihedral angles +119°, –119°

Total energy: –403.8028617 hartrees

Figure 5.6.3. Optimized structure of 6,6,7,7-tetramethyl-2-quinuclidone (**318**).

O=C–N–C dihedral angles: +118°, –118°

Total energy: –560.726844 hartrees

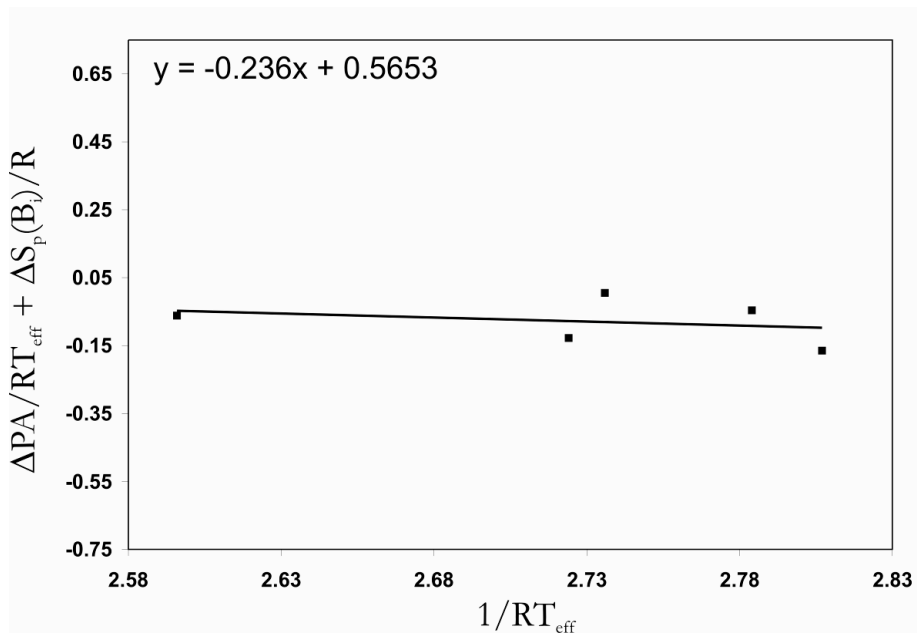
Figure 5.6.4. Optimized structure of *N*-protonated 6,6,7,7-tetramethyl-2-quinuclidone (**318**• H^+).

O=C–N–C dihedral angles: $+116^\circ$, -116°

Total energy: -561.03524 hartrees

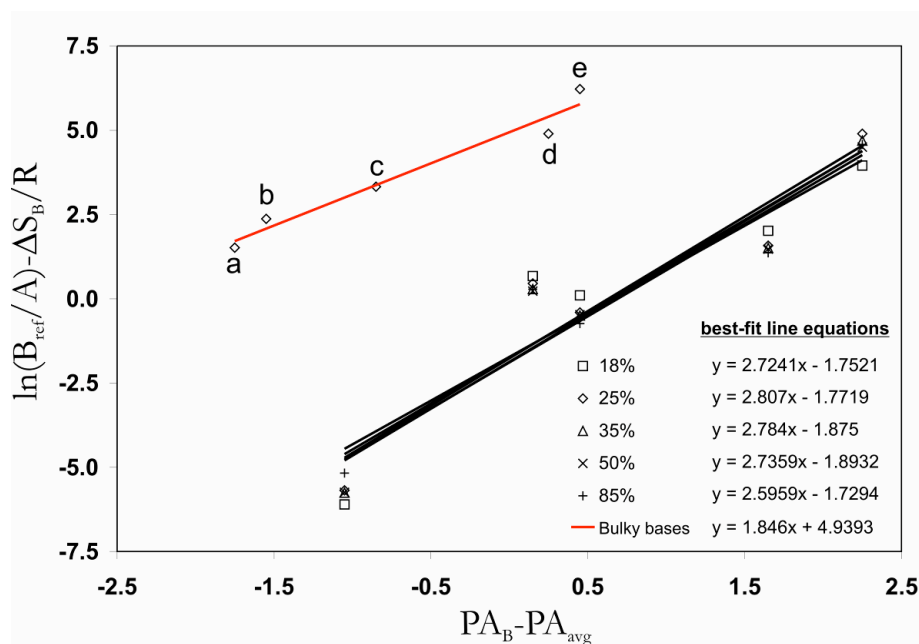
5.6.4 EXTENDED KINETIC METHOD PLOTS

Figure 5.6.5. Plot of the extended kinetic method of **311** with direct entropy correction.

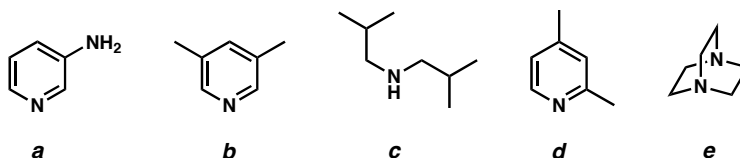


The y-intercepts from the entropy corrected kinetic method were plotted against the slopes at 18%, 25%, 35%, 50%, and 85% normalized collision energies. The slope of the line shown below is equal to $[PA_{\text{quin}} - PA_{\text{avg}}]$.

Figure 5.6.6. Entropy corrected kinetic plot using bulky bases.



The second trend observed is associated with the proton affinity of the carbonyl oxygen of 2-quinuclidone (**311**). Bulky bases: (*a*) 3-aminopyridine; (*b*) 3,5-lutidine; (*c*) diisobutylamine; (*d*) 2,4-lutidine; (*e*) 1,4-diazabicyclo[2.2.2]-octane.



5.6.5 *MS*² SPECTRA OF ISOTOPICALLY LABELED DERIVATIVES AND THEIR HYDROLYSIS PRODUCTS

Fragmentation patterns of all isotopically labeled compounds (**332–335**) are in agreement with mechanism proposed in Scheme 5.3.1a.

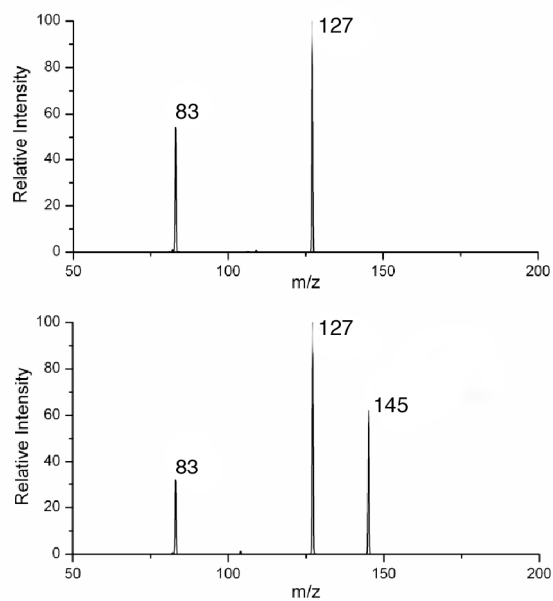
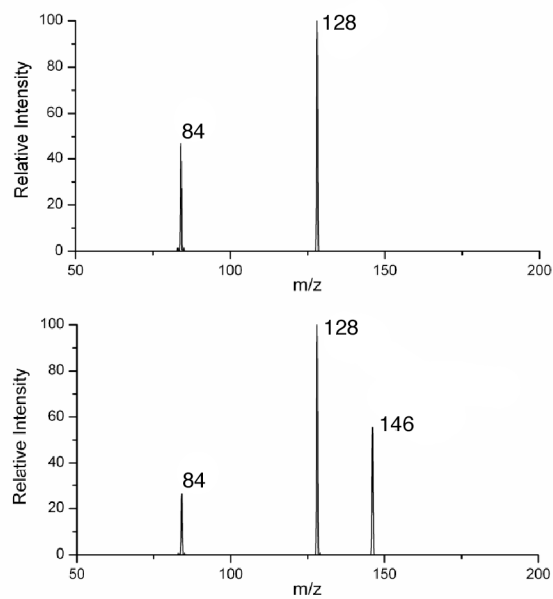
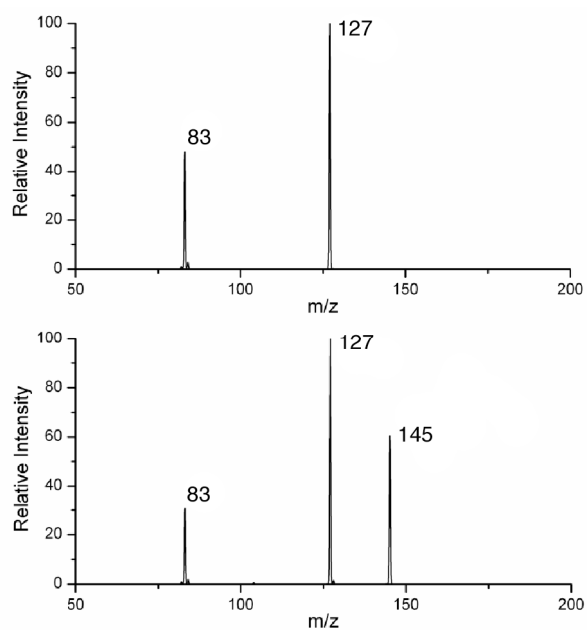
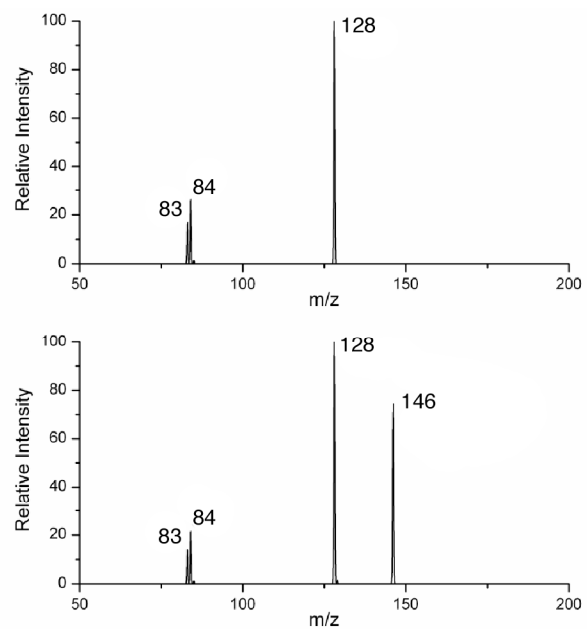
Figure 5.6.7. MS^2 spectrum of **332** (^{15}N).Figure 5.6.8. MS^2 spectrum of **333** ($^{13}C_2$).

Figure 5.6.9. MS^2 spectrum of **334** (D).Figure 5.6.10. MS^2 spectrum of **335** (D_2).

5.7 NOTES AND REFERENCES

- (1) Greenberg, A., Breneman, C. M., Liebman, J. F., Eds. *The Amide Linkage: Selected Structural Aspects in Chemistry, Biochemistry, and Materials Science*; Wiley: New York, 2000.
- (2) Smith, R. M.; Hansen, D. E. *J. Am. Chem. Soc.* **1998**, *120*, 8910–8913.
- (3) (a) Wiberg, K. B. *Acc. Chem. Res.* **1999**, *32*, 922–929. (b) Kemnitz, C. R.; Loewen, M. J. *J. Am. Chem. Soc.* **2007**, *129*, 2521–2528.
- (4) (a) Greenberg, A.; Venanzi, C. A. *J. Am. Chem. Soc.* **1993**, *115*, 6951–6957. (b) Greenberg, A.; Moore, D. T.; DuBois, T. D. *J. Am. Chem. Soc.* **1996**, *118*, 8658–8668.
- (5) Greenberg, A. Twisted Bridgehead Bicyclic Lactams. In *Structure and Reactivity*; Liebman, J. F., Greenberg, A., Eds.; VCH: New York, 1988; pp 139–178.
- (6) (a) Bennet, A. J.; Wang, Q.-P.; Slebocka-Tilk, H.; Somayaji, V.; Brown, R. S.; Santarsiero, B. D. *J. Am. Chem. Soc.* **1990**, *112*, 6383–6385. (b) Ballester, P.; Tadayoni, B. M.; Branda, N.; Rebek, J., Jr. *J. Am. Chem. Soc.* **1990**, *112*, 3685–3686. (c) Kirby, A. J.; Komarov, I. V.; Feeder, N. *J. Am. Chem. Soc.* **1998**, *120*, 7101–7102. (d) Lopez, X.; Mujika, J. I.; Blackburn, G. M.; Karplus, M. *J. Phys. Chem. A* **2003**, *107*, 2304–2315. (e) Mujika, J. I.; Mercero, J. M.; Lopez, X. *J. Am. Chem. Soc.* **2005**, *127*, 4445–4453.
- (7) (a) Poland, B. W.; Xu, M.-Q.; Quioco, F. A. *J. Biol. Chem.* **2000**, *275*, 16408–16413. (b) Romanelli, A.; Shekhtman, A.; Cowburn, D.; Muir, T. W. *Proc. Natl. Acad. Sci. U.S.A.* **2004**, *101*, 6397–6402. (c) Johansson, D. G. A.; Wallin, G.;

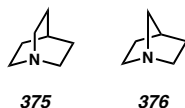
- Sandber, A.; Macao, B.; Åqvist, J.; Härd, T. *J. Am. Chem. Soc.* **2009**, *131*, 9475–9477.
- (8) For reviews of the *cis–trans* isomerization of peptides, see: (a) Wawra, S.; Fischer, G. Amide *Cis–Trans* Isomerization in Peptides and Proteins. In *cis–trans Isomerization in Biochemistry*; Dugave, C., Ed.; Wiley-VCH: Weinheim, 2006; pp 167–193. (b) Fischer, G. Enzymes Catalyzing Peptide Bond *Cis–Trans* Isomerizations. In *cis–trans Isomerization in Biochemistry*; Dugave, C., Ed.; Wiley-VCH: Weinheim, 2006; pp 195–224. (c) Dugave, C.; Demange, L. *Chem. Rev.* **2003**, *103*, 2475–2532.
- (9) Lukeš, R. *Coll. Czech. Chem. Commun.* **1938**, *10*, 148–152.
- (10) Brecht, J. *Liebigs Ann. Chem.* **1924**, *437*, 1–13.
- (11) (a) Johnson, J. R.; Woodward, R. B.; Robinson, R. The Constitution of the Penicillins. *The Chemistry of Penicillin*; Clark, H. T., Johnson, J. R., Robinson, R., Eds.; Princeton University Press: Princeton, NJ, 1949; pp 440–454. (b) Wasserman, H. H. *Heterocycles* **1977**, *7*, 1–15. (c) Wasserman, H.H. *Nature* **2006**, *441*, 699–700.
- (12) Yakhontov, L. N.; Rubsitov, M. V. *J. Gen. Chem. USSR* **1957**, *27*, 83–87.
- (13) Pracejus, H.; Kehlen, M.; Matschiner, H. *Tetrahedron* **1965**, *21*, 2257–2270.
- (14) (a) Pracejus, H. *Chem. Ber.* **1959**, *92*, 988–998. (b) Pracejus, H. *Chem. Ber.* **1965**, *98*, 2897–2905. (c) Levkoeva, E. I.; Nikitskaya, E. S.; Yakhontov, L. N. *Dokl. Akad. Nauk SSSR* **1970**, *192*, 342–345. (d) Greenberg, A.; Wu, G.; Tsai, J.-C.; Chiu, Y.-Y. *Struct. Chem.* **1993**, *4*, 127–129.

- (15) (a) Hall, H. K.; Shaw, R. G.; Deutschmann, A. *J. Org. Chem.* **1980**, *45*, 3722–3724. (b) Blackburn, G. M.; Skaife, C. J.; Kay, I. T. *J. Chem. Res., Miniprint* **1980**, 3650–3669. (c) Buchanan, G. L.; Kitson, D. H.; Mallinson, P. R.; Sim, G. A.; White, D. N. J.; Cox, P. J. *J. Chem. Soc., Perkin Trans. 2* **1983**, 1709–1712. (d) Somayaji, V.; Brown, R. S. *J. Org. Chem.* **1986**, *51*, 2676–2686. (e) Williams, R. M.; Lee, B. H. *J. Am. Chem. Soc.* **1986**, *108*, 6431–6433. (f) Williams, R. M.; Lee, B. Y.; Miller, M. M.; Anderson, O. P. *J. Am. Chem. Soc.* **1989**, *111*, 1073–1081. (g) Wang, Q.-P.; Bennet, A. J.; Brown, R. S.; Santarsiero, B. D. *Can. J. Chem.* **1990**, *68*, 1732–1739. (h) Boivin, J.; Gaudin, D.; Labrecque, D.; Jankowski, K. *Tetrahedron Lett.* **1990**, *31*, 2281–2282. (i) Wang, Q.-P.; Bennet, A. J.; Brown, R. S.; Santarsiero, B. D. *J. Am. Chem. Soc.* **1991**, *113*, 5757–5765. (j) Lease, T. G.; Shea, K. J. *J. Am. Chem. Soc.* **1993**, *115*, 2248–2260. (k) Kirby, A. J.; Komarov, I. V.; Wothers, P. D.; Feeder, N. *Angew. Chem., Int. Ed.* **1998**, *37*, 785–786. (l) Bashore, C. G.; Samardjiev, I. J.; Bordner, J.; Coe, J. W. *J. Am. Chem. Soc.* **2003**, *125*, 3268–3272. (m) Ribelin, T. P.; Judd, A. S.; Akritopoulou-Zanze, I.; Henry, R. F.; Cross, J. L.; Whittern, D. N.; Djuric, S. W. *Org. Lett.* **2007**, *9*, 5119–5122. (n) Szostak, M.; Aube, J. *Org. Lett.* **2009**, *11*, 3878–3881.
- (16) Mujika, J. I.; Mercero, J. M.; Lopez, X. *J. Phys. Chem. A* **2003**, *107*, 6099–6107.
- (17) Clayden, J.; Moran, W. J. *Angew. Chem., Int. Ed.* **2006**, *45*, 7118–7120.
- (18) Tani, K.; Stoltz, B. M. *Nature* **2006**, *441*, 731–734.

- (19) A separate C–H activation approach was pursued incorporating the loss of dinitrogen. However, neither **311** nor any products consistent with its decomposition were observed.
- (20) Aubé, J.; Milligan, G. L. *J. Am. Chem. Soc.* **1991**, *113*, 8965–8966.
- (21) (a) Golden, J. E.; Aubé, J. *Angew. Chem., Int. Ed.* **2002**, *41*, 4316–4318. (b) Lei, Y.; Wroblewski, A. D.; Golden, J. E.; Powell, D. R.; Aubé, J. *J. Am. Chem. Soc.* **2005**, *127*, 4552–4553. (c) Yao, L.; Aubé, J. *J. Am. Chem. Soc.* **2007**, *129*, 2766–2767.
- (22) The ratio of **311:326** was determined by exposure to MeOH and analysis of the ring-opened products.
- (23) Pretsch, E.; Bühlmann, P.; Affolter, C. *Structure Determination of Organic Compounds. Tables of Spectral Data*, 3rd ed.; Springer-Verlag: New York, 2000.
- (24) Dunitz, J. D.; Winkler, F. K. *Acta Crystallogr., Sect. B: Struct. Sci.* **1975**, *31*, 251–263.
- (25) Wiberg, K. B.; Laidig, K. E. *J. Am. Chem. Soc.* **1987**, *109*, 5935–5943.
- (26) (a) Zheng, X.; Cooks, R. G. *J. Phys. Chem. A* **2002**, *106*, 9939–9946. (b) Bouchoux, G.; Sablier, M.; Berruyer-Penaud, F. *J. Mass Spectrom.* **2004**, *39*, 986–997.
- (27) (a) Wu, Z.; Fenselau, C.; Cooks, G. R. *Rapid Commun. Mass. Spectrom.* **1994**, *8*, 777–780. (b) Cerda, B. A.; Wesdemiotis, C. *J. Am. Chem. Soc.* **1995**, *117*, 9734–9739. (c) Armentrout, P. B. *J. Am. Soc. Mass Spectrom.* **2000**, *11*, 371–379.

- (28) Hunter, E. P.; Lias, S. G. Proton Affinity Evaluation. In *NIST Chemistry WebBook, NIST Standard Reference Database Number 69*, Linstrom, P. J., Mallard, W. G., Eds.; National Institute of Standards and Technology, Gaithersburg, MD, 2005; 20899 (<http://webbook.nist.gov>).
- (29) Previous calculations have determined a 22.8 kcal/mol difference in energy for the site of protonation of **311**. See ref 4b.
- (30) See subsection 5.6.4 for details.
- (31) Hunter, E. P.; Lias, S. G.; *J. Phys. Chem. Ref. Data* **1998**, *27*, 413–656.
- (32) (a) McLafferty, F. W. *Anal. Chem.* **1956**, *28*, 306–316. (b) Kingston, D. G. I.; Bursey, J. T.; Bursey, M. M. *Chem. Rev.* **1974**, *74*, 215–242.
- (33) (a) Tomioka, H.; Oshima, K.; Nozaki, H. *Tetrahedron Lett.* **1982**, *23*, 539–542. (b) Kanemoto, S.; Tomioka, H.; Oshima, K.; Nozaki, H. *Bull. Chem. Soc. Jpn.* **1986**, *59*, 105–108.
- (34) (a) Gannon, W. F.; House, H. O. *Org. Synth.* **1973**, *CV 5*, 294–196. (b) Dauphin, G.; Gramain, J.-C.; Kergomard, A.; Renard, M. F.; Veschambre, H. *J. Chem. Soc., Chem. Commun.* **1980**, 318–319.
- (35) See subsection 5.6.5 for details.
- (36) Westheimer, F. H. *Chem. Rev.* **1961**, *61*, 265–273.
- (37) Wiberg, K. B. *Angew., Int. Ed. Engl.* **1986**, *25*, 312–322.

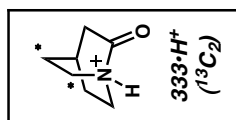
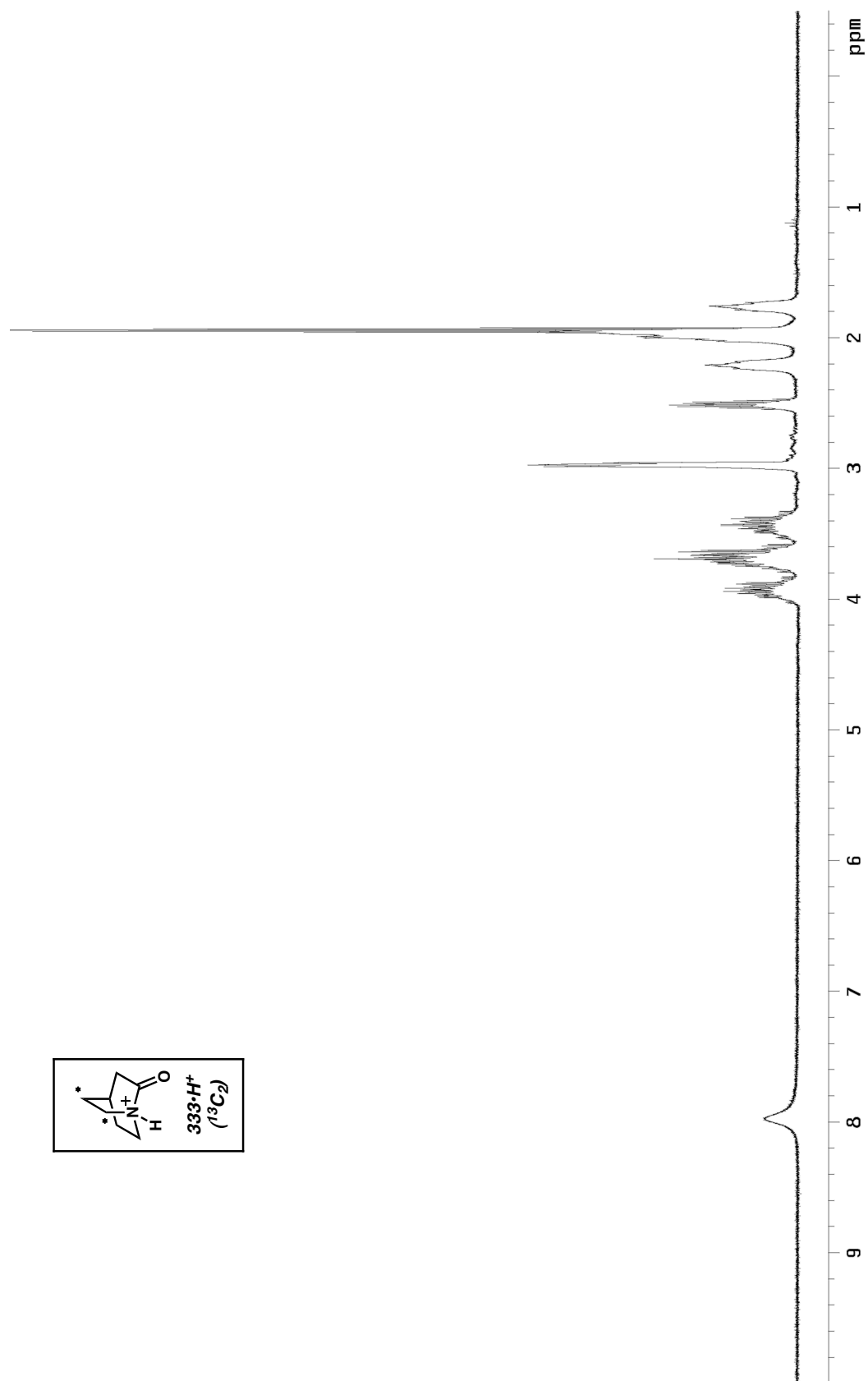
- (38) The parent bicyclic amines **375** and **376** possess a similar pK_a values (10.90 and 10.53, respectively), however their nucleophilic reactivities are significantly different with **375** as the stronger nucleophile. See: Hine, J.; Chen, Y.-J. *J. Org. Chem.* **1987**, *52*, 2091–2094.



- (39) Danheiser, R. L.; Savariar, S.; Cha, D. D. *Organic Syntheses*; Wiley & Sons: New York, 1993; Collect. Vol. VIII, pp 82–86.
- (40) Qin, D.-G.; Zha, H.-Y.; Yao, Z.-H. *J. Org. Chem.* **2002**, *67*, 1038–1040.
- (41) This cyclization has been used for substituted cyclobutanone systems. See ref 20.
- (42) (a) Coll, J. C.; Crist, D. R.; Barrio, M. G.; Leonard, N. J. *J. Am. Chem. Soc.* **1972**, *94*, 7092–7099. (b) Wang, A. H.-J.; Missavage, R. J.; Byrn, S. R.; Paul, I. C. *J. Am. Chem. Soc.* **1972**, *94*, 7100–7104.
- (43) (a) Maier, W. F.; Schleyer, P. v. R. *J. Am. Chem. Soc.* **1981**, *103*, 1891–1900. (b) McEwen, A. B.; Schleyer, P. v. R. *J. Am. Chem. Soc.* **1986**, *108*, 3951–3960.
- (44) Schomaker, J. M.; Pulgam, V. R.; Borhan, B. *J. Am. Chem. Soc.* **2004**, *126*, 13600–13601.
- (45) Gottlieb, H. E.; Kotlyar, V.; Nudelman, A. *J. Org. Chem.* **1997**, *62*, 7512–7515.
- (46) Andersson, M. P.; Uvdal, P. *J. Phys. Chem. A* **2005**, *109*, 2937–2941.
- (47) Boys, S. F.; Bernardi, F. *Mol. Phys.* **1970**, *19*, 553–566.

APPENDIX 5

*Spectra Relevant to Chapter 5:
Synthesis, Structural Analysis, and Gas-Phase Studies
of 2-Quinuclidonium Tetrafluoroborate*

Figure A5.1. ^1H NMR spectrum (300 MHz, CD_3CN) of **333•HBF₄**.

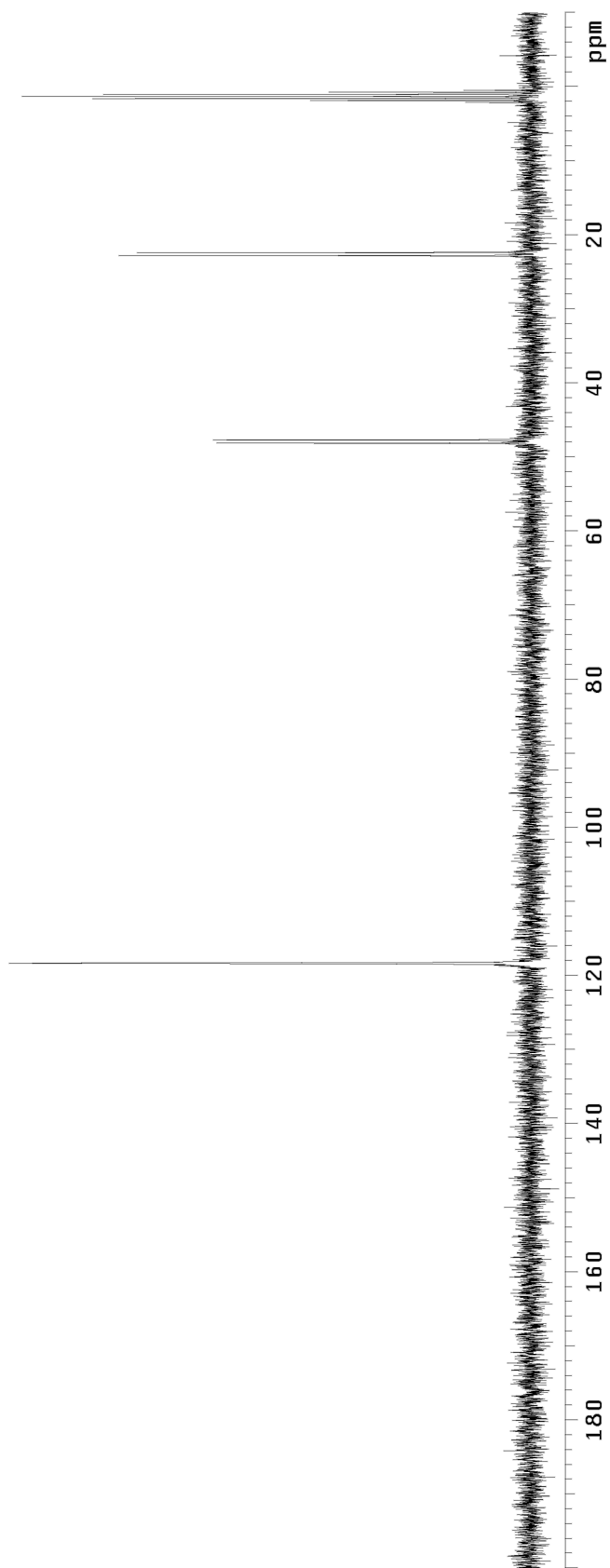
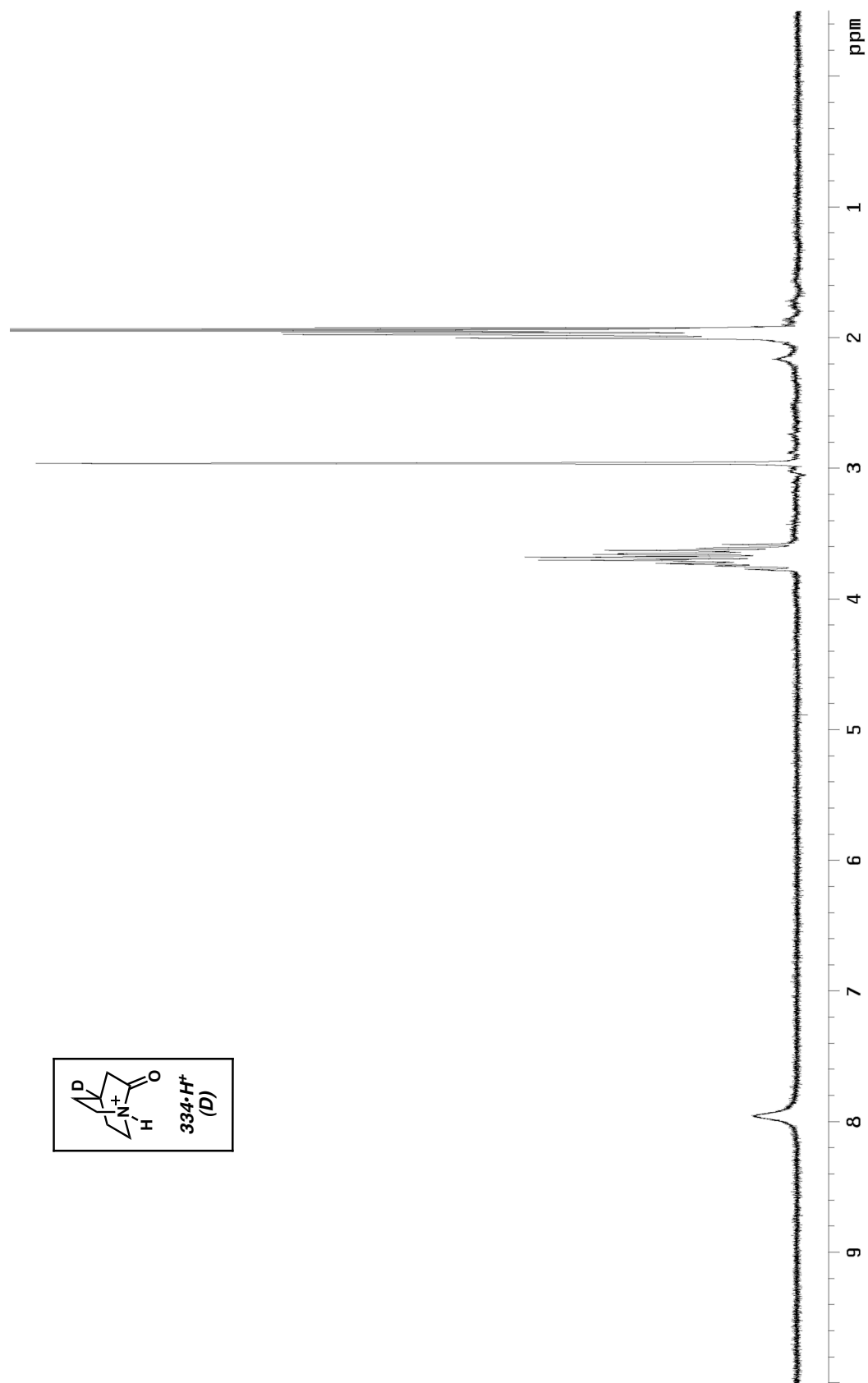


Figure A5.2. ^{13}C NMR spectrum (75 MHz, CD_3CN) of $333\bullet\text{HBF}_4$.

Figure A5.3. ^1H NMR spectrum (300 MHz, CD_3CN) of $334\cdot\text{HBF}_4$.

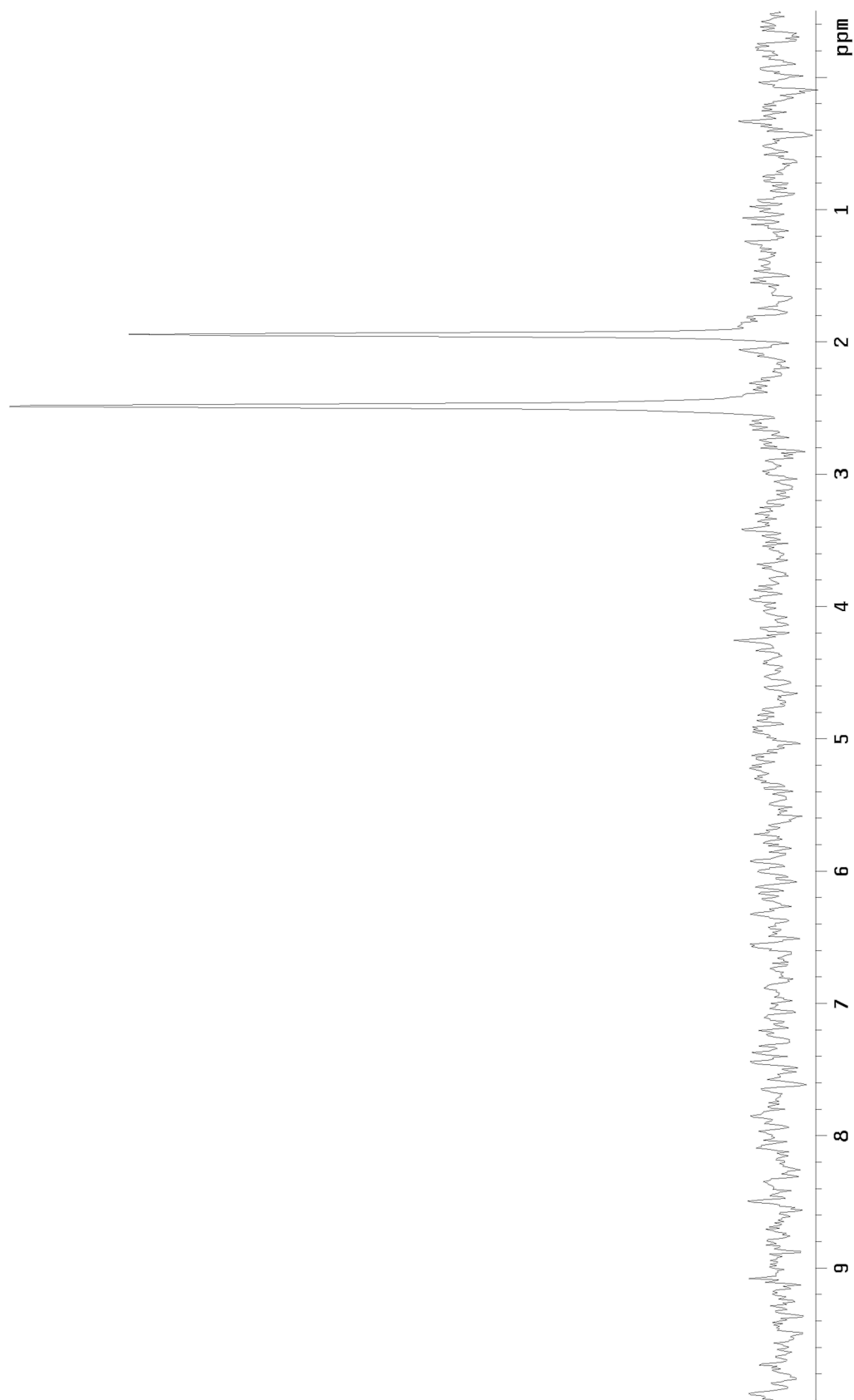
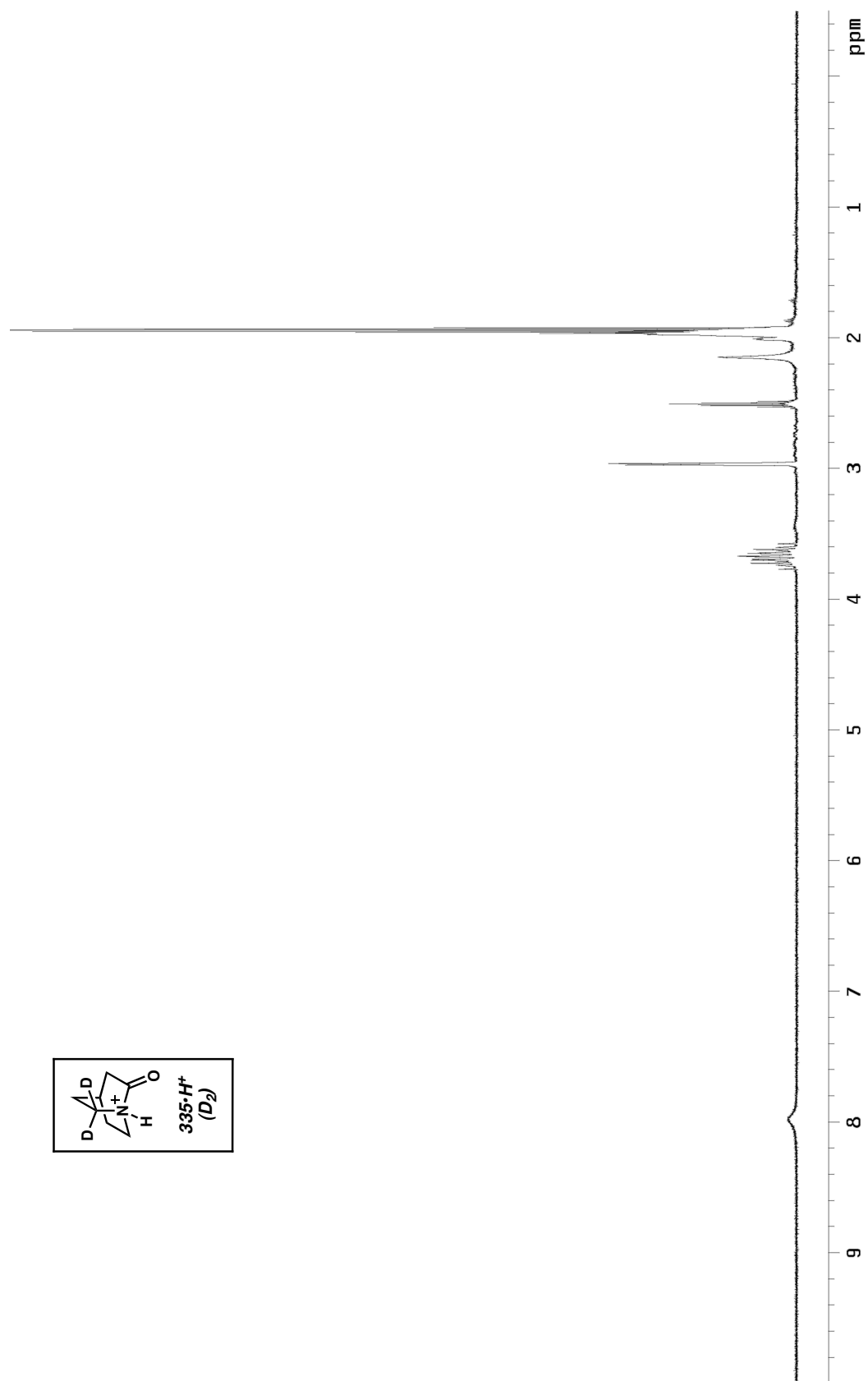


Figure A5.4. ^2H NMR spectrum (76 MHz, CH_3CN) of $334\bullet\text{HBF}_4$.

Figure A5.5. ^1H NMR spectrum (300 MHz, CD_3CN) of $335\cdot\text{HBF}_4$.

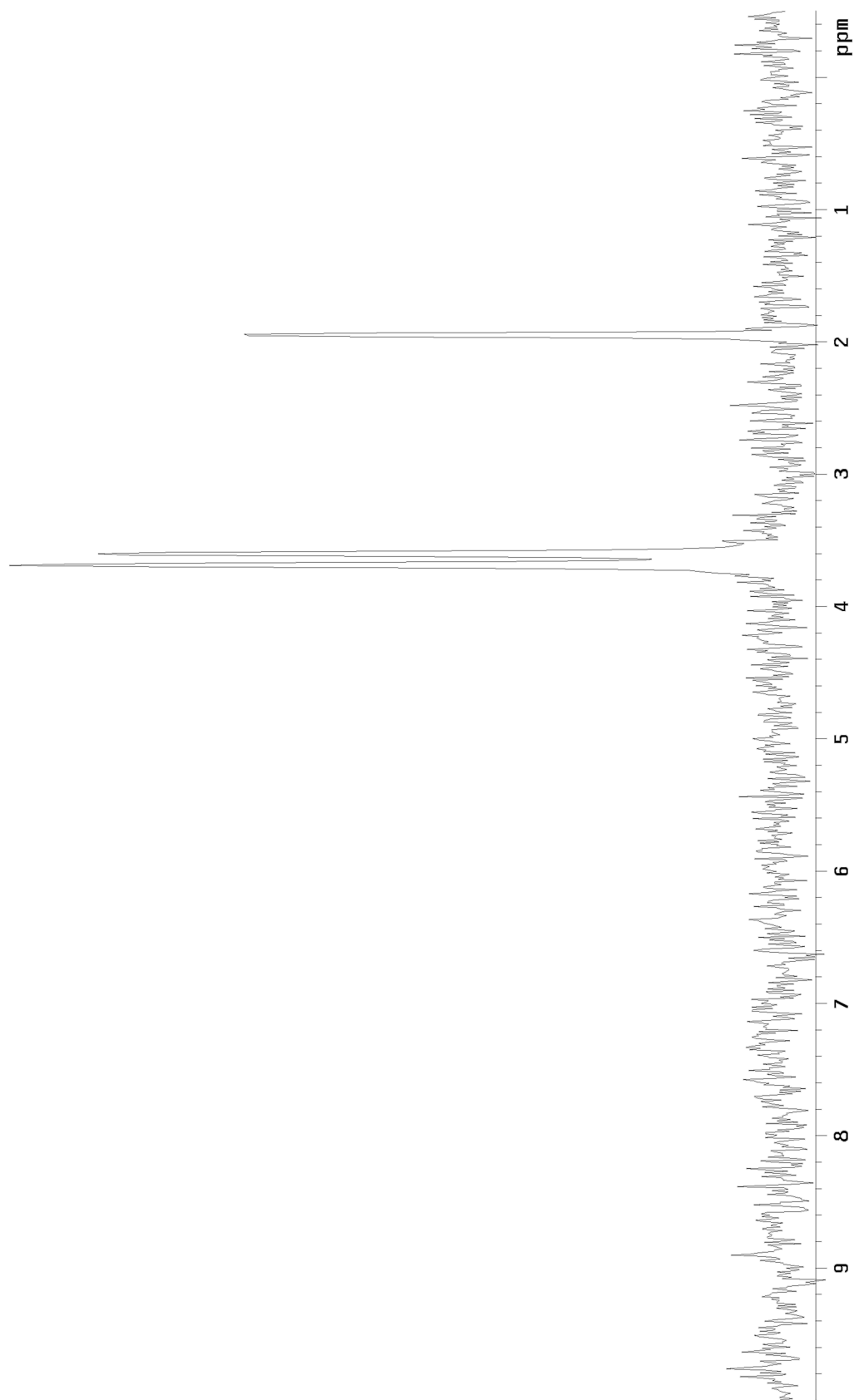
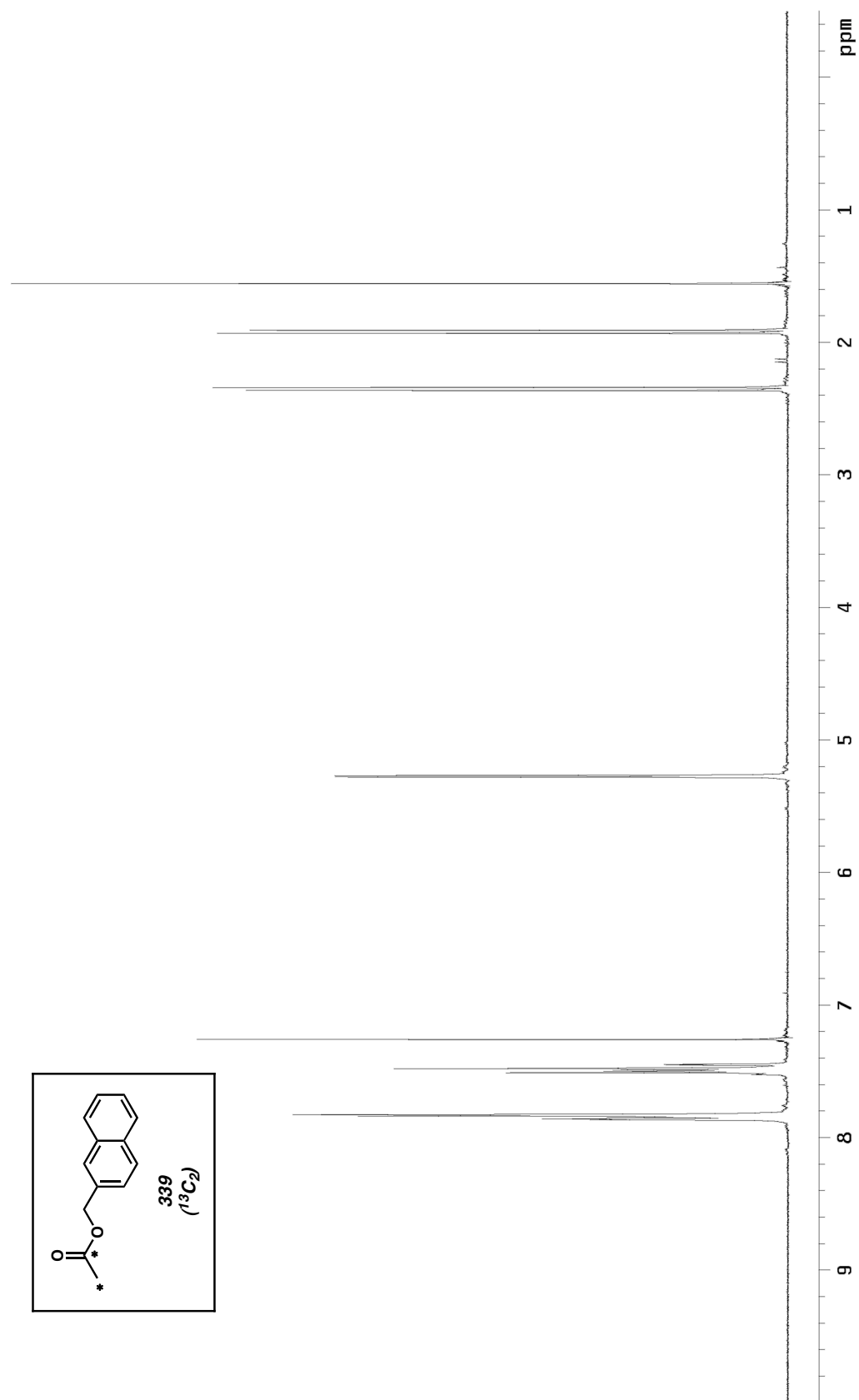


Figure A5.6. ^2H NMR spectrum (75 MHz, CH_3CN) of $335\bullet\text{HBF}_4$.

Figure A5.7. ^1H NMR spectrum (300 MHz, CDCl_3) of 339.

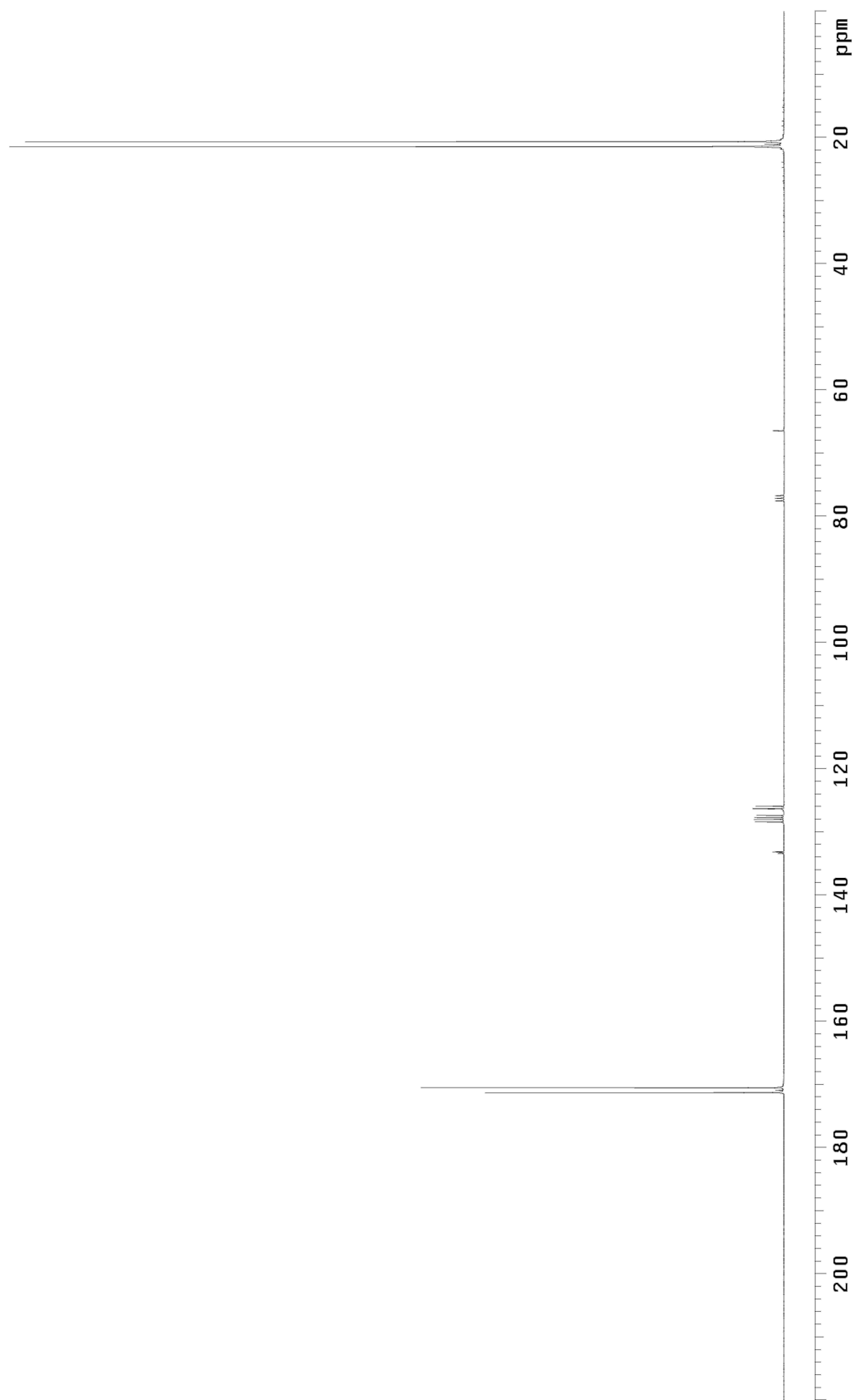
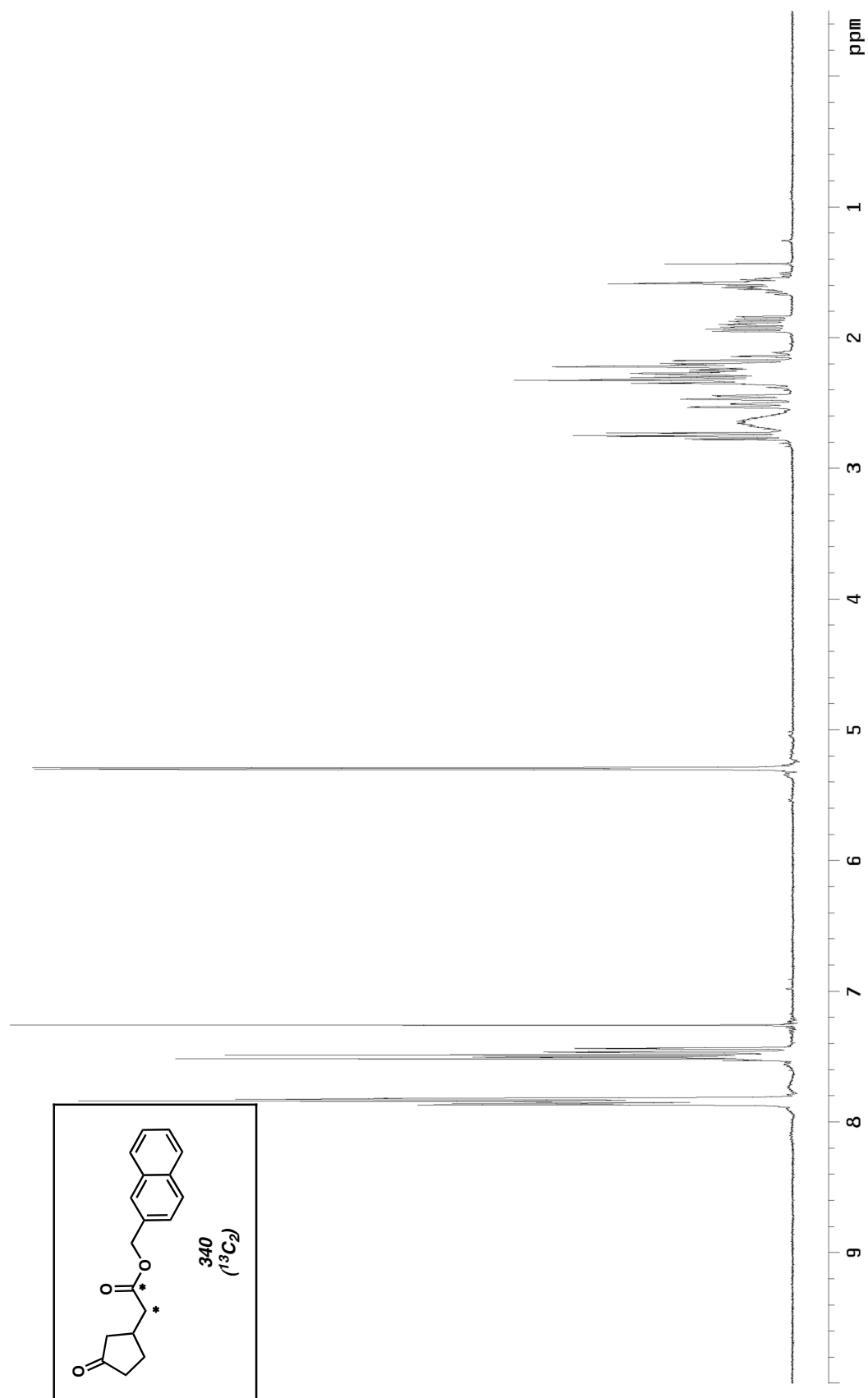


Figure A5.8. ^{13}C NMR spectrum (75 MHz, CDCl_3) of **339**.

Figure A5.9. ^1H NMR spectrum (300 MHz, CDCl_3) of **340**.

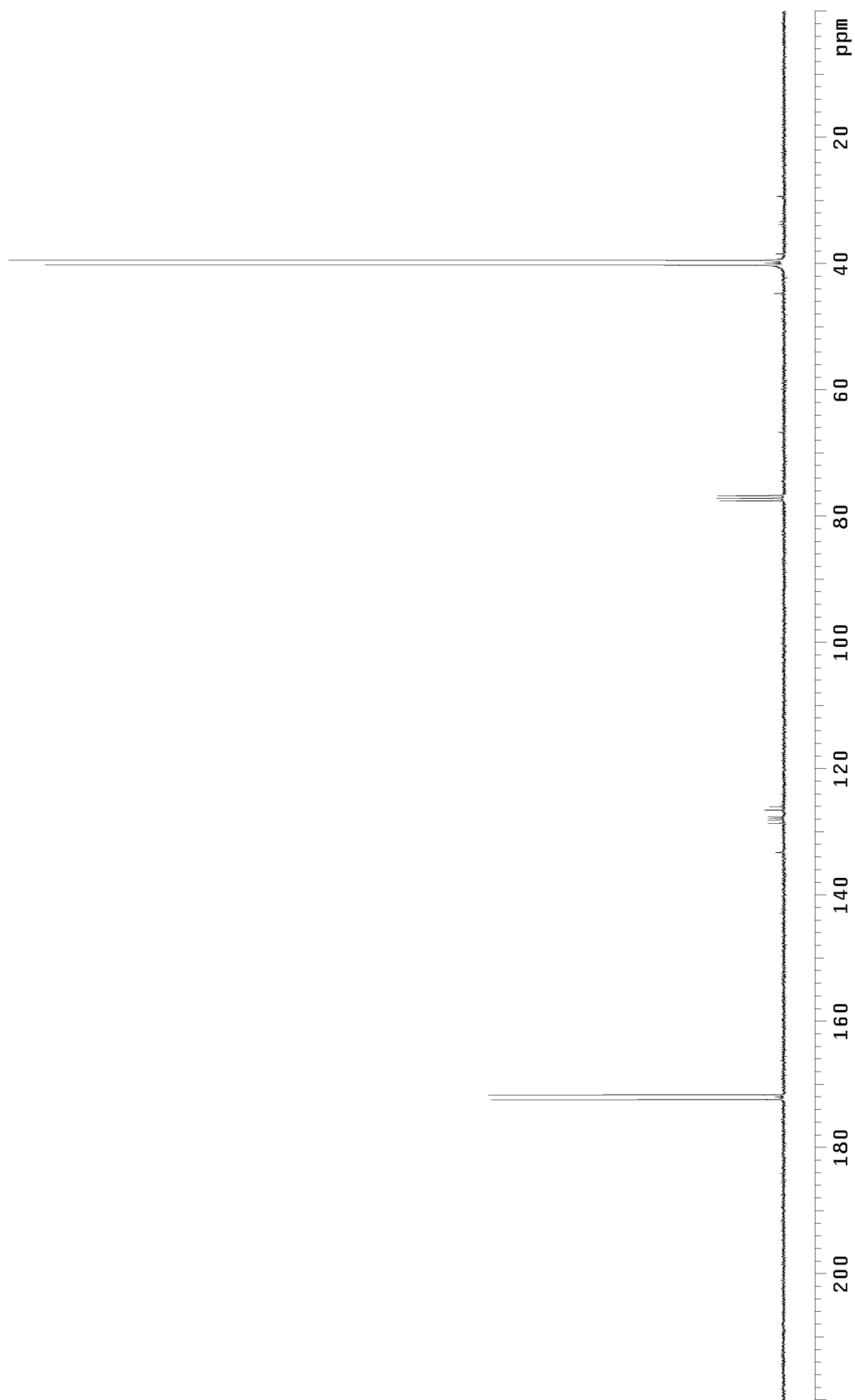
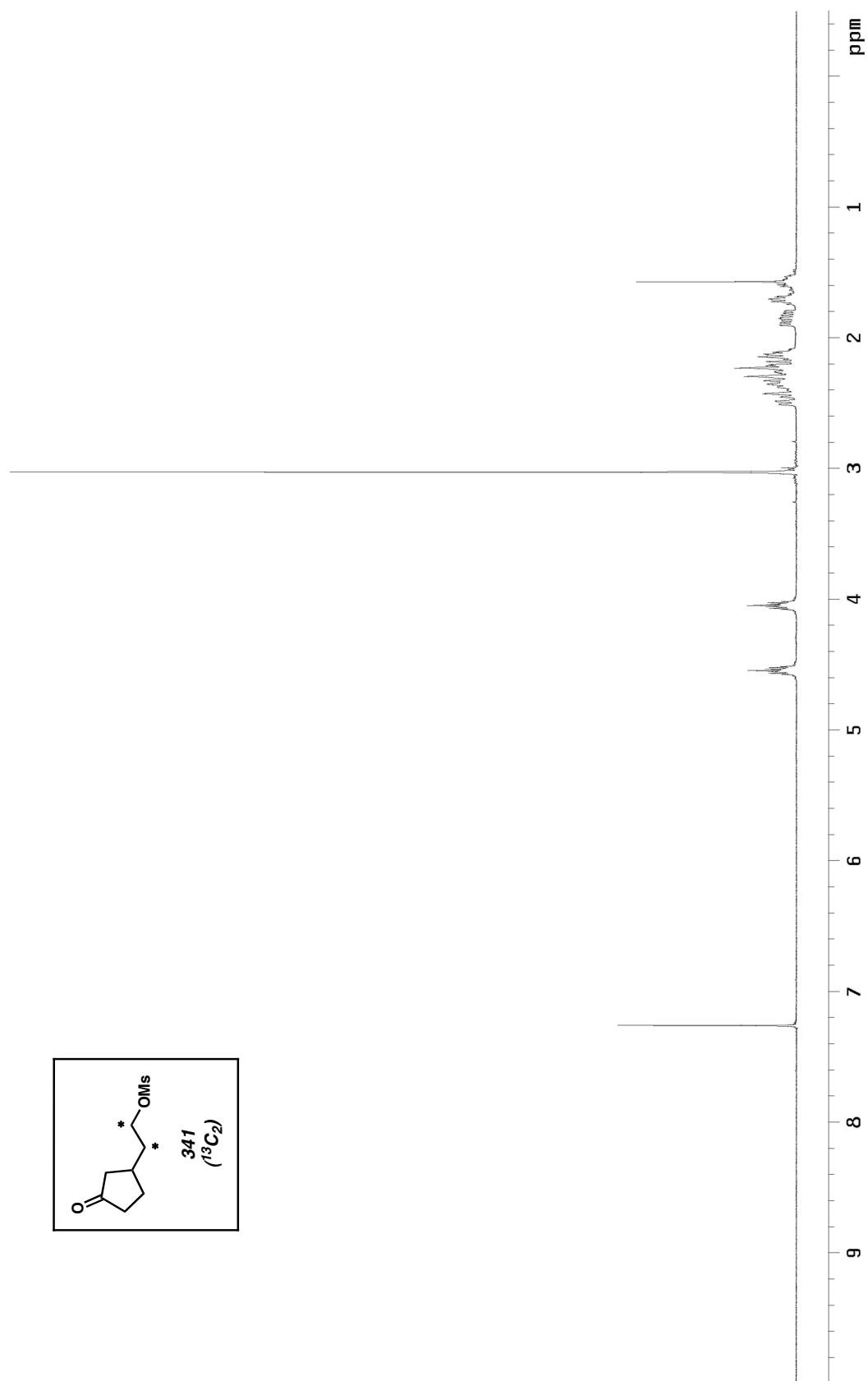


Figure A5.10. ^{13}C NMR spectrum (75 MHz, CDCl_3) of **340**.

Figure A5.11. ^1H NMR spectrum (300 MHz, CDCl_3) of **341**.

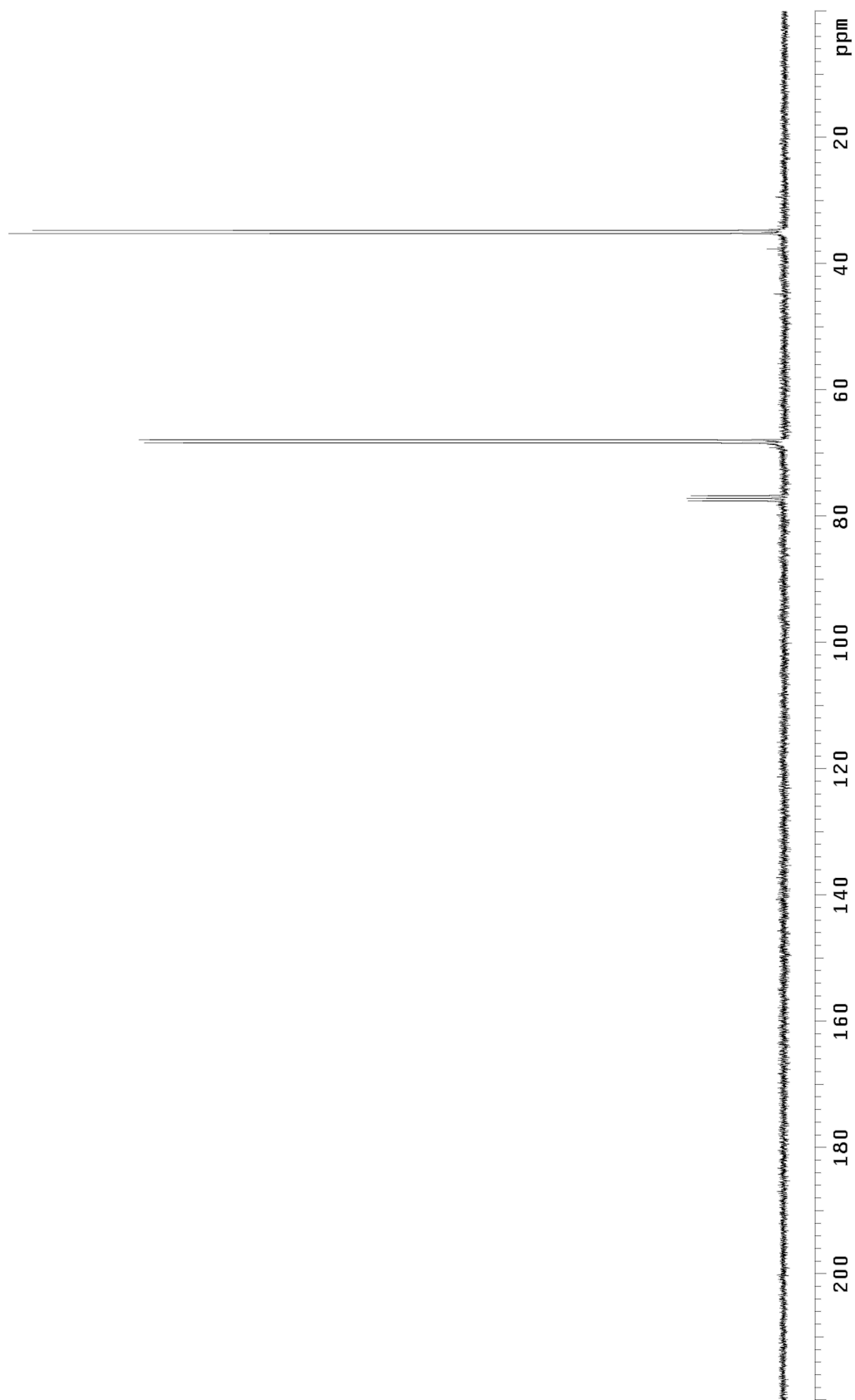
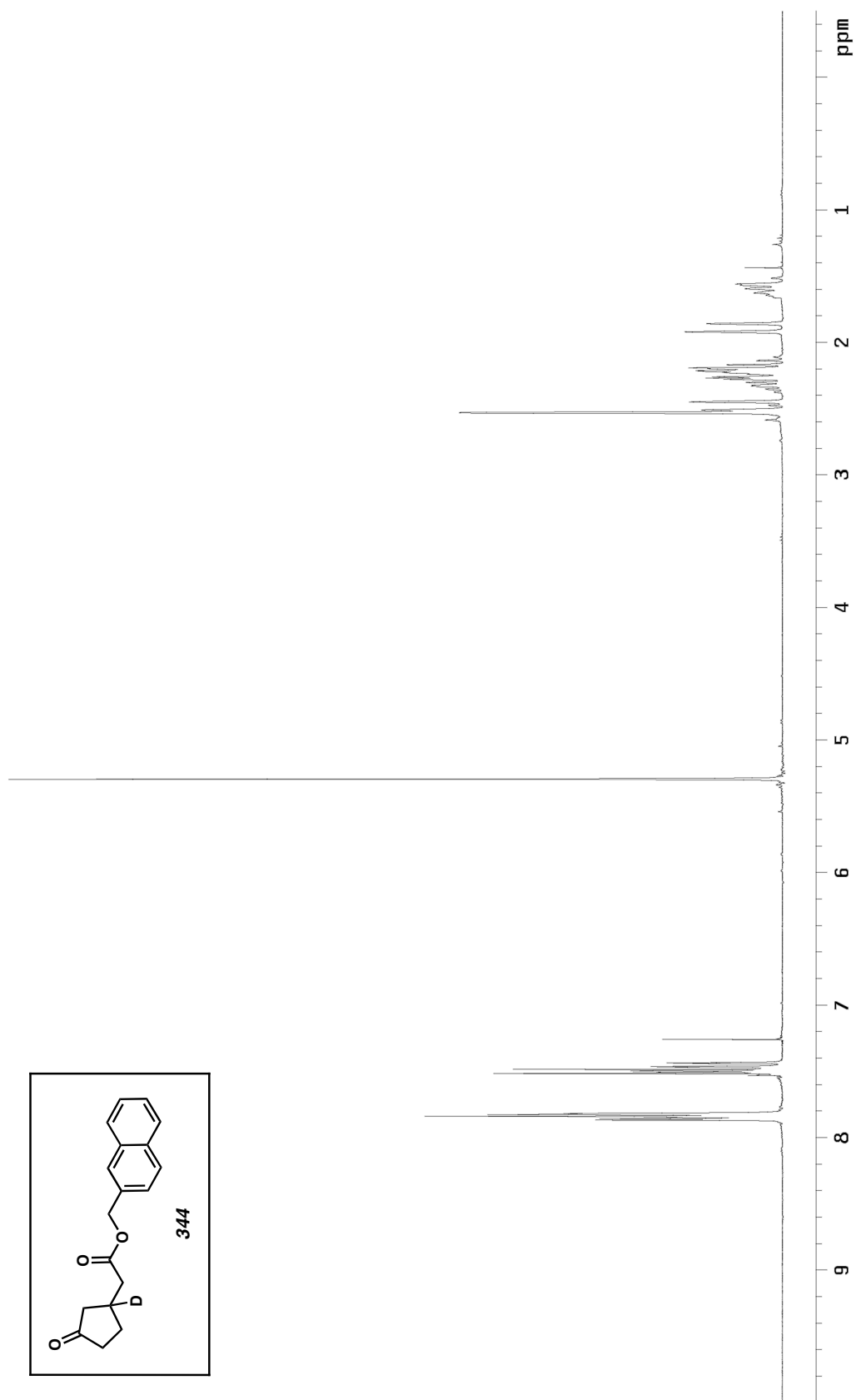


Figure A5.12. ^{13}C NMR spectrum (75 MHz, CDCl₃) of **341**.

Figure A5.13. ^1H NMR spectrum (300 MHz, CDCl_3) of **344**.

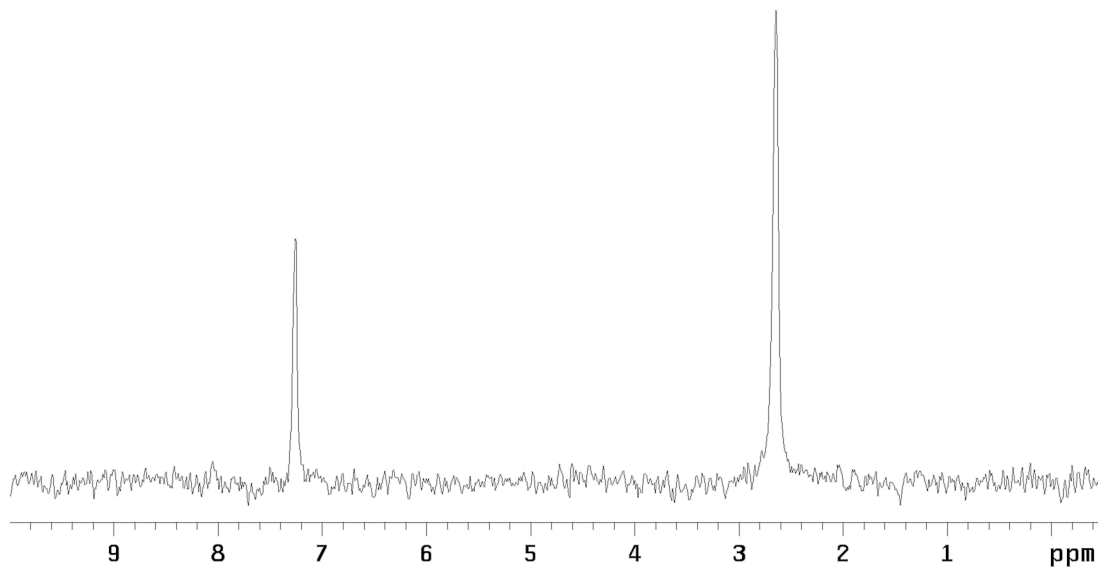


Figure A5.14. ^2H NMR spectrum (76 MHz, CHCl_3) of **344**.

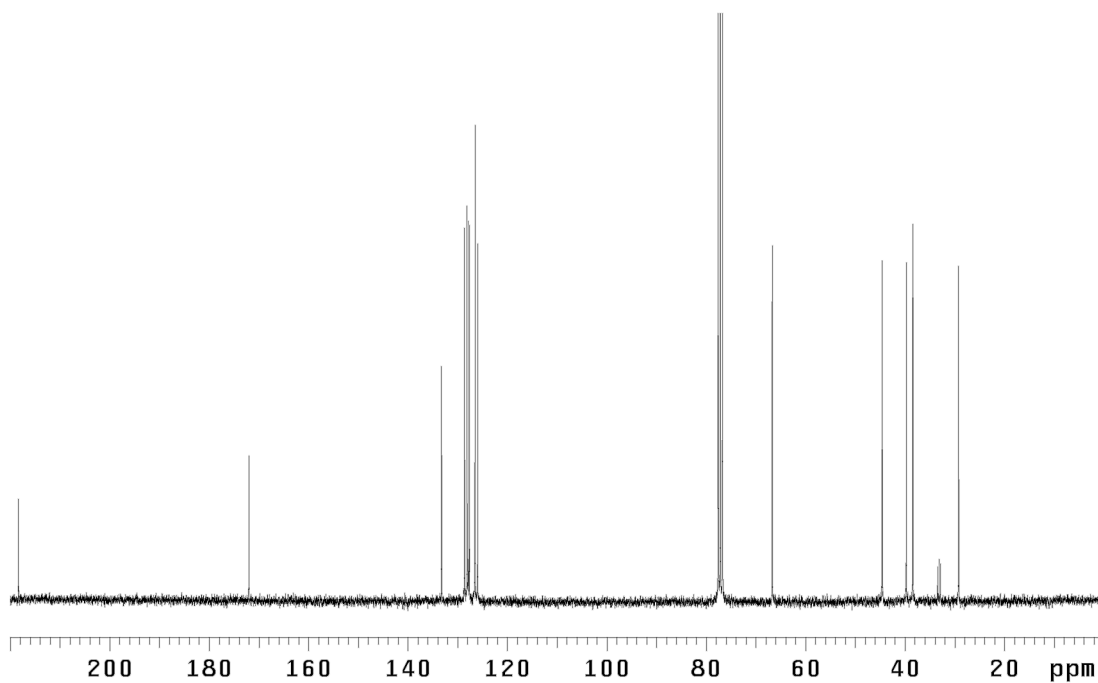
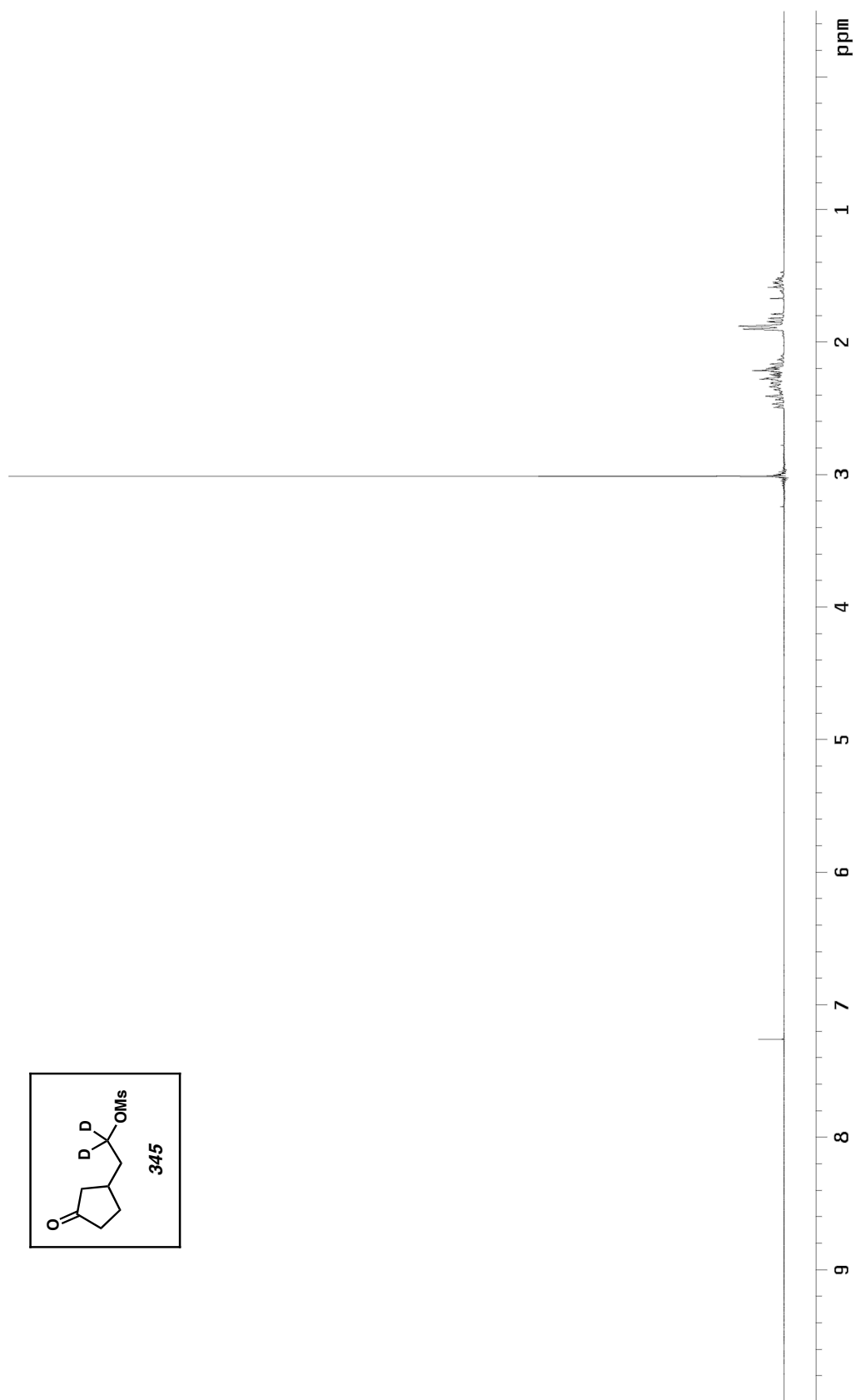


Figure A5.15. ^{13}C NMR spectrum (75 MHz, CDCl_3) of **344**.

Figure A5.16. ^1H NMR spectrum (300 MHz, CDCl_3) of **345**.

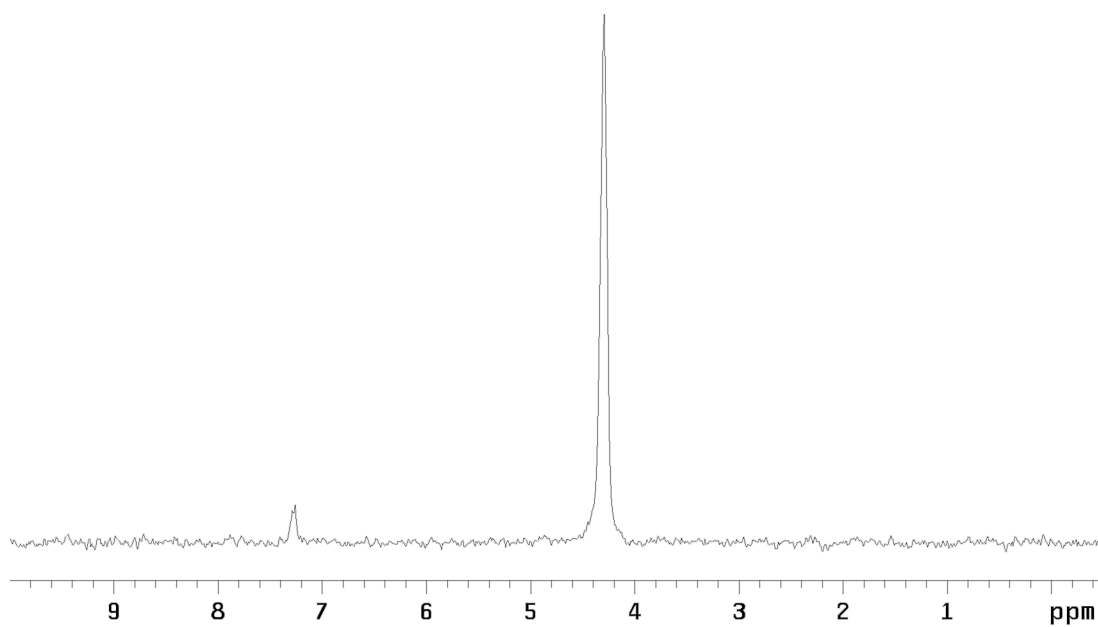


Figure A5.17. ^2H NMR spectrum (76 MHz, CHCl_3) of **345**.

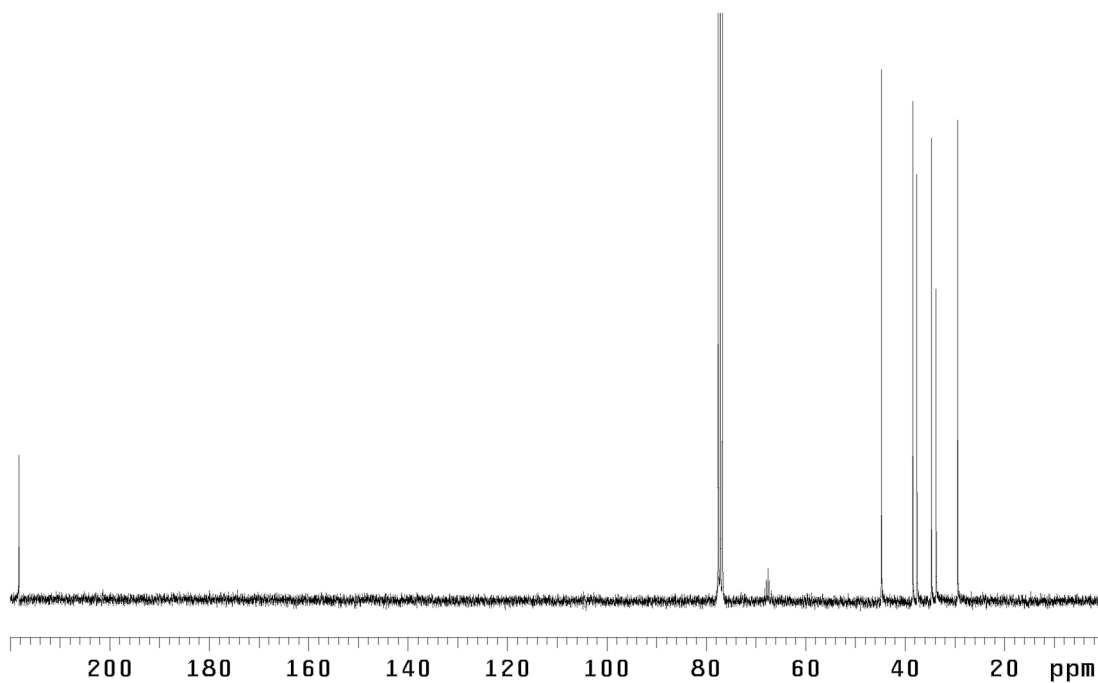
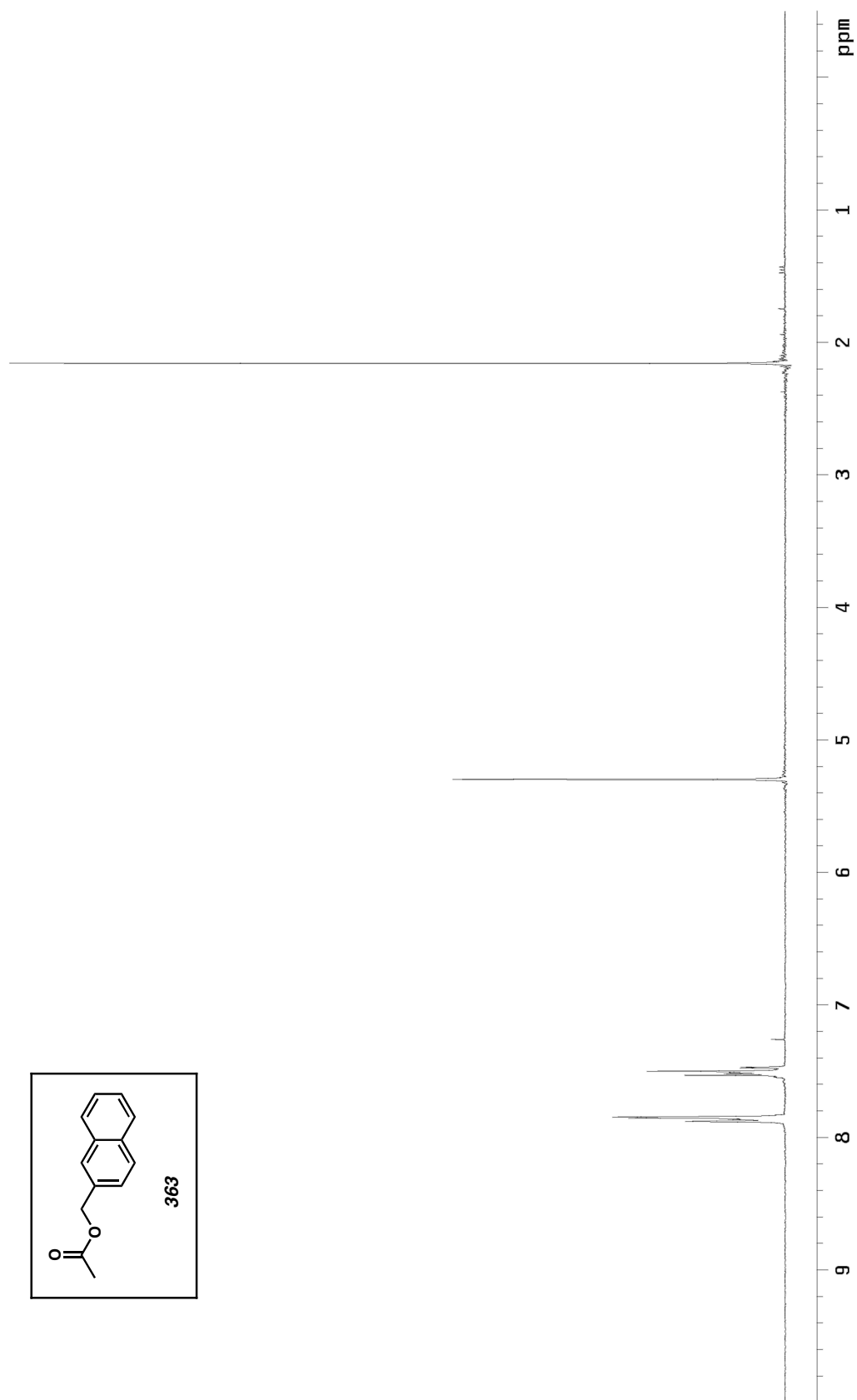


Figure A5.18. ^{13}C NMR spectrum (75 MHz, CDCl_3) of **345**.

Figure A5.19. ^1H NMR spectrum (300 MHz, CDCl_3) of **363**.

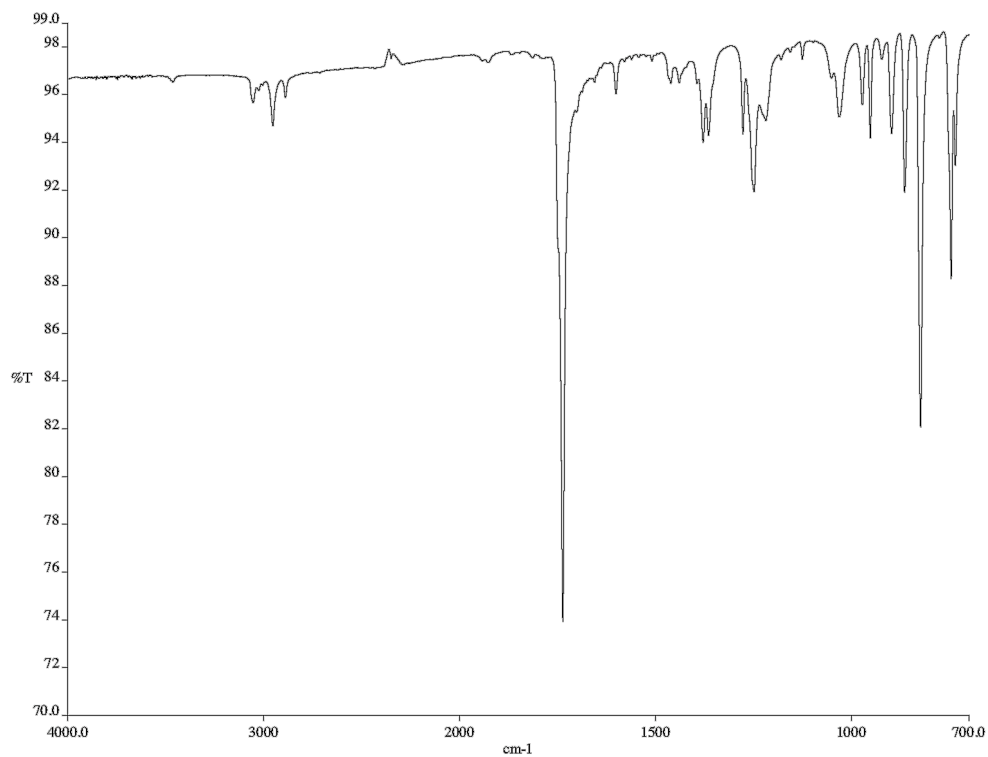


Figure A5.20. Infrared spectrum (neat film/NaCl) of **363**.

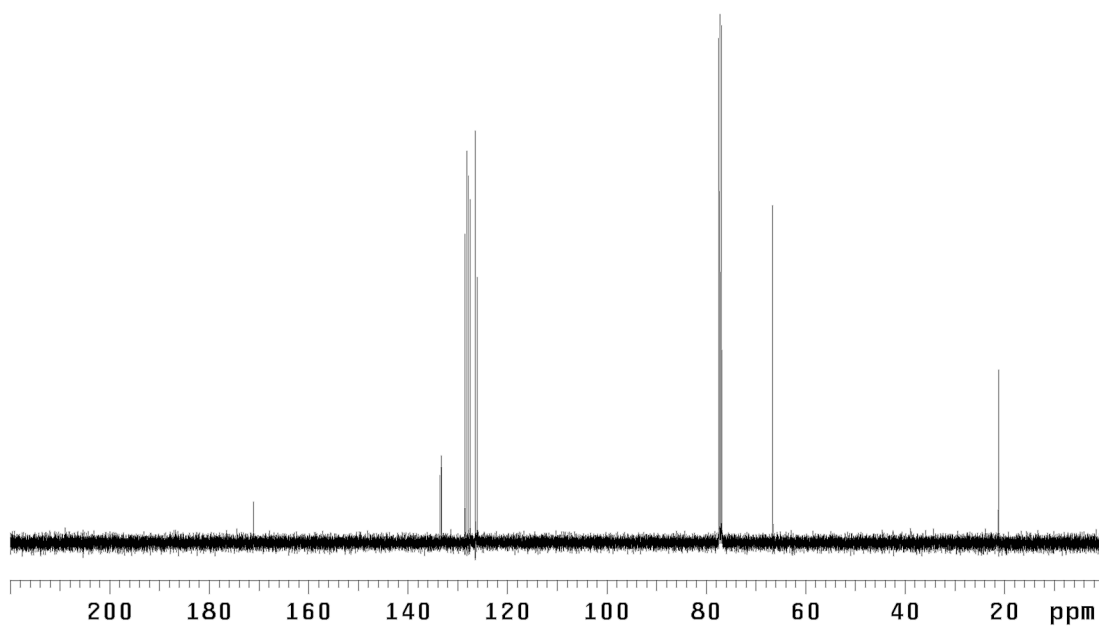
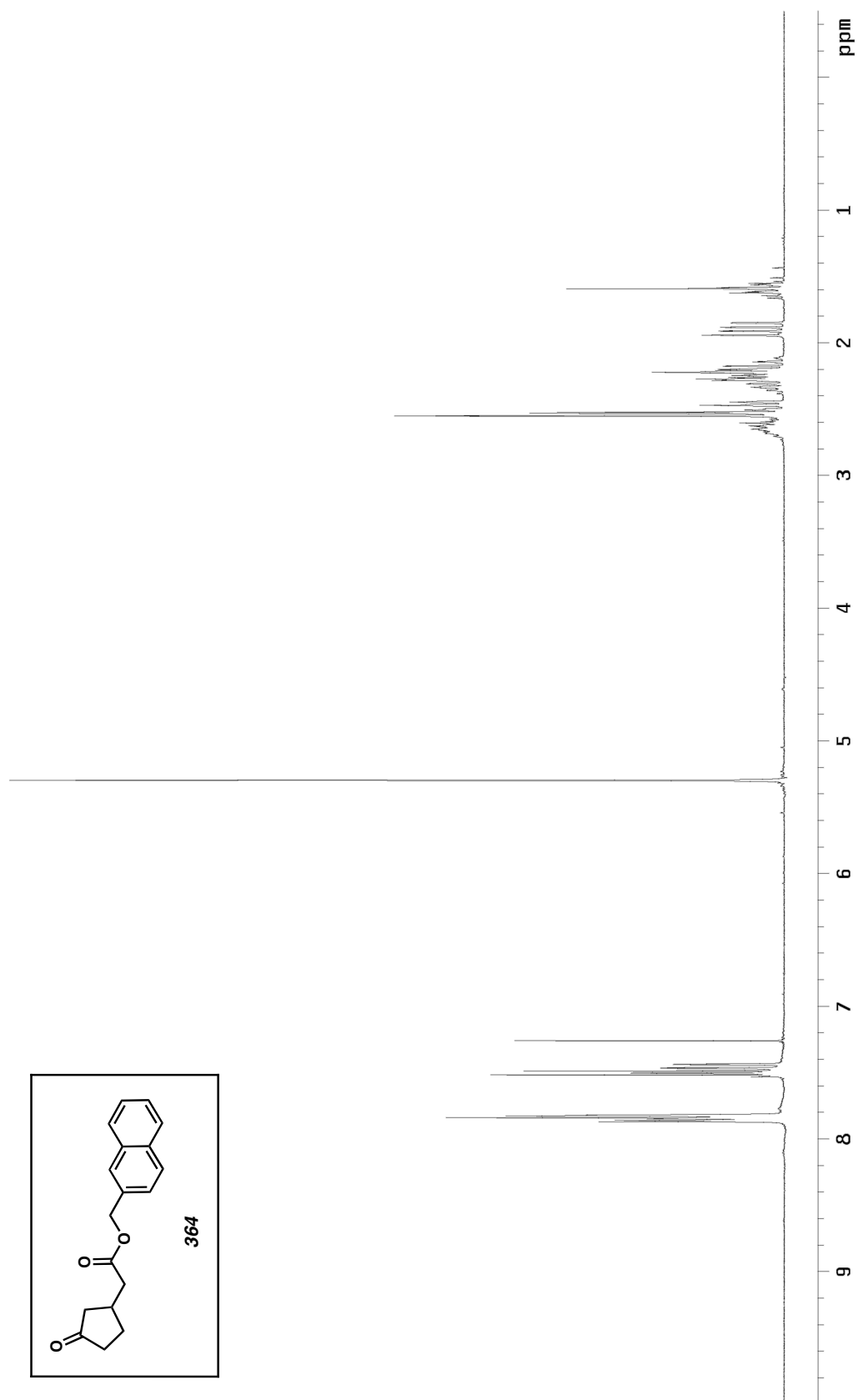


Figure A5.21. ¹³C NMR spectrum (125 MHz, CDCl₃) of **363**.

Figure A5.22. ^1H NMR spectrum (300 MHz, CDCl_3) of **364**.

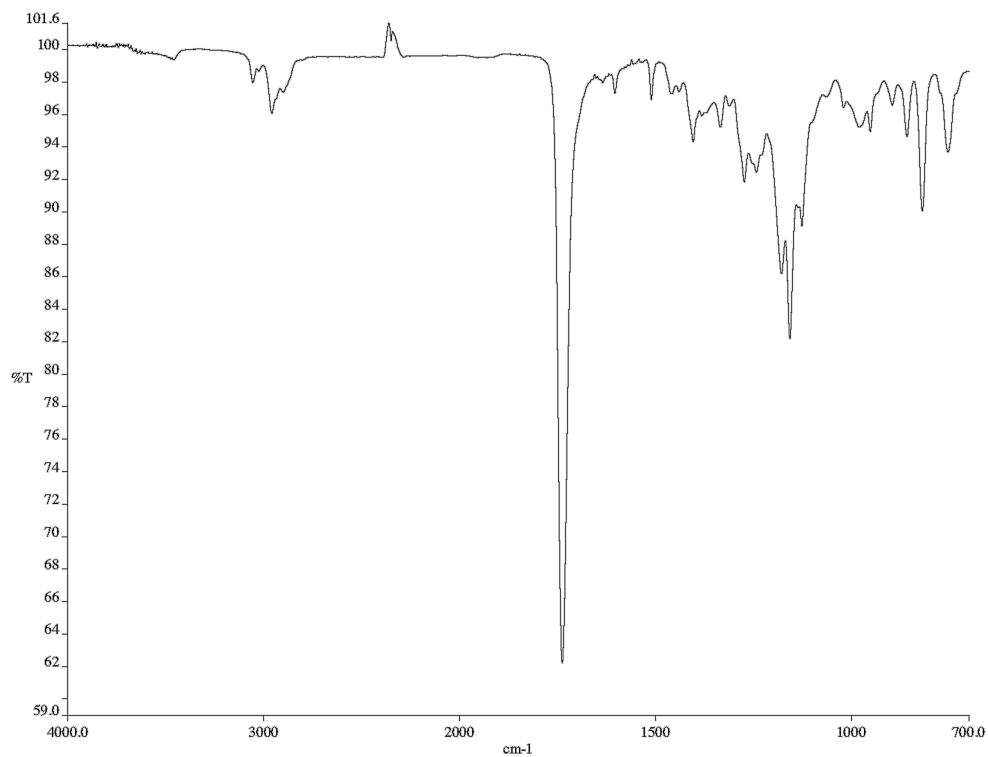


Figure A5.23. Infrared spectrum (neat film/NaCl) of **364**.

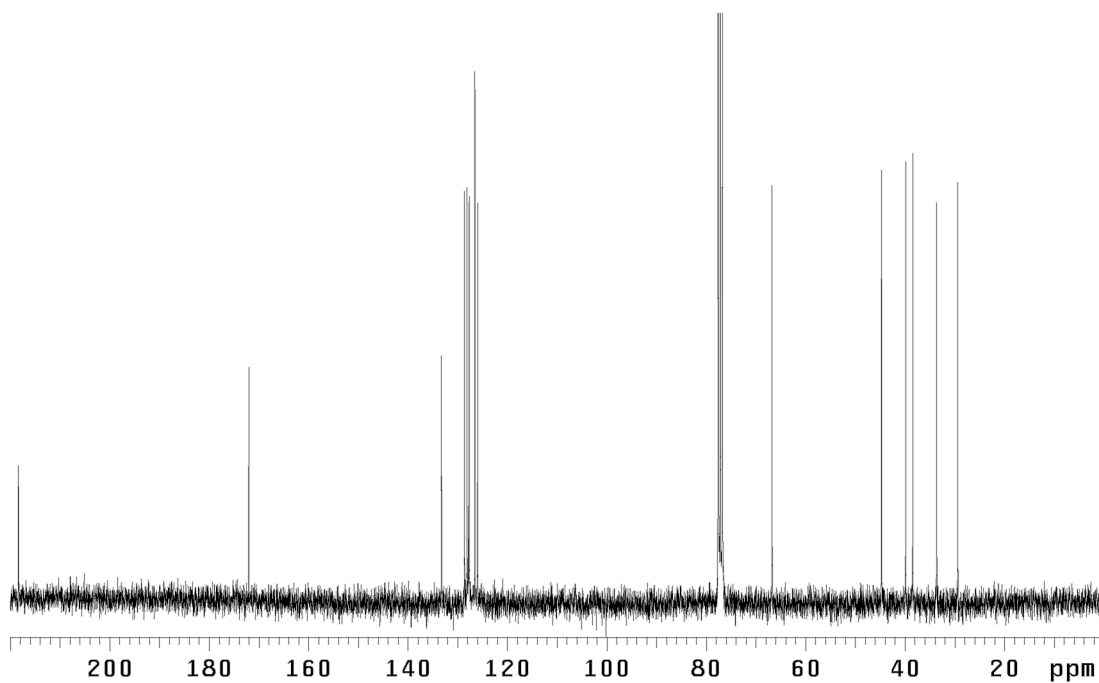


Figure A5.24. ¹³C NMR spectrum (75 MHz, CDCl₃) of **364**.

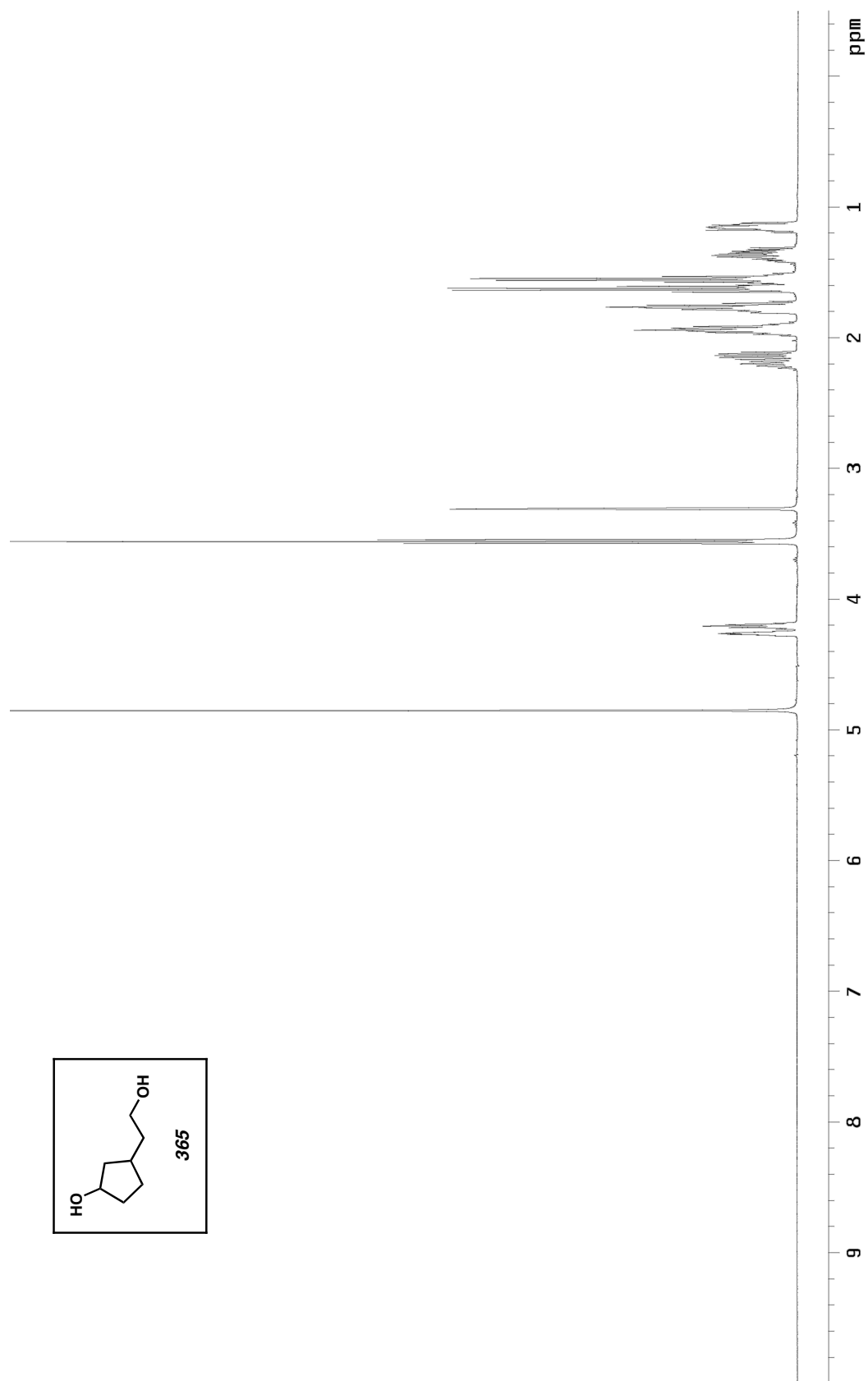


Figure A5.25. ^1H NMR spectrum (500 MHz, CD_3OD) of 365.

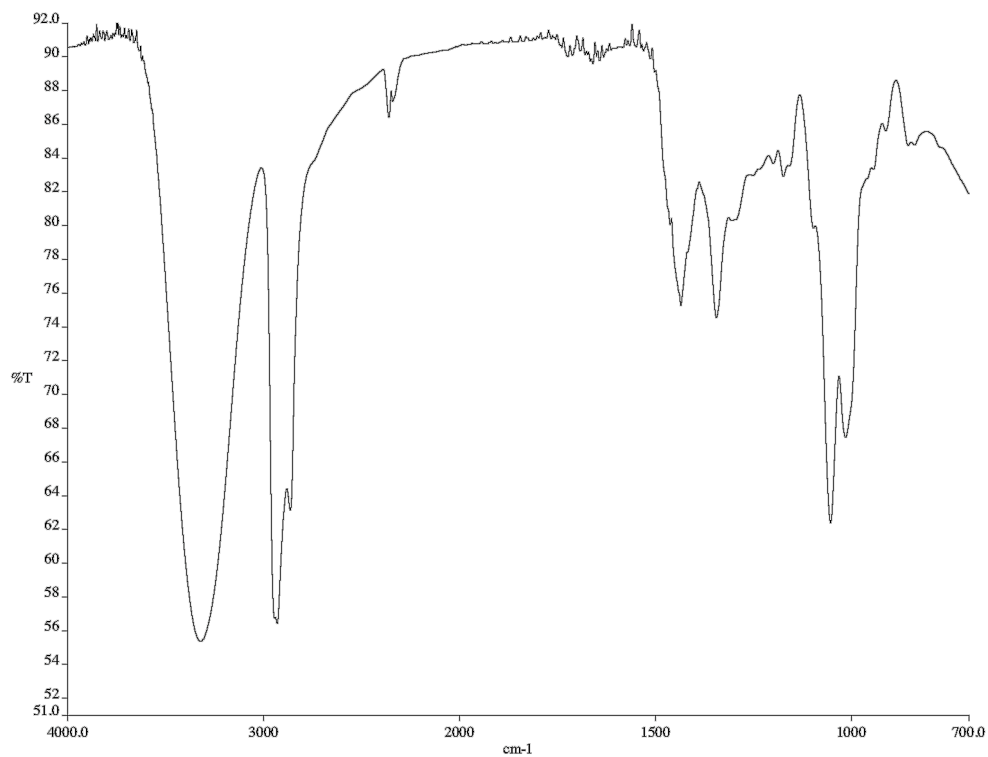


Figure A5.26. Infrared spectrum (neat film/NaCl) of **365**.

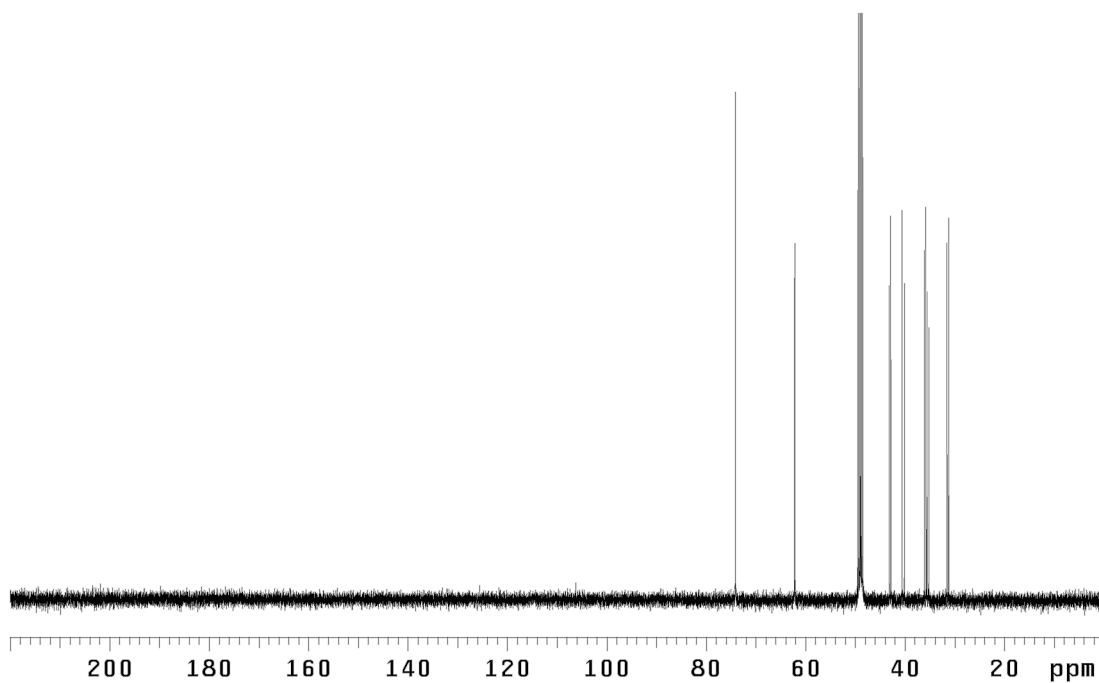
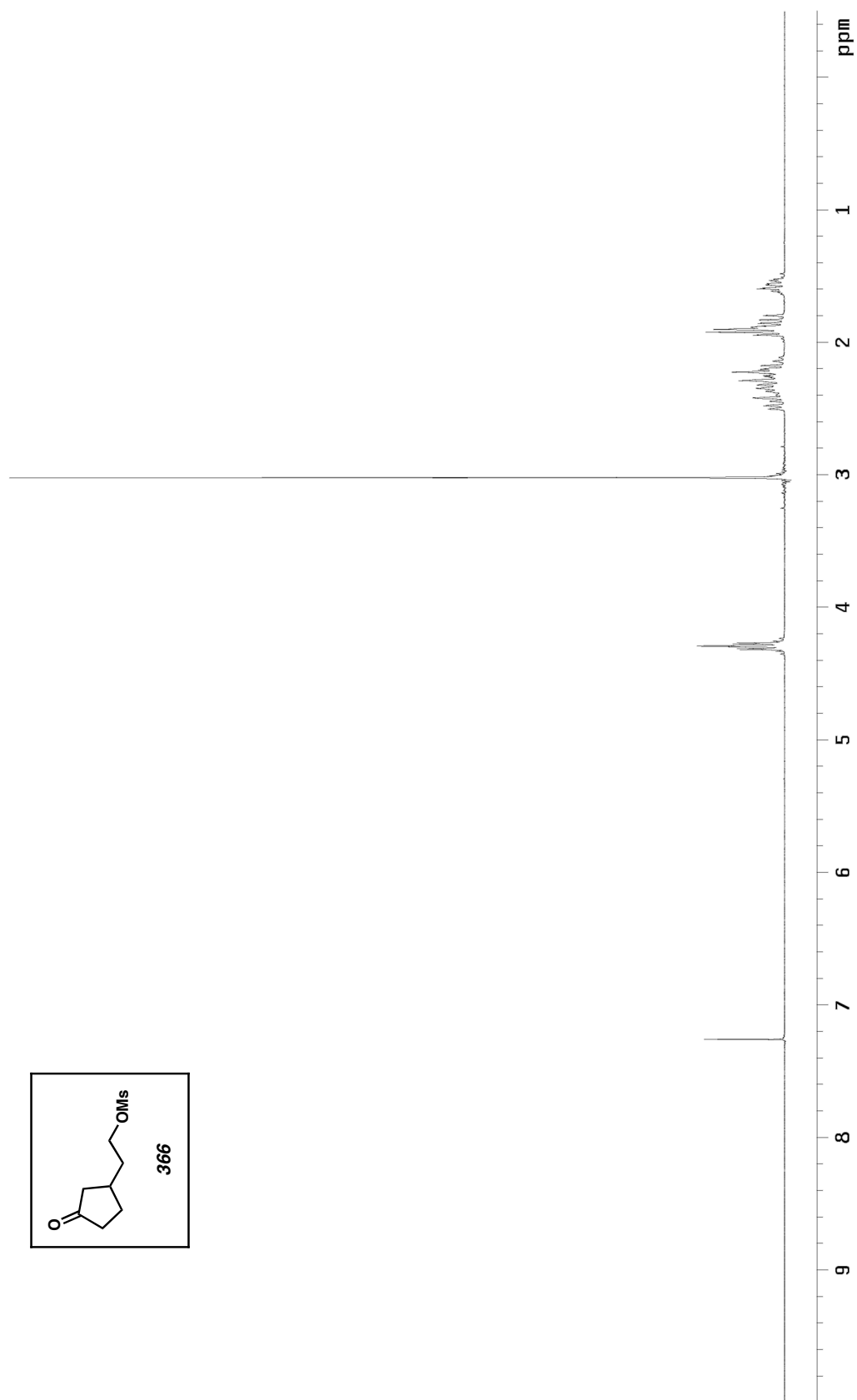


Figure A5.27. ¹³C NMR spectrum (125 MHz, CD₃OD) of **365**.

Figure A5.28. ^1H NMR spectrum (300 MHz, CDCl_3) of **366**.

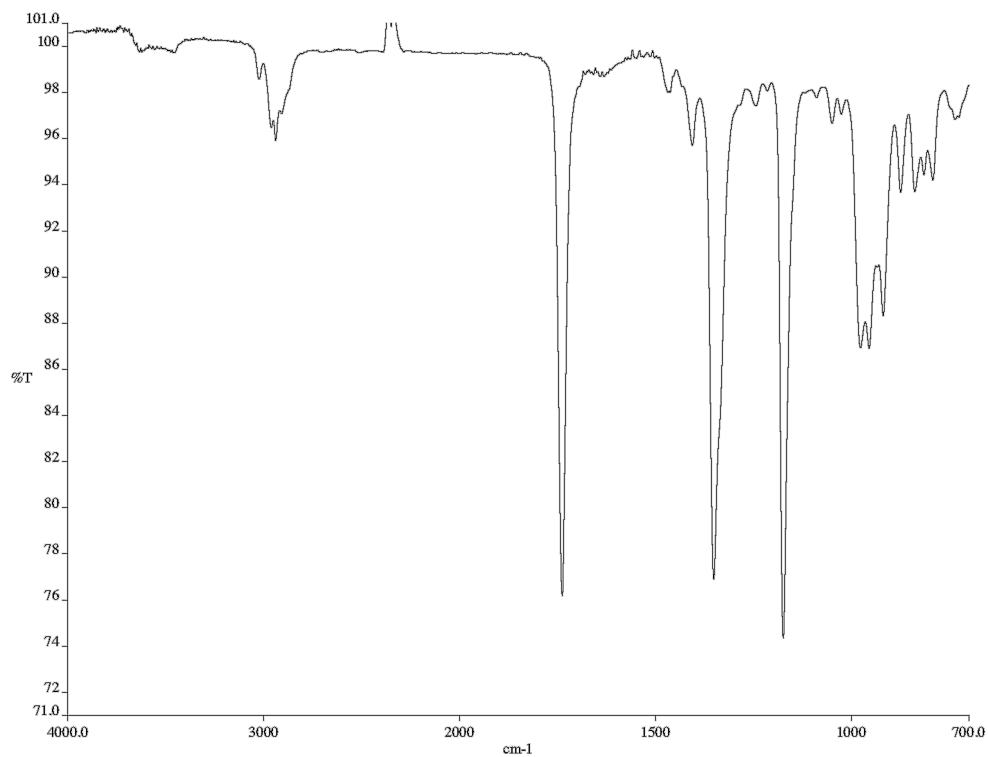


Figure A5.29. Infrared spectrum (neat film/NaCl) of **366**.

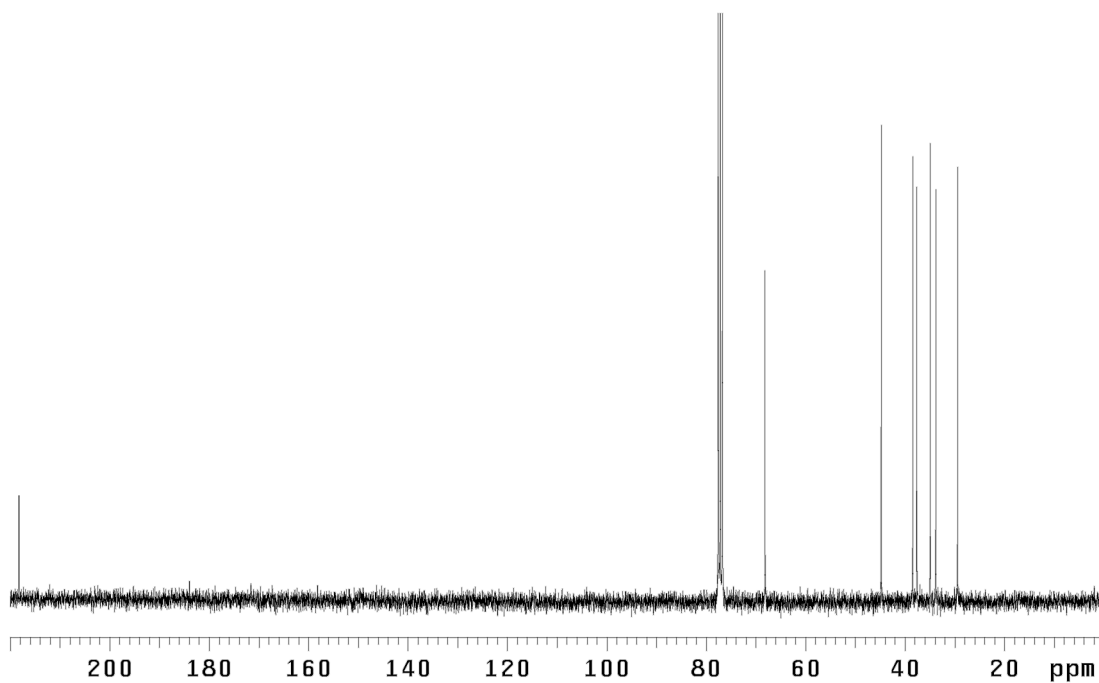
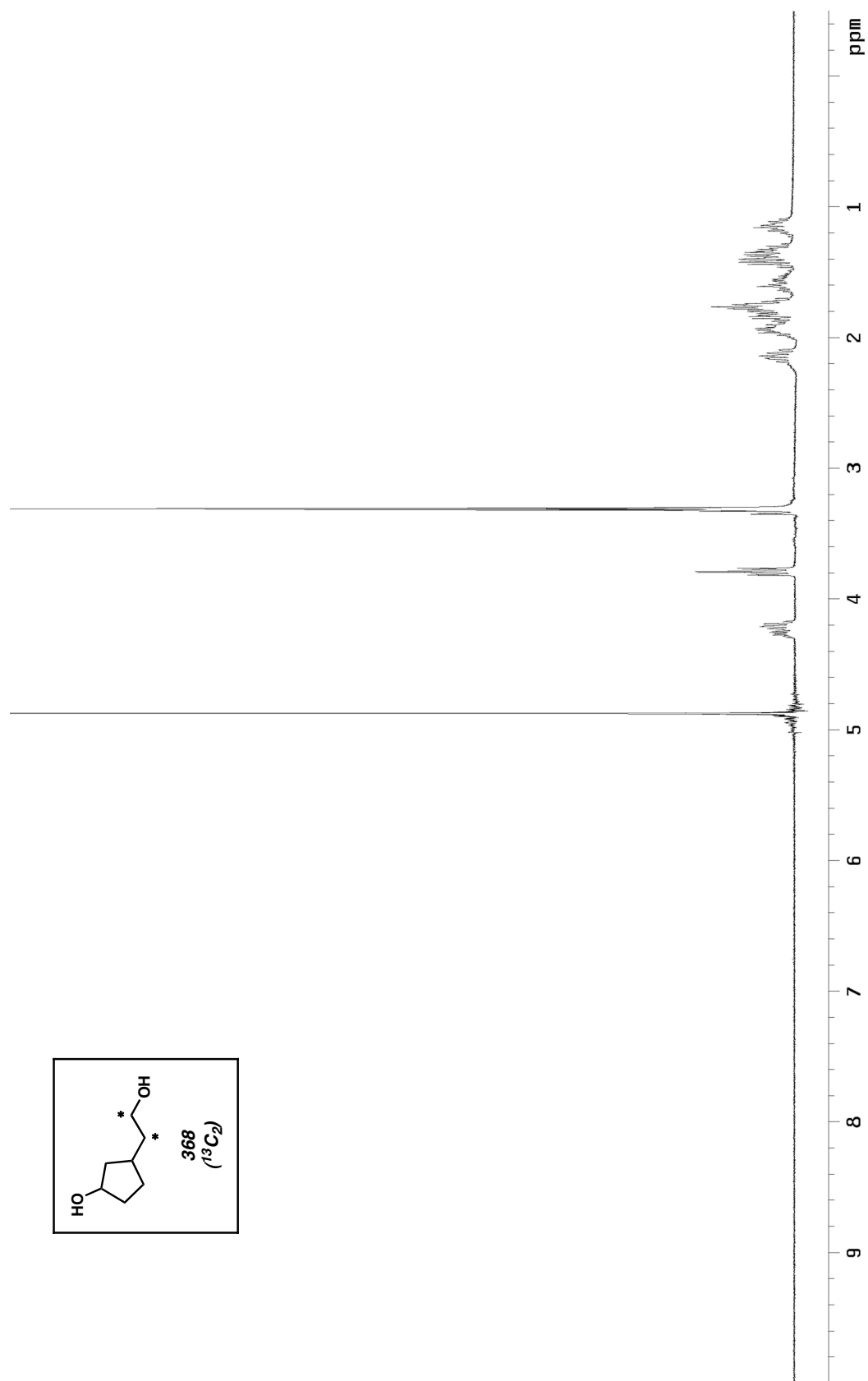


Figure A5.30. ¹³C NMR spectrum (75 MHz, CDCl₃) of **366**.

Figure A5.31. ^1H NMR spectrum (300 MHz, CD_3OD) of 368.

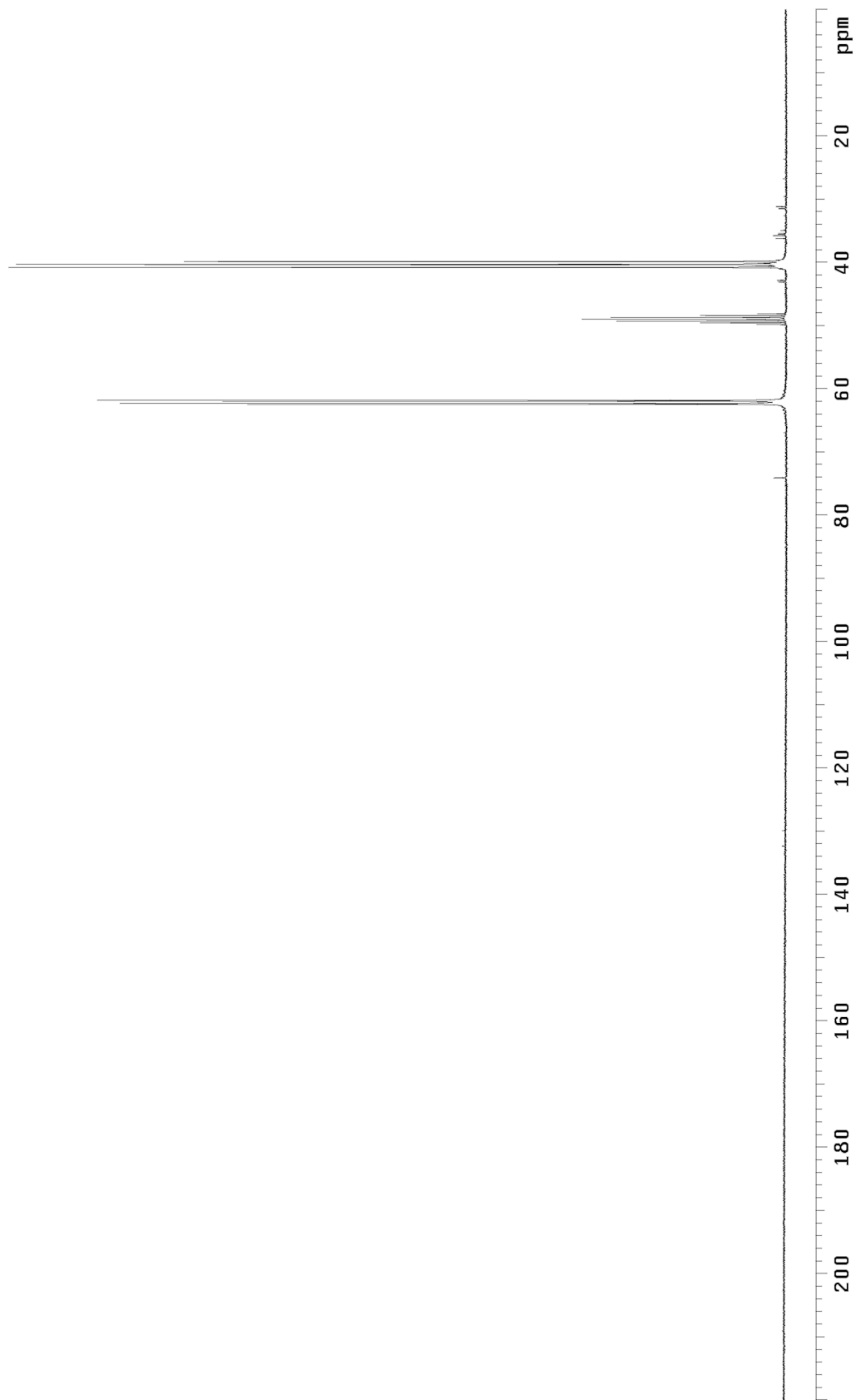
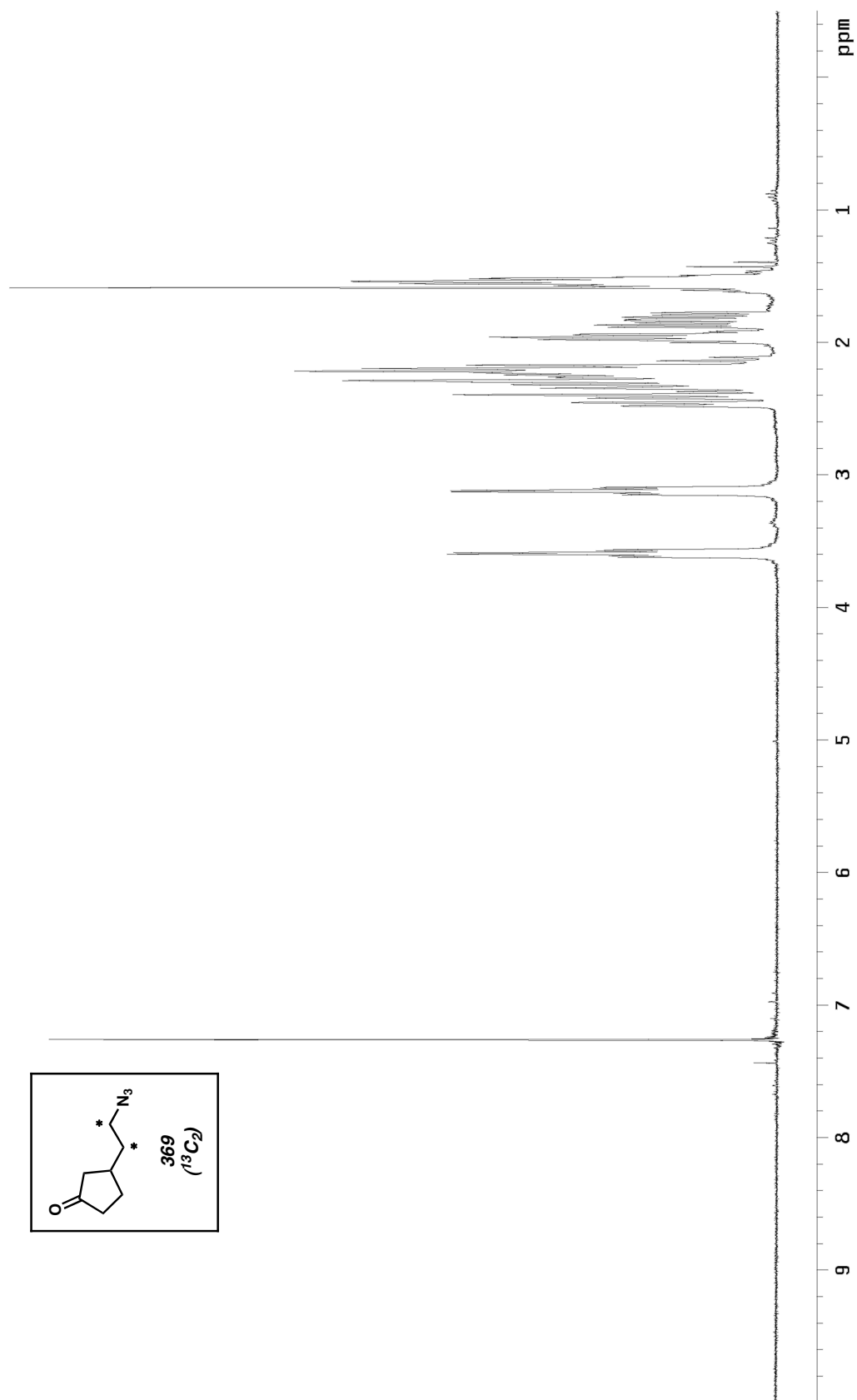


Figure A5.32. ^{13}C NMR spectrum (75 MHz, CD_3OD) of **368**.

Figure A5.33. ^1H NMR spectrum (300 MHz, CDCl_3) of **369**.

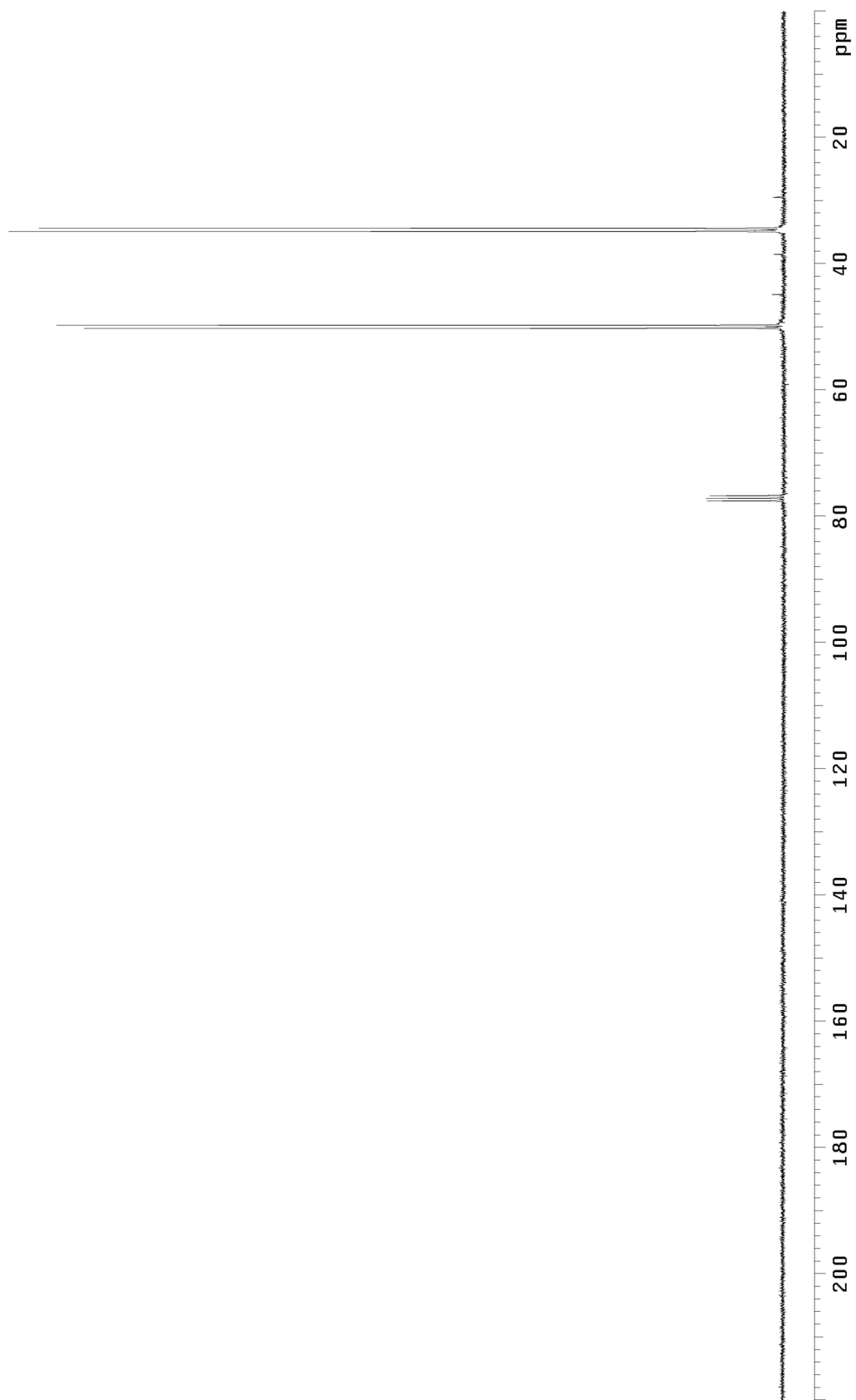
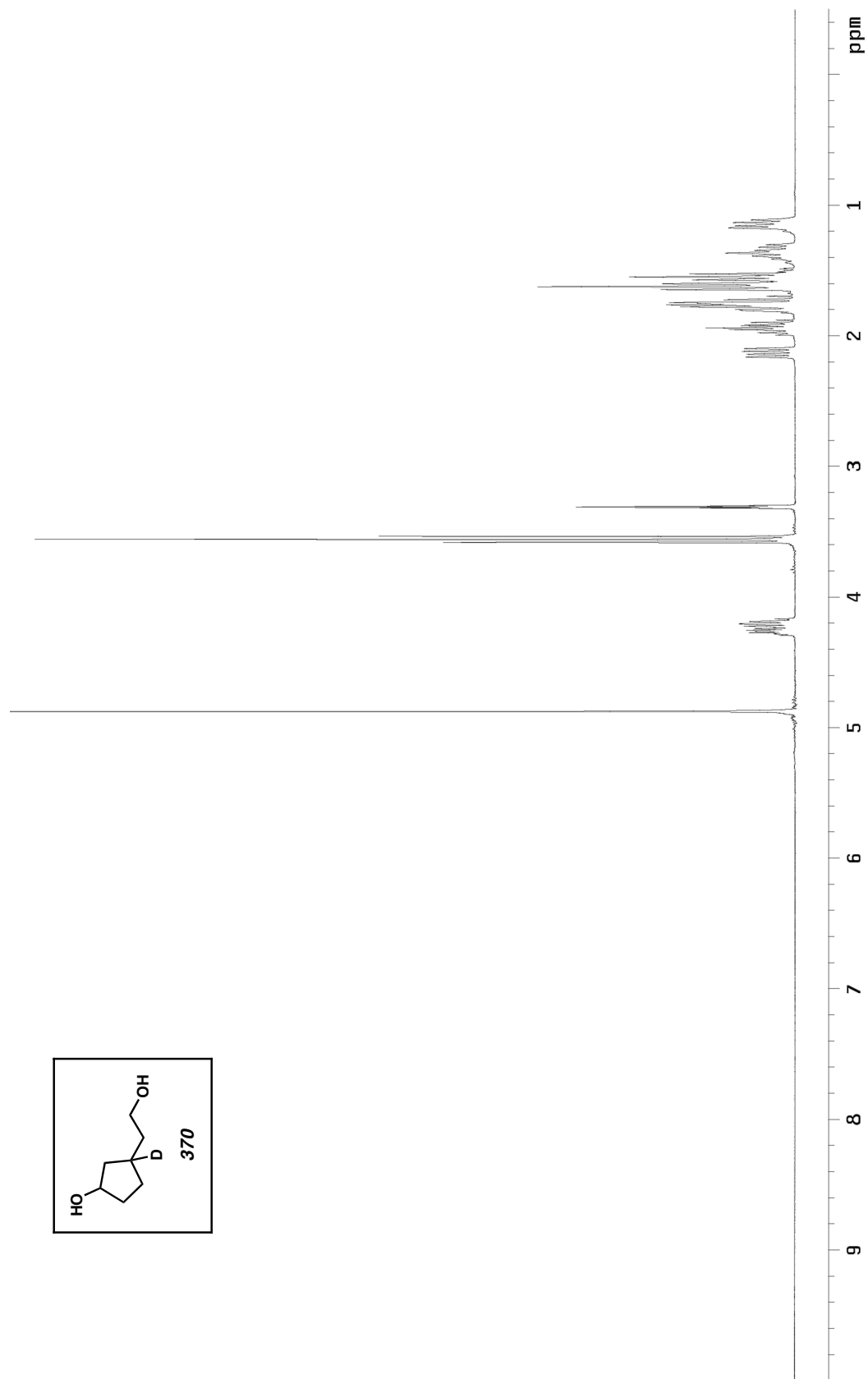


Figure A5.34. ^{13}C NMR spectrum (75 MHz, CDCl_3) of **369**.

Figure A5.35. ^1H NMR spectrum (300 MHz, CD_3OD) of **370**.

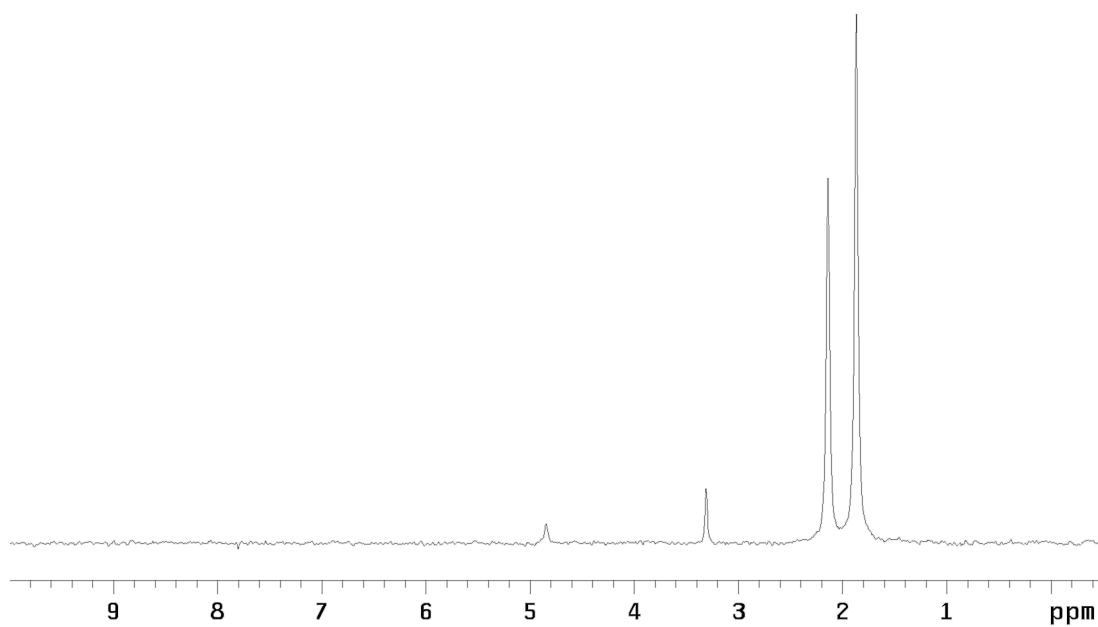


Figure A5.36. ^2H NMR spectrum (76 MHz, CH_3OH) of **370**.

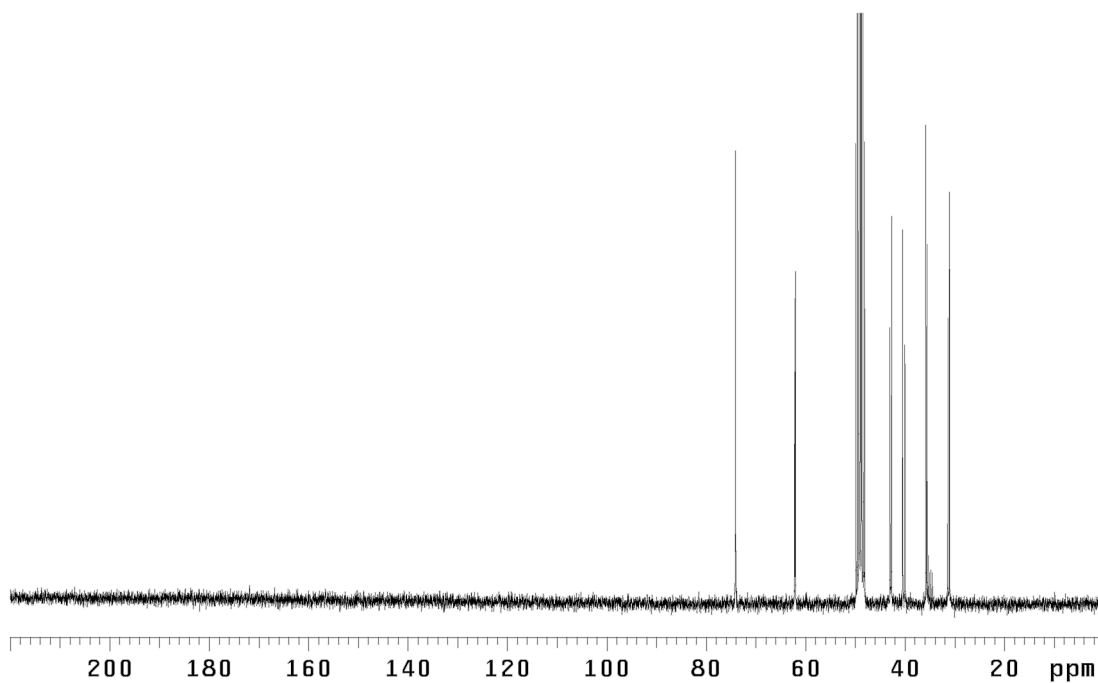
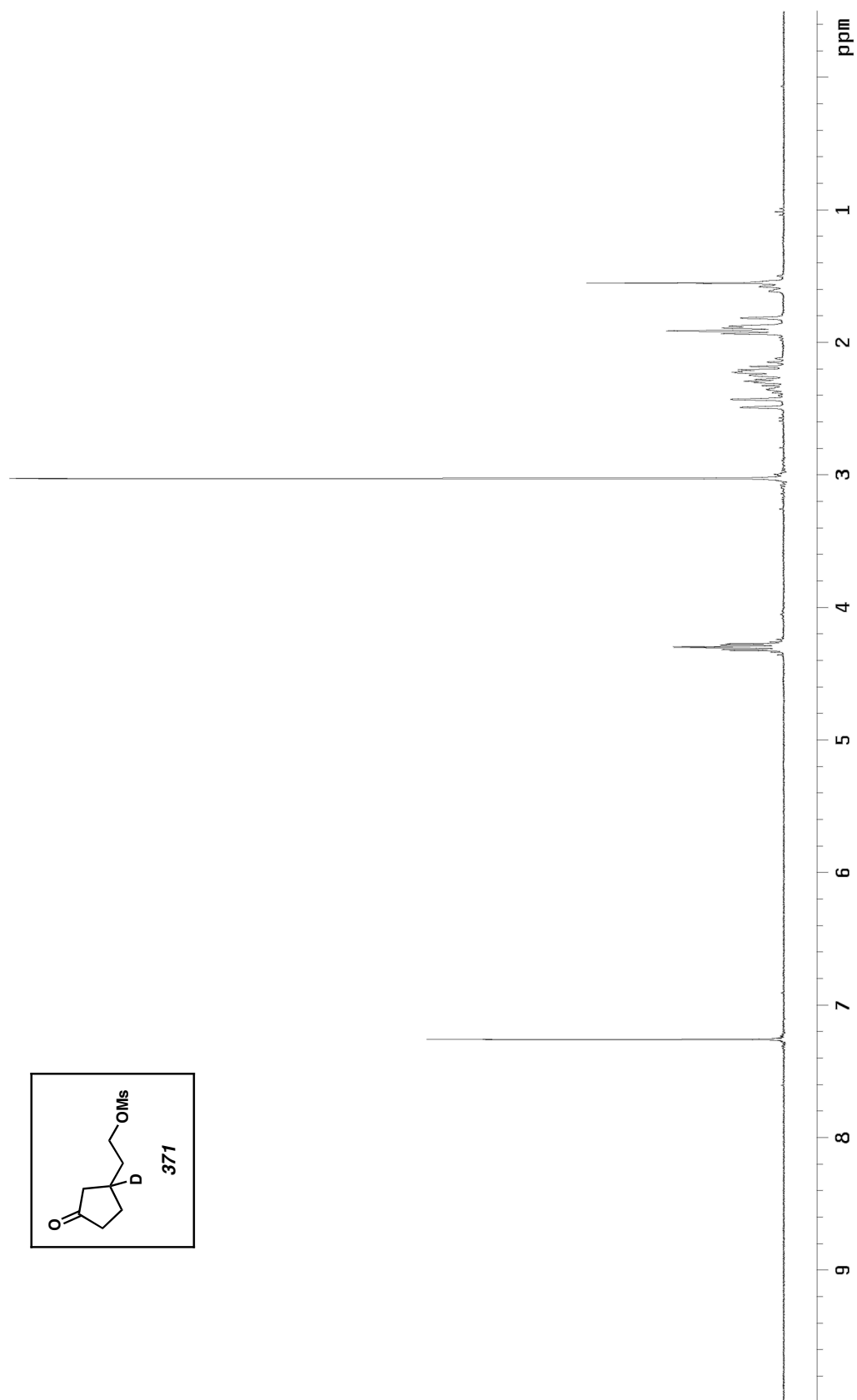


Figure A5.37. ^{13}C NMR spectrum (75 MHz, CD_3OD) of **370**.

Figure A5.38. ¹H NMR spectrum (300 MHz, CDCl₃) of **371**.

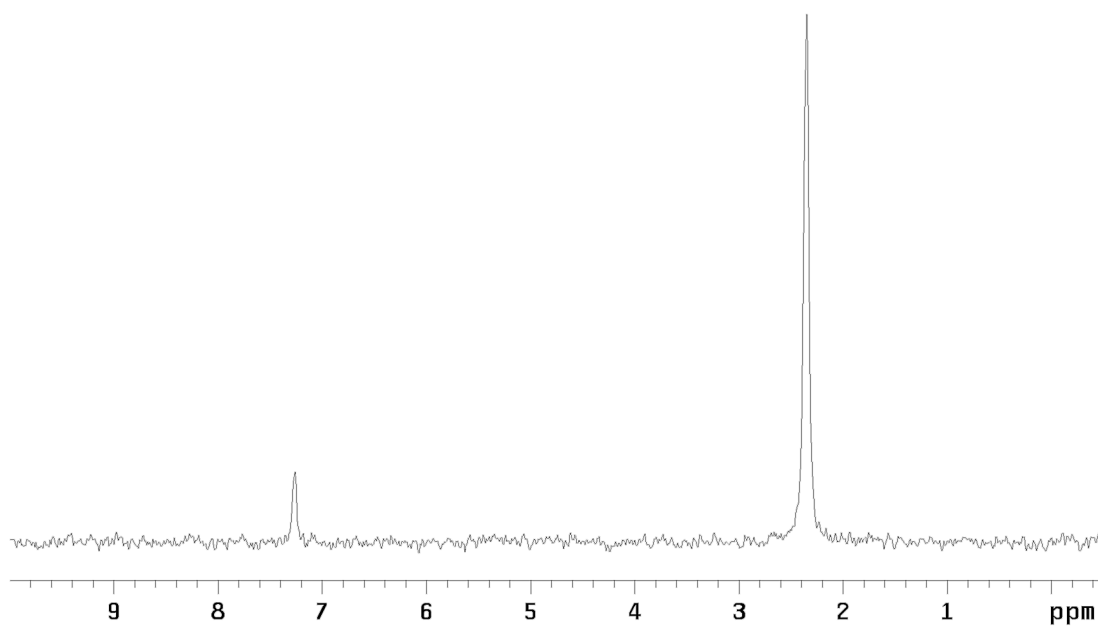


Figure A5.39. ^2H NMR spectrum (76 MHz, CHCl_3) of **371**.

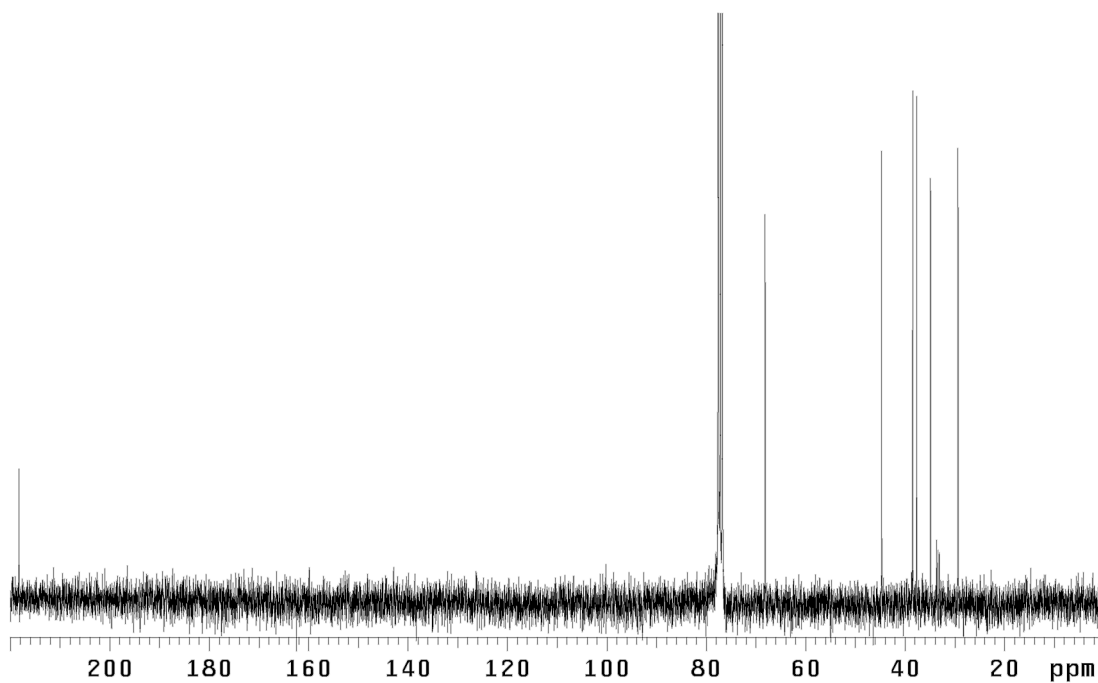
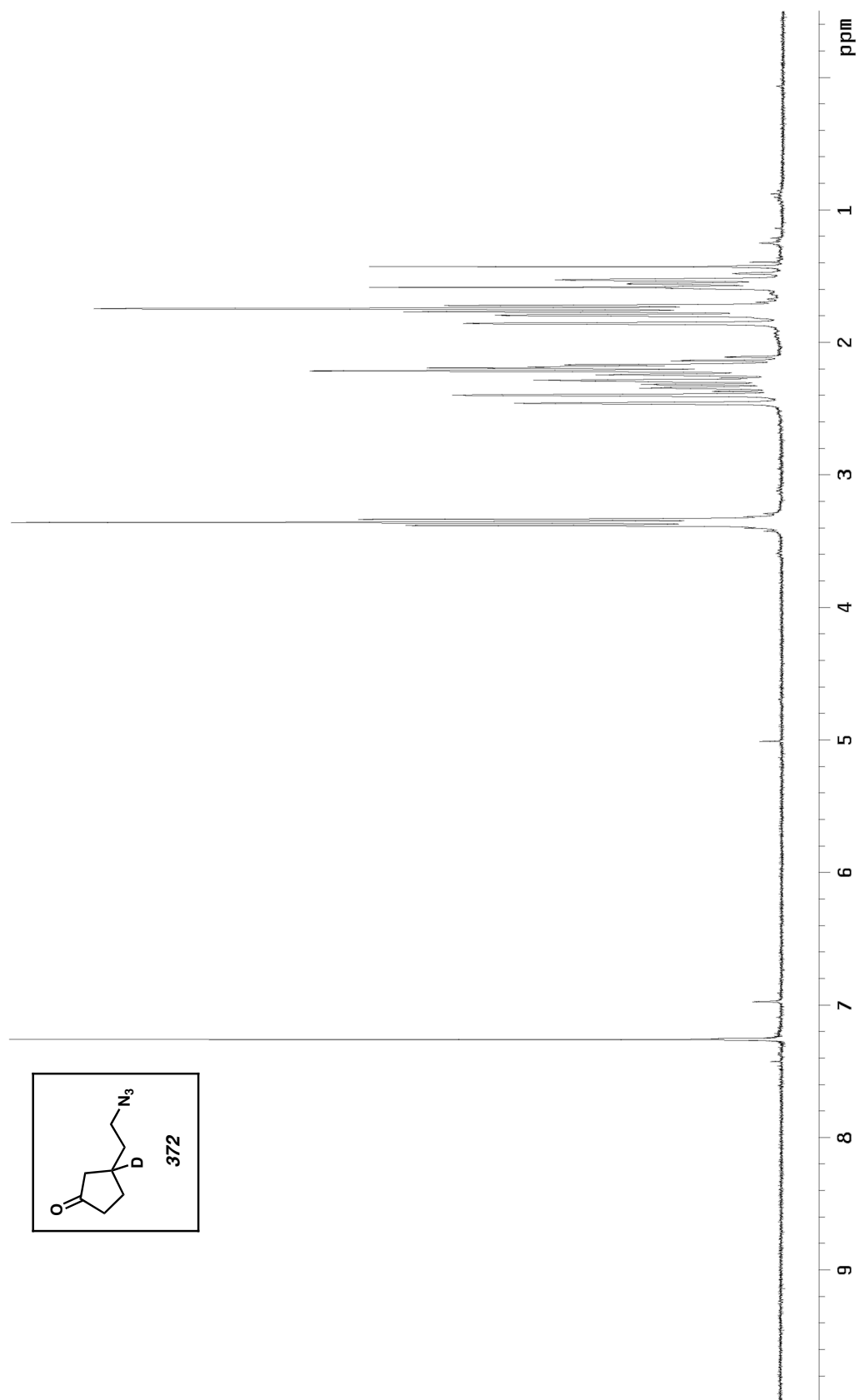


Figure A5.40. ^{13}C NMR spectrum (75 MHz, CDCl_3) of **371**.

Figure A5.41. ^1H NMR spectrum (300 MHz, CDCl_3) of 372.

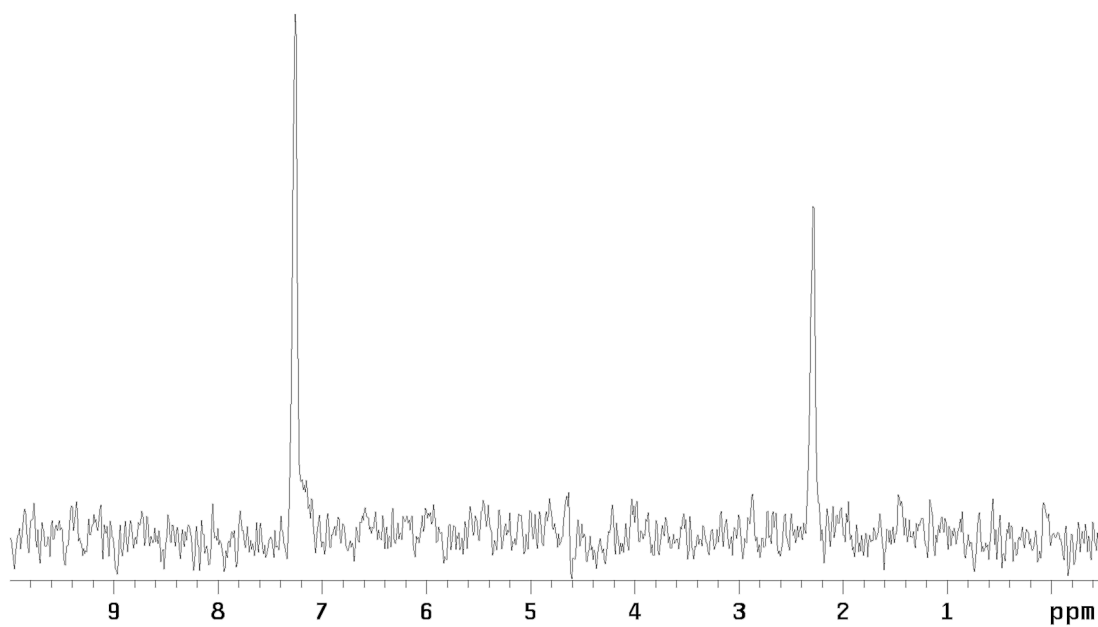


Figure A5.42. ^2H NMR spectrum (76 MHz, CHCl_3) of **372**.

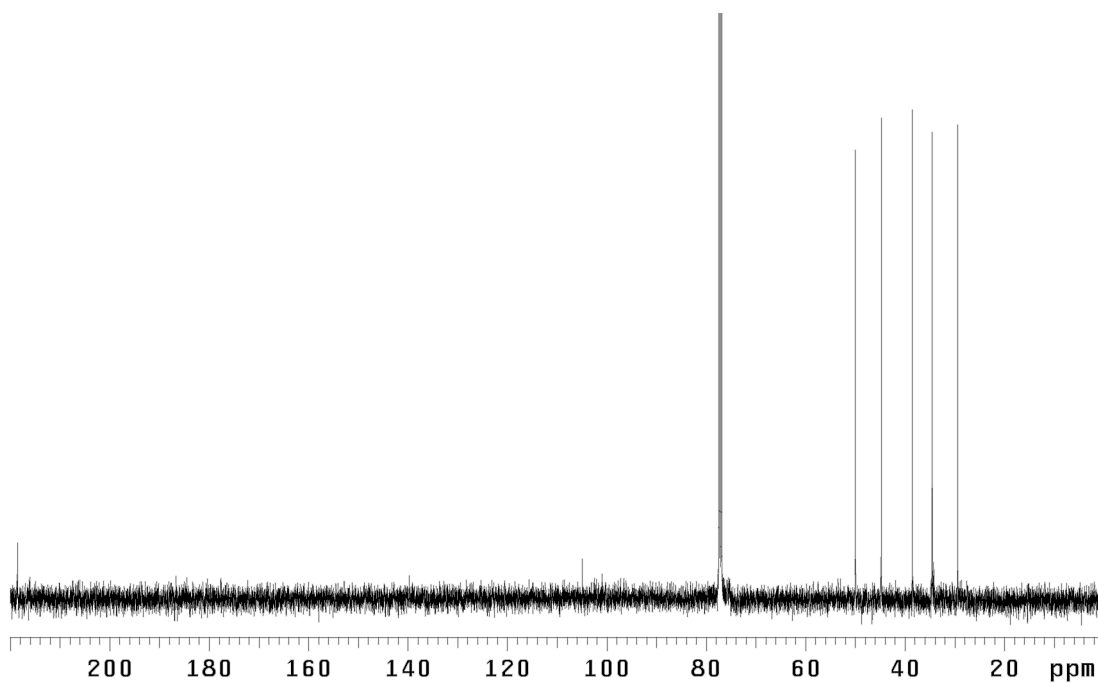


Figure A5.43. ^{13}C NMR spectrum (125 MHz, CDCl_3) of **372**.

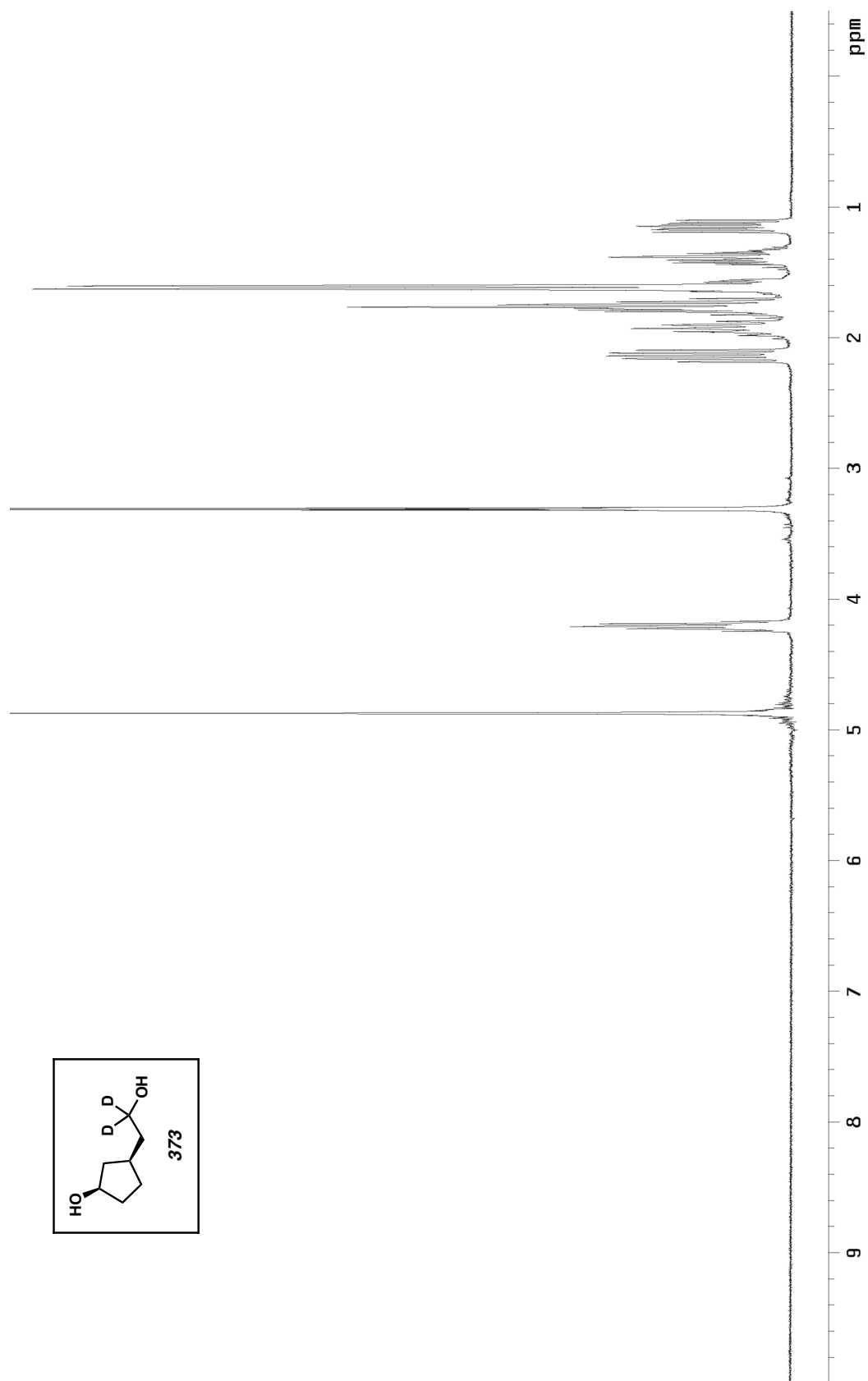


Figure A5.44. ^1H NMR spectrum (300 MHz, CD_3OD) of 373.

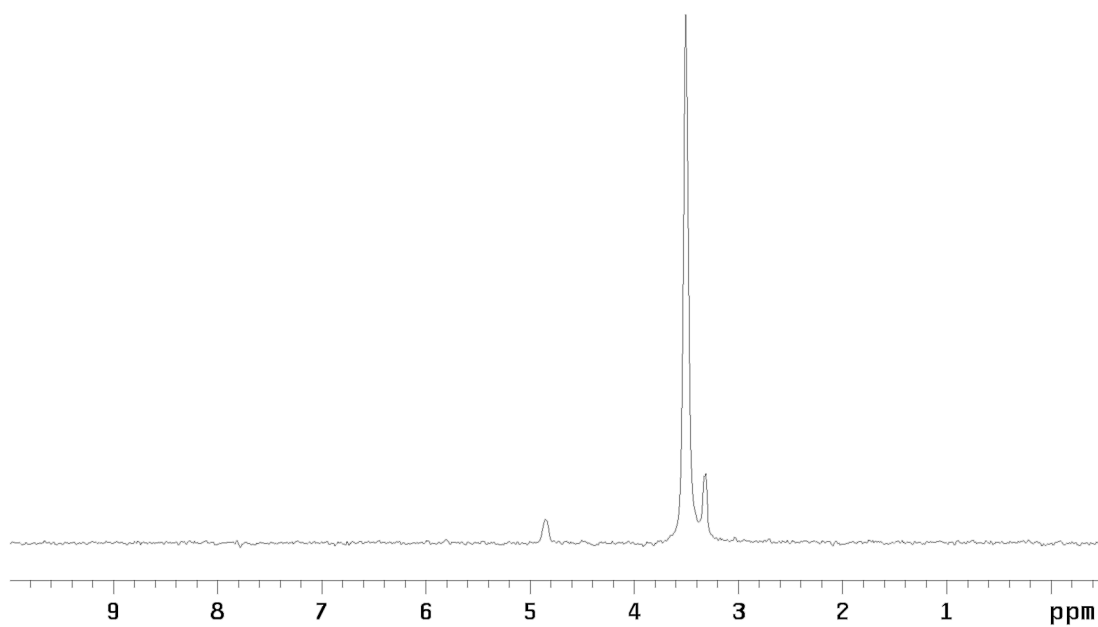


Figure A5.45. ^2H NMR spectrum (76 MHz, CH_3OH) of **373**.

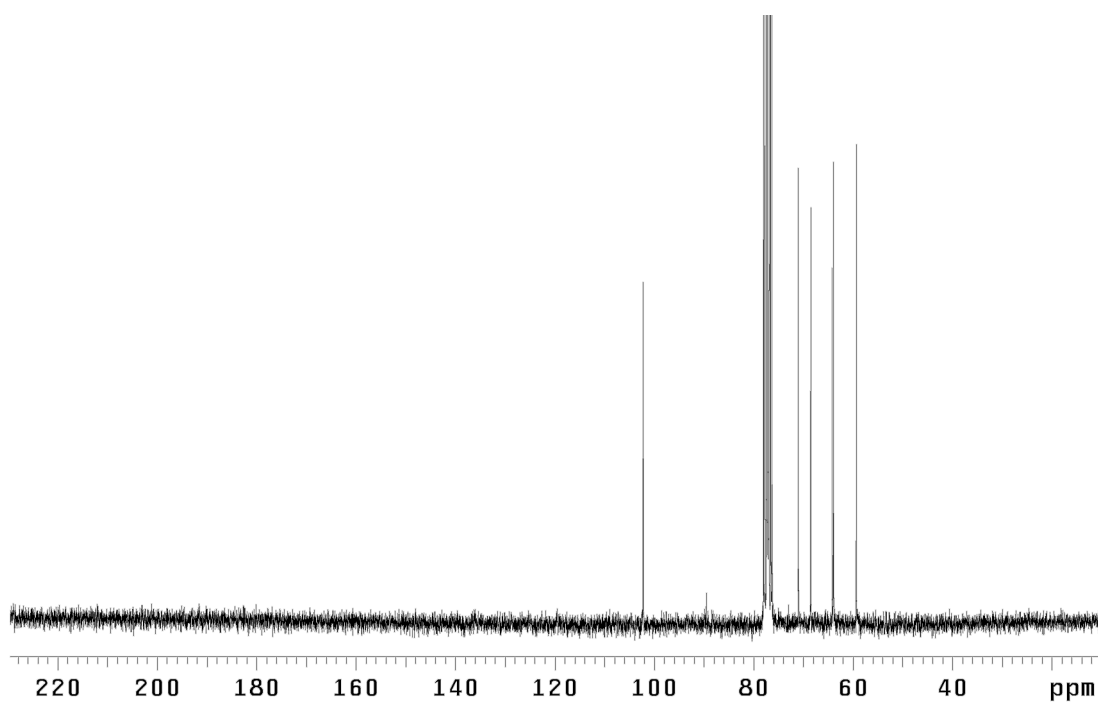
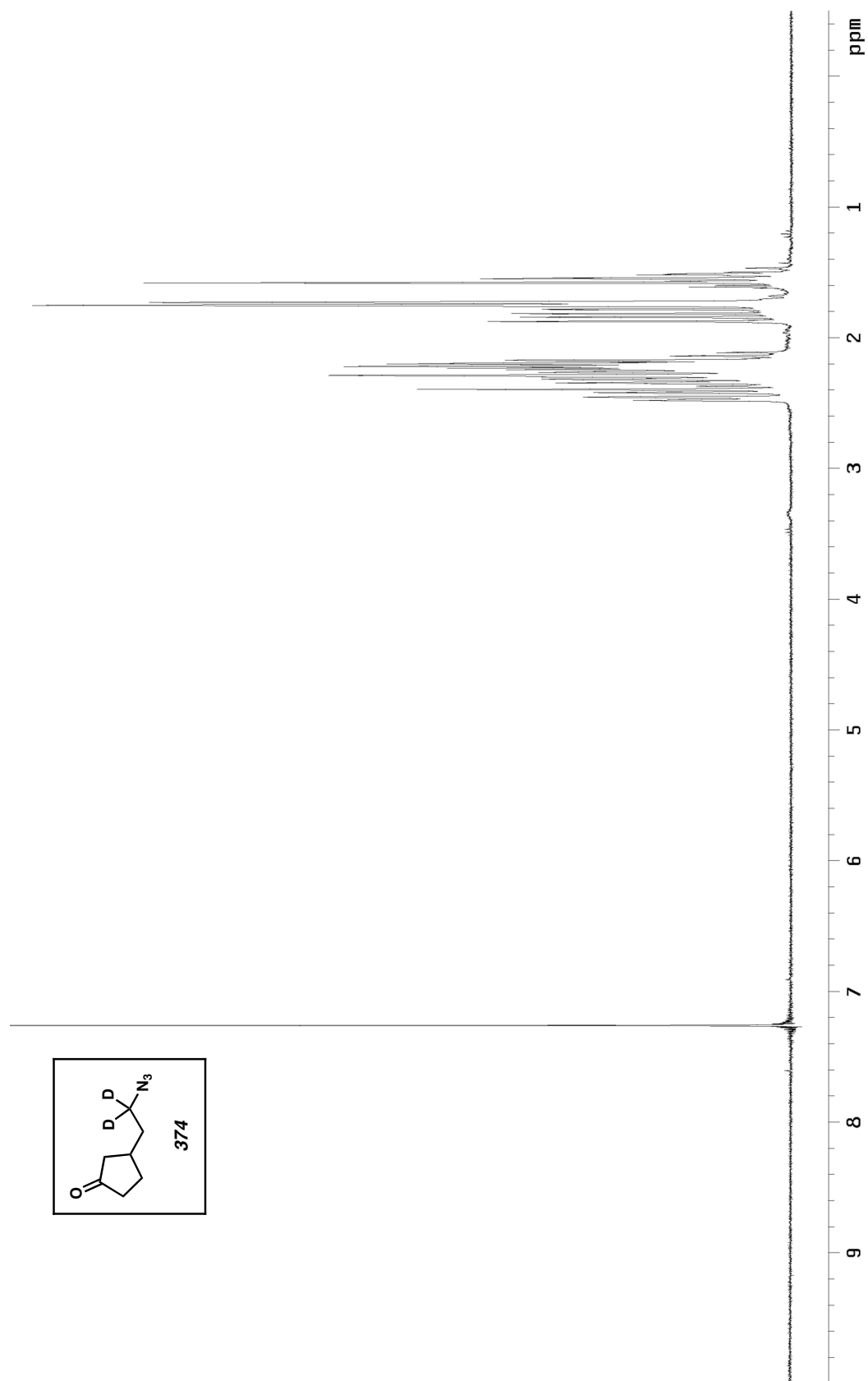


Figure A5.46. ^{13}C NMR spectrum (75 MHz, CD_3OD) of **373**.

Figure A5.47. ^1H NMR spectrum (300 MHz, CDCl_3) of 374.

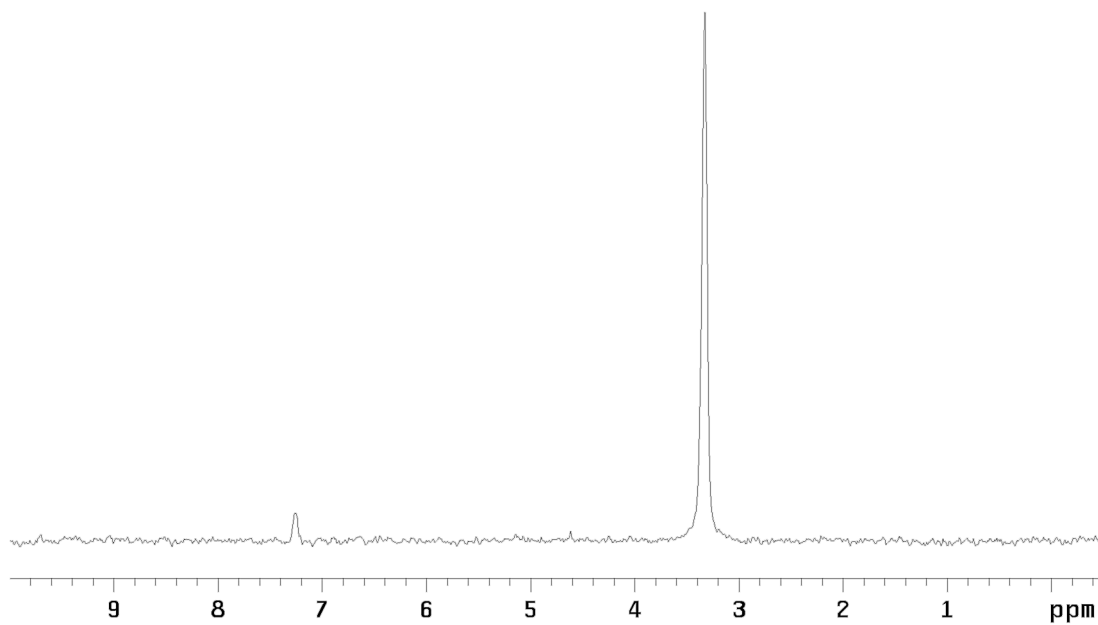


Figure A5.48. ^2H NMR spectrum (76 MHz, CHCl_3) of **374**.

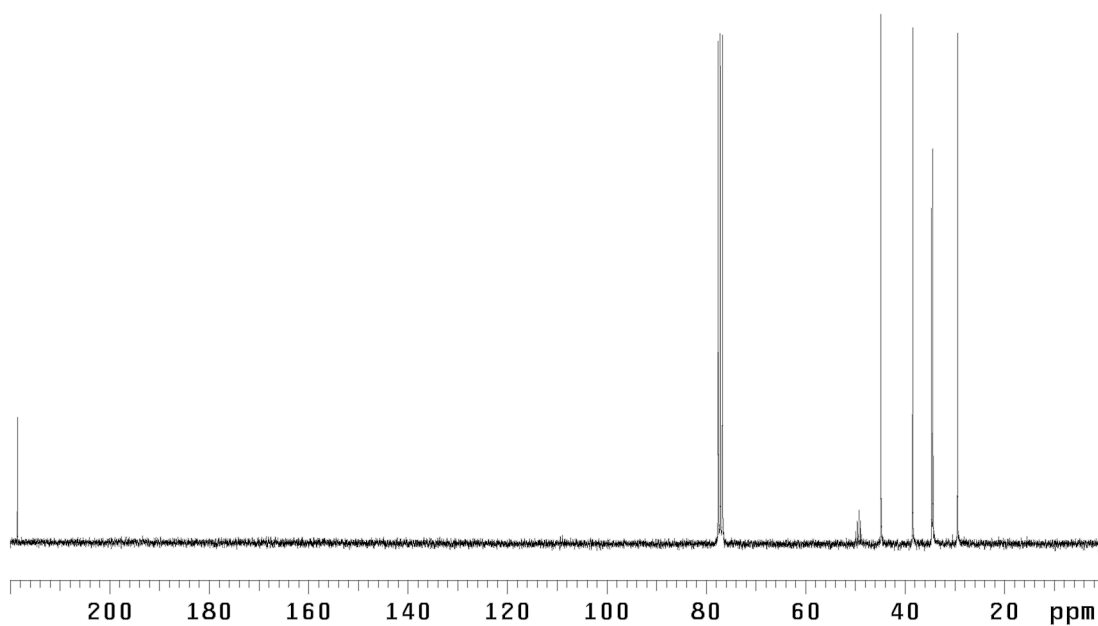


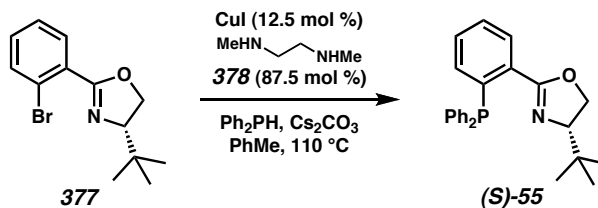
Figure A5.49. ^{13}C NMR spectrum (75 MHz, CDCl_3) of **374**.

APPENDIX 6

*An Improved and Highly Efficient Copper(I)- Catalyzed Preparation of (*S*)-*t*-Bu-PHOX*

A6.1 INTRODUCTION AND BACKGROUND

Phosphinooxazoline (PHOX) ligands¹ have emerged as versatile chiral scaffolds for an array of transition-metal-catalyzed processes. As an important member of this class of P/N-chelates, (*S*)-*t*-Bu-PHOX (**55**)² has been critical to the development of palladium(0)-catalyzed decarboxylative alkylation³ and protonation⁴ technologies in our laboratory. Investigations of these methods prompted the synthesis of numerous PHOX derivatives.⁵ Ultimately, the efficacy of a copper(I) iodide-catalyzed diarylphosphine–aryl bromide coupling reported by Buchwald and co-workers⁶ enabled a mild and modular strategy toward the preparation of these useful ligands.^{3a,7} In this appendix, we detail our improvements to this coupling reaction that increase yields, reduce reagent quantities, and simplify purification.

Scheme A6.1.1. Original CuI-catalyzed coupling for the preparation of (*S*)-*t*-Bu-PHOX

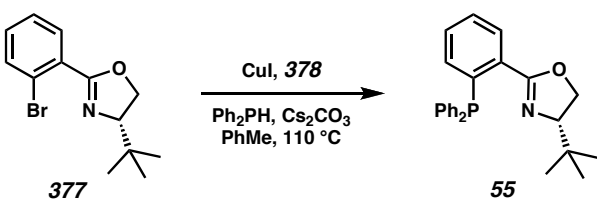
The Ullman-type coupling strategy has proven general for the preparation of a number of structurally and electronically diverse PHOX derivatives.^{7a} However, recent scale-up efforts of our optimal ligand, (*S*)-*t*-Bu-PHOX ((*S*)-**55**), to support applications in natural product total synthesis⁸ revealed a significant limitation to our standard Cu(I)-catalyzed coupling conditions. In particular, various coupling reactions failed to reach complete conversion (i.e., **377** → **55**), thus requiring tedious chromatographic purification. Upon consideration of our standard conditions, we identified several likely problematic factors for scale-up, including relatively high catalyst and ligand loadings, as well as excessive quantities of Cs₂CO₃ and diphenylphosphine. Due to the growing utility of this ligand in asymmetric catalysis,² and consequently, the synthesis of biologically relevant substances, we sought to improve these conditions to facilitate the large-scale preparation of **55**.

A6.2 REACTION OPTIMIZATION

Our efforts to maximize the reaction efficiency for the production of **55** first required a reliable coupling (Table A6.2.1, entry 1). We quickly recognized that it was essential to maintain vigorous stirring throughout the reaction,⁹ a straightforward task on smaller

scales but more difficult as quantities of heterogeneous solids increased. A successful coupling was observed as the CuI was reduced to 5 mol % (entries 2–4) to still provide complete conversions. Decreasing the equivalents of Ph₂PH and Cs₂CO₃ further improved conversion of **377** (entry 5). An increase in substrate concentration resulted in similar reactivity, enabling excellent results with 0.5 mol % CuI and a small excess of Ph₂PH in PhMe at 0.5 M (entries 6 and 7). Copper loadings can be further reduced to 0.1 mol %, although prolonged resulted in incomplete conversion (entry 8).

Table A6.2.1. Optimization of the coupling conditions



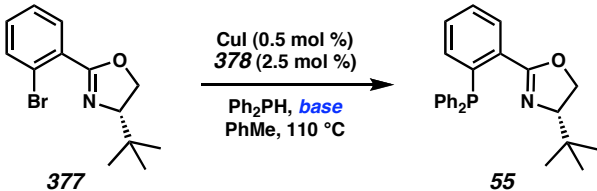
entry	CuI (mol%)	378 (mol%)	Ph ₂ PH (equiv)	Cs ₂ CO ₃ (equiv)	[PhMe] (M)	conversion ^a (%)
1	12.5	87.5	1.88	3.25	0.12	40–97
2	5	35	1.88	3.75	0.12	97
3	1	7	1.88	3.75	0.12	>99
4	0.5	3.5	1.88	3.75	0.12	>99
5	1	5	1.5	1.88	0.12	98
6	1	5	1.25	1.5	0.25	97
7	0.5	2.5	1.25	1.5	0.50	>99
8	0.1	0.5	1.25	1.5	0.50	98

^a Conversion measured by ¹H NMR analysis of crude reaction filtrates after 6–16 h.

With our optimized conditions in hand, we examined several common inorganic bases to determine their utility for this coupling.¹⁰ Standard use of Cs₂CO₃ produced excellent conversions and high yields of **55** on a variety of reaction scales (Table A6.2.2, entries 1 and 2). Surprisingly, other carbonates such as Li₂CO₃ and Na₂CO₃ were

ineffective (entries 3 and 4). Good reactivities were observed for both K_2CO_3 (entries 5 and 6) and K_3PO_4 (entry 7), however lower conversions were achieved.

Table A6.2.2. Inorganic base screen



entry ^a	base	time (h)	conversion (%)	yield (%) ^b
1	Cs_2CO_3	21	>99	94
2 ^c	Cs_2CO_3	21	>99	91
3	Li_2CO_3	24	0	—
4	Na_2CO_3	24	0	—
5	K_2CO_3	24	94	68
6 ^d	K_2CO_3	24	97	72
7	K_3PO_4	24	71	55

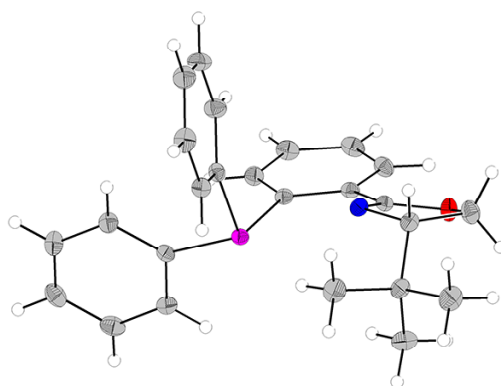
^a Reactions performed at 2.5 mmol of **378** using 1.25 equiv of Ph_2PH and 1.5 equiv of base in PhMe (0.5 M). ^b Isolated yield. ^c Performed on 20 mmol. ^d With 3 equiv of base.

A6.3 CRYSTALLIZATION AND IMPROVED PURIFICATION

During the course of our investigations, we have obtained numerous reaction filtrates composed of varying mixtures of **55** and **377** (e.g., entries 5–7, Table A6.2.2). The previous combination of these two chromatographically similar compounds necessitated difficult column purification. In our search for an alternative purification method, we fortuitously discovered that acetonitrile promotes the rapid and selective crystallization of **55** as large blocks. Application of this procedure to impure samples enabled facile recovery of **55** (yields obtained for entries 5–7, Table A6.2.2) and produced high quality crystals for X-ray analysis (Figure A6.3.1).¹¹ In addition to the new purification

procedure, our newly optimized conditions employing 0.5 mol % catalyst facilitate complete conversion of **377** (entries 1 and 2, Table A6.2.2), thus simplifying the isolation of **55**. A straightforward silica gel plug to remove copper salts and excess diphenylphosphine, followed by concentration of the remaining filtrate, layering with acetonitrile, and final removal of volatiles under vacuum provided ligand **55** as a white crystalline solid in excellent yield and >99% purity as determined by various analytical methods.

Figure A6.3.1. X-ray crystal analysis of (*S*)-*t*-Bu-PHOX ((*S*)-**55**). The molecular structure is drawn with 50% probability ellipsoids.



A6.4 CONCLUSION

In summary, we have described a significant improvement to our original copper(I) iodide catalyzed diarylphosphine–aryl bromide coupling reaction that enables reliable and efficient access to (*S*)-*t*-Bu-PHOX (**55**). Our optimized conditions employ 0.5 mol % of the copper(I) iodide catalyst and feature reduced quantities of Cs₂CO₃ and diphenylphosphine with increased substrate concentrations convenient for large-scale

preparation. Coupling reactions typically proceed to complete conversion, facilitating a simplified purification procedure consisting of a silica gel plug, and our discovery of a selective acetonitrile crystallization provides **55** as a stable, crystalline solid in high yields and >99% purity. We believe our findings can be extended to a general synthesis of PHOX ligands and provide opportunities for future discoveries in asymmetric catalysis.

A6.5 EXPERIMENTAL SECTION

A6.5.1 MATERIALS AND METHODS

Unless otherwise stated, reactions were performed in flame-dried glassware under an argon or nitrogen atmosphere using dry, deoxygenated solvents. Solvents were dried by passage through an activated alumina column under argon. CuI (98%) was purchased from Strem and used as received. Ph₂PH (99%) was purchased from Strem and cannula transferred to a dry Schlenk storage tube under nitrogen to prolong reagent life. Cs₂CO₃ (ReagentPlus, 99%) and diamine **378** were purchased from Sigma Aldrich and used as received. Bromooxazoline **377** was prepared according to ref 7b. The reaction stirring rate was set at ca. 700 setting on an IKAmag RET basic stir/hot plate (a range between 500–800 rpm is sufficient). Reaction temperatures were controlled by an IKAmag temperature modulator. Thin-layer chromatography was performed using E. Merck silica gel 60 F254 precoated plates (0.25 mm) and visualized by UV fluorescence quenching. SiliCycle SiliaFlash P60 Academic Silica Gel (particle size 40–63 μm; pore diameter 60 Å) was used for flash chromatography. ¹H and ¹³C NMR spectra were recorded on a Varian Mercury 300 (at 300 MHz and 75 MHz respectively), or a Varian Inova 500 (at 500 MHz and 126 MHz, respectively) and are reported relative to Me₄Si (δ 0.0 ppm).¹² Data for ¹H NMR spectra are reported as follows: chemical shift (δ ppm) (multiplicity, coupling constant (Hz), integration). ³¹P NMR spectra were recorded on a Varian Mercury 300 (at 121 MHz) and are reported relative to an H₃PO₄ external standard (δ 0.0 ppm). IR spectra were recorded on a Perkin Elmer Paragon 1000 spectrometer and are reported in frequency of absorption (cm⁻¹). Melting points were acquired using a

Buchi Melting Point B-545 instrument and the values are uncorrected. High-resolution mass spectra were acquired from the Caltech Mass Spectral Facility. Crystallographic data have been deposited at the CCDC, 12 Union Road, Cambridge CB2 1EZ, UK, and copies can be obtained on request, free of charge, by quoting the publication citation and the deposition number.

A6.5.2 PREPARATIVE PROCEDURES

(*S*)-*t*-Bu-PHOX ((*S*)-55). To a 250 mL Schlenk flask equipped with a Teflon valve, a 14/20 glass joint, and a large stir bar was added copper(I) iodide (19.0 mg, 0.10 mmol, 0.005 equiv), diphenylphosphine (4.35 mL, 25.0 mmol, 1.25 equiv), diamine **378** (53.3 μ L, 0.50 mmol, 0.025 equiv) and toluene (20 mL). The colorless contents were stirred at ambient temperature for 20 min, and the flask was charged with bromooxazoline **377** (5.642 g, 20.0 mmol, 1.0 equiv), Cs₂CO₃ (9.775 g, 30.0 mmol, 1.5 equiv), and toluene (20 mL, 0.50 M total) to wash the neck and walls of the flask. The Teflon valve was closed and the yellow heterogeneous reaction was placed in a 110 °C oil bath and vigorously stirred. Following consumption of starting material by TLC analysis, the reaction was allowed to cool to ambient temperature, filtered through a pad of Celite, and the filter cake washed with CH₂Cl₂ (2 x 40 mL). The filtrate was concentrated under reduced pressure to a pale yellow semi-solid, dissolved in a minimal amount of dichloromethane (ca. 40 mL) and ethyl ether (ca. 50 mL), and dry-loaded onto 10 g of silica gel. This material was flushed through a silica gel plug eluting with 24:1 hexanes/Et₂O until excess Ph₂PH elutes, then with a 9:1 CH₂Cl₂/Et₂O mixture until the desired product elutes. The combined fractions are concentrated to a viscous pale yellow oil and layered with ca. 5 mL acetonitrile to facilitate crystallization. The flask was swirled while crystals form within seconds, and after ca. 15 minutes, the flask is placed under high vacuum to remove volatiles to afford (*S*)-**55** (7.033 g, 18.15 mmol, 90.8% yield) as white blocks. R_f = 0.64 (4:1 hexanes/Et₂O, developed twice); mp = 114–115 °C (MeCN); ³¹P NMR (121 MHz, CDCl₃) δ -5.33 (s); ¹H NMR (300 MHz, CDCl₃) δ 7.94

(ddd, $J = 7.4, 3.5, 1.3$ Hz, 1H), 7.36 (app dt, $J = 7.4, 1.3$ Hz, 1H), 7.33–7.21 (comp m, 11H), 6.86 (ddd, $J = 7.4, 4.0, 1.3$ Hz, 1H), 4.08 (dd, $J = 10.1, 8.2$ Hz, 1H), 4.01 (dd, $J = 8.0, 8.0$ Hz, 1H), 3.88 (dd, $J = 10.1, 8.0$ Hz, 1H), 0.73 (s, 9H); ^{13}C NMR (126 MHz, CDCl_3) δ 162.8 (d, $J_{\text{CP}} = 2.8$ Hz), 138.9 (d, $J_{\text{CP}} = 25.3$ Hz), 138.7 (d, $J_{\text{CP}} = 12.4$ Hz), 138.4 (d, $J_{\text{CP}} = 9.7$ Hz), 134.5 (d, $J_{\text{CP}} = 21.2$ Hz), 134.2, 133.7 (d, $J_{\text{CP}} = 20.3$ Hz), 132.1 (d, $J_{\text{CP}} = 19.8$ Hz), 130.5, 130.0 (d, $J_{\text{CP}} = 3.2$ Hz), 128.6 (d, $J_{\text{CP}} = 20.2$ Hz), 128.5, 128.4 (2 lines), 128.2, 76.8, 68.4, 33.7, 25.9; IR (Neat Film NaCl) 3053, 2954, 2902, 2867, 1652, 1477, 1434, 1353, 1336, 1091, 1025, 966, 743, 696, 503 cm^{-1} ; HRMS (FAB+) m/z calc'd for $\text{C}_{25}\text{H}_{27}\text{NOP}$ $[\text{M} + \text{H}]^+$: 388.1830, found 388.1831; $[\alpha]_{\text{D}}^{23} -61.5^\circ$ (c 0.925, CHCl_3 , >99% ee); Anal. calc'd. for $\text{C}_{25}\text{H}_{27}\text{NOP}$: C, 77.50; H, 6.76; N, 3.62. Found: C, 77.10; H, 6.62; N, 3.71.

A6.6 NOTES AND REFERENCES

- (1) (a) von Matt, P.; Pfaltz, A. *Angew. Chem., Int. Ed.* **1993**, *32*, 566–568. (b) Sprinz, J.; Helmchen, G. *Tetrahedron Lett.* **1993**, *34*, 1769–1772. (c) Dawson, G. J.; Frost, C. G.; Coote, S. J.; Williams, J. M. J. *Tetrahedron Lett.* **1993**, *34*, 3149–3150. (d) Helmchen, G.; Pfaltz, A. *Acc. Chem. Res.* **2000**, *33*, 336–345.
- (2) For representative examples of **1** in stereoselective transformations, see: (a) von Matt, P.; Loiseleur, O.; Koch, G.; Pfaltz, A.; Lefeber, C.; Feucht, T.; Helmchen, G. *Tetrahedron: Asymmetry* **1994**, *5*, 573–584. (b) Rieck, H.; Helmchen, G. *Angew. Chem., Int. Ed. Engl.* **1995**, *34*, 2687–2689. (c) Baldwin, I. C.; Williams, J. M. J. *Tetrahedron: Asymmetry* **1995**, *6*, 1515–1518. (d) Loiseleur, O.; Meier, P.; Pfaltz, A. *Angew. Chem., Int. Ed. Engl.* **1996**, *35*, 200–202. (e) Ripa, L.; Hallberg, A. *J. Org. Chem.* **1997**, *62*, 595–602. (f) Castro, J.; Moyano, A.; Pericàs, M. A.; Riera, A.; Alvarez-Larena, A.; Piniella, J. F. *J. Am. Chem. Soc.* **2000**, *122*, 7944–7952. (g) Lautens, M.; Hiebert, S. *J. Am. Chem. Soc.* **2004**, *126*, 1437–1447. (h) Legault, C. Y.; Charette, A. B. *J. Am. Chem. Soc.* **2005**, *127*, 8966–8977. (i) Schulz, S. R.; Blechert, S. *Angew. Chem., Int. Ed.* **2007**, *46*, 3966–3970. (j) Cook, M. J.; Rovis, T. *J. Am. Chem. Soc.* **2007**, *129*, 9302–9303. (k) Dounay, A. B.; Humphreys, P. G.; Overman, L. E.; Wroblewski, A. D. *J. Am. Chem. Soc.* **2008**, *130*, 5368–5377. (l) Linton, E. C.; Kozlowski, M. C. *J. Am. Chem. Soc.* **2008**, *130*, 16162–16163.
- (3) (a) Behenna, D. C.; Stoltz, B. M. *J. Am. Chem. Soc.* **2004**, *126*, 15044–15045. (b) Mohr, J. T.; Behenna, D. C.; Harned, A. M.; Stoltz, B. M. *Angew. Chem., Int. Ed.* **2005**, *44*, 6924–6927. (c) Seto, M.; Roizen, J. L.; Stolz, B. M. *Angew. Chem., Int. Ed.* **2008**, *47*, 6873–6876.

- (4) (a) Mohr, J. T.; Nishimata, T.; Behenna, D. C.; Stoltz, B. M. *J. Am. Chem. Soc.* **2006**, *128*, 11348–11349. (b) Marinescu, S. C.; Nishimata, T.; Mohr, J. T.; Stoltz, B. M. *Org. Lett.* **2008**, *10*, 1039–1042.
- (5) For a recently developed *t*-Bu-PHOX practical equivalent, see: Bélanger, E.; Pouliot, M.-F.; Paquin, J.-F. *Org. Lett.* **2009**, *11*, 2201–2204.
- (6) Gelman, D.; Jiang, L.; Buchwald, S. L. *Org. Lett.* **2003**, *5*, 2315–2318.
- (7) (a) Tani, K.; Behenna, D. C.; McFadden, R. M.; Stoltz, B. M. *Org. Lett.* **2007**, *9*, 2529–2531. (b) Krout, M. R.; Mohr, J. T.; Stoltz, B. M. *Org. Synth.* **2009**, *86*, 181–193.
- (8) (a) McFadden, R. M.; Stoltz, B. M. *J. Am. Chem. Soc.* **2006**, *128*, 7738–7739. (b) Behenna, D. C.; Stockdill, J. L.; Stoltz, B. M. *Angew. Chem., Int. Ed.* **2007**, *46*, 4077–2080. (c) White, D. E.; Stewart, I. C.; Grubbs, R. H.; Stoltz, B. M. *J. Am. Chem. Soc.* **2008**, *130*, 810–811. (d) Enquist, J. A., Jr.; Stoltz, B. M. *Nature* **2008**, *453*, 1228–1231. (e) Levine, S. R.; Krout, M. R.; Stoltz, B. M. *Org. Lett.* **2009**, *11*, 289–292. (f) Petrova, K. V.; Mohr, J. T.; Stoltz, B. M. *Org. Lett.* **2009**, *11*, 293–295.
- (9) See subsection A6.5.2 for details.
- (10) For reports utilizing various inorganic bases for copper-catalyzed C–P bond formation, see: (a) Van Allen, D.; Venkataraman, D. *J. Org. Chem.* **2003**, *68*, 4590–4593. (b) Thielges, S.; Bissere, P.; Eustache, J. *Org. Lett.* **2005**, *7*, 681–684. (c) Huang, C.; Tang, X.; Fu, H.; Jiang, Y.; Zhao, Y. *J. Org. Chem.* **2006**, *71*, 5020–5022.

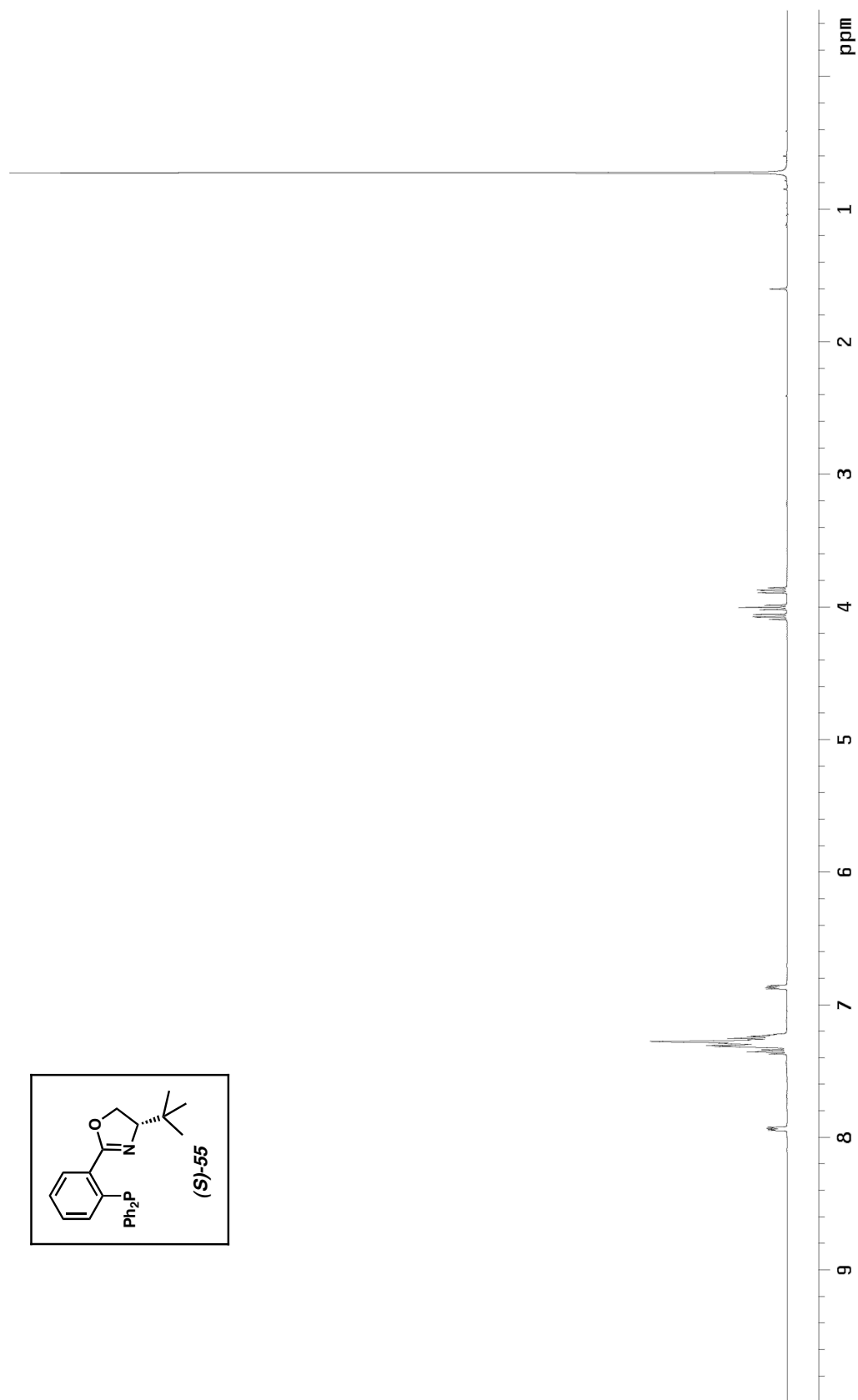
- (11) For a detailed X-ray crystallography report of (S)-**55**, see Appendix 8.
- (12) Gottlieb, H. E.; Kotlyar, V.; Nudelman, A. *J. Org. Chem.* **1997**, *62*, 7512–7515.

APPENDIX 7

Spectra Relevant to Appendix 6:

An Improved and Highly Efficient Copper(I)-

Catalyzed Preparation of (S)-t-Bu-PHOX

Figure A7.1. ^1H NMR spectrum (300 MHz, CDCl_3) of **55**.

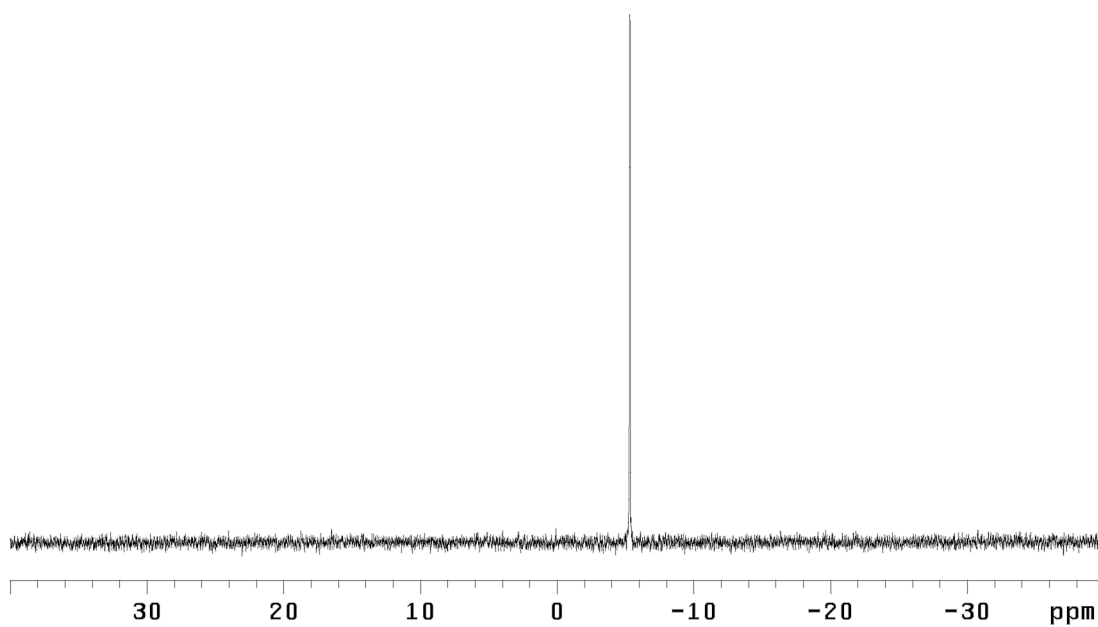


Figure A7.2. ^{31}P NMR spectrum (121 MHz, CDCl_3) of **55**.

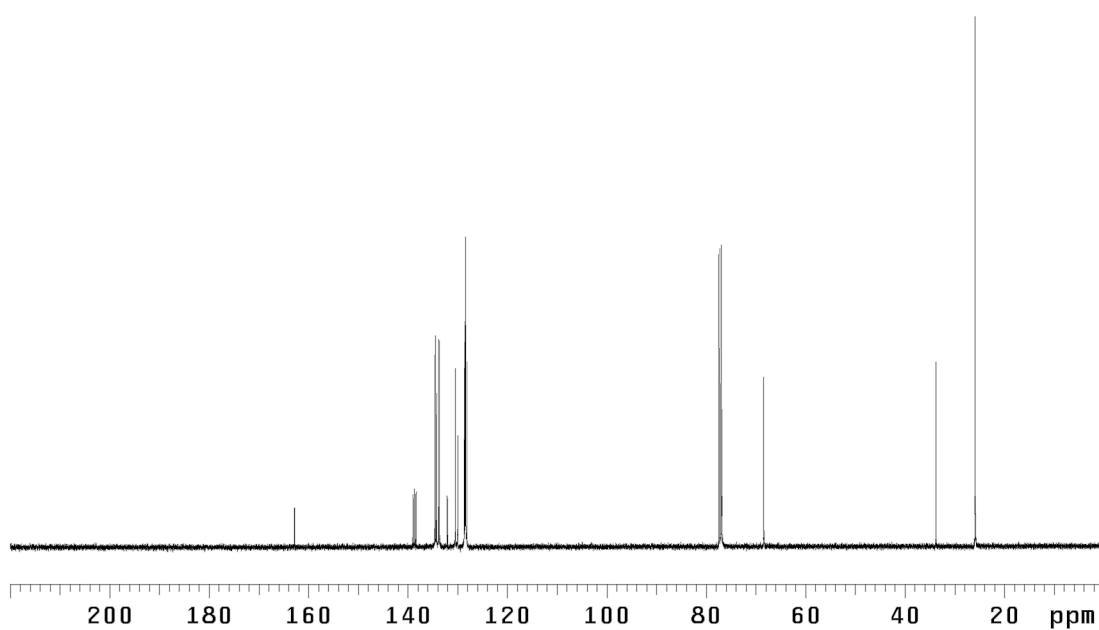


Figure A7.3. ^{13}C NMR spectrum (126 MHz, CDCl_3) of **55**.

APPENDIX 8

X-Ray Crystallography Reports Relevant to Appendix 6:

An Improved and Highly Efficient Copper(I)-

Catalyzed Preparation of (S)-t-Bu-PHOX

A8.1 CRYSTAL STRUCTURE ANALYSIS OF (S)-55

Figure A8.1.1. (S)-t-Bu-PHOX ((S)-55) is shown with 50% probability ellipsoids. Crystallographic data have been deposited at the CCDC, 12 Union Road, Cambridge CB2 1EZ, UK, and copies can be obtained on request, free of charge, by quoting the publication citation and the deposition number 646767.

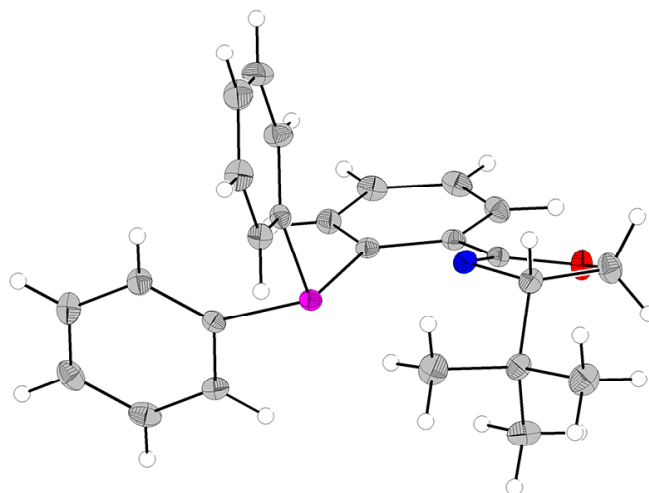


Table A8.1.1. Crystal data and structure refinement for (S)-**55** (CCDC 664767)

Empirical formula	C ₂₅ H ₂₆ NOP
Formula weight	387.44
Crystallization solvent	Acetonitrile
Crystal habit	Block
Crystal size	0.36 x 0.31 x 0.18 mm ³
Crystal color	Colorless

Data Collection

Type of diffractometer	Bruker KAPPA APEX II	
Wavelength	0.71073 Å MoK α	
Data collection temperature	100(2) K	
θ range for 9143 reflections used in lattice determination	2.41 to 40.53°	
Unit cell dimensions	a = 8.5180(4) Å b = 12.7779(7) Å c = 9.7689(5) Å	β = 97.207(3)°
Volume	1054.87(9) Å ³	
Z	2	
Crystal system	Monoclinic	
Space group	P2 ₁	
Density (calculated)	1.220 Mg/m ³	
F(000)	412	
Data collection program	Bruker APEX22 v2.1-0	
θ range for data collection	2.10 to 41.37°	
Completeness to θ = 41.37°	95.2 %	
Index ranges	-14 ≤ h ≤ 15, -22 ≤ k ≤ 22, -17 ≤ l ≤ 17	
Data collection scan type	ω and ϕ scans; 23 settings	
Data reduction program	Bruker SAINT-Plus v7.34A	
Reflections collected	69072	
Independent reflections	13022 [R _{int} = 0.0373]	
Absorption coefficient	0.145 mm ⁻¹	
Absorption correction	None	
Max. and min. transmission	0.9743 and 0.9496	

Table A8.1.1 (cont.)

Structure solution and Refinement

Structure solution program	SHELXS-97 (Sheldrick, 1990)
Primary solution method	Direct methods
Secondary solution method	Difference Fourier map
Hydrogen placement	Geometric positions
Structure refinement program	SHELXL-97 (Sheldrick, 1997)
Refinement method	Full matrix least-squares on F^2
Data / restraints / parameters	13022 / 1 / 256
Treatment of hydrogen atoms	Riding
Goodness-of-fit on F^2	2.289
Final R indices [$I > 2\sigma(I)$, 11270 reflections]	$R1 = 0.0423$, $wR2 = 0.0581$
R indices (all data)	$R1 = 0.0505$, $wR2 = 0.0583$
Type of weighting scheme used	Sigma
Weighting scheme used	$w = 1/\sigma^2(F_o^2)$
Max shift/error	0.001
Average shift/error	0.000
Absolute structure determination	Anomalous differences
Absolute structure parameter	0.00(3)
Largest diff. peak and hole	1.524 and -0.683 e. \AA^{-3}

Special Refinement Details

Refinement of F^2 against ALL reflections. The weighted R-factor (wR) and goodness of fit (S) are based on F^2 , conventional R-factors (R) are based on F , with F set to zero for negative F^2 . The threshold expression of $F^2 > 2\sigma(F^2)$ is used only for calculating R-factors(gt) etc. and is not relevant to the choice of reflections for refinement. R-factors based on F^2 are statistically about twice as large as those based on F , and R-factors based on ALL data will be even larger.

All esds (except the esd in the dihedral angle between two l.s. planes) are estimated using the full covariance matrix. The cell esds are taken into account individually in the estimation of esds in distances, angles and torsion angles; correlations between esds in cell parameters are only used when they are defined

by crystal symmetry. An approximate (isotropic) treatment of cell esds is used for estimating esds involving l.s. planes.

Figure A8.1.2. (*S*)-*t*-Bu-PHOX ((*S*)-**55**).

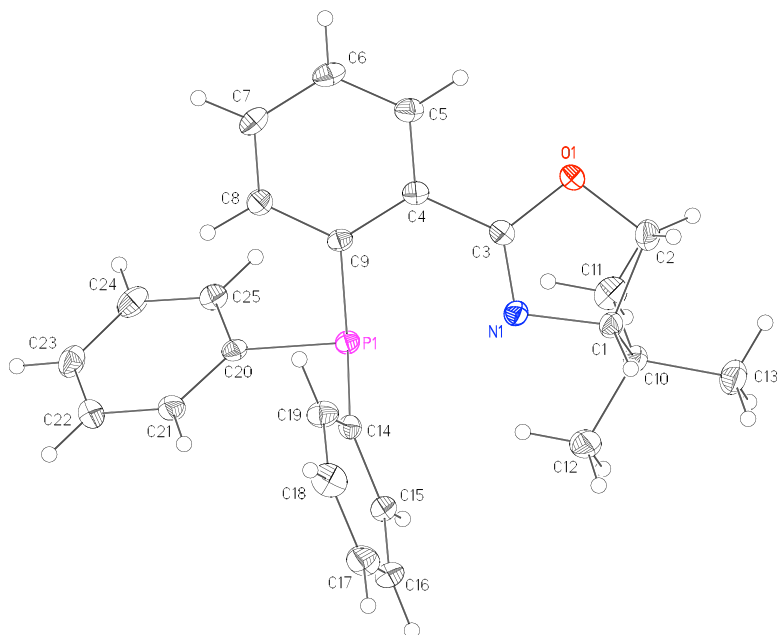


Table A8.1.2. Atomic coordinates ($\times 10^4$) and equivalent isotropic displacement parameters ($\text{\AA}^2 \times 10^3$) for (S)-**55** (CCDC 664767). $U(\text{eq})$ is defined as the trace of the orthogonalized U^{ij} tensor

	x	y	z	U_{eq}
P(1)	7718(1)	4116(1)	2536(1)	13(1)
O(1)	8058(1)	5288(1)	-1715(1)	19(1)
N(1)	9337(1)	4870(1)	390(1)	15(1)
C(1)	10510(1)	4686(1)	-575(1)	16(1)
C(2)	9702(1)	5154(1)	-1939(1)	21(1)
C(3)	8065(1)	5156(1)	-320(1)	14(1)
C(4)	6591(1)	5402(1)	244(1)	14(1)
C(5)	5450(1)	6014(1)	-535(1)	18(1)
C(6)	4131(1)	6364(1)	15(1)	20(1)
C(7)	3926(1)	6091(1)	1355(1)	19(1)
C(8)	5020(1)	5441(1)	2116(1)	17(1)
C(9)	6372(1)	5079(1)	1587(1)	14(1)
C(10)	10981(1)	3522(1)	-605(1)	17(1)
C(11)	9566(1)	2835(1)	-1141(1)	24(1)
C(12)	11601(1)	3187(1)	868(1)	25(1)
C(13)	12299(1)	3405(1)	-1523(1)	26(1)
C(14)	9205(1)	4935(1)	3546(1)	14(1)
C(15)	10662(1)	4483(1)	4024(1)	17(1)
C(16)	11856(1)	5067(1)	4765(1)	22(1)
C(17)	11618(1)	6114(1)	5024(1)	25(1)
C(18)	10175(1)	6572(1)	4563(1)	25(1)
C(19)	8981(1)	5986(1)	3831(1)	20(1)
C(20)	6482(1)	3698(1)	3851(1)	14(1)
C(21)	6716(1)	3972(1)	5241(1)	18(1)
C(22)	5804(1)	3526(1)	6164(1)	23(1)
C(23)	4632(1)	2810(1)	5716(1)	22(1)
C(24)	4359(1)	2548(1)	4332(1)	21(1)
C(25)	5287(1)	2982(1)	3414(1)	17(1)

Table A8.1.3. Bond lengths [\AA] and angles [$^\circ$] for (S)-**55** (CCDC 664767)

P(1)-C(14)	1.8322(8)	N(1)-C(1)-C(10)	111.33(6)
P(1)-C(20)	1.8396(8)	C(2)-C(1)-C(10)	116.50(7)
P(1)-C(9)	1.8494(8)	O(1)-C(2)-C(1)	104.41(6)
O(1)-C(3)	1.3718(9)	N(1)-C(3)-O(1)	118.51(7)
O(1)-C(2)	1.4542(10)	N(1)-C(3)-C(4)	124.75(7)
N(1)-C(3)	1.2649(10)	O(1)-C(3)-C(4)	116.70(6)
N(1)-C(1)	1.4761(10)	C(5)-C(4)-C(9)	120.46(7)
C(1)-C(2)	1.5412(11)	C(5)-C(4)-C(3)	119.05(7)
C(1)-C(10)	1.5422(11)	C(9)-C(4)-C(3)	120.38(7)
C(3)-C(4)	1.4678(11)	C(6)-C(5)-C(4)	120.99(8)
C(4)-C(5)	1.3960(11)	C(5)-C(6)-C(7)	119.44(8)
C(4)-C(9)	1.4105(11)	C(6)-C(7)-C(8)	119.92(8)
C(5)-C(6)	1.3789(12)	C(7)-C(8)-C(9)	121.83(8)
C(6)-C(7)	1.3868(12)	C(8)-C(9)-C(4)	117.23(7)
C(7)-C(8)	1.3922(11)	C(8)-C(9)-P(1)	121.51(6)
C(8)-C(9)	1.3987(11)	C(4)-C(9)-P(1)	121.00(6)
C(10)-C(11)	1.5293(12)	C(11)-C(10)-C(13)	110.38(7)
C(10)-C(13)	1.5297(11)	C(11)-C(10)-C(12)	109.02(7)
C(10)-C(12)	1.5305(11)	C(13)-C(10)-C(12)	109.38(7)
C(14)-C(19)	1.3900(11)	C(11)-C(10)-C(1)	111.38(7)
C(14)-C(15)	1.3952(11)	C(13)-C(10)-C(1)	108.47(7)
C(15)-C(16)	1.3890(11)	C(12)-C(10)-C(1)	108.16(7)
C(16)-C(17)	1.3812(13)	C(19)-C(14)-C(15)	118.11(7)
C(17)-C(18)	1.3850(13)	C(19)-C(14)-P(1)	123.83(6)
C(18)-C(19)	1.3872(12)	C(15)-C(14)-P(1)	118.03(6)
C(20)-C(21)	1.3925(11)	C(16)-C(15)-C(14)	120.97(8)
C(20)-C(25)	1.3947(11)	C(17)-C(16)-C(15)	120.09(8)
C(21)-C(22)	1.3848(11)	C(16)-C(17)-C(18)	119.63(8)
C(22)-C(23)	1.3835(12)	C(17)-C(18)-C(19)	120.17(8)
C(23)-C(24)	1.3845(12)	C(18)-C(19)-C(14)	121.01(8)
C(24)-C(25)	1.3835(12)	C(21)-C(20)-C(25)	118.23(7)
		C(21)-C(20)-P(1)	125.69(6)
C(14)-P(1)-C(20)	101.95(3)	C(25)-C(20)-P(1)	115.90(6)
C(14)-P(1)-C(9)	103.49(3)	C(22)-C(21)-C(20)	120.52(8)
C(20)-P(1)-C(9)	99.79(3)	C(23)-C(22)-C(21)	120.52(8)
C(3)-O(1)-C(2)	104.53(6)	C(22)-C(23)-C(24)	119.68(8)
C(3)-N(1)-C(1)	107.26(6)	C(25)-C(24)-C(23)	119.74(8)
N(1)-C(1)-C(2)	103.10(6)	C(24)-C(25)-C(20)	121.29(8)

Table A8.1.4. Anisotropic displacement parameters ($\text{\AA}^2 \times 10^4$) for (S)-**55** (CCDC 664767). The anisotropic displacement factor exponent takes the form: $-2\pi^2 [h^2 a^{*2} U^{11} + \dots + 2 h k a^* b^* U^{12}]$

	U ¹¹	U ²²	U ³³	U ²³	U ¹³	U ¹²
P(1)	131(1)	123(1)	144(1)	2(1)	13(1)	9(1)
O(1)	177(3)	262(3)	138(3)	32(2)	24(2)	26(2)
N(1)	138(3)	168(3)	152(3)	-17(3)	21(2)	7(3)
C(1)	134(4)	198(4)	161(4)	-20(3)	29(3)	-28(3)
C(2)	203(4)	253(4)	201(4)	39(4)	75(3)	10(3)
C(3)	163(4)	124(3)	140(3)	2(3)	13(3)	-23(3)
C(4)	142(3)	118(3)	159(3)	-5(3)	0(3)	-13(3)
C(5)	161(4)	171(4)	188(4)	35(3)	-11(3)	-16(3)
C(6)	150(4)	169(4)	259(4)	34(3)	-23(3)	18(3)
C(7)	135(4)	175(4)	264(4)	-2(3)	29(3)	23(3)
C(8)	163(4)	164(4)	171(4)	-1(3)	22(3)	3(3)
C(9)	122(3)	129(3)	153(3)	-12(3)	-3(3)	-9(3)
C(10)	156(4)	196(4)	171(4)	-23(3)	35(3)	14(3)
C(11)	223(4)	198(4)	306(5)	-49(4)	31(4)	-12(4)
C(12)	241(5)	263(5)	231(4)	9(4)	12(4)	87(4)
C(13)	223(4)	299(5)	274(5)	-27(4)	91(4)	33(4)
C(14)	137(3)	160(4)	134(3)	16(3)	24(3)	-16(3)
C(15)	153(4)	180(4)	173(4)	4(3)	20(3)	17(3)
C(16)	138(4)	301(5)	220(4)	4(4)	2(3)	-5(3)
C(17)	225(4)	288(5)	220(4)	-19(4)	-11(4)	-111(4)
C(18)	311(5)	159(4)	270(5)	-22(4)	8(4)	-44(4)
C(19)	200(4)	169(4)	223(4)	-7(3)	-8(3)	25(3)
C(20)	118(3)	129(3)	162(3)	21(3)	3(3)	13(3)
C(21)	160(4)	211(5)	173(3)	2(3)	4(3)	-23(3)
C(22)	212(4)	300(5)	166(4)	17(4)	38(3)	-2(4)
C(23)	182(4)	227(4)	272(4)	71(4)	85(3)	11(3)
C(24)	150(4)	170(4)	320(5)	-1(4)	37(3)	-25(3)
C(25)	160(4)	156(4)	193(4)	-15(3)	9(3)	0(3)

APPENDIX 9

Notebook Cross-Reference

The following notebook cross-reference has been included to facilitate access to the original spectroscopic data obtained for the compounds presented in this thesis. For each compound, both hardcopy and electronic characterization folders have been created that contain copies of the original ^1H NMR, ^{13}C NMR, ^{31}P NMR, ^2H NMR, and IR spectra. All notebooks and spectral data are stored in the Stoltz archives.

Table A9.1. Notebook cross-reference for compounds of Chapter 3 and Appendix 2

compound	¹ H NMR	¹³ C NMR	IR
178	MRK-XI-101	MRK-XI-101	MRK-XI-101
180	TJ-III-55a	TJ-III-55a	TJ-III-55a
181	MRK-VI-227b	MRK-VI-227b	
183	MRK-XII-279		
184	MRK-XI-167	MRK-XI-167	MRK-XI-167
185	CEH-I-281	CEH-I-281	CEH-I-281
186	MRK-X-301c		
187	MRK-XIII-125b		
188	MRK-IX-227d	MRK-IX-227d	MRK-IX-227d
189	MRK-IX-297	MRK-IX-297	MRK-IX-297
190	MRK-VIII-87aa	MRK-VIII-87aa	MRK-VIII-87aa
191	MRK-IX-79-2	MRK-X-127c	MRK-VIII-123-2
192	MRK-IX-83-3		
193	MRK-X-51a	MRK-X-51a	MRK-X-51a
197	MRK-XIII-155c	MRK-XIII-155c	MRK-XIII-155c
198	MRK-IX-87-2	MRK-IX-87-2	MRK-IX-87-2
200	MRK-X-179-5	MRK-X-179-5	MRK-VIII-173-2
201	MRK-XII-195-1	MRK-X-181-3	MRK-XII-195-1
203	MRK-X-123-1	MRK-X-123-1	MRK-X-123-1
208	MRK-X-255		
209	MRK-XI-121c	MRK-XI-121c	MRK-XI-121c
211	MRK-XI-151b	MRK-XI-151b	MRK-XI-151b
212	MRK-XI-99	MRK-XI-99	MRK-XI-99
213	MRK-XII-53b	MRK-XII-53b	MRK-XII-53b
214	MRK-XII-123f	MRK-XII-123f	MRK-XII-123f
215	MRK-XII-117c	MRK-XII-117c	MRK-XII-117c
216	MRK-XII-117a	MRK-XII-117a	MRK-XII-117a
217	MRK-XII-123c3	MRK-XII-123c3	MRK-XII-123c3
218	MRK-XII-127	MRK-XII-127	MRK-XII-127
220	MRK-XII-213a	MRK-XII-213a	MRK-XII-213a
221	MRK-XII-199b	MRK-XII-199b	MRK-XII-199b
222	MRK-XII-227d3	MRK-XII-227d3	MRK-XII-227d3

223	MRK-XII-209-1	MRK-XII-209-1	MRK-XII-239-3
224	MRK-XIII-99c	MRK-XIII-99c	MRK-XIII-99c
225	TJ-III-67	TJ-III-67	MRK-VIII-89
227	MRK-VI-277		
228	MRK-VI-201b	MRK-VI-201b	MRK-VII-135b
229	MRK-VII-33b	MRK-VII-33b	MRK-VII-33b
231	TJ-III-55b	TJ-III-55b	TJ-III-55b
232	TJ-III-83	TJ-III-83	TJ-III-83e
233	TJ-III-135	TJ-III-135	TJ-III-135
235	TJ-I-285a	TJ-I-285a	TJ-I-285a2
236	TJ-I-303a	TJ-I-303a	TJ-I-303a
237	TJ-III-203	TJ-III-203	TJ-III-203
238	TJ-I-43f	TJ-I-43f	TJ-I-43f
239	TJ-III-123	TJ-III-123	TJ-II-47d
240	TJ-III-145	TJ-III-145	TJ-III-145
241	TJ-IV-39	TJ-IV_39	TJ-II-115
242	TJ-III-193a	TJ-III-193a	TJ-III-193a
243	TJ-III-301major TJ-III-301minor	TJ-III-301major TJ-III-301minor	TJ-III-301major TJ-III-301minor
245	MRK-XII-293	MRK-XII-293	MRK-XII-233-3
253	MRK-VII-71-4	MRK-VII-71-4	MRK-VII-71-4
254	MRK-IX-71-1	MRK-IX-71-1	MRK-IX-71-1
255	MRK-VI-273		
256	MRK-X-53a	MRK-X-53a	MRK-X-53a

Table A9.2. Notebook cross-reference for compounds of Chapter 4 and Appendix 4

compound	¹ H NMR	¹³ C NMR	IR
275	MRK-XI-207b	MRK-XI-207b	MRK-XI-207b
276	SRL-I-51	SRL-I-51	SRL-I-113
277	KVP-I-179	KVP-I-179	KVP-I-179
278	KVP-I-199	KVP-I-199	KVP-I-199
279	MRK-XII-33-1	MRK-XII-33-1	MRK-XII-33-1
287	SRL-I-47-3		
288	SRL-I-287	SRL-I-287	SRL-I-287

289	SRL-I-269		
290	SRL-II-31	SRL-II-31	SRL-II-31
292	SRL-II-39	SRL-II-39	SRL-II-39
293	MRK-XI-261	MRK-XI-261	MRK-XI-261
294	SRL-II-55-1a	SRL-II-55-1a	SRL-II-55-1a
295	MRK-XI-303	MRK-XI-303	MRK-XI-303
304	SRL-I-47-1	SRL-I-47-1	SRL-I-47-1
307	MRK-XII-47		
308	MRK-XII-49B		
309	MRK-XI-257-1	MRK-XI-257-1	MRK-XI-253b

Table A9.3. Notebook cross-reference for compounds of Chapter 5 and Appendix 5

compound	¹H NMR	¹³C NMR	IR	²H
333	MRK-VII-303	MRK-VII-303		
334	MRK-VIII-31			MRK-VIII-31
335	MRK-VIII-55			MRK-VIII-55
339	MRK-VII-253	MRK-VII-253		
340	MRK-VII-261d	MRK-VII-261d		
341	MRK-VIII-49	MRK-VII-49		
344	MRK-VII-283b	MRK-VII-283b		MRK-VII-283b
345	MRK-VIII-51c	MRK-VIII-51c		MRK-VIII-51c
363	MRK-VII-179	MRK-VII-179	MRK-VII-179	
364	MRK-VII-233b	MRK-VII-233b	MRK-VII-233b	
365	MRK-VIII-71	MRK-VIII-71	MRK-VIII-71	
366	MRK-VII-293	MRK-VII-293	MRK-VII-293	
368	MRK-VIII-35	MRK-VIII-35		
369	MRK-VIII-59	MRK-VIII-59		
370	MRK-VIII-57b	MRK-VIII-57b		MRK-VIII-57b
371	MRK-VIII-63	MRK-VIII-63		MRK-VIII-63
372	MRK-VIII-69	MRK-VIII-69		MRK-VIII-69
373	MRK-VIII-47	MRK-VIII-47		MRK-VIII-47
374	MRK-VIII-53	MRK-VIII-53		MRK-VIII-53

Table A9.4. Notebook cross-reference for compounds of Appendix 6 and Appendix 7

compound	¹H NMR	¹³C NMR	³¹P
55	MRK-X-229	MRK-X-151	MRK-X-229

COMPREHENSIVE BIBLIOGRAPHY

Akutagawa, S.; Tani, K. Asymmetric Isomerization of Allylamines. In *Catalytic Asymmetric Synthesis*; Ojima, I., Ed.; Wiley-VCH: New York, 2002; pp 145–161.

Achenbach, H.; Waibel, R.; Addae-Mensah, I. *Phytochemistry* **1985**, *24*, 2325–2328.

Agar, J.; Kaplan, F.; Roberts, B. W. *J. Org. Chem.* **1974**, *39*, 3451–3452.

Ahmad, N.; Robinson, S. D.; Uttley, M. F. *J. Chem. Soc., Dalton Trans.* **1972**, 843–847.

Al-Dabbas, M. M.; Hashinaga, F.; Abdelgaleil, S. A. M.; Suganuma, T.; Akiyama, K.; Hayashi, H. *J. Ethnopharmacol.* **2005**, *97*, 237–240.

Allin, S. M.; Gaskell, S. N.; Elsegood, M. R. J.; Martin, W. P. *Tetrahedron Lett.* **2007**, *48*, 5669–5671.

Aloise, A. D.; Layton, M. E.; Shair, M. D. *J. Am. Chem. Soc.* **2000**, *122*, 12610–12611.

Ananda, G. D. S.; Steele, J.; Stoodley, R. J. *J. Chem. Soc., Perkin Trans. 1* **1988**, 1765–1771.

Andersson, M. P.; Uvdal, P. *J. Phys. Chem. A* **2005**, *109*, 2937–2941.

Aoyama, Y.; Araki, Y.; Konoike, T. *Synlett* **2001**, *9*, 1452–1454.

- Armentrout, P. B. *J. Am. Soc. Mass Spectrom.* **2000**, *11*, 371–379.
- Arndt, F.; Eistert, B. *Ber. Dtsch. Chem. Ges. B* **1935**, *68*, 200–208.
- Arp, F. O.; Fu, G. C. *J. Am. Chem. Soc.* **2005**, *127*, 10482–10483.
- Asakura, K.; Kanemasa, T.; Minagawa, K.; Kagawa, K.; Ninomiya, M. *Brain Res.* **1999**, *823*, 169–176.
- Asakura, K.; Kanemasa, T.; Minagawa, K.; Kagawa, K.; Yagami, T.; Nakajima, M.; Ninomiya, M. *Brain Res.* **2000**, *873*, 94–101.
- Aubé, J.; Milligan, G. L. *J. Am. Chem. Soc.* **1991**, *113*, 8965–8966.
- Austin, J. F.; Kim, S.-G.; Sinz, C. J.; Xiao, W.-J.; MacMillan, D. W. C. *Proc. Natl. Acad. Sci. U.S.A.* **2004**, *101*, 5482–5487.
- Austin, J. F.; MacMillan, D. W. C. *J. Am. Chem. Soc.* **2002**, *124*, 1172–1173.
- Bader, M.; Ganten, D. *J. Mol. Med.* **2008**, *86*, 615–621.
- Bal, B. S.; Childers, W. E.; Pinnick, H. W. *Tetrahedron* **1981**, *37*, 2091–2096.
- Baldwin, I. C.; Williams, J. M. J. *Tetrahedron: Asymmetry* **1995**, *6*, 1515–1518.
- Ballester, P.; Tadayoni, B. M.; Branda, N.; Rebek, J., Jr. *J. Am. Chem. Soc.* **1990**, *112*, 3685–3686.

Barluenga, J.; Diéguez, A.; Rodríguez, F.; Flórez, J.; Fañanás, F. J. *J. Am. Chem. Soc.* **2002**, *124*, 9056–9057.

Barton, M.; Yanagisawa, M. *Can. J. Physiol. Pharmacol.* **2008**, *86*, 485–498.

Bashore, C. G.; Samardjiev, I. J.; Bordner, J.; Coe, J. W. *J. Am. Chem. Soc.* **2003**, *125*, 3268–3272.

Bégué, J.-P.; Bonnet-Delpon, D.; Crousse, B. *Synlett* **2004**, 18–29.

Behenna, D. C.; Stockdill, J. L.; Stoltz, B. M. *Angew. Chem., Int. Ed.* **2007**, *46*, 4077–4080.

Behenna, D. C.; Stockdill, J. L.; Stoltz, B. M. *Angew. Chem., Int. Ed.* **2007**, *46*, 4077–2080.

Behenna, D. C.; Stoltz, B. M. *J. Am. Chem. Soc.* **2004**, *126*, 15044–15055.

Bélangier, E.; Pouliot, M.-F.; Paquin, J.-F. *Org. Lett.* **2009**, *11*, 2201–2204.

Bennet, A. J.; Wang, Q.-P.; Slebocka-Tilk, H.; Somayaji, V.; Brown, R. S.; Santarsiero, B. D. *J. Am. Chem. Soc.* **1990**, *112*, 6383–6385.

Berson, J. A.; Dervan, P. B. *J. Am. Chem. Soc.* **1972**, *94*, 7597–7598.

Bisai, A.; West, S. P.; Sarpong, R. *J. Am. Chem. Soc.* **2008**, *130*, 7222–7223.

Blackburn, G. M.; Skaife, C. J.; Kay, I. T. *J. Chem. Res., Miniprint* **1980**, 3650–3669.

Blasdel, L. K.; Myers, A. G. *Org. Lett.* **2005**, *7*, 4281–4283.

Asymmetric Catalysis on Industrial Scale: Challenges, Approaches and Solutions;

Blaser, H.-U., Schmidt, E., Eds.; Wiley-VCH: Weinheim, 2004.

Bohlmann, F.; Jakupovic, J.; Lonitz, M. *Chem. Ber.* **1977**, *110*, 301–314.

Boivin, J.; Gaudin, D.; Labrecque, D.; Jankowski, K. *Tetrahedron Lett.* **1990**, *31*, 2281–2282.

Bouchoux, G.; Sablier, M.; Berruyer-Penaud, F. *J. Mass Spectrom.* **2004**, *39*, 986–997.

Boys, S. F.; Bernardi, F. *Mol. Phys.* **1970**, *19*, 553–566.

Bredt, J. *Liebigs Ann. Chem.* **1924**, *437*, 1–13.

Breit, B.; Breuninger, D. *J. Am. Chem. Soc.* **2004**, *126*, 10244–10245.

Brown, J. M.; Golding, B. T.; Stofko, J. J., Jr. *J. Chem. Soc., Perkin Trans. 2* **1978**, 436–441.

Buchanan, G. L.; Kitson, D. H.; Mallinson, P. R.; Sim, G. A.; White, D. N. J.; Cox, P. J. *J. Chem. Soc., Perkin Trans. 2* **1983**, 1709–1712.

Carpenter, N. E.; Kucera, D. J.; Overman, L. E. *J. Org. Chem.* **1989**, *54*, 5846–5848.

Castro, J.; Moyano, A.; Pericàs, M. A.; Riera, A.; Alvarez-Larena, A.; Piniella, J. F. *J. Am. Chem. Soc.* **2000**, *122*, 7944–7952.

Cazeau, P.; Duboudin, F.; Moulines, F.; Babot, O.; Dunogues, J. *Tetrahedron* **1987**, *43*, 2075–2088.

Ceccherelli, P.; Curini, M.; Marcotullio, M. C.; Rosati, O. *Tetrahedron Lett.* **1990**, *31*, 3071–3074.

Cerda, B. A.; Wesdemiotis, C. *J. Am. Chem. Soc.* **1995**, *117*, 9734–9739.

Chou, T.-S.; Lee, S.-J.; Yao, N.-K. *Tetrahedron* **1989**, *45*, 4113–4124.

Quaternary Stereocenters: Challenges and Solutions for Organic Synthesis; Christoffers, J., Baro, A., Eds.; Wiley: Weinheim, 2005.

Quaternary Stereocenters: Challenges and Solutions for Organic Synthesis, Christoffers, J., Baro, A., Eds.; Wiley: Weinheim, 2005.

Claus, R. E.; Schreiber, S. L. *Organic Syntheses*; Wiley & Sons: New York, 1990; Collect. Vol. VII, pp 168–171.

Clausen, A. M.; Dziadul, B.; Cappuccio, K. L.; Kaba, M.; Starbuck, C.; Hsiao, Y.; Dowling, T. M. *Org. Process Res. Dev.* **2006**, *10*, 723–726.

Clayden, J.; Moran, W. J. *Angew. Chem., Int. Ed.* **2006**, *45*, 7118–7120.

Coll, J. C.; Crist, D. R.; Barrio, M. G.; Leonard, N. J. *J. Am. Chem. Soc.* **1972**, *94*, 7092–7099.

Cook, M. J.; Rovis, T. *J. Am. Chem. Soc.* **2007**, *129*, 9302–9303.

Corey, E. J. *Angew. Chem., Int. Ed.* **2002**, *41*, 1650–1667.

Corey, E. J.; Andersen, N. H.; Carlson, R. M.; Paust, J.; Vedejs, E.; Vlattas, I.; Winter, R. E. K. *J. Am. Chem. Soc.* **1968**, *90*, 3245–3247.

Corey, E. J.; Bakshi, R. K.; Shibata, S.; Chen, C.-P.; Singh, V. K. *J. Am. Chem. Soc.* **1987**, *109*, 7925–7926.

Corey, E. J.; Cheng, X.-M. *The Logic of Chemical Synthesis*; Wiley: New York, 1995; pp 1–91.

Corey, E. J.; Helal, C. J. *Angew. Chem., Int. Ed.* **1998**, *37*, 1986–2012.

Cox, E. D.; Cook, J. M. *Chem. Rev.* **1995**, *95*, 1797–1842.

Cozzi, P. G.; Hilgraf, R.; Zimmermann, N. *Eur. J. Org. Chem.* **2007**, *36*, 5969–5994.

Crich, D.; Quintero, L. *Chem. Rev.* **1989**, *89*, 1413–1432.

Cuevas-Yañez, E.; García, M. A.; de la Mora, M. A.; Muchowski, J. M.; Cruz-Almanza, R. *Tetrahedron Lett.* **2003**, *44*, 4815–4817.

d'Augustin, M.; Palais, L.; Alexakis, A. *Angew. Chem., Int. Ed.* **2005**, *44*, 1376–1378.

Danheiser, R. L.; Savariar, S.; Cha, D. D. *Organic Syntheses*; Wiley & Sons: New York, 1993; Collect. Vol. VIII, pp 82–86.

Danishefsky, S. J.; Mantlo, N. *J. Am. Chem. Soc.* **1988**, *110*, 8129–8133.

Dauphin, G.; Gramain, J.-C.; Kergomard, A.; Renard, M. F.; Veschambre, H. *J. Chem. Soc., Chem. Commun.* **1980**, 318–319.

Dawson, G. J.; Frost, C. G.; Coote, S. J.; Williams, J. M. J. *Tetrahedron Lett.* **1993**, *34*, 3149–3150.

De Clercq, E. *Med. Res. Rev.* **2002**, *22*, 531–565.

Metal-Catalyzed Cross-Coupling Reactions; de Meijere, A., Diederich, F., Eds.; Wiley-VCH: Weinheim, 2004; Vols. 1 and 2.

Deardorff, D. R.; Myles, D. C. *Organic Syntheses*; Wiley & Sons: New York, 1993; Collect. Vol. VIII, pp 13–15.

Deardorff, D. R.; Windham, C. Q.; Craney, C. L. *Organic Syntheses*; Wiley & Sons, New York, 1998; Collect. Vol. IX, pp 487–492.

Denissova, I.; Barriault, L. *Tetrahedron* **2003**, *59*, 10105–10146.

- Depew, K. M.; Marsden, S. P.; Zatorska, D.; Zatorski, A.; Bornmann, W. G.; Danishefsky, S. J. *J. Am. Chem. Soc.* **1999**, *121*, 11953–11963.
- Dess, D. B.; Martin, J. C. *J. Am. Chem. Soc.* **1991**, *113*, 7277–7287.
- Diels, O.; Alder, K. *Justus Liebigs Ann. Chem.* **1928**, *460*, 98–122.
- Do, N.; McDermott, R. E.; Ragan, J. A. *Org. Synth.* **2008**, *85*, 138–146.
- Dolling, U.-H.; Davis, P.; Grabowski, E. J. J. *J. Am. Chem. Soc.* **1984**, *106*, 446–447.
- Douglas, C. J.; Overman, L. E. *Proc. Natl. Acad. Sci. U.S.A.* **2004**, *101*, 5363–5367.
- Dounay, A. B.; Humphreys, P. G.; Overman, L. E.; Wroblewski, A. D. *J. Am. Chem. Soc.* **2008**, *130*, 5368–5377.
- Dounay, A. B.; Overman, L. E. *Chem. Rev.* **2003**, *103*, 2945–2963.
- Dounay, A. B.; Overman, L. E.; Wroblewski, A. D. *J. Am. Chem. Soc.* **2005**, *127*, 10186–10187.
- Drexler, H.-J.; You, J.; Zhang, S.; Fischer, C.; Baumann, W.; Spannenberg, A.; Heller, D. *Org. Process Res. Dev.* **2003**, *7*, 355–361.
- Drucker, D.; Easley, C.; Kirkpatrick, P. *Nat. Rev. Drug Discovery* **2007**, *6*, 109–110.
- Dugave, C.; Demange, L. *Chem. Rev.* **2003**, *103*, 2475–2532.

Dunitz, J. D.; Winkler, F. K. *Acta Crystallogr., Sect. B: Struct. Sci.* **1975**, *31*, 251–263.

Eder, U.; Sauer, G.; Wiechert, R. *Angew. Chem., Int. Ed. Engl.* **1971**, *10*, 496–497.

Enquist, J. A., Jr.; Stoltz, B. M. *Nature* **2008**, *453*, 1228–1231.

Erkkilä, A.; Majander, I.; Pihko, P. M. *Chem. Rev.* **2007**, *107*, 5416–5470.

Evans, D. A.; Fitch, D. M.; Smith, T. E.; Cee, V. J. *J. Am. Chem. Soc.* **2000**, *122*, 10033–10046.

Evans, P. A.; Baum, E. W. *J. Am. Chem. Soc.* **2004**, *126*, 11150–11151.

Evans, P. A.; Robinson, J. E.; Baum, E. W.; Fazal, A. N. *J. Am. Chem. Soc.* **2002**, *124*, 8782–8783.

Farina, V.; Reeves, J. T.; Senanayake, C. H.; Song, J. J. *Chem. Rev.* **2006**, *106*, 2734–2793.

Fischer, C.; Fu, G. C. *J. Am. Chem. Soc.* **2005**, *127*, 4594–4595.

Fischer, G. Enzymes Catalyzing Peptide Bond *Cis–Trans* Isomerizations. In *cis–trans Isomerization in Biochemistry*; Dugave, C., Ed.; Wiley-VCH: Weinheim, 2006; pp 195–224.

Fraga, B. M. *Nat. Prod. Rep.* **2006**, *23*, 943–972.

Fraga, B. M. *Nat. Prod. Rep.* **2007**, *24*, 1350–1381.

Fraga, B. M. *Nat. Prod. Rep.* **2008**, *25*, 1180–1209.

Frey, B.; Hünig, S.; Koch, M.; Reissig, H.-U. *Synlett* **1991**, 854–856.

Frey, B.; Schnaubelt, J.; Reißig, H.-U. *Eur. J. Org. Chem.* **1999**, 1385–1393.

Frisch, A. C.; Beller, M. *Angew. Chem., Int. Ed.* **2005**, *44*, 674–688.

Fujimoto, H.; Nakamura, E.; Okuyama, E.; Ishibashi, M. *Chem. Pharm. Bull.* **2000**, *48*,
1436–1441.

Gajewski, J. J.; Hawkins, C. M.; Jimenez, J. L. *J. Org. Chem.* **1990**, *55*, 674–679.

Gannon, W. F.; House, H. O. *Org. Synth.* **1973**, *CV 5*, 294–196.

Gelman, D.; Jiang, L.; Buchwald, S. L. *Org. Lett.* **2003**, *5*, 2315–2318

George, K. M. Natural Product Total Synthesis: I. The Total Synthesis of
(+)-Isoschizandrin. II. Progress Toward the Total Synthesis of Variecolin. Ph.D.
Thesis, University of Pennsylvania, Philadelphia, PA, 2005.

Gibbons, E. G. *J. Am. Chem. Soc.* **1982**, *104*, 1767–1769.

Giese, B.; Kopping, B.; Gobel, T.; Dickhaut, J.; Thoma, G.; Kulicke, K. J.; Trach, F.
Org. React. **1996**, *48*, 301–856.

Golden, J. E.; Aubé, J. *Angew. Chem., Int. Ed.* **2002**, *41*, 4316–4318.

Gottlieb, H. E.; Kotlyar, V.; Nudelman, A. *J. Org. Chem.* **1997**, *62*, 7512–7515.

Greenberg, A. Twisted Bridgehead Bicyclic Lactams. In *Structure and Reactivity*; Liebman, J. F., Greenberg, A., Eds.; VCH: New York, 1988; pp 139–178.

Greenberg, A., Breneman, C. M., Liebman, J. F., Eds. *The Amide Linkage: Selected Structural Aspects in Chemistry, Biochemistry, and Materials Science*; Wiley: New York, 2000.

Greenberg, A.; Moore, D. T.; DuBois, T. D. *J. Am. Chem. Soc.* **1996**, *118*, 8658–8668.

Greenberg, A.; Venanzi, C. A. *J. Am. Chem. Soc.* **1993**, *115*, 6951–6957.

Greenberg, A.; Wu, G.; Tsai, J.-C.; Chiu, Y.-Y. *Struct. Chem.* **1993**, *4*, 127–129.

Grimme, W. *J. Am. Chem. Soc.* **1972**, *94*, 2525–2526.

Grubbs, R. H.; Grey, R. A. *J. Am. Chem. Soc.* **1973**, *95*, 5765–5767.

Gulías, M.; Rodríguez, J. R.; Castedo, L.; Mascareñas, J. L. *Org. Lett.* **2003**, *5*, 1975–1977.

Hajos, Z. G.; Parrish, D. R. *J. Org. Chem.* **1973**, *38*, 3244–3249.

Hall, H. K.; Shaw, R. G.; Deutschmann, A. *J. Org. Chem.* **1980**, *45*, 3722–3724.

Hammond, G. S.; DeBoer, C. D. *J. Am. Chem. Soc.* **1964**, *86*, 899–902.

Han, S. B.; Hassan, A.; Krische, M. J. *Synthesis* **2008**, 2669–2679.

Hanson, J. R. *Nat. Prod. Rep.* **1986**, *3*, 123–132.

Hanson, J. R. *Nat. Prod. Rep.* **1992**, *9*, 481–489.

Hanson, J. R. *Nat. Prod. Rep.* **1996**, *13*, 529–535.

Harrison, D. M. *Nat. Prod. Rep.* **1988**, *5*, 387–415.

Hashimoto, S.-i.; Komeshima, N.; Koga, K. *J. Chem. Soc., Chem. Commun.* **1979**, 437–438.

Hayashi, T.; Konishi, M.; Fukushima, M.; Mise, T.; Kagotani, M.; Tajika, M.; Kumada, M. *J. Am. Chem. Soc.* **1982**, *104*, 180–186.

Hayashi, Y. Catalytic Asymmetric Diels–Alder Reactions. In *Cycloaddition Reactions in Organic Synthesis*; Kobayashi, S., Jørgensen, K. A., Eds.; Wiley-VCH: Weinheim, 2002; pp 5–55.

Heck, R. F. *Acc. Chem. Res.* **1979**, *12*, 146–151.

Helmchen, G.; Pfaltz, A. *Acc. Chem. Res.* **2000**, *33*, 336–345.

Hensens, O. D.; Zink, D.; Williamson, J. M.; Lotti, V. J.; Chang, R. S. L.; Goetz, M. A.

J. Org. Chem. **1991**, *56*, 3399–3403.

Hine, J.; Chen, Y.-J. *J. Org. Chem.* **1987**, *52*, 2091–2094.

Hino, T.; Nakagawa, M. Chemistry and Reactions of Cyclic Tautomers of Tryptamines and Tryptophans. In *The Alkaloids*; Brossi, A., Ed.; Academic Press: San Diego, 1988; Vol. 34, pp 1–75.

Hodson, D.; Holt, G.; Wall, D. K. *J. Chem. Soc. C* **1970**, 971–973.

Hoveyda, A. H. Asymmetric Catalysis in Target-Oriented Synthesis. In *Stimulating Concepts in Chemistry*; Vögtle, F., Stoddart, J. F., Shibasaki, M., Eds.; Wiley-VCH: Weinheim, 2000; pp 145–160.

Hsiao, Y.; Rivera, N. R.; Rosner, T.; Krska, S. W.; Njolito, E.; Wang, F.; Sun, Y.; Armstrong, J. D., III; Grabowski, E. J. J.; Tillyer, R. D.; Spindler, F.; Malan, C. J. *Am. Chem. Soc.* **2004**, *126*, 9918–9919.

Huang, C.; Tang, X.; Fu, H.; Jiang, Y.; Zhao, Y. *J. Org. Chem.* **2006**, *71*, 5020–5022.

Huddleston, R. R.; Krische, M. J. *Synlett* **2003**, 12–21.

Hughes, D. L.; Dolling, U.-H.; Ryan, K. M.; Schoenewaldt, E. F.; Grabowski, E. J. J. *J. Org. Chem.* **1987**, *52*, 4745–4752.

Humber, D. C.; Pinder, A. R.; Williams, R. A. *J. Chem. Soc.* **1967**, 2335–2340.

Humphrey, G. R.; Kuethe, J. T. *Chem. Rev.* **2006**, *106*, 2875–2911.

Hunter, E. P.; Lias, S. G. Proton Affinity Evaluation. In *NIST Chemistry WebBook, NIST Standard Reference Database Number 69*, Linstrom, P. J., Mallard, W. G., Eds.; National Institute of Standards and Technology, Gaithersburg, MD, 2005; 20899 (<http://webbook.nist.gov>).

Hunter, E. P.; Lias, S. G.; *J. Phys. Chem. Ref. Data* **1998**, *27*, 413–656.

Iimura, S.; Overman, L. E.; Paulini, R.; Zakarian, A. *J. Am. Chem. Soc.* **2006**, *128*, 13095–13101.

Ito, M.; Matsuomi, M.; Murugesu, M. G.; Kobayashi, Y. *J. Org. Chem.* **2001**, *66*, 5881–5889.

Comprehensive Asymmetric Catalysis, Supplement 1 & 2; Jacobsen, E. N., Pfaltz, A., Yamamoto, H., Eds.; Springer-Verlag: Berlin, 2004.

Comprehensive Asymmetric Catalysis, Vol. I–III; Jacobsen, E. N., Pfaltz, A., Yamamoto, H., Eds.; Springer-Verlag: Berlin, 2000.

Jensen, K. B.; Thorhauge, J.; Hazell, R. G.; Jørgensen, K. A. *Angew. Chem., Int. Ed.* **2001**, *40*, 160–163.

Johansson, D. G. A.; Wallin, G.; Sandberg, A.; Macao, B.; Åqvist, J.; Härd, T. *J. Am.*

Chem. Soc. **2009**, *131*, 9475–9477.

Johnson, J. R.; Woodward, R. B.; Robinson, R. The Constitution of the Penicillins. *The Chemistry of Penicillin*; Clark, H. T., Johnson, J. R., Robinson, R., Eds.; Princeton University Press: Princeton, NJ, 1949; pp 440–454.

Joshi, D. V.; Boyce, S. F. *J. Org. Chem.* **1957**, *22*, 95–97.

Enantioselective Synthesis of β -Amino Acids; Juaristi, E., Soloshonok, V. A., Eds; Wiley & Son: Hoboken, 2005.

Jun, C.-H.; Moon, C. W.; Lim, S.-G.; Lee, H. *Org. Lett.* **2002**, *4*, 1595–1597.

Kanemoto, S.; Tomioka, H.; Oshima, K.; Nozaki, H. *Bull. Chem. Soc. Jpn.* **1986**, *59*, 105–108.

Kaplan, F.; Meloy, G. K. *J. Am. Chem. Soc.* **1966**, *88*, 950–956.

Kawai, K.-i.; Nozawa, K.; Nakajima, S. *J. Chem. Soc., Perkin Trans. 1* **1994**, 1673–1674.

Kawamura, S.-i.; Yamakoshi, H.; Nojima, M. *J. Org. Chem.* **1996**, *61*, 5953–5958.

Kedzierska, K.; Crowe, S. M.; Turville, S.; Cunningham, A. L. *Rev. Med. Virology* **2003**, *13*, 39–56.

Kemnitz, C. R.; Loewen, M. J. *J. Am. Chem. Soc.* **2007**, *129*, 2521–2528.

Kennedy, M.; McKervey, M. A. *J. Chem. Soc., Perkin Trans. 1* **1991**, 2565–2574.

Khanina, M. A.; Kulyyasov, A. T.; Bagryanskaya, I. Y.; Gatilov, Y. V.; Adekenov, S. M.; Raldugin, V. A. *Chem. Nat. Compd.* **1998**, *34*, 145–147.

Kingston, D. G. I.; Bursey, J. T.; Bursey, M. M. *Chem. Rev.* **1974**, *74*, 215–242.

Kirby, A. J.; Komarov, I. V.; Feeder, N. *J. Am. Chem. Soc.* **1998**, *120*, 7101–7102.

Kirby, A. J.; Komarov, I. V.; Wothers, P. D.; Feeder, N. *Angew. Chem., Int. Ed.* **1998**, *37*, 785–786.

Kirmansjah, L.; Fu, G. C. *J. Am. Chem. Soc.* **2008**, *129*, 11340–11341.

Kirmse, W. *Eur. J. Org. Chem.* **2002**, 2193–2256.

Kiso, Y.; Tamao, K.; Miyake, N.; Yamamoto, K.; Kumada, M. *Tetrahedron Lett.* **1974**, *15*, 3–6.

Kobayashi, Y.; Nakata, K.; Ainai, T. *Org. Lett.* **2005**, *7*, 183–186.

Kraus, G. A.; Roth, B. *J. Org. Chem.* **1980**, *45*, 4825–4830.

Krishnan, S.; Bagdanoff, J. T.; Ebner, D. C.; Ramtohul, Y. K.; Tambar, U. K.; Stoltz, B. M. *J. Am. Chem. Soc.* **2008**, *130*, 13745–13754.

Krout, M. R.; Mohr, J. T.; Stoltz, B. M. *Org. Synth.* **2009**, *86*, 181–193.

Kutney, J. P.; Singh, A. K. *Can. J. Chem.* **1982**, *60*, 1842–1846.

Kwon, O.; Su, D.-S.; Meng, D.; Deng, W.; D'Amico, D. C.; Danishefsky, S. J. *Angew. Chem., Int. Ed.* **1998**, *37*, 1877–1880.

Lautens, M.; Hiebert, S. *J. Am. Chem. Soc.* **2004**, *126*, 1437–1447.

Le Marquand, P.; Tam, W. *Angew. Chem., Int. Ed.* **2008**, *47*, 2926–2928.

Lease, T. G.; Shea, K. J. *J. Am. Chem. Soc.* **1993**, *115*, 2248–2260.

Legault, C. Y.; Charette, A. B. *J. Am. Chem. Soc.* **2005**, *127*, 8966–8977.

Lehner, T. *Trends Immunol.* **2002**, *23*, 347–351.

Lei, Y.; Wroblewski, A. D.; Golden, J. E.; Powell, D. R.; Aubé, J. *J. Am. Chem. Soc.* **2005**, *127*, 4552–4553.

Lelais, G.; MacMillan, D. W. C. *Aldrichimica Acta* **2006**, *39*, 79–87.

Levine, S. R.; Krout, M. R.; Stoltz, B. M. *Org. Lett.* **2009**, *11*, 289–292.

Levkoeva, E. I.; Nikitskaya, E. S.; Yakhontov, L. N. *Dokl. Akad. Nauk SSSR* **1970**, *192*, 342–345.

Limanto, J.; Snapper, M. L. *J. Am. Chem. Soc.* **2000**, *122*, 8071–8072.

Limanto, J.; Snapper, M. L. *J. Org. Chem.* **1998**, *63*, 6440–6441.

Limanto, J.; Tallarico, J. A.; Porter, J. R.; Khuong, K. S.; Houk, K. N.; Snapper, M. L. *J. Am. Chem. Soc.* **2002**, *124*, 14748–14758.

Lindgren, B. O.; Nilsson, T. *Acta Chem. Scand.* **1973**, *27*, 888–890.

Lindsay, E. A.; Berry, Y.; Jamie, J. F.; Bremner, J. B. *Phytochemistry* **2000**, *55*, 403–406.

Linton, E. C.; Kozlowski, M. C. *J. Am. Chem. Soc.* **2008**, *130*, 16162–16163.

Liu, Q.; Ferreira, E. M.; Stoltz, B. M. *J. Org. Chem.* **2007**, *72*, 7352–7358.

Liu, Y.; Wang, L.; Jung, J. H.; Zhang, S. *Nat. Prod. Rep.* **2007**, *24*, 1401–1429.

Lo, P. C.-K.; Snapper, M. L. *Org. Lett.* **2001**, *3*, 2819–2821.

Loiseleur, O.; Meier, P.; Pfaltz, A. *Angew. Chem., Int. Ed. Engl.* **1996**, *35*, 200–202.

Lopez, X.; Mujika, J. I.; Blackburn, G. M.; Karplus, M. *J. Phys. Chem. A* **2003**, *107*, 2304–2315.

Lubell, W. D.; Kitamura, M.; Noyori, R. *Tetrahedron: Asymmetry* **1991**, *2*, 543–554.

Luche, J. L.; Gemal, A. L. *J. Am. Chem. Soc.* **1979**, *101*, 5848–5849.

Luh, T.-Y.; Leung, M.-k.; Wong, K.-T. *Chem. Rev.* **2000**, *100*, 3187–3204.

Lukeš, R. *Coll. Czech. Chem. Commun.* **1938**, *10*, 148–152.

Ma, J.-A. *Angew. Chem., Int. Ed.* **2003**, *42*, 4290–4299.

Maier, M. E. *Angew. Chem., Int. Ed.* **2000**, *39*, 2073–2077.

Maier, W. F.; Schleyer, P. v. R. *J. Am. Chem. Soc.* **1981**, *103*, 1891–1900.

Marinescu, S. C.; Nishimata, T.; Mohr, J. T.; Stoltz, B. M. *Org. Lett.* **2008**, *10*, 1039–1042.

Marmster, F. P.; Murphy, G. K.; West, F. G. *J. Am. Chem. Soc.* **2003**, *125*, 14724–14725.

Asymmetric Phase Transfer Catalysis; Maruoka, K., Ed.; Wiley-VCH: Weinheim, 2008.

May, J. A.; Stoltz, B. M. *J. Am. Chem. Soc.* **2002**, *124*, 12426–12427.

McEwen, A. B.; Schleyer, P. v. R. *J. Am. Chem. Soc.* **1986**, *108*, 3951–3960.

McFadden, R. M. Applications of Palladium-Catalyzed Enantioselective Decarboxylative Alkylation in Natural Products Total Synthesis. Ph.D. Thesis, California Institute of Technology, Pasadena, CA, December 2007.

McFadden, R. M.; Stoltz, B. M. *J. Am. Chem. Soc.* **2006**, *128*, 7738–7739.

McGrath, N. A.; Lee, C. A.; Araki, H.; Brichacek, M.; Njardarson, J. T. *Angew. Chem., Int. Ed.* **2008**, *47*, 9450–9453.

McLafferty, F. W. *Anal. Chem.* **1956**, *28*, 306–316.

McQuillin, F. J.; Parrack, J. D. *J. Chem Soc.* **1956**, 2973–2978.

Mehta, G.; Singh, V. *Chem. Rev.* **1999**, *99*, 881–930.

Meyers, A. I.; Hanreich, R.; Wanner, K. T. *J. Am. Chem. Soc.* **1985**, *107*, 7776–7778.

Michaut, A.; Rodriguez, J. *Angew. Chem., Int. Ed.* **2006**, *45*, 5740–5750.

Miyaoka, H.; Kajiwara, Y.; Hara, M.; Suma, A.; Yamada, Y. *Tetrahedron: Asymmetry* **1999**, *10*, 3189–3196.

Miyaoka, H.; Kajiwara, Y.; Hara, Y.; Yamada, Y. *J. Org. Chem.* **2001**, *66*, 1429–1435.

Mohamed, A. E.-H., Ahmed, A. A.; Wollenweber, E.; Bohm, B.; Asakawa, Y. *Chem. Pharm. Bull.* **2006**, *54*, 152–155.

Mohr, J. T.; Behenna, D. C.; Harned, A. M.; Stoltz, B. M. *Angew. Chem., Int. Ed.* **2005**, *44*, 6924–6927.

Mohr, J. T.; Ebner, D. C.; Stoltz, B. M. *Org. Biomol. Chem.* **2007**, *5*, 3571–3576.

- Mohr, J. T.; Krout, M. R.; Stoltz, B. M. *Nature* **2008**, *455*, 323–332.
- Mohr, J. T.; Krout, M. R.; Stoltz, B. M. *Org. Synth.* **2009**, *86*, 194–211.
- Mohr, J. T.; Nishimata, T.; Behenna, D. C.; Stoltz, B. M. *J. Am. Chem. Soc.* **2006**, *128*, 11348–11349.
- Mohr, J. T.; Stoltz, B. M. *Chem.—Asian J.* **2007**, *2*, 1476–1491.
- Mohr, K.; Schindler, O.; Reichstein, T. *Helv. Chim. Acta.* **1954**, *37*, 462–471.
- Molander, G. A.; Alonso-Alija, C. J. *J. Org. Chem.* **1998**, *63*, 4366–4373.
- Molander, G. A.; Harris, C. R. *J. Am. Chem. Soc.* **1995**, *117*, 3705–3716.
- Molander, G. A.; Harris, C. R. *Tetrahedron* **1998**, *54*, 3321–3354.
- Molander, G. A.; Machrouhi, F. *J. Org. Chem.* **1999**, *64*, 4119–4123.
- Molander, G. A.; Quirnbach, M. S.; Silva, Jr., L. F.; Spencer, K. C.; Balsells, J. *Org. Lett.* **2001**, *3*, 2257–2260.
- Moore, J. P.; Stevenson, M. *Nat. Rev. Mol. Cell. Biol.* **2000**, *1*, 40–49.
- Morita, Y.; Suzuki, M.; Noyori, R. *J. Org. Chem.* **1989**, *54*, 1785–1787.
- Mujika, J. I.; Mercero, J. M.; Lopez, X. *J. Am. Chem. Soc.* **2005**, *127*, 4445–4453.

Mujika, J. I.; Mercero, J. M.; Lopez, X. *J. Phys. Chem. A* **2003**, *107*, 6099–6107.

Nájera, C.; Sansano, J. M. *Chem. Rev.* **2007**, *107*, 4584–4671.

Handbook of Organopalladium Chemistry for Organic Synthesis; Negishi, E.-i., de Meijere, A., Eds.; Wiley & Sons: New York, 2002; Vol 1.

Netherton, M. R.; Fu, G. C. Palladium-Catalyzed Cross-Coupling Reactions of Unactivated Alkyl Electrophiles with Organometallic Compounds. In *Topics in Organometallic Chemistry: Palladium in Organic Synthesis*; Tsuji, J., Ed.; Springer: New York, 2005; pp 85–108.

Newman, D. J.; Cragg, G. M. *J. Nat. Prod.* **2007**, *70*, 461–477.

Nicolaou, K. C.; Baran, P. S.; Zhong, Y.-L.; Choi, H.-S.; Fong, K. C.; He, Y.; Yoon, W. *H. Org. Lett.* **1999**, *1*, 883–886.

Nicolaou, K. C.; Snyder, S. A.; Montagnon, T.; Vassilikogiannakis, G. *Angew. Chem., Int. Ed.* **2002**, *41*, 1668–1698.

Noyori, R.; Kitamura, M.; Ohkuma, T. *Proc. Natl. Acad. Sci. U.S.A.* **2004**, *101*, 5356–5362.

Nugent, W. A.; RajanBabu, T. V.; Burk, M. J. *Science* **2002**, *259*, 479–483.

Overman, L. E. *Pure Appl. Chem.* **1994**, *66*, 1423–11430.

Overman, L. E.; Larrow, J. F.; Stearns, B. A.; Vance, J. M. *Angew. Chem., Int. Ed.* **2000**, *39*, 213–215.

Overman, L. E.; Paone, D. V.; Stearns, B. A. *J. Am. Chem. Soc.* **1999**, *121*, 7702–7703.

Özkan, I.; Zora, M. *J. Org. Chem.* **2003**, *68*, 9635–9642.

Paliani, G.; Sorriso, S.; Cataliotti, R. *J. Chem. Soc., Perkin Trans. 2* **1976**, 707–710.

Palomo, C.; Oiarbide, M.; García, J. M. *Chem.—Eur. J.* **2002**, *8*, 37–44.

Paquette, L. A.; Dahnke, K.; Doyon, J.; He, W.; Wyant, K.; Friedrich, D. *J. Org. Chem.* **1991**, *56*, 6199–6205.

Paquette, L. A.; Sauer, D. R.; Cleary, D. G.; Kinsella, M. A.; Blackwell, C. M.; Anderson, L. G. *J. Am. Chem. Soc.* **1992**, *114*, 7375–7387.

Paras, N. A.; MacMillan, D. W. C. *J. Am. Chem. Soc.* **2001**, *123*, 4370–4371.

Pecile, C.; Föffani, A.; Gheretti, S. *Tetrahedron* **1964**, *20*, 823–829.

Petasis, N. A.; Patane, M. A. *Tetrahedron* **1992**, *48*, 5757–5821.

Petrova, K. V.; Mohr, J. T.; Stoltz, B. M. *Org. Lett.* **2009**, *11*, 293–295.

Pettit, G. R.; Nelson, P. S. *Can. J. Chem.* **1986**, *64*, 2097–2102.

Pictet, A.; Spengler, T. *Ber. Dtsch. Chem. Ges.* **1911**, *44*, 2030–2036.

Piers, E.; Boulet, S. L. *Tetrahedron Lett.* **1997**, *38*, 8815–8818.

Pinder, A. R.; Williams, R. A. *J. Chem. Soc.* **1963**, 2773–2778.

Poland, B. W.; Xu, M.-Q.; Quioco, F. A. *J. Biol. Chem.* **2000**, *275*, 16408–16413.

Pracejus, H. *Chem. Ber.* **1959**, *92*, 988–998.

Pracejus, H. *Chem. Ber.* **1965**, *98*, 2897–2905.

Pracejus, H.; Kehlen, M.; Matschiner, H. *Tetrahedron* **1965**, *21*, 2257–2270.

Presset, M.; Coquerel, Y.; Rodriguez, J. *J. Org. Chem.* **2009**, *74*, 415–418.

Pretsch, E.; Bühlmann, P.; Affolter, C. *Structure Determination of Organic Compounds.*

Tables of Spectral Data, 3rd ed.; Springer-Verlag: New York, 2000.

Qin, D.-G.; Zha, H.-Y.; Yao, Z.-H. *J. Org. Chem.* **2002**, *67*, 1038–1040.

Ragan, J. A.; Makowski, T. W.; am Ende, D. J.; Clifford, P. J.; Young, G. R.; Conrad, A.

K.; Eisenbeis, S. A. *Org. Process Res. Dev.* **1998**, *2*, 379–381.

Ragan, J. A.; Murry, J. A.; Castaldi, M. J.; Conrad, A. K.; Jones, B. P.; Li, B.;

Makowski, T. W.; McDermott, R.; Sitter, B. J.; White, T. D.; Young, G. R. *Org.*

Process Res. Dev. **2001**, *5*, 498–507.

Raheem, I. T.; Thiara, P. S.; Jacobsen, E. N. *Org. Lett.* **2008**, *10*, 1577–1580.

Raheem, I. T.; Thiara, P. S.; Peterson, E. A.; Jacobsen, E. N. *J. Am. Chem. Soc.* **2007**, *129*, 13404–13405.

Rai, A. N.; Basu, A. *Tetrahedron Lett.* **2003**, *44*, 2267–2269.

Reetz, M. T.; Eipper, A.; Tielmann, P.; Mynott, R. *Adv. Synth. Catal.* **2002**, *344*, 1008–1016.

Reetz, M. T.; Steinbach, R.; Wenderoth, B. *Synth. Commun.* **1981**, *11*, 261–266.

Reetz, M. T.; Wenderoth, B.; Peter, R.; Steinbach, R.; Westerman, J. *J. Chem. Soc., Chem. Commun.* **1980**, 1202–1204.

Reisman, S. E.; Doyle, A. G.; Jacobsen, E. N. *J. Am. Chem. Soc.* **2008**, *130*, 7198–7199.

Ribelin, T. P.; Judd, A. S.; Akritopoulou-Zanze, I.; Henry, R. F.; Cross, J. L.; Whittern, D. N.; Djuric, S. W. *Org. Lett.* **2007**, *9*, 5119–5122.

Rieck, H.; Helmchen, G. *Angew. Chem., Int. Ed. Engl.* **1995**, *34*, 2687–2689.

Ripa, L.; Hallberg, A. *J. Org. Chem.* **1997**, *62*, 595–602.

Romanelli, A.; Shekhtman, A.; Cowburn, D.; Muir, T. W. *Proc. Natl. Acad. Sci. U.S.A.* **2004**, *101*, 6397–6402.

Sarpong, R.; Su, J. T.; Stoltz, B. M. *J. Am. Chem. Soc.* **2003**, *125*, 13624–13625.

Sathe, V. M.; Rao, A. S. *Indian J. Chem.* **1971**, *9*, 95–97.

Sato, A.; Morishita, T.; Hosoya, T. S-19777 as Endothelin Antagonist, Its Manufacture with *Emericella Aurantiobrunnea*, and Its Use as Pharmaceutical. Japan Patent JP 10306087, 1998.

Sato, Y.; Sodeoka, M.; Shibasaki, M. *J. Org. Chem.* **1989**, *54*, 4738–4739.

Indoles. Part Four. The Monoterpenoid Indole Alkaloids; Saxton, J. E., Ed.; Wiley & Sons: New York, 1983.

Schmidt, E. K. G. *Angew. Chem., Int. Ed. Engl.* **1973**, *12*, 777–778.

Schneider, M. *Angew. Chem.* **1975**, *87*, 717–718.

Scholl, M.; Ding, S.; Lee, C. W.; Grubbs, R. H. *Org. Lett.* **1999**, *1*, 953–956.

Schomaker, J. M.; Pulgam, V. R.; Borhan, B. *J. Am. Chem. Soc.* **2004**, *126*, 13600–13601.

Schreiber, S. L.; Claus, R. E.; Reagan, J. *Tetrahedron Lett.* **1982**, *23*, 3867–3870.

Schroeder, G. M.; Trost, B. M. *Chem.—Eur. J.* **2005**, *11*, 174–184.

Schulz, S. R.; Blechert, S. *Angew. Chem., Int. Ed.* **2007**, *46*, 3966–3970.

Schwartz, M. A.; Willbrand, A. M. *J. Org. Chem.* **1985**, *50*, 1359–1365.

Seayad, J.; Seayad, A. M.; List, B. *J. Am. Chem. Soc.* **2006**, *128*, 1086–1087.

Senanayake, C. H.; Jacobsen, E. N. Chiral (Salen)Mn(III) Complexes in Asymmetric Epoxidations: Practical Synthesis of *cis*-Aminoindanol and Its Application to Enantiopure Drug Synthesis. In *Process Chemistry in the Pharmaceutical Industry*; Gadamasetti, K. G., Ed.; Marcel Dekker, New York, 1999; pp 347–368.

Seto, M.; Roizen, J. L.; Stoltz, B. M. *Angew. Chem., Int. Ed.* **2008**, *47*, 6873–6876.

Sherden, N. H.; Behenna, D. C.; Virgil, S. C.; Stoltz, B. M. *Angew. Chem., Int. Ed.* **2009**, *48*, 6840–6843.

Shultz, C. S.; Krska, S. W. *Acc. Chem Res.* **2007**, *40*, 1320–1326.

Silva, L. F., Jr. *Tetrahedron* **2002**, *58*, 9137–9161.

Smith, A. B., III.; Nolen, E. G., Jr.; Shirai, R.; Blase, F. R.; Ohta, M.; Chida, N.; Hartz, R. A.; Fitch, D. M.; Clark, W. M.; Sprengeler, P. A. *J. Org. Chem.* **1995**, *60*, 7837–7848.

Smith, A. B., III; Agosta, W. C. *J. Am. Chem. Soc.* **1974**, *96*, 3289–3295.

Smith, R. M.; Hansen, D. E. *J. Am. Chem. Soc.* **1998**, *120*, 8910–8913.

Somayaji, V.; Brown, R. S. *J. Org. Chem.* **1986**, *51*, 2676–2686.

Son, S.; Fu, G. C. *J. Am. Chem. Soc.* **2008**, *130*, 2756–2757.

Sorriso, S.; Piazza, G.; Foffani, A. *J. Chem. Soc. B* **1971**, 805–809.

Sprinz, J.; Helmchen, G. *Tetrahedron Lett.* **1993**, *34*, 1769–1772.

Srikrishna, A.; Vijaykumar, D. *J. Chem. Soc., Perkin Trans. 1* **2000**, 2583–2589.

Stewart, I. C.; Ung, T.; Pletnev, A. A.; Berlin, J. M.; Grubbs, R. H.; Schrodi, Y. *Org. Lett.* **2007**, *9*, 1589–1592.

Stork, G.; Danheiser, R. L. *J. Org. Chem.* **1973**, *38*, 1775–1776.

Stork, G.; Rosen, P.; Goldman, N. L. *J. Am. Chem. Soc.* **1961**, *83*, 2965–2966.

Stork, G.; Rosen, P.; Goldman, N.; Coombs, R. V.; Tsuji, J. *J. Am. Chem. Soc.* **1965**, *87*, 275–286.

Stork, G.; van Tamalen, E. E.; Friedman, L. J.; Burgstahler, A. W. *J. Am. Chem. Soc.* **1951**, *73*, 4501.

Streuff, J.; White, D. E.; Virgil, S. C.; Stoltz, B. M. *Nat. Chem.* **2010**, *2*, 192–196.

Su, J. T.; Sarpong, R.; Stoltz, B. M.; Goddard, W. A., III. *J. Am. Chem. Soc.* **2004**, *126*, 24–25.

Sudrik, S. G.; Chavan, S. P.; Chandrakumar, K. R. S.; Sourav, P.; Date, S. K.; Chavan, S. P.; Sonawane, H. R. *J. Org. Chem.* **2002**, *67*, 1574–1579.

Suh, Y.-G.; Kim, S.-A.; Jung, J.-K.; Shin, D.-Y.; Min, K.-H.; Koo, B.-A.; Kim, H.-S. *Angew. Chem., Int. Ed.* **1999**, *38*, 3545–3547.

Sundberg, R. J. *Indoles*; Academic Press: San Diego, 1996.

Szostak, M.; Aube, J. *Org. Lett.* **2009**, *11*, 3878–3881.

Taber, D. F.; Saleh, S. A. *Tetrahedron Lett.* **1982**, *23*, 2361–2364.

Takahashi, H.; Hosoe, T.; Nozawa, K.; Kawai, K.-i. *J. Nat. Prod.* **1999**, *62*, 1712–1713.

Takeda, K.; Haraguchi, H.; Okamoto, Y. *Org. Lett.* **2003**, *5*, 3705–3707.

Tallarico, J. A.; Randall, M. L.; Snapper, M. L. *J. Am. Chem. Soc.* **1996**, *118*, 9196–9197.

Tambar, U. K.; Ebner, D. C.; Stoltz, B. M. *J. Am. Chem. Soc.* **2006**, *128*, 11752–11753.

Tambar, U. K.; Kano, T.; Stoltz, B. M. *Org. Lett.* **2005**, *7*, 2413–2416.

Tambar, U. K.; Kano, T.; Zepernick, J. F.; Stoltz, B. M. *J. Org. Chem.* **2006**, *71*, 8357–8364.

Tambar, U. K.; Kano, T.; Zepernick, J. F.; Stoltz, B. M. *Tetrahedron Lett.* **2007**, *48*,

345–350.

Tambar, U. K.; Stoltz, B. M. *J. Am. Chem. Soc.* **2005**, *127*, 5340–5341.

Tani, K.; Behenna, D. C.; McFadden, R. M.; Stoltz, B. M. *Org. Lett.* **2007**, *9*, 2529–2531.

Tani, K.; Stoltz, B. M. *Nature* **2006**, *441*, 731–734.

Taylor, M. S.; Jacobsen, E. N. *J. Am. Chem. Soc.* **2004**, *126*, 10558–10559.

Taylor, M. S.; Jacobsen, E. N. *Proc. Natl. Acad. Sci. U.S.A.* **2004**, *101*, 5368–5373.

Testero, S. A.; Suárez, A. G.; Spanevello, R. A.; Mangione, M. I. *Trends Org. Chem.* **2003**, *10*, 35–49.

Tezuka, Y.; Takahashi, A.; Maruyama, M.; Tamamura, T.; Kutsuma, S.; Naganawa, H.; Takeuchi, T. Novel Antibiotics, AB5362-A, B, and C, Their Manufacture, Their Use as Fungicides, and Phoma Species AB5362. Japan Patent JP 10045662, 1998.

Thielges, S.; Bisseret, P.; Eustache, J. *Org. Lett.* **2005**, *7*, 681–684.

Tietze, L. F.; Stadler, C.; Böhnke, N.; Brasche, G.; Grube, A. *Synlett* **2007**, 485–487.

Tomioka, H.; Oshima, K.; Nozaki, H. *Tetrahedron Lett.* **1982**, *23*, 539–542.

Toyota, M.; Yonehara, Y.; Horibe, I.; Minagawa, K.; Asakawa, Y. *Phytochemistry* **1999**,

52, 689–694.

Trecker, D. J.; Henry, J. P. *J. Am. Chem. Soc.* **1964**, *86*, 902–905.

Trost, B. M. *Proc. Natl. Acad. Sci. U.S.A.* **2004**, *101*, 5348–5355.

Trost, B. M.; Bream, R. N.; Xu, J. *Angew. Chem., Int. Ed.* **2006**, *45*, 3109–3112.

Trost, B. M.; Chan, D. M. T. *J. Am. Chem. Soc.* **1979**, *101*, 6429–6432.

Trost, B. M.; Chan, D. M. T. *J. Am. Chem. Soc.* **1979**, *101*, 6432–6433.

Trost, B. M.; Cramer, N.; Bernsmann, H. *J. Am. Chem. Soc.* **2007**, *129*, 3086–3087.

Trost, B. M.; Cramer, N.; Silverman, S. M. *J. Am. Chem. Soc.* **2007**, *129*, 12396–12397.

Trost, B. M.; Jiang, C. *Synthesis* **2006**, 369–396.

Trost, B. M.; Silverman, S. M.; Stambuli, J. P. *J. Am. Chem. Soc.* **2007**, *129*, 12398–
12399.

Trost, B. M.; Stambuli, J. P.; Silverman, S. M.; Schwörer, W. *J. Am. Chem. Soc.* **2006**,
128, 13328–13329.

Ukai, T.; Kawazura, H.; Ishii, Y.; Bonnet, J. J.; Ibers, J. A. *J. Organomet. Chem.* **1974**,
65, 253–266.

Ukai, T.; Kawazura, H.; Ishii, Y.; Bonnet, J. J.; Ibers, J. A. *J. Organomet. Chem.* **1974**, *65*, 253–266.

Van Allen, D.; Venkataraman, D. *J. Org. Chem.* **2003**, *68*, 4590–4593.

Varseev, G. N.; Maier, M. E. *Angew. Chem., Int. Ed.* **2009**, *48*, –3685–3688.

Veale, C. A.; Rheingold, A. L.; Moore, J. A. *J. Org. Chem.* **1985**, *50*, 2141–2145.

Villieras, J.; Rambaud, M. *Organic Syntheses*; Wiley & Sons: New York, 1993; Collect. Vol. VIII, pp 265–267.

Vineyard, B. D.; Knowles, W. S.; Sabacky, M. J.; Bachman, G. L.; Weinkauff, D. J. *J. Am. Chem. Soc.* **1977**, *99*, 5946–5952.

von Matt, P.; Loiseleur, O.; Koch, G.; Pfaltz, A.; Lefeber, C.; Feucht, T.; Helmchen, G. *Tetrahedron: Asymmetry* **1994**, *5*, 573–584.

von Matt, P.; Pfaltz, A. *Angew. Chem., Int. Ed.* **1993**, *32*, 566–568.

Vuagnoux-d'Augustin, M.; Alexakis, A. *Chem.—Eur. J.* **2007**, *13*, 9647–9662.

Walker, S. D. A Synthetic Approach to the Variocolin Class of Sesterterpenoids: Total Synthesis of (±)-5-Deoxyvariecolin, (±)-5-Deoxyvariecolol and (±)-5-Deoxyvariecolactone. A New Cycloheptenone Annulation Method Employing the Bifunctional Reagent (Z)-5-Iodo-1-tributylstannylpent-1-ene. Ph.D. Thesis,

University of British Columbia, Vancouver, Canada, 2002.

Wang, A. H.-J.; Missavage, R. J.; Byrn, S. R.; Paul, I. C. *J. Am. Chem. Soc.* **1972**, *94*, 7100–7104.

Wang, C.-C. *J. Nat. Prod.* **1996**, *59*, 409–411.

Wang, J.; Burdzinski, G.; Kubicki, J.; Platz, M. S. *J. Am. Chem. Soc.* **2008**, *130*, 11195–11209.

Wang, J.; Zhang, Z. *Tetrahedron* **2008**, *64*, 6577–6605.

Wang, Q.-P.; Bennet, A. J.; Brown, R. S.; Santarsiero, B. D. *Can. J. Chem.* **1990**, *68*, 1732–1739.

Wang, Q.-P.; Bennet, A. J.; Brown, R. S.; Santarsiero, B. D. *J. Am. Chem. Soc.* **1991**, *113*, 5757–5765.

Wang, Y.; Wang, J.; Su, J.; Huang, F.; Jiao, L.; Liang, Y.; Yang, D.; Zhang, S.; Wender, P. A.; Yu, Z.-X. *J. Am. Chem. Soc.* **2007**, *129*, 10060–10061.

Wanner, M. J.; van der Haas, R. N. S.; de Cuba, K. R.; van Maarseveen, J. H.; Hiemstra, H. *Angew. Chem., Int. Ed.* **2007**, *46*, 7485–7487.

Wasserman, H. H. *Heterocycles* **1977**, *7*, 1–15. (c) Wasserman, H.H. *Nature* **2006**, *441*, 699–700.

Watts, L.; Fitzpatrick, J. D.; Pettit, R. *J. Am. Chem. Soc.* **1965**, *87*, 3253–3254.

Wawra, S.; Fischer, G. Amide *Cis–Trans* Isomerization in Peptides and Proteins. In *cis–trans Isomerization in Biochemistry*; Dugave, C., Ed.; Wiley-VCH: Weinheim, 2006; pp 167–193.

Werner, E. A. *J. Chem. Soc.* **1919**, 1093–1102

Westheimer, F. H. *Chem. Rev.* **1961**, *61*, 265–273.

White, D. E.; Stewart, I. C.; Grubbs, R. H.; Stoltz, B. M. *J. Am. Chem. Soc.* **2008**, *130*, 810–811.

Wiberg, K. B. *Acc. Chem. Res.* **1999**, *32*, 922–929.

Wiberg, K. B. *Angew., Int. Ed. Engl.* **1986**, *25*, 312–322.

Wiberg, K. B.; Laidig, K. E. *J. Am. Chem. Soc.* **1987**, *109*, 5935–5943.

Wilds, A. L.; Meader, A. L., Jr. *J. Org. Chem.* **1948**, *13*, 763–779.

Williams, J. M. J. *Synlett* **1996**, 705–710.

Williams, R. M.; Lee, B. H. *J. Am. Chem. Soc.* **1986**, *108*, 6431–6433.

Williams, R. M.; Lee, B. Y.; Miller, M. M.; Anderson, O. P. *J. Am. Chem. Soc.* **1989**, *111*, 1073–1081.

Wilson, S. R.; Turner, R. B. *J. Org. Chem.* **1973**, *38*, 2870–2873.

Woodward, R. B.; Bader, F. E.; Bickel, H.; Frey, A. J.; Kierstead, R. W. *J. Am. Chem. Soc.* **1956**, *78*, 2023–2025.

Wu, Q.-X.; Shi, Y.-P.; Jia, Z.-J. *Nat. Prod. Rep.* **2006**, *23*, 699–734.

Wu, Z.; Fenselau, C.; Cooks, G. R. *Rapid Commun. Mass. Spectrom.* **1994**, *8*, 777–780.

Xiong, Z.; Yang, J.; Li, Y. *Tetrahedron: Asymmetry* **1996**, *7*, 2607–2612.

Xu, F.; Armstrong, J. D., III; Zhou, G. X.; Simmons, B.; Hughes, D.; Ge, Z.; Grabowski, E. J. *J. Am. Chem. Soc.* **2004**, *126*, 13002–13009.

Yakhontov, L. N.; Rubsitov, M. V. *J. Gen. Chem. USSR* **1957**, *27*, 83–87.

Yamago, S.; Nakamura, E. *Org. React.* **2002**, *61*, 1–217.

Yamamoto, A.; Ito, Y.; Hayashi, T. *Tetrahedron Lett.* **1989**, *30*, 375–378.

Yao, L.; Aubé, J. *J. Am. Chem. Soc.* **2007**, *129*, 2766–2767.

Yates, P.; Eaton, P. *J. Am. Chem. Soc.* **1960**, *82*, 4436–4437.

Yet, L. *Chem. Rev.* **2000**, *100*, 2963–3007

Yoganathan, K.; Rossant, C.; Glover, R. P.; Cao, S.; Vittal, J. J.; Ng, S.; Huang, Y.;

Buss, A. D.; Butler, M. S. *J. Nat. Prod.* **2004**, *67*, 1681–1684.

Yoon, T. P.; Jacobsen, E. N. *Science* **2003**, *229*, 1691–1693.

Yu, W.; Mei, Y.; Kang, Y.; Hua, Z.; Jin, Z. *Org. Lett.* **2004**, *6*, 3217–3219.

Zhao, Y.; Zhou, Y.; Liang, L.; Yang, X.; Du, F.; Li, L.; Zhang, H. *Org. Lett.* **2009**, *11*,
555–558.

Zheng, G. Z.; Chan, T. H. *Organometallics* **1995**, *14*, 70–79.

Zheng, X.; Cooks, R. G. *J. Phys. Chem. A* **2002**, *106*, 9939–9946.

Zhou, J.; Fu, G. C. *J. Am. Chem. Soc.* **2003**, *125*, 14726–14727.

INDEX

A

acyclopentene.....83, 87, 89, 90, 152, 153, 154, 156, 157
alkaloid15, 19, 21, 22
annulation 26, 47, 48, 49, 92, 94, 95, 101
anti-HIV38, 45, 59, 64
antihypertensive38, 64
asymmetric3, 4, 5, 6, 8, 9, 11, 13, 14, 15, 16, 17, 18, 19, 20, 26, 27, 28, 54, 56, 66, 77, 79, 80, 84, 85, 86,
89, 92, 100, 172, 317, 318, 319, 322, 324, 325, 326, 328, 332, 338, 340, 342, 345, 348, 502, 506

C

carissone317, 326, 329, 331, 332
catalysis 1, 2, 4, 7, 11, 13, 15, 20, 26, 28, 29, 65, 502, 506
CCR545
collision-induced dissociation
 CID418, 419, 420, 421, 423, 424, 426, 432
 collision-induced dissociation.....418
cross-coupling12, 13, 14, 25
cyclobutadiene68, 69, 77, 78, 105, 106, 107, 110, 131
cyclooctadienone 76, 80, 81, 82, 83, 95, 96, 124, 142, 173, 174

D

diastereoselective5, 15, 19, 46, 53, 55, 92, 99, 327, 330, 332
diazoketone73, 74, 75, 76, 82, 83, 122, 123, 124, 139, 140, 141, 142
distortion.....412, 416, 426, 430

E

eight-membered ring38, 59, 64, 65, 66, 68, 100
enantiomer2, 39, 55

enantioselective 1, 2, 3, 4, 5, 6, 7, 8, 15, 16, 17, 19, 20, 22, 23, 25, 27, 28, 29, 52, 53, 66, 84, 86, 101, 318, 325, 328
eudesmane 325, 326, 331, 332
eudesmol 326, 331, 332

G

gas phase 417, 423, 430

I

immunosuppressant 38

K

kinetic method 417, 419, 425, 432, 452

M

metathesis 25, 327, 330

microwave 16, 76, 80, 81, 82, 100, 124, 141, 142

N

nickel 12, 13

O

organometallic 12, 14, 330

ozonolysis 53, 70, 71, 72, 73, 78, 79

P

palladium 12, 15, 16, 24, 25, 26, 27, 49, 66, 84, 85, 101, 318, 319, 321, 328, 332, 501

phosphinooxazoline 16, 24, 501

proton affinity

PA 417, 418, 419, 425, 428

proton affinity417, 425, 427, 453

Q

quaternary stereocenter.....15, 18, 26, 46, 58, 59, 66, 83, 84, 93, 95, 96, 97, 100, 317, 326, 327, 332

2-quinuclidone410, 411, 412, 413, 419, 426, 427, 430, 431, 449, 450, 451, 453

R

regioselective70, 97, 99, 100, 317

resonance stabilization409, 423

retrosynthetic analysis 2, 66, 327, 413

rhodium10, 93

ring contraction 66, 83, 84, 87, 89

S

Schmidt–Aubé.....413, 414, 417, 421, 427, 428, 430

sesquiterpenoids.....325, 326, 332

sesterterpenoid38, 41, 46, 64

(*S*)-*t*-Bu-PHOX 84, 102, 319, 501, 502, 505, 509

T

tandem25, 66, 67, 68, 74, 75, 80, 82, 100, 432

total synthesis2, 8, 13, 16, 26, 28, 29, 47, 95, 99, 100, 329, 331, 332, 371, 502

twisted amide410, 417, 418, 423, 425, 426, 427

V

variecolactone40, 43, 45, 60, 64

variecolin .38, 39, 40, 41, 42, 43, 44, 45, 46, 47, 48, 49, 50, 51, 53, 54, 56, 58, 59, 64, 65, 66, 67, 68, 74, 76,
77, 82, 91, 92, 93, 94, 95, 99, 100

variecolol.....40, 45, 64

vinylogous ...66, 84, 85, 86, 101, 146, 147, 148, 149, 150, 317, 318, 319, 320, 321, 322, 323, 324, 325, 328,
329, 330, 332, 337, 339, 340, 341, 342, 344, 346, 347, 349, 350, 352, 354, 359

W

Wolff/Cope rearrangement.....66, 67, 68, 74, 76, 80, 82, 92, 100, 142

X

X-ray39, 40, 79, 90, 91, 137, 156, 415, 416, 430, 504, 505

ABOUT THE AUTHOR

Michael R. Krout was born on November 2, 1979 in Lewisburg, PA to Raymond and Debra Krout. He spent his childhood with his older brother, Jan, and twin brother, Eric, in the small rural town of Mifflinburg, PA. His enthusiasm for science was stimulated by a challenging course instructed by Mr. Daryl Dreese, who emphasized the fundamental skills of observation and creativity in science. Michael attended Mifflinburg Area High where he competed in varsity football and pursued advanced math and science studies.

In 1998, he began undergraduate studies at Indiana University of Pennsylvania in Indiana, PA. Although he majored in biochemistry, an audited summer course (for “fun”) in organic chemistry, lectured by John T. Wood, triggered a new challenge and inspired his pursuit of advanced organic coursework and two summer internships that solidified his zeal for organic chemistry. In 2002, Michael graduated summa cum laude with a B.S. in biochemistry, along with minors in biology, chemistry, and mathematics.

In 2003, Michael ameliorated his chemistry skills for eight months in the Department of Medicinal Chemistry at Merck in West Point, PA, and then moved to sunny Pasadena, CA to pursue doctoral studies with Professor Brian M. Stoltz (an IUP alum!) at the California Institute of Technology. In 2009, he earned his Ph.D. in chemistry for investigations involving progress toward the asymmetric total synthesis of variegolin and gas-phase studies of the twisted amide 2-quinuclidone. Three weeks prior to his defense in August of 2009, he married his fiancée, Kristy Dax. In October of 2009, Michael began his NIH-sponsored postdoctoral studies under the direction of Professor David Y. Gin at the Memorial Sloan-Kettering Cancer Center in New York, NY.